

Harnessing the immunostimulatory properties of oncolytic reovirus for anticancer immunotherapy

Groeneveldt, P.C.

Citation
Groeneveldt, P. C. (2023, November 23). *Harnessing the immunostimulatory properties of oncolytic reovirus for anticancer immunotherapy*. Retrieved from https://hdl.handle.net/1887/3663612

Version:	Publisher's Version
License:	Licence agreement concerning inclusion of doctoral thesis in the Institutional Repository of the University of Leiden
Downloaded from:	https://hdl.handle.net/1887/3663612

Note: To cite this publication please use the final published version (if applicable).

Harnessing the immunostimulatory properties of oncolytic reovirus for anticancer immunotherapy

Christianne Groeneveldt

© 2023 Christianne Groeneveldt

ISBN: 978-94-6483-394-2
Printing: Ridderprint, ridderprint.nl
Cover: Evelien Jagtman, evelienjagtman.com
Layout and design: Tara Schollema, persoonlijkproefschrift.nl

The research described in this thesis was performed at the Department of Medical Oncology of the Leiden University Medical Center, Leiden and was financially supported by a PhD fellowship from Leiden University Medical Center, the Dutch Cancer Society Bas Mulder Award (11056) and the Support Casper campaign by the Dutch foundation 'Stichting Overleven met Alvleesklierkanker' (project numbers SOAK 17.04, 19.03 and 22.02).

Printing of this thesis was financially supported by the Department of Medical Oncology and the Stichting Overleven met Alvleesklierkanker.

All rights reserved. No part of this thesis may be reproduced, stored, or transmitted in any way or by any means without permission of the author.

Harnessing the immunostimulatory properties of oncolytic reovirus for anticancer immunotherapy

Proefschrift

ter verkrijging van
de graad van doctor aan de Universiteit Leiden,
op gezag van rector magnificus prof.dr.ir. H. Bijl,
volgens besluit van het college voor promoties
te verdedigen op donderdag 23 november 2023
klokke 10.00 uur

door

Pietje Centina Groeneveldt
geboren te Dordrecht
in 1995

PROMOTORES
Prof. dr. S.H. van der Burg
Prof. dr. T. van Hall

CO-PROMOTOR
Dr. A.G. van Montfoort

LEDEN PROMOTIECOMMISSIE

Prof. dr. E.J.H.J Wiertz	UMC Utrecht
Prof. dr. T.D. de Gruijl	Amsterdam UMC
Prof. dr. M.H.M. Heemskerk	
Prof. dr. R.E.M Toes	
Prof. dr. M. Yazdanbakhsh	

TABLE OF CONTENTS

Chapter 1	General Introduction	7
PART A	**EXPLOITATION OF THE REOVIRUS-SPECIFIC T-CELL RESPONSE FOR ANTICANCER THERAPY**	
Chapter 2	Preconditioning of the tumor microenvironment with oncolytic reovirus converts CD3-bispecific antibody treatment into effective immunotherapy *Journal for ImmunoTherapy of Cancer 2020;8:e001191*	25
Chapter 3	Preinduced reovirus-specific T-cell immunity enhances the anticancer efficacy of reovirus therapy *Journal for ImmunoTherapy of Cancer 2022;10:e004464*	69
PART B	**THE EFFECT OF PREEXISTING IMMUNITY ON REOVIRUS THERAPY**	
Chapter 4	Preexisting immunity: barrier or bridge to effective oncolytic virus therapy? *Cytokine & Growth Factor Reviews 2023;70:1-12*	115
Chapter 5	Neutralizing antibodies impair the efficacy of reovirus as oncolytic agent but permit effective combination with T-cell-based immunotherapy *Manuscript submitted*	147
Addendum I	$CD4^+$ T-cell depletion abrogates NAb production and improves the efficacy of reovirus monotherapy	185
PART C	**BLOCKADE OF TGF-β SIGNALING TO IMPROVE REOVIRUS-BASED IMMUNOTHERAPY**	
Chapter 6	Immunotherapeutic potential of TGF-β inhibition and oncolytic viruses *Trends in Immunology 2020;41(5):406-420*	195
Chapter 7	Intratumoral differences dictate the outcome of TGF-β blockade on the efficacy of viro-immunotherapy *Cancer Research Communications 2023;3(2):325–337*	223
Addendum II	TGF-β blockade improves Reo&αPD-L1 therapy in the murine colon MC38 tumor model	259
Chapter 8	Summarizing Discussion and Future Perspectives	265
Appendices	Nederlandse samenvatting voor niet-ingewijden	288
	List of publications	295
	About the author	298
	About the cover	299
	Dankwoord	300



CHAPTER 1

General Introduction

THE IMMUNE SYSTEM AS A DEFENSE AGAINST PATHOGENS

The immune system protects the body against invading microorganisms. Invaders, such as viruses and bacteria, can enter the body from the outside after breaching mucosal layers. Two branches of the immune system can be distinguished, the innate and the adaptive arms. As the first line of defense, the innate immune response is initiated immediately after pathogen-specific structures are recognized by pattern-recognizing receptors such as Toll-like receptors (TLRs) or retinoic acid-inducible gene 1 (RIG-1)-like receptors (1). One important function of innate immunity is the rapid recruitment of phagocytic immune cells such as neutrophils and macrophages to sites of infection through the production of cytokines and chemokines, to quickly eliminate the pathogen. Additionally, infected cells produce interferon molecules that initiate signaling cascades to enhance pathogen detection and restrict pathogen replication (2). Innate immunity responds relatively similar to different pathogens, which is why it is considered a non-specific immune response. In contrast, the adaptive immune response is highly antigen-specific and relies on the presence of specific receptors on immune cells derived from the thymus (T cells) or the bone marrow (B cells). The adaptive immune response is initiated by antigen-presenting cells (APCs), especially dendritic cells, that process and present pathogen-derived antigens to T cells. $CD4^+$ T cells play a key role in coordinating immune responses, including the stimulation of $CD8^+$ T cells and B cells. Whereas $CD8^+$ T cells engage in the eradication of intracellular pathogens via interactions between the T-cell receptor (TCR) and foreign peptides presented in major histocompatibility class I molecules (MHC-I), a B-cell response involves the production of antibodies that promote phagocytosis of the pathogen and prohibit infection (**Figure 1**).

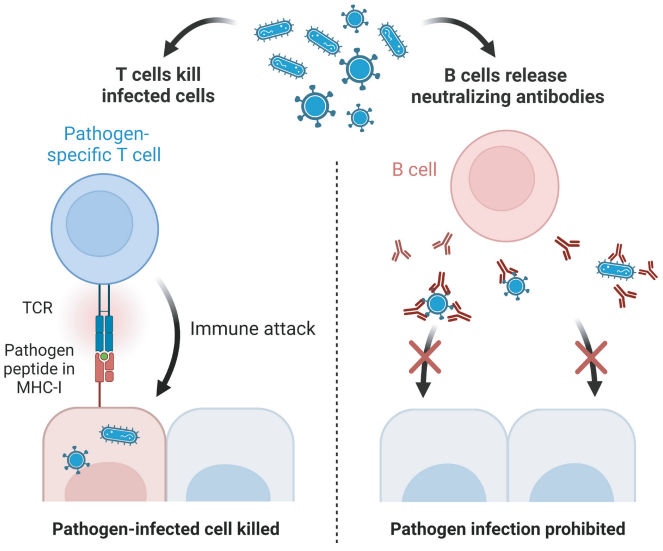


Figure 1. Adaptive immune responses upon exposure to pathogens. $CD8^+$ T cells are primed to recognize pathogen-derived peptides in MHC-I molecules on the surface of infected cells, leading to T-cell mediated killing of these infected cells. Activated B cells produce neutralizing antibodies, which bind to the pathogen and prevent the infection of cells.

EMPLOYING THE IMMUNE SYSTEM IN THE BATTLE AGAINST CANCER

The immune system not only mounts protective immune responses when it recognizes 'non-self' pathogens, it also can employ the same mechanisms to fight cancer. Although malignant cells are more similar to the host than pathogens, they still differ genetically from normal cells and, therefore, can be recognized by the immune system. Mutations in tumor cells might also give rise to the specific recognition of tumor cells by immune cells, a trait called immunogenicity. The potential of the immune system to recognize and control cancer is exploited in what is known as cancer immunotherapy. A big advantage of immunotherapy is that the tumor-specific immune response can eliminate a primary tumor, and established immune memory could also prevent cancer from recurring.

The therapeutic activation of tumor-specific T cells is especially promising due to their ability to selectively recognize and kill tumor cells. Indeed, multiple T-cell-based immunotherapeutic strategies have revolutionized the treatment of cancer. An example of T-cell-based immunotherapy is the use of immune checkpoint inhibitors, where inhibitory signals on T cells or their ligand on tumor cells are blocked to reactivate dysfunctional tumor-specific T cells (3). Another example is adoptive T-cell therapy (ACT), where tumor-specific T cells are isolated and expanded *ex vivo* before re-administration to the patient (4). Additionally, cancer vaccines, including synthetic peptides, viral vectors, and DNA or RNA vectors aim to enhance the frequency of tumor-specific T cells for enhanced eradication of the tumor (5). Lastly, the use of agonistic monoclonal antibodies is emerging, which aims to improve tumor-specific T-cell responses by targeting co-stimulatory molecules (6).

Although the above-mentioned T-cell-based immunotherapeutic strategies have demonstrated remarkable clinical responses in the treatment of solid tumors, there is much room for improvement. Successful responses to T-cell-based immuno-therapeutic interventions in solid tumors mostly occur in patients where tumors have an immune-infiltrated tumor phenotype, which displays a preexisting but often dysfunctional immune response (**Figure 2**) (7,8). However, a large proportion of solid tumors does not have an immune-infiltrated phenotype, but an immune-silent phenotype. These tumors are much less susceptible to T-cell-based immunotherapeutic strategies (9). Various factors contribute to this decreased susceptibility, for instance, a lack of antigens that can be targeted due to lower immunogenicity and/or lower mutational burden, an absence of tumor-specific T-cell priming or activation, or impaired trafficking and infiltration of tumor-specific T cells into the tumor beds (10-13). An example of a tumor type with an immune-silent phenotype is pancreatic cancer, which often responds poorly to various immunotherapeutic strategies (14). The lack of effective responses to immunotherapy in this type of tumor is a huge unmet need. Therefore, strategies to transform the immune-silent phenotype of unresponsive solid tumors

to an immune-infiltrated phenotype are desperately needed to enhance the efficacy of T-cell-based immunotherapeutic strategies. In other words, we need to find ways to increase the frequency of T cells in solid tumors to enhance the efficacy of T-cell-based immunotherapy.

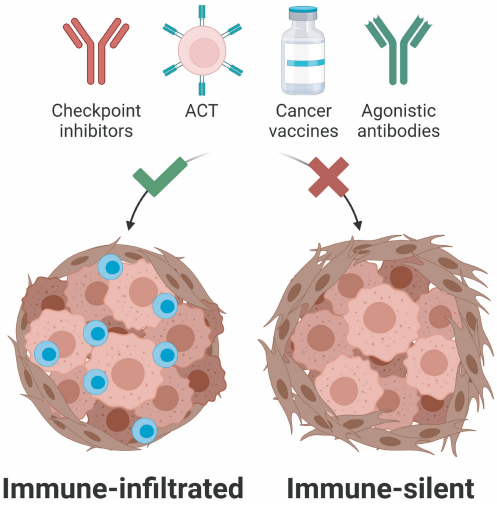


Figure 2. Immunophenotype of solid tumors determines response to T-cell-based immunotherapy. In immune-infiltrated tumors, T cells (blue) can migrate through the stromal regions (brown) into the tumor nests (red) but are often dysfunctional. Immunotherapeutic strategies such as checkpoint inhibition, adoptive cell transfer (ACT), vaccination and the use of agonistic antibodies can be effective. These therapies are less effective or non-effective in immune-silent tumors where intratumoral T cells are absent.

ONCOLYTIC VIRUSES AS IMMUNOSTIMULATORY AGENTS

One promising strategy to increase intratumoral T-cell density is treatment with oncolytic viruses (OVs) (15). The use of OVs as anticancer agents is emerging and inspired by the U.S. Food and Drug Administration (FDA) and European Medicines Agency (EMA) approval of talimogene laherparepvec (T-Vec) in 2015. T-vec is a herpes simplex virus type 1 (HSV-1) encoding granulocyte-macrophage colony-stimulating factor (GM-CSF) that increased survival and demonstrated favorable tolerability in advanced-stage melanoma patients (16). Besides T-vec, two other OVs have been approved globally for the treatment of cancer; a picornavirus named Rigvir was approved in 2004 for the treatment of melanoma in Latvia, and in China the use of a genetically modified adenovirus named H101 was approved in 2005 for the treatment of nasopharyngeal carcinoma in combination with chemotherapy. Currently, there is an immense pipeline of over 200 registered clinical trials investigating the therapeutic application of various OVs as single agents or as part of combination therapies (17).

OVs can demonstrate anticancer activity by their preferential replication in transformed cells, either as a natural characteristic or after genetic modification. Continued replication of the OV in malignant cells can eventually induce oncolysis, which might impair tumor outgrowth. Besides their oncolytic function, accumulating (pre)clinical evidence suggests that OVs might elicit a stronger antitumor effect through their capacity to function as immunostimulatory agents. Indeed, the percentage of scientific publications containing the search terms 'oncolytic virus' (OV) and 'immune response' (IR) increases yearly (**Figure 3**).

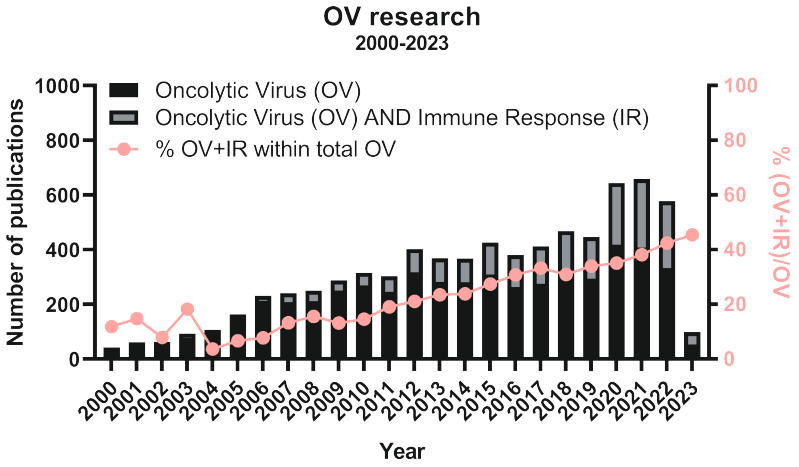


Figure 3. Number of publications focusing on immunostimulatory properties of OVs since 2000. Number of publications from the years 2000-2023 containing the search term 'Oncolytic Viruses' (OV), either alone or in combination with search term 'Immune Response' (IR). Right y-axis depicts percentage of OV+IR papers within total number of OV publications. Data obtained from PubMed Central® on 23-02-2023.

The idea to use OVs as immunostimulatory agents for anticancer therapy is supported by observations that OV treatment could induce an environment that is particularly favorable for the priming of T cells (**Figure 4**). For instance, the release of virus-derived nucleic acids, pathogen-associated molecular patterns (PAMPs), and/or damage-associated molecular patterns (DAMPs) during OV infection optimally induce the maturation of dendritic cells (18,19). Simultaneously, dying tumor cells are a source of virus and tumor antigens, leading to the priming of tumor- and virus-specific $CD4^+$ and $CD8^+$ T-cell responses (20,21). This process is further enhanced by the OV-induced interferon (IFN) response, which involves the release of T-cell-attracting chemokines, promotes antigen presentation, and recruits immune cells to the tumor (22). Thus, the OV-induced tumor-reactive immune response is believed to be not only a crucial aspect of the therapeutic efficacy of OVs themselves (23,24) but may also be utilized to sensitize tumors for other types of immunotherapy by enhancing immunogenicity or by attracting activated $CD4^+$ and $CD8^+$ T cells to nonresponsive tumors (15,25).

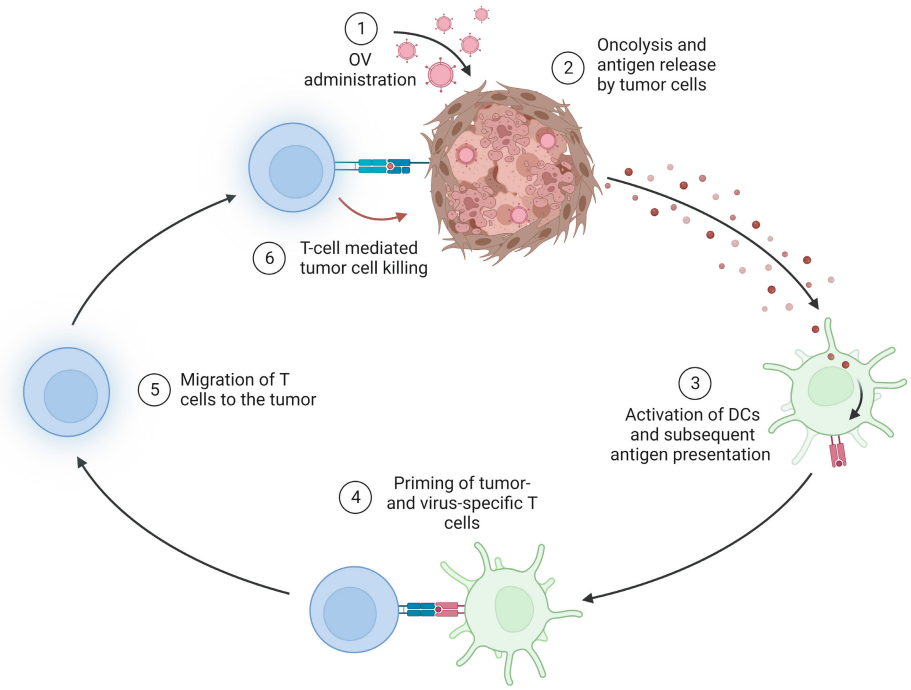


Figure 4. Model of the immunostimulatory properties of OVs. OV replication causes oncolysis, which can induce the release of tumor-specific and virus-specific antigens. The subsequent uptake and presentation of these antigens by dendritic cells (DCs) leads to the induction of tumor- and virus-specific T cells. OV infection and replication also can induce a type I interferon (IFN) response that causes the release of T cell-attracting chemokines. The tumor- and virus-specific T cells are attracted by these chemokines and migrate towards the tumor to exert their function.

ONCOLYTIC REOVIRUS

Various viruses can demonstrate oncolytic and immunostimulatory potential, including Vaccinia virus, HSV-1, and Adenovirus (26,27). In particular, the mammalian reovirus type 3 Dearing strain (T3D) is one of the leading OVs under clinical evaluation and displays an excellent safety record in clinical trials (28,29). Previously known as Reolysin®, reovirus type 3 Dearing is currently manufactured as pelareorep for therapeutic anticancer application by Canadian company Oncolytics Biotech Inc.

Reoviruses are non-enveloped, double-stranded (ds) RNA viruses. The outer and inner capsids protect its genome, which consists of 10 dsRNA segments termed large (L1-3), medium (M1-3), or small (S1-4) (30). These gene segments encode 8 structural proteins (λ1-3, μ1-2, and σ1-3) and 2 non-structural proteins, μNS and σNS (**Figure 5**). Reoviruses were first isolated in the 1950s from pediatric stool samples and were termed reovirus (respiratory enteric orphan virus), since at the time of discovery reoviruses were not associated with any known disease. In most individuals, reovirus infection occurs asymptomatically during childhood, confirming its classification as an orphan virus.

Besides T3D, two other reovirus serotypes circulate in humans, named serotype 1 Lang (T1L) and serotype 2 Jones (T2J).

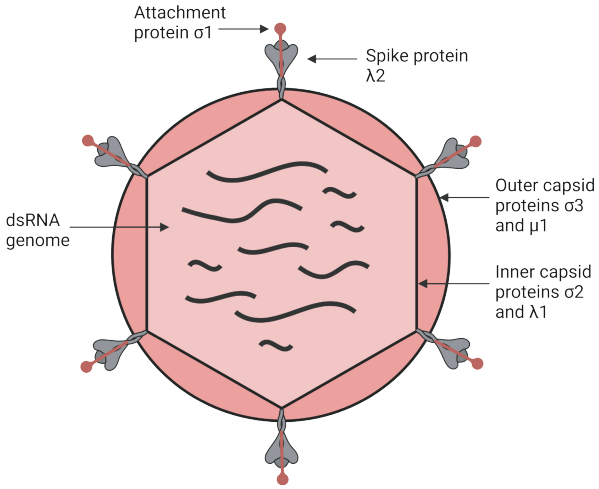


Figure 5. Schematic representation of mammalian reovirus Type 3 Dearing. Depicted are the locations of reovirus proteins and its double stranded RNA (dsRNA) genome.

Reovirus T3D (hereafter named reovirus) shows an inherent preference for replication in malignant but not healthy cells (31,32). Early, pivotal studies demonstrated that high activity of the intracellular Ras signaling pathway allowed for efficient reovirus replication (33). The Ras signaling pathway is upregulated in many cancer types, often due to an activating oncogenic mutation, where it regulates various cellular processes such as cell proliferation and survival (34). Upon infection with reovirus, healthy cells activate their natural defenses upon recognition of the double-stranded RNA structures, which includes the phosphorylation of double-stranded-RNA-dependent protein kinase (PKR). Phosphorylation of PKR leads to phosphorylation of eukaryotic initiation factor 2α, which can inhibit the translation of viral genes (35). However, in cancer cells with a highly active RAS pathway, the phosphorylation of PKR is inhibited, and viral translation is not prohibited. Besides an activated Ras pathway, other factors might also contribute to the preferential replication of reovirus in tumor cells, such as the increased expression of the reovirus entry-receptor junctional adhesion molecule A (36-38) or cellular proteases such as cathepsin B and L (39) which allow efficient viral uncoating and thus replication in tumor cells. Ultimately, sensitivity to reovirus-induced oncolysis is likely to be dependent on multiple cellular and molecular determinants, many of which still need to be uncovered.

The preferential replication of reovirus in tumor cells, combined with its non-pathogenic nature in humans, makes reovirus attractive to use as an oncolytic agent for anticancer therapy. Already in 1998, Coffey et al demonstrated that a single intratumoral injection of reovirus could result in the regression of established NIH 3T3 tumors or human U87 glioblastoma tumors in 80% of severe combined immunodeficient mice (40).

Other preclinical studies demonstrated that reovirus could induce regressions of subcutaneous and orthotopic gliomas (41), as well as colorectal C26 liver metastases (42) or prostrate xenograft tumors (43). But, although reovirus has demonstrated some tumor regressions as a monotherapy in certain cancer types, results from clinical trials all point toward a growing consensus that reovirus is unlikely to have sufficient clinical efficacy as a single agent. Various aspects might contribute to the limited efficacy of oncolytic reovirus as monotherapy, such as a limited oncolytic potential of the virus itself or the large heterogeneity of cells within tumors, including virus-resistant cell populations. In addition, early investigations suggested that the presence of neutralizing antibodies (NAbs) in patients, either preexisting or induced upon therapy, might limit the therapeutic efficacy of reovirus, especially when reovirus is administered intravenously (44). However, knowledge regarding the effect of (preexisting) NAbs on the efficacy of reovirus therapy remains underexplored.

Instead of applying reovirus as monotherapy, its potential might be better manifested in rationally-designed combination strategies (45,46). For instance, the administration of reovirus in combination with radiotherapy (47,48) or chemotherapeutic agents (49-51) has resulted in an enhanced therapeutic outcome compared to reovirus alone, which could often be attributed to increased direct cytotoxicity. But, not much is known about the immunostimulatory properties of oncolytic reovirus, and consequently, research into the possible benefit of combining oncolytic reovirus with immunotherapy is lacking. Only a few studies have explored the immunostimulatory properties of reovirus, for example by combining reovirus administration with immune checkpoint blockade. Indeed, intratumorally or systemically administered reovirus sensitized tumors to subsequent blockade of the PD-1/PD-L1 axis in preclinical models of multiple myeloma (52), glioma (22), and breast cancer (53). However, since the efficacy of immune checkpoint blockade mostly relies on the presence of tumor-specific T cells, the combination of reovirus and immune checkpoint blockade might be predominantly successful in immunogenic tumors where tumor-specific T cells can be elicited. This highlights the need for new viro-immunotherapeutic strategies that can benefit patients with less immunogenic, immune-silent tumors where T cells are mostly absent.

TGF-β SIGNALING AS ANOTHER BARRIER TO EFFECTIVE IMMUNOTHERAPY

The exploitation of OVs, and in particular oncolytic reovirus, to transform the tumor microenvironment (TME) of solid, immune-silent tumors to enhance the efficacy of T-cell-based immunotherapy is a new and exciting avenue. But, the lack of intratumoral T cells in immune-silent tumors might not be the only problem that limits effective T-cell-based immunotherapy in solid tumors. The pleiotropic cytokine transforming growth factor β (TGF-β) is considered one of the key factors responsible for the exclusion and suppression of immune cells from the tumor. In pre-malignant cells, TGF-β acts as a

tumor-suppressing cytokine that induces apoptosis and regulates proliferation (54). However, in certain types of cancer, such as pancreatic cancer, non-small cell lung cancer, and colon cancer (55-57), tumor cells can become insensitive to TGF-β-induced cytostatic effects, and TGF-β functionally switches into a tumor-promoting cytokine by stimulating cancer cell migration and invasion, extracellular matrix (ECM) remodeling, epithelial-to-mesenchymal transition (EMT) and the formation of an immunosuppressive TME (58). Amongst others, its immunosuppressive functions include inhibiting the generation, intratumoral influx, and function of $CD4^+$ and $CD8^+$ T cells, as well as dendritic cells (59). These characteristics hint towards a potential beneficial effect of TGF-β blockade on the efficacy of T-cell-based immunotherapy. Preclinical evidence already demonstrated that TGF-β blockade could enhance the efficacy of checkpoint blockade (60), but whether TGF-β blockade could work synergistically with OV therapy to optimally improve the therapeutic efficacy of T-cell-based immunotherapy is not yet investigated.

AIM OF THIS THESIS

The studies described in this thesis aimed to elucidate the immunostimulatory potential of oncolytic reovirus and to investigate how these immunostimulatory characteristics could be exploited for effective anticancer immunotherapy (**Figure 6**). After reovirus administration to the tumor (**1**), we hypothesize that a potent immune response will be elicited (**2**). We aim to identify how this immune response can be employed for antitumor immunotherapy (**3**), but also whether the emergence of reovirus-specific immune responses (**4**) might prevent or contribute to the antitumor effect of oncolytic reovirus. Lastly, we will assess whether blocking immuno-inhibitory signaling pathways in the tumor influences the function of reovirus (**5**) or the reovirus-induced immune response (**6**) and can thus be employed to improve the efficacy of viro-immunotherapy.

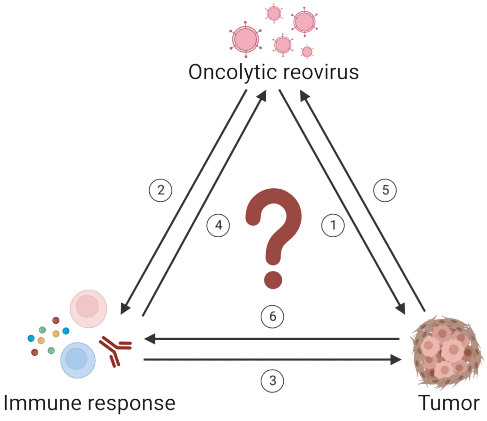


Figure 6. Harnessing the immunostimulatory potential of oncolytic reovirus for anticancer immunotherapy. Arrows and numbers indicate various processes that will be investigated in this thesis, to ultimately understand how the immunostimulatory properties of oncolytic reovirus can be employed for effective anticancer therapy.

OUTLINE OF THIS THESIS

Here, we first studied the reovirus-induced immune response in detail in immunocompetent mice bearing murine pancreatic KPC3 tumors in **Chapter 2**. We observed that intratumoral administration of reovirus leads to a fast interferon response, which is followed by an influx of immune cells, especially $CD8^+$ T cells. A proportion of these $CD8^+$ T cells recognized reovirus itself, but not the tumor. Therefore, we employed CD3-bispecific antibodies (CD3-bsAbs) that could activate these $CD8^+$ T cells, irrespective of their virus-specificity, to kill tumor cells. The combination of reovirus and CD3-bsAbs proved to be highly effective in inducing tumor regression and survival. The reovirus-specific $CD8^+$ T-cell response is further dissected in **Chapter 3**. Here, we identified the immunodominant $CD8^+$ T-cell epitope of reovirus in the applied mouse strain, which allowed us to study the kinetics, distribution, and phenotype of reovirus-specific T cells. We show that reovirus-specific T cells are potent effector cells that are enriched in the tumor after intratumoral reovirus administration, which suggested that they may recognize and kill reovirus-infected tumor cells. A synthetic long peptide (SLP) vaccine containing this reovirus-derived $CD8^+$ T-cell epitope was designed to induce high levels of reovirus-specific T cells before virotherapy. Upon intratumoral reovirus administration, these T cells were reactivated and migrated toward the tumor, which lead to significantly delayed tumor growth. Together, the research in **Chapters 2 and 3** demonstrates two different manners in which reovirus-specific T cells can be exploited for effective anticancer therapy.

Since a substantial percentage of the human population has supposedly encountered reovirus during their lifetime, we wondered whether preexisting immunity would have implications on the efficacy of reovirus (combination) therapy. **Chapter 4** reviews the current literature on the effect of preexisting immunity against various OVs on their efficacy when used as anticancer therapeutic agents. In **Chapter 5**, the effect of preexisting immunity on reovirus replication and its oncolytic potential, as well as the efficacy of reovirus-based immunotherapeutic strategies is experimentally addressed. We observed that the presence of preexisting neutralizing antibodies impairs reovirus replication and the reovirus-induced interferon response and hampers the use of reovirus as oncolytic agent. We demonstrated in **Addendum I** that depletion of $CD4^+$ T cells can abrogate NAb production and enhance the anticancer efficacy of reovirus as monotherapy. Furthermore, we demonstrated in **Chapter 5** that the reovirus-induced intratumoral T-cell influx was not impaired by preexposure, and that potent antitumor responses can still be observed in the context of preexisting immunity.

Lastly, we investigated whether TGF-β blockade might further improve the efficacy of viro-immunotherapy. **Chapter 6** provides an extensive summary of preclinical and clinical evidence that illustrates how the combined inhibition of TGF-β signaling and the use of OVs might increase the efficacy of immunotherapy. We then investigated whether TGF-β blockade could improve the efficacy of reovirus-based immunotherapeutic

strategies in **Chapter 7** and **Addendum II**. We demonstrated that TGF-β blockade significantly improved the efficacy of reovirus and CD3-bsAbs or reovirus and αPD-L1 in the preclinical MC38 colon carcinoma model, but surprisingly impaired the efficacy of reovirus and CD3-bsAbs in the pancreatic KPC3 tumor model. We elaborated on various intertumoral differences that might be contributing to this differential effect, such as baseline T-cell density, stromal composition, or the different effects of TGF-β blockade on the reovirus-induced T-cell influx into the tumor. Finally, **Chapter 8** provides a summary and discussion of the findings of this thesis in the context of recent literature.

REFERENCES

1. Amarante-Mendes GP, Adjemian S, Branco LM, Zanetti LC, Weinlich R, Bortoluci KR. Pattern Recognition Receptors and the Host Cell Death Molecular Machinery. Front Immunol **2018**;9
2. Kopitar-Jerala N. The Role of Interferons in Inflammation and Inflammasome Activation. Front Immunol **2017**;8:873
3. Robert C. A decade of immune-checkpoint inhibitors in cancer therapy. Nature Communications **2020**;11:3801
4. Kirtane K, Elmariah H, Chung CH, Abate-Daga D. Adoptive cellular therapy in solid tumor malignancies: review of the literature and challenges ahead. J Immunother Cancer **2021**;9:e002723
5. Lin MJ, Svensson-Arvelund J, Lubitz GS, Marabelle A, Melero I, Brown BD*, et al.* Cancer vaccines: the next immunotherapy frontier. Nature Cancer **2022**;3:911-26
6. Mayes PA, Hance KW, Hoos A. The promise and challenges of immune agonist antibody development in cancer. Nature Reviews Drug Discovery **2018**;17:509-27
7. Chen DS, Mellman I. Elements of cancer immunity and the cancer-immune set point. Nature **2017**;541:321-30
8. Fridman WH, Pagès F, Sautès-Fridman C, Galon J. The immune contexture in human tumours: impact on clinical outcome. Nature Reviews Cancer **2012**;12:298-306
9. Bonaventura P, Shekarian T, Alcazer V, Valladeau-Guilemond J, Valsesia-Wittmann S, Amigorena S*, et al.* Cold Tumors: A Therapeutic Challenge for Immunotherapy. Front Immunol **2019**;10
10. Goodman AM, Kato S, Bazhenova L, Patel SP, Frampton GM, Miller V*, et al.* Tumor Mutational Burden as an Independent Predictor of Response to Immunotherapy in Diverse Cancers. Mol Cancer Ther **2017**;16:2598-608
11. Herbst RS, Soria J-C, Kowanetz M, Fine GD, Hamid O, Gordon MS*, et al.* Predictive correlates of response to the anti-PD-L1 antibody MPDL3280A in cancer patients. Nature **2014**;515:563-7
12. Ayers M, Lunceford J, Nebozhyn M, Murphy E, Loboda A, Kaufman DR*, et al.* IFN-γ-related mRNA profile predicts clinical response to PD-1 blockade. J Clin Invest **2017**;127:2930-40
13. Galon J, Costes A, Sanchez-Cabo F, Kirilovsky A, Mlecnik B, Lagorce-Pagès C*, et al.* Type, Density, and Location of Immune Cells Within Human Colorectal Tumors Predict Clinical Outcome. Science **2006**;313:1960-4
14. Timmer FEF, Geboers B, Nieuwenhuizen S, Dijkstra M, Schouten EAC, Puijk RS*, et al.* Pancreatic Cancer and Immunotherapy: A Clinical Overview. Cancers (Basel) **2021**;13
15. Harrington K, Freeman DJ, Kelly B, Harper J, Soria J-C. Optimizing oncolytic virotherapy in cancer treatment. Nature Reviews Drug Discovery **2019**
16. Andtbacka RHI, Kaufman HL, Collichio F, Amatruda T, Senzer N, Chesney J*, et al.* Talimogene Laherparepvec Improves Durable Response Rate in Patients With Advanced Melanoma. J Clin Oncol **2015**;33:2780-8
17. Lauer UM, Beil J. Oncolytic viruses: challenges and considerations in an evolving clinical landscape. Future Oncology **2022**;18:2713-32
18. Brown MC, Holl EK, Boczkowski D, Dobrikova E, Mosaheb M, Chandramohan V*, et al.* Cancer immunotherapy with recombinant poliovirus induces IFN-dominant activation of dendritic cells and tumor antigen–specific CTLs. Sci Transl Med **2017**;9:eaan4220
19. Benencia F, Courrèges MC, Conejo-García JR, Mohamed-Hadley A, Zhang L, Buckanovich RJ*, et al.* HSV oncolytic therapy upregulates interferon-inducible chemokines and recruits immune effector cells in ovarian cancer. Molecular Therapy **2005**;12:789-802
20. Gauvrit A, Brandler S, Sapede-Peroz C, Boisgerault N, Tangy F, Gregoire M. Measles virus induces oncolysis of mesothelioma cells and allows dendritic cells to cross-prime tumor-specific CD8 response. Cancer Res **2008**;68:4882-92
21. Delaunay T, Violland M, Boisgerault N, Dutoit S, Vignard V, Münz C*, et al.* Oncolytic viruses sensitize human tumor cells for NY-ESO-1 tumor antigen recognition by CD4+ effector T cells. Oncoimmunology **2017**;7:e1407897-e

22. Samson A, Scott KJ, Taggart D, West EJ, Wilson E, Nuovo GJ, *et al.* Intravenous delivery of oncolytic reovirus to brain tumor patients immunologically primes for subsequent checkpoint blockade. Sci Transl Med **2018**;10:eaam7577
23. Diaz RM, Galivo F, Kottke T, Wongthida P, Qiao J, Thompson J, *et al.* Oncolytic Immunovirotherapy for Melanoma Using Vesicular Stomatitis Virus. Cancer Res **2007**;67:2840-8
24. Moesta AK, Cooke K, Piasecki J, Mitchell P, Rottman JB, Fitzgerald K, *et al.* Local Delivery of OncoVEXmGM-CSF Generates Systemic Antitumor Immune Responses Enhanced by Cytotoxic T-Lymphocyte–Associated Protein Blockade. Clin Cancer Res **2017**;23:6190-202
25. Zamarin D, Holmgaard RB, Subudhi SK, Park JS, Mansour M, Palese P, *et al.* Localized Oncolytic Virotherapy Overcomes Systemic Tumor Resistance to Immune Checkpoint Blockade Immunotherapy. Sci Transl Med **2014**;6:226ra32-ra32
26. Takasu A, Masui A, Hamada M, Imai T, Iwai S, Yura Y. Immunogenic cell death by oncolytic herpes simplex virus type 1 in squamous cell carcinoma cells. Cancer Gene Therapy **2016**;23:107
27. Ma J, Ramachandran M, Jin C, Quijano-Rubio C, Martikainen M, Yu D, *et al.* Characterization of virus-mediated immunogenic cancer cell death and the consequences for oncolytic virus-based immunotherapy of cancer. Cell death & disease **2020**;11:48
28. Mahalingam D, Goel S, Aparo S, Patel Arora S, Noronha N, Tran H, *et al.* A Phase II Study of Pelareorep (REOLYSIN(®)) in Combination with Gemcitabine for Patients with Advanced Pancreatic Adenocarcinoma. Cancers (Basel) **2018**;10:160
29. Sborov DW, Nuovo GJ, Stiff A, Mace T, Lesinski GB, Benson DM, *et al.* A Phase I Trial of Single-Agent Reolysin in Patients with Relapsed Multiple Myeloma. Clinical Cancer Research **2014**;20:5946-55
30. Shatkin AJ, Sipe JD, Loh P. Separation of ten reovirus genome segments by polyacrylamide gel electrophoresis. J Virol **1968**;2:986-91
31. Duncan MR, Stanish SM, Cox DC. Differential sensitivity of normal and transformed human cells to reovirus infection. J Virol **1978**;28:444-9
32. Shmulevitz M, Marcato P, Lee PWK. Unshackling the links between reovirus oncolysis, Ras signaling, translational control and cancer. Oncogene **2005**;24:7720-8
33. Strong JE, Coffey MC, Tang D, Sabinin P, Lee PW. The molecular basis of viral oncolysis: usurpation of the Ras signaling pathway by reovirus. The EMBO journal **1998**;17:3351-62
34. Gimple RC, Wang X. RAS: Striking at the Core of the Oncogenic Circuitry. Front Oncol **2019**;9
35. Clemens MJ. PKR--a protein kinase regulated by double-stranded RNA. The international journal of biochemistry & cell biology **1997**;29:945-9
36. Kelly KR, Espitia CM, Zhao W, Wendlandt E, Tricot G, Zhan F, *et al.* Junctional adhesion molecule-A is overexpressed in advanced multiple myeloma and determines response to oncolytic reovirus. Oncotarget **2015**;6:41275-89
37. Zhang M, Luo W, Huang B, Liu Z, Sun L, Zhang Q, *et al.* Overexpression of JAM-A in non-small cell lung cancer correlates with tumor progression. PLoS One **2013**;8:e79173
38. McSherry EA, McGee SF, Jirstrom K, Doyle EM, Brennan DJ, Landberg G, *et al.* JAM-A expression positively correlates with poor prognosis in breast cancer patients. Int J Cancer **2009**;125:1343-51
39. Alain T, Kim TS, Lun X, Liacini A, Schiff LA, Senger DL, *et al.* Proteolytic disassembly is a critical determinant for reovirus oncolysis. Mol Ther **2007**;15:1512-21
40. Coffey MC, Strong JE, Forsyth PA, Lee PWK. Reovirus Therapy of Tumors with Activated Ras Pathway. Science **1998**;282:1332-4
41. Wilcox ME, Yang W, Senger D, Rewcastle NB, Morris DG, Brasher PM, *et al.* Reovirus as an oncolytic agent against experimental human malignant gliomas. Journal of the National Cancer Institute **2001**;93:903-12
42. Smakman N, van der Bilt JD, van den Wollenberg DJ, Hoeben RC, Borel Rinkes IH, Kranenburg O. Immunosuppression promotes reovirus therapy of colorectal liver metastases. Cancer Gene Ther **2006**;13:815-8

43. Thirukkumaran CM, Nodwell MJ, Hirasawa K, Shi Z-Q, Diaz R, Luider J*, et al.* Oncolytic Viral Therapy for Prostate Cancer: Efficacy of Reovirus as a Biological Therapeutic. Cancer Research **2010**;70:2435-44
44. Hirasawa K, Nishikawa SG, Norman KL, Coffey MC, Thompson BG, Yoon CS*, et al.* Systemic reovirus therapy of metastatic cancer in immune-competent mice. Cancer Res **2003**;63:348-53
45. Zhao X, Chester C, Rajasekaran N, He Z, Kohrt HE. Strategic Combinations: The Future of Oncolytic Virotherapy with Reovirus. Molecular cancer therapeutics **2016**;15:767-73
46. Müller L, Berkeley R, Barr T, Ilett E, Errington-Mais F. Past, Present and Future of Oncolytic Reovirus. Cancers **2020**;12:3219
47. Twigger K, Vidal L, White CL, De Bono JS, Bhide S, Coffey M*, et al.* Enhanced in vitro and in vivo cytotoxicity of combined reovirus and radiotherapy. Clin Cancer Res **2008**;14:912-23
48. McEntee G, Kyula JN, Mansfield D, Smith H, Wilkinson M, Gregory C*, et al.* Enhanced cytotoxicity of reovirus and radiotherapy in melanoma cells is mediated through increased viral replication and mitochondrial apoptotic signalling. Oncotarget **2016**;7:48517-32
49. Heinemann L, Simpson GR, Boxall A, Kottke T, Relph KL, Vile R*, et al.* Synergistic effects of oncolytic reovirus and docetaxel chemotherapy in prostate cancer. BMC Cancer **2011**;11:221
50. Pandha HS, Heinemann L, Simpson GR, Melcher A, Prestwich R, Errington F*, et al.* Synergistic effects of oncolytic reovirus and cisplatin chemotherapy in murine malignant melanoma. Clin Cancer Res **2009**;15:6158-66
51. Sei S, Mussio JK, Yang QE, Nagashima K, Parchment RE, Coffey MC*, et al.* Synergistic antitumor activity of oncolytic reovirus and chemotherapeutic agents in non-small cell lung cancer cells. Mol Cancer **2009**;8:47
52. Kelly KR, Espitia CM, Zhao W, Wu K, Visconte V, Anwer F*, et al.* Oncolytic reovirus sensitizes multiple myeloma cells to anti-PD-L1 therapy. Leukemia **2018**;32:230-3
53. Mostafa AA, Meyers DE, Thirukkumaran CM, Liu PJ, Gratton K, Spurrell J*, et al.* Oncolytic Reovirus and Immune Checkpoint Inhibition as a Novel Immunotherapeutic Strategy for Breast Cancer. Cancers (Basel) **2018**;10
54. David CJ, Massagué J. Contextual determinants of TGFβ action in development, immunity and cancer. Nature Reviews Molecular Cell Biology **2018**;19:419-35
55. Shen W, Tao GQ, Zhang Y, Cai B, Sun J, Tian ZQ. TGF-beta in pancreatic cancer initiation and progression: two sides of the same coin. Cell & Bioscience **2017**;7:39
56. Calon A, Espinet E, Palomo-Ponce S, Tauriello DV, Iglesias M, Cespedes MV*, et al.* Dependency of colorectal cancer on a TGF-beta-driven program in stromal cells for metastasis initiation. Cancer Cell **2012**;22:571-84
57. Chae YK, Chang S, Ko T, Anker J, Agte S, Iams W*, et al.* Epithelial-mesenchymal transition (EMT) signature is inversely associated with T-cell infiltration in non-small cell lung cancer (NSCLC). Scientific reports **2018**;8:2918
58. Connolly EC, Freimuth J, Akhurst RJ. Complexities of TGF-beta targeted cancer therapy. Int J Biol Sci **2012**;8:964-78
59. Batlle E, Massague J. Transforming Growth Factor-beta Signaling in Immunity and Cancer. Immunity **2019**;50:924-40
60. Mariathasan S, Turley SJ, Nickles D, Castiglioni A, Yuen K, Wang Y*, et al.* TGFbeta attenuates tumour response to PD-L1 blockade by contributing to exclusion of T cells. Nature **2018**;554:544-8



PART A

Exploitation of the reovirus-specific T-cell response for anticancer therapy



CHAPTER 2

Preconditioning of the tumor microenvironment with oncolytic reovirus converts CD3-bispecific antibody treatment into effective immunotherapy

Christianne Groeneveldt[1], Priscilla Kinderman[1], Diana J. M. van den Wollenberg[2], Ruben L. van den Oever[1], Jim Middelburg[1], Dana A. M. Mustafa[3], Rob C. Hoeben[2], Sjoerd H. van der Burg[1], Thorbald van Hall[1#] and Nadine van Montfoort[1#]

1 Department of Medical Oncology, Oncode Institute, Leiden University Medical Center, 2333 ZA, Leiden, The Netherlands

2 Department of Cell and Chemical Biology, Leiden University Medical Center, 2300 RC, Leiden, The Netherlands

3 Department of Pathology, the Tumor Immuno-Pathology Laboratory, Erasmus MC, University Medical Center Rotterdam, Rotterdam, 3000 CA, The Netherlands

Corresponding authors

Journal for ImmunoTherapy of Cancer 2020;8:e001191. doi:10.1136/jitc-2020-001191

ABSTRACT

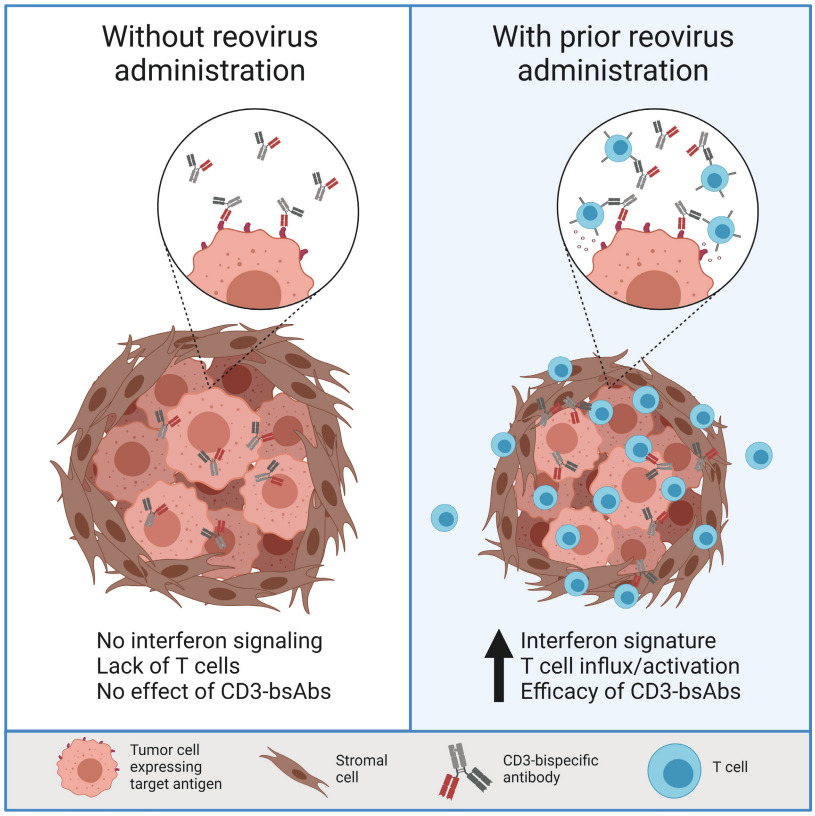
Background. T-cell-engaging CD3-bispecific antibodies (CD3-bsAbs) are promising modalities for cancer immunotherapy. Although this therapy has reached clinical practice for hematological malignancies, the absence of sufficient infiltrating T cells is a major barrier to efficacy in solid tumors. In this study, we exploited oncolytic reovirus as a strategy to enhance the efficacy of CD3-bsAbs in immune-silent solid tumors.

Methods. The mutant *p53* and *K-ras*-induced murine pancreatic cancer model KPC3 resembles human pancreatic ductal adenocarcinomas with a desmoplastic tumor microenvironment, low T-cell density, and resistance to immunotherapy. Immune-competent KPC3-tumor bearing mice were intratumorally injected with reovirus type 3 Dearing strain and the reovirus-induced changes in the tumor microenvironment and spleen were analyzed over time by NanoString analysis, RT-qPCR, and multicolor flow cytometry. The efficacy of reovirus in combination with systemically injected CD3-bsAbs was evaluated in immune-competent mice with established KPC3 or B16.F10 tumors, and in the close-to-patient $HER2^+$ breast cancer model BT474 engrafted in NSG mice with human PBMCs as effector cells.

Results. Replication-competent reovirus induced an early IFN signature, followed by a strong influx of NK cells and $CD8^+$ T cells, at the cost of $FoxP3^+$ Tregs. Viral replication declined after seven days and was associated with systemic activation of lymphocytes and the emergence of intratumoral reovirus-specific $CD8^+$ T cells. Although tumor-infiltrating T cells were mostly reovirus-specific and not tumor-specific, they served as non-exhausted effector cells for the subsequently systemically administered CD3-bsAbs. Combination treatment of reovirus and CD3-bsAbs led to the regression of large, established KPC3, B16F10, and BT474 tumors. Reovirus as a preconditioning regimen performed significantly better than simultaneous or early administration of CD3-bsAbs. This combination treatment induced regressions of distant lesions that were not injected with reovirus, and systemic administration of both reovirus and CD3-bsAbs also led to tumor control. This suggests that this therapy might also be effective for metastatic disease.

Conclusions. Oncolytic reovirus administration represents an effective strategy to induce a local IFN response and strong T-cell influx, thereby sensitizing the tumor microenvironment for subsequent CD3-bsAb therapy. This combination therapy warrants further investigation in patients with non-inflamed solid tumors.

GRAPHICAL ABSTRACT



INTRODUCTION

T-cell-engaging bispecific antibodies (bsAbs) are emerging as a potent therapeutic cancer modality (1). These immunoglobulin-based biologicals can induce dramatic responses in advanced malignancies, as was demonstrated with the use of a CD3xCD19 bsAb for the treatment of non-Hodgkin's lymphoma (2). Currently, more than 40 other T-cell-redirecting bsAbs are in clinical development for both hematological malignancies and solid tumors (3). CD3-bsAbs are comprised of one arm engaging a tumor-associated antigen (TAA) expressed on the cell surface of cancer cells, and a second arm targeting T cells via CD3 (4). By tethering T cells to tumor cells, these CD3-bsAbs create a functional immunological synapse (5). This results in selective T-cell-mediated killing of the target-expressing tumor cells, for which both $CD4^+$ and $CD8^+$ T cells can be employed (6). Since binding and activation of T cells occurs via CD3, these CD3-bsAbs can activate T cells in an MHC class I- and T-cell receptor (TCR)-independent manner. CD3-bsAbs can redirect a large proportion of the polyclonal T-cell pool towards the tumor, and thereby bypass the need for endogenous tumor-specific T cells (7). Despite the many advantages of these CD3-bsAbs, clinical development has been hampered by several factors, including low response rates in solid, immune-silent tumors (7). Factors associated with poor response to immunotherapy include the absence of an interferon gene signature and lack of T cells in the tumor beds, generally referred to as a 'cold' microenvironment (8,9).

Oncolytic viruses (OVs) are increasingly recognized as potent anticancer moieties due to their virtue of selective replication in transformed cells and the ability to ignite an antiviral immune response in the malignant lesion (10). It has been demonstrated that OVs can sensitize resistant tumors for checkpoint blockade therapy (11-13). The mammalian reovirus type 3 Dearing strain (T3D), which is not associated with symptomatic disease in humans, is one of the leading oncolytic viruses under clinical evaluation and displays an excellent safety record in clinical trials (14,15). Reoviruses show an inherent preference for replication in transformed, but not in healthy cells (16,17). Although reovirus has demonstrated some tumor regressions as a monotherapy in certain cancer types, such as in prostate xenograft models and prostate cancer patients, its potency might be better manifested in rationally-designed combination strategies (18,19). In this study, we employed oncolytic reovirus as a strategy to enhance the antitumor efficacy of CD3-bsAbs in solid tumors. Using fully immunocompetent mouse tumor models, we demonstrated that injection with replication-competent reovirus converted immunologically cold pancreatic adenocarcinoma tumors to inflamed sites with a strong IFN signature and abundance of virus-specific $CD8^+$ T cells. This effect depended on viral replication, which was controlled by the immune system within two weeks. Subsequent systemic administration of bsAb resulted in regressions of local and distant large tumors. These findings provide evidence that preconditioning the tumor microenvironment with oncolytic reovirus is an attractive strategy to prime immune-silent tumors for effective CD3-bsAb therapy.

MATERIAL & METHODS

Reovirus

The wild-type reovirus strain R124 (here referred to as reovirus) was previously isolated from a heterogeneous reovirus Type 3 Dearing (T3D) stock (VR-824) obtained from the American Type Culture Collection (ATCC) by two rounds of plaque purification using HER911 cells (20). All experiments were performed using cesium chloride (CsCl)-purified stocks (see Supplementary materials). The total amount of particles was calculated based on OD260 values where 1 OD equals $2.10x10^{12}$ reovirus particles/mL (21). The infectious titer was quantified by plaque assay on HER911 cells (22). Reovirus particles were inactivated by exposure to shortwave ultraviolet light (254 nm) for 15 minutes at room temperature on a low-attachment 6-well plate (Corning™) (23). Afterward, the total amount of viral particles was determined based on the OD_{260} values. A correction value was calculated to ensure an equal number of viral particles for treatments with infectious and inactivated reovirus (UVi).

Bispecific antibodies

The CD3xTRP1 bispecific antibody (bsAb) used is a knob-into-hole bispecific based on murine IgG2a with an Fc Silent™ mutation, featuring one arm with an anti-mouse CD3e scFv based on the clone 145-2C11, and the other arm containing the TA99 clone directed against TRP1 (bAb0136; Absolute Antibody). The CD3xHER2 bsAb comprises an anti-human CD3 scFv based on the clone OKT3, together with an anti-HER2 arm based on clone 4D5-8 (Trastuzumab) (bAb0183; Absolute Antibody).

Cell lines

The murine pancreatic cancer cell line KPC3 is a low-passage derivate of a primary KPC tumor with mutant *p53* and *K-ras* (24) from a female C57BL/6 mouse. KPC3.TRP1 cells were generated as described (25) and selected for expression of TRP1 by cell sorting using an αTRP1 antibody (clone: TA99). The murine melanoma cell line B16.F10 (ATCC-CRL6475) and the human breast cancer cell line BT474 (ATCC-HTB-20) were purchased from the American Type Culture Collection. More information can be found in the **Supplementary Methods**.

Animal experiments

Male or female C57BL/6J mice (Charles River Laboratories, France) of 8 weeks old were used for the KPC3 and B16.F10 models, respectively. KPC3 or KPC3.TRP1 tumors were inoculated by subcutaneous injection of $1x10^5$ (for antitumor efficacy experiments) or $2x10^5$ (for intratumoral analysis experiments) cells in the right flank in 100-200 µL PBS/0.1% BSA. For bilateral experiments, a second tumor was subcutaneously engrafted one week after the primary tumor on the alternate flank. B16.F10 tumors were engrafted by subcutaneous injection of $5x10^4$ cells in a volume of 100 µL PBS/0.1% BSA. Female NOD.Cg-Prkdc^{scid}Il2rg^{tm1Wjl}SzJ/ (NSG) mice of 6 weeks old (Charles River Laboratories, France) were used for the BT474 model. BT474 tumors were orthotopically

engrafted by injecting $5x10^6$ cells in a volume of 100 µL 50:50 PBS/0.1% BSA : Growth Factor Reduced matrigel (Corning®) in the fourth mammary fat pad of isoflurane-anesthetized mice. Human PBMCs from a buffy-coat of an anonymous consented donor (Sanquin Blood bank, Amsterdam, The Netherlands), HLA-A29:02-matched to BT474 (26), were isolated by Ficoll-Paque density-gradient centrifugation. $5x10^6$ PBMCs were intravenously administered to each mouse in a volume of 100 µL PBS/0.1% BSA.

Mice with palpable tumors were allocated into groups with similar average tumor volumes and assigned a treatment regimen. Intratumoral reovirus administration was performed by injection of 10^7 plaque-forming units (pfu) of reovirus or PBS as a control in a volume of 30 µL on 3 consecutive days unless otherwise indicated, while mice were under isoflurane anesthesia. Intravenous reovirus administration was performed by injection of 10^7 or 10^8 pfu of reovirus in a volume of 100 µL in the tail vein on 3 consecutive days. Treatment with CD3xTRP1 or CD3xHER2 bsAbs consisted of 3 intraperitoneal injections of 12,5 µg antibody in 100 µL PBS given every other day. Treatment with FTY720 (Cayman Chemical) occurred by supplementing the mice with 2,5 µg/mL FTY720 in their drinking water and a daily oral dose of 2 µg FTY720/g body weight administered orally via pipetting into the mouth. During all experiments, tumors were measured 3-6 times a week in 3 dimensions using a caliper, in a blinded manner concerning the experimental group. For antitumor efficacy experiments, mice were euthanized when tumors reached the experimental endpoint, which equals a volume of 1000 mm^3 (one-tumor model) or a combined volume of 1500 mm^3 (bilateral tumor model). Mice were censored from analysis when they had to be euthanized due to humane endpoints before reaching the experimental endpoint. For intratumoral analysis experiments, mice were sacrificed at indicated days after treatment before tumors and/or spleens were collected. Tumors were divided into representative parts, which were either snap-frozen in liquid N_2 and stored at -80 °C until further analysis, fixed in 4% formaldehyde (AddedPharma) for immunohistochemistry or immediately processed to single cells suspensions to analyze the cellular composition by flow cytometry. These procedures are described in detail in the **Supplementary Methods**.

Quantification of reovirus replication by RT-qPCR

Reovirus replication was quantified by quantitative reverse transcription polymerase chain reaction (RT-qPCR) of reovirus genomic segment 4 (S4) on RNA of cells, tumors, and other organs, as described in the **Supplementary Methods**. Reovirus S4 copy numbers were determined based on a standard curve, generated with serial dilutions of plasmid pcDNA_S4. Log_{10} S4 copy numbers were calculated using a previously described formula (27).

NanoString analysis

Total RNA was isolated from a representative piece (10-30 mg) of each tumor as described in the **Supplementary Methods**. RNA quality and integrity (RQI) were determined using the Experion™ Automated Electrophoresis System (Bio-Rad).

Only samples with an RQI score > 8 were included for NanoString analysis. Multiplex gene expression was measured using the PanCancer Mouse Immune Profiling panel (NanoString Technologies). 200 ng of total RNA was hybridized for 17 hours and quantified by scanning 490 Field of Views (FOV) using the Digital Analyzer (nCounter Flex). Data were processed and normalized using nSolver Analysis Software (version 4.0) and the Advanced Analysis module (NanoString). NanoString-defined markers were used to analyze cell type scores. Expression of reovirus-induced host genes was confirmed by RT-qPCR as described in the **Supplementary Methods**.

Statistics

All graphs were prepared and statistical analyses were performed using the GraphPad Prism software (version 8). All data represent mean±SEM and key data are representative of 2-5 experiments with similar results. Survival between groups was compared using Kaplan-Meier curves and the statistical log-rank test (Mantel-Cox). For RT-qPCR analysis, samples were excluded when RNA concentration and purity were too low. When comparing S4 RT-qPCR data between two groups, average Log_{10} values were compared using a two-tailed unpaired t test. For comparing more groups versus PBS treatment, average Log_{10} values were compared using an ordinary one-way analysis of variance (ANOVA) including Dunnett's post-hoc test. For flow cytometry data, tumor samples were excluded when evidence for draining lymph node contamination was present. The means of flow cytometric data of two experimental groups were compared using two-tailed unpaired t tests. For comparing multiple groups versus PBS treatment or negative control, a one-way analysis of variance (ANOVA) including Dunnett's post-hoc test was performed. For comparing multiple groups with each other, a one-way analysis of variance (ANOVA) including Tukey's post-hoc test was used. The association between two ranked variables was done by Spearman rank correlation. Significance levels are labeled with asterisks, with *p<0.05, **<0.01, ***p<0.001, and ****p<0.0001. Non-significant differences are indicated by ns.

RESULTS

Reovirus efficiently replicates but does not affect tumor growth in the KPC3 pancreatic cancer model

Human pancreatic tumors are often not susceptible to immunotherapeutic strategies, including checkpoint inhibition (28,29). The murine pancreatic cancer model KPC3 is an early derivate from the genetic pancreatic ductal adenocarcinoma (PDAC) KPC mouse model, which recapitulates many of the histopathological and immunological key features observed in human PDAC (30), including acinar tubular structures, a dense desmoplastic stroma, and absence of $CD3^+$ T cells (**Figure S1A, B**). We previously demonstrated that the outgrowth of KPC3 tumors with heterologous expression of the *Trp1* gene (KPC3.TRP1) could significantly be delayed by early CD3xTRP1 bsAb therapy (25). However, CD3xTRP1 bsAb treatment failed to exhibit any effect on larger KPC3.

TRP1 tumors (**Figure S1C, D**), although tumor cells were efficiently killed *in vitro* in an antigen-dependent fashion (**Figure S1E**). We hypothesized that the low T-cell density observed in established KPC3 tumors represents a major barrier to the efficacy of CD3-bsAb therapy and therefore explored the use of oncolytic reovirus to overcome this barrier.

We first tested the ability of reovirus to infect and replicate in KPC3 cells *in vitro* and observed a high number of genomic viral copies (**Figure 1A**) and reoviral protein $\sigma3^+$ cells (**Figure 1B**) after infection with very low multiplicities of infection (MOIs). Total viral copy numbers and viral load per cell increased with higher MOIs, and additionally, reovirus demonstrated a dose-dependent oncolytic activity *in vitro* (**Figure 1C**). Oncolytic activity appeared moderate as half of the cell culture was killed after 2 days, whereas all cells contained high levels of replicating virus. As expected, reovirus did not replicate after UV-inactivation (UVi) in KPC3 cell cultures (**Figure 1A**) (23). To test the replication capacity of reovirus *in vivo*, KPC3 tumor-bearing mice were intratumorally injected on three consecutive days with either 10^7 or 10^8 plaque-forming units (pfu)/mouse starting at day 13 when the tumors were established (**Figure 1D**). Both viral doses resulted in high levels of genomic reovirus copies after three days, indicating efficient replication *in vivo* (**Figure 1E**)**.** Hotspots of viral replication were seen in tumor tissue slides stained for σ3, suggesting that viral replication is not evenly distributed in the tumor (**Figure 1F**). Despite this very efficient replication, reovirus administration failed to make a large impact on tumor growth (**Figure 1G**). Since optimal replication was observed with 10^7 pfu/mouse, we selected this dose for further experiments.

Replication-competent reovirus induces a potent interferon response in the tumor

Next, we studied the kinetics of reovirus replication in KPC3 tumor-bearing mice (**Figure 2A**). Intratumoral administration of reovirus yielded high viral copy numbers that peaked around 1 to 3 days and gradually decreased back to baseline levels around day 11 post-injection (**Figure 2B**). UVi reovirus did not show any amplification. Thus, reovirus has a limited time window of replication in the tumor microenvironment which lasted up to 10 days, suggesting that replication is restricted by antiviral immunity of the host. Transcriptome analysis of whole KPC3 tumors using NanoString technology was performed to investigate the antiviral immune response (**Figure 2C and Figure S2A**). A heatmap of all genes differentially expressed on at least one of the time points revealed that the number of upregulated genes peaked 7 days after reovirus administration (**Figure 2C**). More than 100 immune-related genes were upregulated (FDR $p < 0.1$ and fold change > 2 compared to PBS) and this number severely declined after 11 days, in parallel with viral replication (**Figure 2C and Figure S2A**). Although UVi reovirus might still have the capacity to engage pattern-recognition receptors, as was previously demonstrated (31), this inactivated reovirus did not induce upregulation of immune genes (**Figure 2C and Figure S2A**). This suggested that the ability to replicate was essential for the immunostimulatory effects of reovirus in the tumor microenvironment (TME).

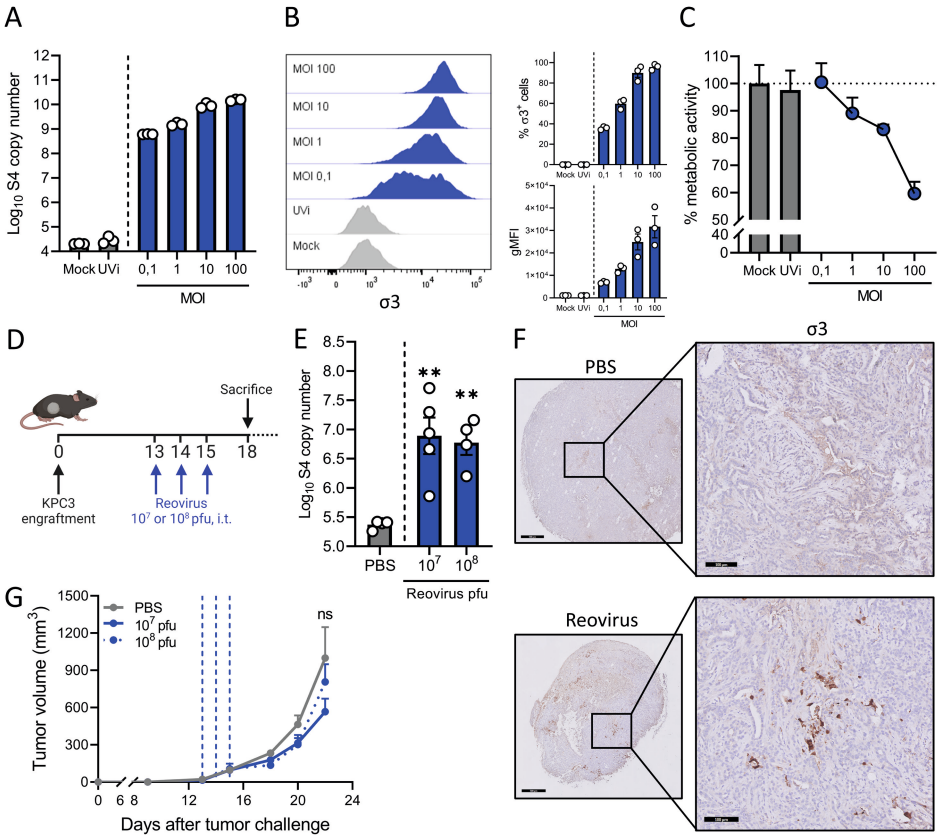


Figure 1. Reovirus efficiently replicates but does not affect tumor growth in the KPC3 pancreatic cancer model. (**A**) Numbers of reovirus S4 copies in KPC3 cells after reovirus infection. KPC3 cells (125.000/well) were infected with increasing MOIs of reovirus, PBS (Mock), or UVi (equal number of viral particles as MOI 100) as controls. Samples (n=3) were harvested 24 hours after infection and reovirus genomic RNA segment 4 (S4) copy numbers were determined by RT-qPCR. (**B**) Frequency of σ3-positive KPC3 cells 48 hours after infection with increasing MOIs of reovirus, or PBS (Mock) or UVi reovirus as controls, analyzed by flow cytometry. Bar graphs represent mean±SEM of triplicates. (**C**) Analysis of the oncolytic activity of reovirus. KPC3 cells (5000/well) were plated and infected with reovirus or controls. Metabolic activity was determined 48 hours after infection. Data represent mean±SEM of triplicates. (**D**) Design of experiment described in E-G. Mice (n=4-6/group) with established KPC3 tumors were treated with intratumoral injections of 10^7 or 10^8 pfu of reovirus on three consecutive days. PBS was used as a control. (**E**) Three days after the last reovirus injection, tumors were harvested and reovirus S4 copy numbers were determined in tumor lysates by RT-qPCR. (**F**) Representative images obtained from immunohistochemical staining of tumors for σ3. Shown are tumors treated with PBS or reovirus 10^7 pfu. Scale bars equal 500 µm and 100 µm for overview and magnification, respectively. (**G**) Mean tumor volumes after treatment with PBS or reovirus 10^7 or 10^8 pfu. Dashed vertical lines indicate days of injections. Data are presented as mean±SEM (n=4-6/group). Significance versus PBS treatment in figures E and G is determined using an ordinary one-way ANOVA with Dunnett's post-hoc test. Significance levels: ns=not significant and **p<0.01. MOI, multiplicities of infection; UVi, UV-inactivated; pfu, plaque-forming units.

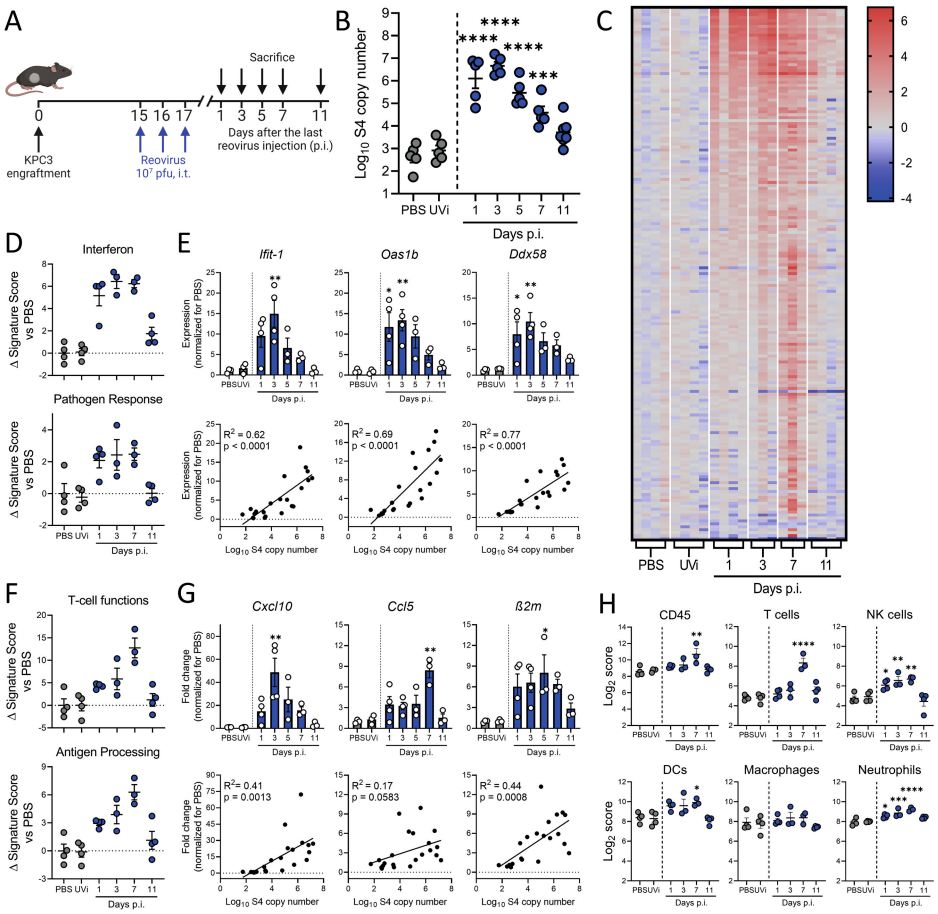


Figure 2. Replication-competent reovirus induces a potent interferon response in the tumor. (**A**) Design of the experiment described in figures B-H. Mice (n=5/group) with established KPC3 tumors were intratumorally injected with 10^7 pfu of reovirus on three consecutive days. PBS or UVi were used as controls and were harvested 3 days after the last injection. (**B**) Tumors were harvested at designated days after reovirus injection (p.i.) and viral S4 copy numbers were determined in tumor lysates by RT-qPCR. (**C**) Heatmap of all genes that were differentially expressed in the tumor (n=3-4/group) on any day after reovirus treatment (FDR $p < 0.1$ and fold change > 2 compared to PBS), as analyzed by NanoString. (**D**) Changes in signature scores on indicated days after reovirus treatment. All scores are normalized for the average score of PBS. (**E**) Relative expression of interferon response genes (upper panel) as determined by RT-qPCR, and the correlation between expression and reovirus S4 copy numbers (lower panel). (**F**) Changes in signature scores on indicated days after reovirus treatment. All scores are normalized for the average score of PBS. (**G**) Relative expression of genes involved in T-cell attraction and antigen processing (upper panel) as determined by RT-qPCR, and the correlation between expression and reovirus S4 copy numbers (lower panel). (**H**) Kinetics of specific cell type scores after reovirus treatment. All data are presented as mean±SEM. Significance versus PBS treatment is determined using an ordinary one-way ANOVA with Dunnett's post-hoc test. Correlation is determined using Pearson's correlation tests. Significance levels: *p<0.05, **p<0.01, ***p<0.001, and ****p<0.0001. Pfu, plaque-forming units; UVi, UV-inactivated reovirus.

Analysis of gene expression signatures roughly revealed two patterns: an early expressed profile, including pathways such as 'interferon' and 'pathogen response', peaking at day 1 to 5, and a late expressed profile, with pathways such as 'T-cell functions' and 'antigen processing', which peaked at day 7 (**Figure 2D-G and Figure S2B**). Expression of early interferon response genes was validated for some prime examples such as *Ifit-1, Oas1b,* and *Ddx58* using RT-qPCR (**Figure 2E**). These antiviral genes were strongly upregulated after treatment with replication-competent reovirus, but not UVi, and expression levels correlated strongly ($R^2 > 0.6$) and significantly ($p < 0.0001$) with the number of viral copy numbers in the tumor (**Figure 2E**). We also validated the expression of some genes involved in the late pathways (**Figure 2F**), such as T-cell-attracting chemokines *CxclL10, Ccl5,* and MHC class I component *β2M*, and observed increased expression levels after reovirus, but not UVi treatment (**Figure 2G**). The expression levels of these genes also significantly correlated with the number of viral copies present in the tumor, although to a lesser extent ($R^2 < 0.5$) than the early induced genes. Lastly, we analyzed the kinetics of NanoString-defined cell type scores in our dataset (**Figure 2H**). A marginal increase in CD45 score was observed on day 7, and when lineage-specific scores were examined, the score for T cells (identified by expression of *Cd3g*, *Cd3e*, *Cd3d,* and *Sh2d1a*) was most significantly upregulated at day 7 after reovirus treatment. Interestingly, natural killer (NK) cells, dendritic cells (DCs), and neutrophil scores were also enhanced on day 7. Macrophage score remained largely unaffected by reovirus treatment. Overall, we observed that reovirus replication induced a potent interferon response, including highly increased expression of inflammatory genes and T-cell-attracting chemokines.

Replication-competent reovirus recruits virus-specific T cells to the tumor

To validate that the reovirus-induced inflammatory response increased tumor infiltration by immune cells, we analyzed the cellular composition of the TME by flow cytometry and immunohistochemistry (IHC) (**Figure 3 and Figure S3**). Interestingly, the total number of $CD45^+$ immune cells in the reovirus-treated tumors was hardly altered (**Figure 3A**). However, the percentage of $CD3^+$ T cells within the $CD45^+$ population was significantly increased after reovirus administration, starting 5 days after the last reovirus injection (**Figure 3B**). This effect was replication-dependent since UVi reovirus treatment failed to increase the intratumoral T-cell density (**Figure 3B and Figure S4A**). Within the $CD3^+$ T-cell population, the $CD8^+$ T cells were significantly more enriched compared to the $CD4^+$ T cells, as seen by a significantly increased $CD8^+/CD4^+$ ratio (**Figure 3C-D**). In the tumors of reovirus-injected mice, the presence of $CD8^+$ T cells could be observed in both the border and the interior of tumors (**Figure 3E**)**.**

To gain a broader view of the TME, we performed a high-dimensional flow cytometric analysis of the lymphoid and myeloid cell compartments in the tumors 5 days after reovirus administration (**Figure 3F and Figure S4B-G**). This analysis confirmed the increased contribution of $CD8^+$ T cells (a 2,6-fold increase compared to PBS), as the total $CD45^+$ immune infiltrate increased only 1,4-fold (**Figure S4B**).

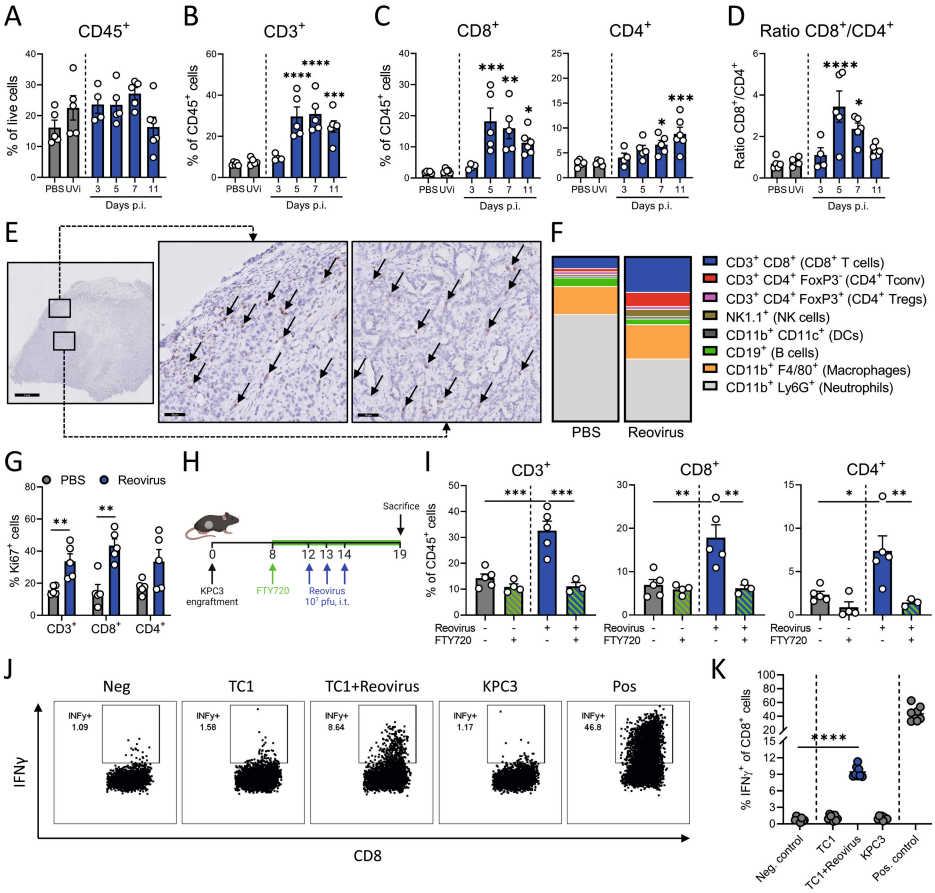


Figure 3. Replication-competent reovirus recruits virus-specific T cells to the tumor. (**A**) Frequency of CD45⁺ immune cells in the tumor on indicated days after reovirus or UVi treatment (n=5/group). (**B**) Frequency of CD3⁺ T cells within CD45⁺ immune cells in the tumor. (**C**) Frequency of CD8⁺ and CD4⁺ T cells within CD45⁺ immune cells in tumors after reovirus treatment. (**D**) Ratio between intratumoral CD8⁺ and CD4⁺ T cells. (**E**) Representative images obtained from immunohistochemical staining of tumors for CD8 (light brown). Arrows indicate CD8⁺ T cells. Scale bars equal 1 mm and 50 µm for overview and magnification, respectively. (**F**) Composition of CD45⁺ immune infiltrate in the tumor, 5 days after reovirus treatment. (**G**) Frequency of Ki67⁺ cells within CD3⁺, CD8⁺, and CD4⁺ T-cell populations in the tumor. (**H**) Design of experiment described in I. Mice (n=3-5/group) with established KPC3 tumors were intratumorally injected with reovirus (10^7 pfu) on three consecutive days and were treated with FTY720 (2,5 µg/mL FTY720 in drinking water and daily oral administration of 2 µg/g body weight). (**I**) Frequency of CD3⁺, CD8⁺, and CD4⁺ T-cell populations in the tumor. (**J**) Representative flow cytometry plots for the frequency of IFNγ⁺ cells within the intratumoral CD8⁺ T-cell population 7 days after reovirus treatment. Single-cell suspensions from tumor samples (n=8/group) were cocultured with indicated targets for six hours. Medium was used as negative (Neg.) and PMA/ionomycin was as positive (Pos.) controls, respectively. (**K**) Quantification of IFNγ⁺ cells within CD8⁺ T-cell population. See next page for continuation of figure legend. All data are presented as mean±SEM. Statistical tests used: Panels A-D: ordinary one-way ANOVA with Dunnett's post-hoc test. Panel G: Multiple unpaired t tests. Panel I: ordinary one-way ANOVA with Tukey's post-hoc test. Panel K: unpaired t test between Neg. control and TC1+Reovirus. Significance levels: *p<0.05, **p<0.01, ***p<0.001, and ****p<0.0001. UVi, UV-inactivated reovirus.

The frequency of NK cells and CD4 cells also significantly increased, and within the $CD4^+$ T-cell population, the frequency of $FoxP3^+$ $CD4^+$ regulatory T cells dramatically dropped from 40% to 10% (**Figure S4C, D**). This resulted in an enhanced ratio of $CD8^+$ cytotoxic T cells to $FoxP3^+$ regulatory T cells in the TME (**Figure S4E**). Additionally, reovirus induced activation of T cells, as indicated by increased expression of activation marker CD44 and loss of adhesion marker CD62L (**Figure S4F**). Interestingly, we observed a large population of neutrophils ($CD11b^+Ly6G^+$) in untreated KPC3 tumors, the frequency of which dramatically decreased after reovirus administration (**Figure S4G**). Other myeloid cell lineages, such as macrophages ($CD11b^+$ $F4/80^+$) and $CD11c^+$ macrophages ($CD11b^+$ $CD11c^+$) remained unaffected (**Figure S4G**). Overall, these analyses revealed that replication-competent reovirus converts an immunologically cold tumor-microenvironment with low T-cell infiltration into a site with a strongly enhanced abundance of activated effector T cells and NK cells and reduced frequency of neutrophils and immunosuppressive regulatory T cells.

Next, we investigated the mechanism underlying the increased T-cell density in the tumor after reovirus administration. First, we assessed the proliferation of T cells by measuring the frequency of intratumoral $Ki67^+$ T cells (**Figure 3G**). The fraction of $Ki67^+$ T cells was significantly increased after reovirus treatment, especially in $CD8^+$ T cells. We subsequently examined if the increased T-cell frequencies were solely the result of local proliferation in the tumor or were the result of increased attraction to the tumor. To this end, T-cell egress from lymph nodes was blocked with FTY720 during this experiment (**Figure 3H, I and Figure S4H, I**) (32). Interestingly, the reovirus-induced increase in intratumoral $CD3^+$ T cells, both $CD4^+$ and $CD8^+$ subsets, was completely abrogated under FTY720 conditions, whereas the abundance of total $CD45^+$ immune cell infiltrate into the tumor was not affected.

Finally, we examined the specificity of the tumor-infiltrating $CD8^+$ T cells. Tumor-infiltrating lymphocytes were cocultured for 6 hours with KPC3 tumor cells, MHC class I-matched control TC-1 tumor cells, or TC-1 cells infected with reovirus (**Figure 3J, K**). No tumor-specific response to KPC3 could be detected, but 10% of the $CD8^+$ T cells responded to reovirus-infected TC1 cells by producing IFNγ. This population of reovirus-specific T cells was specifically enriched at the site of the tumor since their frequencies were around 1% in the spleen (**Figure S4J**). We concluded that reovirus replication in the tumor leads to strong recruitment of proliferating and activated type 1 T cells, which are reovirus-specific.

Combination treatment of reovirus and CD3-bsAbs induces strong tumor regression of established TRP1-expressing tumors

The observation that reovirus replication ignites a strong influx of T cells in the otherwise immunologically cold KPC tumors provided a strong rationale to evaluate the combination of reovirus with CD3-bsAb therapy. C57BL6/J mice with palpable TRP1-expressing KPC3 tumors were treated intratumorally with reovirus and 4 days later,

when the inflammatory response had reached its full potential, CD3xTRP1 bsAbs were systemically administered (**Figure 4A**). This combination resulted in striking tumor regressions, which started directly after the first bsAb injection, whereas bsAbs or reovirus monotherapy hardly showed any tumor growth delay (**Figure 4B and Figure S5A**). Visualizing the relative change in tumor size after the start of bsAb injection indicated that combination therapy induced tumor regressions in all treated mice, whereas tumors treated with CD3xTRP1 bsAb monotherapy all increased in size (**Figure 4C**). Mice receiving the combination treatment had significantly lower tumor volumes on day 21 (**Figure 4B**) and survived significantly longer (**Figure 4D**) compared to PBS or both monotherapies.

Despite the striking regressions induced by the combination therapy, durable responses were not observed, and all tumors eventually escaped immune control (**Figure 4B-D and Figure S5A**)**.** This escape could not be prevented by an additional treatment round of reovirus and CD3xTRP1 bsAbs (**Figure S5B, C**), or by the addition of checkpoint blockade using αPD-L1 (**Figure S5D-F**). We aimed to explain the escape mechanism and first assessed T-cell presence in end-stage tumors. Immunohistochemical analysis of these samples indicated that $CD3^+$ T cells were still abundantly present in tumors from combination-treated animals (**Figure S6A**). Flow cytometry analysis confirmed the increased presence of mainly $CD8^+$ T cells in the tumors that were treated with reovirus and bsAb (**Figure S6B**) and additionally revealed that most of these T cells still displayed an activated phenotype with high expression of CD44 and an absence of CD62L (**Figure S6C**)**.** Furthermore, no striking differences in the expression of checkpoint molecules PD1, Tim3, and NKG2A were observed between T cells from the combination group and T cells from the bsAb group (**Figure S6C**)**.** These data indicated that the observed tumor escape could not be explained by the absence or exhaustion of intratumoral T cells.

We then looked at tumor-intrinsic factors and analyzed the presence of surface $TRP1^+$ cells within the $CD45^-$ tumor cell population (**Figure 4E, F and Figure S6D**). Importantly, we found that TRP1 expression was lost in nearly all tumor cells after combination treatment, versus 40% in tumors treated with bsAb alone and <20% of cells in the other groups (**Figure 4E, F**). These data imply that the robust immune pressure of combination treatment initially resulted in striking tumor regressions, but also promoted the selective expansion of TRP1-negative tumor cell clones that are insensitive to CD3xTRP1 bsAb targeting. The TRP1 protein was selected as a model antigen in this study, however, it is not an essential molecule for cell growth or survival and could therefore be lost without consequences for tumor growth. We concluded that this combination therapy led to the complete eradication of TRP1-expressing tumor cells, concomitantly leading to the escape of tumor variants that lost the targeted antigen.

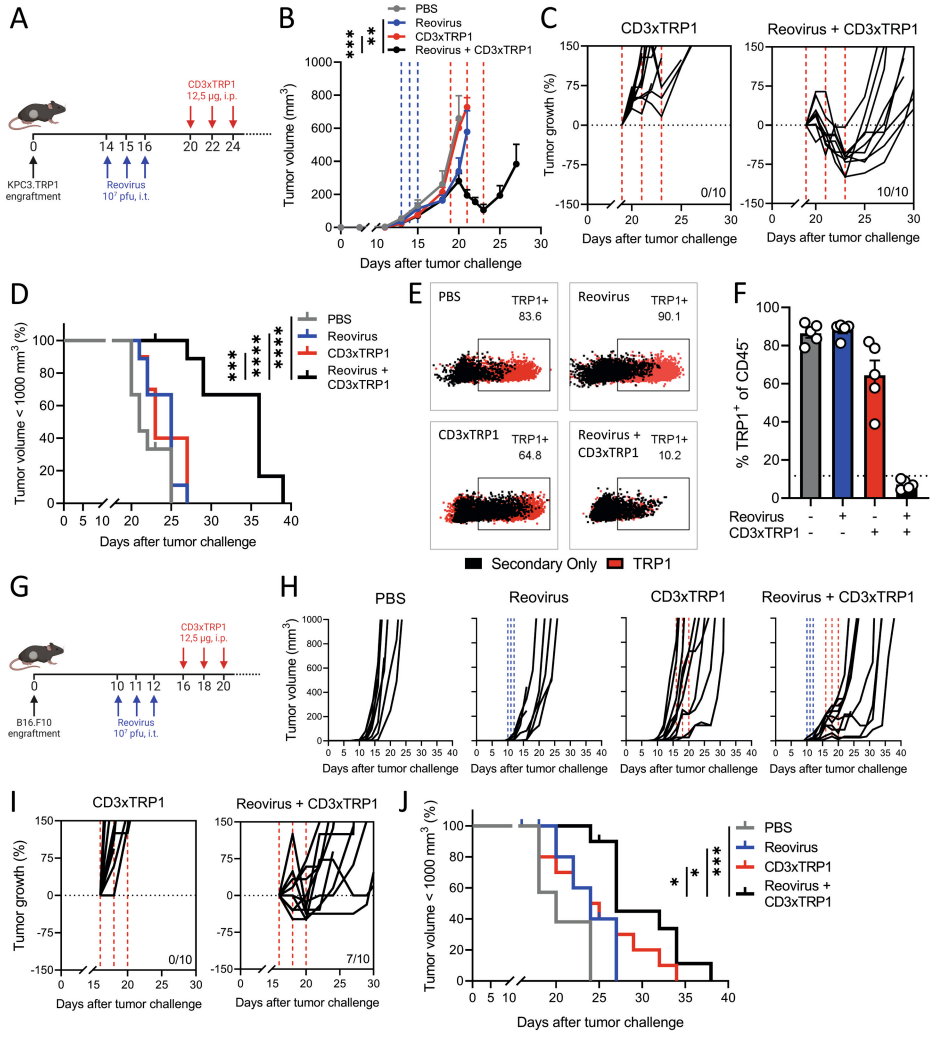


Figure 4. Combination treatment of reovirus and CD3xTRP1 bsAbs induces regression of established TRP1-expressing tumors. (**A**) Design of experiment described in figures B-F. Mice (n=8-10/group) with established KPC3.TRP1 tumors were intratumorally injected with reovirus (10^7 pfu) on three consecutive days. After 4 days, mice received intraperitoneal injections of 12,5 µg CD3xTRP1 bsAbs (CD3xTRP1) or PBS as control. (**B**) Average tumor growth curves±SEM. Dashed lines indicate the timing of injection with Reovirus (blue) or CD3xTRP1 (red). Differences in mean tumor volumes versus Reovirus + CD3xTPR1 treatment on day 21 are determined by one-way ANOVA with Dunnett's post-hoc test. (**C**) Relative changes in tumor volume of individual mice from the start of CD3xTRP1 bsAb treatment. Indicated is the number of mice with tumor regressions. (**D**) Kaplan-Meier survival graphs of mice in indicated treatment groups. (**E**) Overlayed dot plots indicating the percentage of $TRP1^+$ cells on representative tumors of each group. Black dots show background staining of secondary antibody. Red dots show staining using primary αTRP1 antibody followed by the secondary antibody. (**F**) Quantification of TRP1 expression. Dashed line indicates the mean background staining of secondary antibody. Data represent mean±SEM. (**G**) Design of experiment described in figures H-J. Mice (n=8-10/group) with established B16.F10 tumors were intratumorally injected with reovirus (10^7 pfu) on three consecutive days. After 4 days, mice received intraperitoneal injections of 12,5 µg CD3xTRP1 bsAbs or PBS as control.

>>

>> (**H**) Individual growth curves of B16.F10-bearing mice receiving indicated treatments. (**I**) Relative changes in tumor volume from the start of CD3xTRP1 bsAb treatment. Indicated is the number of mice with tumor regressions. (**J**) Kaplan-Meier survival graphs of mice in indicated treatment groups. Log-rank test was used to compare differences in survival. Significance levels: *p<0.05, **p<0.01, ***p<0.001, and ****p<0.0001. Pfu, plaque-forming units; bsAbs, bispecific antibodies.

To demonstrate the efficacy of this combination treatment in another immunologically cold tumor model, we employed the murine melanoma model B16.F10 (33), which spontaneously expresses the melanocyte-lineage antigen TRP1. Although all B16.F10 cells expressed TRP1 on their cell surface, the level of expression in B16.F10 was a magnitude lower compared to KPC.TRP1 (**Figure S7A**). In vitro, reovirus was able to efficiently replicate in B16.F10 cells, however, the number of viral copy numbers and the frequency of $\sigma3^+$ cells were lower compared to KPC3 (**Figure S7B, C**)**.** Interestingly, despite viral replication in B16.F10 cells, oncolysis hardly occurred, even at a MOI of 100 (**Figure S7D**). *In vivo,* reovirus was able to efficiently replicate (**Figure S7E**) and to increase the T cell density in established subcutaneous B16.F10 tumors after intratumoral injection (**Figure S7F**). Earlier, we reported that CD3xTRP1 significantly delayed tumor growth in B16.F10 tumors, when given early after tumor challenge (25). Similar to the KPC3.TRP1 model, the combination regimen of reovirus and CD3xTRP1 was required to induce tumor regressions in established B16.F10 tumors (**Figure 4G, H**). Whereas CD3xTRP1 monotherapy delayed tumor growth in some animals (**Figure 4H**)**,** therapy-mediated tumor regressions were exclusively found in 7 out of 10 animals of the combination group (**Figure 4I**). The combination treatment also significantly prolonged survival (**Figure 4J**)**.**

The combination of reovirus and CD3-bsAbs is effective in a human, orthotopic HER2$^+$ breast cancer model

Additionally, we aimed to investigate the efficacy of the combination of reovirus and CD3-bsAbs in a more clinically relevant setting. We employed the human epidermal growth factor receptor (HER2) positive breast cancer model BT474 (34), as a close-to-patient model to test CD3xHER2 bsAb therapy. BT474 cells express high levels of HER2 and were susceptible to reovirus replication (**Figure 5A, B**). BT474 tumors were engrafted orthotopically in the fourth mammary fat pad of NSG mice, and human PBMCs were intravenously administered as a source of effector cells before reovirus and bsAb administration (**Figure 5C**). In contrast to our experiments in immunocompetent mice, reovirus alone already showed some efficacy by impairing tumor growth (**Figure 5D**). Whereas CD3xHER2 monotherapy had no therapeutic efficacy in comparison to the PBS-treated group, the combination of reovirus with CD3xHER2 bsAbs induced strong tumor regressions in all animals (**Figure 5D**) and a significant average tumor shrinkage calculated from the moment of PBMC injection (**Figure 5E**). Collectively, these results show that the efficacy of bsAb therapy in immunologically cold, solid tumors such as KPC3, B16.F10, and BT474 can be greatly enhanced by prior sensitization with reovirus.

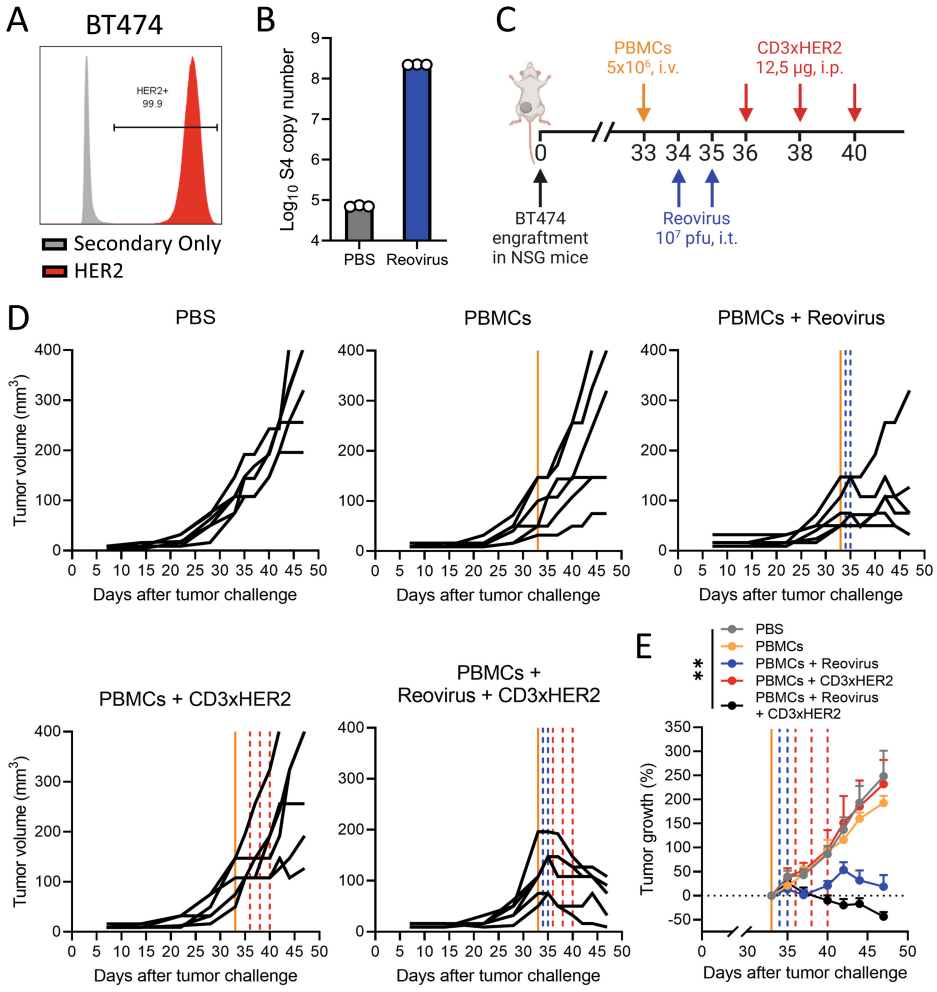


Figure 5. Combination of reovirus and CD3-bsAbs is effective in a human, orthotopic HER2⁺ breast cancer model. (**A**) HER2 expression percentages on BT474 cells, as analyzed by flow cytometry using a 2-step protocol. (**B**) Number of reovirus S4 copies in BT474 cells after reovirus infection. BT474 cells (200.000/well) were infected with reovirus MOI 10 or PBS (Mock) as a control. Samples (n=3) were harvested 24 hours after infection and the number of viral S4 copies was determined by RT-qPCR. (**C**) Design of experiment described in figures D-E. Mice (n=6/group) with established BT474 tumors were intravenously injected with $5x10^6$ human PBMCs, and thereafter intratumorally injected with reovirus (10^7 pfu) on two consecutive days. After 4 days, mice received intraperitoneal injections of 12,5 µg CD3xHER2 bsAbs (CD3xHER2) or PBS as control. (**D**) Individual growth curves of BT474-bearing mice receiving indicated treatments. Lines indicate the timing of injection with PBMCs (orange), Reovirus (blue), or CD3xHER2 (red). (**E**) Average relative changes (±SEM) in tumor volume from the start of CD3xHER2 bsAb treatment. Significance versus PBS on day 42 was calculated using one-way ANOVA with Dunnett's post-hoc test. Significance level: **p<0.01. MOI, multiplicities of infection; bsAbs, bispecific antibodies.

Treatment sequence is important for the synergistic effect of the reovirus and CD3-bsAb combination therapy

Here, we used two separate treatment modalities applied sequentially, but alternatively, genes coding for T-cell-engaging antibodies can also be introduced into oncolytic viruses as transgenes (35). For this reason, we investigated whether timing was important for the observed synergistic effect and if comparable tumor regressions could also be observed if reovirus and CD3xTRP1 bsAbs were administered simultaneously or in reversed order (**Figure 6**). Interestingly, steady tumor growth without any regressions was observed when we switched the sequence of treatment arms and first administered bsAbs (**Figure 6A, D**). Simultaneous administration of bsAb on the day of reovirus injection did induce regressions in tumor volume, but tumors started to regrow fast (**Figure 6B, D**).

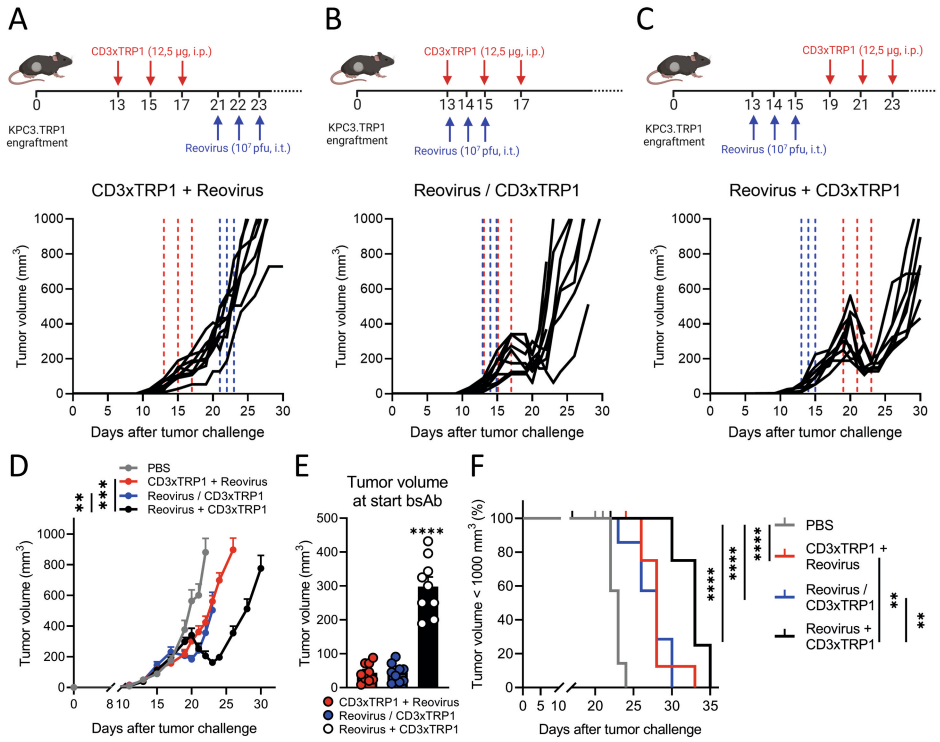


Figure 6. Treatment sequence is important for the synergistic effect of the reovirus and CD3-bsAb combination therapy. Treatment schedule and individual tumor growth curves of mice (n=8-10/group) that received intraperitoneal injections (12,5 µg/mouse) of CD3xTRP1 bsAbs before (**A**), simultaneously with (**B**) or after (**C**) intratumoral reovirus injections (10^7 pfu/mouse). Dashed vertical lines indicate the timing of injection with Reovirus (blue) or CD3xTRP1 (red). (**D**) Average tumor growth curves (±SEM) of experimental groups shown in A-C compared to PBS treatment. Significance versus Reovirus + CD3xTPR1 treatment on day 23 is determined by comparing tumor volumes using a one-way ANOVA with Dunnett's post-hoc test. (**E**) Mean±SEM tumor volume at the start of CD3xTRP1 bsAb treatment for treatment schedules CD3xTRP1 + Reovirus (day 13), Reovirus/CD3xTRP1 (day 13), and Reovirus + CD3xTRP1 (day 19). Ordinary one-way ANOVA with Tukey's post-hoc test was used to compare means. >>

>> (**F**) Kaplan-Meier survival curves of mice in different treatment schedules. Log-rank test was used to compare differences in survival. Significance levels: *p<0.05 and **** p<0.0001. Pfu, plaque-forming units; bsAbs, bispecific antibodies.

Our previous regimen of reovirus before bsAbs led to significantly smaller tumor volumes on day 23 after the tumor challenge, indicating more durable and deeper regressions compared to the other regimens (**Figure 6C, D**). Importantly, simultaneous treatment with reovirus and bsAbs did induce small regressions, but these occurred when tumor volumes were still relatively low at the start of bsAb treatment (**Figure 6E**)**.** In contrast, pre-treatment with reovirus caused tumors to undergo steeper regressions, even though the tumor volume was significantly higher at the start of bsAb treatment. All combination treatment regimens significantly improved survival in comparison to the untreated group, but the exploitation of reovirus as a preconditioning regimen performed significantly better compared to both other schedules (**Figure 6F**). In conclusion, these data highlight the importance of sensitization of tumors with reovirus preceding bispecific antibody treatment to optimally harness the full potential of this combination.

Intratumorally injected reovirus sensitizes local and distant cold tumors for subsequent treatment with CD3xTRP1 therapy

In previous experiments, we observed that intratumoral delivery of reovirus also induced systemic activation of both $CD8^+$ and $CD4^+$ T cells in the spleen, reflected by increased expression of CD44, KLRG1, and PD1, and absence of adhesion molecule CD62L (**Figure 7A**). To evaluate the possible systemic effects of local reovirus administration, a bilateral tumor model was used. Mice were engrafted with a subcutaneous KPC3 tumor on the right flank and one week later received another tumor on the left flank (**Figure 7B**). After reovirus treatment, we assessed the presence of reovirus copy numbers in both the injected (local) and the non-injected (distant) tumor. To our surprise, we detected a significantly increased number of viral genomic copies in the distant tumor after reovirus treatment, although at lower numbers than in the injected tumor (**Figure 7C**). Interestingly, no increase in reovirus copy numbers could be observed in other organs except for the tumor-draining lymph node (TDLN) (**Figure 7D**). The presence of reovirus in the distant tumor also led to an increased expression of a selection of ISGs (**Figure 7E**) and a subsequent increased influx of $CD8^+$ T cells, indicating that locally injected reovirus can find its way to distant tumors, and is associated with the recruitment of immune cells there (**Figure 7F**). We then investigated whether our combination treatment could also effectively control the growth of distant tumors. As expected, monotherapy with CD3xTRP1 bsAbs did not affect the tumor growth of local or distant tumors (**Figure 7G**). Strikingly, combination treatment also induced regression of the distant KPC3.TRP1 tumors (**Figure 7H**). This effect was TRP1-targeted since no regressions were observed in distant tumors not expressing TRP1 (KPC3). These findings suggest that the combination of reovirus and CD3-bsAbs might also be effective in metastatic disease.

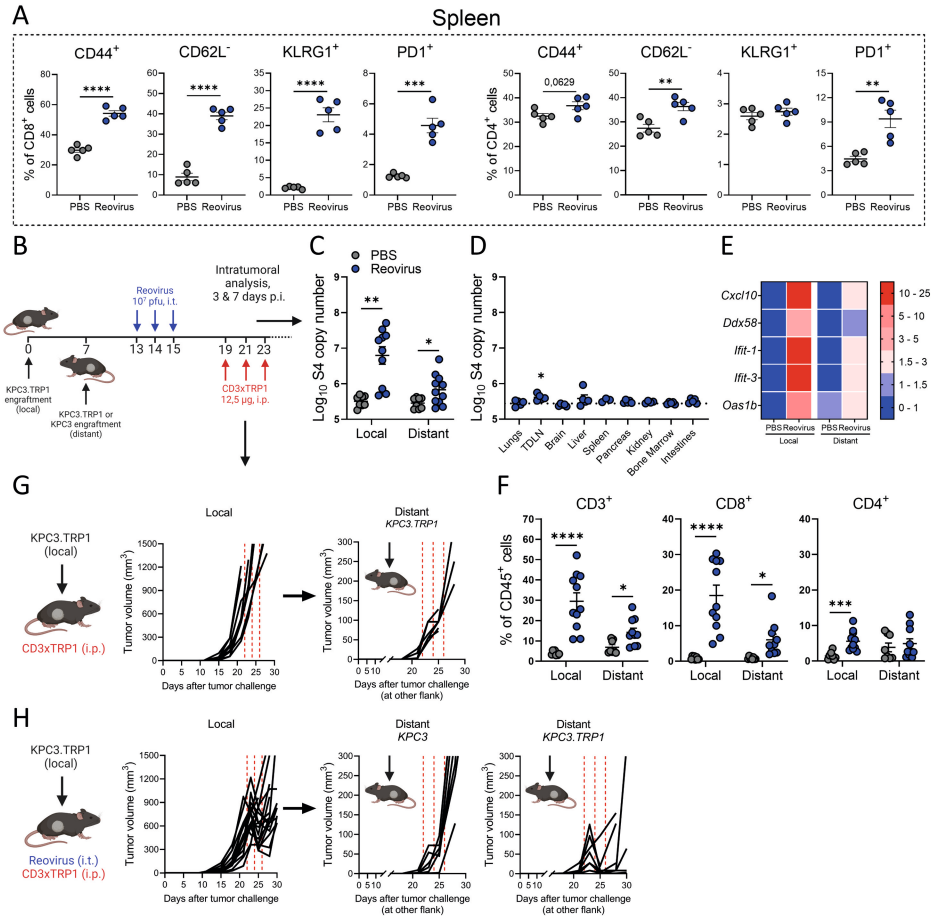


Figure 7. Intratumorally injected reovirus sensitizes local and distant cold tumors for subsequent treatment with CD3xTRP1 therapy. (**A**) Expression of activation markers on splenic CD8⁺ or CD4⁺ T cells 5 days after reovirus or PBS administration (n=5/group). (**B**) Treatment schedule of experiment described in C-G. Mice (n=8-10/group) were subcutaneously inoculated with KPC3.TRP1 cells in the right flank. Seven days later, another KPC3.TRP1 or KPC3 tumor was inoculated in the left flank. Mice received intratumoral injections of reovirus (10^7 pfu) in the primary right tumor. Then, mice were sacrificed for intratumoral analysis at 3 and 7 days after the last reovirus injection (panels C-F; pooled results of 2 independent experiments with similar results) or mice received subsequent intraperitoneal injections of 12,5 µg CD3xTRP1 bsAbs and tumor size was monitored (panels G and H). (**C**) S4 copy numbers in local and distant tumors 3 days after reovirus treatment or PBS as control. (**D**) S4 copy numbers present in other organs of reovirus-treated mice 3 days after reovirus administration. Dashed horizontal line represents average S4 copy numbers in PBS-treated mice. (**E**) Heatmap of relative expression of interferon response genes in the local and distant tumors as determined by RT-qPCR. Numbers indicate fold change versus PBS-treated local tumors. (**F**) Frequency of T cells in local and distant tumors of mice 7 days after local reovirus administration. Data presented as mean±SEM. Differences between PBS and reovirus in panels A and C-F were determined with unpaired t tests. (**G**) Individual tumor growth curves of local and distant tumors of mice (n=8/group) treated with CD3xTRP1. Dashed red lines indicate the timing of injection.

>>

>> (**H**) Individual tumor growth curves of local and distant TRP1-expressing (KPC3.TRP1) or WT KPC3 tumors of mice after intratumoral treatment with reovirus and subsequent intraperitoneal injections with CD3xTRP1. Dashed lines indicate the timing of injection with Reovirus (blue) or CD3xTRP1 (red). Significance levels: *p<0.05, **p<0.01, ***p<0.001, and ****p<0.0001. Pfu, plaque-forming units; bsAbs, bispecific antibodies.

Intravenous administration of reovirus is also effective in preconditioning the tumor microenvironment

In the present study, reovirus was injected intratumorally to ensure efficient delivery at the tumor site. However, in most clinical studies, intravenous infusion of reovirus has been applied (36) and effective delivery to tumor sites, including the brain, was demonstrated (11). Therefore, we tested the therapeutic efficacy of systemic delivery of reovirus (**Figure 8A**). Intravenous administration of 10^7 and 10^8 pfu/injection resulted in detectable numbers of reovirus genomic copies in the tumor, although in significantly lower numbers compared to intratumoral administration of 10^7 pfu of reovirus (**Figure 8B**). Increased expression of a selection of ISGs was observed in comparison to the PBS group (**Figure 8C**), suggesting that intravenously administered reovirus can induce an interferon response in the TME. Intravenous administration of reovirus was effective as a preconditioning method since tumor outgrowth was temporarily halted, but no regressions were observed as was the case after intratumoral administration (**Figure 8D-F**)**.** Mice treated with any of the combination treatments had smaller tumor volumes (**Figure 8E**) and significantly prolonged survival times (**Figure 8F**) in comparison to the untreated group. These data imply that preconditioning of the TME with both intravenous and local administration of reovirus is effective to turn CD3-bsAbs into a potent immunotherapy for solid cancers. Collectively, our data demonstrate that replication-competent reovirus turns an otherwise unsuccessful CD3-bsAb therapy into a powerful systemic treatment.

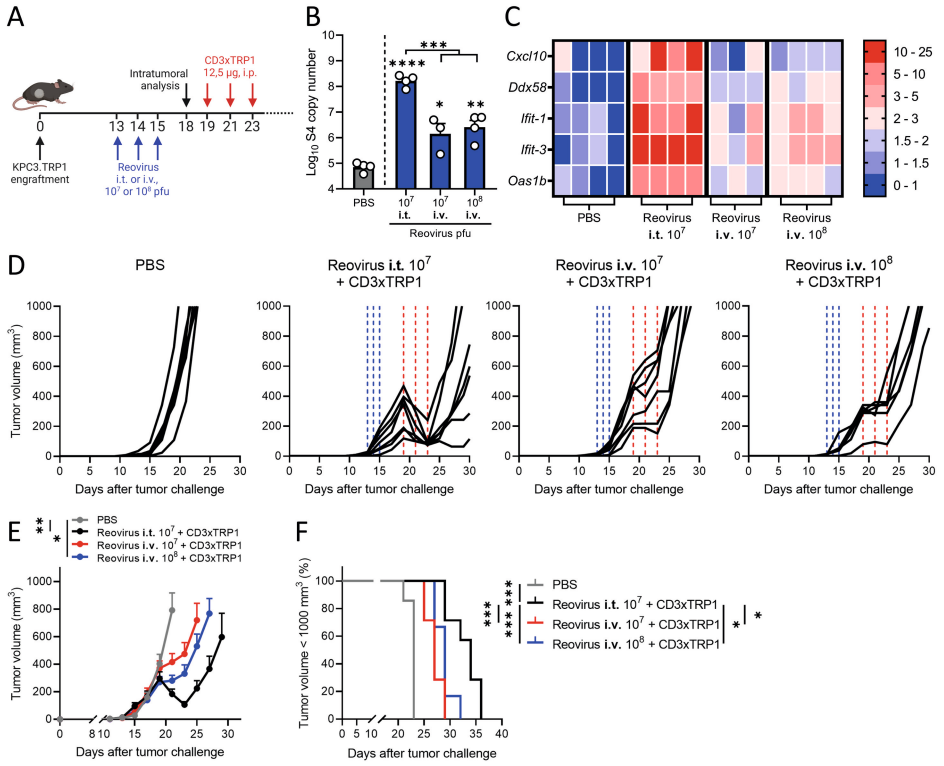


Figure 8. Intravenous administration of reovirus is also effective in pre-conditioning the tumor microenvironment. (**A**) Design of experiment described in figures B-F. KPC3.TRP1-bearing mice were intratumorally or intravenously injected with reovirus (10^7 or 10^8 pfu) on three consecutive days. Tumors were harvested 3 days after the last reovirus injection for intratumoral analysis (n=3-4/group), or mice received intraperitoneal injections of 12,5 µg CD3xTRP1 bsAbs (CD3xTRP1) or PBS as control (n=6-7/group). (**B**) Viral S4 copy number in tumor lysates by RT-qPCR. Mean±SEM. (**C**) Heatmap of relative expression of interferon response genes in tumors versus PBS treatment, as determined by RT-qPCR. (**D**) Individual tumor growth curves of KPC3.TRP1-bearing mice (n=6-8/group) that were intratumorally or intravenously injected with reovirus (10^7 or 10^8 pfu) on three consecutive days. After 4 days, mice received intraperitoneal injections of 12,5 µg CD3xTRP1 bsAbs (CD3xTRP1) or PBS as control. Dashed vertical lines indicate the timing of injection with Reovirus (blue) or CD3xTRP1 (red). (**E**) Average±SEM tumor growth curves. Differences in mean tumor volumes versus PBS treatment on day 21 are determined by one-way ANOVA with Dunnett's post-hoc test. (**F**) Kaplan-Meier survival curves of mice. Log-rank test was used to compare differences in survival. Significance levels: *p<0.05, **p<0.01, and ****p<0.0001. Pfu, plaque-forming units; bsAbs, bispecific antibodies.

DISCUSSION

In this study, we demonstrated that preconditioning the tumor microenvironment with oncolytic reovirus is an attractive strategy to prime immunologically cold tumors for T-cell-engaging antibody therapy. Tumor-selective replication of competent reovirus converted the tumor microenvironment to an inflamed site with a strong IFN signature

and T-cell-attracting chemokines, followed by an enhanced influx of NK cells and activated T cells. Subsequent systemic administration of T-cell-engaging antibodies induced strong tumor regressions of reovirus-injected and distant non-injected lesions, implying that this strategy may be effective for the treatment of metastatic disease.

Although OVs are considered potent anticancer modalities, reovirus and several others have demonstrated limited therapeutic efficacy when used as a monotherapy. Since oncolytic activity may not be the main asset of reovirus as an anticancer therapeutic, we focused on its potential to modify the TME. RNA viruses, typically replicate with fast kinetics and induce a very potent type I interferon response (37). Indeed, our analysis of reovirus-induced immune dynamics revealed a very fast and potent induction of intratumoral interferon response, followed by a robust influx of T cells. UV-inactivated, replication incompetent reovirus did not induce an interferon gene signature and T-cell influx in the TME, although it still contains pathogen-associated molecular patterns (PAMPs) that may be recognized by pattern-recognition receptors (PRRs) (38). Although UV-inactivated reovirus has shown to be effective in the induction of tumor-specific T cells by human dendritic cells in an *in vitro* setting,(31) in our *in vivo* setting replication was required to induce a potent interferon response and subsequent T-cell infiltration into the tumor. In contrast, a modified vaccinia virus did induce intratumoral inflammation and T-cell influx after inactivation, indicating that this OV holds sufficient viral PAMPs in the absence of viral replication (39).

Intratumoral injections lead to 'islands' of reovirus production within the tumor, resulting in local amplification and release of virus particles. Concomitantly, we found viral spread in the animals from injected tumors to distant non-injected tumors, without affecting healthy tissues except for low levels in the TDLN. Previous work already showed that various cell types such as T cells, DCs, monocytes, and granulocytes can act as cellular carriers and deliver infectious reovirus particles to tumor cells, even in the context of preexisting antiviral immunity (40-42). We speculate that one of these immune cell types is involved in carrying infectious reovirus particles via the TDLN to distant tumors. Further research is required to elucidate the exact cellular carrier or if reovirus can migrate without any cellular carrier.

Local versus systemic delivery of OVs is a huge topic of debate. Local delivery of OVs is in clinical practice for T-VEC (13,43) and is used in many preclinical studies including the present study to ensure efficient delivery to the tumor site (12). However, in most clinical studies, reovirus is administered intravenously (11,36). One advantage of intravenous delivery is that it does not rely on injectable tumor lesions, which are not available in the majority of cancer types. Here, we showed that intravenously injected reovirus is able to reach the tumor and sensitize tumors for subsequent CD3-bsAb therapy. However, the antitumor efficiency of the combination with CD3-bsAbs is lower when compared to intratumorally injected reovirus. Even a ten-fold higher dose of systemically administered reovirus significantly underperformed intratumoral delivery, suggesting

that intravenous delivery would need to be improved to reach its full potential. One previously suggested method to enhance reovirus delivery is to load reovirus on the aforementioned cellular carriers (40). Nevertheless, the efficacy of the intravenously delivered reovirus in this model is an important finding since it paves the way for the clinical application of such a combination regardless of the tumor location and route of administration.

Reovirus and other OVs have already demonstrated to combine well with checkpoint blockade, a therapy that depends on the presence of tumor-specific T cells (10-12). OVs and T-cell-engaging antibody therapy is an emerging and exciting new field of research. We demonstrated that prior sensitization with reovirus greatly enhanced the efficacy of CD3-bsAb therapy in immunologically cold tumors. However, others introduced bispecific T-cell engagers (BiTE) as transgenes into OVs (44-47). For instance, treatment with oncolytic measles virus encoding CD3-BiTEs demonstrated delayed tumor growth and prolonged survival in immunocompetent C57BL/6J mice harboring subcutaneous MC38 or B16 tumors (44). Similarly, an oncolytic adenovirus engineered with a CD3xEGFR BiTE and an oncolytic vaccinia virus encoding a CD3xEPHA2 BiTE showed antitumor activity in xenograft models and an oncolytic adenovirus encoding a CD3xEpCAM BiTE was able to activate endogenous T cells kill tumor cells in primary human tumor samples of malignant peritoneal ascites and pleural exudates (45-47). Although encoding bsAbs or BiTEs in OVs has several advantages such as reduction of treatment burden for patients (35), our data imply that these strategies do not exploit the full potential of this combination therapy as the T-cell influx peaks around a week after reovirus application, when viral genomic copies start to decline. In the studies with BiTE-encoding OVs, the kinetics of expression of the transgene may not parallel the kinetics of the OV-induced T-cell activation, especially since BiTE molecules have a very short half-life due to their small size and the absence of a stabilizing Fc tail (3). Most of the T-cell engaging activity might already be declined at the peak of T-cell-attracting chemokines. We therefore advocate to separate the administration of OVs from bsAbs and consider OV injection as a preconditioning strategy. Further research is however warranted to fully understand the optimal regiment of OV and bsAb delivery, including the biodistribution of the OVs and bsAbs, and how this differs between OVs, bsAbs and even tumor types.

The mechanism of action of CD3-bsAbs is not yet completely understood. For instance, in our studies, we did not assess whether CD3xTRP1 bsAbs first bind TRP1 in the tumor and then engage T cells that are infiltrating into the tumor due to reovirus-induced inflammation, or if bsAbs bind T cells in the lymph node, spleen or the circulation and subsequently activate these T cells upon binding of TRP1 in the tumor (4). Elucidating this mode of action might be important to further harness the full potential of CD3-bsAbs as a monotherapy and in combination with OVs since it will guide future improvements in therapeutic efficacy.

Importantly, our data demonstrated that the combination of OV and CD3-bsAbs is an extremely powerful therapy that imposed a strong, immunological selective pressure on the tumors, leading to initial regressions but later on in relapsed tumors that lost expression of the antigen. We used the melanoma-associated antigen TRP1 as a well-known model antigen. This surface-expressed protein is involved in melanin production but is not essential for cell growth or survival. The use of this particular model antigen allowed us to investigate therapy resistance on the one hand, but on the other can be considered a limitation of our study. It emphasizes the importance of the careful selection of the targeted antigen when this combination strategy is translated to the clinic. For effective bsAb therapy in humans, the ideal target antigen needs to be selectively and abundantly expressed on tumor cells but should also be essential for tumorigenesis. One such target is human epidermal growth factor 2 (HER2), and we employed human CD3xHER2 as the second bsAb to demonstrate proof-of-concept of our combination strategy in the $HER2^+$ BT474 model. In this model, we observed some close-to-complete regressions, but we were not able to determine durable responses in these animals due to increasing viremia over time, which we attributed to the lack of a functional adaptive immune system in these NSG mice. Although HER2 and other classical tumor-associated antigens such as EpCAM and epidermal growth factor receptor (EGFR) represent attractive targets, they are not entirely tumor-specific. So-called 'on-target, off-tumor toxicity' might limit the therapeutic potential of these targets (48,49). Instead, targeting of highly tumor-specific antigen glypican-3 (GPC3) or the tumor-specific mutant of EGFR (EGFRvIII) showed limited and manageable toxicity, and striking antitumor efficacy in immunocompetent mouse models or patients with recurrent glioblastoma (50,51). These data illustrate that further extensive target discovery and testing are required to create safe and effective bsAbs for clinical use. The intracellular proteome might even be considered a good target for bsAbs, via surface display of tumor-specific peptide/MHC complexes (52).

Together, our data demonstrate that combined local reovirus treatment and systemic T-cell-engaging antibody therapy induces strong tumor regressions of both local and distant solid tumors. Both CD3-bsAbs and OVs are already undergoing rigorous clinical testing, suggesting a possible fast translation of our work to the clinic.

DECLARATIONS

Acknowledgments. The authors thank Lisa Griffioen, Noortje de Bie, and Marjolein Sluijter for their technical assistance, the Animal Facility of the LUMC for their excellent care of the animals, and Michael Fiebig (Absolute Antibody) for his collaboration. The hybridoma 4F2 (reovirus σ3), developed by T. S. Dermody from the University of Pittsburgh School of Medicine, was obtained from the Developmental Studies Hybridoma Bank, created by the NICHD of the NIH and maintained at The University of Iowa, Department of Biology, Iowa City, IA 52242.

Author contributions. Conceptualization, TvH and NvM; Methodology, CG, PK, DvdW, RvdO, JM, DM, RH, TvH and NvM; Formal analysis, CG, PK, DM; Investigation, CG, PK, RvdO; Resources, DvdW, RH; Writing – Original Draft, CG, TvH, NvM; Writing - Review & Editing, All authors; Visualization, CG; Supervision, SHvdB, TvH and NvM, Funding acquisition, SHvdB, TvH, and NvM. All authors approved the final version of the manuscript.

Funding. This work was financially supported by the Dutch Cancer Society Bas Mulder Award 11056 (to NvM), a PhD fellowship from Leiden University Medical Center (to CG), and the Support Casper campaign by the Dutch foundation 'Stichting Overleven met Alvleesklierkanker' (supportcasper.nl) project numbers SOAK 17.04 and 19.03.

Competing interests. None declared.

Ethics approval. All mouse studies were approved by the institutional Animal Welfare Body of Leiden University Medical Center and carried out under project licenses AVD1160020187004 or AVD116002015271, issued by the competent authority on animal experiments in the Netherlands (named CCD). Experiments were performed following the Dutch Act on Animal Experimentation and EU Directive 2010/63/EU ("On the protection of animals used for scientific purposes") at the animal facility of the Leiden University Medical Center (LUMC), The Netherlands.

Data availability statement. All data relevant to this study are included in the main text or the supplementary materials and are available on reasonable request.

REFERENCES

1. Runcie K, Budman DR, John V, Seetharamu N. Bi-specific and tri-specific antibodies- the next big thing in solid tumor therapeutics. Molecular medicine (Cambridge, Mass) **2018**;24:50
2. Bargou R, Leo E, Zugmaier G, Klinger M, Goebeler M, Knop S*, et al.* Tumor Regression in Cancer Patients by Very Low Doses of a T Cell–Engaging Antibody. Science **2008**;321:974-7
3. Labrijn AF, Janmaat ML, Reichert JM, Parren P. Bispecific antibodies: a mechanistic review of the pipeline. Nature Reviews Drug Discovery **2019**;18:585-608
4. Mandikian D, Takahashi N, Lo AA, Li J, Eastham-Anderson J, Slaga D*, et al.* Relative Target Affinities of T-Cell–Dependent Bispecific Antibodies Determine Biodistribution in a Solid Tumor Mouse Model. Molecular cancer therapeutics **2018**;17:776-85
5. Offner S, Hofmeister R, Romaniuk A, Kufer P, Baeuerle PA. Induction of regular cytolytic T cell synapses by bispecific single-chain antibody constructs on MHC class I-negative tumor cells. Molecular Immunology **2006**;43:763-71
6. Mack M, Gruber R, Schmidt S, Riethmüller G, Kufer P. Biologic properties of a bispecific single-chain antibody directed against 17-1A (EpCAM) and CD3: tumor cell-dependent T cell stimulation and cytotoxic activity. J Immunol **1997**;158:3965-70
7. Dahlén E, Veitonmäki N, Norlén P. Bispecific antibodies in cancer immunotherapy. Therapeutic advances in vaccines and immunotherapy **2018**;6:3-17
8. Herbst RS, Soria J-C, Kowanetz M, Fine GD, Hamid O, Gordon MS*, et al.* Predictive correlates of response to the anti-PD-L1 antibody MPDL3280A in cancer patients. Nature **2014**;515:563-7
9. Chen DS, Mellman I. Elements of cancer immunity and the cancer-immune set point. Nature **2017**;541:321-30
10. Groeneveldt C, van Hall T, van der Burg SH, ten Dijke P, van Montfoort N. Immunotherapeutic potential of TGF-β inhibition and oncolytic viruses. Trends in Immunology **2020**;41:406-20
11. Samson A, Scott KJ, Taggart D, West EJ, Wilson E, Nuovo GJ*, et al.* Intravenous delivery of oncolytic reovirus to brain tumor patients immunologically primes for subsequent checkpoint blockade. Science translational medicine **2018**;10
12. Bourgeois-Daigneault MC, Roy DG, Aitken AS, El Sayes N, Martin NT, Varette O*, et al.* Neoadjuvant oncolytic virotherapy before surgery sensitizes triple-negative breast cancer to immune checkpoint therapy. Science translational medicine **2018**;10
13. Ribas A, Dummer R, Puzanov I, VanderWalde A, Andtbacka RHI, Michielin O*, et al.* Oncolytic Virotherapy Promotes Intratumoral T Cell Infiltration and Improves Anti-PD-1 Immunotherapy. Cell **2017**;170:1109-19 e10
14. Mahalingam D, Goel S, Aparo S, Patel Arora S, Noronha N, Tran H*, et al.* A Phase II Study of Pelareorep (REOLYSIN(®)) in Combination with Gemcitabine for Patients with Advanced Pancreatic Adenocarcinoma. Cancers (Basel) **2018**;10:160
15. Sborov DW, Nuovo GJ, Stiff A, Mace T, Lesinski GB, Benson DM*, et al.* A Phase I Trial of Single-Agent Reolysin in Patients with Relapsed Multiple Myeloma. Clinical Cancer Research **2014**;20:5946-55
16. Duncan MR, Stanish SM, Cox DC. Differential sensitivity of normal and transformed human cells to reovirus infection. J Virol **1978**;28:444-9
17. Shmulevitz M, Marcato P, Lee PWK. Unshackling the links between reovirus oncolysis, Ras signaling, translational control and cancer. Oncogene **2005**;24:7720-8
18. Thirukkumaran CM, Nodwell MJ, Hirasawa K, Shi Z-Q, Diaz R, Luider J*, et al.* Oncolytic Viral Therapy for Prostate Cancer: Efficacy of Reovirus as a Biological Therapeutic. Cancer research **2010**;70:2435-44
19. Zhao X, Chester C, Rajasekaran N, He Z, Kohrt HE. Strategic Combinations: The Future of Oncolytic Virotherapy with Reovirus. Molecular cancer therapeutics **2016**;15:767-73
20. van den Wollenberg DJM, Dautzenberg IJC, van den Hengel SK, Cramer SJ, de Groot RJ, Hoeben RC. Isolation of reovirus T3D mutants capable of infecting human tumor cells independent of junction adhesion molecule-A. PLoS One **2012**;7:e48064-e

21. Smith RE, Zweerink HJ, Joklik WK. Polypeptide components of virions, top component and cores of reovirus type 3. Virology **1969**;39:791-810
22. Fallaux FJ, Kranenburg O, Cramer SJ, Houweling A, Van Ormondt H, Hoeben RC, *et al.* Characterization of 911: a new helper cell line for the titration and propagation of early region 1-deleted adenoviral vectors. Human gene therapy **1996**;7:215-22
23. Hiller BE, Berger AK, Danthi P. Viral gene expression potentiates reovirus-induced necrosis. Virology **2015**;484:386-94
24. Hingorani SR, Wang L, Multani AS, Combs C, Deramaudt TB, Hruban RH, *et al.* Trp53R172H and KrasG12D cooperate to promote chromosomal instability and widely metastatic pancreatic ductal adenocarcinoma in mice. Cancer cell **2005**;7:469-83
25. Benonisson H, Altıntaş I, Sluijter M, Verploegen S, Labrijn AF, Schuurhuis DH, *et al.* CD3-Bispecific Antibody Therapy Turns Solid Tumors into Inflammatory Sites but Does Not Install Protective Memory. Molecular cancer therapeutics **2019**;18:312-22
26. Rozanov DV, Rozanov ND, Chiotti KE, Reddy A, Wilmarth PA, David LL, *et al.* MHC class I loaded ligands from breast cancer cell lines: A potential HLA-I-typed antigen collection. J Proteomics **2018**;176:13-23
27. Mijatovic-Rustempasic S, Tam KI, Kerin TK, Lewis JM, Gautam R, Quaye O, *et al.* Sensitive and specific quantitative detection of rotavirus A by one-step real-time reverse transcription-PCR assay without antecedent double-stranded-RNA denaturation. Journal of clinical microbiology **2013**;51:3047-54
28. Brahmer JR, Tykodi SS, Chow LQM, Hwu W-J, Topalian SL, Hwu P, *et al.* Safety and activity of anti-PD-L1 antibody in patients with advanced cancer. The New England journal of medicine **2012**;366:2455-65
29. Royal RE, Levy C, Turner K, Mathur A, Hughes M, Kammula US, *et al.* Phase 2 Trial of Single Agent Ipilimumab (Anti-CTLA-4) for Locally Advanced or Metastatic Pancreatic Adenocarcinoma. Journal of Immunotherapy **2010**;33:828-33
30. Lee JW, Komar CA, Bengsch F, Graham K, Beatty GL. Genetically Engineered Mouse Models of Pancreatic Cancer: The KPC Model (LSL-Kras(G12D/+) ;LSL-Trp53(R172H/+) ;Pdx-1-Cre), Its Variants, and Their Application in Immuno-oncology Drug Discovery. Curr Protoc Pharmacol **2016**;73:14.39.1-14.39.20
31. Prestwich RJ, Ilett EJ, Errington F, Diaz RM, Steele LP, Kottke T, *et al.* Immune-mediated antitumor activity of reovirus is required for therapy and is independent of direct viral oncolysis and replication. Clin Cancer Res **2009**;15:4374-81
32. Fransen MF, Schoonderwoerd M, Knopf P, Camps MG, Hawinkels LJ, Kneilling M, *et al.* Tumor-draining lymph nodes are pivotal in PD-1/PD-L1 checkpoint therapy. JCI Insight **2018**;3:e124507
33. Mosely SIS, Prime JE, Sainson RCA, Koopmann J-O, Wang DYQ, Greenawalt DM, *et al.* Rational Selection of Syngeneic Preclinical Tumor Models for Immunotherapeutic Drug Discovery. Cancer Immunology Research **2017**;5:29-41
34. Iorns E, Drews-Elger K, Ward TM, Dean S, Clarke J, Berry D, *et al.* A new mouse model for the study of human breast cancer metastasis. PLoS One **2012**;7:e47995
35. Twumasi-Boateng K, Pettigrew JL, Kwok YYE, Bell JC, Nelson BH. Oncolytic viruses as engineering platforms for combination immunotherapy. Nature Reviews Cancer **2018**;18:419-32
36. Harrington KJ, Vile RG, Melcher A, Chester J, Pandha HS. Clinical trials with oncolytic reovirus: moving beyond phase I into combinations with standard therapeutics. Cytokine Growth Factor Rev **2010**;21:91-8
37. Baum A, García-Sastre A. Induction of type I interferon by RNA viruses: cellular receptors and their substrates. Amino Acids **2010**;38:1283-99
38. Goubau D, Schlee M, Deddouche S, Pruijssers AJ, Zillinger T, Goldeck M, *et al.* Antiviral immunity via RIG-I-mediated recognition of RNA bearing 5'-diphosphates. Nature **2014**;514:372-5

39. Dai P, Wang W, Yang N, Serna-Tamayo C, Ricca JM, Zamarin D*, et al.* Intratumoral delivery of inactivated modified vaccinia virus Ankara (iMVA) induces systemic antitumor immunity via STING and Batf3-dependent dendritic cells. Science Immunology **2017**;2:eaal1713
40. Ilett EJ, Prestwich RJ, Kottke T, Errington F, Thompson JM, Harrington KJ*, et al.* Dendritic cells and T cells deliver oncolytic reovirus for tumour killing despite pre-existing anti-viral immunity. Gene Ther **2009**;16:689-99
41. Berkeley RA, Steele LP, Mulder AA, van den Wollenberg DJM, Kottke TJ, Thompson J*, et al.* Antibody-Neutralized Reovirus Is Effective in Oncolytic Virotherapy. Cancer Immunology Research **2018**;6:1161-73
42. Adair RA, Roulstone V, Scott KJ, Morgan R, Nuovo GJ, Fuller M*, et al.* Cell Carriage, Delivery, and Selective Replication of an Oncolytic Virus in Tumor in Patients. Science translational medicine **2012**;4:138ra77-ra77
43. Andtbacka RHI, Kaufman HL, Collichio F, Amatruda T, Senzer N, Chesney J*, et al.* Talimogene Laherparepvec Improves Durable Response Rate in Patients With Advanced Melanoma. Journal of Clinical Oncology **2015**;33:2780-8
44. Speck T, Heidbuechel JPW, Veinalde R, Jaeger D, von Kalle C, Ball CR*, et al.* Targeted BiTE Expression by an Oncolytic Vector Augments Therapeutic Efficacy Against Solid Tumors. Clinical Cancer Research **2018**;24:2128-37
45. Fajardo CA, Guedan S, Rojas LA, Moreno R, Arias-Badia M, de Sostoa J*, et al.* Oncolytic Adenoviral Delivery of an EGFR-Targeting T-cell Engager Improves Antitumor Efficacy. Cancer research **2017**;77:2052-63
46. Yu F, Wang X, Guo ZS, Bartlett DL, Gottschalk SM, Song X-T. T-cell engager-armed oncolytic vaccinia virus significantly enhances antitumor therapy. Molecular Therapy **2014**;22:102-11
47. Freedman JD, Hagel J, Scott EM, Psallidas I, Gupta A, Spiers L*, et al.* Oncolytic adenovirus expressing bispecific antibody targets T-cell cytotoxicity in cancer biopsies. EMBO Mol Med **2017**;9:1067-87
48. Yu L, Wang J. T cell-redirecting bispecific antibodies in cancer immunotherapy: recent advances. Journal of Cancer Research and Clinical Oncology **2019**;145:941-56
49. Haense N, Atmaca A, Pauligk C, Steinmetz K, Marmé F, Haag GM*, et al.* A phase I trial of the trifunctional anti Her2 × anti CD3 antibody ertumaxomab in patients with advanced solid tumors. BMC Cancer **2016**;16:420
50. Ishiguro T, Sano Y, Komatsu SI, Kamata-Sakurai M, Kaneko A, Kinoshita Y*, et al.* An anti-glypican 3/CD3 bispecific T cell-redirecting antibody for treatment of solid tumors. Science translational medicine **2017**;9
51. O'Rourke DM, Nasrallah MP, Desai A, Melenhorst JJ, Mansfield K, Morrissette JJD*, et al.* A single dose of peripherally infused EGFRvIII-directed CAR T cells mediates antigen loss and induces adaptive resistance in patients with recurrent glioblastoma. Science translational medicine **2017**;9:eaaa0984
52. Holland CJ, Crean RM, Pentier JM, de Wet B, Lloyd A, Srikannathasan V*, et al.* Specificity of bispecific T cell receptors and antibodies targeting peptide-HLA. The Journal of Clinical Investigation **2020**;130:2673-88

SUPPLEMENTARY METHODS

Cell culture

All cells were cultured at 37 °C in a humidified atmosphere containing 5% CO_2 in Iscove's Modified Dulbecco's medium (IMDM; Invitrogen) supplemented with 8% fetal calf serum (FCS; Bodinco, Alkmaar, The Netherlands), 2mM L-glutamine (Gibco), 100 µg/mL penicillin and 100 µg/mL streptomycin (Gibco). The tumor cell line TC-1 was additionally cultured in the presence of 400 µg/ml Geneticin (G418; Life Technologies), 1% nonessential amino acids (Life Technologies), and 1 mM sodium pyruvate (Life Technologies). Cell lines were assured to be free of *Mycoplasma* by regular PCR analysis. Authentication of the cell lines was done by Short Tandem Repeat (STR) profiling (IDEXX BioAnalytics, Ludwigsburg, Germany) and cells of low passage number were used for all experiments.

In vivo αPD-L1 treatment

Mice were treated on indicated days with intraperitoneal injections of 200 µg PD-L1-blocking antibody (clone 10F.9G2; GoInVivo™ Purified anti-mouse CD274 Antibody; BioLegend).

CsCl purification of reovirus stock

For purification, a freeze-thaw lysate containing reovirus particles was incubated with 0,1% Triton (Sigma-Aldrich, Zwijndrecht, the Netherlands) and 25 units/ml Benzonase (Santa Cruz, Bio-Connect B.V. Huissen, the Netherlands) for 15 min on ice followed by 15 min at 37 °C. After two extractions with Halotec CL10 (FenS B.V. Goes, the Netherlands) to remove cellular debris, the cleared lysate was loaded onto a discontinuous CsCl gradient (1.45 and 1.2 g/cm^3 in phosphate-buffered saline (PBS)). After centrifugation in a SW28 rotor (Beckman Coulter, Woerden, the Netherlands) at 69000 × g for 14 hours at 4 °C, the lower band containing the infectious particles was harvested and desalted in an Amicon Ultra 100K device according to the manufacturer's protocol (Millipore, Merck Chemicals BV, Amsterdam, the Netherlands). The CsCl-purified reoviruses were recovered in reovirus storage buffer (RSB: 10mM Tris-HCl; pH 7.5, 150mM NaCl, 10mM $MgCl_2$ • 6 H2O), aliquoted and stored at 4 °C until use.

In vitro viability assays

The oncolytic capacity of reovirus was assessed using a colorimetric assay to determine metabolic activity. In short, KPC3 and B16.F10 cells were seeded in a concentration of 5000 (KPC3) and 2500 (B16.F10) cells/well and left to attach overnight. The next day, cells were infected with designated MOIs of reovirus. Cell viability was assessed after 48 hours using the CellTiter 96® AQ_{ueous} One Solution Cell Proliferation Assay (Promega). 20 µL/well of CellTiter 96® AQ_{ueous} One Solution Reagent was added for two hours. The ability of CD3xTRP1 bsAbs to induce specific killing was assessed using a colorimetric method for quantifying cellular cytotoxicity. In short, KPC3, KPC3.TRP1 and B16.F10 cells were irradiated at 6000 RAD and plated at a concentration of 30.000 cells/well. Splenocytes were isolated from a naive C57BL/6J mice and B cells were

removed by passaging through nylon wool before use. Splenocytes were added in an E/T ratio of 5:1 and then CD3xTRP1 or CD3xFluorescein bsAbs (CD3xcntrl) were added in a concentration of 1 µg/mL. 48 hours after incubation, 20 µL of Triton-X100 was added to wells containing tumor cells alone to serve as a positive control. 50 µL of supernatant was harvested of all conditions and incubated for 30 minutes with 50 µL of lactate dehydrogenase reaction mix (Pierce LDH Cytotoxicity Assay Kit, ThermoFisher Scientific). Absorbance was measured at 490 using a SpectraMax iD3 multi-mode plate reader (Molecular Devices). Viability was normalized to the viability of non-infected conditions, and % of cytotoxicity was calculated using the positive control as 100 % cytotoxicity. All conditions were performed in triplicate.

Cell preparation and flow cytometry

Tumors were minced in small pieces and additionally incubated with Liberase TL (Roche) for 15 minutes at 37 °C. The reaction was stopped by the addition of medium and the mixture was gently dissociated into a single-cell suspension over a cell strainer. Single-cell suspensions of splenocytes were resuspended in lysis buffer to remove all red blood cells before use. Cells were incubated with Zombie AquaTM Fixable Viability Dye (Biolegend) in PBS at room temperature followed by incubation with 2.4G2 FcR blocking antibodies (clone 2.4G2; BD Biosciences) in FACS buffer (PBS, 0.5% BSA and 1% NaAz) before surface marker staining (**Table S1**). If applicable, cells were fixed and stained for transcription factors and nuclear proteins using the Foxp3 / Transcription Factor Staining Buffer Set (eBiosciences) according to manufacturers' instructions. TRP1 expression on KPC3.TRP1 tumor cells was measured using the αTRP1 primary antibody (clone: TA99) followed by a secondary Alexa Fluor 647-labeled anti-mouse IgG (BioLegend). HER2 expression on BT474 tumor cells was measured using the anti-erbB-2 (Her-2/neu) primary antibody (clone: 4D5-8) followed by a secondary PE-labeled anti-rabbit IgG (BioLegend). The frequency of $\sigma3^+$ cells was determined as a method of quantifying the infection efficiency of reovirus. Cells were harvested 48 hours after infection and fixed with Fixation Buffer (BioLegend) according to the manufacturer's instructions. Afterward, cells were washed with Permeabilization Wash Buffer (BioLegend) and stained with 4F2 hybridoma supernatant (dilution 1:500), recognizing the σ3 protein of reovirus T3D (Developmental Studies Hybridoma Bank) followed by a secondary Alexa Fluor 647-labeled anti-mouse IgG (BioLegend). After completion of staining protocols, samples were fixed in 1% paraformaldehyde and acquired using a BD LSRFortessa™ X20 cell analyzer (BD Biosciences) within 24 hours. Flow cytometry data was analyzed using FlowJo™ Software Version 10 (Becton, Dickinson, and Company).

Ex vivo analysis of TIL specificity

To determine the specificity of T cells in the tumor and spleen, KPC3-bearing mice were treated with the standard regimen reovirus as described above. Single-cell suspensions of individual tumors and spleens, collected at seven days after the last reovirus injection, were co-cultured with irradiated (6000 RAD) target cells. The irrelevant tumor cell line TC-1 was used as a target to facilitate reovirus replication and PMA (20 ng/mL)

and ionomycin (1 µg/mL) were used as positive control. After 1 hour of co-incubation, BD GolgiPlug™ (BD Biosciences) was added in a 1:1000 dilution. After an additional 5 hours, cells were washed and stained for surface markers. Afterward, cells were fixed, permeabilized, and stained for intracellular markers using the Foxp3/Transcription Factor Staining Buffer Set (eBiosciences) according to manufacturers' instructions. After completion of the staining protocol, samples were fixed, measured, and analyzed as described above.

RNA isolation

From *in vitro* samples, total RNA was isolated from cell pellets using the NucleoSpin® RNA Kit (Macherey-Nagel™) according to the manufacturer's instructions. For *in vivo* samples, a representative snap-frozen proportion (10-30 mg) of each tumor or organ was disrupted using a stain-less bead and the TissueLyser LT (Qiagen). Total RNA of *in vivo* samples was using the ReliaPrep™ RNA Tissue Miniprep System (Promega) according to manufacturer's protocol. RNA quality and integrity were determined using the Experion™ Automated Electrophoresis System (Bio-Rad).

RT-qPCR analysis

For S4 analysis, 150 ng of RNA was used to generate cDNA with primer S4EndR (GATGAATGAAGCCTGTCCCACGTCA) and GoScript™ Reverse Transcriptase (Promega). For assessing the transcription levels of host genes *Ifit-1, Ifit-3, Oas1b, Ddx58, Cxcl10, Ccl5,* and *β2M*, 500 ng of RNA was used to generate cDNA using the High-Capacity RNA-to-cDNA™ Kit (ThermoFisher Scientific) according to the manufacturer's protocol. Subsequent qPCR analysis was performed using the Bio-Rad iQ™ SYBR® Green Supermix (Bio-Rad) and the primer sets are displayed in (**Table S2**). The expression of host genes was normalized to reference genes *Mzt2, Ptp4a2, and Ubc* using the Bio-Rad CFX Manager 3.1 Software (Bio-Rad). All primers were quality controlled by assessing the slope, efficiency, and R^2 value of dilution series using cDNA that was synthesized from murine reference RNA. All samples were measured in technical duplicates or triplicates. The used PCR program consisted of the following steps: (1) 3 min at 95 °C; (2) 40 cycles of 10 s at 96 °C followed by 30 s at 60 °C and plate read; (3) 10 s at 95 °C; (4) Melt curve 65–95 °C with an increment of 0.2 °C every 10 s, and plate read.

Immunohistochemistry

Formaldehyde-fixed, paraffin-embedded tissue sections were stained for reoviral protein σ3 or murine CD3. Formalin-fixed tumor pieces were embedded in paraffin and then sectioned randomly at 5 µm and placed on Superfrost® Plus slides (VWR). Sections were dried overnight at 37 °C and stored at 4 °C until staining. Slides were deparaffinized and endogenous peroxidase was blocked with 0,3% hydrogen peroxidase (VWR) in methanol for 20 minutes. After rehydration, antigen retrieval was performed by boiling slides for 10 minutes in 0,01M sodium citrate (Merck). Non-specific binding was blocked using SuperBlock™ (ThermoFisher Scientific) before overnight incubation at 4 °C with rabbit anti-mouse CD3ε D7A6E™ XP® mAb (1:200; Cell Signaling Technology), rat

anti-mouse CD8a (clone 4SM15, 1:1600; eBioscience™) or 4F2 hybridoma supernatant which recognizes the σ3 protein of reovirus (1:150; Developmental Studies Hybridoma Bank). Hereafter, samples were incubated for 30 min at RT with biotinylated goat anti-rabbit, rabbit anti-rat, or goat anti-mouse secondary antibodies (1:200; Agilent), followed by incubation with avidin-biotin complex (VECTASTAIN® Elite® ABC HRP Kit; Vector Laboratories). Peroxidase activity was detected using the 2-component liquid DAB+ system (Agilent) according to the manufacturer's instructions for 5 min. Slides were counterstained in hematoxylin (Sigma Aldrich), dehydrated, and mounted using Entellan (Sigma Aldrich). Control sections were processed in parallel, but without incubation with primary antibody. No labeling was observed in the control sections.

SUPPLEMENTARY FIGURES

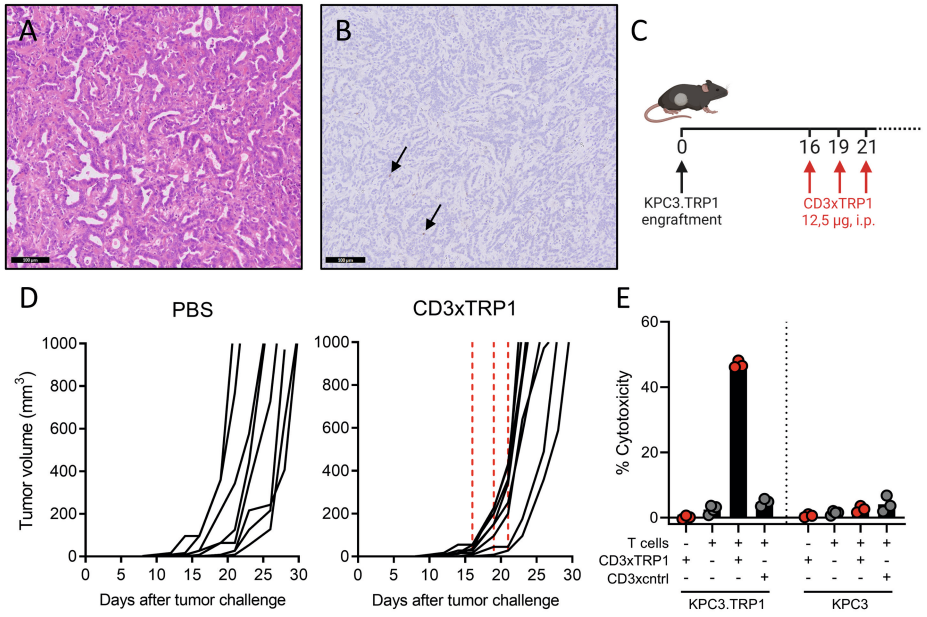


Figure S1. CD3xTRP1 bsAb treatment is not effective in a therapeutic setting in the KPC3.TRP1 model. Hematoxylin and eosin (H&E) staining (**A**) or CD3 immunohistochemical staining (**B**) of representative untreated KPC3 tumor at a size of 1000 mm^3. Arrows indicate $CD3^+$ cells. Scale bar equals 100 µm. (**C**) *In vivo* treatment schedule. Mice (n=8/group) with established KPC3.TRP1 tumors were treated i.p. with 12.5 µg CD3xTRP1 on indicated days, after which tumor growth was monitored. (**D**) Individual tumor growth curves of mice treated with PBS or CD3xTRP1 BsAb. Dashed red vertical lines indicate timing of injection with CD3xTRP1. (**E**) Percentages of cytotoxicity of KPC3.TRP1 or KPC3 cells after *in vitro* co-culture with naive T cells and CD3xTRP1 or CD3xcntrl bsAbs (CD3xFluorescein; bAb0161, Absolute Antibody). Data represent mean±SEM of triplicates. BsAb, bispecific antibody.

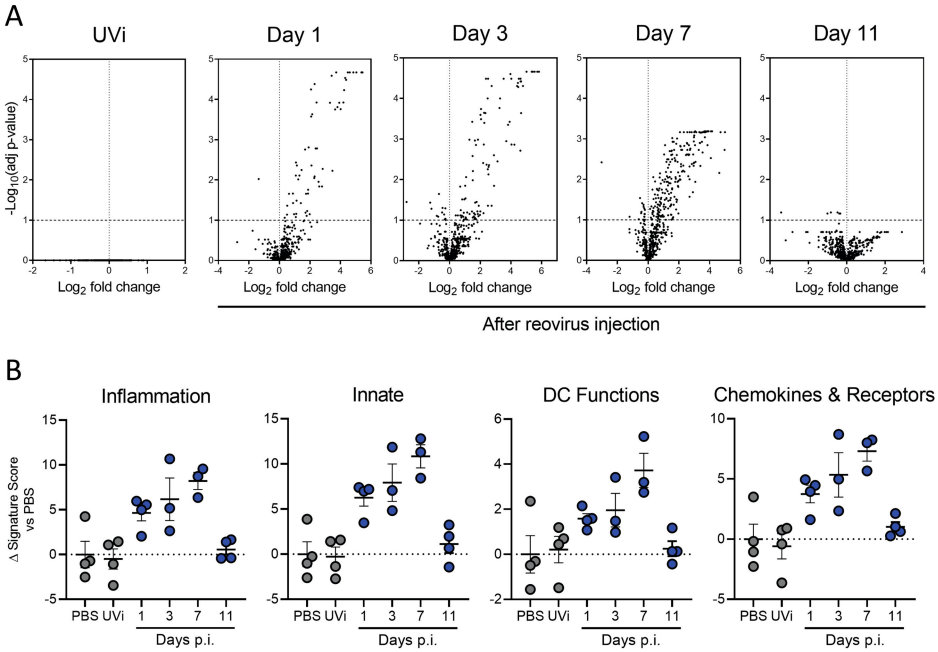


Figure S2. Transcriptomic changes after treatment with replication-competent reovirus. (**A**) Volcano plots showing the differentially expressed genes analyzed by NanoString at various timepoints after treatment with replication-competent reovirus or day 3 after treatment with UVi, normalized versus PBS (n=3-4/group). Horizontal dashed line indicates FDR p-value of 0.1. (**B**) Changes in signature scores on indicated days after reovirus treatment. All scores are normalized for average score of PBS. Data are presented as mean±SEM. UVi, UV-inactivated reovirus.

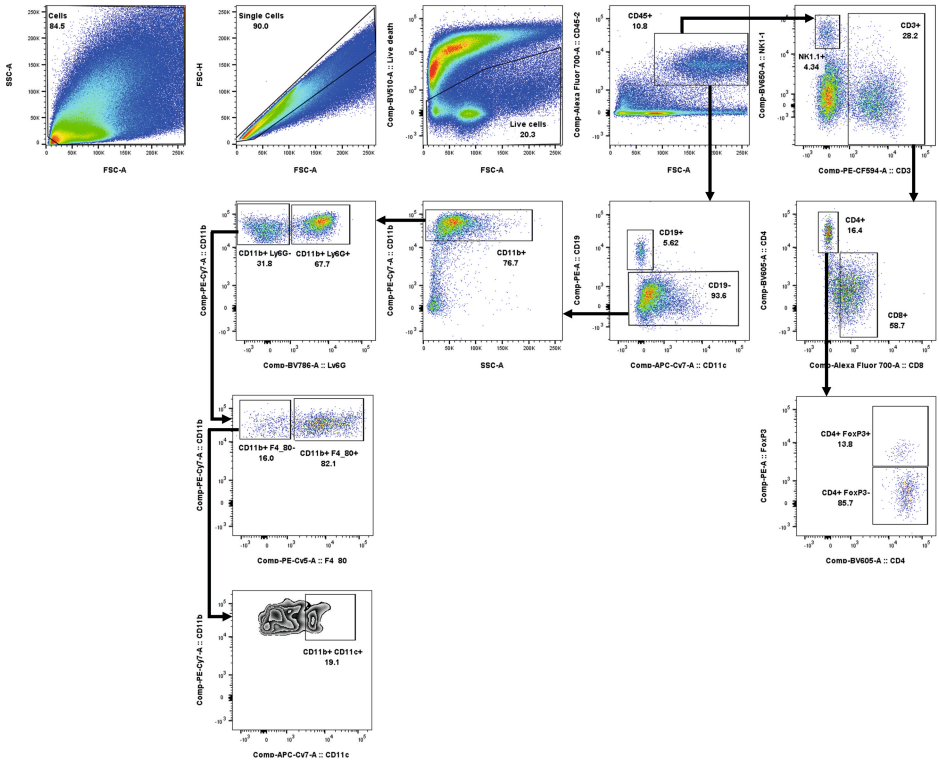


Figure S3. Gating strategy for flow cytometric analyses of the lymphoid and myeloid cell compartment in the tumor after reovirus treatment. Cells of the lymphoid and myeloid compartment were gated according to visualized strategy. Specific antibodies used for flow cytometry can be found in **Table S1**. Data was analyzed by FlowJo™ software.

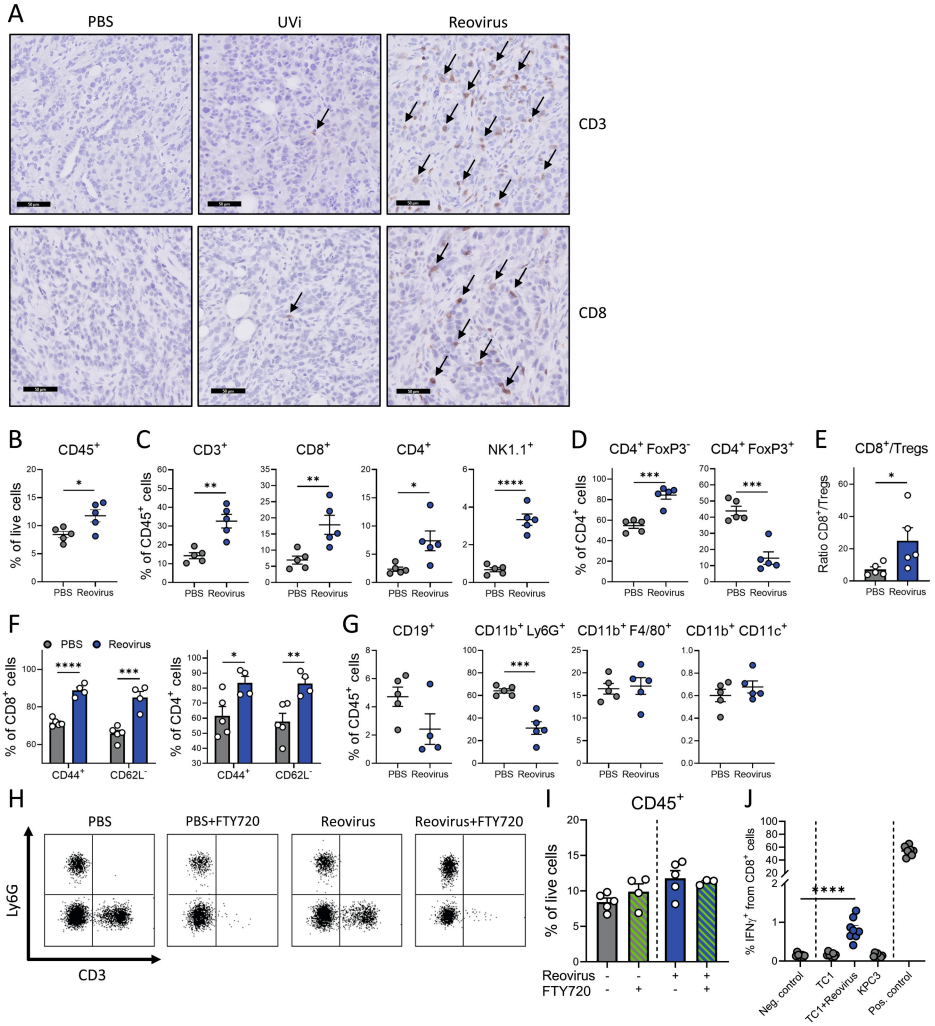


Figure S4. Extended analysis of changes in immune cell composition in the tumor 5 days after reovirus treatment. (**A**) CD3 and CD8 immunohistochemical staining of representative KPC3 tumors injected with PBS, UVi or replication-competent reovirus. Arrows indicate $CD3^+$ or $CD8^+$ cells. Scale bar equals 50 µm. (**B**) Frequency of $CD45^+$ immune cells out of all live cells. (**C**) Frequency of $CD3^+$, $CD8^+$ and $CD4^+$ T cells and $NK1.1^+$ cells out of $CD45^+$ immune cells in tumors after administration of reovirus or PBS. (**D**) Frequency of $CD4^+$ $FoxP3^-$ (conventional $CD4^+$ T cells) and $CD4^+$ $FoxP3^+$ (regulatory T cells). (**E**) Ratio between $CD8^+$ T cells and $CD4^+FoxP3^+$ cells (regulatory T cells) within the $CD45^+$ immune cell population in the tumor after treatment with reovirus or PBS. Statistical difference between groups is determined using a Mann Whitney U test. (**F**) Activation status of intratumoral $CD8^+$ and $CD4^+$ T cells after reovirus or PBS treatment. (**G**) Percentages of other immune cells within the $CD45^+$ population after treatment with reovirus or PBS. Significance of data visualized in B-D, F and G is determined using unpaired t tests. (**H**) Presence of $CD3^+$ T cells and $Ly6G^+$ cells in tail blood of mice treated as indicated, without or with FTY720. Representative flow cytometry dot plot of one mouse per group is shown. (**I**) Frequency of $CD45^+$ immune cells in de tumor. Data is representative for 2 independent experiments. (**J**) Presence of $IFNγ^+$ $CD8^+$ cells in the spleen after ex vivo co-culture with indicated targets. All data are presented as mean±SEM (n=5/group for A-I, n=8/group for J). In figure I, significance between groups is determined using an ordinary one-way ANOVA with Tukey's post-hoc test. In (J), significance versus negative control is determined using an unpaired t test. Significance levels are indicated with asterisks, with *p<0.05, **p<0.01, ***p<0.001, and ****p<0.0001. UVi, UV-inactivated reovirus.

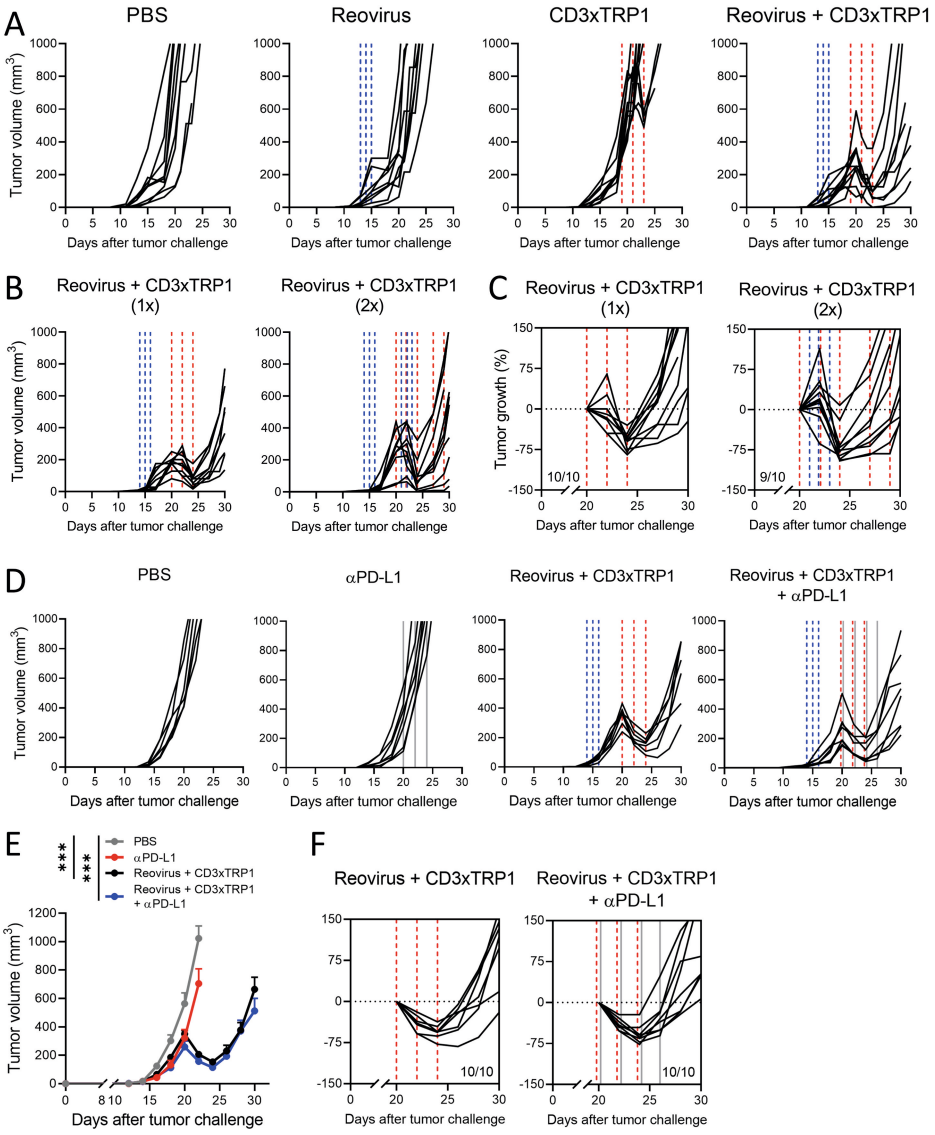


Figure S5. Strategies to prevent immune escape after combined reovirus and CD3xTRP1 bsAb combination treatment. (**A**) Individual tumor growth curves of experiment described in Figure 4B. Dashed vertical lines indicate timing of treatment with Reovirus (blue) or CD3xTRP1 (red). (**B**) Individual tumor growth curves of groups receiving one round or two rounds of reovirus + CD3xTRP1 therapy (n=10/group). (**C**) Relative changes in tumor volume of individual mice from the start of CD3xTRP1 bsAb treatment. Indicated is the number of mice with tumor regressions. (**D**) Individual growth curves of KPC3.TRP1-bearing mice receiving indicated treatments. Grey lines indicate timing of treatment with αPD-L1. (**E**) Average tumor growth curves. Differences in mean tumor volumes versus PBS treatment on day 22 is determined by ordinary one-way ANOVA with Dunnett's post-hoc test. (**F**) Relative changes in tumor volume from start of CD3xTRP1 bsAb treatment. Indicated is the number of mice with tumor regressions. All data are presented as mean±SEM. Significance level: ***p<0.001. BsAb, bispecific antibody.

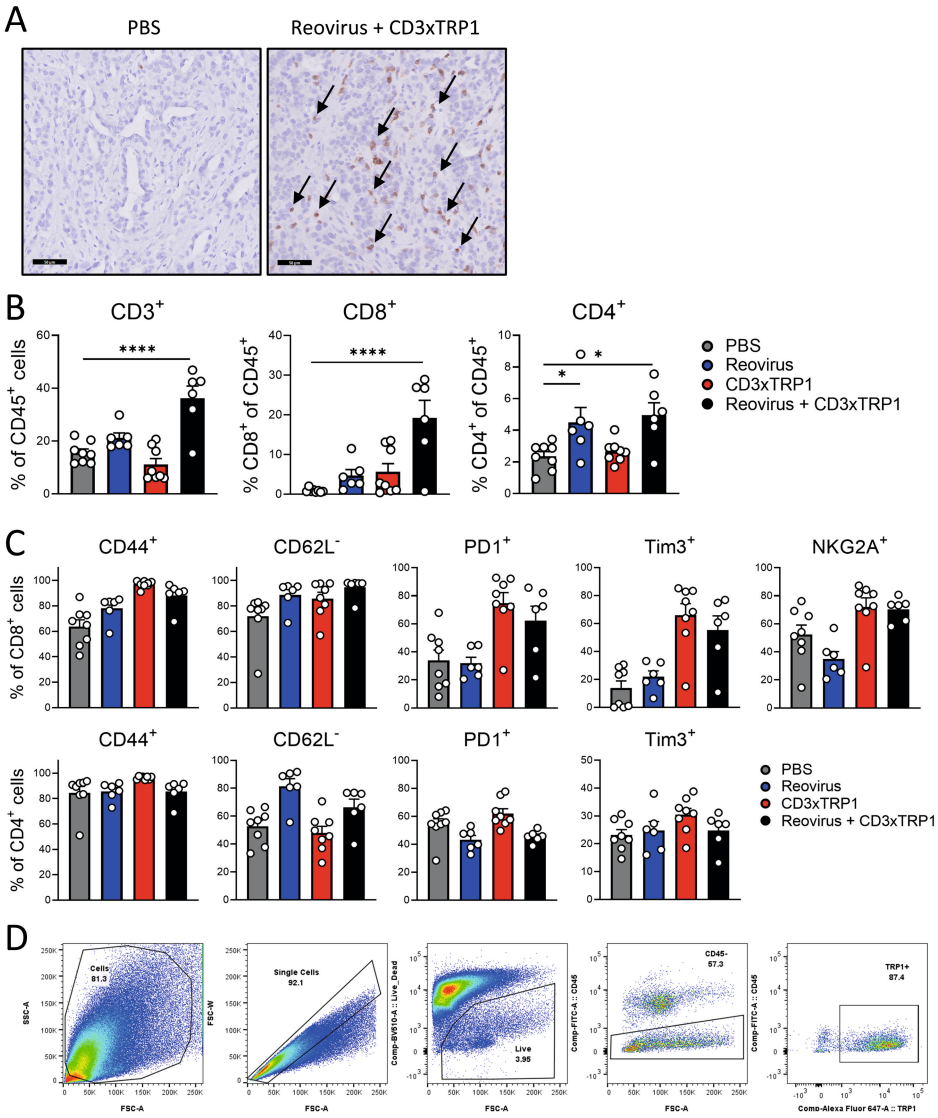


Figure S6. Analysis of mechanisms underlying escape to reovirus and CD3xTRP1 bsAb combination treatment. (**A**) Representative images obtained from immunohistochemical CD3 staining (light brown) of tumors treated with PBS or reovirus + CD3xTRP1. Arrows indicate $CD3^+$ cells. Scale bars equal 100 µm. (**B**) Flow cytometric analysis of the frequency of tumor-infiltrating T cells (TILs) in end stage tumor samples (n=6-8/group). Significance versus PBS treatment is determined using an ordinary one-way ANOVA with Dunnett's post-hoc test. (**C**) Expression of activation markers and checkpoint receptors on TILs. All data are presented as mean±SEM with white dots indicating individual mice. (**D**) Gating strategy to determine TRP1 expression by a 2-step flow cytometry protocol. A sample from the PBS group is depicted. Significance levels are indicated with asterisks, with *p<0.05, **p<0.01, ***p<0.001, and ****p<0.0001. BsAb, bispecific antibody.

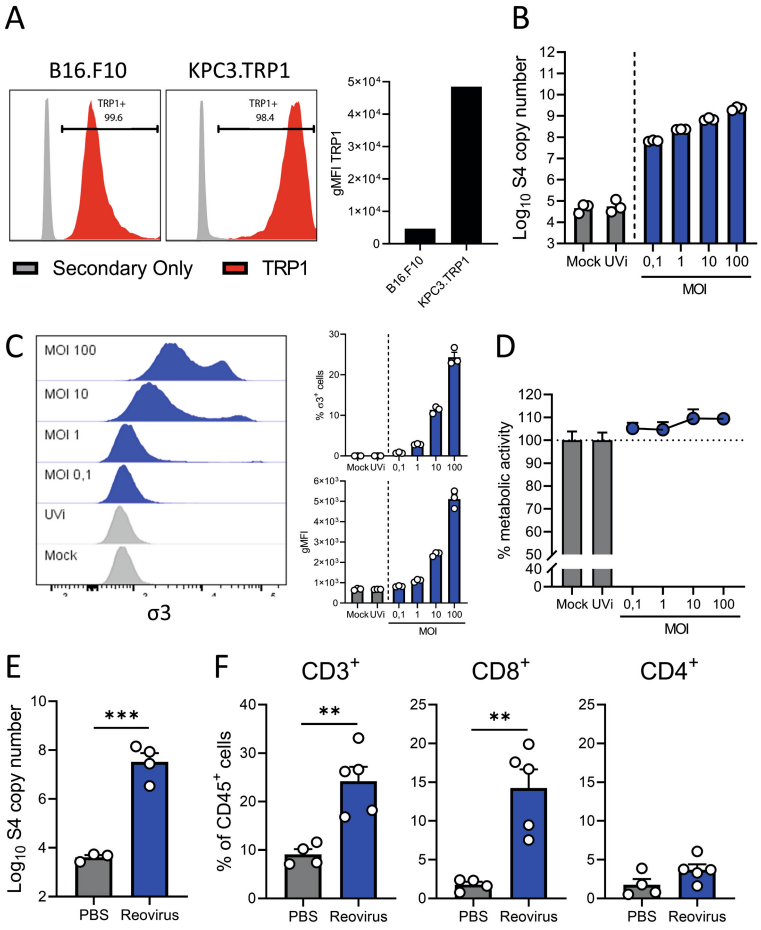


Figure S7. Characterization of reovirus efficacy in B16.F10. (**A**) TRP1 expression percentages and intensities on B16.F10 and KPC3.TRP1 cells, as analysed by flow cytometry using a 2-step protocol. (**B**) Number of reovirus S4 copies in B16.F10 cells after reovirus infection. B16.F10 cells (62.500/well) were infected with increasing MOIs of reovirus, or PBS (Mock) or UVi (equal number of viral particles as MOI 100) as controls. Samples (n=3) were harvested 24 hours after infection and the number of viral S4 copies was determined by RT-qPCR. (**C**) Frequency of σ3$^+$ B16.F10 cells 48 hours after infection with increasing MOIs of reovirus (blue histograms), or PBS or UVi as controls (grey histograms). (**D**) Analysis of oncolytic activity of reovirus. B16.F10 cells (2500/well) were plated and infected with reovirus or controls. Metabolic activity was determined 48 hours after infection. (**E**) S4 copy numbers in tumors harvested 5 days after reovirus treatment (n=3-4/group). (**F**) Flow cytometric analysis of the frequency of tumor-infiltrated T cells (TILs) in B16.F10 tumor samples, 7 days after reovirus treatment (n=3-4/group). All data are presented as mean±SEM and individual values. In figures E-F, significance versus PBS treatment is determined using an unpaired t test. Significance levels are indicated with asterisks, with *p<0.05, **p<0.01, and ***p<0.001. UVi, UV-inactivated reovirus. MOI, multiplicity of infection.

SUPPLEMENTARY TABLES

Table S1. List of antibodies used for flow cytometric analysis.

	Marker	*Clone*	*Fluorochrome*	*Supplier*
Lymphoid panel	CD45.2	104	APC-Cy7	eBioscience
	CD3	145-2C11	PE-CF594	BD Biosciences
	CD8α	53-6.7	Alexa Fluor 700	eBioscience
	CD4	RM4-5	BV605	BioLegend
	CD44	IM-7	BV785	BioLegend
	CD62L	MEL-14	BV421	BioLegend
	NK1.1	Pk136	BV650	BD Biosciences
	PD-1	RMP1-30	FITC	eBioscience
	Tim3	RMT3-23	APC	BioLegend
	NKG2A	16A11	PE	eBioscience
	CD43	1b11	PE-Cy5	BioLegend
	KLRG-1	2F1	PE-Cy7	eBioscience
Myeloid panel	CD45.2	104	FITC	BioLegend
	CD19	eBio1D3	PE	eBioscience
	CD11b	M1/70	PE-Cy7	BioLegend
	Ly6G	1A8	BV785	BioLegend
	F4/80	BM8	PE-Cy5	BioLegend
	CD11c	N418	APC-Cy7	BioLegend
Treg panel	CD45.2	104	FITC	BioLegend
	CD3	145-2C11	PE-CF594	BD Biosciences
	CD8α	53-6.7	Alexa Fluor 700	eBioscience
	CD4	RM4-5	BV605	BioLegend
	FoxP3	FJK-16s	PE	eBioscience
	Ki67	B56	BV711	BD Biosciences
Intracellular T-cell activation panel	CD45.2	104	APC-Cy7	eBioscience
	CD3	145-2C11	PE-CF594	BD Biosciences
	CD8α	53-6.7	Alexa Fluor 700	eBioscience
	INFγ	XMG1.2	APC	BioLegend

Table S2. List of primers used for RT-qPCR analysis.

Gene	*Forward*	*Reverse*
S4Q	5′-CGCTTTTGAAGGTCGTGTATCA-3′	5′-CTGGCTGTGCTGAGATTGTTTT-3′
Ifit-1	5′-CTGGACAAGGTGGAGAAGGT-3′	5′-AGGGTTTTCTGGCTCCACTT-3′
Ifit-3	5′-GTGCAACCAGGTCGAACATT-3′	5′- AGGTGACCAGTCGACGAATT-3′
Oas1b	5′-AGCATGAGAGACGTTGTGGA-3′	5′-GCGTAGAATTGTTGGTTAGGCT-3′
Ddx58	5′-AAGGCCACAGTTGATCCAAA-3′	5′-TTGGCCAGTTTTCCTTGTCG-3′
Cxcl10	5′-ACGAACTTAACCACCATCT-3′	5′-TAAACTTTAACTACCCATTGATACATA-3′
Ccl5	5′-ATTGCTTGCTCTAGTCCTA-3′	5′-ATGCTGATTTCTTGGGTTT-3′
β2M	5′-CTCGGTGACCCTGGTCTTT-3′	5′-CCGTTCTTCAGCATTTGGAT-3′
Mzt2	5′-TCGGTGCCCATATCTCTGTC-3′	5′-CTGCTTCGGGAGTTGCTTTT-3′
Ptp4a2	5′-AGCCCCTGTGGAGATCTCTT-3′	5′-AGCATCACAAACTCGAACCA-3′
Ubc	5′-GCCCAGTGTTACCACCAAGA-3′	5′-CCCATCACACCCAAGAACA-3′



CHAPTER 3

Preinduced reovirus-specific T-cell immunity enhances the anticancer efficacy of reovirus therapy

Christianne Groeneveldt[1], Priscilla Kinderman[1], Jordi J. C. van Stigt Thans[1], Camilla Labrie[1], Lisa Griffioen[1], Marjolein Sluijter[1], Diana J. M. van den Wollenberg[2], Rob C. Hoeben[2], Joke M. M. den Haan[3], Sjoerd H. van der Burg[1], Thorbald van Hall[1], Nadine van Montfoort[4#]

[1] Department of Medical Oncology, Oncode Institute, Leiden University Medical Center, 2333 ZA, Leiden, The Netherlands

[2] Department of Cell and Chemical Biology, Leiden University Medical Center, 2300 RC, Leiden, The Netherlands

[3] Department of Molecular Cell Biology and Immunology, Amsterdam University Medical Center, Cancer Center Amsterdam, Amsterdam Infection and Immunity Institute, Vrije Universiteit Amsterdam, Amsterdam, The Netherlands

[4] Department of Gastroenterology and Hepatology, Leiden University Medical Center, 2333 ZA, Leiden, The Netherlands

[#] Corresponding author

Journal for ImmunoTherapy of Cancer 2022;10:e004464. doi:10.1136/jitc-2021-004464

ABSTRACT

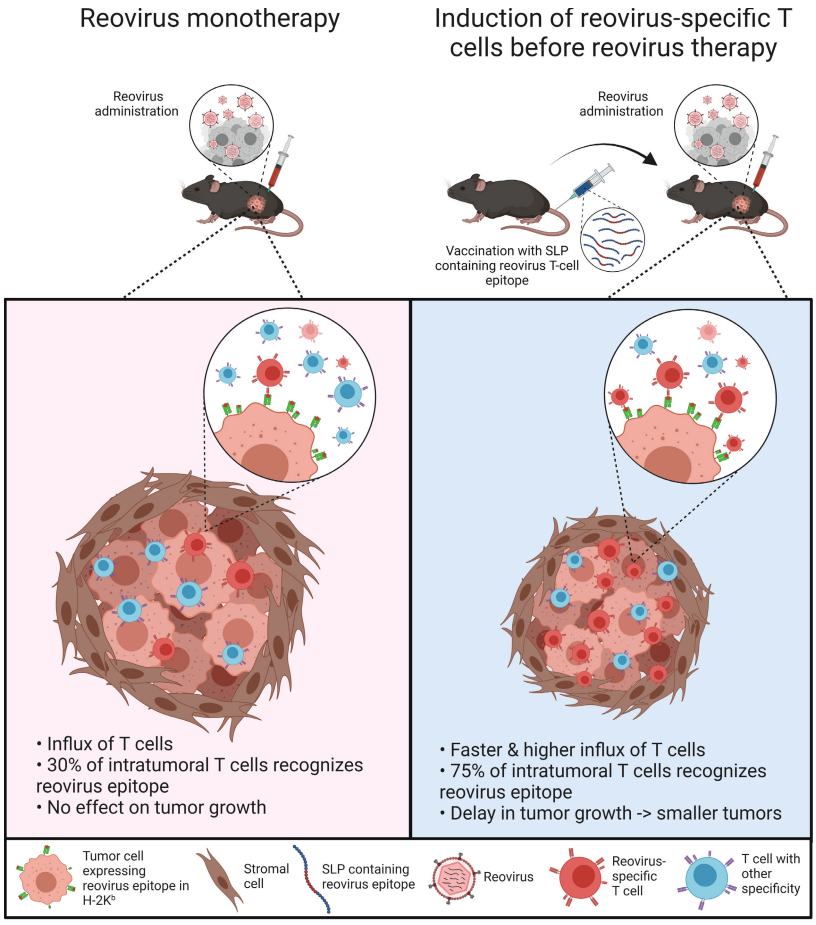
Background. Many solid tumors do not respond to immunotherapy due to their immunologically cold tumor microenvironment (TME). We and others found that oncolytic viruses, including reovirus type 3 Dearing, can enhance the efficacy of immunotherapy by recruiting $CD8^+$ T cells to the TME. A significant part of the incoming $CD8^+$ T cells is directed towards reovirus itself, which may be detrimental to the efficacy of OVs. However, here we aim to exploit these incoming virus-specific T cells as anticancer effector cells.

Methods. We performed an in-depth characterization of the reovirus-induced T-cell response in immune-competent mice bearing pancreatic KPC3 tumors. The immunodominant $CD8^+$ T-cell epitope of reovirus was identified using epitope prediction algorithms and peptide arrays, and the quantity and quality of reovirus-specific T cells after reovirus administration were assessed using high dimensional flow cytometry. A synthetic long peptide (SLP)-based vaccination strategy was designed to enhance the intratumoral frequency of reovirus-specific $CD8^+$ T cells.

Results. Reovirus administration did not induce tumor-specific T cells but rather induced high frequencies of reovirus-specific $CD8^+$ T-cell response directed to the immunodominant epitope. Priming of reovirus-specific T cells required a low-frequent population of cross-presenting dendritic cells which was absent in *Batf3*$^{-/-}$ mice. While intratumoral and intravenous reovirus administration induced equal systemic frequencies of reovirus-specific T cells, reovirus-specific T cells were highly enriched in the TME exclusively after intratumoral administration. Here, they displayed characteristics of potent effector cells with high expression of KLRG1, suggesting they may be responsive against local reovirus-infected cells. To exploit these reovirus-specific T cells as anticancer effector cells, we designed an SLP-based vaccination strategy to induce a strong T-cell response before virotherapy. These high frequencies of circulating reovirus-specific T cells were reactivated upon intratumoral reovirus administration and significantly delayed tumor growth.

Conclusions. These findings provide proof of concept that oncolytic virus-specific T cells, despite not being tumor-specific, can be exploited as potent effector cells for anticancer treatment when primed before virotherapy. This is an attractive strategy for low-immunogenic tumors lacking tumor-specific T cells.

GRAPHICAL ABSTRACT



INTRODUCTION

Oncolytic viruses (OVs) are increasingly recognized as potent anticancer agents due to their preferential replication in cancerous cells and stimulation of host antitumor immunity (1). The mammalian reovirus type 3 Dearing strain (T3D) is one of the leading oncolytic viruses under clinical evaluation and displays an excellent safety record in clinical trials (2,3). Reoviruses show an inherent preference for replication in and lysis of transformed, but not healthy cells (4-6). As a monotherapy, reovirus has demonstrated moderate antitumor efficacy, for example in prostate xenograft models and prostate cancer patients (7,8). Recent advances in the field have shown that beyond their oncolytic capacity, OVs are useful as potent immunostimulatory agents. For example, they can enhance the efficacy of immune checkpoint blockade in immunogenic tumors by further enhancing the intratumoral density of tumor-specific $CD8^+$ T cells that can be reinvigorated by checkpoint blockade (1,9,10).

We questioned whether the immunostimulatory properties of OVs can also be beneficial for non-immunogenic tumors that lack tumor-specific T cells and thus are completely non-responsive to immune checkpoint therapy. We recently demonstrated that intratumoral reovirus administration strongly enhances the infiltration of $CD8^+$ T cells in a non-immunogenic murine pancreatic cancer model (11). A large proportion of these tumor-infiltrating lymphocytes (TILs) did not recognize the tumor but was directed towards reovirus itself. *Despite* being reovirus-specific, these T cells could be exploited by CD3-bispecific antibodies (CD3-bsAbs) to induce tumor regressions of established tumors. Here, we aim to exploit the incoming T cells as anticancer effector cells *because* they are virus-specific.

For this aim, we first investigated the requirements for an effective reovirus-specific T-cell response. We mapped the reovirus T-cell epitope, which allowed us to specifically study the kinetics, distribution, and phenotype of reovirus-specific T cells. We demonstrated that *Batf3*-driven cDC1s are involved in the priming of reovirus-specific T cells and that intratumoral reovirus administration is not required for priming but is strongly preferred for an efficient intratumoral influx of reovirus-specific T cells. In the tumor, reovirus-specific T cells have a profound effector phenotype. Priming of these T cells using a vaccination strategy before intratumoral reovirus therapy strongly improved its antitumor effect.

Our findings provide proof of concept that the presence of a pre-installed pool of oncolytic virus-specific T cells, despite not being tumor-specific, can effectively delay tumor growth after OV therapy. Exploiting these virus-specific T cells during OV administration is an attractive strategy for low-immunogenic tumors that lack tumor-specific T cells.

MATERIAL & METHODS

Reovirus

The wild-type reovirus strain R124 (here referred to as Reo) was previously isolated from a heterogeneous reovirus Type 3 Dearing (T3D) stock (VR-824) obtained from the American Type Culture Collection (ATCC) by two rounds of plaque purification using HER911 cells (12). Reovirus mutant Jin-3 was isolated from JAM-A-deficient U118MG cells after passaging of the wild-type T3D strain R124 (12). All experiments were performed using cesium chloride (CsCl)-purified stocks as described earlier (11). The total amount of particles was calculated based on OD_{260} values where 1 OD equals $2.10x10^{12}$ reovirus particles/mL (13), and the infectious titer was quantified by plaque assay on HER911 cells (14).

Cell lines and culture

The murine pancreatic cancer cell line KPC3 is a low-passage derivate of a primary KPC tumor with mutant *p53* and *K-ras* from a female C57BL/6 mouse (11,15). All cells were cultured at 37 °C in a humidified atmosphere containing 5% CO_2 in Iscove's Modified Dulbecco's Medium (IMDM; Invitrogen) supplemented with 8% fetal calf serum (FCS; Bodinco, Alkmaar, The Netherlands), 2mM L-glutamine (Gibco), 100 µg/mL penicillin and 100 µg/mL streptomycin (Gibco). The tumor cell line TC1 expresses the HPV16-derived oncogenes E6 and E7 and activated Ras oncogene and was additionally cultured in the presence of 400 µg/ml Geneticin (G418; Life Technologies), 1% nonessential amino acids (Life Technologies), and 1 mM sodium pyruvate (Life Technologies) (16). The cell line TC1. B7 was retrovirally transduced to express high levels of co-stimulatory molecule CD86. The DC line D1 was originally obtained from P. Ricciardi-Castagnoli (University of Milano-Bicocca, Milan, Italy) (17). Fre.D^b and Fre.K^b cell lines are stable transfectants of the Fisher rat embryo (Fre) cell line (18). Cell lines were assured to be free of *Mycoplasma* by regular PCR analysis. Authentication of the cell lines was done by Short Tandem Repeat (STR) profiling (IDEXX BioAnalytics, Ludwigsburg, Germany) and cells of low passage number were used for all experiments.

Animal experiments

Male C57BL/6J mice (H-2^b) were purchased from Charles River Laboratories (France). Male and female *Batf3*-deficient mice (The Jackson Laboratory, USA) were bred at the animal facility of Amsterdam University Medical Center. Mice were housed in individually ventilated cages with no more than 5 mice/cage. After one week of acclimatization after transport, mice (6-8 weeks old) were inoculated with subcutaneous KPC3 or TC1 tumors as described before (11). Intratumoral reovirus administration was performed under isoflurane anesthesia by injection of $1x10^7$ plaque-forming units (pfu) of reovirus or PBS as a control in a volume of 30 µL PBS on 3 consecutive days unless otherwise indicated. Intravenous administration of reovirus after tumor challenge was performed by injection of $3x10^7$ pfu of reovirus in a total volume of 100 µL PBS in the tail vein. Intratumoral peptide injection was performed under isoflurane anesthesia by injection of 50 µg peptide in 30 µL PBS.

For vaccination experiments, naive male C57BL/6J mice received the reovirus-derived SLP (DKMRVLSVSPKYSDLLTYVDAYVGV) or the HPV E7-derived SLP (GQAEPDRAHYNIVTFCCKCDS) (GenScript, Leiden, The Netherlands) to induce reovirus- or HPV-specific T-cell immunity. 50 nmol SLP was mixed with 20 µg CpG (ODN1826; InvivoGen) and subcutaneously injected in the tail-base region in 50 µL PBS. This injection was repeated after 2 weeks to boost the efficacy of vaccination. For immunization experiments, mice were immunized by intravenously injecting $1x10^7$ pfu of reovirus in a volume of 100 µL PBS in the tail vein. This injection was repeated after 2 weeks. After vaccination or immunization, mice were engrafted with a subcutaneous KPC3 tumor ($1x10^5$ cells in 100 µL PBS/0.1% BSA) and received reovirus intratumorally as described.

When checkpoint blockade was applied, mice were treated on indicated days with intraperitoneal injections of 200 µg PD-L1-blocking antibody (clone 10F.9G2; GoInVivo™ Purified anti-mouse CD274 Antibody; BioLegend). To deplete $CD8^+$ T cells after vaccination, mice were injected with 50 µg anti-CD8 antibody (Clone 2.43; produced *in-house*). Depletion of $CD8^+$ T cells was verified by flow cytometry before mice received intratumoral reovirus injections.

To reduce the number of experimental animals, some research questions were addressed in one experiment, thereby sharing the control group. This is indicated in the respective figure legends. Cages were randomly allocated to a certain treatment group by an independent researcher and treatments were given in a different order each time. During all experiments, tumors were measured 3 times a week in 3 dimensions using a caliper, in a blinded manner concerning the experimental group. For intratumoral analysis experiments, mice were sacrificed at indicated days after treatment before organs and blood were collected. For experiments where tumor growth was the experimental outcome, mice were sacrificed when the tumor volume exceeded 1000 mm^3 or when ulceration occurred. Tumors were divided into representative parts, which were either snap-frozen in liquid N2 and stored at -80 °C until further analysis, or immediately processed to single cells suspensions for flow cytometry analysis.

Cell preparation and flow cytometry

Tumors, liver, lungs, spleens, and (TD)LNs were dissociated into a single-cell suspension as described before (11). Liver, blood, and splenocytes were incubated with red blood cell lysis buffer for 3 minutes at room temperature (RT) before use. All cells were incubated with Zombie AquaTM Fixable Viability Dye (Biolegend) in PBS for 20 minutes at RT followed by incubation with 2.4G2 FcR blocking antibodies (clone 2.4G2; BD Biosciences) in FACS buffer (PBS, 0.5% BSA, and 1% sodium azide) for 20 minutes on ice. If applicable, cells were incubated with Reo $\mu1_{133\text{-}140}$ tetramer conjugated to APC or the HPV $E7_{49\text{-}57}$ tetramer conjugated to PE (both generated *in-house*) for 1 hour at RT in FACS buffer, after which surface markers (**Table S1**) were added directly to the tetramer mixture for 30 minutes of incubation at RT. After completion of staining protocols,

samples were fixed in 1% paraformaldehyde and acquired using a BD LSRFortessa™ X20 4L cell analyzer (BD Biosciences, San Jose, CA, USA) at the Flow cytometry Core Facility (FCF) of Leiden University Medical Center (LUMC) in Leiden, Netherlands (https://www.lumc.nl/research/facilities/fcf). Data were analyzed using FlowJo™ Software Version 10 (Becton, Dickinson, and Company). Opt-SNE plots (19) were generated using standard settings in OMIQ data analysis software (Omiq, Inc. www.omiq.ai).

Generation of reovirus-specific T-cell bulk

To generate a reovirus-specific T-cell bulk, a KPC3-bearing C57BL/6J mouse was intratumorally injected with 10^7 pfu of reovirus on three consecutive days. 6 days after the last reovirus injection, the mouse was sacrificed by cervical dislocation and the spleen was harvested and processed to a single-cell suspension. After red blood cell lysis, $30x10^6$ splenocytes were co-cultured in culture medium supplemented with 50 mM β-mercaptoethanol for 4 hours with $1.5x10^8$ infectious reovirus particles, equaling a multiplicity of infection (MOI) of 5. Hereafter, splenocytes were washed and plated at 300.000 cells/well in a round-bottom 96-well plate. Bulk cultures were restimulated weekly with irradiated reovirus-infected TC1 cells (6000 RAD) and irradiated naive splenocytes (3000 RAD) as feeders. Initially, bulk cultures were sustained with recombinant IL-2 (10 CU/mL) and later supplemented with 5% (v/v) conditioned medium from Con A- and PMA-stimulated rat splenocytes (18). When necessary, cellular debris was removed by Ficoll-Paque density-gradient centrifugation following the manufacturer's instructions. The specificity of the T-cell bulk was initially assessed using intracellular cytokine staining.

Peptide prediction

Peptide prediction was performed using the NetMHC 4.0 Server (Technical University of Denmark). Sequences of all segments (S1-4, M1-3, and L1-3, **Table S2**) of reovirus type 3 Dearing strain isolate R124 were obtained from the Nucleotide database of the National Center for Biotechnology Information (NCBI, Bethesda MD, USA) (20) and individually loaded into the NetMHC 4.0 Server. Peptide length was set at 8-11 amino acids and thresholds for predicted affinity were set at <0.5% (strong binders) and >2.0% (weak binders) for murine MHC-I molecule H-2K^b. Predicted peptides of all segments were combined and sorted on binding affinity (nM) and rank. Peptides (**Table S3**) with rank <0.200 were ordered as a micro-scale crude peptide library (GenScript, Leiden, The Netherlands) and their recognition by the reovirus-specific T-cell bulk was assessed using intracellular cytokine staining.

Intracellular cytokine staining

T cells from the reovirus-specific T-cell bulk or ex vivo tissues were co-cultured with reovirus-infected target cells (E/T = 1:1) or peptides (1 μg/mL). Unless otherwise indicated, the irrelevant cell line TC1 was used as target. Alternatively, serial dilutions of peptides ranging from 10 μM to 10 pM were added to T cells from the reovirus-specific T-cell bulk. When peptides were presented in the context of D1 cells,

peptides were incubated with D1 cells for one hour before overnight incubation with lipopolysaccharides (LPS, 10 ug/mL). For SLP processing experiments, D1 cells were pre-incubated for 1 hour with SLPs in concentrations between 10 µM and 1 pM after which lipopolysaccharide (LPS; 10 µg/mL) was added to each well for an additional 23 hours. Effector cells and target cells, peptides, or peptide-loaded D1 cells were co-cultured for 6 hours in the presence of BD GolgiPlug™ (BD Biosciences). PMA (20 ng/mL) and ionomycin (1 µg/mL) were used as a positive control. After incubation, cells were washed and stained for CD8α (53-6.7; BioLegend). Thereafter, cells were fixed with Fixation Buffer (BioLegend) according to the manufacturer's instructions, followed by staining for intracellular IFNγ (XMG1.2; BioLegend). After completion of the staining protocol, samples were fixed in 1% paraformaldehyde and acquired using a BD LSRFortessa™ X20 cell analyzer (BD Biosciences).

RNA isolation and RT-qPCR

A representative snap-frozen proportion (10-30 mg) of each tumor or organ was disrupted using a stain-less bead and the TissueLyser LT (Qiagen). Total RNA of *in vivo* samples was using the ReliaPrep™ RNA Tissue Miniprep System (Promega) according to the manufacturer's protocol. Reovirus genomic copies and expression levels of host genes (**Table S4**) in tumors were measured by RT-qPCR as previously described (11). Reovirus S4 copy numbers were determined based on a standard curve, generated with serial dilutions of plasmid pcDNA_S4. Log_{10} S4 copy numbers were calculated using a previously described formula (21). The expression of host genes was normalized to reference genes *Mzt2* and *Ptp4a2* using the Bio-Rad CFX Manager 3.1 Software (Bio-Rad).

Western blotting

Expression of reovirus µ1 protein in KPC3 tumors was analyzed by Western blotting. Briefly, snap-frozen KPC3 tumor pieces were lysed in radioimmunoprecipitation assay (RIPA) buffer containing protease and phosphatase inhibitors using a stain-less bead and the TissueLyser LT (Qiagen). Proteins (40 µg) were separated on a 4-15% mini-protean TGX gel (Bio-Rad) and then transferred to a 0.2 µM nitrocellulose membrane (Bio-Rad). After blocking for 1h at RT with Pierce™ Protein-Free (TBS) Blocking Buffer (ThermoFisher Scientific), the membrane was incubated overnight at 4°C with anti-µ1 (clone 10F6; Developmental Studies Hybridoma Bank, 1:200) or anti-β-actin (Cell Signaling Technology; 1:1000), followed by horseradish peroxidase (HRP)-conjugated goat anti-mouse IgG+IgM+IgA (Abcam, 1:1000) or HRP-conjugated goat anti-rabbit IgG (Cell Signaling Technology, 1:2000) at RT for 1 hour. Proteins were detected on the Chemidoc imaging XRS+ system (Bio-Rad) using the Clarity Western ECL Substrate kit (Bio-Rad).

Statistics

Group size was calculated using the PS: Power and Sample Size Calculation program (Vanderbilt University, version 3.1.6) (22). For experiments where tumor growth was the experimental read-out, mice were excluded when tumor engraftment was not successful (1% of all tumor engraftments). For RT-qPCR analysis, samples were excluded when

RNA concentration and purity were too low. For flow cytometry data, tumor samples were excluded when evidence for draining lymph node contamination was present. All graphs were prepared and statistical analyses were performed using the GraphPad Prism software (version 8.0.2). Statistical tests used for each figure are described in the figure legends. Experimental data were assumed to be normally distributed in all cases, except in the case of RT-qPCR data where standard deviations in Reo groups were significantly different compared to PBS groups. Significance levels are labeled with asterisks, with *p<0.05, **p<0.01, ***p<0.001, and ****p<0.0001. Non-significant differences are indicated by ns.

RESULTS

Identification of immunodominant reovirus CD8⁺ T-cell epitope

The use of oncolytic viruses is an attractive approach to increase $CD8^+$ T-cell influx in solid tumors with an immune-silent phenotype. Indeed, intratumoral injections with oncolytic reovirus in mice bearing murine pancreatic KPC3 tumors or epithelial lung TC1 tumors significantly enhance the frequency of $CD8^+$ T cells in these tumors (**Figure 1A-B, S1A,B**) (11). When these tumor-infiltrating lymphocytes (TILs) were examined for their specificity, we observed that TILs from reovirus-injected tumors only responded when the irrelevant, reovirus-infected TC1 cell line was used as a target (**Figure 1C, S1C**). This suggests that TILs of reovirus-treated mice were mainly reovirus-specific but not tumor-specific. To enable more detailed studies on the role of T cells during reovirus therapy, we set forth to identify the reovirus-derived epitopes recognized by the T cells. Since reovirus-specific T cells were also found in the spleen (**Figure 1C, S1C**), we utilized this splenic population of reovirus-specific $CD8^+$ T cells to generate a reovirus-specific T-cell bulk culture that could be used for epitope identification (**Figure 1D**). After a few rounds of in vitro restimulation with reovirus-infected target cells, a large proportion of the bulk recognized reovirus-infected target cells (**Figure 1E**). The response of reovirus-specific T-cell bulk was restricted by murine H-$2K^b$, as IFNγ was only produced in response to reovirus-infected Fisher rat embryo (FRE) FRE.K^b cells and not to infected FRE.D^b cells, even though infection efficiency was similar in both cell lines (**Figure 1F, S2A, B**).

Next, we determined the H-$2K^b$-specific reovirus-derived peptides that are recognized by reovirus-specific T cells. Predicted epitopes with a length between 8-11 amino acids from the sequences of all reovirus type 3 Dearing segments were divided into 10 pools and tested for their recognition by the reovirus-specific T-cell bulk using intracellular IFNγ staining (**Figure 1G, S3**). Peptide pools #2, #6, #7, and #9 were predominantly recognized. Therefore, peptides from these 4 pools were individually tested. Although some peptides such as peptides #29 and #42 induced IFNγ production, especially two length variant peptides #9 (*VSPKYSDL*) and #34 (*VSPKYSDLL*) activated a high percentage of T cells, comparable to the response against reovirus-infected target cells (**Figure**

1H). This indicated that these peptides might be recognized by the majority of T cells from the reovirus-specific T-cell bulk.

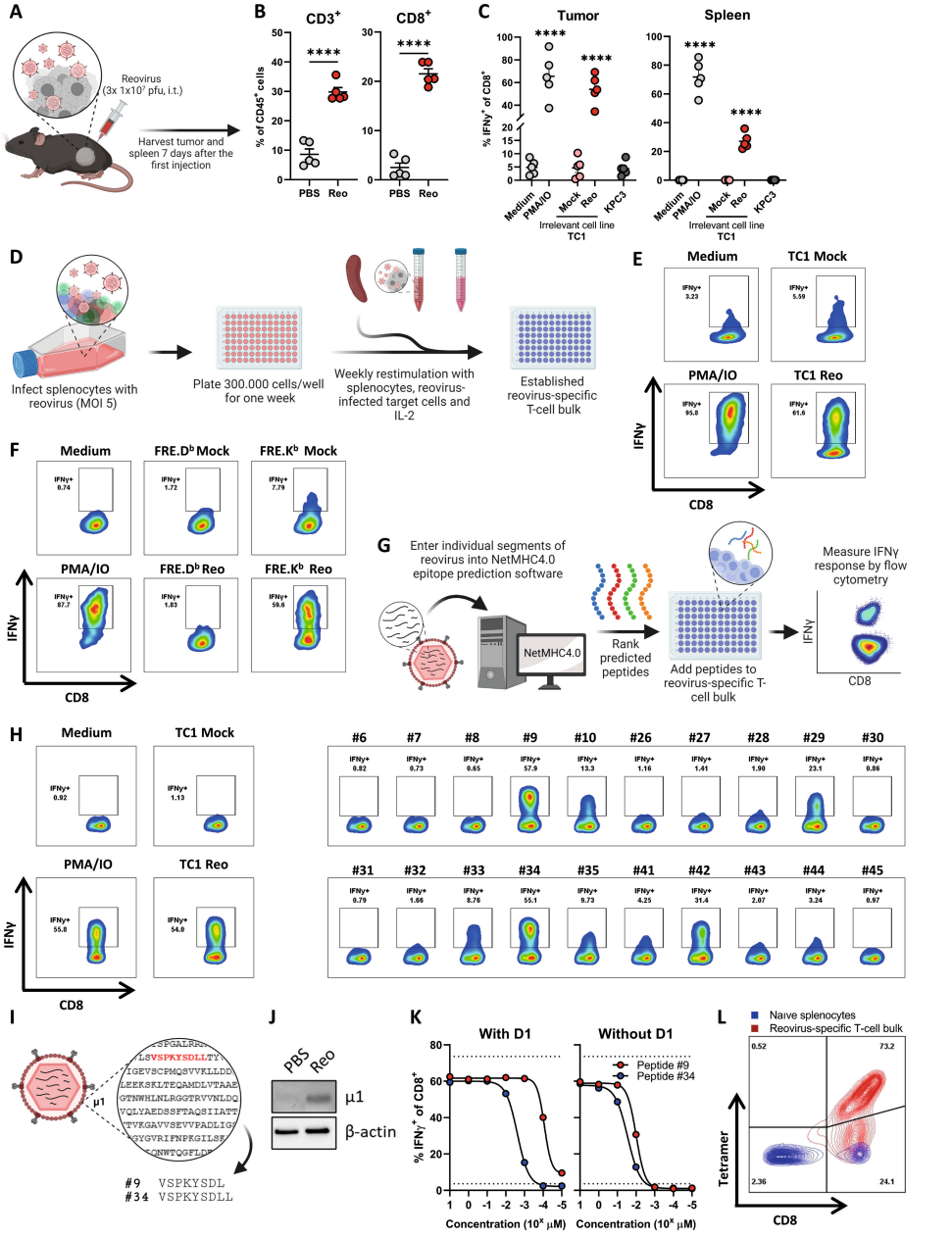


Figure 1. Identification of immunodominant reovirus CD8⁺ T-cell epitope. (**A**) Design of the experiment described in B-C. Mice (n=5/group) with established KPC3 tumors were intratumorally (i.t.) injected with reovirus (10^7 plaque-forming units (pfu)) on 3 consecutive days. Tumors and spleen were analyzed ex vivo 7 days after the first reovirus injection. (**B**) Frequency of CD3⁺ and CD8⁺ T cells within the total CD45⁺ immune cell population in KPC3 tumors after reovirus administration.

>>

>> (**C**) Frequency of interferon gamma (IFNγ)$^+$ cells within the intratumoral and splenic CD8$^+$ T-cell population as measured with intracellular cytokine staining. Single-cell suspensions (n=5/group) were cocultured with indicated targets. PMA/ionomycin (IO) was used as a positive control, and the irrelevant cell line TC1 was used as target cell line for reovirus infection. (**D**) Schematic overview of generation of reovirus-specific T-cell bulk. (**E, F**) Frequency of IFNγ$^+$ cells within reovirus-specific T-cell bulk after coculture with indicated targets. (**G**) Schematic overview of peptide prediction and testing. (**H**) Frequency of IFNγ$^+$ cells within reovirus-specific T-cell bulk after coculture with individual peptides from positive pools (Supplementary Figure S3). (**I**) Schematic overview of sequence and location of two dominant peptides. (J) Expression of reovirus μ1 protein in reovirus-treated KPC3 tumor. (**K**) Frequency of IFNγ$^+$ cells within reovirus-specific T cell bulk after coculture with titrated amounts of peptide #9 or #34. Peptides were added directly or pre-loaded for 1 hour on LPS-matured D1 dendritic cells. (**L**) Binding of generated H-2K^b-*VSPKYSDL* (Reo μ1$_{133\text{-}140}$)-tetramer to naive splenocytes or reovirus-specific T-cell bulk, as measured with flow cytometry. Data are presented as mean±SEM. Statistical tests used: (B): unpaired t-test between PBS and Reo groups. (C): ordinary one-way analysis of variance (ANOVA) with Dunnett's post hoc test. Statistical difference was compared to medium control group. Significance level: ****p<0.0001.

Peptides #9 and #34 are derived from the reovirus outer-capsid protein μ1, a protein that is expressed in reovirus-treated tumors (**Figure 1I, J**). Peptide #9 was found in H-2K^b on the surface of reovirus-infected cells in another study, indicating that this peptide can be processed and presented (23). Subsequently, peptides #9 and #34 were titrated and co-cultured with reovirus-specific T cells, either added directly or in the presence of professional antigen-presenting cells (**Figure 1K**). This showed that the T cells responded to lower concentrations of peptide #9 when compared to peptide #34 and, therefore, peptide #9 (named Reo μ1$_{133\text{-}140}$) was used to generate a reovirus-specific H-2K^b-tetramer. This tetramer did specifically bind to T cells from the reovirus-specific T-cell bulk and not to naive splenocytes (**Figure 1L**), indicating that this tetramer allows selective staining of reovirus-specific T cells.

Intratumoral delivery of reovirus induces a systemic reovirus-specific T-cell response that is enriched in the tumor

We used this Reo μ1$_{133\text{-}140}$ tetramer (Tm) to interrogate reovirus-specific T-cell immunity in the blood of KPC3 tumor-bearing mice after intratumoral administration of reovirus (**Figure 2A**). We observed a reovirus-specific, Tm$^+$ CD8$^+$ T-cell population 5 days after the first intratumoral injection (**Figure 2B**), the frequency of which peaked at day 7 with percentages ranging from 1.7% to 12.8% Tm$^+$ cells out of all CD8$^+$ T cells. Next, we examined the location and frequency of reovirus-specific T cells in the spleen, tumor-draining lymph node (TDLN), and tumor 7 days after intratumoral reovirus administration. Reovirus-specific T cells were found in small frequencies in the TDLN, in the spleen, and at high frequencies in the tumor (**Figure 2C, D**). A similar distribution of Tm$^+$ CD8$^+$ T cells over the lymphoid organs and tumors was observed in TC1 tumor-bearing mice after intratumoral injection with reovirus (**Figure S4**). Tm$^+$ CD8$^+$ T cells were also present in tumors of mice that were injected with Jin-3 (12,24), a variant of the reovirus Type 3 Dearing strain with enhanced tropism (**Figure S5**). These data suggest that the reovirus epitope is conserved among virus isolates and in different tumor models. Interestingly, the frequencies of Tm$^+$ CD8$^+$ T cells in blood, spleen, and

TDLN dropped drastically on day 12 after intratumoral reovirus administration but were retained at relatively high levels in the tumor (**Figure 2E**).

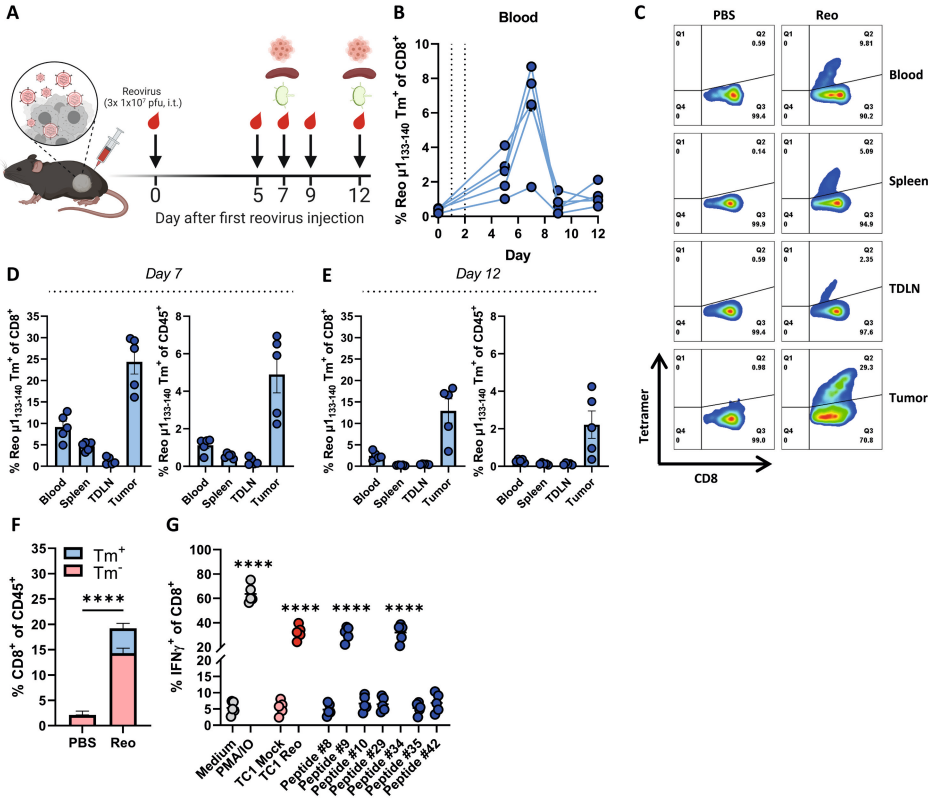


Figure 2. Intratumoral delivery of reovirus induces a systemic reovirus-specific T-cell response that is enriched in the tumor. (**A**) Design of the experiment described in B-D. Mice (n=5/group) with established KPC3 tumors were intratumorally (i.t.) injected with reovirus (10^7 plaque-forming units (pfu)) on 3 consecutive days. Blood, tumors, spleens, and tumor-draining lymph nodes (TDLN) were analyzed using flow cytometry on indicated days. (**B**) Frequency of Reo $\mu1_{133\text{-}140}$ tetramer $(Tm)^+$ $CD8^+$ T cells in the blood on indicated days after intratumoral reovirus administration. (**C**) Representative flow cytometry plots of Tm^+ $CD8^+$ T cells in indicated organs on day 7 after the first reovirus injection. (**D, E**) Quantification of Tm^+ cells out of $CD8^+$ T cells and total $CD45^+$ immune cell population in indicated organs. (**F**) Separation of Tm^+ cells from Tm^- cells within the total $CD8^+$ T cell population of reovirus-treated KPC3 tumors. (**G**) Frequency of interferon gamma $(IFN\gamma)^+$ cells within the intratumoral $CD8^+$ T-cell population after coculture with indicated targets as measured with intracellular cytokine staining. PMA/ionomycin (IO) was used as a positive control. All data are presented as mean±SEM. Statistical tests used: (F): unpaired t-test between PBS and Reo group. (G): ordinary one-way analysis of variance (ANOVA) with Dunnett's post hoc test. Statistical difference was compared to medium control group. Significance level: ****$p<0.0001$.

Whilst a substantial population within $CD8^+$ TILs was Tm^+, there was also a Tm^- $CD8^+$ T-cell fraction (**Figure 2F**). We already demonstrated that this Tm^- fraction was not tumor-specific (**Figure 1, Figure S1**), suggesting that reovirus administration either led to the influx of bystander T cells or reovirus-specific T cells directed to another reovirus-derived epitope. To test this, TILs from reovirus-treated mice were co-cultured with the other peptides that were also recognized by the splenocyte-derived reovirus-specific T-cell bulk (**Figure 1H**). However, none of these peptides elicited a detectable response in the TILs (**Figure 2G**). This suggests that a large majority of the reovirus-specific T-cell response is directed against an immunodominant $CD8^+$ T-cell epitope, similar to what is observed for LCMV (25), influenza (26), and the oncolytic vesicular stomatitis virus (VSV) (27).

cDC1s are involved in the priming of reovirus-specific T cells

Because intratumoral administration of reovirus also resulted in high numbers of systemic reovirus-specific T cells, we were interested in which cell types are involved in the priming of these reovirus-specific T cells. Within the family of antigen-presenting cells, the low-frequent population of basic leucine zipper transcriptional factor ATF-like 3 (*Batf3*)-driven cross-presenting dendritic cells (cDC1) are highly specialized in shaping $CD8^+$ T-cell responses through uptake and processing of exogenous antigens for their presentation in the context of MHC-I molecules, including viral antigens (28-32). Therefore, we studied reovirus-specific immunity in *Batf3*$^{-/-}$ mice, which contained significantly decreased numbers of cDC1 in the spleen and peripheral organs (**Figure S6A, B**) (32,33). Both wild-type C57BL/6J and *Batf3*$^{-/-}$ mice were engrafted with a KPC3 tumor and received intratumoral reovirus injections (**Figure 3A**). An in-depth analysis of the tumor immune cell infiltrate revealed that the total $CD45^+$ immune cell population (**Figure 3B**) or the reovirus-induced influx of NK (**Figure 3C**) and $CD4^+$ T cells (**Figure 3D**) was not affected by *Batf3*-deficiency. However, the influx of total $CD8^+$ T cells was significantly decreased in reovirus-treated *Batf3*$^{-/-}$ mice (**Figure 3E**). This lower $CD8^+$ T-cell influx probably reflects the impaired systemic priming of reovirus-specific $CD8^+$ T cells, since *Batf3*$^{-/-}$ mice displayed significantly lower frequencies of reovirus-specific $CD8^+$ T cells in the tumor, as well as in the blood, spleen, and TDLN (**Figure 3E**). The attraction of $CD8^+$ T cells to the tumor was most likely not the limiting factor in *Batf3*$^{-/-}$ mice since reovirus replication and the reovirus-induced expression of ISGs, including the T-cell attracting chemokines *Cxcl9* and *Cxcl10*, were not affected (**Figure 3F, G**). Combined, these data indicate that cDC1s play an important role in the priming of reovirus-specific T cells.

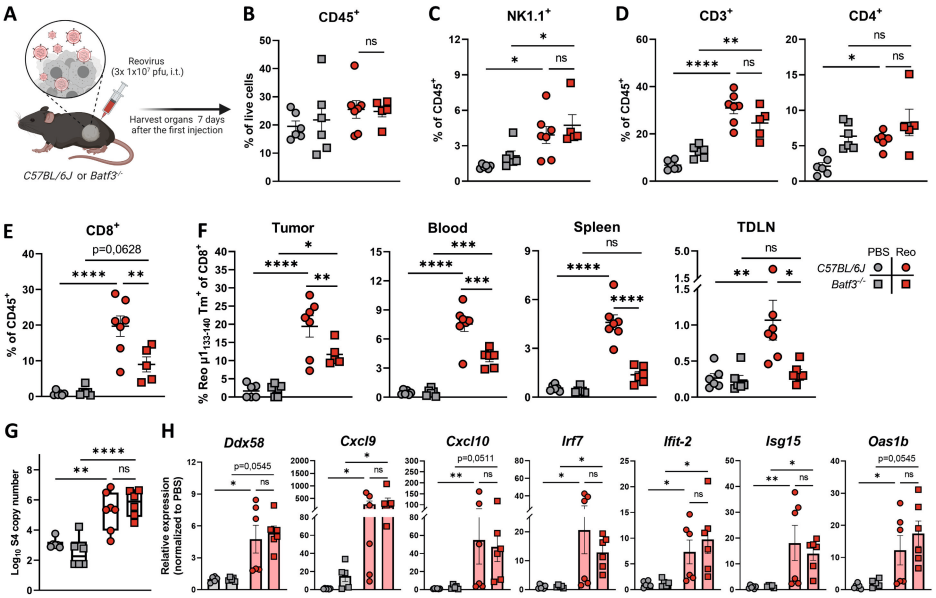


Figure 3. cDC1s are involved in priming of reovirus-specific T cells. (**A**) Design of the experiment described in (B-H). *C57BL/6J* or *Batf3*$^{-/-}$ mice (n=5–7/group) with established KPC3 tumors were intratumorally (i.t.) injected with reovirus (10^7 plaque-forming units (pfu)) on 3 consecutive days. Blood, tumors, spleens, and tumor-draining lymph nodes (TDLN) were analyzed 7 days after the first reovirus injection using flow cytometry. (**B**) Total CD45$^+$ immune cell population in KPC3 tumors of *C57BL/6J* or *Batf3*$^{-/-}$ mice after reovirus administration. (**C**) Intratumoral frequency of NK1.1$^+$ cells within CD45$^+$ immune cells. (**D**) Intratumoral frequency of CD3$^+$ and CD4$^+$ T cells within CD45$^+$ immune cells. (**E**) Intratumoral frequency of CD8$^+$ T cells within CD45$^+$ immune cells. (**F**) Frequency of Reo $\mu1_{133\text{-}140}$ tetramer (Tm)$^+$ CD8$^+$ T cells in indicated organs after intratumoral reovirus administration. (**G**) Intratumoral presence of reovirus genomic segment 4 (S4) copy numbers as measured by quantitative reverse transcription PCR (RT-qPCR). (**H**) Relative expression of various interferon response genes as determined by RT-qPCR. All data are presented as mean±SEM. One tumor of the *Batf3*$^{-/-}$ Reo group in figures B-E was excluded due to lymph node contamination. Statistical tests used: (B-G): ordinary one-way analysis of variance (ANOVA) with Tukey's post hoc test. (H): Nonparametric Kruskal-Wallis test with Dunn's multiple comparisons test. Significance levels: *p<0.05, **p<0.01, ***p<0.001, and ****p<0.0001.

Tumor-infiltrated reovirus-specific T cells have a pronounced effector phenotype

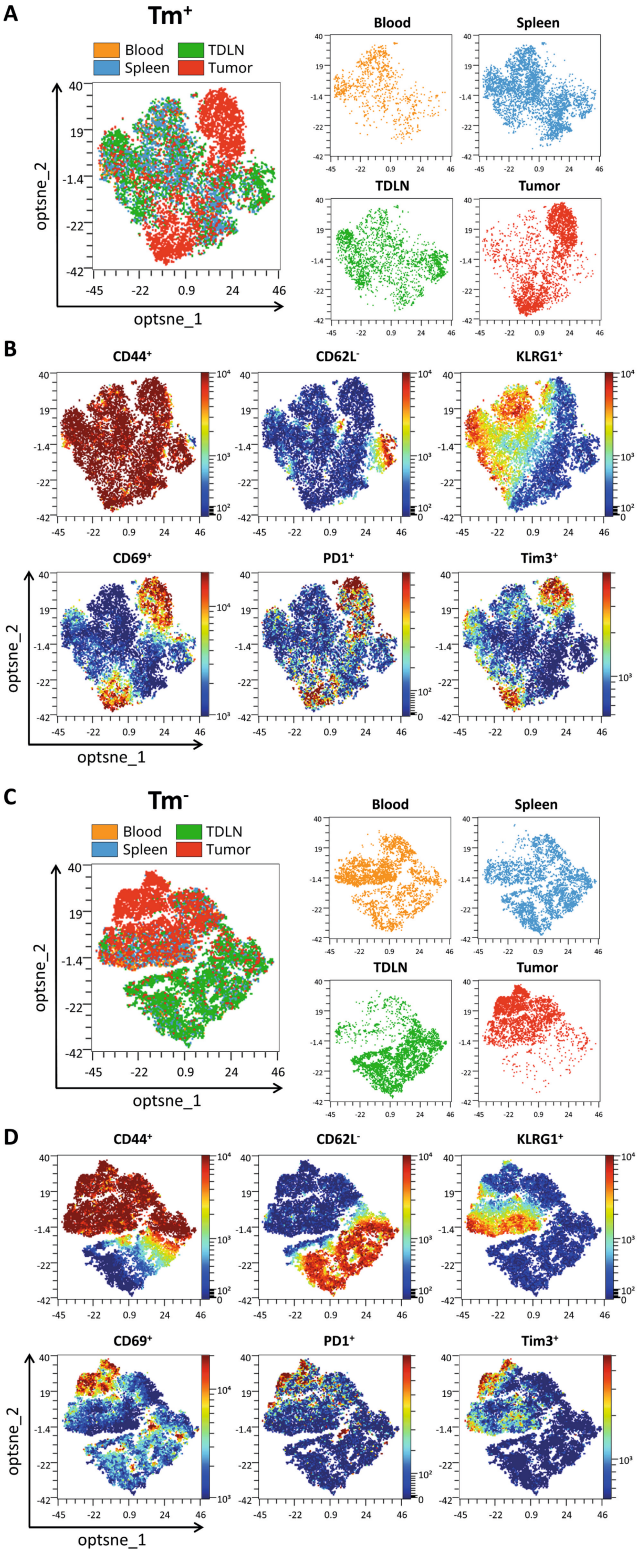
Next, we assessed the phenotype of Reo $\mu1_{133\text{-}140}$-specific CD8$^+$ T cells (Tm$^+$) and investigated whether their phenotype is influenced by their location. Tm$^+$ CD8$^+$ T-cell populations from blood, spleen, TDLN, and tumor were analyzed with OMIQ analysis software that clustered cells based on their expression of CD44, CD62L, KLRG1, CD69, PD1, and Tim3. The tumor-residing Tm$^+$ CD8$^+$ T cells clustered separately from Tm$^+$ CD8$^+$ T cells found in other organs (**Figure 4A**). Tumor-residing Tm$^+$ CD8$^+$ T cells had a higher expression of activation markers CD69, PD1, and Tim3 compared to Tm$^+$ CD8$^+$ T cells in other organs (**Figure 4B**). This suggests that reovirus-specific TILs obtain a unique and distinct phenotype upon reaching the tumor, most likely because this is where reovirus is replicating and the reovirus epitope is presented (**Figure 1J**).

When the same analysis was applied to tetramer-negative $CD8^+$ T cells (**Figure 4C**), we observed a cluster within this population with a similar phenotype as Tm^+ $CD8^+$ T cells, with high expression of CD69, PD1, and Tim3 (**Figure 4D**). These Tm^- $CD8^+$ T cells may also be reovirus-specific, but recognize other, yet unidentified reovirus-derived epitopes. The other intratumoral Tm^- $CD8^+$ T cell cluster, with low expression of CD69, PD1, and Tim3 overlaps with $CD8^+$ T cells that are found in the blood and the spleen, suggesting that this population encompasses mainly 'bystander' $CD8^+$ T cells.

Direct comparison and quantification of expression profiles of Tm^+ and Tm^- $CD8^+$ T cells revealed that in all indicated organs, Tm^+ $CD8^+$ T cells have a significantly more activated phenotype compared to Tm^- $CD8^+$ T cells (**Figure 4E**). This effector phenotype of Tm^+ $CD8^+$ T cells remained stable until 12 days after intratumoral reovirus administration (**Figure S7**). Collectively, these data show that reovirus-specific T cells are highly activated and demonstrate a pronounced effector phenotype when present in the tumor, which distinguishes them from 'bystander' $CD8^+$ T cells. Targeting these reovirus-specific T cells might therefore be an attractive solution for low-immunogenic tumors where tumor-specific T cells are absent.

Route of reovirus administration impacts intratumoral influx, but not priming of reovirus-specific T cells

We next investigated whether intravenous administration of reovirus, which is the route applied in the clinic, also recruits antigen-specific T cells to the tumor. Therefore, the frequency and location of reovirus-specific $CD8^+$ T cells were compared between intravenous and intratumoral administration of reovirus (**Figure 5A**). Interestingly, both intravenous, as well as intratumoral reovirus administration in tumor-bearing mice resulted in similar systemic frequencies of reovirus-specific T cells, suggesting effective systemic priming occurs independently of the reovirus administration route (**Figure 5B**). Surprisingly, equal levels of reovirus-specific T cells were also found in mice without a tumor, demonstrating that active reovirus replication in the tumor is not essential for the priming of a potent systemic reovirus-specific T-cell response (**Figure 5B**).


A
Tm+
Blood
Spleen
TDLN
Tumor
optsne_2
optsne_1
B
CD44+
CD62L-
KLRG1+
CD69+
PD1+
Tim3+
C
Tm-
D

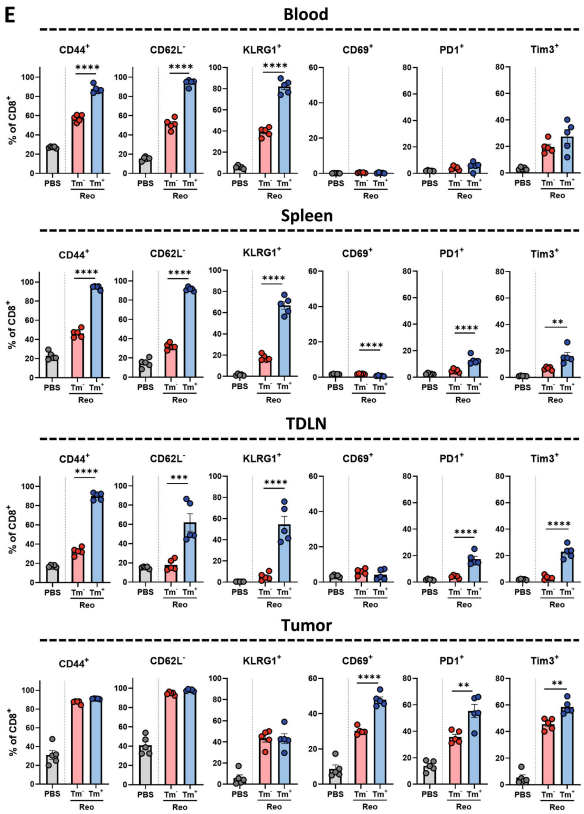


Figure 4. Tumor-infiltrated reovirus-specific T cells have a potent effector phenotype. (**A/C**) Opt-SNE cluster plots of Reo $\mu1_{133-140}$ tetramer $(Tm)^+$ (A) or Tm^- (C) $CD8^+$ T cells from indicated organs. 1000 Tm^+ $CD8^+$ T cells or the maximum possible number of cells if Tm^+ $CD8^+$ T cells <1000 were subsampled from individual organs of each mouse. (**B/D**) Expression intensity profile of activation markers on Tm^+ (B) or Tm^- (D) $CD8^+$ T cells. (**E**) Quantification of expression of activation markers on Tm^- or Tm^+ $CD8^+$ T cells in the blood, spleen, tumor-draining lymph node (TDLN), or tumor (n=5/group) of mice treated with Reo, compared to untreated (PBS). Samples were harvested 7 days after the first intratumoral reovirus injection and the expression of indicated markers was measured using flow cytometry. All data are presented as mean±SEM. Statistical tests used: (E): ordinary one-way analysis of variance (ANOVA) with Tukey's post hoc test. Significance levels: *p<0.05, **p<0.01, ***p<0.001, and ****p<0.0001.

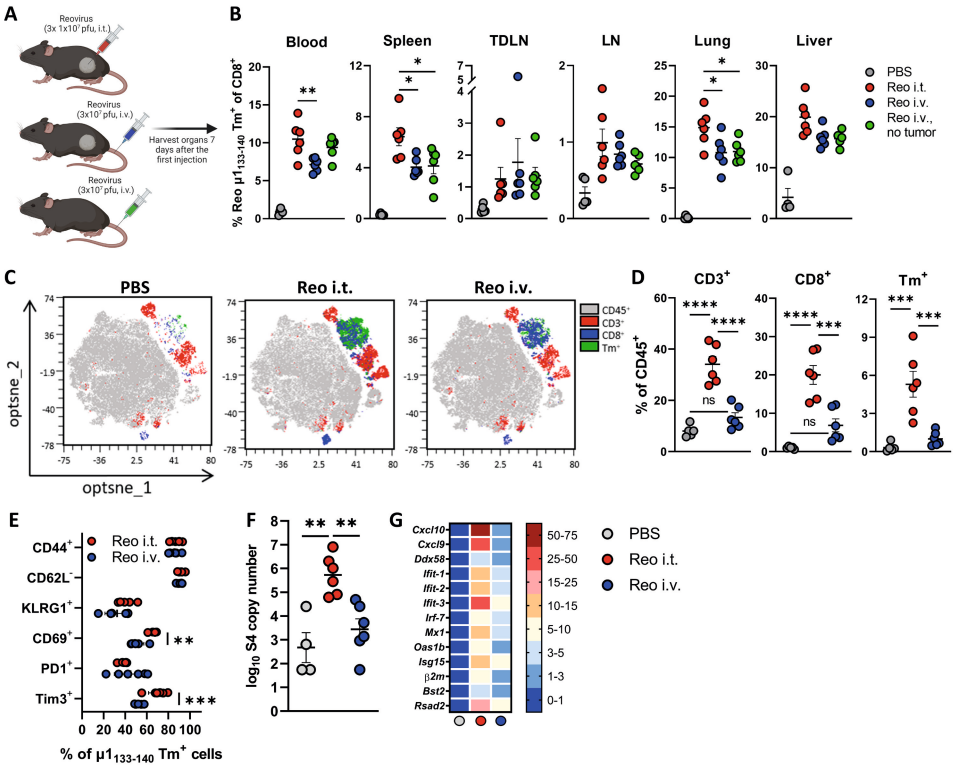


Figure 5. Route of reovirus administration impacts intratumoral influx, but not priming of reovirus-specific T cells. (**A**) Schematic overview of reovirus administration routes, in mice with or without a tumor. (**B**) Frequency of Reo $\mu1_{133\text{-}140}$ Tm^+ $CD8^+$ T cells in indicated organs 7 days after reovirus administration. (**C**) Opt-SNE plots highlighting the intratumoral presence of $CD3^+$, $CD8^+$, and Tm^+ T cells after indicated treatments. 10.000 $CD45^+$ cells were subsampled from each sample or the maximum possible number of cells if $CD45^+$ cells <10000. (**D**) Intratumoral frequency of $CD3^+$, $CD8^+$, and Tm^+ T cells within $CD45^+$ immune cells after indicated treatments. (**E**) Expression of activation markers on Tm^+ $CD8^+$ T cells in the tumor after intratumoral or intravenous reovirus administration. (**F**) Intratumoral presence of reovirus genomic segment 4 (S4) copy numbers as measured by quantitative reverse transcription PCR (RT-qPCR). (**G**) Heatmap depicting relative expression of various interferon response genes as determined by RT-qPCR. Data are presented as mean±SEM. Statistical tests used: (B, D, F): ordinary one-way analysis of variance (ANOVA) with Tukey's post hoc test. (E): ordinary two-way ANOVA with Sidak's post hoc test. Significance levels: *p<0.05, **p<0.01, ***p<0.001, and ****p<0.0001.

Although systemic priming of reovirus-specific CD8$^+$ T cells was equally effective, we observed that the reovirus-induced influx of (reovirus-specific) CD8$^+$ T cells was severely impaired in tumors of mice that received reovirus intravenously, although a small population of T cells could still be observed (**Figure 5C, D**). Additionally, while the expression levels of CD44, CD62L, KLRG1, and PD1 on the few intratumoral Tm$^+$ CD8$^+$ T cells after intravenous reovirus administration were relatively similar to the Tm$^+$ CD8$^+$ T cells that were present after intratumoral reovirus administration, their expression of CD69 and Tim3 was significantly lower (**Figure 5E**). The number of reovirus genomic copies (**Figure 5F**) and the reovirus-induced expression of ISGs (**Figure 5G**) in the tumor was also significantly lower in mice that received intravenous administration of reovirus, suggesting that T-cell influx is connected with either reovirus replication or reovirus-induced expression of ISGs or a combination of both. In conclusion, these data indicate that systemic frequency and location of reovirus-specific CD8$^+$ T cells are not influenced by the route of reovirus administration, but that intratumoral reovirus administration is preferred to induce higher densities of these reovirus-specific CD8$^+$ T cells in the tumor.

Reovirus-specific T cells are amenable to peptide-mediated reactivation

We next asked if the limited influx of reovirus-specific T cells in the tumor upon intravenous reovirus administration could be enhanced by local repeated T-cell receptor (TCR)-triggering. To uncouple reactivation and expansion of reovirus-specific T cells from other reovirus-mediated effects, we intratumorally injected the reovirus-derived Reo $\mu1_{133\text{-}140}$ peptide (*VSPKYSDL*) instead of replicating reovirus (**Figure 6A**). Injection of Reo $\mu1_{133\text{-}140}$ peptide in the tumor after intravenous reovirus administration significantly enhanced the percentage of intratumoral (reovirus-specific) T cells similar to that observed when reovirus was intratumorally administered (**Figure 6B**). Within the intratumoral and splenic CD8$^+$ T-cell populations, the frequency of reovirus-specific T cells was significantly increased when Reo $\mu1_{133\text{-}140}$ peptide was injected, suggesting that reactivation of reovirus-specific T cells led to specific expansion of this population (**Figure 6C**). The additional administration of peptide Reo $\mu1_{133\text{-}140}$ also specifically enhanced the effector phenotype of reovirus-specific T cells, as demonstrated by high CD44, PD1, and Tim3 expression in the tumor and the spleen (**Figure 6D**), implying that T cells induced by intravenously applied reovirus can be turned into fully activated effector cells with a phenotype comparable to those generated via intratumoral application.

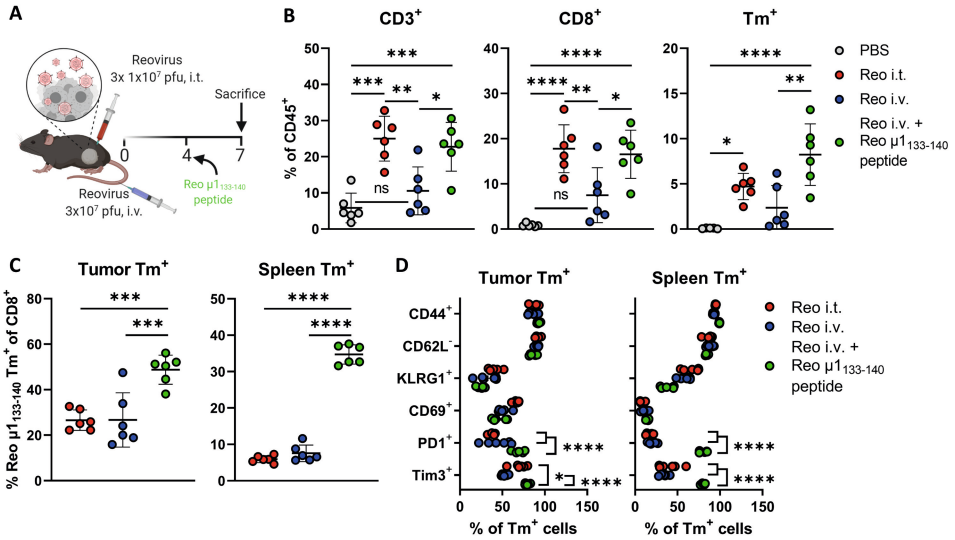


Figure 6. Reovirus-specific T cells are amenable to peptide-mediated reactivation. (**A**) Design of the experiment described in (B-E). Mice (n=6/group) with established KPC3 tumors were intratumorally (i.t.) injected with reovirus (10^7 plaque-forming units (pfu)) on days 0, 1, and 2, or intravenously (i.t.) injected on day 0 with $3x10^7$ pfu of reovirus. One group of mice that received reovirus i.v. additionally received an i.t. injection with the Reo $\mu1_{133-140}$ peptide (50 μg) on day 4, after which mice were sacrificed on day 7 for ex vivo analysis. (**B**) Intratumoral frequency of $CD3^+$, $CD8^+$ and Tm^+ T cells within the $CD45^+$ population. (**C**) Frequency of Reo $\mu1_{133-140}$ Tm^+ $CD8^+$ T cells out of $CD8^+$ T cell population in tumor and spleen. (**D**) Expression of activation markers on Tm^+ $CD8^+$ T cells in the tumor and spleen after indicated treatments. All data are presented as mean±SEM. Statistical tests used: (B-C): ordinary one-way analysis of variance (ANOVA) with Tukey's post hoc test. (D) ordinary two-way ANOVA with Tukey's post hoc test. Significance levels: *p<0.05, **p<0.01, ***p<0.001, and ****p<0.0001.

Induction of vaccine-induced reovirus-specific T-cell immunity enhances the anticancer efficacy of reovirus therapy

We showed that reovirus-specific T cells are potent effector cells that are present in the tumor, which makes them very attractive to use as anticancer effector cells, especially when tumor-specific T cells are unavailable. We hypothesized that these reovirus-specific T cells, when available in sufficiently high numbers, would be able to kill virus-infected cells in the tumor microenvironment that display viral epitopes on their cell surface. To optimally stimulate the frequency of this reovirus-specific T-cell population, we developed a vaccination strategy to install a preexisting pool of circulating reovirus-specific T cells before tumor inoculation. We designed a synthetic long peptide (SLP) that was derived from the natural sequence of the reovirus μ1 protein and contains the immunodominant Reo $\mu1_{133-140}$ epitope of reovirus. *In vitro*, the SLP was processed and presented efficiently by murine dendritic D1 cells and was able to induce activation of T cells from the reovirus-specific T-cell bulk (**Figure S8**). Next, we vaccinated naive mice with the SLP, using a prime-boost schedule (**Figure 7A**) that induced high frequencies of Tm^+ $CD8^+$ T cells in the circulation (**Figure 7B**). These circulating Tm^+ $CD8^+$ T cells displayed a potent effector phenotype as evidenced by their expression of activation markers CD44, KLRG1, PD1, and Tim3 (**Figure 7C**).

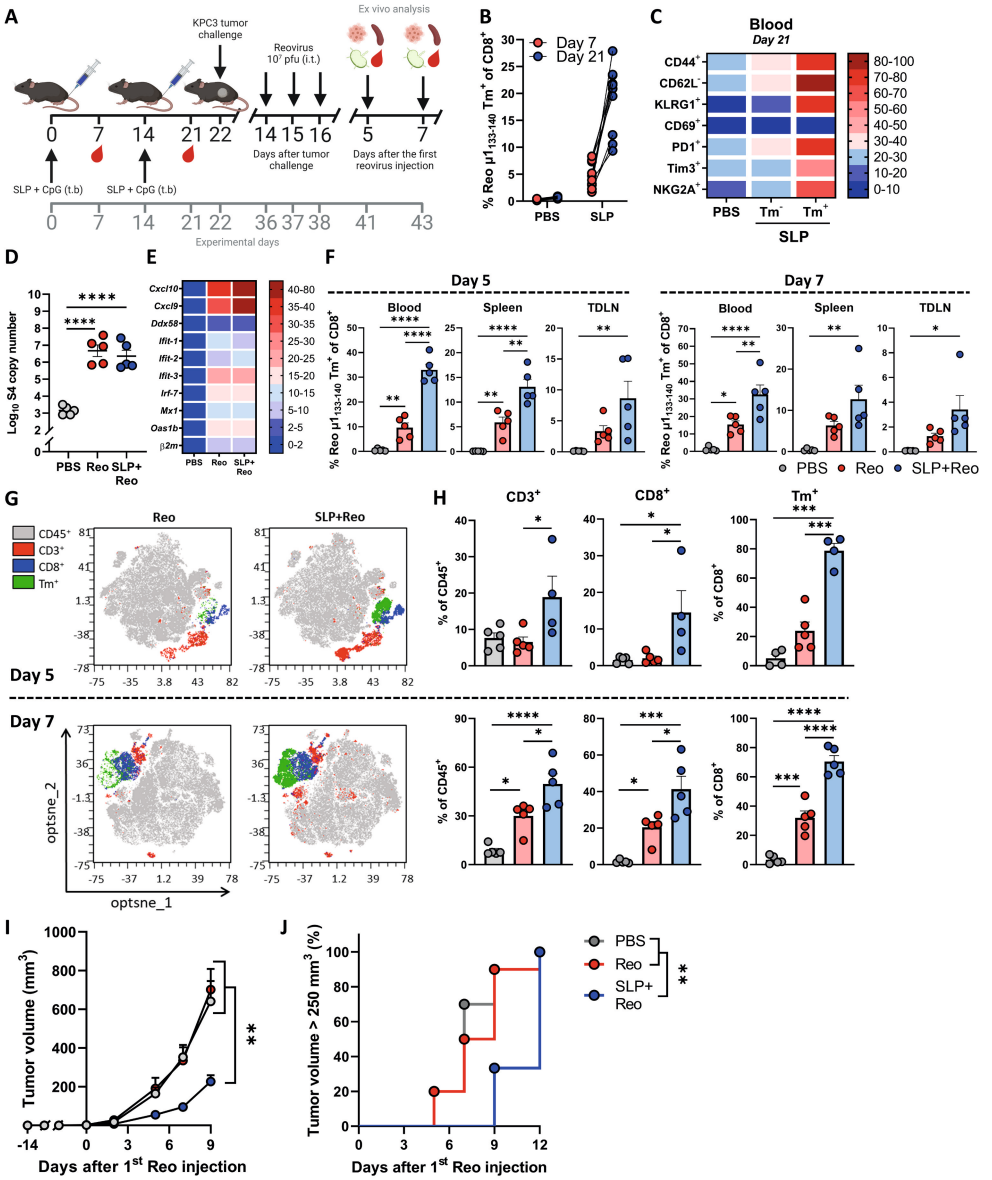


Figure 7. Induction of vaccine-induced reovirus-specific T-cell immunity enhances the anticancer efficacy of reovirus therapy. (**A**) Design of the experiment described in (B-H). Naive mice (n=10/group) were vaccinated on days 0 and 14 by injecting 100 µg SLP together with 20 µg CpG in the tail-base region. On day 22, KPC3 tumor challenge was performed. Mice with established KPC3 tumors were intratumorally (i.t.) injected with reovirus (10^7 plaque-forming units (pfu)) on days 14, 15, and 16 after the tumor challenge. Mice were sacrificed on day 5 (n=5/group) and 7 (n=5/group) after the first i.t. reovirus injection for ex vivo analysis. (**B**) Frequency of Reo $\mu1_{133\text{-}140}$ Tm^+ cells within $CD8^+$ T cells 7 days after priming vaccination and 7 days after boosting vaccination. (**C**) Heatmap showing activation profile of Tm^+ $CD8^+$ T cells in blood on day 21. (**D**) Intratumoral presence of reovirus genomic segment 4 (S4) copy numbers on day 5 after the first reovirus injection, as measured by quantitative reverse transcription PCR (RT-qPCR). (**E**) Heatmap depicting relative expression of various interferon response genes on day 5, as determined by RT-qPCR. >>

>> (**F**) Frequency of Tm^+ cells within $CD8^+$ T cells in blood, spleen, and tumor-draining lymph node (TDLN), 5 and 7 days after reovirus treatment. (**G**) Opt-SNE plots highlighting the intratumoral presence of $CD3^+$, $CD8^+$, and Tm^+ T cells after indicated treatments, on days 5 and 7. 10000 $CD45^+$ cells were subsampled from each sample or the maximum possible number of cells if $CD45^+$ cells <10000. (**H**) Intratumoral frequency of $CD3^+$, $CD8^+$, and Tm^+ T cells within $CD45^+$ immune cells on days 5 and 7. (**I**) Average growth curves of mice (n=9-10/group) receiving indicated treatments. (**J**) Kaplan-Meier graph showing accumulation of animals reaching tumor size > 250 mm^3. All data are presented as mean±SEM. One tumor of SLP+Reo Day 5 group in figure H was excluded due to lymph node contamination. One mouse of SLP+Reo group in figures I and J was excluded due to unsuccessful tumor engraftment. Statistical tests used: (D, F, H): ordinary one-way analysis of variance (ANOVA) with Tukey's post hoc test. (I): ordinary two-way ANOVA with Tukey's post hoc test. (J): Mantel-Cox Log-rank test. Significance levels: *p<0.05, **p<0.01, ***p<0.001, and ****p<0.0001.

Vaccinated mice were subsequently implanted with a KPC3 tumor and palpable tumors were injected intratumorally on 3 consecutive days with reovirus. Notably, the preexisting presence of reovirus-specific T cells did not affect reovirus replication (**Figure 7D**) or reovirus-induced expression of ISGs in the tumor (**Figure 7E**). We next assessed frequencies of reovirus-specific $CD8^+$ T cells on days 5 and 7 after the first intratumoral reovirus injection. The presence of a vaccine-induced, reovirus-specific T-cell response significantly increased the frequency of reovirus-specific T cells in the blood, spleen, and TDLN upon intratumoral reovirus administration (**Figure 7F**). As expected, boosting of the preexisting reovirus-specific T-cell response by intratumoral reovirus administration mediated an earlier and higher intratumoral influx of $CD8^+$ T cells (SLP+Reo) than when this response had to be kick-started by intratumoral reovirus (Reo) administration (**Figure 7G, H**). In particular, the specificity of the intratumoral $CD8^+$ T-cell population was highly enriched for reovirus when mice were first primed by SLP vaccination. Around 75% of intratumoral $CD8^+$ T cells were reovirus-specific in the SLP+Reo group compared to an average of 25% in the Reo only group (**Figure 7G, H**).

This also resulted in a stronger antitumor effect. While intratumoral reovirus administration monotherapy does not affect tumor growth at the used dosage, a significant delay in tumor growth was observed when mice were vaccinated before intratumoral reovirus treatment, resulting in smaller tumors at later time points (**Figure 7I, J**). The enhanced antitumor effect was mediated by $CD8^+$ T cells since the SLP+Reo-induced antitumor effect was significantly decreased when CD8 T cells were depleted after vaccination (**Figure S9A-D**). Within the CD8 T-cell population, the reovirus-specific T cells were specifically responsible since vaccination with an irrelevant SLP vaccine targeting the HPV16 $E7_{49-57}$ epitope did not enhance the antitumor effect of Reo monotherapy (**Figure S10A-C**).

Although SLP+Reo delayed tumor outgrowth, tumors eventually reached the experimental endpoint. When we assessed these end-stage tumors for the presence of T cells, we observed that there was still a large population of reovirus-specific T cells present (**Figure S11A, B**). We investigated whether these T cells could be reinvigorated by combining SLP+Reo therapy with checkpoint blockade (αPD-L1), to possibly prolong

the delay in tumor growth. However, the addition of αPD-L1 did not enhance the efficacy of SLP+Reo therapy (**Figure S12A-C**). We next investigated whether we could enhance the antitumor effect of SLP+Reo therapy by additional reovirus administrations. Surprisingly, the continued intratumoral administration of reovirus also did not improve the antitumor effect of SLP+Reo therapy (**Figure S13A-C**). These observations suggest that there is a maximum level of control that reovirus-specific T cells can exert on the growth of the tumor.

Therapeutic boosting of a reovirus-induced, preexisting T-cell pool delays tumor growth

Lastly, we investigated whether SLP+Reo therapy can also be applied in a more therapeutically relevant setting. Since a large majority of the human population has encountered reovirus before, most cancer patients will have circulating reovirus-specific T cells. We investigated whether this preexisting reovirus-induced T-cell pool might also be exploited to improve the efficacy of reovirus therapy. Additionally, we investigated whether the SLP vaccine is still effective when applied in mice that already have a tumor. We immunized mice with live reovirus to induce preexisting immunity, and subsequently boosted the immunization-induced reovirus-specific T-cell response with the SLP, either before (BT – before tumor) or after (AT – after tumor) tumor inoculation (**Figure 8A**). In both immunized groups, reovirus-specific T-cell responses in the blood could be boosted to similar levels compared to naive mice that were vaccinated according to the prime-boost schedule, even when mice received the SLP after tumor inoculation, thus in a therapeutic setting (**Figure 8B**). No toxicity through changes in body weight could be observed (**Figure S14**), but tumor growth was significantly delayed in both immunized groups. This suggests that boosting the reovirus-specific T-cell response with an SLP in humans with preexisting immunity might also be safe and effective to enhance the efficacy of reovirus monotherapy (**Figure 8C, D**).

Taken together, we showed proof-of-concept data that high intratumoral frequencies of preinduced reovirus-specific T cells can be exploited to effectively impact tumor growth upon reovirus treatment, thereby circumventing the need for tumor-specific T cells. These data advocate for the use of vaccines aimed at inducing strong OV-specific T-cell responses to enhance the efficacy of OV monotherapy in tumors with low immunogenicity.

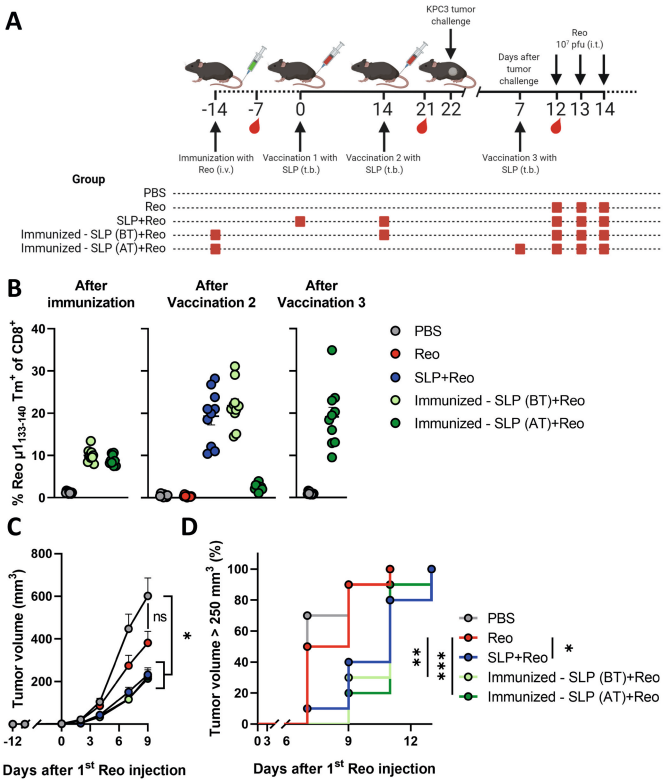


Figure 8. Therapeutic boosting of a reovirus-induced, preexisting T-cell pool delays tumor growth. (**A**) Design of the experiment described in (B-D). Naive mice (n=10/group) were immunized on day -14 by injecting reovirus (10^7 plaque-forming units (pfu)). Vaccination occurred on days 0 and/or 14 by injecting 100 µg SLP together with 20 µg CpG in the tail-base region. On day 22, KPC3 tumor challenge was performed. One group was vaccinated with the SLP on day 7 after tumor challenge. Intratumoral administration with reovirus (10^7 pfu) occurred on days 12, 13, and 14 after the tumor challenge. (**B**) Frequency of Reo $\mu1_{133-140}$ Tm^+ cells within $CD8^+$ T cells after immunization or vaccination. (**C**) Average growth curves of mice (n=10/group) receiving indicated treatments. (**D**) Kaplan-Meier graph showing accumulation of animals reaching tumor size > 250 mm^3. All data are presented as mean±SEM. Statistical tests used: (C): ordinary two-way ANOVA with Tukey's post hoc test. (D): Mantel-Cox Log-rank test. Significance levels: *p<0.05, **p<0.01, and ***p<0.001.

DISCUSSION

The mammalian reovirus type 3 Dearing strain (T3D), clinically known as Pelareorep, is one of the leading oncolytic viruses (OVs) under clinical evaluation (34). As monotherapy, reovirus has undergone clinical evaluation in trials across a range of indications, most of which have employed intravenous administration of reovirus. As recently reviewed by Müller et al, the clinical efficacy of reovirus as monotherapy has been modest (34). Current clinical attempts are therefore focussed on combinational approaches, involving for example chemotherapeutic or immunotherapeutic strategies (2,35). Indeed, we and others recently demonstrated that reovirus has high potential as

a strategy to enhance the efficacy of immunotherapy by recruiting $CD8^+$ T cells to the tumor (11,36,37). Whereas stimulation of intratumoral T-cell influx represents an important pillar in the immunotherapeutic efficacy of reovirus, the dynamics of T-cell responses during reovirus therapy are not completely understood. The identification of the immunodominant $CD8^+$ T-cell epitope of reovirus enabled us to track reovirus-specific T cells and study the dynamics of this response during oncolytic virus therapy. Induction of preexisting T-cell immunity by means of vaccination did, surprisingly, not hamper viral replication, but on the contrary, empowered reovirus therapy against immunologically cold tumors.

One important consideration in the clinical use of OVs is the choice of the administration route, which is mostly focused on the efficient delivery of the OV itself to the tumor site and less on the OV-induced immune response (38,39). Interestingly, we observed that priming of reovirus-specific T cells does not depend on a specific route of administration. In fact, replication at a tumor site is not even required to mount an efficient systemic reovirus-specific T-cell response. However, intratumoral administration is required to induce an efficient influx of (reovirus-specific) $CD8^+$ T cells into the tumor. Interestingly, we found that injection of cognate peptide in the tumor was able to reactivate reovirus-specific T cells, as was previously shown for intratumoral OT-I cells recognizing the SIINFEKL peptide (40), thereby increasing the density and activation of virus-specific T-cell density in the TME.

Reovirus-specific T cells can be found throughout the body after both systemic and local reovirus administration, but only express high levels of CD69, PD1, and Tim3 after intratumorally applied reovirus or peptide. Increased cell-surface CD69 can be driven by either TCR stimulation or cytokines such as IFNα and IFNβ (41), which are both provided by the presence of replicating reovirus in the tumor. PD1 is rapidly induced on T cells following TCR-mediated activation and this expression decreases with antigen clearance (42), Tim3 is identified as being selectively expressed on IFNγ–secreting $CD4^+$ and $CD8^+$ T cells, and expression is induced after repeated TCR-stimulation (43,44). Given that all three surface markers are associated with previous antigen exposure, co-expression of these markers suggests tumor-residing reovirus-specific T cells have encountered their cognate antigen in the TME during active reovirus infection and thus recognize reovirus-infected tumor cells.

Although reovirus-specific T cells were enriched in the tumor, they did not make up the total TIL population. Since other TILs displayed similar phenotypic characteristics as reovirus-specific T cells, we hypothesize that those TILs might also be reovirus-specific but simply recognize other, yet unidentified epitopes. Identifying these epitopes and their inclusion in the vaccination strategy might further enhance SLP+Reo therapy efficacy. Tetramer-negative TILs with a much less pronounced effector phenotype might be 'bystander' T cells that are attracted to the tumor by the reovirus-induced release of chemokines and cytokines. It is not likely that tetramer-negative TILs are tumor-specific

since the administration of reovirus in both KPC3 and TC1 tumors did not induce any reactivity towards autologous tumor cells *ex vivo*. Whereas a body of literature has shown that several OVs, including reovirus, can induce tumor-specific T-cell responses (45-49), this seems to be restricted to immunogenic models with high mutational load or expression of tumor-associated or artificial antigens. Therefore, the exploitation of virus-specific T cells may represent a solution for targeting low-immunogenic tumors to which tumor-specific responses are out of the question.

Recent evidence from murine and human studies has shown that previously established antiviral T cells can also be found in tumors (40,50-53). Taking advantage of this preexisting, pathogen-specific immune cell population is an exciting new approach in the cancer immunotherapy field. This is particularly attractive in the setting of an oncolytic virus that selectively replicates in tumor cells, thereby specifically directing the virus-specific T cells to the infected tumor cells.

An important consideration when employing virus-specific T cells as anticancer effectors is that tumor cell-killing relies on the expression of the virus-derived epitopes on tumor cells. The continuous expression of viral epitopes is likely restricted by antiviral immunity (possibly by the emergence of neutralizing antibodies or innate immune responses), thereby installing a maximum level of tumor cell-killing that can be achieved by the virus-specific T cells before the virus is cleared. The emergence of antiviral immunity might also explain why continued intratumoral reovirus administration or the addition of checkpoint blockade does not improve the antitumor effect of SLP+Reo therapy. More insight into the various layers of antiviral immunity that might limit viral replication and epitope presentation in the tumor is necessary to enhance the therapeutic window of this strategy. Furthermore, it would also be interesting to study whether an initial wave of tumor cell-killing by virus-specific T cells can induce a second wave of tumor-specific T cells, so-called epitope spreading.

However, exploiting antiviral $CD8^+$ T cells also has multiple advantages over utilizing tumor-specific T cells. Antiviral T cells often display strong effector and memory responses and lack exhaustion markers including expression of CD39, which is associated with chronic antigen exposure in the tumor (51). Since antiviral T cells are generated against 'non-self' epitopes, there is no central tolerance and minimal auto-reactivity is expected. Various approaches have already demonstrated that pathogen-specific T cells can be repurposed to attack tumors (40). For instance, antibody-peptide epitope conjugates were used to redirect cytomegalovirus (CMV)-specific $CD8^+$ T cells to kill tumor cells *in vitro* and in NOD/SCID mice that were injected with expanded CMV-specific $CD8^+$ T cells and were engrafted with orthotopic human breast cancer tumors or hepatocellular carcinomas (54). Also, repurposing of severe acute respiratory syndrome-coronavirus-2 (SARS-CoV-2)-specific $CD8^+$ T-cell responses, present in a large population of coronavirus disease 2019 (COVID-19) resolvers, has been suggested as an anticancer immunotherapy approach (55).

Our approach uniquely involves the use of a non-pathogenic virus that has previously been tested in patients as an oncolytic agent with excellent safety records (34). Moreover, using an OV adds tumor-specificity to the system due to specific replication in malignant cells, thereby converting the tumor cells into target cells for the previously established virus-specific T cells. Therefore, inducing and subsequently exploiting an oncolytic virus-specific $CD8^+$ T-cell response might be considered a more generalized immunotherapy approach to combat cancer that does not require the presence of tumor-specific $CD8^+$ T cells.

DECLARATIONS

Acknowledgments. The authors thank Kees Franken en Robert Cordfunke from the protein-facility of LUMC for the generation of the Reo $\mu1_{133\text{-}140}$ tetramer to detect reovirus-specific T cells. The authors thank Vera Kemp (Department of Cell and Chemical Biology) for providing reovirus variant Jin-3 and Marit van Elsas for providing the HPV E7-derived SLP and HPV $E7_{49\text{-}57}$ tetramer. The authors gratefully acknowledge the operators of the Flow cytometry Core Facility (FCF) of the LUMC and the Animal Facility of the LUMC for their excellent support and care of the animals, respectively. The hybridoma 10F6 (reovirus μ1), developed by T. S. Dermody from the University of Pittsburgh School of Medicine, was obtained from the Developmental Studies Hybridoma Bank, created by the NICHD of the NIH and maintained at The University of Iowa, Department of Biology, Iowa City, IA 52242. Figures depicting experimental designs were created with BioRender.com.

Author contributions. Conceptualization, CG and NvM; Methodology, CG, PK, JJCvST, DvdW, RH, TvH, NvM; Formal analysis, CG; Investigation, CG, PK, JJCvST, CL, LG, MS; Resources, DvdW, RH, JMMdH; Writing – Original Draft, CG, NvM; Writing - Review & Editing, All authors; Visualization, CG; Supervision, SHvdB, TvH, NvM; Funding acquisition, SHvdB, TvH, NvM. All authors approved the final version of the manuscript.

Funding. This work was financially supported by the Dutch Cancer Society Bas Mulder Award 11056 (to NvM), a PhD fellowship from Leiden University Medical Center (to CG), and the Support Casper campaign by the Dutch foundation 'Stichting Overleven met Alvleesklierkanker' (supportcasper.nl) project number SOAK 17.04 (to SHvdB, TvH, and NvM).

Competing interests. CG, NvM, and TvH filed a patent (P335646NL) regarding the research described in this manuscript. All other authors declare no competing interests.

Ethics approval. All mouse studies were individually prepared, reviewed, approved, and registered by the institutional Animal Welfare Body of Leiden University Medical Center and carried out under project license AVD1160020187004, issued by the competent authority on animal experiments in the Netherlands (named CCD). Experiments were performed following the Dutch Act on Animal Experimentation and EU Directive 2010/63/EU ("On the protection of animals used for scientific purposes") at the animal facility of the Leiden University Medical Center (LUMC), The Netherlands.

Data availability statement. All data relevant to this study are included in the main text or the supplementary materials and are available on reasonable request.

REFERENCES

1. Groeneveldt C, van Hall T, van der Burg SH, Ten Dijke P, van Montfoort N. Immunotherapeutic Potential of TGF-β Inhibition and Oncolytic Viruses. Trends Immunol **2020**;41:406-20
2. Mahalingam D, Goel S, Aparo S, Patel Arora S, Noronha N, Tran H*, et al.* A Phase II Study of Pelareorep (REOLYSIN(®)) in Combination with Gemcitabine for Patients with Advanced Pancreatic Adenocarcinoma. Cancers (Basel) **2018**;10:160
3. Sborov DW, Nuovo GJ, Stiff A, Mace T, Lesinski GB, Benson DM*, et al.* A Phase I Trial of Single-Agent Reolysin in Patients with Relapsed Multiple Myeloma. Clinical Cancer Research **2014**;20:5946-55
4. Duncan MR, Stanish SM, Cox DC. Differential sensitivity of normal and transformed human cells to reovirus infection. J Virol **1978**;28:444-9
5. Shmulevitz M, Marcato P, Lee PWK. Unshackling the links between reovirus oncolysis, Ras signaling, translational control and cancer. Oncogene **2005**;24:7720-8
6. Smakman N, van den Wollenberg DJ, Borel Rinkes IH, Hoeben RC, Kranenburg O. Sensitization to apoptosis underlies KrasD12-dependent oncolysis of murine C26 colorectal carcinoma cells by reovirus T3D. J Virol **2005**;79:14981-5
7. Thirukkumaran CM, Nodwell MJ, Hirasawa K, Shi Z-Q, Diaz R, Luider J*, et al.* Oncolytic Viral Therapy for Prostate Cancer: Efficacy of Reovirus as a Biological Therapeutic. Cancer research **2010**;70:2435-44
8. Zhao X, Chester C, Rajasekaran N, He Z, Kohrt HE. Strategic Combinations: The Future of Oncolytic Virotherapy with Reovirus. Molecular cancer therapeutics **2016**;15:767-73
9. Samson A, Scott KJ, Taggart D, West EJ, Wilson E, Nuovo GJ*, et al.* Intravenous delivery of oncolytic reovirus to brain tumor patients immunologically primes for subsequent checkpoint blockade. Science translational medicine **2018**;10
10. Bourgeois-Daigneault MC, Roy DG, Aitken AS, El Sayes N, Martin NT, Varette O*, et al.* Neoadjuvant oncolytic virotherapy before surgery sensitizes triple-negative breast cancer to immune checkpoint therapy. Science translational medicine **2018**;10
11. Groeneveldt C, Kinderman P, van den Wollenberg DJM, van den Oever RL, Middelburg J, Mustafa DAM*, et al.* Preconditioning of the tumor microenvironment with oncolytic reovirus converts CD3-bispecific antibody treatment into effective immunotherapy. J Immunother Cancer **2020**;8:e001191
12. van den Wollenberg DJM, Dautzenberg IJC, van den Hengel SK, Cramer SJ, de Groot RJ, Hoeben RC. Isolation of reovirus T3D mutants capable of infecting human tumor cells independent of junction adhesion molecule-A. PloS One **2012**;7:e48064-e
13. Smith RE, Zweerink HJ, Joklik WK. Polypeptide components of virions, top component and cores of reovirus type 3. Virology **1969**;39:791-810
14. Fallaux FJ, Kranenburg O, Cramer SJ, Houweling A, Van Ormondt H, Hoeben RC*, et al.* Characterization of 911: a new helper cell line for the titration and propagation of early region 1-deleted adenoviral vectors. Human gene therapy **1996**;7:215-22
15. Hingorani SR, Wang L, Multani AS, Combs C, Deramaudt TB, Hruban RH*, et al.* Trp53R172H and KrasG12D cooperate to promote chromosomal instability and widely metastatic pancreatic ductal adenocarcinoma in mice. Cancer cell **2005**;7:469-83
16. Lin K-Y, Guarnieri FG, Staveley-O'Carroll KF, Levitsky HI, August JT, Pardoll DM*, et al.* Treatment of Established Tumors with a Novel Vaccine That Enhances Major Histocompatibility Class II Presentation of Tumor Antigen. Cancer Res **1996**;56:21-6
17. Winzler C, Rovere P, Rescigno M, Granucci F, Penna G, Adorini L*, et al.* Maturation Stages of Mouse Dendritic Cells in Growth Factor–dependent Long-Term Cultures. Journal of Experimental Medicine **1997**;185:317-28
18. van Hall T, van Bergen J, van Veelen PA, Kraakman M, Heukamp LC, Koning F*, et al.* Identification of a Novel Tumor-Specific CTL Epitope Presented by RMA, EL-4, and MBL-2 Lymphomas Reveals Their Common Origin. J Immunol **2000**;165:869-77

19. Belkina AC, Ciccolella CO, Anno R, Halpert R, Spidlen J, Snyder-Cappione JE. Automated optimized parameters for T-distributed stochastic neighbor embedding improve visualization and analysis of large datasets. Nature Communications **2019**;10:5415
20. van den Wollenberg DJ, Dautzenberg IJ, van den Hengel SK, Cramer SJ, de Groot RJ, Hoeben RC. Isolation of reovirus T3D mutants capable of infecting human tumor cells independent of junction adhesion molecule-A. PLoS One **2012**;7:e48064
21. Mijatovic-Rustempasic S, Tam KI, Kerin TK, Lewis JM, Gautam R, Quaye O*, et al.* Sensitive and specific quantitative detection of rotavirus A by one-step real-time reverse transcription-PCR assay without antecedent double-stranded-RNA denaturation. Journal of clinical microbiology **2013**;51:3047-54
22. Dupont WD, Plummer WD, Jr. Power and sample size calculations. A review and computer program. Controlled clinical trials **1990**;11:116-28
23. Murphy JP, Kim Y, Clements DR, Konda P, Schuster H, Kowalewski DJ*, et al.* Therapy-Induced MHC I Ligands Shape Neo-Antitumor CD8 T Cell Responses during Oncolytic Virus-Based Cancer Immunotherapy. J Proteome Res **2019**;18:2666-75
24. van de Merbel AF, van der Horst G, van der Mark MH, Bots STF, van den Wollenberg DJM, de Ridder CMA*, et al.* Reovirus mutant jin-3 exhibits lytic and immune-stimulatory effects in preclinical human prostate cancer models. Cancer Gene Ther **2021**
25. Woopen C, Straub T, Schweier O, Aichele U, Düker K, Boehm T*, et al.* Immunological tolerance to LCMV antigens differently affects control of acute and chronic virus infection in mice. European Journal of Immunology **2018**;48:120-7
26. Belz GT, Xie W, Altman JD, Doherty PC. A Previously Unrecognized H-2Db-Restricted Peptide Prominent in the Primary Influenza A Virus-Specific $CD8^+$ T-Cell Response Is Much Less Apparent following Secondary Challenge. J Virol **2000**;74:3486-93
27. Schreiber L-M, Urbiola C, Das K, Spiesschaert B, Kimpel J, Heinemann F*, et al.* The lytic activity of VSV-GP treatment dominates the therapeutic effects in a syngeneic model of lung cancer. British Journal of Cancer **2019**;121:647-58
28. Noubade R, Majri-Morrison S, Tarbell KV. Beyond cDC1: Emerging Roles of DC Crosstalk in Cancer Immunity. Front Immunol **2019**;10
29. Desai P, Tahiliani V, Abboud G, Stanfield J, Salek-Ardakani S. Batf3-Dependent Dendritic Cells Promote Optimal CD8 T Cell Responses against Respiratory Poxvirus Infection. J Virol **2018**;92
30. Davenport BJ, Bullock C, McCarthy MK, Hawman DW, Murphy KM, Kedl RM*, et al.* Chikungunya Virus Evades Antiviral $CD8^+$ T Cell Responses To Establish Persistent Infection in Joint-Associated Tissues. J Virol **2020**;94
31. Dai P, Wang W, Yang N, Serna-Tamayo C, Ricca JM, Zamarin D*, et al.* Intratumoral delivery of inactivated modified vaccinia virus Ankara (iMVA) induces systemic antitumor immunity via STING and Batf3-dependent dendritic cells. Sci Immunol **2017**;2:eaal1713
32. Hildner K, Edelson BT, Purtha WE, Diamond M, Matsushita H, Kohyama M*, et al.* Batf3 Deficiency Reveals a Critical Role for $CD8\alpha^+$ Dendritic Cells in Cytotoxic T Cell Immunity. Science **2008**;322:1097-100
33. van Dinther D, Veninga H, Iborra S, Borg EGF, Hoogterp L, Olesek K*, et al.* Functional CD169 on Macrophages Mediates Interaction with Dendritic Cells for $CD8^+$ T Cell Cross-Priming. Cell Rep **2018**;22:1484-95
34. Müller L, Berkeley R, Barr T, Ilett E, Errington-Mais F. Past, Present and Future of Oncolytic Reovirus. Cancers **2020**;12:3219
35. Mahalingam D, Wilkinson GA, Eng KH, Fields P, Raber P, Moseley JL*, et al.* Pembrolizumab in Combination with the Oncolytic Virus Pelareorep and Chemotherapy in Patients with Advanced Pancreatic Adenocarcinoma: A Phase Ib Study. Clin Cancer Res **2020**;26:71-81
36. Samson A, Scott KJ, Taggart D, West EJ, Wilson E, Nuovo GJ*, et al.* Intravenous delivery of oncolytic reovirus to brain tumor patients immunologically primes for subsequent checkpoint blockade. Sci Transl Med **2018**;10:eaam7577

37. Mostafa AA, Meyers DE, Thirukkumaran CM, Liu PJ, Gratton K, Spurrell J*, et al.* Oncolytic Reovirus and Immune Checkpoint Inhibition as a Novel Immunotherapeutic Strategy for Breast Cancer. Cancers (Basel) **2018**;10
38. Macedo N, Miller DM, Haq R, Kaufman HL. Clinical landscape of oncolytic virus research in 2020. Journal for ImmunoTherapy of Cancer **2020**;8:e001486
39. Kaufman HL, Bommareddy PK. Two roads for oncolytic immunotherapy development. Journal for ImmunoTherapy of Cancer **2019**;7:26
40. Rosato PC, Wijeyesinghe S, Stolley JM, Nelson CE, Davis RL, Manlove LS*, et al.* Virus-specific memory T cells populate tumors and can be repurposed for tumor immunotherapy. Nature Communications **2019**;10:567
41. Shiow LR, Rosen DB, Brdičková N, Xu Y, An J, Lanier LL*, et al.* CD69 acts downstream of interferon-α/β to inhibit S1P1 and lymphocyte egress from lymphoid organs. Nature **2006**;440:540-4
42. Chikuma S, Terawaki S, Hayashi T, Nabeshima R, Yoshida T, Shibayama S*, et al.* PD-1-Mediated Suppression of IL-2 Production Induces CD8$^+$ T Cell Anergy In Vivo. J Immunol **2009**;182:6682-9
43. Monney L, Sabatos CA, Gaglia JL, Ryu A, Waldner H, Chernova T*, et al.* Th1-specific cell surface protein Tim-3 regulates macrophage activation and severity of an autoimmune disease. Nature **2002**;415:536-41
44. Borst L, Sluijter M, Sturm G, Charoentong P, Santegoets SJ, van Gulijk M*, et al.* NKG2A is a late immune checkpoint on CD8 T cells and marks repeated stimulation and cell division. Int J Cancer **2021**:1-17
45. Diaz RM, Galivo F, Kottke T, Wongthida P, Qiao J, Thompson J*, et al.* Oncolytic Immunovirotherapy for Melanoma Using Vesicular Stomatitis Virus. Cancer Res **2007**;67:2840-8
46. Wang G, Kang X, Chen KS, Jehng T, Jones L, Chen J*, et al.* An engineered oncolytic virus expressing PD-L1 inhibitors activates tumor neoantigen-specific T cell responses. Nature Communications **2020**;11:1395
47. Woller N, Gürlevik E, Fleischmann-Mundt B, Schumacher A, Knocke S, Kloos AM*, et al.* Viral Infection of Tumors Overcomes Resistance to PD-1-immunotherapy by Broadening Neoantigenome-directed T-cell Responses. Molecular therapy : the journal of the American Society of Gene Therapy **2015**;23:1630-40
48. Prestwich RJ, Ilett EJ, Errington F, Diaz RM, Steele LP, Kottke T*, et al.* Immune-mediated antitumor activity of reovirus is required for therapy and is independent of direct viral oncolysis and replication. Clin Cancer Res **2009**;15:4374-81
49. Brown MC, Holl EK, Boczkowski D, Dobrikova E, Mosaheb M, Chandramohan V*, et al.* Cancer immunotherapy with recombinant poliovirus induces IFN-dominant activation of dendritic cells and tumor antigen–specific CTLs. Sci Transl Med **2017**;9:eaan4220
50. Erkes DA, Smith CJ, Wilski NA, Caldeira-Dantas S, Mohgbeli T, Snyder CM. Virus-Specific CD8$^+$ T Cells Infiltrate Melanoma Lesions and Retain Function Independently of PD-1 Expression. J Immunol **2017**;198:2979-88
51. Simoni Y, Becht E, Fehlings M, Loh CY, Koo SL, Teng KWW*, et al.* Bystander CD8$^+$ T cells are abundant and phenotypically distinct in human tumour infiltrates. Nature **2018**;557:575-9
52. Saini SK, Ørskov AD, Bjerregaard AM, Unnikrishnan A, Holmberg-Thydén S, Borch A*, et al.* Human endogenous retroviruses form a reservoir of T cell targets in hematological cancers. Nat Commun **2020**;11:5660
53. Bentzen AK, Marquard AM, Lyngaa R, Saini SK, Ramskov S, Donia M*, et al.* Large-scale detection of antigen-specific T cells using peptide-MHC-I multimers labeled with DNA barcodes. Nature Biotechnology **2016**;34:1037-45
54. Millar DG, Ramjiawan RR, Kawaguchi K, Gupta N, Chen J, Zhang S*, et al.* Antibody-mediated delivery of viral epitopes to tumors harnesses CMV-specific T cells for cancer therapy. Nature Biotechnology **2020**;38:420-5
55. Gujar S, Pol JG, Kim Y, Kroemer G. Repurposing CD8$^+$ T cell immunity against SARS-CoV-2 for cancer immunotherapy: a positive aspect of the COVID-19 pandemic? Oncoimmunology **2020**;9:1794424

SUPPLEMENTARY FIGURES

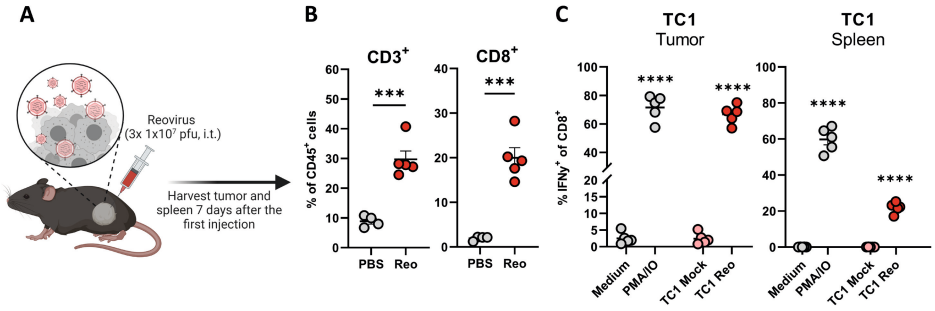


Figure S1. Local and systemic presence of reovirus-specific T cells in the TC1 model. (**A**) Design of the experiment described in B-C. Mice (n=5–8/group) with established TC1 tumors were intratumorally (i.t.) injected with reovirus (10^7 plaque-forming units (pfu)) on 3 consecutive days. Mice were sacrificed 7 days after the first reovirus injection for ex vivo analysis of tumors and spleens. (**B**) Frequency of $CD3^+$ and $CD8^+$ T cells within the total $CD45^+$ immune cell population in TC1 tumors after reovirus administration. (**C**) Frequency of interferon γ $(IFNγ)^+$ cells within the intratumoral and splenic $CD8^+$ T-cell population as measured with intracellular cytokine staining. Single-cell suspensions (n=5/group) were cocultured with indicated targets for 6 hours. Medium was used as negative control and PMA/ionomycin (IO) was used as positive control. Data are presented as mean±SEM. Statistical tests used: (B): unpaired t-test between PBS and Reo groups. (C): ordinary one-way analysis of variance (ANOVA) with Dunnett's post hoc test. Statistical difference was compared to medium control group. Significance levels: ***p<0.001 and ****p<0.0001.

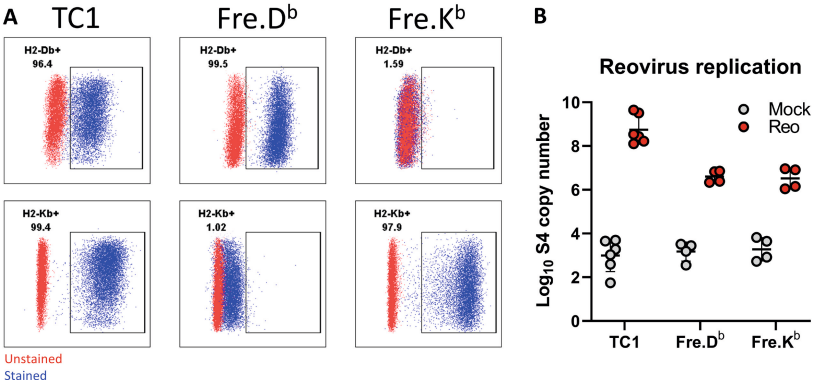


Figure S2. MHC class I expression and reovirus replication in TC1, Fre.K^b and Fre.D^b cells. (**A**) K^b and D^b expression on TC1, Fre.K^b and Fre.D^b cells as measured with flow cytometry. (**B**) Reovirus genomic segment 4 (S4) copy number in TC1, Fre.K^b and Fre.D^b cells after reovirus infection. Cells ($1.5x10^5$/well) were infected with multiplicities of infection (MOI)=10. Samples (n=2-3) were harvested 24 hours after infection and reovirus S4 copy numbers were determined by quantitative reverse transcription PCR (RT-qPCR). Individual data points represent 2-3 biological duplicates with each 2 technical replicates.

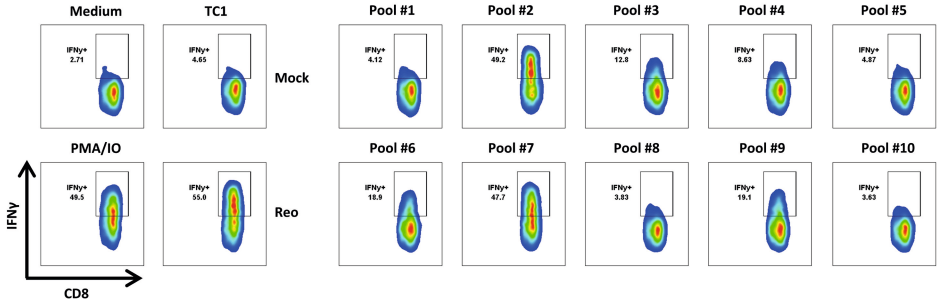


Figure S3. T-cell recognition of positive peptide pools. (**A**) Frequency of interferon γ (IFNγ)$^+$ cells within the reovirus-specific T-cell bulk as measured with intracellular cytokine staining. T cells were cocultured with peptide pools (1 µg/mL for each peptide) for 6 hours. Medium was used as negative control and phorbol 12-myristate 13-acetate (PMA)/ionomycin (IO) was used as positive control.

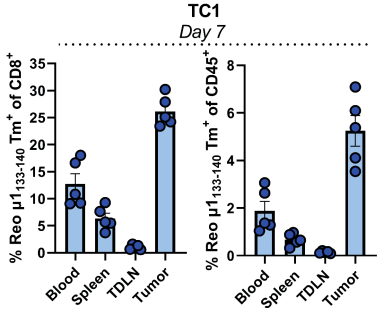


Figure S4. Frequency and distribution of reovirus-specific T cells in TC1-bearing mice. Quantification of Tm$^+$ cells out of CD8$^+$T cells and total CD45$^+$ immune cell population in indicated organs on day 7 after the first intratumoral reovirus injection in mice bearing established TC1 tumors. Data are presented as mean±SEM.

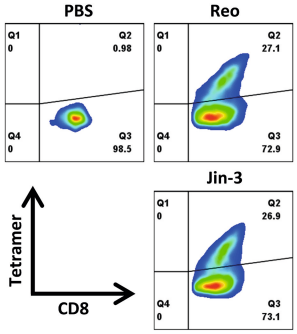


Figure S5. Reovirus-specific T cells in tumors after intratumoral Reo or Jin-3 administration. Representative flow cytometry plots of Tm$^+$ CD8$^+$T cells in tumors injected with Reo or Jin-3 according to the schedule described in Figure 2A. Tumors were harvested on day 7 after the first intratumoral reovirus injection.

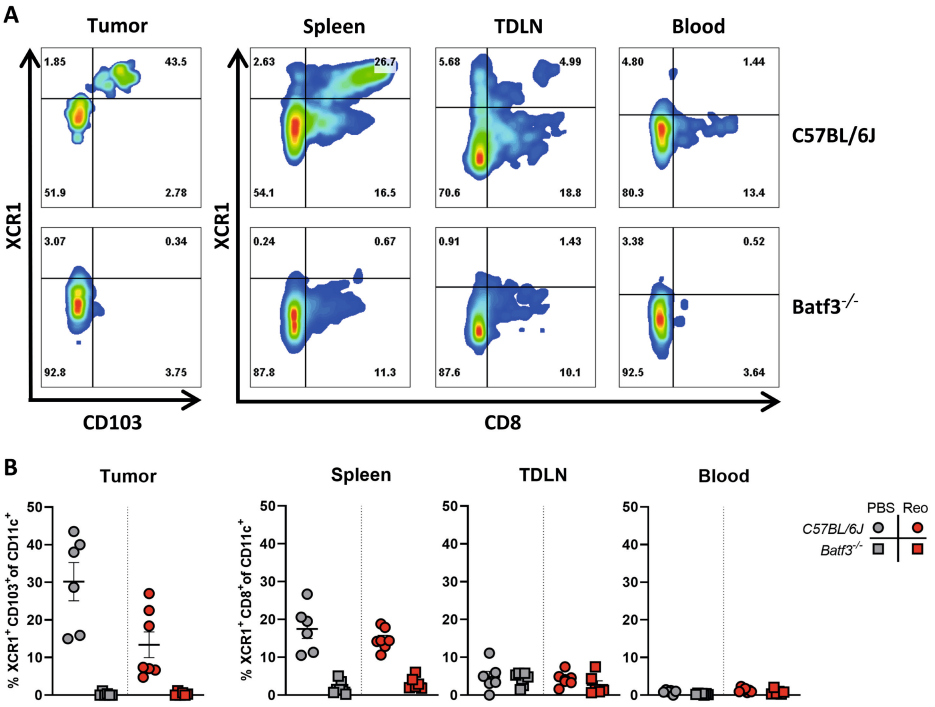


Figure S6. cDC1 absence in *Batf3*$^{-/-}$ mice. (**A**) Flow cytometry plots of cDC1s (characterized by XCR1 and CD103 expression in tumors, and XCR1 and CD8 expression in other organs) in tumors, spleens, tumor-draining lymph nodes (TDLN), and blood of KPC3-bearing, PBS-treated C57BL/6J mice or *Batf3*$^{-/-}$ mice. (**B**) Quantification of cDC1s (n=5-7/group). All data are presented as mean±SEM.

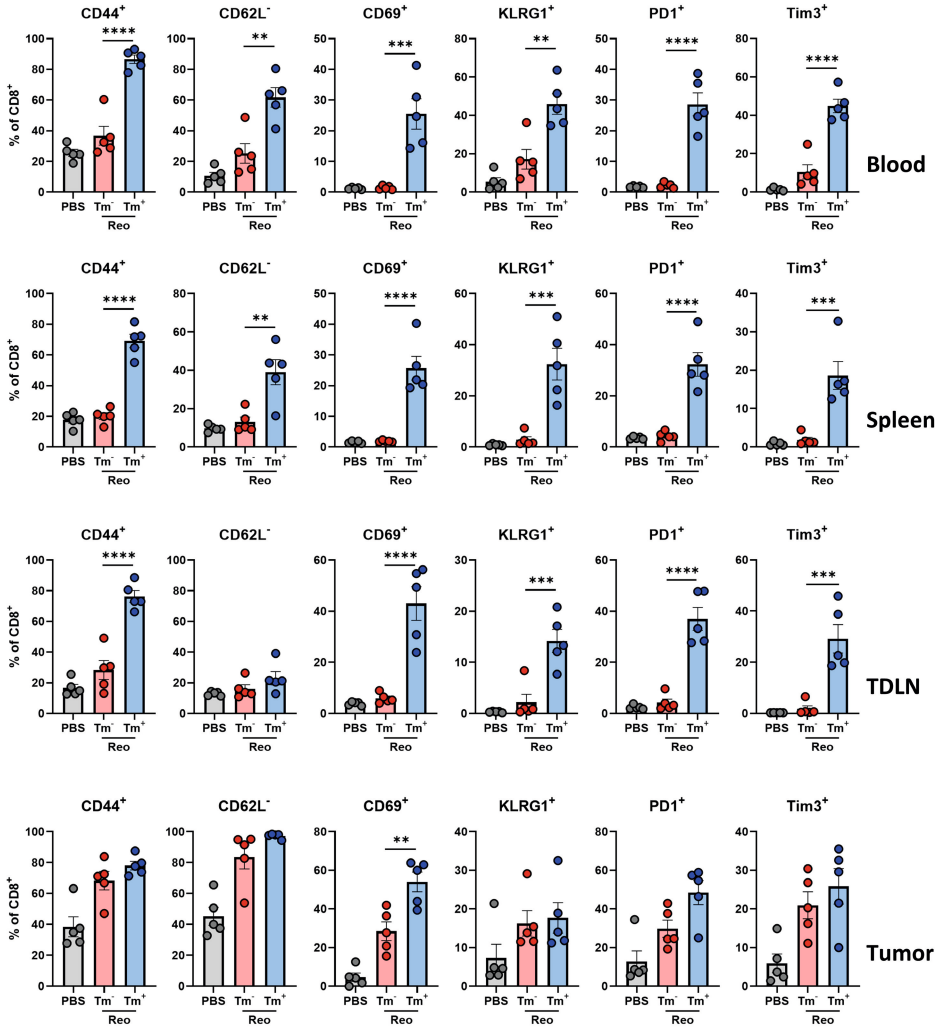


Figure S7. Phenotype of reovirus-specific T cells on day 12. Expression of activation markers on Tm^- or Tm^+ $CD8^+$ T cells in blood, spleen, tumor-draining lymph node (TDLN), and tumor, 12 days after the first intratumoral reovirus injection. All data are presented as mean±SEM. Statistical tests used: (A): ordinary one-way analysis of variance (ANOVA) with Tukey's post hoc test. Significance levels: *p<0.05, **p<0.01, ***p<0.001, and ****p<0.0001.

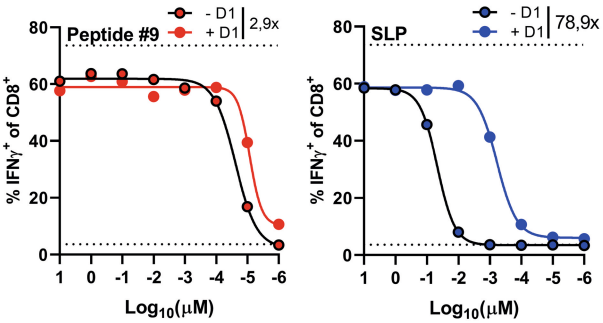


Figure S8. Processing of SLPs by D1 cells and activation of reovirus-specific T cells. Frequency of IFNγ⁺ cells within reovirus-specific T-cell bulk after coculture with peptide #9 or the SLP (10 μM to 10 pM). Peptides were added directly or in the context of D1 cells as antigen-presenting cells and incubated with T cells for 6 hours. Before coculture with T cells, D1 cells were pre-incubated for 1 hour with peptide #9 or SLP after which lipopolysaccharide (LPS; 10 μg/mL) was added to each well for an additional 23 hours.

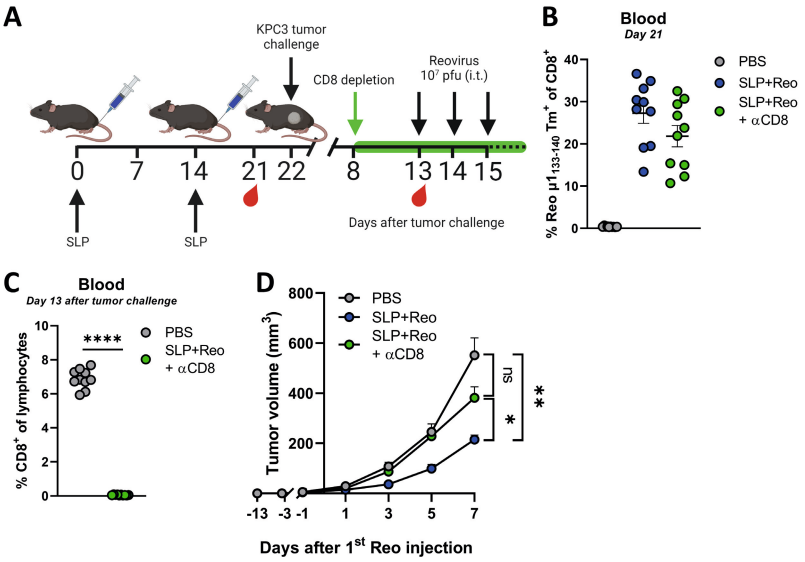


Figure S9. Depletion of CD8 T cells diminishes SLP+Reo effect. (**A**) Design of the experiment described in (B-D). Mice were vaccinated on days 0 and/or 14 by injecting 100 μg SLP together with 20 μg CpG in the tail-base region. On day 22, KPC3 tumor challenge was performed. 8 days after KPC3 tumor inoculation, CD8⁺ T-cell depletion was initiated (Clone 2.42, 50 μg intraperitoneal). Mice with established KPC3 tumors were intratumorally (i.t.) injected with reovirus (10^7 plaque-forming units (pfu)) on days 13, 14, and 15 after the tumor challenge. (**B**) Frequency of Reo $\mu1_{133\text{-}140}$ Tm⁺ cells within CD8⁺ T cells after vaccination. (**C**) Frequency of CD8⁺ T cells in blood after CD8⁺ T-cell depletion. (**D**) Average growth curves of mice (n=10/group) receiving indicated treatments. All data are presented as mean±SEM. Statistical tests used: (C) unpaired t-test. (D): ordinary two-way ANOVA with Tukey's post hoc test. Significance levels: *p<0.05, **p<0.01, ****p<0.0001. The control group is shared with Figure S12.

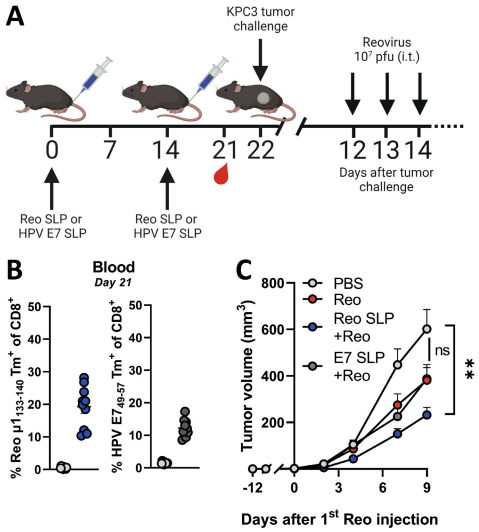


Figure S10. Irrelevant SLP vaccination impairs the antitumor efficacy of SLP+Reo therapy. (**A**) Design of the experiment described in (B-C). Mice were vaccinated with an SLP containing the reovirus epitope (Reo SLP) or an irrelevant SLP containing an HPV E7 epitope (E7 SLP) on days 0 and 14 by injecting 100 μg SLP together with 20 μg CpG in the tail-base region. On day 22, KPC3 tumor challenge was performed. Mice with established KPC3 tumors were intratumorally (i.t.) injected with reovirus (10^7 plaque-forming units (pfu)) on days 12, 13, and 14 after the tumor challenge. (**B**) Frequency of Reo $\mu1_{133-140}$ or HPV16 $E7_{49-57}$ Tm^+ cells within $CD8^+$ T cells after vaccination. (**C**) Average growth curves of mice (n=10/group) receiving indicated treatments. All data are presented as mean±SEM. Statistical tests used: (C): ordinary two-way ANOVA with Tukey's post hoc test. Significance level: **p<0.01. Control groups are shared with Figure S13 and Figure 8.

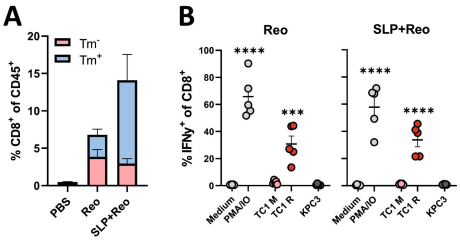


Figure S11. Presence of reovirus-specific but not tumor-specific T cells in end-stage tumors after SLP+Reo therapy. (**A**) Separation of Tm^+ cells from Tm^- cells within the total $CD8^+$ T cell population of end-stage KPC3 tumors after Reo or SLP+Reo therapy. (**B**) Frequency of interferon γ $(IFNγ)^+$ cells within the intratumoral $CD8^+$ T-cell population of end-stage KPC3 tumors that received Reo or SLP+Reo therapy. Single-cell suspensions (n=5/group) were cocultured with indicated targets. PMA/ionomycin (IO) was used as a positive control, and the irrelevant cell line TC1 was used as target cell line for reovirus infection. Data are presented as mean±SEM. Statistical tests used: (B): ordinary one-way analysis of variance (ANOVA) with Dunnett's post hoc test. Statistical difference was compared to medium control group. Significance level: ****p<0.0001.

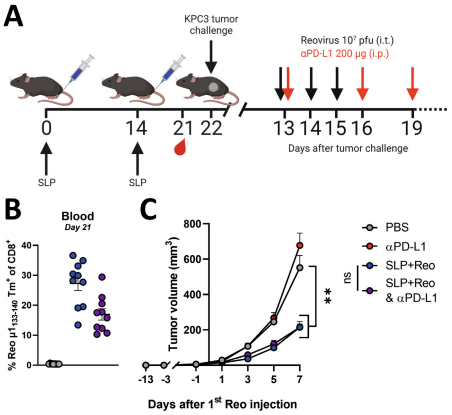


Figure S12. The antitumor effect of SLP+Reo therapy cannot be improved by the addition of αPD-L1 therapy. (**A**) Design of the experiment described in (B-C). Mice were vaccinated with an SLP containing the reovirus epitope on days 0 and 14 by injecting 100 μg SLP together with 20 μg CpG in the tail-base region. On day 22, KPC3 tumor challenge was performed. Mice with established KPC3 tumors were intratumorally (i.t.) injected with reovirus (10^7 plaque-forming units (pfu)) on days 13, 14, and 15 after the tumor challenge. αPD-L1 was administered intraperitoneally (i.p.) on days 14, 16, and 19. (**B**) Frequency of Reo $\mu1_{133\text{-}140}$ Tm^+ cells within $CD8^+$ T cells after vaccination. (**C**) Average growth curves of mice (n=10/group) receiving indicated treatments. All data are presented as mean±SEM. Statistical tests used: (C): ordinary two-way ANOVA with Tukey's post hoc test. Significance level: **p<0.01. The control group is shared with Figure S9.

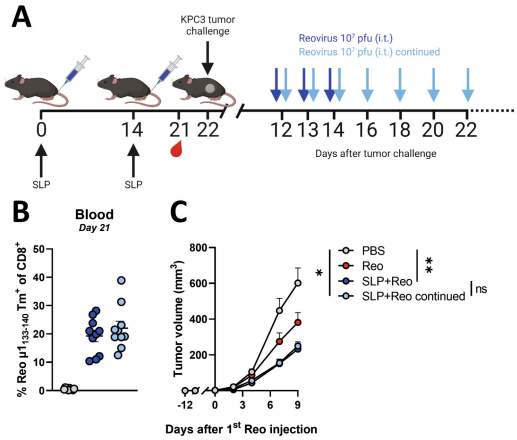


Figure S13. Continuation of intratumoral reovirus administration does not improve the antitumor effect of SLP+Reo therapy. (**A**) Design of the experiment described in (B-C). Mice were vaccinated with an SLP containing the reovirus epitope on days 0 and 14 by injecting 100 μg SLP together with 20 μg CpG in the tail-base region. On day 22, KPC3 tumor challenge was performed. Mice with established KPC3 tumors were intratumorally (i.t.) injected with reovirus (10^7 plaque-forming units (pfu)) on days 12, 13, and 14 after the tumor challenge. One group continued to receive intratumoral reovirus injections every 2 days after day 14. (**B**) Frequency of Reo $\mu1_{133\text{-}140}$ Tm^+ cells within $CD8^+$ T cells after vaccination. (**C**) Average growth curves of mice (n=10/group) receiving indicated treatments. All data are presented as mean±SEM. Statistical tests used: (C): ordinary two-way ANOVA with Tukey's post hoc test. Significance levels: *p<0.05 and **p<0.01. Control groups are shared with Figure S10 and Figure 8.

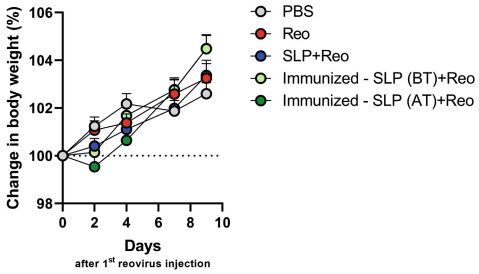


Figure S14. Boosting the reovirus-specific T-cell response does not affect body weight.
Increase in body weight (%) starting from the moment of the first intratumoral reovirus injection.

SUPPLEMENTARY TABLES

Table S1. List of antibodies used for flow cytometric analysis.

	Marker	*Clone*	*Fluorochrome*	*Supplier*
Lymphoid panel	CD45.2	104	FITC	eBioscience
	CD3	145-2C11	PE-CF594	BD Biosciences
	CD8α	53-6.7	Alexa Fluor 700	eBioscience
	Reo $\mu1_{133-140}$ tetramer		APC	In house
	HPV $E7_{49-57}$ tetramer		PE	In house
	CD44	IM-7	BV785	BioLegend
	CD62L	MEL-14	BV421	BioLegend
	NK1.1	Pk136	BV650	BD Biosciences
	PD-1	29F.1A12	APC-Cy7	BioLegend
	Tim3	RMT3-23	PE	BioLegend
	NKG2A	16A11	PE	eBioscience
	KLRG-1	2F1	PE-Cy7	eBioscience
	CD103	2E7	BV711	BioLegend
	CD69	H1.2F3	BV605	BioLegend
Myeloid panel	CD45.2	104	FITC	BioLegend
	CD11b	M1/70	PE-Cy7	BioLegend
	CD11c	N418	APC-Cy7	BioLegend
	CD8α	53-6.7	Alexa Fluor 700	eBioscience
	CD103	2E7	BV711	BioLegend
	XCR1	ZET	PE	BioLegend
	CD4	RM4-5	APC	BioLegend
Intracellular T-cell activation panel	CD45.2	104	FITC	eBioscience
	CD3	145-2C11	PE-CF594	BD Biosciences
	CD8α	53-6.7	Alexa Fluor 700	eBioscience
	IFNγ	XMG1.2	APC	BioLegend

Table S2. GenBank accession numbers of Reovirus Type 3 Dearing isolate R124 segments.

Segment	*GenBank accession number*	*Link*
Segment S1	GU991665	https://www.ncbi.nlm.nih.gov/nuccore/325112732
Segment S2	GU991666	https://www.ncbi.nlm.nih.gov/nuccore/325112734
Segment S3	GU991667	https://www.ncbi.nlm.nih.gov/nuccore/325112736
Segment S4	GU991668	https://www.ncbi.nlm.nih.gov/nuccore/325112738
Segment M1	GU991662	https://www.ncbi.nlm.nih.gov/nuccore/325112726
Segment M2	GU991663	https://www.ncbi.nlm.nih.gov/nuccore/406601112
Segment M3	GU991664	https://www.ncbi.nlm.nih.gov/nuccore/325112730
Segment L1	GU991659	https://www.ncbi.nlm.nih.gov/nuccore/325112720
Segment L2	GU991660	https://www.ncbi.nlm.nih.gov/nuccore/325112722
Segment L3	GU991661	https://www.ncbi.nlm.nih.gov/nuccore/325112724

Table S3. Predicted H2-K^b reovirus epitopes tested in intracellular cytokine staining.

N	*Peptide*	*Allele*	*nM*	*Rank*	*Segment*	
1	ISDVYAPL	H-2-K^b	4.2	0.010	M1	Pool #1
2	SAVLFSPL	H-2-K^b	3.9	0.010	L3	
3	MVYDYSEL	H-2-K^b	5.9	0.015	S4	
4	SSYAWFIL	H-2-K^b	6.0	0.015	L1	
5	ISPAHAYL	H-2-K^b	7.4	0.020	M3	
6	LMYKYMPI	H-2-K^b	6.6	0.020	L2	Pool #2
7	INFVSAML	H-2-K^b	8.3	0.025	M3	
8	LSLNFVTGL	H-2-K^b	10.5	0.030	S1	
9	VSPKYSDL	H-2-K^b	10.9	0.030	M2	
10	VSYSGSGL	H-2-K^b	13.3	0.040	S1	
11	ISITSAAL	H-2-K^b	14.0	0.040	M3	Pool #3
12	AVQLFRPL	H-2-K^b	14.3	0.040	L2	
13	VAVQLFRPL	H-2-K^b	14.2	0.040	L2	
14	QGYYMAQL	H-2-K^b	14.1	0.040	L1	
15	VNPYYRLM	H-2-K^b	17.4	0.050	L2	
16	SNQAFYDLL	H-2-K^b	15.9	0.050	L2	Pool #4
17	VGYLQYPM	H-2-K^b	17.2	0.050	L1	
18	LNANYFGHL	H-2-K^b	18.6	0.060	M1	
19	KSRLRYLPL	H-2-K^b	20.8	0.060	L2	
20	MSIPYQHV	H-2-K^b	23.9	0.070	M3	
21	VSIRAPRL	H-2-K^b	21.5	0.070	M1	Pool #5
22	AAFLFKTV	H-2-K^b	25.8	0.080	S2	
23	WSFVYWGL	H-2-K^b	25.6	0.080	L1	
24	HSYSSFSKL	H-2-K^b	25.4	0.080	L1	
25	SMFKHHVKL	H-2-K^b	25.2	0.080	L1	
26	STHLWSPL	H-2-K^b	29.1	0.090	L3	Pool #6
27	MTPMYLQQL	H-2-K^b	30.5	0.090	L3	
28	IMGVFFNGV	H-2-K^b	30.1	0.090	L1	
29	ITVNPYYRL	H-2-K^b	32.3	0.100	L2	
30	KIFQAAQL	H-2-K^b	33.0	0.100	L1	
31	ITWDFFLSV	H-2-K^b	33.9	0.100	L1	Pool #7
32	SPNYRFRQSM	H-2-K^b	39.7	0.125	S1	
33	TVVNYVQL	H-2-K^b	39.6	0.125	M2	
34	VSPKYSDLL	H-2-K^b	42.7	0.125	M2	
35	KAFMTLANM	H-2-K^b	41.6	0.125	L3	
36	STRKYFAQTL	H-2-K^b	36.2	0.125	L1	Pool #8
37	CSAVLFSPL	H-2-K^b	43.6	0.150	L3	
38	VSIRGRWMARL	H-2-K^b	49.7	0.150	L3	
39	LSYDLRWTRL	H-2-K^b	49.4	0.150	L2	
40	SDYKFMYM	H-2-K^b	51.5	0.150	L1	

Table S3. Continued.

N	*Peptide*	*Allele*	*nM*	*Rank*	*Segment*	
41	IAPMRFVL	H-2-K^b	53.2	0.175	M2	Pool #9
42	SNQAFYDL	H-2-K^b	61.7	0.175	L2	
43	HFYRYETL	H-2-K^b	52.8	0.175	L2	
44	SRLRYLPL	H-2-K^b	62.1	0.175	L2	
45	LMYKYMPIM	H-2-K^b	57.3	0.175	L2	
46	MNYYLLATF	H-2-K^b	66.9	0.200	M2	Pool #10
47	AGWLYNGV	H-2-K^b	70.5	0.200	L3	
48	TWYLAAARM	H-2-K^b	68.4	0.200	L1	

Table S4. List of primers used for RT-qPCR analysis.

Gene	*Forward*	*Reverse*
S4Q	5′-CGCTTTTGAAGGTCGTGTATCA-3′	5′-CTGGCTGTGCTGAGATTGTTTT-3′
Ifit-1	5′-CTGGACAAGGTGGAGAAGGT-3′	5′-AGGGTTTTCTGGCTCCACTT-3′
Ifit-2	5′-TGCTCTTGACTGTGAGGAGG-3′	5′-ATCCAGACGGTAGTTCGCAA-3′
Ifit-3	5′-GTGCAACCAGGTCGAACATT-3′	5′- AGGTGACCAGTCGACGAATT-3′
Irf7	5′-GACCGTGTTTACGAGGAACC-3′	5′-GCTGTACAGGAACACGCATC-3′
Isg15	5′-GGAACGAAAGGGGCCACAGCA-3′	5′-CCTCCATGGGCCTTCCCTCGA-3′
Oas1b	5′-AGCATGAGAGACGTTGTGGA-3′	5′-GCGTAGAATTGTTGGTTAGGCT-3′
Ddx58	5′-AAGGCCACAGTTGATCCAAA-3′	5′-TTGGCCAGTTTTCCTTGTCG-3′
Cxcl9	5′-TGGAGTTCGAGGAACCCTAGT-3′	5′-AGGCAGGTTTGATCTCCGTT-3′
Cxcl10	5′-ACGAACTTAACCACCATCT-3′	5′-TAAACTTTAACTACCCATTGATACATA-3′
Mx1	5′-GATGGTCCAAACTGCCTTCG-3′	5′-TTGTAAACCTGGTCCTGGCA-3′
β2M	5′-CTCGGTGACCCTGGTCTTT-3′	5′-CCGTTCTTCAGCATTTGGAT-3′
Mzt2	5′-TCGGTGCCCATATCTCTGTC-3′	5′-CTGCTTCGGGAGTTGCTTTT-3′
Ptp4a2	5′-AGCCCCTGTGGAGATCTCTT-3′	5′-AGCATCACAAACTCGAACCA-3′



PART B

The effect of preexisting immunity on reovirus therapy



CHAPTER 4

Preexisting Immunity: Barrier or Bridge to Effective Oncolytic Virus Therapy?

Christianne Groeneveldt[1*#], Jasper van den Ende[2*], Nadine van Montfoort[3]

[1] Department of Medical Oncology, Oncode Institute, Leiden University Medical Center, 2333 ZA Leiden, The Netherlands
[2] Master Infection & Immunity, Utrecht University, 3584 CS Utrecht, The Netherlands
[3] Department of Gastroenterology and Hepatology, Leiden University Medical Center, 2333 ZA, Leiden, The Netherlands
[*] These authors contributed equally
[#] Corresponding author

Cytokine & Growth Factor Reviews 2023;doi.org/10.1016/j.cytogfr.2023.01.002

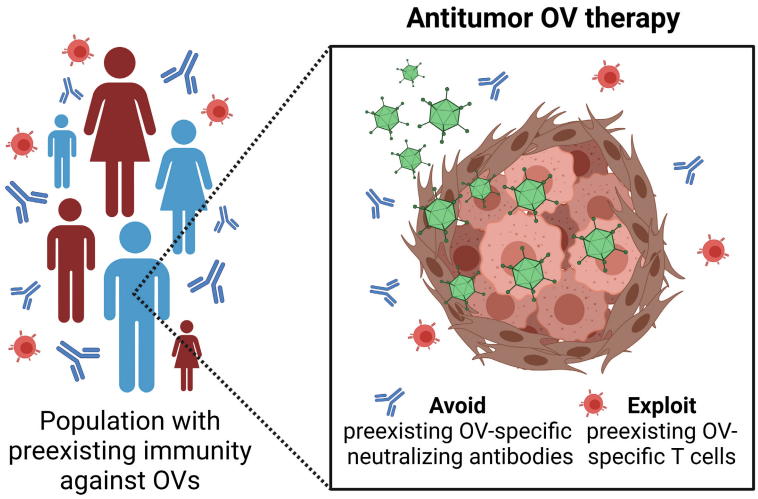
ABSTRACT

Oncolytic viruses (OVs) represent a highly promising treatment strategy for a wide range of cancers, by mediating both the direct killing of tumor cells as well as mobilization of antitumor immune responses. As many OVs circulate in the human population, preexisting OV-specific immune responses are prevalent. Indeed, neutralizing antibodies (NAbs) are abundantly present in the human population for commonly used OVs, such as Adenovirus type 5 (Ad5), Herpes Simplex Virus-1 (HSV-1), Vaccinia virus, Measles virus, and Reovirus. This review discusses (pre)clinical evidence regarding the effect of preexisting immunity against OVs on two distinct aspects of OV therapy; OV infection and spread, as well as the immune response induced upon OV therapy. Combined, this review provides evidence that consideration of preexisting immunity is crucial in realizing the full potential of the highly promising therapeutic implementation of OVs. Future investigation of current gaps in knowledge highlighted in this review should yield a more complete understanding of this topic, ultimately allowing for better and more personalized OV therapies.

List of Abbreviations

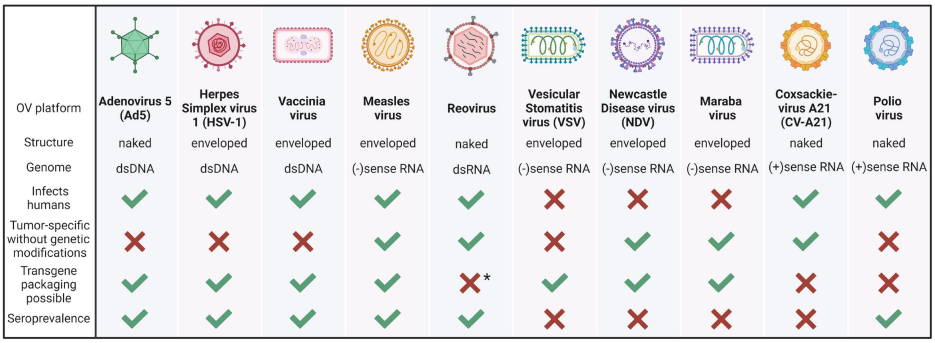
Ad5; Adenovirus serotype 5
ADE; antibody-dependent enhancement
ATPP; Antibody-Targeted Pathogen-derived Peptides
BiTE; bispecific T-cell engager
CMV; Cytomegalovirus
CV-A21; Coxsackievirus A21
DAMP; damage-associated molecular pattern
DC; dendritic cells
EBV; Eppstein-Barr virus
EEVs; extracellular enveloped viruses
FcγRs; Fc-gamma receptors
FDA; Food and Drug Administration
HBsAg; Hepatitis B surface antigen
HSV-1; Herpes simplex virus type 1
ISG; interferon-stimulated gene
MHC; major histocompatibility complex
NAbs; neutralizing antibodies
NDV; Newcastle disease virus
NOD; non-obese diabetic
NOG; NOD.Cg-Prkdc^{scid}Il2rg^{tm1Sug}/ShiJic
NSG; NOD.Cg-Prkdc^{scid} Il2rg^{tm1Wjl}/SzJ
OV; oncolytic virus
OVA; ovalbumin
PAMP; pathogen-associated molecular pattern
TME; tumor microenvironment
T-VEC; talimogene laherparepvec
VSV; Vesicular Stomatitis Virus

GRAPHICAL ABSTRACT



INTRODUCTION

Oncolytic viruses (OVs) are increasingly being recognized as a promising therapeutic modality for the treatment of a variety of cancers (1,2). Selective replication of OVs in cancerous cells, which can either be a result of natural viral tropism or artificially achieved by genetic modification, makes them highly specific antitumor agents with minimal off-target effects. An overview of the most prominently investigated OVs is provided in **Figure 1**. Increasing interest in the clinical potential of OVs has been driven by the Food and Drug Administration (FDA) approval of the modified Herpes Simplex Virus type 1 (HSV-1) talimogene laherparepvec (T-VEC), which was shown to significantly improve survival in patients with late-stage melanoma (3-5). Currently, there is an immense pipeline of over 200 registered clinical trials investigating the therapeutic application of various OVs as single agents or as part of combination therapies (6).



OV platform	Adenovirus 5 (Ad5)	Herpes Simplex virus 1 (HSV-1)	Vaccinia virus	Measles virus	Reovirus	Vesicular Stomatitis virus (VSV)	Newcastle Disease virus (NDV)	Maraba virus	Coxsackie-virus A21 (CV-A21)	Polio virus
Structure	naked	enveloped	enveloped	enveloped	naked	enveloped	enveloped	enveloped	naked	naked
Genome	dsDNA	dsDNA	dsDNA	(-)sense RNA	dsRNA	(-)sense RNA	(-)sense RNA	(-)sense RNA	(+)sense RNA	(+)sense RNA
Infects humans	✓	✓	✓	✓	✓	✗	✗	✗	✓	✓
Tumor-specific without genetic modifications	✗	✗	✗	✓	✓	✗	✓	✓	✓	✗
Transgene packaging possible	✓	✓	✓	✓	✗*	✓	✓	✓	✗	✗
Seroprevalence	✓	✓	✓	✓	✓	✗	✗	✗	✗	✓

Figure 1. Properties of commonly investigated oncolytic virus (OV) platforms. dsDNA indicates double-stranded DNA. Green checkmarks indicate that a characteristic does apply to the specific OV platform, red crosses indicate that it does not. The presence of seropositivity is derived from clinical trial data (serum samples measured before treatment), or population studies. References for general information about each OV and seropositivity data: Ad5 (7-10), HSV-1 (3,11-13), Vaccinia virus (14-17), Measles virus (18-22), Reovirus (23-29), VSV (30-32), NDV (33), Maraba virus (34), CV-A21 (35-37), Polio virus (38-40). *For Reovirus, only packaging of very small transgenes is possible, such as granulocyte-macrophage colony-stimulating factor (GM-CSF) (41).

Multiple mechanisms of action are known to contribute to the therapeutic efficacy of OVs, as was previously reviewed by us and others (42,43). Direct oncolysis is the result of viral repurposing of the infected cell for the production of viral genomic material and proteins, which eventually results in the release of progeny viral particles through cell lysis (44). Besides direct killing, there is accumulating evidence that shows that OVs can also stimulate strong immune-mediated antitumor effects (45). Local inflammation recruits immune cells to the tumor microenvironment (TME), where viral infection and killing of tumor cells result in the release of both pathogen- and damage-associated molecular patterns (PAMPs and DAMPs) and type I interferons (46). These PAMPs and DAMPs mediate the potent activation of dendritic cells (DCs) for antigen presentation. In combination with high tumor antigen availability due to oncolysis, this constitutes

an OV-induced 'perfect storm' which establishes conditions uniquely favorable for efficient priming and subsequent influx of both virus- and tumor-specific $CD4^+$ and $CD8^+$ T cells (**Figure 2**). Recent investigations into the OV-mediated delivery of immune-stimulating transgenes into the TME, such as cytokines, costimulatory T-cell ligands, checkpoint inhibitors, or even tumor antigens, further illustrate the crucial importance of immunity in the context of OV therapy (47,48). Furthermore, OV therapy can promote the availability of tumor antigens. Most notably, OV-induced oncolysis of infected cells can result in the release of otherwise inaccessible tumor antigens, improving the immune response against cancer cells expressing these epitopes (49). Furthermore, OVs can be employed as so-called oncolytic vaccines, which encode or are coated with tumor antigens to steer the immune response toward antitumor specificity (50,51).

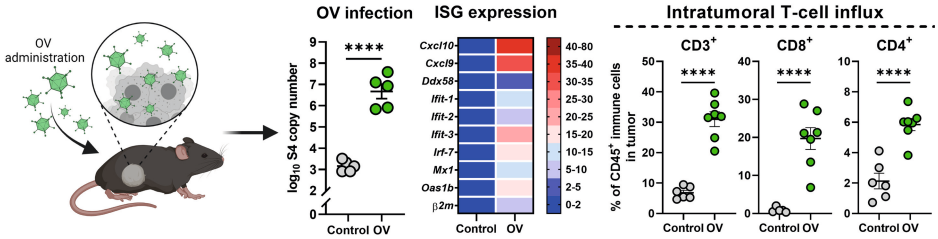


Figure 2. Mechanism of action of immune-stimulatory effects of OVs in the tumor microenvironment. OV administration leads to infection of tumor cells, which induces the upregulation of interferon-stimulated genes (ISGs) including T-cell attracting chemokines. The OV-induced expression of ISGs is followed by an increased influx of T cells into the tumor. Data is derived from studies where oncolytic reovirus is injected intratumorally in immunocompetent C57BL/6J mice bearing murine pancreatic KPC3 tumors (52,53). OV infection and ISG expression was determined by reverse transcription quantitative polymerase chain reaction (RT-qPCR) and intratumoral T-cell influx was measured by flow cytometry.

Despite the immense therapeutic potential of OVs, some patients do not respond to OV therapy. One of the proposed limiting factors for effective OV therapy is the presence of preexisting immunity in patients (54). Therapeutic application necessitates the use of non-pathogenic OVs, but the fact that they are benign is often a result of the efficient immune response that is induced upon infection. Thus, previous exposure is likely to result in the presence of a potent preexisting immune response. In antiviral immune responses, circulating viral particles are recognized and subsequently neutralized by antibodies, whereas virus-infected cells are targeted by virus-specific cytotoxic $CD8^+$ T cells. Therefore, possible effects of preexisting immunity on OV infection and spread predominantly involve a preexisting humoral response. Indeed, assessment of OV-specific neutralizing antibodies (NAbs) in serum in both the general population and OV clinical trial cohorts, also termed seroprevalence, shows that preexisting immune responses are abundantly present. This is primarily the case for viruses that, besides their application as OVs, also circulate in the human population or are used as vectors for vaccination, such as Adenovirus serotype 5 (Ad5), HSV-1, or Vaccinia virus (**Figure 1**). Seroprevalence is much less common for OVs that mainly infect non-human hosts, such

as Vesicular Stomatitis Virus (VSV) or Newcastle Disease virus (NDV). So far, the general consensus has been that the presence of preexisting immunity decreases OV efficacy by enhancing viral clearance, thus limiting the window of therapeutic action. This has resulted in patient exclusion criteria based on the presence of neutralizing antibodies in some clinical trials, for example (NCT01227551) (55). However, emerging evidence suggests that OV-specific preexisting immunity might actually potentiate antitumor effects in some cases. Thus, a nuanced assessment of the effects of preexisting immunity in the context of OV therapy is warranted.

Here, we provide an overview of the currently available mechanistic insights regarding the effect of preexisting immunity in two distinct phases of OV therapy: 1) OV infection and spread upon administration, and 2) development of the OV therapy-induced immune response, while discussing the many variables that contribute to the effect of preexisting immunity in these phases. Furthermore, we discuss how preexisting immunity can be evaded or even utilized to enhance the therapeutic efficacy of OVs. By shining a light on the complex nature of preexisting immunity in the context of OV therapies, the collection of (pre)clinical data discussed here should prove instructive for future decisions regarding both fundamental investigation as well as the therapeutic application of OVs.

THE EFFECT OF PREEXISTING IMMUNITY ON OV INFECTION AND SPREAD

Until recently, interest regarding the effects of preexisting immunity has been largely focused on the early phases of OV therapy, which comprise the initial infection of tumor cells by the OV, its subsequent spread throughout the circulation, and the dissemination to distant tumors and tissues. Although neutralizing antibodies for commonly used OVs are present in the human population as well as cancer patients (**Figure 1**), their effect on the therapeutic efficacy of OVs is highly dependent on many variables, including the route of administration and the specific OV platform used.

Intratumoral OV therapy is largely unaffected by preexisting immunity

In the field of OV therapy, local versus systemic delivery is a huge topic of debate (56). Local, intratumoral delivery of OVs is in clinical practice for T-VEC (57,58) and is often used in preclinical studies to ensure efficient delivery to the tumor site (59). Theoretically, intratumorally administered OVs might be less accessible to preexisting antibodies than circulating OVs (**Figure 3A**), although this could vary depending on tumor vascularization (60). Direct cell-to-cell spread after infection with several OVs, including HSV-1, Vaccinia virus, and Measles virus, was shown to be unaffected by the presence of neutralizing antibodies in both *in vitro* and *in vivo* contexts (61,62). However, several other studies have reported that preexisting immunity can limit intratumoral viral replication or spread (63-65). For example, induction of preexisting immunity by intramuscular exposure to

Ad5 before intratumoral injection of this OV into subcutaneous HPD-1NR pancreatic carcinomas, resulted in rapid clearance of viral load from the tumor in hamsters (66).

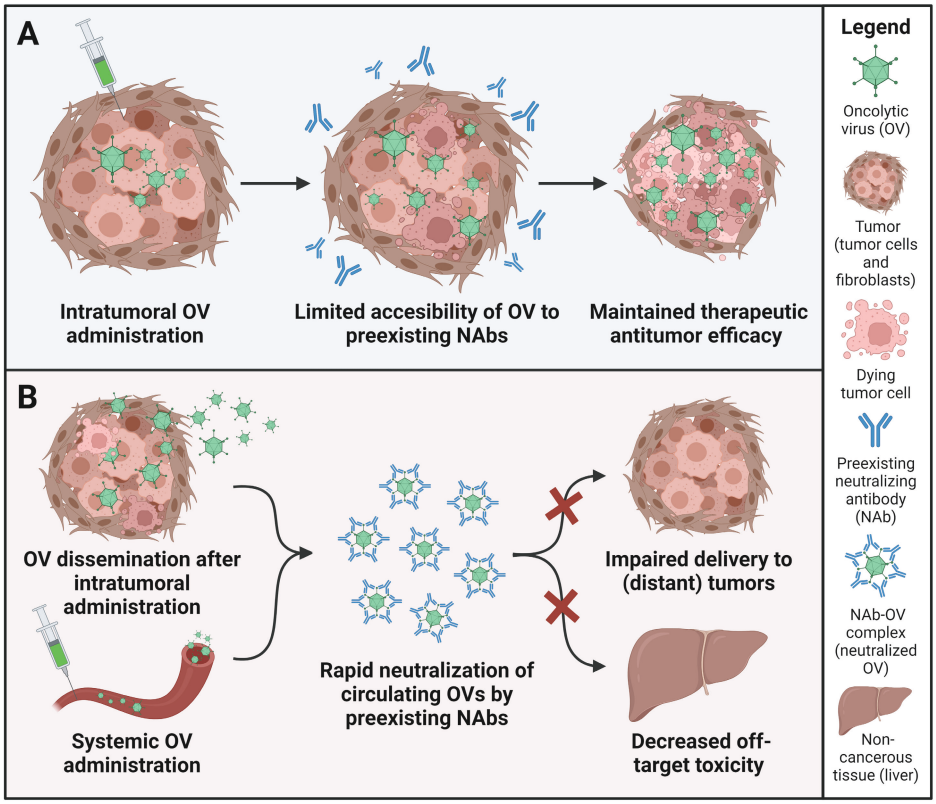


Figure 3. Route of administration contributes to the effect of preexisting neutralizing antibodies (NAbs) on OV efficacy. (**A**) Intratumorally injected OVs might be less accessible to preexisting NAbs (in blue), leading to maintained therapeutic antitumor efficacy. (**B**) OVs that disseminate into the circulation after intratumoral injection, as well as OVs that are systemically administered, are susceptible to rapid neutralization. This can limit the delivery efficiency to (distant) tumors, but also decrease off-target toxicity.

Interestingly, although preexisting immunity against Ad5 and other OVs including HSV-1 and Coxsackievirus A21 (CV-A21) can result in reduced intratumoral viral replication, preexisting immunity against these OVs does not mitigate the OV-induced effect on primary tumor growth or animal survival upon intratumoral OV therapy (63-69). These results highlight the discrepancy between viral replication and therapeutic efficacy in the setting of intratumoral administration (70). Indeed, clinical trials investigating the efficacy of various OVs with high seroprevalence that were injected directly into a variety of readily accessible tumors, such as melanomas, have been relatively successful (4,55,71-73). One of these trials, investigating the efficacy of intratumoral Ad5 treatment of pancreatic ductal adenocarcinoma, showed there was no significant correlation between preexisting anti-Ad5 antibody titers and changes in tumor size upon therapy (74). Thus, both the preclinical and clinical data suggest that, even though OV replication

might be decreased, preexisting immunity should generally not be considered an obstacle to primary tumor clearance in the setting of intratumoral OV therapy.

Rapid neutralization of OVs shed by infected tumors prevents viral dissemination

Although intratumoral OV therapy consists of direct injection of OVs into the tumor microenvironment, spillover and viral shedding as a consequence of oncolysis will introduce OVs into the circulation. These circulating OVs are readily accessible to preexisting antibodies and thus subject to neutralization, which can impact OV therapy in a variety of ways (**Figure 3B**). For instance, in the case of multiple tumors, preexisting immunity might prevent intratumorally administered OVs from disseminating to distant tumors. An example of this was shown to occur upon injection of CV-A21 into one of two bilateral subcutaneous YUMM 2.1 melanomas in immunocompetent C57BL/6 mice (69). For naive animals, viral genomic material was present in the blood and both tumors, but intraperitoneal preexposure to CV-A21 completely precluded viral recovery from the circulation and the distant tumor. Likewise, another study showed that passive immunization with Vaccinia-specific immunoglobulins strongly reduced dissemination to lung, bone, and lymph node metastases in BALB/c mice upon injection of a primary 4T1 mammary carcinoma with luciferase-expressing Vaccinia virus (75). As such, preexisting immunity is likely detrimental to therapeutic efficacy in a setting of metastatic disease, where therapy should affect both the injected and distant tumors.

Importantly, preexisting NAbs can reduce toxicity associated with intratumoral OV therapy by limiting viral dissemination to off-target tissues. This was investigated in a study using an intratumoral injection of subcutaneous PymT-induced breast adenocarcinoma with a luciferase-expressing replication-deficient Ad5 in FVB/n mice (63). Here, intranasal exposure to Ad5 before OV therapy strongly reduced luciferase activity in the liver, which is a major site of Adenovirus off-target toxicity, while only slightly reducing transgene expression in the tumor. Similar results were obtained for intratumoral treatment of subcutaneous HaK kidney tumors with an Ad5 OV in Syrian hamsters (64). Here, intramuscular preexposure to Ad5 completely abrogated recovery of viral genome copies from the liver and lungs, as well as infectious virus from the liver, whereas naive animals exhibited dissemination to these tissues and active viral replication in the liver. Importantly, tumor growth was similarly inhibited for both naive and preexposed animals. Thus, it appears that NAbs prevent OV dissemination to distant tumors upon intratumoral therapy, but can also be beneficial by limiting dissemination and infection of off-target tissues.

The efficacy of systemic OV therapy is abrogated by preexisting immunity

Clinically speaking, systemic OV administration is often preferable to intratumoral injection, as it limits patient discomfort and allows for the treatment of tumors that are not easily accessible (76). However, since therapeutic efficacy in this context is completely dependent on dissemination via the circulation, preexisting immunity

represents a major hurdle to this route of administration (**Figure 3B**). Indeed, the preclinical efficacy of most systemically-administered OV therapies, including Measles virus, VSV, HSV-1, and Ad5, is severely abrogated by preexisting immunity (77-80). For example, a study investigating the efficacy of intravenous VSV-GFP treatment in BALB/c mice bearing subcutaneous CT26 colon carcinomas demonstrated that intravenous VSV exposure before OV therapy completely abrogated transgene expression and recovery of infectious virus from the tumor, which was not observed in naive animals (81). Similar attenuation was observed upon passive immunization with antibody-containing serum, but not for animals receiving a transfer of T cells from donor mice exposed to VSV. Passive immunization with purified Ad5-specific antibodies was also shown to inhibit intratumoral Ad5 replication and clearance of subcutaneous LNCaP prostate cancer tumors in BALB/c nude mice treated intravenously with Ad5, while Ad5 treatment demonstrated antitumor activity in a setting without Ad5 NAbs (80). As such, the accessibility of these systemically administered OVs to NAbs appears to be the main reason for their diminished therapeutic efficacy in an immunized host.

The specific site of intravenous delivery might be an important consideration for therapeutic outcome, as it influences the effect of preexisting immunity on OV efficacy. This was shown for HSV-1 therapy in BALB/c mice carrying hepatic metastases established by subcapsular injection of CT26 colon carcinoma cells (82). Here, intraperitoneal preexposure attenuated HSV-1-induced tumor clearance upon tail vein, but not portal vein delivery of HSV-1. As delivery into the portal vein reduces the distance to its target, it likely minimizes the window in which preexisting antibodies can abrogate therapeutic efficacy through the neutralization of OVs. Thus, this observation supports a model in which the required distance of OV dissemination is inversely related to the attenuating effect of preexisting immunity. Together, these studies support the role of preexisting antibodies as a likely contributing factor to the limited efficacy of clinical trials investigating systemic OV delivery and show that nuanced consideration of delivery sites is warranted.

EVADING PREEXISTING IMMUNITY FOR IMPROVED OV INFECTION AND SPREAD

To improve the infection and spread by OVs, many studies have explored modifications of OV therapy to evade neutralization by NAbs (54). Especially in the context of systemic therapy, such strategies might strongly increase therapeutic efficacy.

Cell carriage can rescue the efficacy of systemic OV therapy despite preexisting immunity

Avoiding recognition of OVs by neutralizing antibodies might be achieved by utilizing infected cells as 'Trojan horses' to deliver OVs to tumors (**Figure 4A, C**). Early clinical trials demonstrated that systemically delivered Reovirus was able to reach and actively

infect distant tumors, despite the presence of Reovirus-specific NAbs (83). Interestingly, replication-competent Reovirus could be recovered from circulating PBMCs, granulocytes, and platelets but not plasma. This suggests that immune cell carriage can be employed for shuttling and handing off OVs to distant tumors, as a means to evade OV clearance by neutralizing antibodies. Indeed, mechanistic studies have shown that Reovirus can be internalized by various immune cells, including DCs and T cells (84,85). One study assessed the consequences of cell carriage by subcutaneously implanting B16 melanomas, treating C57BL/6 mice intravenously with either free or cell-carried Reovirus, and then assessing the number of metastatic colonies in the tumor-draining lymph node (86). For both naive and Reovirus preexposed animals, Reovirus-loaded mature DCs and T cells outperformed free OVs in limiting lymph node metastases, likely as a result of more efficient draining and thus viral delivery to lymph nodes by immune cells. Similarly, T cells loaded with Measles virus facilitated delivery of Measles virus to tumors in the presence of NAbs (87). Other studies have investigated stem cells as potential OV carriers, as they are naturally resistant to chemotherapeutic drugs and can survive in the tumor microenvironment (88). As an example of such a strategy, Ad5-infected neural stem cells were less susceptible to *in vitro* serum neutralization and led to more efficient *in vivo* infection of intracranial GL261 gliomas when delivered in multiple cycles, compared to naked OVs (89).

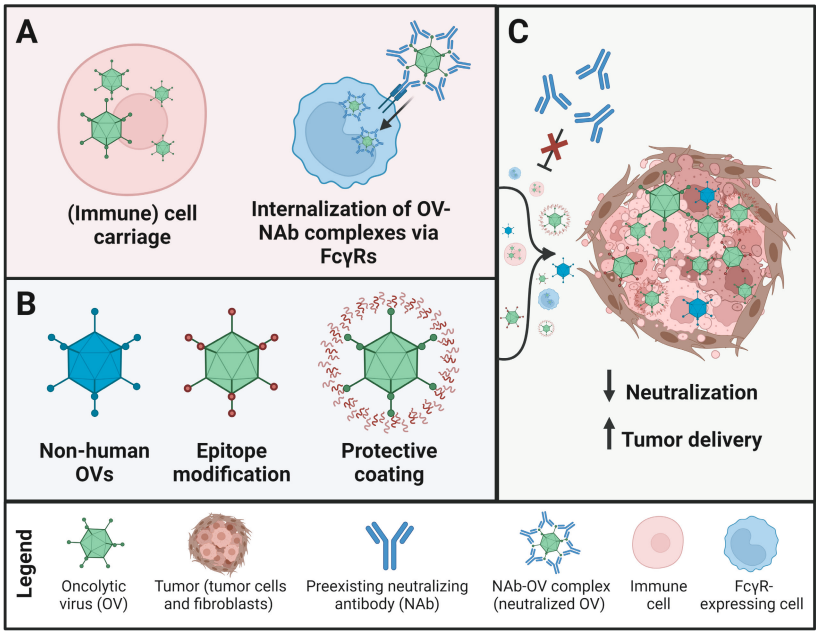


Figure 4. Strategies to evade neutralization by preexisting neutralizing antibodies (NAbs). (**A**) OVs can be carried by various (immune) cells, such as dendritic cells (DCs), T cells or stem cells to avoid neutralization. Alternatively, OV-NAb complexes can be internalized by cells expressing antibody-binding Fc-gamma receptors. (**B**) Usage of non-human OVs, epitope modification or a protective coating to decrease recognition and clearance by NAbs. (**C**) Employment of evasion strategies described in (A) and (B) lead to decreased neutralization and improved delivery of the OV to the tumor.

Interestingly, when using a cell carrier system for OV delivery, the presence of NAbs might even be beneficial. For instance, antibody-Reovirus complexes can effectively be internalized by human monocytes and delivered to tumor cells, resulting in infection and lysis of Mel-624 melanoma cells. This internalization is mediated via the antibody-binding Fc-gamma receptors (FcγRs), expressed on the surface of monocytes and other immune cells (90). Similarly, antibody-neutralized CV-A21 was shown to be ineffective at killing Mel-624 cells *in vitro* unless carried and handed off by monocytes (90). Furthermore, A549 lung carcinoma cell lines artificially expressing FcγRs have been shown to internalize antibody-neutralized Ad5 (91). The antibody-dependent enhancement (ADE) of viral infection through internalization of antibody-virus complexes by FcγR-expressing cells has been described to occur for a range of viruses, such as Influenza virus, Measles virus, Coronaviruses, and most notably Flaviviruses (92,93). In contrast to Reovirus, these viruses can efficiently replicate in their carrier cells, ultimately resulting in cell death. Since this broadens viral tropism and eliminates immune cells, ADE is often associated with poorer disease outcomes. As such, the ability of some OVs to productively replicate in FcγR-expressing cells might preclude them from beneficial cell carriage, as it would result in the rapid elimination of carrier cells before they can facilitate viral dissemination to distant tumors. Nevertheless, it appears that delivery of OVs via (immune) cell carriage could be a promising new approach for systemic delivery of OVs, especially in preexposed individuals.

Non-human OVs demonstrate oncolytic activity towards human tumors but are less susceptible to neutralization

Another way to avoid recognition by preexisting immune responses is the use of alternative viral strains, which are sufficiently different from their human-infecting homologs but also display oncolytic effects (**Figure 4B, C**). The capacity of non-human OVs to kill human tumor cells has been demonstrated for various viruses, such as an HSV-1 virus derived from goats that was able to replicate in different human cell lines and induce apoptosis (94,95). Additionally, Adenoviruses isolated from non-human primates were shown to effectively infect and kill a wide range of human cancer cell lines *in vitro*, while not being neutralized by pooled human donor serum (96). Similarly, an avian Reovirus was able to infect hepatocellular carcinoma cells and induce apoptosis *in vitro* but is likely less susceptible to neutralization in humans, since structural analysis demonstrated that its neutralizing epitopes were distinctly different from its human homolog (97). Other examples of non-human virus species that are in development as oncolytic agents have been described elsewhere (98,99). The (pre)clinical efficacy of most of these non-human viruses remains to be proven, but they represent an attractive alternative to currently used OVs.

Genetic modification limits neutralization by OV-specific preexisting antibodies

Alternatively, antibody-binding sites of OVs can be altered by genetic modification, preventing neutralization by preexisting antibodies (**Figure 4B, C**). For example, the introduction of point mutations in the gD glycoprotein of HSV-1 was shown to result

in increased resistance to *in vitro* neutralization by monoclonal antibodies (100). More radical modification is also possible by exchanging surface glycoproteins of OVs with those from other viruses with lower rates of preexposure in the population. This so-called envelope exchange has been utilized for the generation of chimeric Measles virus strains with surface proteins originating from the Canine Distemper virus, which retain their oncolytic activity *in vitro* and *in vivo* (77,79,101). Indeed, this modified Measles virus demonstrated potent oncolytic antitumor efficacy in athymic nude mice bearing intraperitoneal SKOV3.ip1 ovarian cancers and passively immunized with measles-immune human antibody serum, while the efficacy of the non-modified Measles virus was strongly diminished (79). Similar chimerism has also been explored for Ad5, by switching its serotype to that of the related Ad3 or Ad35 to evade neutralization (102-104).

Shielding or coating of OVs prevents immune recognition

Modification of neutralizing epitopes on OVs or the use of OVs from other hosts thus appear promising for the evasion of preexisting immunity present in the population. Nevertheless, both modified and non-human OVs will likely still be affected by the antiviral immune response induced by repeated therapeutic administrations. Thus, shielding surface epitopes of OVs with a non-immunogenic coat to prevent recognition might be an alternative strategy (**Figure 4B, C**). This can be achieved by genetic modification of the OV, as was shown for the insertion of an albumin-binding domain in the main capsid protein of Ad5 (105). Intravenous administration of a luciferase-expressing Ad5 virus into nude mice bearing subcutaneous B16-CAR melanomas that were intraperitoneally preexposed to Ad5 led to complete neutralization, as the Ad5-mediated luciferase expression within tumors was completely abolished. In contrast, the albumin-binding Ad5 did not suffer from significant loss of luciferase signal in tumors. Similarly, in nude mice bearing subcutaneous A549 or Sk-mel28 tumors that were intraperitoneally preexposed to Ad5, the oncolytic antitumor efficacy of intravenously administered albumin-binding Ad5 was maintained while the Ad5 without the albumin-binding domain was completely inefficacious. As another example, Vaccinia virus has been successfully modified to increase the release of so-called extracellular enveloped viruses (EEVs) upon infection, which have an additional membrane layer and are thereby less susceptible to immune-mediated clearance compared to Vaccinia virus particles themselves (75). This EEV-enhanced Vaccinia virus displayed improved spread to metastases in the lungs and lymph nodes after intratumoral delivery in BALB/c mice inoculated with 4T1 tumors in the mammary fat pad, compared to a Vaccinia virus variant that was less capable to produce EEVs. Similarly, a significant survival advantage was provided by the EEV-enhanced strain over the wild-type virus in BALB/c mice bearing subcutaneous JC tumors.

Alternatively, OVs can be artificially coated by the attachment of ionic polymers, graphene sheets, or liposomes to shield them from antibody recognition (78,106). For example, multilayer ionic polymer coating of Measles virus resulted in improved

control of subcutaneous LL/2-CD64 lung cancer tumors compared to the non-coated virus in Measles-preimmunized C57BL/6N mice (107). In another study, shielding of Ad11 using a hybrid membrane comprised of artificial lipid membranes and red blood cell membranes protected the virus from neutralizing antibodies, prolonged its circulation, and enhanced its antitumor efficacy in the murine TC1 lung cancer model (108). Further (pre)clinical evaluation of the strategies described above would be interesting to optimally enhance the efficacy of (systemically delivered) OV therapy in preexposed patients.

EFFECTS OF PREEXISTING IMMUNITY ON THE OV THERAPY-INDUCED IMMUNE RESPONSE

Besides viral replication and oncolysis, the induction of a potent immune response is a second, but equally important pillar of OV therapy (45) (see also section 1). However, if and how the presence of preexisting immunity also affects the OV-induced immune response remains underexplored. Here, we gathered (pre)clinical evidence that describes the effect of preexisting immunity regarding the induction of virus- and tumor-specific immune responses.

Repeated OV exposure can limit the induction of a tumor-specific immune response

Indications that preexisting immunity can affect OV-induced immune responses can be derived from studies utilizing multiple dosages of OVs. Specifically, it has been shown that homologous boosting regimens impair the induction of a tumor-specific T-cell response, in contrast to heterologous prime-boost schedules utilizing a combination of distinct OV platforms. An example of this was shown for intratumoral OV therapy of hamsters with subcutaneously implanted HaK kidney tumors or HPD-1NR pancreatic carcinomas (109). In both models, a heterologous treatment schedule comprising three intratumoral Ad5 injections followed by three intratumoral Vaccinia injections displayed significantly superior antitumor efficacy compared to 6 doses of either virus alone. This heterologous OV therapy resulted in improved induction of tumor-specific T cells compared to treatment with either virus alone, and these T cells were responsible for therapeutic efficacy since the depletion of $CD3^+$ T cells completely abrogated the antitumor effect of this combination therapy. OVs encoding a transgene appear to be similarly affected by dosage regimens. For instance, in a CT26 metastasis model where tumors express β-galactosidase, two intravenous doses of either β-galactosidase-expressing Vaccinia virus or the related β-galactosidase-expressing Fowlpox virus resulted in inferior overall survival compared to sequential treatment with both viruses (110). Heterologous boosting led to higher β-galactosidase-specific $CD8^+$ T-cell responses compared to homologous boosting, and homologous boosting was associated with the induction of a strong antiviral antibody response.

Although repeated OV administration can hamper the OV-induced tumor-specific T-cell response, evidence for the mechanisms underlying this problem remains elusive. This phenomenon could simply be explained by lower clearance of the OV by NAbs, but another possible explanation could be derived from the immunodominance of previously encountered viral T-cell epitopes. Besides the notion that most viral epitopes are inherently more immunogenic than most tumor epitopes, an OV-specific T-cell response is boosted upon the reintroduction of previously recognized viral epitopes. Both aspects might result in an immunodominant OV-specific T-cell response over the tumor-specific T-cell response (**Figure 5**). This phenomenon, sometimes referred to as 'original antigenic sin' (111), has been extensively studied for vector-based vaccines and Influenza infections but has not gained a lot of attention in the field of OV research (112). Nevertheless, as similar viral strains are often used in both fields, data showing problematic viral epitope immunodominance for vector vaccines highlights current gaps in OV research and might indicate shared mechanisms. Of note, it could be that different OV platforms vary in their inherent immunogenicity, making them more or less dominant over the tumor-specific immune response. Indeed, research on viral vectors has shown that viral backbones can differ in the type and potency of immune responses they induce (113), indicating the same might be true for OVs.

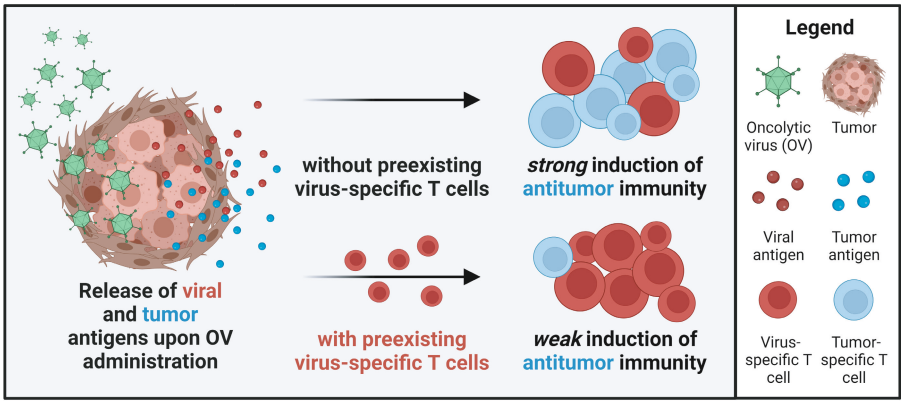


Figure 5. Immunodominance of OV-specific T-cell responses over tumor-specific T-cell responses. Viral epitopes are often more immunogenic compared to most tumor epitopes. Additionally, in the setting of preexisting immunity or repeated dosage, the preexisting OV-specific T-cell response is boosted upon repeated recognition of the viral epitopes. These combined aspects may result in an impaired induction of an antitumor T-cell response compared to a strong virus-specific T-cell response.

The possible immunodominance of the viral backbone over transgenes could especially be relevant for OVs which encode tumor antigens. For instance, investigation of intramuscular delivery of Hepatitis B surface antigen (HBsAg) and ovalbumin (OVA) antigen in BALB/c mice using an Ad5-based vector revealed prior exposure to Ad5 strongly reduced the HBsAg- and OVA-specific $CD8^+$ T-cell responses (114). Instead, isolated $CD8^+$ T cells were mainly reactive to Ad5 epitopes. Skewing of immunity towards an antiviral response was replicated in antibody-deficient $IgH^{-/-}$ mice, indicating it is the

established Ad5-specific cellular immunity, and not the Ad5-specific humoral response, that limits the priming and expansion of HBsAg/OVA-specific $CD8^+$ T cells. Similarly, induction of $CD4^+$ and $CD8^+$ T-cell responses specific for an Influenza virus antigen, which was intramuscularly delivered using a Vaccinia virus vector, was completely abrogated by prior exposure to Vaccinia virus (115). Highlighting the relevance of such preclinical observations, clinical data suggests similar immunodominance occurs in humans. For example, several trials of Ad-vectored vaccines have reported correlations between preexisting Ad-specific $CD4^+$ T cells (116,117) or antibodies (118) and strongly decreased induction of $CD4^+$ T-cell, $CD8^+$ T-cell and antibody responses directed against the delivered vaccine antigen. Although these studies utilized Adenovirus to deliver Ebolavirus and HIV epitopes irrelevant to OV therapy, these observations might be relevant to the field of OV research. Furthermore, the discussed data on OV boosting regimens might suggest that preexisting immunity could also affect responses to tumor antigens released after oncolysis, due to the simultaneous release of viral epitopes.

Intramuscular, intravenous, and intratumoral OV administration are likely to result in distinct dynamics of viral epitope exposure to the immune system and thus influence the development of antiviral immunodominance, but a direct comparison of routes of administration has yet to be performed. Regardless of the underlying mechanisms, heterologous prime-boost regimens appear to be beneficial for some OV therapies by improving tumor-specific immune responses and tumor clearance. Consequently, clinical trials of such strategies are promising and currently ongoing. For example, sequential systemic therapy with Ad5 and Maraba virus, both encoding the tumor antigen MAGE-A3, showed preclinical efficacy and is currently being tested for the treatment of advanced metastatic solid tumors and non-small cell lung cancer (NCT02285816, NCT02879760) (119-121).

Preexisting OV-specific immunity can also improve therapeutic anticancer efficacy by enhancing tumor-specific T-cell responses

The data described above suggested that OV administration might result in the dominance of OV-specific T-cell responses over tumor-specific T-cell responses upon repeated exposure. However, other studies suggest that preexisting OV-specific immunity does not hamper, but can actually promote the induction of a systemic tumor-specific immune response. An example of this was shown for immunocompetent C57BL/6J mice with subcutaneously implanted bilateral B16.F10 melanomas, of which one was injected with NDV (122). In this setting, prior subcutaneous footpad exposure to NDV led to improved control of tumor size as well as extended survival upon intratumoral NDV treatment, even though viral replication was compromised. For both the injected and distant tumor, the ratio of conventional $CD4^+$ T cells over regulatory T cells as well as the expression of genes related to immune-mediated cytotoxicity were strongly increased by preexposure to NDV. In the distant, but not the injected tumor of preexposed animals, an increase in $CD8^+$ T-cell influx could be observed, which was not the case for the distant tumors of naive animals. Prior NDV exposure did not significantly increase

the amount of virus-specific $CD8^+$ T cells in the spleen but instead caused a strong increase in the amount of tumor-specific $CD8^+$ T cells. $CD8^+$ T-cell depletion completely abrogated the antitumor effect of NDV in immunized mice, suggesting that $CD8^+$ T cells were indispensable for the therapeutic efficacy of NDV in a preexposed setting. Similar effects of preexisting immunity on therapeutic OV efficacy were recently shown for the intratumoral treatment of BALB/c mice with subcutaneously implanted bilateral CT26 colon carcinomas using a highly modified HSV-1, expressing several cytokines and a PD-L1 blocking peptide (123). Control of both the injected and distant tumors was improved by subcutaneous preexposure to HSV-1, as was overall survival. Strikingly, the outgrowth of the distant tumor was completely unaffected by intratumoral OV therapy of the local tumor in naive animals, showing preexisting immunity was required for systemic efficacy in this setting. Gene expression profiling of tumors again revealed a skewing toward cytotoxic and inflammatory responses. Additionally, isolated splenocytes from preexposed mice were more reactive to tumor cells compared to splenocytes from naive animals, indicating an increased induction of tumor-specific immunity.

Thus, it appears that preexisting immunity can also promote the induction of a tumor-specific immune response upon therapy with these OVs. These tumor-specific responses have a systemic impact with efficacy on distant tumors and could thus have the potential to treat metastatic disease. Whether this phenomenon extends to other OV platforms and its underlying mechanisms, however, remains to be explored. One possibility could be that preexisting antiviral $CD4^+$ T cells aid the development of tumor-specific $CD8^+$ T cell responses. $CD4^+$ T-cell help has been well established as a crucial factor in the induction of robust $CD8^+$ T-cell responses but is generally considered to be restricted to responses specific to the same antigen (124). Nevertheless, some studies have indicated that $CD4^+$ T cells might also mediate more general immune-stimulating effects upon activation by their cognate antigen, such as an increase in naive lymphocyte recruitment to lymph nodes (125). Indeed, it was recently shown in C57BL/6 mice that were intramuscularly vaccinated with tetanus toxoid before intratumoral OVA-coated Ad5 therapy, that additional coating of the Ad5 with major histocompatibility complex (MHC) class II-restricted tetanus toxoid peptides led to increased infiltration of tumor-specific $CD8^+$ T cells into subcutaneous B16.OVA melanomas (126). As the tetanus toxoid coating resulted in potent stimulation of preexisting pathogen-specific $CD4^+$ T-helper cells, it appears likely that pathogen-specific $CD4^+$ T-cell help can potentiate tumor-specific $CD8^+$ T-cell responses. In another study, it was revealed that prior vaccination against poliovirus substantially improved the antitumor efficacy of intratumoral polio treatment in C57BL/6 mice bearing murine melanoma B16.F10 tumors, and that this antitumor effect was mediated by the recall of $CD4^+$ T cells and the induction of tumor-specific T cells that could delay tumor outgrowth in naive mice after adoptive cell transfer (127). So far, preexisting virus-specific $CD4^+$ T cells have been largely overlooked in the OV research field, but these observations suggest that they might play an important part in modulating the OV-induced immune response, especially in a setting where preexposure has occurred.

EXPLOITING PREEXISTING VIRUS-SPECIFIC IMMUNITY FOR EFFECTIVE ANTICANCER IMMUNOTHERAPY

Regardless of the induction of a tumor-specific immune response in a preexposed setting, increasing amounts of evidence suggest that preexisting antiviral effector responses might also be engaged to directly contribute to tumor clearance and thus therapeutic efficacy. Studies have shown that antiviral $CD8^+$ T cells commonly survey a range of both murine and human tumors, including melanomas, brain metastases, endometrial, lung, and colorectal cancers (128,129). Upon immune cell profiling, tumor-specific $CD8^+$ T cells found in patient tumors expressed high levels of T-cell exhaustion, likely as a result of chronic antigen exposure in the tumor (129). $CD8^+$ T cells specific for common viral pathogens, such as Cytomegalovirus (CMV), Eppstein-Barr virus (EBV), or Influenza virus, on the other hand, exhibited phenotypes more in line with active effector cells. Indeed, virus-specific T cells, as determined by staining with HLA tetramers specific for these viruses, could be potently activated after isolation from tumor tissue by providing relevant viral peptides (128). Various strategies are described to employ antiviral T cells for anticancer therapy, either by reactivation using their cognate antigens, or in a specificity-independent manner.

Preexisting antiviral T cells can be activated and engaged for anticancer therapy

The engagement of preexisting antiviral T cells for antitumor activity is an appealing avenue for immunotherapy, in particular for the treatment of low-immunogenic tumors (**Figure 6**). One way to achieve this is by delivering viral epitopes into the tumor, resulting in the activation of antiviral T cells present in the tumor microenvironment. For example, preexisting Reovirus-specific $CD8^+$ T cells, induced by vaccination with a synthetic viral peptide containing the Reovirus $CD8^+$ T-cell epitope, were efficiently recruited into subcutaneous KPC3 pancreatic tumors upon intratumoral injection of Reovirus (53). In this study, the presence of this preinstalled pool of Reovirus-specific effector cells significantly delayed tumor outgrowth after intratumoral Reovirus administration, an effect not observed when Reovirus was administered to naive animals. Similar effects on tumor growth were observed in animals that were immunized with Reovirus before vaccination, showing that vaccine-mediated boosting of preexisting Reovirus-specific $CD8^+$ T cells can improve OV therapeutic efficacy. Similarly, intratumoral delivery of the Vaccinia virus-derived B8R protein by a recombinant adeno-associated virus reactivated preinduced Vaccinia-specific $CD4^+$ and $CD8^+$ T cells and retarded outgrowth of murine DT6606 pancreatic tumors (130).

Besides direct infection with a virus, other innovative strategies can also be employed to reactivate virus-specific T cells. Although these studies often investigate the use of non-OV-specific T cells, these observations should also be instructive for the employment of preexisting OV-specific T cells. For example, injection of B16 melanomas with the viral peptide SIINFEKL resulted in improved tumor control and survival over an irrelevant peptide in C57BL/6J mice that had previously received a transfer of OT-1 $CD8^+$ T cells

which target this epitope (128). Similarly, intratumoral injection of murine CMV (MCMV)-derived T-cell epitopes triggered the expansion of MCMV-specific CD4⁺ and CD8⁺ T cells in TC1-bearing immunocompetent mice that were preexposed to MCMV (131). Injection of MHC-I-restricted MCMV epitopes into TC1 tumors induced a T-cell/IFN-γ signature, delayed tumor outgrowth, and improved survival. Expanding on such an approach is the idea that the conjugation of virus-derived epitopes to tumor-targeting antibodies might improve their specificity and facilitate systemic efficacy. This was demonstrated in a study where CMV-derived epitopes conjugated to an antibody targeting the tumor antigen MMP14 could be used for efficient recruitment of preexisting antiviral CD8⁺ T cells towards various MMP14-expressing tumors (132). This resulted in improved control of orthotopic MDA-MB-231 breast tumors, as well as orthotopic SNU-475 liver or subcutaneous MGH-1 lung tumors.

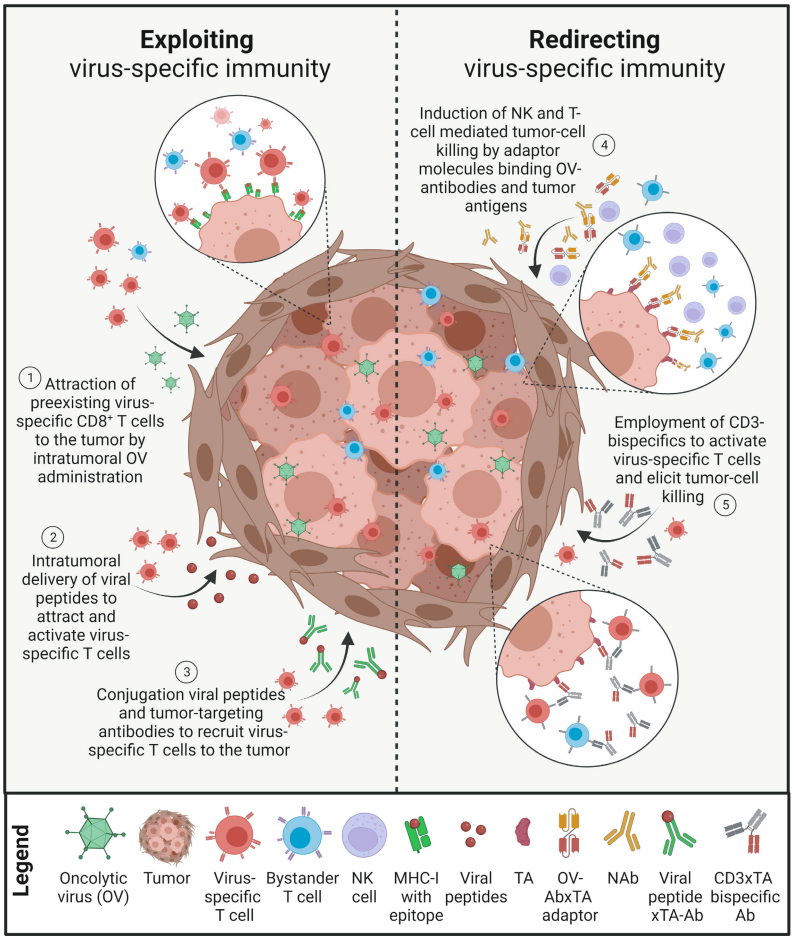


Figure 6. Strategies to exploit or redirect (preexisting) virus-specific T cells for antitumor immunotherapy. Multiple avenues can be employed to exploit the specificity of (oncolytic) virus-specific immunity for anticancer immunotherapy. (1) Preexisting OV-specific T cells can be attracted to the tumor by intratumoral OV administration and activated by presentation of OV >>

>> epitopes on the surface of tumor cells in MHC-I proteins. (2) Intratumoral delivery of viral peptides leads to activation of intratumoral virus-specific T cells. (3) Complexes of viral peptides together with a tumor-targeting antibody can recruit OV-specific T cells to the tumor. (4) Adaptor molecules binding to both OV-specific antibodies and tumor antigens induce NK- and T-cell-mediated killing of tumor cells. (5) Utilization of CD3-bispecific antibodies transforms OV-specific T cells into tumor-attacking T cells. NK; natural killer, MHC-I; major histocompatibility molecule class I; TA; tumor antigen, Ab; antibody.

A similar principle was applied in a model where immunodeficient female non-obese diabetic (NOD).Cg-Prkdc^{scid}Il2rg^{tm1Sug}/ShiJic (NOG) mice bearing MDA-MB-231 breast cancer xenografts received an adoptive transfer of expanded human EBV-specific CD8$^+$ T cells, which were subsequently directed to the tumor by use of immunoconjugates called Antibody-Targeted Pathogen-derived Peptides (ATPPs) (133). Here, MHC class I peptides are conjugated to antibodies specific for a tumor antigen that is expressed on the tumor cell surface. This tumor-specific delivery of EBV peptides activated EBV-specific T cells and delayed tumor outgrowth in combination with PD-1 checkpoint blockade. Similarly, in NOD.Cg-Prkdc^{scid} Il2rg^{tm1Wjl}/SzJ (NSG) mice bearing the same MDA-MB-231 tumors, CMV-specific T cells could be redirected to exert antitumor efficacy via a CD8$^+$ T-cell epitope-delivering antibody (termed TEDbody), which was engineered to deliver a viral MHC-I epitope peptide into the cytosol of target tumor cells by fusion with a tumor-specific cytosol-penetrating antibody (134).

Thus, delivery of viral epitopes into the tumor microenvironment, through a variety of ways, can be utilized to engage preexisting antiviral T cell populations for antitumor effect. An exciting strategy involves the exploitation of 'molecular mimicry', where preexisting virus-specific T cells can demonstrate cross-reactivity toward tumors after restimulation with tumor-specific antigens that display high similarities to their cognate viral antigens (135). For instance, in a cohort of melanoma patients with high anti-CMV antibody levels, it was suggested that molecular mimicry between CMV and tumor antigens played a role in the response to anti-PD1 therapy blockade by activation of cross-reactive T cells. Another enticing opportunity is the reactivation of T cells that are induced by exposure to a common virus or established antiviral vaccines, which have already been abundantly tested for clinical safety and are administered to a majority of the human population. As examples of this, T cells specific for Influenza virus (136), Yellow Fever virus (137), or even SARS-CoV-2 (138) might be employed for anticancer therapy.

Redirecting the specificity of preexisting virus-specific responses for their use as anticancer effector cells

As an alternative approach to using the specificity of preexisting antiviral immune responses, the inherent specificities could also be redirected to the tumor by using bispecific molecules (139). Such retargeting of preexisting virus-specific antibodies and T cells for antitumor activity using bispecific molecules might be used to improve OV efficacy (140) (**Figure 6**). For instance, a recent study described the design of a bispecific adaptor molecule containing an Ad5 antibody-binding epitope and a domain

that binds polysialic acid, a surface adhesion molecule associated with a range of cancers (141). Immunocompetent C57BL/6 mice were immunized with Ad5 to develop anti-Ad5 antibodies, which were subsequently recruited to the tumor with the bispecific adaptor molecule. This treatment led to improved tumor control and survival of mice with subcutaneous polysialic acid-expressing MC38 colon carcinomas, CMT-64 lung carcinomas, and B16F10 melanomas compared to naive mice. Further studies in MC38 tumors established a model in which the retargeted Ad5 antibodies recruited and activated NK cells, which mediated initial tumor cell killing through antibody-dependent cellular cytotoxicity (ADCC) and thereby induced the priming of a tumor-specific $CD8^+$ T-cell response (142).

Besides virus-specific antibodies, preexisting OV-specific T cells can also be directly recruited for antitumor efficacy using CD3-bispecific molecules (also known as bispecific T-cell engagers (BiTEs)). For instance, intratumoral Reovirus administration to subcutaneous KPC3 pancreatic tumors expressing tumor antigen TRP1 led to a strong influx of virus-specific $CD8^+$ T cells, which could be subsequently engaged for delayed tumor growth by intraperitoneal administration of a bispecific antibody targeting both CD3 and TRP1 (52). When tested in a bilateral model, this combination therapy led to delayed tumor growth for both the injected and non-injected distant tumors, showing such strategies could be efficacious in a setting of metastatic disease. Current undertakings in this field especially involve the use of OVs encoding BiTEs, where the OV acts both as an immunostimulatory agent, as well as a vector for BiTE delivery into the tumor (143). Together, these results showcase the potential of bypassing the specificity of preexisting antiviral immunity using bispecific molecules for effective anticancer therapy.

CONCLUDING REMARKS

In this review, we discussed how preexisting immunity against OVs can act as a barrier, but also as a bridge to effective anticancer therapy. As is evident from the data described here, a preexisting OV-specific humoral response against commonly-used OVs might limit viral replication and spread, especially when the OV is administered intravenously. Importantly, even for OVs that do not abundantly circulate in the human population, the observations discussed here are highly relevant, as therapeutic regimens usually entail multiple OV administrations. Each dose will invariably lead to the development of an antiviral immune response that modulates the efficacy of the next round of therapy.

Effects of preexisting immunity on OV infection and spread have been relatively well explored and suggest that, although various OV modifications can help evade a preexisting immune response, a nuanced case-by-case assessment appears warranted and variables such as the location of the tumor(s), the specific OV used, as well as

the route of OV administration should be taken into account. For example, treatment of a single, easily accessible tumor by intratumoral OV injection would likely not be compromised by preexisting immunity. In the case of metastatic disease, on the other hand, the therapeutic efficacy of both intratumoral and systemic OV administration will be strongly limited by preexisting immunity, making modifications to evade it beneficial or even necessary. Currently, a variable that remains largely unexplored in this context is the confounding effect of tumor location. As discussed, the distance between the site of intravenous OV administration and the target tumor appears to modulate the effect of preexisting immunity on therapeutic efficacy (82), indicating administration sites should be optimized based on tumor localization.

While, generally speaking, preexisting humoral immunity is considered to be a barrier to effective anticancer OV therapy and should be circumvented, preexisting OV-specific cellular immune responses might rather be considered a beneficial factor for OV therapy. Additionally, the route of OV administration, which has been abundantly explored and discussed here in the context of OV infection and spread, remains strongly underappreciated regarding its effect on the induced immune response. Vaccine studies have uncovered clear evidence showing that the site of administration is a crucial determinant of the type and quality of subsequently induced responses (144), highlighting the need for evaluation of this factor in OV research. Regardless of its effects on the induction of a tumor-specific immune response, exciting novel data suggests preexisting OV-specific adaptive immunity can be engaged for direct antitumor effects. However, careful investigation is warranted, since preexisting OV-specific T cells might also be involved in inducing viral clearance (66). Further research in the field of OV research should elucidate how OV replication, the OV-induced immune response, and the ultimate therapeutic effects of OVs all interrelate, and how both preexisting humoral and adaptive immunity influence these aspects.

In conclusion, consideration of preexisting immunity is crucial in realizing the full potential of the highly promising therapeutic implementation of OVs. Future investigation of the current gaps in knowledge highlighted here should yield a more complete understanding of the topic, ultimately allowing for better and more personalized OV therapies.

DECLARATIONS

CRediT author statement. *Christianne Groeneveldt:* Conceptualization, Literature collection, Writing – original draft preparation, Visualization, Writing – review & editing. *Jasper van den Ende:* Conceptualization, Literature collection, Writing – original draft preparation, Visualization, Writing – review & editing. *Nadine van Montfoort:* Conceptualization, Writing – review & editing, Supervision.

Funding. This work was financially supported by a PhD fellowship from Leiden University Medical Center (to C.G.) and the Support Casper campaign by the Dutch foundation 'Overleven met Alvleesklierkanker' (supportcasper.nl) (SOAK 22.02, to N.v.M). All figures were created with BioRender software (BioRender.com).

Declarations of Competing Interest. The authors declare that they have no known competing financial interests or personal relationships that could have appeared to influence the work reported in this paper.

REFERENCES

1. Yun C-O, Hong J, Yoon A-R. Current clinical landscape of oncolytic viruses as novel cancer immunotherapeutic and recent preclinical advancements. **2022**;13
2. Macedo N, Miller DM, Haq R, Kaufman HL. Clinical landscape of oncolytic virus research in 2020. Journal for ImmunoTherapy of Cancer **2020**;8:e001486
3. Kohlhapp FJ, Kaufman HL. Molecular Pathways: Mechanism of Action for Talimogene Laherparepvec, a New Oncolytic Virus Immunotherapy. Clin Cancer Res **2016**;22:1048-54
4. Andtbacka RHI, Kaufman HL, Collichio F, Amatruda T, Senzer N, Chesney J*, et al.* Talimogene Laherparepvec Improves Durable Response Rate in Patients With Advanced Melanoma. J Clin Oncol **2015**;33:2780-8
5. Ferrucci PF, Pala L, Conforti F, Cocorocchio E. Talimogene Laherparepvec (T-VEC): An Intralesional Cancer Immunotherapy for Advanced Melanoma. Cancers **2021**;13:1383-
6. Lauer UM, Beil J. Oncolytic viruses: challenges and considerations in an evolving clinical landscape. Future Oncology **2022**;18:2713-32
7. Nwanegbo E, Vardas E, Gao W, Whittle H, Sun H, Rowe D*, et al.* Prevalence of Neutralizing Antibodies to Adenoviral Serotypes 5 and 35 in the Adult Populations of The Gambia, South Africa, and the United States. Clinical and Vaccine Immunology **2004**;11:351-7
8. Hemminki O, Parviainen S, Juhila J, Turkki R, Linder N, Lundin J*, et al.* Immunological data from cancer patients treated with Ad5/3-E2F-Δ24-GMCSF suggests utility for tumor immunotherapy. Oncotarget **2015**;6:4467-81
9. Fueyo J, Gomez-Manzano C, Alemany R, Lee PSY, McDonnell TJ, Mitlianga P*, et al.* A mutant oncolytic adenovirus targeting the Rb pathway produces anti-glioma effect in vivo. Oncogene **2000**;19:2-12
10. Mantwill K, Klein FG, Wang D, Hindupur SV, Ehrenfeld M, Holm PS*, et al.* Concepts in Oncolytic Adenovirus Therapy. Int J Mol Sci **2021**;22:10522-
11. Bradley H, Markowitz LE, Gibson T, McQuillan GM. Seroprevalence of Herpes Simplex Virus Types 1 and 2--United States, 1999-2010. Journal of Infectious Diseases **2014**;209:325-33
12. Puzanov I, Milhem MM, Minor D, Hamid O, Li A, Chen L*, et al.* Talimogene Laherparepvec in Combination With Ipilimumab in Previously Untreated, Unresectable Stage IIIB-IV Melanoma. Journal of Clinical Oncology **2016**;34:2619-26
13. Aldrak N, Alsaab S, Algethami A, Bhere D, Wakimoto H, Shah K*, et al.* Oncolytic Herpes Simplex Virus-Based Therapies for Cancer. Cells **2021**;10:1541-
14. Costantino V, Trent MJ, Sullivan JS, Kunasekaran MP, Gray R, MacIntyre R. Serological Immunity to Smallpox in New South Wales, Australia. Viruses **2020**;12:554-
15. Downs-Canner S, Guo ZS, Ravindranathan R, Breitbach CJ, O'Malley ME, Jones HL*, et al.* Phase 1 Study of Intravenous Oncolytic Poxvirus (vvDD) in Patients With Advanced Solid Cancers. Molecular Therapy **2016**;24:1492-501
16. Hwang T-H, Moon A, Burke J, Ribas A, Stephenson J, Breitbach CJ*, et al.* A Mechanistic Proof-of-concept Clinical Trial With JX-594, a Targeted Multi-mechanistic Oncolytic Poxvirus, in Patients With Metastatic Melanoma. Molecular Therapy **2011**;19:1913-22
17. Guo ZS, Lu B, Guo Z, Giehl E, Feist M, Dai E, *et al.* Vaccinia virus-mediated cancer immunotherapy: cancer vaccines and oncolytics. J Immunother Cancer **2019**;7:6
18. Lebo EJ, Kruszon-Moran DM, Marin M, Bellini WJ, Schmid S, Bialek SR*, et al.* Seroprevalence of Measles, Mumps, Rubella and Varicella Antibodies in the United States Population, 2009–2010. Open Forum Infectious Diseases **2015**;2:ofv006-ofv
19. Galanis E, Hartmann LC, Cliby WA, Long HJ, Peethambaram PP, Barrette BA*, et al.* Phase I Trial of Intraperitoneal Administration of an Oncolytic Measles Virus Strain Engineered to Express Carcinoembryonic Antigen for Recurrent Ovarian Cancer. Cancer Research **2010**;70:875-82
20. Lin L-T, Richardson C. The Host Cell Receptors for Measles Virus and Their Interaction with the Viral Hemagglutinin (H) Protein. Viruses **2016**;8:250-

21. Allagui F, Achard C, Panterne C, Combredet C, Labarrière N, Dréno B*, et al.* Modulation of the Type I Interferon Response Defines the Sensitivity of Human Melanoma Cells to Oncolytic Measles Virus. Current Gene Therapy **2017**;16:419-28
22. Engeland CE, Ungerechts G. Measles Virus as an Oncolytic Immunotherapy. Cancers **2021**;13:544-
23. Tai JH, Williams JV, Edwards KM, Wright PF, Crowe JJE, Dermody TS. Prevalence of Reovirus-Specific Antibodies in Young Children in Nashville, Tennessee. The Journal of Infectious Diseases **2005**;191:1221-4
24. White CL, Twigger KR, Vidal L, De Bono JS, Coffey M, Heinemann L*, et al.* Characterization of the adaptive and innate immune response to intravenous oncolytic reovirus (Dearing type 3) during a phase I clinical trial. Gene Therapy **2008**;15:911-20
25. Lolkema MP, Arkenau H-T, Harrington K, Roxburgh P, Morrison R, Roulstone V*, et al.* A Phase I Study of the Combination of Intravenous Reovirus Type 3 Dearing and Gemcitabine in Patients with Advanced Cancer. Clinical Cancer Research **2011**;17:581-8
26. Vidal L, Pandha HS, Yap TA, White CL, Twigger K, Vile RG*, et al.* A Phase I Study of Intravenous Oncolytic Reovirus Type 3 Dearing in Patients with Advanced Cancer. Clinical Cancer Research **2008**;14:7127-37
27. Comins C, Spicer J, Protheroe A, Roulstone V, Twigger K, White CM*, et al.* REO-10: A Phase I Study of Intravenous Reovirus and Docetaxel in Patients with Advanced Cancer. Clinical Cancer Research **2010**;16:5564-72
28. Shmulevitz M, Pan L-Z, Garant K, Pan D, Lee PWK. Oncogenic Ras Promotes Reovirus Spread by Suppressing IFN-β Production through Negative Regulation of RIG-I Signaling. Cancer Res **2010**;70:4912-21
29. Müller L, Berkeley R, Barr T, Ilett E, Errington-Mais F. Past, Present and Future of Oncolytic Reovirus. Cancers **2020**;12:3219
30. Cline BL. Ecological Associations of Vesicular Stomatitis Virus in Rural Central America and Panama. The American Journal of Tropical Medicine and Hygiene **1976**;25:875-83
31. Cook J, Peng KWW, Witzig TE, Broski SM, Villasboas JC, Paludo J*, et al.* Clinical Activity of Single Dose Systemic Oncolytic VSV Virotherapy in Patients with Relapsed Refractory T-Cell Lymphoma. Blood Advances **2022**;6:3268-79
32. Bishnoi S, Tiwari R, Gupta S, Byrareddy S, Nayak D. Oncotargeting by Vesicular Stomatitis Virus (VSV): Advances in Cancer Therapy. Viruses **2018**;10:90-
33. Schirrmacher V. Molecular Mechanisms of Anti-Neoplastic and Immune Stimulatory Properties of Oncolytic Newcastle Disease Virus. Biomedicines **2022**;10:562-
34. Pol J, Atherton M, Bridle B, Stephenson K, Le Boeuf F, Hummel J*, et al.* Development and applications of oncolytic Maraba virus vaccines. Oncolytic Virotherapy **2018**;Volume 7:117-28
35. Tanaka W, Komabayashi K, Ikeda Y, Aoki Y, Itagaki T, Mizuta K. Seroprevalence of coxsackievirus A21 neutralizing antibodies in Yamagata, Japan, between 1976 and 2019; coxsackievirus A21 has rarely affected young children. Journal of Medical Virology **2022**;94:2877-81
36. Andtbacka RHI, Curti B, Daniels GA, Hallmeyer S, Whitman ED, Lutzky J*, et al.* Clinical Responses of Oncolytic Coxsackievirus A21 (V937) in Patients With Unresectable Melanoma. Journal of Clinical Oncology **2021**;39:3829-38
37. Bradley S, Jakes AD, Harrington K, Pandha H, Melcher A, Errington-Mais F. Applications of coxsackievirus A21 in oncology. Oncolytic virotherapy **2014**;3:47-55
38. Li J, Zhang Z, Zhang H, Li M, Li X, Lu L*, et al.* Seroprevalence of poliovirus antibodies before and after polio vaccine switch in 2012 and 2017 in Beijing. Human Vaccines & Immunotherapeutics **2021**;17:389-96
39. Díaz-Quiñónez JA, Díaz-Ortega JL, Cruz-Hervert P, Ferreira-Guerrero E, Delgado-Sánchez G, Ferreyra-Reyes L*, et al.* Seroprevalence of Poliomyelitis Antibodies Among Children Aged 1 to 4 Years Old and Factors Associated With Poliovirus Susceptibility; Mexican Health and Nutrition Survey, 2012. Clinical infectious diseases : an official publication of the Infectious Diseases Society of America **2018**;67:S110-s4

40. Alfonso VH, Voorman A, Hoff NA, Weldon WC, Gerber S, Gadoth A*, et al.* Poliovirus immunity among adults in the Democratic Republic of the Congo: a cross-sectional serosurvey. BMC Infectious Diseases **2022**;22:30
41. Kemp V, van den Wollenberg DJM, Camps MGM, van Hall T, Kinderman P, Pronk-van Montfoort N*, et al.* Arming oncolytic reovirus with GM-CSF gene to enhance immunity. Cancer Gene Therapy **2018**
42. Groeneveldt C, van Hall T, van der Burg SH, Ten Dijke P, van Montfoort N. Immunotherapeutic Potential of TGF-β Inhibition and Oncolytic Viruses. Trends Immunol **2020**;41:406-20
43. Kooti W, Esmaeili Gouvarchin Ghaleh H, Farzanehpour M, Dorostkar R, Jalali Kondori B, Bolandian M. Oncolytic Viruses and Cancer, Do You Know the Main Mechanism? Front Oncol **2021**;11
44. Mullen JT, Tanabe KK. Viral Oncolysis. The Oncologist **2002**;7:106-19
45. Lemos de Matos A, Franco LS, McFadden G. Oncolytic Viruses and the Immune System: The Dynamic Duo. Molecular Therapy - Methods & Clinical Development **2020**;17:349-58
46. Russell L, Peng KW, Russell SJ, Diaz RM. Oncolytic Viruses: Priming Time for Cancer Immunotherapy. BioDrugs **2019**;33:485-501
47. de Graaf JF, de Vor L, Fouchier RAM, van den Hoogen BG. Armed oncolytic viruses: A kick-start for anti-tumor immunity. Cytokine & Growth Factor Reviews **2018**;41:28-39
48. Nguyen T, Avci NG, Shin DH, Martinez-Velez N, Jiang H. Tune Up In Situ Autovaccination against Solid Tumors with Oncolytic Viruses. Cancers **2018**;10:171
49. Russell SJ, Barber GN. Oncolytic Viruses as Antigen-Agnostic Cancer Vaccines. Cancer cell **2018**;33:599-605
50. Feola S, Russo S, Martins B, Lopes A, Vandermeulen G, Fluhler V*, et al.* Peptides-Coated Oncolytic Vaccines for Cancer Personalized Medicine. Frontiers in Immunology **2022**;13:1-16
51. Capasso C, Hirvinen M, Garofalo M, Romaniuk D, Kuryk L, Sarvela T*, et al.* Oncolytic adenoviruses coated with MHC-I tumor epitopes increase the antitumor immunity and efficacy against melanoma. Oncoimmunology **2016**;5:e1105429
52. Groeneveldt C, Kinderman P, van den Wollenberg DJM, van den Oever RL, Middelburg J, Mustafa DAM*, et al.* Preconditioning of the tumor microenvironment with oncolytic reovirus converts CD3-bispecific antibody treatment into effective immunotherapy. J Immunother Cancer **2020**;8:e001191
53. Groeneveldt C, Kinderman P, van Stigt Thans JJC, Labrie C, Griffioen L, Sluijter M*, et al.* Preinduced reovirus-specific T-cell immunity enhances the anticancer efficacy of reovirus therapy. Journal for ImmunoTherapy of Cancer **2022**;10:e004464
54. Shin DH, Nguyen T, Ozpolat B, Lang F, Alonso M, Gomez-Manzano C*, et al.* Current strategies to circumvent the antiviral immunity to optimize cancer virotherapy. Journal for ImmunoTherapy of Cancer **2021**;9:e002086-e
55. ClinicalTrials.gov. A Study of Intratumoral CAVATAK™ in Patients With Stage IIIc and Stage IV Malignant Melanoma (VLA-007 CALM). 2010.
56. Kaufman HL, Bommareddy PK. Two roads for oncolytic immunotherapy development. Journal for ImmunoTherapy of Cancer **2019**;7:26
57. Andtbacka RHI, Kaufman HL, Collichio F, Amatruda T, Senzer N, Chesney J*, et al.* Talimogene Laherparepvec Improves Durable Response Rate in Patients With Advanced Melanoma. Journal of Clinical Oncology **2015**;33:2780-8
58. Ribas A, Dummer R, Puzanov I, VanderWalde A, Andtbacka RHI, Michielin O*, et al.* Oncolytic Virotherapy Promotes Intratumoral T Cell Infiltration and Improves Anti-PD-1 Immunotherapy. Cell **2017**;170:1109-19 e10
59. Bourgeois-Daigneault MC, Roy DG, Aitken AS, El Sayes N, Martin NT, Varette O*, et al.* Neoadjuvant oncolytic virotherapy before surgery sensitizes triple-negative breast cancer to immune checkpoint therapy. Science translational medicine **2018**;10

60. Thurber GM, Schmidt MM, Wittrup KD. Antibody tumor penetration: Transport opposed by systemic and antigen-mediated clearance. Advanced Drug Delivery Reviews **2008**;60:1421-34
61. Hooks JJ, Burns W, Hayashi K, Geis S, Notkins AL. Viral spread in the presence of neutralizing antibody: mechanisms of persistence in foamy virus infection. Infection and Immunity **1976**;14:1172-8
62. Simmons A, Nash AA. Role of antibody in primary and recurrent herpes simplex virus infection. J Virol **1985**;53:944-8
63. Bramson JL, Hitt M, Gauldie J, Graham FL. Pre-existing immunity to adenovirus does not prevent tumor regression following intratumoral administration of a vector expressing IL-12 but inhibits virus dissemination. Gene Therapy **1997**;4:1069-76
64. Dhar D, Spencer JF, Toth K, Wold WSM. Effect of Preexisting Immunity on Oncolytic Adenovirus Vector INGN 007 Antitumor Efficacy in Immunocompetent and Immunosuppressed Syrian Hamsters. J Virol **2009**;83:2130-9
65. Herrlinger U, Kramm CM, Aboody-Guterman KS, Silver JS, Ikeda K, Johnston KM*, et al.* Pre-existing herpes simplex virus 1 (HSV-1) immunity decreases, but does not abolish, gene transfer to experimental brain tumors by a HSV-1 vector. Gene Therapy **1998**;5:809-19
66. Li X, Wang P, Li H, Du X, Liu M, Huang Q*, et al.* The Efficacy of Oncolytic Adenovirus Is Mediated by T-cell Responses against Virus and Tumor in Syrian Hamster Model. Clinical Cancer Research **2017**;23:239-49
67. Chahlavi A, Rabkin SD, Todo T, Sundaresan P, Martuza RL. Effect of prior exposure to herpes simplex virus 1 on viral vector-mediated tumor therapy in immunocompetent mice. Gene Therapy **1999**;6:1751-8
68. Lambright ES, Kang EH, Force S, Lanuti M, Caparrelli D, Kaiser LR*, et al.* Effect of Preexisting Anti-Herpes Immunity on the Efficacy of Herpes Simplex Viral Therapy in a Murine Intraperitoneal Tumor Model. Molecular Therapy **2000**;2:387-93
69. Burnett WJ, Burnett DM, Parkman G, Ramstead A, Contreras N, Gravley W*, et al.* Prior Exposure to Coxsackievirus A21 Does Not Mitigate Oncolytic Therapeutic Efficacy. Cancers **2021**;13:4462-
70. Davola ME, Mossman KL. Oncolytic viruses: how "lytic" must they be for therapeutic efficacy? OncoImmunology **2019**;8:e1581528
71. Annels NE, Mansfield D, Arif M, Ballesteros-Merino C, Simpson GR, Denyer M*, et al.* Phase I Trial of an ICAM-1-Targeted Immunotherapeutic-Coxsackievirus A21 (CVA21) as an Oncolytic Agent Against Non Muscle-Invasive Bladder Cancer. Clinical Cancer Research **2019**;25:5818-31
72. Andtbacka RHI, Curti BD, Kaufman H, Daniels GA, Nemunaitis JJ, Spitler LE*, et al.* Final data from CALM: A phase II study of Coxsackievirus A21 (CVA21) oncolytic virus immunotherapy in patients with advanced melanoma. Journal of Clinical Oncology **2015**;33:9030-
73. Andtbacka RHI, Ross MI, Agarwala SS, Taylor MH, Vetto JT, Neves RI*, et al.* Final results of a phase II multicenter trial of HF10, a replication-competent HSV-1 oncolytic virus, and ipilimumab combination treatment in patients with stage IIIB-IV unresectable or metastatic melanoma. Journal of Clinical Oncology **2017**;35:9510-
74. Bazan-Peregrino M, Garcia-Carbonero R, Laquente B, Álvarez R, Mato-Berciano A, Gimenez-Alejandre M*, et al.* VCN-01 disrupts pancreatic cancer stroma and exerts antitumor effects. Journal for ImmunoTherapy of Cancer **2021**;9:e003254-e
75. Kirn DH, Wang Y, Liang W, Contag CH, Thorne SH. Enhancing Poxvirus Oncolytic Effects through Increased Spread and Immune Evasion. Cancer Research **2008**;68:2071-5
76. Ferguson MS, Lemoine NR, Wang Y. Systemic Delivery of Oncolytic Viruses: Hopes and Hurdles. Advances in Virology **2012**;2012:1-14
77. Miest TS, Yaiw K-C, Frenzke M, Lampe J, Hudacek AW, Springfeld C*, et al.* Envelope-chimeric Entry-targeted Measles Virus Escapes Neutralization and Achieves Oncolysis. Molecular Therapy **2011**;19:1813-20

78. Xia M, Luo D, Dong J, Zheng M, Meng G, Wu J*, et al.* Graphene oxide arms oncolytic measles virus for improved effectiveness of cancer therapy. Journal of Experimental & Clinical Cancer Research **2019**;38:408-
79. Bah ES, Nace RA, Peng KW, Muñoz-Alía MÁ, Russell SJ. Retargeted and Stealth-Modified Oncolytic Measles Viruses for Systemic Cancer Therapy in Measles Immune Patients. Mol Cancer Ther **2020**;19:2057-67
80. Chen Y, Yu D-C, Charlton D, Henderson DR. Pre-Existent Adenovirus Antibody Inhibits Systemic Toxicity and Antitumor Activity of CN706 in the Nude Mouse LNCaP Xenograft Model: Implications and Proposals for Human Therapy. Human Gene Therapy **2000**;11:1553-67
81. Power AT, Wang J, Falls TJ, Paterson JM, Parato KA, Lichty BD*, et al.* Carrier Cell-based Delivery of an Oncolytic Virus Circumvents Antiviral Immunity. Molecular Therapy **2007**;15:123-30
82. Delman KA, Bennett JJ, Zager JS, Burt BM, McAuliffe PF, Petrowsky H*, et al.* Effects of Preexisting Immunity on the Response to Herpes Simplex-Based Oncolytic Viral Therapy. Human Gene Therapy **2000**;11:2465-72
83. Adair RA, Roulstone V, Scott KJ, Morgan R, Nuovo GJ, Fuller M*, et al.* Cell Carriage, Delivery, and Selective Replication of an Oncolytic Virus in Tumor in Patients. Science Translational Medicine **2012**;4
84. Ilett EJ, Bárcena M, Errington-Mais F, Griffin S, Harrington KJ, Pandha HS*, et al.* Internalization of Oncolytic Reovirus by Human Dendritic Cell Carriers Protects the Virus from Neutralization. Clinical Cancer Research **2011**;17:2767-76
85. Ilett E, Kottke T, Donnelly O, Thompson J, Willmon C, Diaz R*, et al.* Cytokine Conditioning Enhances Systemic Delivery and Therapy of an Oncolytic Virus. Molecular Therapy **2014**;22:1851-63
86. Ilett EJ, Prestwich RJ, Kottke T, Errington F, Thompson JM, Harrington KJ*, et al.* Dendritic cells and T cells deliver oncolytic reovirus for tumour killing despite pre-existing anti-viral immunity. Gene Therapy **2009**;16:689-99
87. Ong HT, Hasegawa K, Dietz AB, Russell SJ, Peng KW. Evaluation of T cells as carriers for systemic measles virotherapy in the presence of antiviral antibodies. Gene Therapy **2007**;14:324-33
88. Zhou Y-C, Zhang Y-N, Yang X, Wang S-B, Hu P-Y. Delivery systems for enhancing oncolytic adenoviruses efficacy. International Journal of Pharmaceutics **2020**;591:119971-
89. Batalla-Covello J, Ngai HW, Flores L, McDonald M, Hyde C, Gonzaga J*, et al.* Multiple Treatment Cycles of Neural Stem Cell Delivered Oncolytic Adenovirus for the Treatment of Glioblastoma. Cancers **2021**;13:6320-
90. Berkeley RA, Steele LP, Mulder AA, van den Wollenberg DJM, Kottke TJ, Thompson J*, et al.* Antibody-Neutralized Reovirus Is Effective in Oncolytic Virotherapy. Cancer Immunology Research **2018**;6:1161-73
91. Leopold PL, Wendland RL, Vincent T, Crystal RG. Neutralized Adenovirus-Immune Complexes Can Mediate Effective Gene Transfer via an Fc Receptor-Dependent Infection Pathway. J Virol **2006**;80:10237-47
92. Yang X, Zhang X, Zhao X, Yuan M, Zhang K, Dai J*, et al.* Antibody-Dependent Enhancement: "Evil" Antibodies Favorable for Viral Infections. Viruses **2022**;14
93. Mok DZL, Chan KR. The Effects of Pre-Existing Antibodies on Live-Attenuated Viral Vaccines. Viruses **2020**;12:520
94. Montagnaro S, Damiano S, Ciarcia R, Puzio MV, Ferrara G, Iovane V*, et al.* Caprine herpesvirus 1 (CpHV-1) as a potential candidate for oncolytic virotherapy. Cancer Biol Ther **2019**;20:42-51
95. Forte IM, Indovina P, Montagnaro S, Costa A, Iannuzzi CA, Capone F*, et al.* The Oncolytic Caprine Herpesvirus 1 (CpHV-1) Induces Apoptosis and Synergizes with Cisplatin in Mesothelioma Cell Lines: A New Potential Virotherapy Approach. Viruses **2021**;13:2458-

96. Bots STF, Kemp V, Cramer SJ, van den Wollenberg DJM, Hornsveld M, Lamfers MLM*, et al.* Nonhuman Primate Adenoviruses of the Human Adenovirus B Species Are Potent and Broadly Acting Oncolytic Vector Candidates. Human Gene Therapy **2022**;33:275-89
97. Kozak R, Hattin L, Biondi M, Corredor J, Walsh S, Xue-Zhong M*, et al.* Replication and Oncolytic Activity of an Avian Orthoreovirus in Human Hepatocellular Carcinoma Cells. Viruses **2017**;9:90-
98. Koppers-Lalic D, Hoeben RC. Non-human viruses developed as therapeutic agent for use in humans. Rev Med Virol **2011**;21:227-39
99. Hoeben RC, Louz D, Koppers-Lalic D. Biosafety of non-human therapeutic viruses in clinical gene therapy. Curr Gene Ther **2013**;13:492-9
100. Tuzmen C, Cairns TM, Atanasiu D, Lou H, Saw WT, Hall BL*, et al.* Point Mutations in Retargeted gD Eliminate the Sensitivity of EGFR/EGFRvIII-Targeted HSV to Key Neutralizing Antibodies. Molecular Therapy - Methods & Clinical Development **2020**;16:145-54
101. Neault S, Bossow S, Achard C, Bell JC, Diallo JS, Leber MF*, et al.* Robust envelope exchange platform for oncolytic measles virus. Journal of Virological Methods **2022**;302:114487-
102. Roberts DM, Nanda A, Havenga MJE, Abbink P, Lynch DM, Ewald BA*, et al.* Hexon-chimaeric adenovirus serotype 5 vectors circumvent pre-existing anti-vector immunity. Nature **2006**;441:239-43
103. Zafar S, Quixabeira DCA, Kudling TV, Cervera-Carrascon V, Santos JM, Grönberg-Vähä-Koskela S*, et al.* Ad5/3 is able to avoid neutralization by binding to erythrocytes and lymphocytes. Cancer Gene Therapy **2021**;28:442-54
104. Stepanenko AA, Sosnovtseva AO, Valikhov MP, Chernysheva AA, Cherepanov SA, Yusubalieva GM*, et al.* Superior infectivity of the fiber chimeric oncolytic adenoviruses Ad5/35 and Ad5/3 over Ad5-delta-24-RGD in primary glioma cultures. Molecular Therapy - Oncolytics **2022**;24:230-48
105. Rojas LA, Condezo GN, Moreno R, Fajardo CA, Arias-Badia M, San Martín C*, et al.* Albumin-binding adenoviruses circumvent pre-existing neutralizing antibodies upon systemic delivery. Journal of Controlled Release **2016**;237:78-88
106. Naito T, Kaneko Y, Kozbor D. Oral vaccination with modified vaccinia virus Ankara attached covalently to TMPEG-modified cationic liposomes overcomes pre-existing poxvirus immunity from recombinant vaccinia immunization. Journal of General Virology **2007**;88:61-70
107. Nosaki K, Hamada K, Takashima Y, Sagara M, Matsumura Y, Miyamoto S*, et al.* A novel, polymer-coated oncolytic measles virus overcomes immune suppression and induces robust antitumor activity. Molecular Therapy - Oncolytics **2016**;3:16022-
108. Huang H, Sun M, Liu M, Pan S, Liu P, Cheng Z*, et al.* Full encapsulation of oncolytic virus using hybrid erythroctye-liposome membranes for augmented anti-refractory tumor effectiveness. Nano Today **2022**;47:101671
109. Tysome JR, Li X, Wang S, Wang P, Gao D, Du P*, et al.* A Novel Therapeutic Regimen to Eradicate Established Solid Tumors with an Effective Induction of Tumor-Specific Immunity. Clinical Cancer Research **2012**;18:6679-89
110. Irvine KR, Chamberlain RS, Shulman EP, Surman DR, Rosenberg SA, Restifo NP. Enhancing Efficacy of Recombinant Anticancer Vaccines With Prime/Boost Regimens That Use Two Different Vectors. JNCI Journal of the National Cancer Institute **1997**;89:1595-601
111. Fazekas de St.Groth S, Webster RG. Disquisitions on Original Antigenic Sin. Journal of Experimental Medicine **1966**;124:331-45
112. Zhang A, Stacey HD, Mullarkey CE, Miller MS. Original Antigenic Sin: How First Exposure Shapes Lifelong Anti-Influenza Virus Immune Responses. J Immunol **2019**;202:335-40
113. Shirley JL, de Jong YP, Terhorst C, Herzog RW. Immune Responses to Viral Gene Therapy Vectors. Mol Ther **2020**;28:709-22
114. Schirmbeck R, Reimann J, Kochanek S, Kreppel F. The Immunogenicity of Adenovirus Vectors Limits the Multispecificity of CD8 T-cell Responses to Vector-encoded Transgenic Antigens. Molecular Therapy **2008**;16:1609-16

115. Altenburg AF, van Trierum SE, de Bruin E, de Meulder D, van de Sandt CE, van der Klis FRM*, et al.* Effects of pre-existing orthopoxvirus-specific immunity on the performance of Modified Vaccinia virus Ankara-based influenza vaccines. Scientific Reports **2018**;8:6474-
116. Frahm N, DeCamp AC, Friedrich DP, Carter DK, Defawe OD, Kublin JG*, et al.* Human adenovirus-specific T cells modulate HIV-specific T cell responses to an Ad5-vectored HIV-1 vaccine. Journal of Clinical Investigation **2012**;122:359-67
117. Buchbinder SP, Mehrotra DV, Duerr A, Fitzgerald DW, Mogg R, Li D*, et al.* Efficacy assessment of a cell-mediated immunity HIV-1 vaccine (the Step Study): a double-blind, randomised, placebo-controlled, test-of-concept trial. The Lancet **2008**;372:1881-93
118. Ledgerwood JE, Costner P, Desai N, Holman L, Enama ME, Yamshchikov G*, et al.* A replication defective recombinant Ad5 vaccine expressing Ebola virus GP is safe and immunogenic in healthy adults. Vaccine **2010**;29:304-13
119. Pol JG, Zhang L, Bridle BW, Stephenson KB, Rességuier J, Hanson S*, et al.* Maraba Virus as a Potent Oncolytic Vaccine Vector. Molecular Therapy **2014**;22:420-9
120. ClinicalTrials.gov. MG1 Maraba/MAGE-A3, With and Without Adenovirus Vaccine With Transgenic MAGE-A3 Insertion in Incurable MAGE-A3-Expressing Solid Tumours - Full Text View - ClinicalTrials.gov. 2014.
121. ClinicalTrials.gov. Oncolytic MG1-MAGEA3 With Ad-MAGEA3 Vaccine in Combination With Pembrolizumab for Non-Small Cell Lung Cancer Patients - Full Text View - ClinicalTrials.gov. 2016.
122. Ricca JM, Oseledchyk A, Walther T, Liu C, Mangarin L, Merghoub T*, et al.* Pre-existing Immunity to Oncolytic Virus Potentiates Its Immunotherapeutic Efficacy. Molecular Therapy **2018**;26:1008-19
123. Ding J, Murad YM, Sun Y, Lee IF, Samudio I, Liu X*, et al.* Pre-Existing HSV-1 Immunity Enhances Anticancer Efficacy of a Novel Immune-Stimulating Oncolytic Virus. Viruses **2022**;14:2327-
124. Borst J, Ahrends T, Bąbała N, Melief CJM, Kastenmüller W. CD4+ T cell help in cancer immunology and immunotherapy. Nature Reviews Immunology **2018**;18:635-47
125. Kumamoto Y, Mattei LM, Sellers S, Payne GW, Iwasaki A. CD4 + T cells support cytotoxic T lymphocyte priming by controlling lymph node input. Proceedings of the National Academy of Sciences **2011**;108:8749-54
126. Tähtinen S, Feola S, Capasso C, Laustio N, Groeneveldt C, Ylösmäki EO*, et al.* Exploiting Preexisting Immunity to Enhance Oncolytic Cancer Immunotherapy. Cancer Research **2020**;80:2575-85
127. Brown MC, McKay ZP, Yang Y, Beasley GM, Ashley DM, Bigner DD*, et al.* Intratumor Childhood Vaccine-Specific $CD4^+$ T cell Recall Coordinates Antitumor $CD8^+$ T cells and Eosinophils. bioRxiv **2022**:2022.03.14.484260
128. Rosato PC, Wijeyesinghe S, Stolley JM, Nelson CE, Davis RL, Manlove LS*, et al.* Virus-specific memory T cells populate tumors and can be repurposed for tumor immunotherapy. Nature Communications **2019**;10:567
129. Simoni Y, Becht E, Fehlings M, Loh CY, Koo SL, Teng KWW*, et al.* Bystander $CD8^+$ T cells are abundant and phenotypically distinct in human tumour infiltrates. Nature **2018**;557:575-9
130. Cao D, Song Q, Li J, Chard Dunmall LS, Jiang Y, Qin B*, et al.* Redirecting anti-Vaccinia virus T cell immunity for cancer treatment by AAV-mediated delivery of the VV B8R gene. Molecular Therapy - Oncolytics **2022**;25:264-75
131. Çuburu N, Bialkowski L, Pontejo SM, Sethi SK, Bell ATF, Kim R*, et al.* Harnessing anti-cytomegalovirus immunity for local immunotherapy against solid tumors. Proc Natl Acad Sci U S A **2022**;119:e2116738119
132. Millar DG, Ramjiawan RR, Kawaguchi K, Gupta N, Chen J, Zhang S*, et al.* Antibody-mediated delivery of viral epitopes to tumors harnesses CMV-specific T cells for cancer therapy. Nature Biotechnology **2020**;38:420-5

133. Sefrin JP, Hillringhaus L, Mundigl O, Mann K, Ziegler-Landesberger D, Seul H*, et al.* Sensitization of Tumors for Attack by Virus-Specific CD8+ T-Cells Through Antibody-Mediated Delivery of Immunogenic T-Cell Epitopes. **2019**;10
134. Jung K, Son M-J, Lee S-Y, Kim J-A, Ko D-H, Yoo S*, et al.* Antibody-mediated delivery of a viral MHC-I epitope into the cytosol of target tumor cells repurposes virus-specific CD8+ T cells for cancer immunotherapy. Molecular Cancer **2022**;21:102
135. Chiaro J, Kasanen HHE, Whalley T, Capasso C, Grönholm M, Feola S*, et al.* Viral Molecular Mimicry Influences the Antitumor Immune Response in Murine and Human Melanoma. Cancer Immunol Res **2021**;9:981-93
136. Chaganty BKR, Qiu S, Lu Y, Lopez-Berestein G, Ozpolat B, Fan Z. Redirecting host preexisting influenza A virus immunity for cancer immunotherapy. Cancer Immunology, Immunotherapy **2022**;71:1611-23
137. Aznar MA, Molina C, Teijeira A, Rodriguez I, Azpilikueta A, Garasa S*, et al.* Repurposing the yellow fever vaccine for intratumoral immunotherapy. EMBO Mol Med **2020**;12:1-17
138. Gujar S, Pol JG, Kim Y, Kroemer G. Repurposing $CD8^+$ T cell immunity against SARS-CoV-2 for cancer immunotherapy: a positive aspect of the COVID-19 pandemic? Oncoimmunology **2020**;9:1794424
139. Ordóñez-Reyes C, Garcia-Robledo JE, Chamorro DF, Mosquera A, Sussmann L, Ruiz-Patiño A*, et al.* Bispecific Antibodies in Cancer Immunotherapy: A Novel Response to an Old Question. Pharmaceutics **2022**;14:1243-
140. Conti M. Boosting effect of pre-existing immunity on anti-cancer immunotherapies. Frontiers in Drug, Chemistry and Clinical Research **2021**;4:1-6
141. Niemann J, Woller N, Brooks J, Fleischmann-Mundt B, Martin NT, Kloos A*, et al.* Molecular retargeting of antibodies converts immune defense against oncolytic viruses into cancer immunotherapy. Nature Communications **2019**;10:3236-
142. Pinto S, Pahl J, Schottelius A, Carter PJ, Koch J. Reimagining antibody-dependent cellular cytotoxicity in cancer: the potential of natural killer cell engagers. Trends in Immunology **2022**;43:932-46
143. Heidbuechel JPW, Engeland CE. Oncolytic viruses encoding bispecific T cell engagers: a blueprint for emerging immunovirotherapies. Journal of Hematology & Oncology **2021**;14:63
144. Rosenbaum P, Tchitchek N, Joly C, Rodriguez Pozo A, Stimmer L, Langlois S*, et al.* Vaccine Inoculation Route Modulates Early Immunity and Consequently Antigen-Specific Immune Response. Frontiers in Immunology. Volume 122021. p 645210.



CHAPTER 5

Neutralizing antibodies impair the efficacy of reovirus as oncolytic agent but permit effective combination with T-cell-based immunotherapy

Christianne Groeneveldt[1], Priscilla Kinderman[2], Lisa Griffioen[1], Olivia Rensing[2], Camilla Labrie[1], Diana J. M. van den Wollenberg[3], Rob C. Hoeben[3], Matt Coffey[4], Houra Loghmani[4], Els M. E. Verdegaal[1], Marij J. P. Welters[1], Sjoerd H. van der Burg[1], Thorbald van Hall[1] and Nadine van Montfoort[2]

[1] Department of Medical Oncology, Oncode Institute, Leiden University Medical Center, 2333 ZA, Leiden, The Netherlands

[2] Department of Gastroenterology and Hepatology, Leiden University Medical Center, 2333 ZA, Leiden, The Netherlands

[3] Department of Cell and Chemical Biology, Leiden University Medical Center, 2300 RC, Leiden, The Netherlands

[4] Oncolytics Biotech Incorporated, Calgary, AB, Canada

[#] Corresponding author

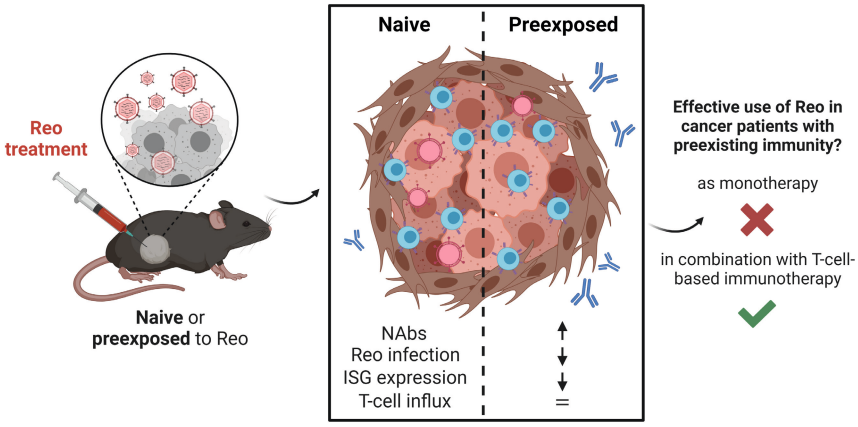
Manuscript submitted

ABSTRACT

Oncolytic reovirus type 3 Dearing (Reo) is an attractive anticancer agent for the treatment of solid tumors. Direct killing of tumor cells (oncolysis) as well as induction of intratumoral T-cell influx contribute to its anticancer efficacy. Since the majority of the human population has been preexposed to Reo, neutralizing antibodies (NAbs) are prevalent in cancer patients and might present a barrier to effective Reo therapy. Here, we confirmed that NAbs are present in the majority of cancer patients and thus investigated the effect of preexposure-induced and therapy-induced NAbs on the anticancer efficacy of Reo therapy in preclinical mouse models. The presence of preexposure-induced NAbs reduced Reo tumor infection and the expression of interferon-stimulated genes in immunocompetent mice and prevented Reo-mediated control of tumor growth. In B-cell deficient mice, the lack of NAbs provided enhanced tumor growth control after Reo monotherapy. Importantly, the intratumoral T-cell influx was not affected by the presence of preexposure-induced or therapy-induced NAbs. Consequently, combinatorial antitumor strategies comprising Reo and T-cell-engagers or checkpoint inhibitors remained effective in these settings. Altogether, our data provide preclinical evidence that NAbs hamper the efficacy of Reo when used as oncolytic agent, but that potent antitumor responses induced by combined Reo and T-cell-based immunotherapy can still be achieved. Given the high prevalence of seropositivity for Reo in cancer patients, these data strongly advocate for the use of Reo as part of a T-cell-based combinatorial approach to unleash its full potential and allow maximal anticancer efficacy, without obstruction by preexisting immune responses.

Synopsis: The presence of neutralizing antibodies hampers the oncolytic function of reovirus, but not its T-cell-attracting capacity. Since the majority of humans has been preexposed to reovirus, this implicates that reovirus should exclusively be used as part of T-cell-based immunotherapeutic strategies to ensure optimal efficacy in cancer patients.

GRAPHICAL ABSTRACT



INTRODUCTION

Oncolytic viruses (OVs) represent a highly promising treatment strategy for a wide range of cancers, by mediating both the direct killing of tumor cells as well as the induction of potent immune responses. These immunostimulatory properties of OVs can be exploited to convert a cold tumor-microenvironment (TME) of solid tumors into a T-cell-infiltrated TME, leading to an increased response to other forms of immunotherapy (1). Oncolytic reovirus type 3 Dearing (Reo) is one of the leading OVs for clinical development (2). In our previous studies using the preclinical murine pancreatic KPC3 tumor model, Reo demonstrated great immunostimulatory potential by inducing a strong interferon response in these tumors, which subsequently attracted a wave of $CD8^+$ T cells. These immunostimulatory characteristics enabled Reo to significantly enhance the efficacy of otherwise unsuccessful CD3-bispecific antibody therapy in these tumors (3).

In the clinic, Reo is often administered intravenously and has demonstrated limited potential when applied as monotherapy (4-6). Although various aspects might contribute to this limited efficacy, one potential barrier to the clinical success of Reo is preexisting immunity against the virus (7). The majority of individuals have acquired preexisting immunity against reovirus after non-symptomatic exposure, indicated by the detection of neutralizing antibodies (NAbs) in patient sera before treatment with Reo (5,8-12). It was demonstrated that Reo can still reach the TME in the presence of NAbs, which was explained by Reo cell carriage via circulating immune cells (13). Since additional studies demonstrated that the uptake and delivery of Reo particles to the tumor via these cellular carriers was enhanced in the presence of NAbs (14,15), this may have led to a common belief that NAbs do not represent a barrier and may even be beneficial for reovirus therapy. But, to the best of our knowledge, a direct comparison of the antitumor efficacy of Reo therapy in settings with and without preexisting NAbs has not been performed.

To this purpose, we developed an experimental setting in immunocompetent mice to study the effect of preexposure- or therapy-induced NAbs on both the oncolytic, as well as the immunostimulatory capacity of Reo. NAbs hampered Reo infection and the Reo-induced expression of interferon-stimulated genes (ISGs), and prevented Reo-mediated control of tumor growth. However, NAbs did not impair the Reo-induced intratumoral T-cell influx and T-cell-based viro-immunotherapeutic combination strategies remained effective, even in the context of clinically preferred intravenous administration. Combined, this study demonstrates that preexisting immunity is detrimental to Reo monotherapy, but Reo can still be employed to sustain effective T-cell-based immunotherapy.

MATERIAL & METHODS

Serum from healthy volunteers and cancer patients

Serum samples from the various cancer patient cohorts were obtained during various Phase I/II studies that were approved by the Medical Ethics Committee of the LUMC, and all patients gave written informed consent before inclusion in the respective studies. The use of serum samples and corresponding geographical data (gender, age) from these cohorts was approved by the LUMC Biobank Review Committee under reference number RP23.023. Patients with recurrent Epithelial Ovarian Cancer from the 'Ovarium Carcinoma' cohort (study number NCT01637532) were treated to evaluate the safety and feasibility of tocilizumab in combination with carboplatin/(pegylated liposomal) doxorubicin and interferon-α2b (Peg-Intron) (16). Patients in the 'Melanoma' cohort (study number P04.085) were treated with adoptive T-cell transfer consisting of tumor-reactive autologous T cells (17). Patients from the 'Cervical Carcinoma' cohort were included in the CIRCLE study investigating cellular immunity against anogenital lesions (18). Patients with metastatic colorectal cancer from the 'Colon Carcinoma' cohort (study number ISRCTN43704292) were enrolled in a phase I/II trial investigating the safety and efficacy of a p53-synthetic long peptide (SLP) vaccine (19). Serum from healthy donors was obtained through the Leiden University Medical Center (LUMC) Voluntary Donor Service (LuVDS, Leiden, The Netherlands) after ethical approval under reference number LuVDS22.049. The age of healthy donors was matched to the age range within the cancer patient cohorts.

Reovirus

The wild-type reovirus strain R124 (here referred to as Reo) was previously isolated from a heterogeneous reovirus Type 3 Dearing (T3D) stock (VR-824) obtained from the American Type Culture Collection (ATCC) by two rounds of plaque purification using HER911 cells (20). All experiments were performed using cesium chloride (CsCl)-purified stocks as described earlier (3). The total amount of particles was calculated based on OD_{260} values where 1 OD equals $2.10x10^{12}$ reovirus particles/mL (21), and the infectious titer was quantified by plaque assay on HER911 cells (22). Clinical-grade Reo (Pelareorep) was provided by Oncolytics Biotech Incorporated (Calgary, AB, Canada).

Cell lines

The murine pancreatic cancer cell line KPC3 (RRID:CVCL_A9ZK) is a low-passage derivate of a primary KPC tumor with mutant *trp53* and *K-ras* from a female C57BL/6 mouse (3,23). KPC3.TRP1 cells (RRID:CVCL_A9ZL) were generated as described (24) and selected for expression of tyrosine-related protein (TRP1) by cell sorting using an αTRP1 antibody (clone: TA99). The MC38 cell line (RRID: CVCL_B288) is a chemically-induced murine colon carcinoma and was obtained from Prof. F. Ossendorp (Leiden University Medical Center, The Netherlands). The human breast cancer cell line BT474 (RRID:CVCL_0179) was purchased from the ATCC (ATCC-HTB-20). KPC3(.TRP1), MC38, and BT474 cells were cultured at 37 °C in a humidified atmosphere containing 5% CO_2

in Iscove's Modified Dulbecco's Medium (IMDM; Gibco) supplemented with 8% fetal calf serum (FCS; Bodinco, Alkmaar, The Netherlands), 2mM L-glutamine (Gibco), 100 U/mL penicillin and 100 µg/mL streptomycin (Gibco). The human embryonic retinoblast cell line HER911 (RRID:CVCL_1K15) was cultured in Dulbecco's Modified Eagle's Medium (DMEM; Gibco), supplemented as described above. The tumor cell line TC1 (RRID:CVCL_4699) expresses the HPV16-derived oncogenes E6 and E7 and activated Ras oncogene and was cultured in IMDM medium as described above but with the addition of 400 µg/ml Geneticin (G418; Life Technologies), 1% nonessential amino acids (Life Technologies), and 1 mM sodium pyruvate (Life Technologies) (25). Cell lines were assured to be free of *Mycoplasma* by regular PCR analysis. The authentication of the cell lines was done by Short Tandem Repeat (STR) profiling (IDEXX BioAnalytics, Ludwigsburg, Germany) and only cells of low passage number were used for experiments.

Antibodies for in vivo administration

The CD3xTRP1 bispecific antibody (bsAb) used is a knob-into-hole bispecific based on murine IgG2a with an Fc Silent™ mutation, featuring one arm with an anti-mouse CD3e scFv based on the clone 145-2C11, and the other arm containing the TA99 clone directed against TRP1 (bAb0136; Absolute Antibody). PD-L1 blockade was performed using a PD-L1-blocking antibody (clone 10F.9G2; GoInVivo™ Purified anti-mouse CD274 Antibody; BioLegend). αCD20 antibodies (clone 18B12) were obtained from Absolute Antibody, and αCD8 (clone 2.43), αCD4 (GK1.5) and αNK1.1 (clone PK136) antibodies were all obtained from BioXcell.

Animal experiments

Male C57BL/6J mice (RRID:IMSR_JAX:000664) (6-8 weeks old) were purchased from Charles River Laboratories (France). Male B6.129S2-Ighm^{tm1Cgn}/J mice (µMT) (RRID:IMSR_JAX:002288) (6-8 weeks old) were purchased from The Jackson Laboratory. Male and female nonobese diabetic (NOD).Cg-Prkdc^{scid}Il2rg^{tm1Wjl}/SzJ (NSG) mice (RRID:IMSR_JAX:005557) (6-16 weeks old) were obtained from The Jackson Laboratory and maintained at the breeding facility of the LUMC in Leiden, The Netherlands. All mouse experiments were individually prepared, reviewed, ethically approved, and registered by the institutional Animal Welfare Body of the LUMC and carried out under project license AVD1160020187004, issued by the competent authority on animal experiments in The Netherlands (named CCD). Experiments were performed following the Dutch Act on Animal Experimentation and EU Directive 2010/63/EU ("On the protection of animals used for scientific purposes") at the animal facility of the LUMC. Mice were housed in individually ventilated cages with no more than 5 mice/cage and experiments were initiated after one week of acclimatization after transport.

For preexposure, mice were injected intravenously with 10^7 plaque-forming units (pfu) of Reo in a volume of 100 µL phosphate-buffered saline (PBS, Fresenius Kabi) at two consecutive times with a 2-week interval. In depletion experiments, depletion using αCD20, αNK, αCD8, or αCD4 antibodies (100 µg in 100 µL PBS, intraperitoneally (i.p.))

was initiated 5 and 2 days before the first Reo preexposure, and hereafter depletion was maintained by weekly injections until indicated. Alternatively, αCD4 injections were initiated before the second Reo preexposure or before tumor challenge. Depletion of designated cell populations was verified by flow cytometry before mice received further interventions.

After preexposure or at the start of the experiment, mice were inoculated in the right flank with subcutaneous KPC3(.TRP1) tumors ($1x10^5$ cells in 100 µL PBS/0.1% bovine serum albumin (BSA, Sigma-Aldrich) or MC38 tumors ($5x10^5$ cells in 200 µL PBS/0.1% BSA). BT474 tumors were orthotopically engrafted by injecting $5x10^6$ cells in a volume of 100 µL 1:1 (v/v) PBS/0.1% BSA : Growth Factor Reduced matrigel (Corning®) in the fourth mammary fat pad of isoflurane-anesthetized female NSG mice. Mice with palpable tumors were allocated into groups with similar average tumor volumes and assigned a treatment regimen. Intratumoral Reo administration was performed under isoflurane anesthesia by injection of 10^7 pfu of Reo or PBS as a control in a volume of 30 µL on 3 consecutive days unless otherwise indicated. Intravenous Pelareorep administration was performed by injection of $2x10^8$ pfu of Pelareorep in a volume of 100 µL PBS in the tail vein on indicated days, with 5-day intervals. Treatment with CD3xTRP1 bsAbs consisted of 3 i.p. injections of 12.5 µg antibody in 100 µL PBS, given every other day or with 5-day intervals. αPD-L1 antibodies were administered on indicated days by i.p. injection of 200 µg antibody in 100 µL PBS.

Cages were randomly allocated to a certain treatment group by an independent researcher and treatments were given in a different order each time. During all experiments, tumor size and/or body weight were measured 3 times a week in 3 dimensions using a caliper, in a blinded manner concerning preexposure status, genotype, or depletion group when possible. Blood was collected in lithium heparin-coated microvettes (Sarstedt) from the tail vein on indicated days for interim analysis of immune cells. Plasma was obtained by centrifugation (14.000 rpm, 15 min, 4 °C) and stored at -80 °C for assessment of neutralizing antibodies. For tumor growth experiments, mice were sacrificed when the tumor volume exceeded 1000 mm^3 or when ulceration occurred. Therapy response was determined as follows: NR = no response; CR = complete response and PR = partial response (regression or constant tumor volumes for at least 7 days). For intratumoral analysis experiments, mice were sacrificed at indicated days after treatment, and tumors, spleens, tumor-draining lymph nodes (TDLN), and blood were collected. Tumors were divided into representative parts, which were either snap-frozen in liquid N2 and stored at -80 °C until further analysis, fixed in 4% formaldehyde (AddedPharma) for immunohistochemistry or immediately processed to single cells suspensions to analyze the cellular composition by flow cytometry.

Neutralization assay

HER911 cells were seeded in flat-bottom 96-well plates in a density of $1x10^4$ cells/well and allowed to adhere overnight in the incubator (37 °C, 5% CO_2, 90% humidity). The next day, human serum samples or murine plasma samples were heat-inactivated by incubation at 56 °C for 30 minutes. For human serum samples, a two-fold dilution series (starting with 1:5) was prepared in DMEM with 2% FCS. Nanogam® (Sanquin, Amsterdam, The Netherlands), a pool of immunoglobulins of >1000 donors, was used as a positive control. For murine plasma samples, a 2-fold or 4-fold dilution series was prepared (starting with 1:25, 1:50, or 1:100) in DMEM with 2% FCS. Serum or plasma samples were mixed with 150 pfu/well of Reo and incubated for 30 minutes at 37 °C to allow the binding of NAbs to Reo particles. Next, the serum/plasma:Reo samples were transferred in duplo onto the HER911 cells. Cell growth was determined at 3 days post-infection by crystal violet staining. In short, cells were fixed with ice-cold methanol (Merck) for 10 minutes at -20 °C. Hereafter, cells were incubated with 0.5% crystal violet (Sigma-Aldrich) in 20% methanol for 20 minutes at room temperature (RT). Plates were extensively washed with H_2O and air dried. After drying, plates were incubated with 100 uL of methanol for 20 minutes at RT before measuring the optical density (OD) at 570 nm using a SpectraMax iD3 multi-mode plate reader (Molecular Devices). The measured OD_{570} value of the positive (Reo only) control was set to 100% and that of the negative (medium only) control to 0%. The OD_{570} of the samples were normalized using these controls and IC_{50} values were calculated using nonlinear regression analysis and sera with IC_{50} < 10 were regarded as negative.

Cell preparation and flow cytometry

Tumors were minced in small pieces and incubated with Liberase TL (Roche) for 15 minutes at 37 °C. The reaction was stopped by the addition of culture medium with 8% FCS and the mixture was gently dissociated into a single-cell suspension over a cell strainer (Corning). Spleens and TDLNs were dissociated into a single-cell suspension over a cell strainer. Blood and splenocytes were incubated with lysis buffer (Pharmacy LUMC) for 3 minutes at RT to remove all red blood cells before use. Cells were incubated with Zombie AquaTM Fixable Viability Dye (BioLegend) in PBS for 20 minutes at RT followed by incubation with 2.4G2 FcR blocking antibodies (clone 2.4G2; BD Biosciences) in FACS buffer (PBS, 0.5% BSA, and 1% sodium azide) for 20 minutes on ice. If applicable, cells were incubated with Reo $\mu1_{133\text{-}140}$ tetramer (Tm) conjugated to APC or the Reo $\mu1_{422\text{-}430}$ Tm conjugated to PE (both generated *in-house*) for 1 hour at RT in FACS buffer, after which surface markers (**Table S1**) were added directly to the tetramer mixture and incubated for 30 minutes at RT. After completion of the staining protocol, samples were fixed in 1% paraformaldehyde (Pharmacy LUMC) and acquired using a BD LSRFortessa™ X20 4L cell analyzer (BD Biosciences, San Jose, CA, USA) at the Flow cytometry Core Facility (FCF) of the LUMC (https://www.lumc.nl/research/facilities/fcf). Data were analyzed using FlowJo™ Software Version 10 (Becton, Dickinson, and Company). Opt-SNE plots (26) were generated using standard settings in OMIQ data analysis software (Omiq, Inc. www.omiq.ai).

Intracellular cytokine staining

Ex vivo tumor single-cell suspensions were cocultured with Reo-infected TC1 cells (MOI 10) or Reo-derived peptides (1 µg/mL) to assess recognition. Sequences of Reo-derived peptides (**Table S2**) were obtained from a study by Murphy *et al* where the MHC-I ligandome of Reo-infected ovarian surface epithelial cells (ID8; H2-K^b/H2-D^b) was investigated using comparative mass spectrometry (27). Identified Reo-derived peptides were ordered as a micro-scale crude peptide library (GenScript, Leiden, The Netherlands). Effector cells and target cells or peptides were cocultured for 6 hours in the presence of BD GolgiPlug™ (BD Biosciences). PMA (20 ng/mL) and ionomycin (1 µg/mL) were used as a positive control. After incubation, cells were washed and stained for CD8α (clone 53-6.7; BioLegend). Thereafter, cells were fixed with Fixation Buffer (BioLegend) according to the manufacturer's instructions, followed by staining for intracellular IFNγ (clone XMG1.2; BioLegend). After completion of the staining protocol, samples were fixed in 1% paraformaldehyde and acquired using the BD LSRFortessa™ X20 4L cell analyzer.

Western blotting

The presence of antibodies against Reo proteins in the plasma of naive or preexposed mice was investigated by Western blotting. HER911 cells were infected with reovirus (multiplicity of infection = 10) for 24 hours, after which cells were lysed in radioimmunoprecipitation assay (RIPA) buffer (Bioke) containing protease and phosphatase inhibitors (ThermoFisher Scientific). Proteins (10-15 µg) were separated on a 4-15% mini-protean TGX gel (Bio-Rad) and then transferred to a 0.2 µM nitrocellulose membrane (Bio-Rad). After blocking for 1 hour at RT with Pierce™ Protein-Free Blocking Buffer (ThermoFisher Scientific), the membrane was incubated overnight at 4°C with pooled plasma from preexposed or naive mice (n=5-6) (1:200). As a positive control, the membrane was incubated with anti-µ1 (clone 10F6; Developmental Studies Hybridoma Bank, 1:200). The next day, membranes were incubated with horseradish peroxidase (HRP)-conjugated goat anti-mouse IgG+IgM+IgA (Abcam, 1:1000) at RT for 1 hour. Proteins were detected on the Chemidoc imaging XRS+ system (Bio-Rad) using the Clarity Western ECL Substrate kit (Bio-Rad).

RNA isolation and RT-qPCR

A representative snap-frozen proportion (10-30 mg) of each tumor or organ was disrupted in lysis buffer (Promega) using a stainless bead and the TissueLyser LT (Qiagen). Total RNA of tumor samples was isolated using the ReliaPrep™ RNA Tissue Miniprep System (Promega) according to the manufacturer's protocol. 500 ng of RNA was used to generate cDNA using the High-Capacity RNA-to-cDNA™ Kit (ThermoFisher Scientific) according to the manufacturer's protocol. Reo genomic copies and expression levels of host genes (**Table S3**) in tumors were measured by RT-qPCR as previously described (3). Reo S4 copy numbers were determined based on a standard curve, generated with serial dilutions of plasmid pcDNA_S4. Log_{10} S4 copy numbers were calculated using a previously described formula (28). The expression of host genes

was normalized to reference genes *Mzt2* and *Ptp4a2* using the Bio-Rad CFX Manager 3.1 Software (Bio-Rad).

Immunohistochemistry

Formaldehyde-fixed, paraffin-embedded tissue sections were stained for cleaved caspase-3. Formalin-fixed tumor pieces were embedded in paraffin and then sectioned randomly at 4 µm and placed on Superfrost® Plus slides (VWR). Sections were dried overnight at 37 °C and stored at 4 °C until staining. Slides were deparaffinized and endogenous peroxidase was blocked with 0.3% hydrogen peroxidase (VWR) in methanol for 20 minutes. After rehydration, antigen retrieval was performed by boiling slides for 10 minutes in 0.01M sodium citrate (pH=6.0; Merck). Non-specific binding was blocked using SuperBlock™ (ThermoFisher Scientific) before overnight incubation at 4 °C with rabbit anti-mouse cleaved caspase-3 antibody (clone Asp175, 1:400; Cell Signaling Technology). Hereafter, slides were incubated for 30 min at RT with a biotinylated goat anti-rabbit secondary antibody (1:200; Agilent), followed by incubation with avidin-biotin complex (VECTASTAIN® Elite® ABC HRP Kit; Vector Laboratories). Peroxidase activity was detected using the 2-component liquid DAB+ system (Agilent) according to the manufacturer's instructions for 5 min. Slides were counterstained with hematoxylin (Sigma-Aldrich), dehydrated, and mounted using Entellan (Sigma-Aldrich). Control sections were processed in parallel but without incubation with the primary antibody. No labeling was observed in the control sections.

IFNγ ELISA

Sorted Reo $\mu1_{133\text{-}140}$ Tm^+ or Reo $\mu1_{422\text{-}430}$ Tm^+ cells (2000 cells/well of a round-bottom 96-wells plate) were cocultured with PMA (20 ng/mL) and ionomycin (1 µg/mL), Reo-infected TC1 cells (20.000 cells/well) or Reo-infected TC1 cells. In some wells, NAb-containing plasma from Reo-preexposed mice (1:1000 dilution) was added. After 48 hours of incubation, supernatants were harvested. For ELISA, Nunc MaxiSorp™ plates (Corning) were coated with purified rat anti-mouse IFNγ antibody (BD Pharmingen) in sodium carbonate/sodium bicarbonate coating buffer (pH 9.6) overnight at 4 °C and then blocked with PBS/1% BSA/0.05% Tween-20 (Merck) for 1 hour at 37 °C. After washing with wash buffer (PBS/0.05% Tween-20), 100 µL of supernatant was added and incubated for 2 hours at RT. The standard curve was prepared using recombinant mouse IFNγ (BioLegend). After washing, biotinylated rat anti-mouse IFNγ antibody (BD Pharmingen) was applied for 1 hour at RT, followed by poly-Streptavidin-HRP conjugate (Sanquin, The Netherlands) for 1 hour at RT. After washing, 50 µL of TMB (3,3',5,5'-Tetramethylbenzidine) (Sigma-Aldrich) was added and the reaction was quenched by the addition of 50 µL 2M H_2SO_4 (Merck). Absorbance was measured at 450 nm using a SpectraMax iD3 multi-mode plate reader (Molecular Devices).

Statistics

Group size was calculated using the PS: Power and Sample Size Calculation program (Vanderbilt University, version 3.1.6) (29). For experiments where tumor growth was the experimental read-out, mice were excluded when tumor engraftment was not successful (1% of all tumor engraftments). For RT-qPCR analysis, samples were excluded when RNA concentration and purity were too low (< 75 ng/µL). For flow cytometry data, tumor samples were excluded when macroscopic evidence for draining lymph node contamination was present.

All graphs were prepared and statistical analyses were performed using the GraphPad Prism software (version 8). All data represent mean±SEM and key observations are based upon multiple experiments with similar results. For the comparison of two groups, an unpaired t test was used. For comparing multiple groups versus PBS treatment or negative control, an one-way analysis of variance (ANOVA) including Dunnett's post hoc test was performed. For comparing multiple groups with each other, an one-way ANOVA including Tukey's post hoc test was used. To compare differences in average tumor growth, an ordinary two-way ANOVA with Tukey's post hoc test was used. IC50 values were calculated using non-linear regression analysis. Survival between groups was compared using Kaplan-Meier curves and the statistical Log-rank test (Mantel-Cox). More information regarding the statistical tests used can be found in the individual figure legends. Significance levels are labeled with asterisks, with *p<0.05, **p<0.01, ***p<0.001, and ****p<0.0001. Non-significant differences are indicated by ns.

RESULTS

Preexisting immunity against Reo is prevalent in the human population

The use of oncolytic reovirus type 3 Dearing (hereafter named Reo) is an emerging anticancer treatment and a promising strategy to enhance the efficacy of immunotherapy. However, various factors, including the presence of preexisting neutralizing antibodies (NAbs) might limit its anticancer potential. Before investigating the effect of preexisting immunity on various aspects of Reo therapy, we determined the level of seropositivity against Reo in healthy volunteers and various cohorts of cancer patients. Using serial dilutions of serum in a virus neutralization assay, we observed that 81.0% of all tested individuals (n=100) carried Reo-specific NAbs (**Figure 1A, B**). The frequency of seropositivity did not differ between healthy volunteers and cancer patients (**Figure 1C**), or between male and female individuals (**Figure 1D**). Reo is known as a 'kindergarten' virus and higher seropositivity might thus be expected in younger individuals, but the level of seropositivity was not correlated with age (**Figure 1E**). Combined, these data confirm that the majority of the human population has been preexposed to Reo, which underscores the relevance to determine the effect of preexposure on the efficacy of Reo-based anticancer therapies.

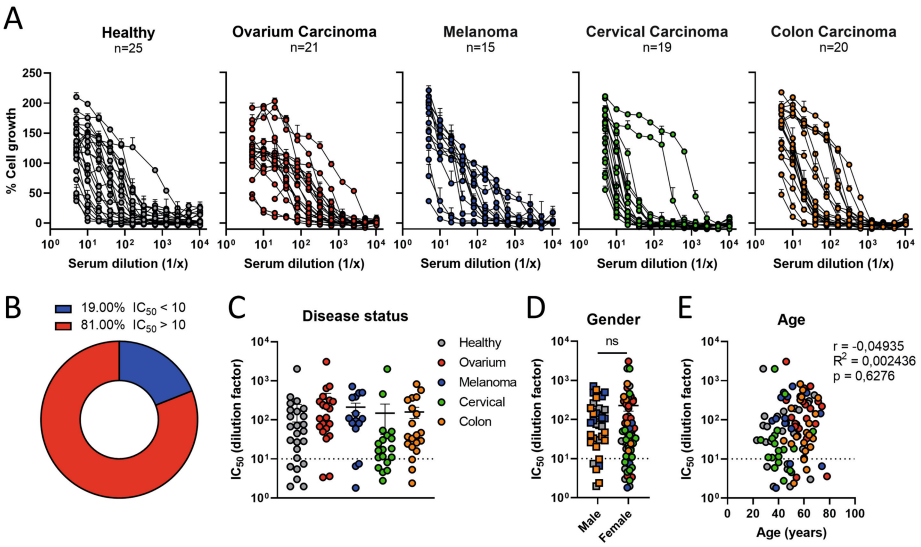


Figure 1. Preexisting immunity against Reo is prevalent in the human population. (**A**) Individual serum samples from healthy volunteers or cancer patients with different primary tumors were subjected to a Reo neutralization assay. Percentage of cell growth is calculated by normalizing for Reo only (0% viable) and Mock (100% viable). (**B**) Percentage of all individuals that tested seropositive (IC_{50} > 10) or seronegative (IC_{50} < 10) for Reo. (**C**) Comparison of IC_{50} values between healthy volunteers and cancer patient cohorts. (**D**) Comparison of IC_{50} values between male and female individuals. (**E**) Correlation analysis between IC_{50} values of individuals and corresponding age in years. Data represent mean±SEM. IC_{50} values were calculated using non-linear regression analysis. Differences between groups in (C) were determined using a Kruskal-Wallis test with Dunn's multiple comparisons test. Differences between groups in (D) were determined using an unpaired t test with Welch's correction, and correlation between IC_{50} values and age in (E) was determined by calculating the Pearson correlation coefficient (r). Significance levels: ns=not significant.

Preexposure impairs intratumoral Reo infection and the Reo-induced interferon response

To study the role of preexisting immunity on Reo antitumor efficacy, we established an experimental model where immunocompetent C57BL/6J mice were preexposed to Reo with a two-week interval (**Figure 2A**). This preexposure led to the presence of high levels of NAbs in the circulation (**Figure 2B, C**), as well as $CD8^+$ T cells recognizing the Reo $\mu1_{133\text{-}140}$ epitope that we identified earlier (**Figure 2D**) (30). These NAb levels remained high over time (**Figure S1**). Western blot analysis using the plasma of preexposed mice as the primary antibody source revealed that Reo-specific antibodies also predominantly recognize the μ1 protein (**Figure 2E**), suggesting that immunodominant Reo-specific T-cell and B-cell responses are both directed to the same viral protein.

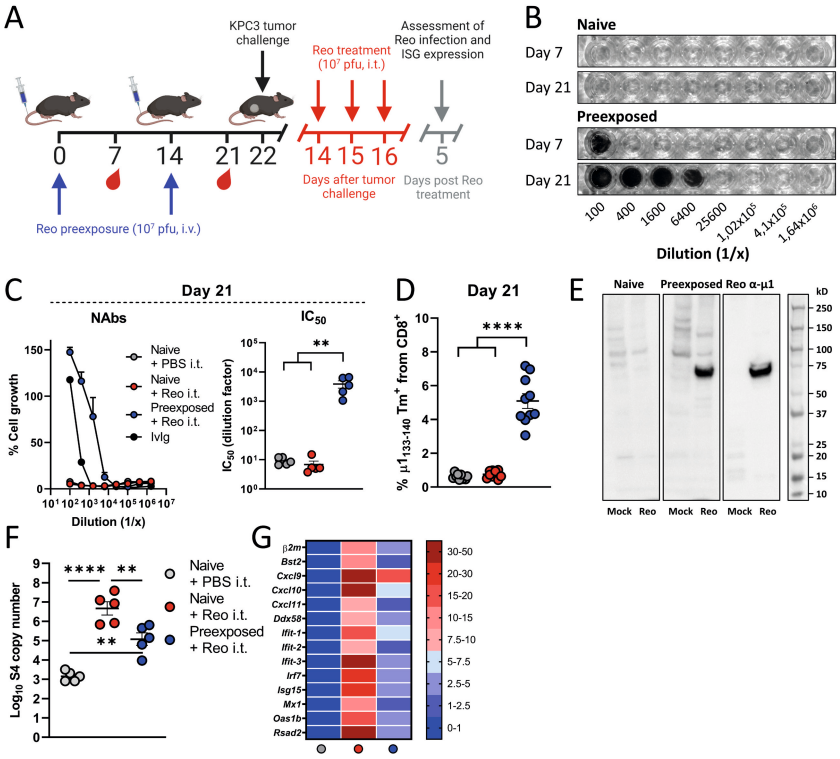


Figure 2. Preexposure impairs Reo infection and the Reo-induced interferon response. (**A**) Overview of experiment described in (B-G). Male C57BL/6J mice (n=5/group) were preexposed by intravenous (i.v.) injection of Reo (10^7 plaque-forming units (pfu)/injection) on days 0 and 14. Blood was drawn on days 7 and 21 for interim analysis. After preexposure, mice were subcutaneously inoculated with KPC3 cells ($1x10^5$/mouse) and received intratumoral (i.t.) Reo injections (10^7 pfu/injection) on indicated days. Tumors were harvested 5 days after Reo administration for *ex vivo* analysis. (**B**) Representative pictures of crystal violet-stained 911 cells after subjection to a neutralization assay with diluted plasma from naive or preexposed mice. (**C**) Reo neutralization assay. Average dilution curves using plasma from naive or preexposed mice and individual IC_{50} values on day 21. (**D**) Frequency of Reo-specific $\mu1_{133-140}$ tetramer $(Tm)^+$ $CD8^+$ T cells in the circulation on day 21. (**E**) Western blot of Mock or Reo-infected 911 cell lysates using antibodies against the Reo μ1 protein or plasma of preexposed mice as primary antibody source. (**F**) Intratumoral presence of genomic copies of Reo S4 segment, as measured by quantitative reverse transcription PCR (RT-qPCR). (**G**) Heatmap depicting relative expression of various interferon response genes on day 5, as determined by RT-qPCR on bulk tumor RNA. Data represent mean±SEM. IC_{50} values were calculated using non-linear regression analysis. Differences between groups in (C), (D), and (F) were determined using an ordinary one-way analysis of variance (ANOVA) with Tukey's post hoc test. Significance levels: **p<0.01 and ****p<0.0001.

As a first step of Reo anticancer efficacy, we investigated whether Reo infection of the tumor was affected by preexisting immunity. After preexposure, mice were engrafted with KPC3 tumors and received intratumoral Reo injections when tumors were palpable. On day 5 post Reo treatment, mice were sacrificed for intratumoral analysis. Importantly, the quantity of intratumoral genomic copies of the Reo S4 segment was significantly decreased in preexposed mice compared to naive mice, implying impaired viral infection (**Figure 2F**). Concomitantly, the expression of a panel of interferon-stimulated genes

(ISGs), such as *Ifit-1, Ifit-2,* and *Ifit-3*, as well as T-cell attracting chemokines *Cxcl10* and *Cxcl11*, was lower in tumors of preexposed mice (**Figure 2G**). Of note, the expression of chemokine *Cxcl9* appeared to be less affected. Altogether, we concluded that Reo preexposure is associated with a strong decrease in Reo genomic copies and ISG expression in tumors upon Reo treatment.

Reo-specific NAbs impair the anticancer efficacy of Reo monotherapy

We next specifically investigated the effect of NAbs after Reo preexposure. μMT mice, which lack B cells and thus cannot produce antibodies (**Figure S2A-D**), were exposed to Reo but succumbed to weight loss (**Figure S2E**) two weeks after inoculation, suggesting that Reo replication was uncontrolled in the absence of NAbs. Then, a tumor challenge experiment was performed in a small number of immunocompromised NSG mice that are also B-cell deficient. Similarly, Reo-exposed NSG mice succumbed to weight loss, and high numbers of Reo genomic copies were detected in tumors, livers, hearts, and plasma of these mice, indicating viremia in the absence of NAbs (**Figure S2F-I**). These data and similar observations by others (31-33) demonstrate that NAbs are necessary to prevent uncontrolled Reo infection in mice.

We then investigated the effect of strongly decreased, but not completely absent, levels of NAbs on Reo infection in immunocompetent C57BL/6J mice by injection of αCD20 antibodies to deplete B cells (**Figure 3A**). Indeed, although the depletion of B cells was efficient in blood (**Figure S3A, B**), neutralization assay (**Figure 3B**) and Western blot analysis (**Figure S4**) showed that residual levels of NAbs were still present in the plasma of preexposed mice. These low NAb levels were sufficient to protect mice from Reo-induced pathology but, importantly, hampered Reo infection (**Figure 3C**) and ISG expression (**Figure 3D**) in the tumor. Even the intratumoral administration of a 10-fold higher dose of Reo to preexposed mice did not increase the presence of genomic Reo S4 copies (**Figure 3D**), demonstrating that even low systemic levels of NAbs significantly hamper intratumoral Reo infection and ISG expression. This suggests that achieving effective infection in most patients will be difficult, including those with low NAb levels.

Due to the crucial role of $CD4^+$ T cells in establishing effective class-switched B-cell responses, we depleted $CD4^+$ T cells during Reo preexposure as another way to influence NAbs (**Figure 3E, S3C, D**). Depletion of $CD4^+$ T cells during preexposure, but not $CD8^+$ T cells or NK cells, completely abrogated NAb production (**Figure 3F**) and significantly increased genomic Reo S4 copies (**Figure 3G**) and the expression of ISGs (**Figure 3H**) in the tumor upon intratumoral Reo treatment. Combined, these data clearly show that the presence of Reo-specific NAbs impairs infection and ISG expression, even when Reo is injected directly into tumors.

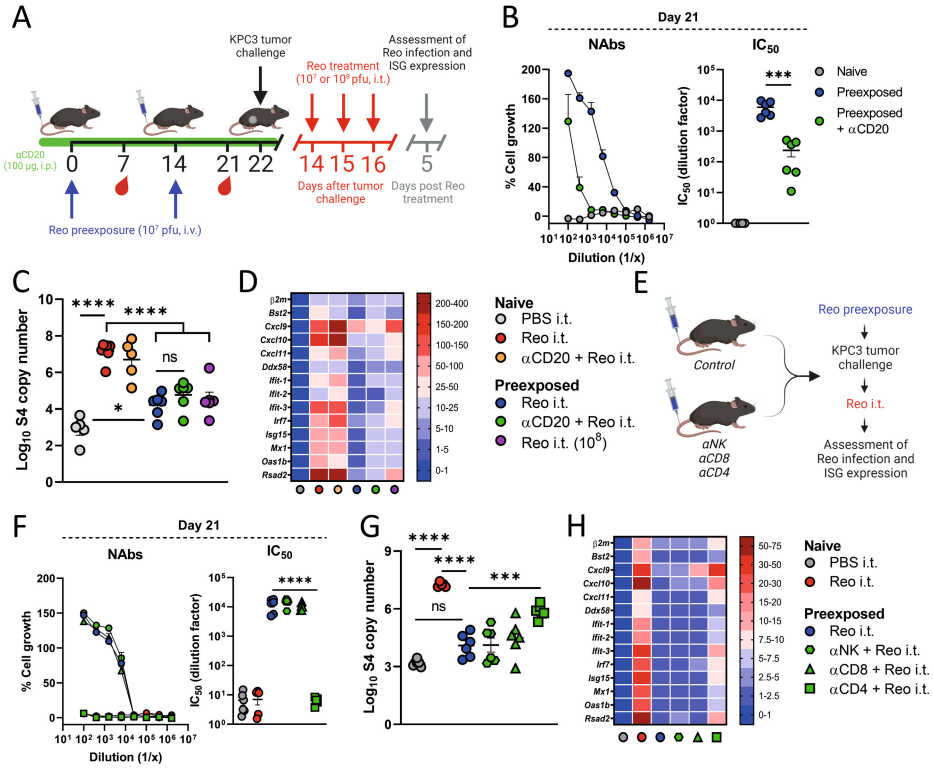


Figure 3. Preexposure-induced Reo-specific NAbs impair Reo infection and ISG expression in the tumor. (**A**) Overview of experiment described in (B-D). Male C57BL/6J mice (n=5-7/group) were preexposed by intravenous (i.v.) injection of Reo (10^7 plaque-forming units (pfu)/injection) on days 0 and 14. Depletion of B cells (**α**CD20, 100 **μ**g/injection, intraperitoneally (i.p.)) was initiated on days -5 and -2 and maintained weekly during the preexposure period. Blood was drawn on days 7 and 21 for interim analysis. After preexposure, mice were subcutaneously inoculated with KPC3 cells (1x10^5/mouse) and received intratumoral (i.t.) Reo injections (10^7 of 10^8 pfu/injection) on indicated days. Tumors were harvested 5 days after Reo administration for *ex vivo* analysis. (**B**) Reo neutralization assay. Average dilution curves using plasma from indicated groups and individual IC_{50} values on day 21. (**C**) Intratumoral presence of genomic copies of Reo S4 segment, as measured by quantitative reverse transcription PCR (RT-qPCR). (**D**) Heatmap depicting relative expression of various interferon response genes on day 5, as determined by RT-qPCR. (**E**) Design of experiment described in (F-H). Experiment was executed exactly as described in (A), but male C57BL/6J mice (n=6/group) received **α**NK, **α**CD8, or **α**CD4 (100 **μ**g/injection, i.p.) during the preexposure period. (**F**) Reo neutralization assay. Average dilution curves using plasma from indicated groups and individual IC_{50} values on day 21. (**G**) Intratumoral presence of genomic copies of Reo S4 segment, as measured by RT-qPCR. (**H**) Heatmap depicting relative expression of various interferon response genes on day 5, as determined by RT-qPCR. Data represent mean±SEM. IC_{50} values were calculated using non-linear regression analysis. To determine differences between groups in (B), (D), and (F), an ordinary one-way analysis of variance (ANOVA) with Tukey's post hoc test was used. Significance levels: ns=not significant, *p<0.05, ***p<0.001, and ****p<0.0001.

Since circulating NAbs can already be detected five days after intratumoral Reo administration (**Figure S5**), these therapy-induced NAbs might hinder the therapeutic potency of intratumoral Reo treatment already at early time points. Therefore, we next evaluated the therapeutic potency of oncolytic Reo in the absence of NAbs in KPC3-bearing B-cell deficient μMT mice (**Figure 4A**). Intratumoral injection with Reo created a therapeutic time window that allowed us to study the role of treatment-induced NAbs before the loss of bodyweight occurred (**Figure 4B**). Reo treatment in μMT mice was associated with significant decreases in tumor volumes, which were not observed in fully immunocompetent, Reo-treated C57BL/6J mice (**Figure 4C**). Similar levels of Reo S4 copies could be found in Reo-treated tumors from μMT mice and C57BL/6J mice, even though tumors from μMT mice were smaller in size (**Figure 4D**). Additionally, the expression of ISGs (**Figure 4E**) and the level of apoptosis, measured by cleaved caspase-3, was higher in tumors of Reo-treated μMT mice compared to those of Reo-treated C57BL/6J mice (**Figure 4F, G**).

To indisputably prove that NAbs impair the antitumor effect of Reo therapy, a NAb transfer experiment was performed. KPC3-bearing NSG mice received naive plasma or NAb-containing plasma from preexposed C57BL/6J mice, at 2 different doses, and subsequently were treated intratumorally with Reo (**Figure 4H, S6**). Even though NAbs were only detected after infusion of the high dose NAb-containing plasma (**Figure 4I**) and NAbs did not reduce the genomic Reo S4 copies in tumors (**Figure 4J**), the transfer of both doses of NAbs reduced the Reo-induced expression of ISGs (**Figure 4K**) and the level of cleaved caspase-3 (**Figure 4L, M**) in the tumor. Importantly, the transfer of NAb-containing plasma, but not naive plasma, completely neutralized the Reo-induced antitumor effect (**Figure 4N**). These combined results show that Reo can have profound antitumor efficacy, but its use as an oncolytic agent is impaired by the presence of NAbs, even at low levels.

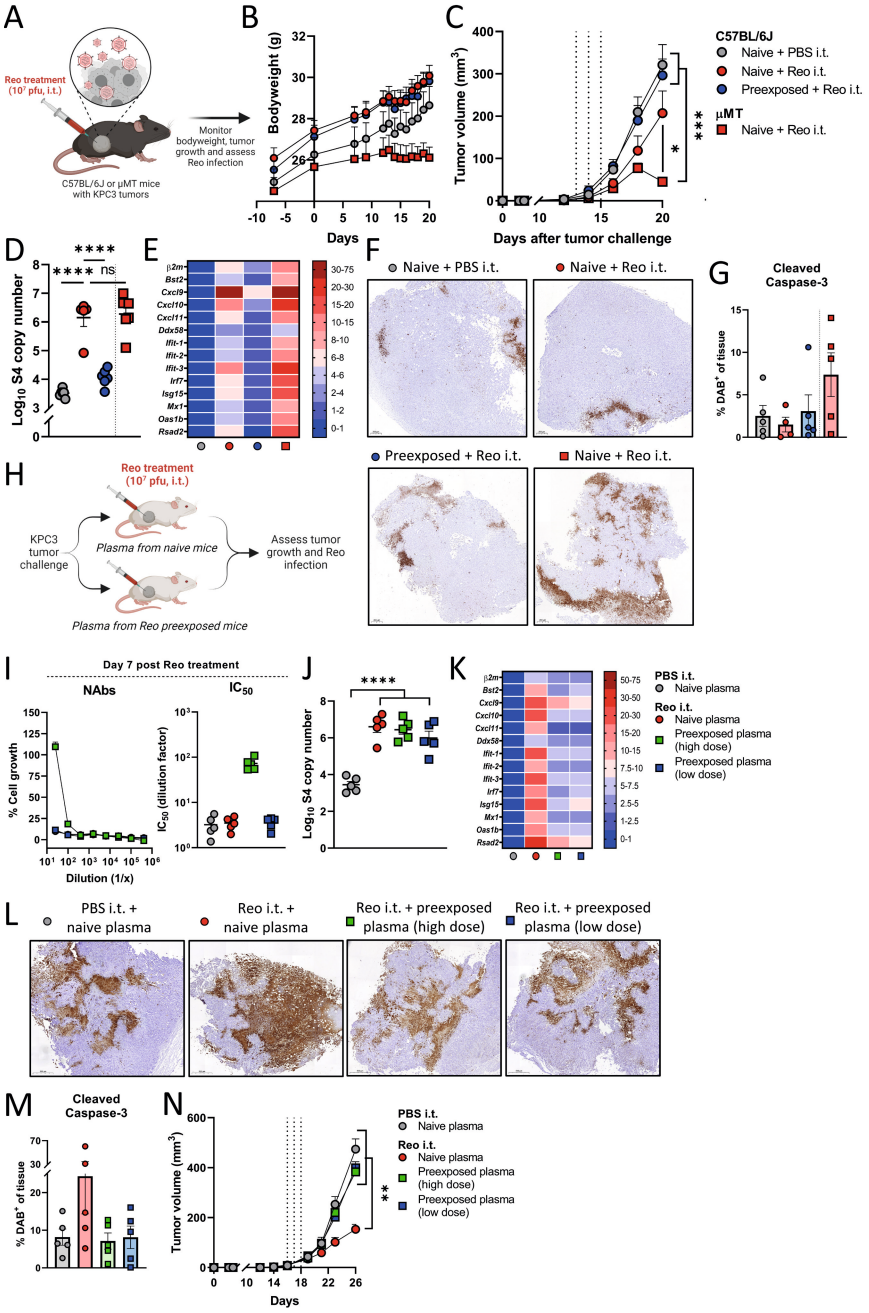


Figure 4. Reo-specific NAbs abrogate the antitumor efficacy of Reo monotherapy. (**A**) Overview of experiment described in (B-G). Male C57BL/6J or µMT mice (n=6/group) were subcutaneously inoculated with KPC3 cells (1x10^5/mouse) and received intratumoral (i.t.) Reo injections (10^7 pfu/injection) on days 13-15. Mice were sacrificed 7 days after Reo administration for *ex vivo* analysis. (**B**) Average bodyweight curves. (**C**) Average tumor volume curves. (**D**) Intratumoral presence of genomic copies of Reo S4 segment, as measured by quantitative reverse transcription PCR (RT-qPCR). >>

>> (**E**) Heatmap depicting relative expression of various interferon response genes, as determined by RT-qPCR. (**F**) Representative images obtained from immunohistochemical staining of KPC3 tumors for apoptosis marker cleaved caspase-3. Scale bar equals 200 µm. (**G**) Quantification of positive DAB signal in sections stained for cleaved caspase-3. (**H**) Overview of experiment described in (I-N). Male and female NSG mice (n=5/group) were subcutaneously inoculated with KPC3 cells ($1x10^5$/mouse) and received intratumoral (i.t.) Reo injections (10^7 pfu/injection) on days 16-18. Plasma from preexposed C57BL/6J mice was injected i.p., 2x/week. Mice were sacrificed 10 days after Reo administration for *ex vivo* analysis. (**I**) Reo neutralization assay. Average dilution curves and individual IC_{50} values using plasma from indicated groups, harvested on day 7 after i.t. Reo administration. (**J**) Intratumoral presence of genomic copies of Reo S4 segment, as measured by quantitative reverse transcription PCR (RT-qPCR). (**K**) Heatmap depicting relative expression of various interferon response genes in tumors, as determined by RT-qPCR. (**L**) Representative images obtained from immunohistochemical staining of KPC3 tumors for apoptosis marker cleaved caspase-3. Scale bar equals 500 µm. (**M**) Quantification of positive DAB signal in sections stained for cleaved caspase-3. (**N**) Average tumor volume curves. Data represent mean±SEM. IC_{50} values were calculated using non-linear regression analysis. Differences between groups in (C) and (N) were determined using an ordinary two-way analysis of variance (ANOVA) with Tukey's post hoc test, and an ordinary one-way ANOVA with Tukey's post hoc test was used to determine differences between groups in (D) and (J). Significance levels: ns=not significant, *p<0.05, **p<0.01, ***p<0.001, and ****p<0.0001.

Preexposure does not affect the Reo-induced intratumoral influx or activation of T cells

Current clinical efforts aim to use Reo not solely as an oncolytic agent, but rather as an immune-stimulatory agent, especially to induce the intratumoral influx of T cells that can be harnessed by T-cell-based immunotherapeutic strategies (34-36). Therefore, we next studied whether the Reo-induced intratumoral T-cell influx therapy is affected by Reo preexposure. Immunocompetent C57BL/6J mice were preexposed to Reo, engrafted with KPC3 tumors, and the frequency, specificity, and effector function of intratumoral T cells after intratumoral Reo treatment were analyzed (**Figure 5A**). Interestingly, the Reo-induced influx of $CD8^+$ T cells was not affected (**Figure 5B, C**). Equally, the intratumoral influx of $CD8^+$ T cells did not differ between Reo-treated µMT mice and Reo-treated C57BL/6J mice, demonstrating that T-cell influx is not affected by the presence or absence of NAbs (**Figure S7A, B**). This might be related to the moderate expression of *Cxcl9* that is still present in tumors of preexposed mice. Of note, the Reo-induced influx of NK cells was lower in preexposed C57BL/6J mice and higher in Reo-treated µMT mice, suggesting that the influx of NK cells is more influenced by the presence of NAbs or ISG expression than the influx of T cells (**Figure 5D, S7C**).

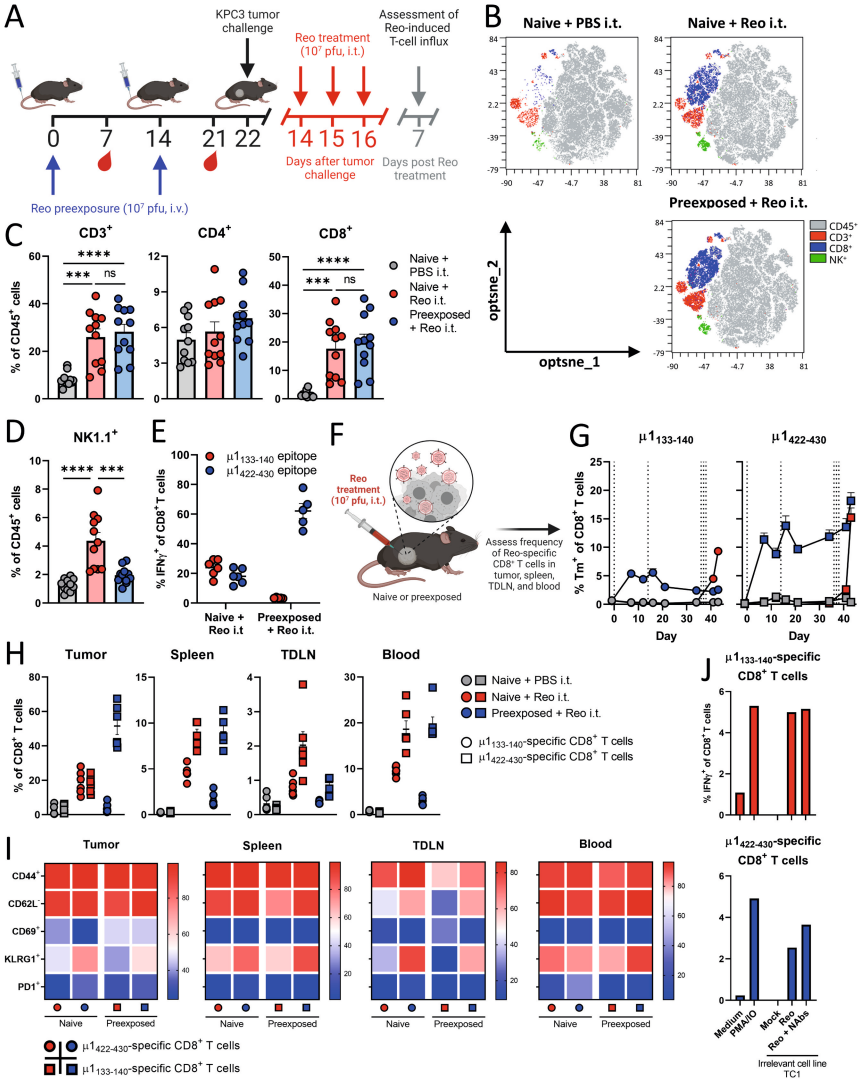


Figure 5. Preexposure does not affect the Reo-induced intratumoral influx or activation of T cells but shifts the frequency of Reo-specific T-cell populations. (**A**) Overview of experiment described in (B-E). Male C57BL/6J mice (n=5-6/group) were preexposed by intravenous (i.v.) injection of Reo (10^7 plaque-forming units (pfu)/injection) on days 0 and 14. After preexposure, mice were subcutaneously inoculated with KPC3 cells ($1x10^5$/mouse) and received intratumoral (i.t.) Reo injections (10^7 pfu/injection) on days 14-16. Tumors were harvested 7 days after Reo administration for *ex vivo* analysis. (**B**) Opt-SNE plots highlighting the intratumoral presence of $CD3^+$, $CD8^+$ T cells, and NK cells after indicated treatments. $1x10^5$ $CD45^+$ cells were subsampled from each sample. (**C**) Intratumoral frequency of $CD3^+$, $CD4^+$, and $CD8^+$ T cells within $CD45^+$ immune cells. (**D**) Intratumoral frequency of NK cells within $CD45^+$ immune cells. (**E**) Frequency of interferon gamma $(IFN\gamma)^+$ cells within the intratumoral $CD8^+$ T-cell population after coculture with indicated peptides, as measured with intracellular cytokine staining. (**F**) Design of experiment described in (G-J). Mice (n=6/group) were preexposed with Reo, inoculated with KPC3 cells, and treated i.t. with Reo as described in (A). (**G**) Kinetics of Reo-specific $\mu1_{133-140}$ and $\mu1_{422-430}$ tetramer $(Tm)^+$ $CD8^+$ T cells in the circulation. (**H**) Frequency of Reo-specific $\mu1_{133-140}$ and $\mu1_{422-430}$ Tm^+ $CD8^+$ T cells in tumor, spleen, tumor-draining lymph node (TDLN), or blood of naive or preexposed mice after intratumoral Reo administration.

>>

>> (**I**) Heatmap showing activation profile of Reo-specific $\mu1_{133-140}$ and $\mu1_{422-430}$ Tm^+ $CD8^+$ T cells in tumor, spleen, TDLN, or blood. (**J**) Production of IFNγ by sorted Reo-specific $\mu1_{133-140}$ or $\mu1_{422-430}$ Tm^+ $CD8^+$ T cells after coculture with indicated targets for 48 hours. Data represent mean±SEM, except in (J) where n=1. In (C) and (D), data from two experiments with the same set-up are pooled and differences between groups were determined using an ordinary one-way analysis of variance (ANOVA) with Tukey's post hoc test. Significance levels: ns=not significant, ***p<0.001, and ****p<0.0001.

Although the intratumoral influx of $CD8^+$ T cells was not affected by the presence of NAbs, the proportion of T cells recognizing our previously identified Reo $\mu1_{133-140}$ epitope was strongly diminished (**Figure S8A**). Intratumoral $CD8^+$ T cells in preexposed mice were still Reo-specific (**Figure S8B**) but now recognized another epitope ($\mu1_{422-430}$) (**Figure 5E, S8C, D**). Further analysis of these two Reo-specific $CD8^+$ T-cell populations using tetramers (**Figure 5F**), revealed different kinetics (**Figure 5G**) and confirmed that especially in tumors of preexposed mice, the frequency of $\mu1_{422-430}$-specific $CD8^+$ T cells dominated over the frequency of those recognizing the $\mu1_{133-140}$ epitope (**Figure 5H**). Both Reo-specific $CD8^+$ T-cell populations exhibited a similar effector phenotype which did not differ between Reo-treated naive and preexposed mice (**Figure 5I**), and a similar capacity to produce IFNγ upon non-specific stimulation with PMA/ionomycin or upon specific stimulation with Reo-infected target cells (**Figure 5J**). Additionally, their recognition of Reo-infected target cells was not impaired when NAb-containing plasma from preexposed mice was added to the system. Altogether, these data demonstrate that the intratumoral presence of functional T cells is not affected by preexposure to Reo.

Combined Reo and T-cell-based immunotherapy retains its efficacy in preexposed mice

Since the total Reo-induced influx and activation of $CD8^+$ T cells was not impaired in preexposed mice, we expected that the combination of Reo and T-cell-based immunotherapy would still be effective in this setting. We first investigated the efficacy of Reo&CD3-bsAb therapy in the KPC3.TRP1 tumor model (**Figure 6A**). As demonstrated before, preexposure induced high levels of NAbs (**Figure 6B**) and the presence of Reo-specific T cells (**Figure 6C**) in the circulation. We treated both naive and preexposed mice bearing KPC3.TRP1 tumors with Reo&CD3-bsAb therapy and observed that tumors of all Reo&CD3-bsAb-treated mice regressed in volume, irrespective of their preexposure status (**Figure 6D**). Although the survival time after Reo&CD3-bsAbs therapy was decreased in preexposed mice compared to naive mice (**Figure 6E**), these data demonstrate that Reo&CD3-bsAb therapy is still effective in a preexisting immunity setting.

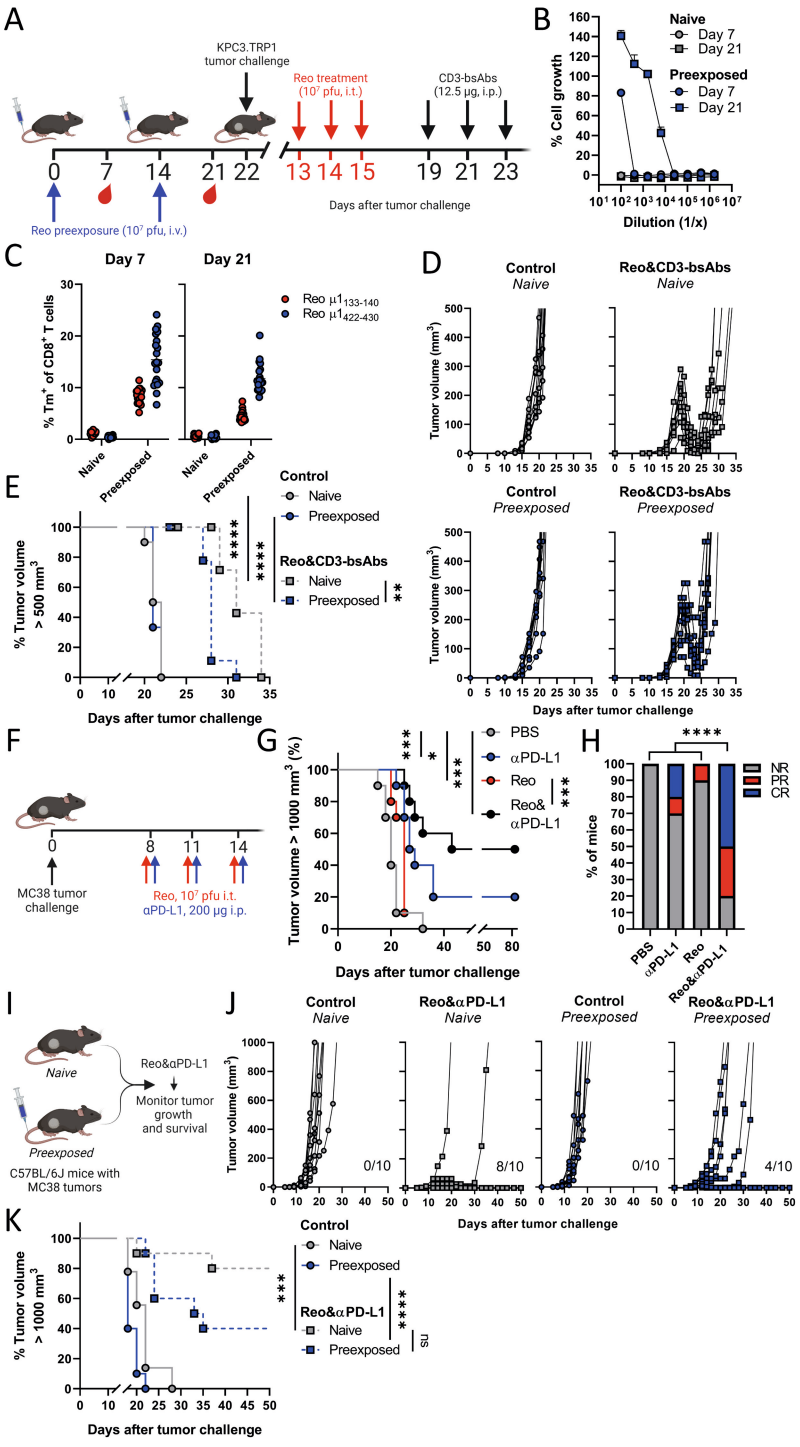


Figure 6. Combined Reo and T-cell-based immunotherapy retains its efficacy in preexposed mice. (**A**) Overview of experiment described in (B-E). Male C57BL/6J mice (n=10/group) were preexposed by intravenous (i.v.) injection of Reo (10^7 plaque-forming units (pfu)/injection) on days 0 and 14. After preexposure, mice were subcutaneously inoculated with KPC3.TRP1 cells >>

>> (1x10^5/mouse) and received intratumoral (i.t.) Reo injections (10^7 pfu/injection) on indicated days, followed by intraperitoneal (i.p.) administration of CD3-bsAbs (12.5 µg/injection). (**B**) Reo neutralization assay. Average dilution curves using plasma harvested on indicated days. (**C**) Reo-specific $\mu1_{133-140}$ and $\mu1_{422-430}$ tetramer (Tm)$^+$ $CD8^+$ T cells in the circulation on indicated days. (**D**) Individual growth curves of naive or preexposed mice receiving Reo&CD3-bsAb therapy. (**E**) Kaplan-Meier survival graphs of mice after indicated treatments. (**F**) Overview of experiment described in (G, H). Male C57BL/6J mice (n=10/group) were subcutaneously engrafted with MC38 cells (5x10^5/mouse) and received Reo (i.t., 10^7 pfu/injection) and αPD-L1 (i.p., 200 µg/injection) on day 8, 11 and 14. (**G**) Kaplan-Meier survival graphs of mice after indicated treatments. (**H**) Frequency of Non-Responders (NR), Partial Responders (PR), or Complete Responders (CR) within each treatment group. (**I**) Overview of experiment described in (J, K). Male C57BL/6J mice (n=10/group) were preexposed as described in (A). After preexposure, mice were subcutaneously inoculated with MC38 cells (5x10^5/mouse) and received Reo&αPD-L1 therapy as described in (F). (**J**) Individual growth curves of naive or preexposed mice receiving Reo&αPD-L1 therapy. Indicated is the number of tumor-free mice in each experimental group. (**K**) Kaplan-Meier survival graphs of mice after indicated treatments. Data represent mean±SEM. Log-rank tests were used to compare differences in survival in (E), (G), and (K). Chi-square test was used to determine statistical differences in response in (H). Significance levels: ns=not significant, *p<0.05, **p<0.01, ***p<0.001, and ****p<0.0001.

To assess the role of Reo preexisting immunity in a different combinatorial immunotherapeutic strategy, we employed the chemically-induced preclinical colon model MC38, which shows a partial response to checkpoint blockade therapy (αPD-L1) (37). We first assessed whether Reo was able to enhance the efficacy of αPD-L1. Reo was administered intratumorally on days 8, 11, and 14 after tumor challenge, and αPD-L1 therapy was applied intraperitoneally on the same days (**Figure 6F**). While αPD-L1 alone delayed tumor growth and induced complete tumor clearance in 20% of animals, Reo&αPD-L1 therapy led to tumor clearance in 50% of animals (**Figure 6G, H**). We concluded that the combination of Reo&αPD-L1 is very effective in the MC38 tumor model, and subsequently investigated the impact of preexposure to Reo on its efficacy (**Figure 6I**). Similar to what was observed for Reo&CD3-bsAbs, preexposure to Reo (**Figure S9A, B**) did influence the efficacy of Reo&αPD-L1 therapy, but complete tumor clearance could still be observed in 40% of preexposed mice (**Figure 6J, K**). These data indicate that Reo preexposure does not preclude the use of Reo and T-cell-based combination therapy for effective tumor control.

Reo-based combination therapy remains effective upon repeated systemic administration

Given that preexposure does not hamper the efficacy of Reo-based combination therapies when Reo is administered intratumorally, we finally investigated the efficacy of Reo-based combination therapy in a more clinically-relevant setting. In the clinic, intravenous administration is preferred over intratumoral administration, since it limits patients' discomfort and allows for the simultaneous targeting of multiple tumor lesions, irrespective of their location. In addition, patients are preferably treated with repeated infusions, which will result in multiple boosting events of Reo-directed immunity that might impair therapeutic efficacy. We therefore investigated the consequences of repeated intravenous (i.v.) Reo infusions on Reo infection and the Reo-induced influx of immune cells (**Figure 7A**). For this experiment, the clinical-grade formulation of Reo, named Pelareorep (Pela in graphs) was used. Indeed, repeated i.v. Pelareorep injections

impaired the presence of virus in tumors (**Figure 7B**). While Reo S4 genomic copies could be found in tumors of mice that received only 1 injection with Pelareorep, this greatly diminished after multiple infusions. A similar pattern was observed with the expression of ISGs (**Figure 7C**). Importantly, while the frequency of NK cells decreased after the first infusion (**Figure 7D**), the frequency of intratumoral CD8$^+$ T cells remained constant over time after repeated i.v. Pelareorep injections (**Figure 7E**). We next investigated whether the combination therapy of i.v. administered Pelareorep combined with CD3-bsAbs would still be effective. We compared the efficacy of i.v. Pelareorep&CD3-bsAb administered as multiple cycles with a 5-day interval, with our previously defined regimen which comprises 1 cycle of 3 consecutive virus infusions followed by CD3-bsAb administrations (**Figure 7F**) (3). Both regimens were equally effective (**Figure 7G, H**), demonstrating that systemic and repeated Reo administration is not a barrier to the antitumor efficacy of combined Reo and T-cell-based immunotherapy. Altogether, these data demonstrate that the use of Reo as an oncolytic agent is hampered by the presence of NAbs, but T cells are still attracted towards the tumor and combined Reo and T-cell-based immunotherapy remained effective.

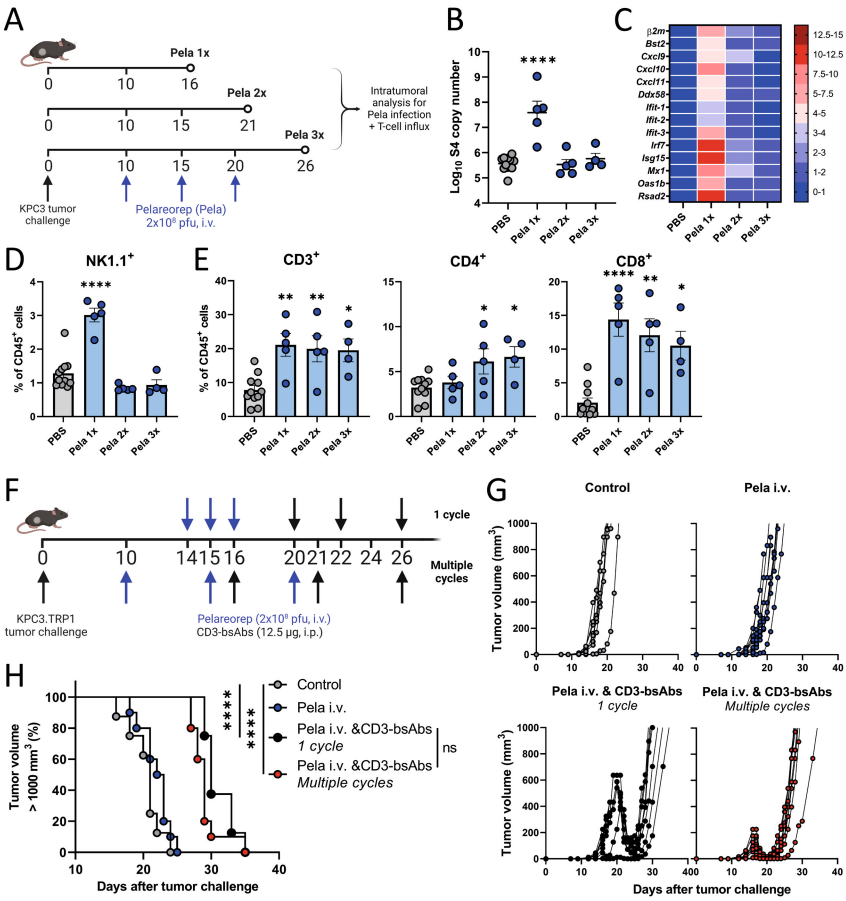


Figure 7. Reo-based combination therapy remains effective upon repeated systemic administration. (**A**) Overview of experiment described in (B-E). Male C57BL/6J mice (n=5/group) >>

>> were subcutaneously inoculated with KPC3 cells (1x10^5/mouse) and intravenously (i.v.) injected with Pelareorep (Pela; 2x10^8 plaque-forming units (pfu)/injection) on indicated days. Mice were sacrificed after 1, 2, or 3 Pela infusions for intratumoral analysis. (**B**) Intratumoral presence of genomic copies of Reo S4 segment, as measured by quantitative reverse transcription PCR (RT-qPCR). (**C**) Heatmap depicting relative expression of various interferon response genes in tumors harvested after 1, 2, or 3 Pela infusions, as determined by RT-qPCR. (**D**) Intratumoral frequency of NK cells within CD45$^+$ immune cells. (**E**) Intratumoral frequency of CD3$^+$, CD4$^+$, and CD8$^+$ T cells within CD45$^+$ immune cells. (**F**) Overview of experiment described in (G, H). Male C57BL/6J mice (n=8-10/group) were subcutaneously inoculated with KPC3.TRP1 cells (1x10^5/mouse) and received i.v. injections with Pela (2x10^8 pfu/injection) and intraperitoneal (i.p.) injections with CD3-bsAbs (12.5 **μ**g/injection) on indicated days. (**G**) Individual tumor growth curves of mice receiving indicated treatments. (**H**) Kaplan-Meier survival graphs of mice after indicated treatments. Data represent mean±SEM. Differences between groups in (B), (D), and (E) against the PBS-treated group was determined using an ordinary one-way analysis of variance (ANOVA) with Dunnett's post hoc test. Log-rank tests were used to compare differences in survival in (H). Significance levels: ns=not significant, *p<0.05, **p<0.01, and ****p<0.0001.

DISCUSSION

Here, we tackled an important topic of debate in the field of oncolytic virus (OV) therapy, by investigating the impact of preexisting immunity, in particular the role of neutralizing antibodies (NAbs), on the antitumor efficacy of oncolytic Reovirus (Reo). Our data demonstrated that preexposure-induced Reo-specific NAbs are detrimental to Reo infection and Reo-induced tumor control when used as monotherapy. In contrast, the Reo-induced influx of T cells was not affected by NAbs and Reo-based combinatorial immunotherapy remained effective in preexposed mice.

It currently remains unknown why the Reo-induced T-cell influx remained unaffected by preexposure, even though the copy numbers of Reo and the expression of ISGs in tumors were impaired. However, a similar observation was made in a study where immunocompetent naive or Newcastle disease virus (NDV)-exposed B16.F10-bearing C57BL/6J mice were intratumorally injected with NDV (38). Although viral replication was decreased in preexposed mice, the NDV-induced intratumoral influx of CD8$^+$ T cells was comparable between naive and preexposed animals. In our studies, it might be possible that the remaining moderate expression of T-cell-attracting chemokine *Cxcl9* in tumors of preexposed mice was sufficient to attract T cells to the tumor. In contrast to *Cxcl10* and *Cxcl11* which are induced by both type I and type II IFN, *Cxcl9* is only induced by type II IFN, which might contribute to this different expression pattern (39). Furthermore, the expression of ISGs was strongly reduced in the presence of NAbs, but not completely abrogated. Since interferons are powerful immune mediators, a very moderate IFN response, either induced by Reo itself, incoming T cells or NK cells, or by the transmission of an antiviral state from a few Reo-infected tumor cells to neighboring tumor cells, might have been sufficient to induce T-cell attraction to the tumor (40,41).

Alternatively, it is possible that administration of Reo to preexposed mice did not completely preclude effective viral infection and ISG expression, but that the presence

of Reo, the expression of ISGs, and the subsequent influx of T cells might follow different kinetics in preexposed mice compared to naive mice. The preexisting NAbs will presumably lead to faster clearance of the virus, even upon intratumoral injection. However, a short presence of Reo in the tumor might already have been sufficient to attract and maintain T cells in the tumor, without the need for continued viral presence.

Lastly, the processing and presentation of viral epitopes are expected to be affected by the presence of NAbs (42), which might also explain why a different Reo-specific $CD8^+$ T-cell population is dominant in tumors of preexposed mice. Although the presence of Reo itself is diminished, this does not directly preclude the presentation of viral epitopes. A continued presentation of viral epitopes might thus retain $CD8^+$ T cells in the tumor. While these observations provide interesting avenues for further research, we concluded here that the impaired Reo infection observed in preexposed mice, or upon repeated intravenous Reo infusions, does not preclude effective intratumoral T-cell influx and thus permits potent antitumor responses upon combinatorial Reo and T-cell-based immunotherapy.

The conclusion that NAbs present a barrier to the antitumor efficacy of Reo monotherapy may be surprising, since previous studies suggested that NAbs are beneficial (14,15). However, the beneficial role of NAbs has only been demonstrated in the context of immune cell carriage. For instance, mechanistic studies have shown that Reo can be taken up and internalized by various immune cells, including human monocytes, DCs, and T cells (13-15,43,44). Here, the presence of NAbs can contribute to enhanced uptake, since Reo/NAb complexes are more efficiently internalized by immune cells compared to Reo particles alone. Thus, NAbs might be beneficial specifically when employing cellular carriers for Reo delivery to tumors, but the effect of NAbs on the antitumor efficacy of Reo remained unknown. Here, we unequivocally demonstrate that the presence of NAbs restricts the antitumor efficacy of Reo therapy, even when administered intratumorally.

Since a large proportion of the human population, including cancer patients, has been preexposed to Reo and thus has circulating NAbs, our data may explain why Reo monotherapy has not yet reached optimal efficacy in prior clinical studies. Still, various approaches, including the above-mentioned use of immune cell carriage, have been proposed to enhance the delivery of Reo particles to tumors in the presence of NAbs (7). For instance, the use of a low dosage of the chemotherapeutic drug cyclophosphamide (CPA) leads to the depletion of regulatory T cells and enhanced tumor-specific $CD8^+$ T-cell responses (45,46), but can also ablate the production of NAbs, leading to enhanced anticancer efficacy of Reo therapy (47,48). Although these preclinical results were encouraging, compiled data from various Phase I clinical trials demonstrated that the effect of CPA or other chemotherapeutic drugs such as gemcitabine and docetaxel only moderately reduced Reo-specific NAb responses (49). Additionally, the use of CPA or other chemotherapeutics to prevent NAb production

might only be relevant for individuals that have not been exposed to Reo before, which is a minority of patients. Alternatively, it might be possible to employ certain apheresis techniques such as plasma exchange (50) or immunoadsorption (51) in seropositive patients, which are already applied in the context of autoimmune diseases and organ transplants. Especially immunoadsorption ensures rapid removal of specific antibodies from the circulation, and might be performed in seropositive patients before Reo therapy to greatly reduce the level of preexisting NAbs. However, the activation of Reo-specific B cells upon the first therapeutic Reo administration will lead to rapidly emerging new NAbs that will hamper the efficacy of subsequent infusions.

The above-mentioned strategies could be employed to reduce, circumvent, or remove NAb responses to increase the efficacy of Reo monotherapy. However, our data strongly suggest that these efforts might not be necessary. We expect that combined Reo and checkpoint blockade, which has already demonstrated potent responses in various preclinical models (52,53), and is currently the subject of various clinical trials, as well as other combinatorial strategies that also rely on the effective Reo-induced influx of T cells, such as T-cell-engagers (3), vaccination (30) or the use of dual-specific CAR T cells (54) should be able to demonstrate potent antitumor responses in the presence of NAbs. Thus, our data are encouraging for ongoing and future clinical trials investigating the efficacy of Reo and T-cell-based immunotherapeutic strategies, even in the context of intravenous Reo administration.

Altogether, given the high prevalence of seropositivity for Reo in cancer patients, this study strongly advocates for the use of Reo as part of a T-cell-based combinatorial approach to unleash its full potential and allow maximal anticancer efficacy, without obstruction by preexisting immune responses.

DECLARATIONS

Acknowledgments. The authors gratefully acknowledge the operators of the Flow Cytometry Core Facility (FCF) of the LUMC and the Animal Facility of the LUMC for their excellent support and care of the animals, respectively. The hybridoma 10F6 (reovirus μ1), developed by T. S. Dermody from the University of Pittsburgh School of Medicine, was obtained from the Developmental Studies Hybridoma Bank, created by the NICHD of the NIH and maintained at The University of Iowa, Department of Biology, Iowa City, IA 52242. All figures regarding experimental designs are created with BioRender.com.
Author contributions. Conceptualization: CG, TvH, NvM. Methodology: CG, PK, LG, CL, DvdW, RH, TvH, NvM. Formal analysis: CG. Investigation: CG, PK, OR. Resources: DvdW, RH, MC, LH, EMEV, MJPW. Writing – Original Draft: CG, NvM. Writing - Review & Editing: CG, SHvdB, TvH, NvM. Visualization: CG. Supervision: NvM. Funding acquisition: TvH, NvM. All authors approved the final version of the manuscript.

Funding. This work was financially supported by a PhD fellowship from Leiden University Medical Center (to CG), a research grant from Oncolytics Biotech Inc. (to TvH and NvM) and the Support Casper campaign by the Dutch foundation 'Stichting Overleven met Alvleesklierkanker' (supportcasper.nl) project number SOAK 22.02 (to NvM).

Competing interests. MC and HL are employees of Oncolytics Biotech Inc. TvH and NvM received funding from Oncolytics Biotech Inc. in the past. All other authors declare no conflict of interest. The funders had no role in the design of the study; in the collection, analyses, or interpretation of data; in the writing of the manuscript, or in the decision to publish the results.

Data availability statement. All data relevant to this study are included in the main text or the supplementary materials and are available on reasonable request.

REFERENCES

1. Groeneveldt C, van Hall T, van der Burg SH, Ten Dijke P, van Montfoort N. Immunotherapeutic Potential of TGF-β Inhibition and Oncolytic Viruses. Trends Immunol **2020**;41:406-20
2. Müller L, Berkeley R, Barr T, Ilett E, Errington-Mais F. Past, Present and Future of Oncolytic Reovirus. Cancers (Basel) **2020**;12
3. Groeneveldt C, Kinderman P, van den Wollenberg DJM, van den Oever RL, Middelburg J, Mustafa DAM*, et al.* Preconditioning of the tumor microenvironment with oncolytic reovirus converts CD3-bispecific antibody treatment into effective immunotherapy. J Immunother Cancer **2020**;8:e001191
4. Morris DG, Feng X, DiFrancesco LM, Fonseca K, Forsyth PA, Paterson AH*, et al.* REO-001: A phase I trial of percutaneous intralesional administration of reovirus type 3 dearing (Reolysin®) in patients with advanced solid tumors. Investigational new drugs **2013**;31:696-706
5. Vidal L, Pandha HS, Yap TA, White CL, Twigger K, Vile RG*, et al.* A Phase I Study of Intravenous Oncolytic Reovirus Type 3 Dearing in Patients with Advanced Cancer. Clinical Cancer Research **2008**;14:7127-37
6. Forsyth P, Roldán G, George D, Wallace C, Palmer CA, Morris D*, et al.* A Phase I Trial of Intratumoral Administration of Reovirus in Patients With Histologically Confirmed Recurrent Malignant Gliomas. Molecular Therapy **2008**;16:627-32
7. Groeneveldt C, van den Ende J, van Montfoort N. Preexisting immunity: Barrier or bridge to effective oncolytic virus therapy? Cytokine & Growth Factor Reviews **2023**;70:1-12
8. Tai JH, Williams JV, Edwards KM, Wright PF, Crowe JJE, Dermody TS. Prevalence of Reovirus-Specific Antibodies in Young Children in Nashville, Tennessee. J Infect Disease **2005**;191:1221-4
9. White CL, Twigger KR, Vidal L, De Bono JS, Coffey M, Heinemann L*, et al.* Characterization of the adaptive and innate immune response to intravenous oncolytic reovirus (Dearing type 3) during a phase I clinical trial. Gene Therapy **2008**;15:911-20
10. Lolkema MP, Arkenau H-T, Harrington K, Roxburgh P, Morrison R, Roulstone V*, et al.* A Phase I Study of the Combination of Intravenous Reovirus Type 3 Dearing and Gemcitabine in Patients with Advanced Cancer. Clinical Cancer Research **2011**;17:581-8
11. Comins C, Spicer J, Protheroe A, Roulstone V, Twigger K, White CM*, et al.* REO-10: A Phase I Study of Intravenous Reovirus and Docetaxel in Patients with Advanced Cancer. Clinical Cancer Research **2010**;16:5564-72
12. Galanis E, Markovic SN, Suman VJ, Nuovo GJ, Vile RG, Kottke TJ*, et al.* Phase II trial of intravenous administration of Reolysin(®) (Reovirus Serotype-3-dearing Strain) in patients with metastatic melanoma. Mol Ther **2012**;20:1998-2003
13. Adair RA, Roulstone V, Scott KJ, Morgan R, Nuovo GJ, Fuller M*, et al.* Cell Carriage, Delivery, and Selective Replication of an Oncolytic Virus in Tumor in Patients. Science Translational Medicine **2012**;4
14. Berkeley RA, Steele LP, Mulder AA, van den Wollenberg DJM, Kottke TJ, Thompson J*, et al.* Antibody-Neutralized Reovirus Is Effective in Oncolytic Virotherapy. Cancer Imm Res **2018**;6:1161-73
15. Ilett E, Kottke T, Donnelly O, Thompson J, Willmon C, Diaz R*, et al.* Cytokine Conditioning Enhances Systemic Delivery and Therapy of an Oncolytic Virus. Molecular Therapy **2014**;22:1851-63
16. Dijkgraaf EM, Santegoets SJ, Reyners AK, Goedemans R, Wouters MC, Kenter GG*, et al.* A phase I trial combining carboplatin/doxorubicin with tocilizumab, an anti-IL-6R monoclonal antibody, and interferon-α2b in patients with recurrent epithelial ovarian cancer. Annals of oncology : official journal of the European Society for Medical Oncology **2015**;26:2141-9
17. Verdegaal E, van der Kooij MK, Visser M, van der Minne C, de Bruin L, Meij P*, et al.* Low-dose interferon-alpha preconditioning and adoptive cell therapy in patients with metastatic melanoma refractory to standard (immune) therapies: a phase I/II study. J Immunother Cancer **2020**;8

18. Santegoets SJ, van Ham VJ, Ehsan I, Charoentong P, Duurland CL, van Unen V*, et al.* The Anatomical Location Shapes the Immune Infiltrate in Tumors of Same Etiology and Affects Survival. Clin Cancer Res **2019**;25:240-52
19. Speetjens FM, Kuppen PJ, Welters MJ, Essahsah F, Voet van den Brink AM, Lantrua MG*, et al.* Induction of p53-specific immunity by a p53 synthetic long peptide vaccine in patients treated for metastatic colorectal cancer. Clin Cancer Res **2009**;15:1086-95
20. van den Wollenberg DJM, Dautzenberg IJC, van den Hengel SK, Cramer SJ, de Groot RJ, Hoeben RC. Isolation of reovirus T3D mutants capable of infecting human tumor cells independent of junction adhesion molecule-A. PLoS One **2012**;7:e48064-e
21. Smith RE, Zweerink HJ, Joklik WK. Polypeptide components of virions, top component and cores of reovirus type 3. Virology **1969**;39:791-810
22. Fallaux FJ, Kranenburg O, Cramer SJ, Houweling A, Van Ormondt H, Hoeben RC*, et al.* Characterization of 911: a new helper cell line for the titration and propagation of early region 1-deleted adenoviral vectors. Human gene therapy **1996**;7:215-22
23. Hingorani SR, Wang L, Multani AS, Combs C, Deramaudt TB, Hruban RH*, et al.* Trp53R172H and KrasG12D cooperate to promote chromosomal instability and widely metastatic pancreatic ductal adenocarcinoma in mice. Cancer cell **2005**;7:469-83
24. Benonisson H, Altıntaş I, Sluijter M, Verploegen S, Labrijn AF, Schuurhuis DH*, et al.* CD3-Bispecific Antibody Therapy Turns Solid Tumors into Inflammatory Sites but Does Not Install Protective Memory. Molecular cancer therapeutics **2019**;18:312-22
25. Lin K-Y, Guarnieri FG, Staveley-O'Carroll KF, Levitsky HI, August JT, Pardoll DM*, et al.* Treatment of Established Tumors with a Novel Vaccine That Enhances Major Histocompatibility Class II Presentation of Tumor Antigen. Cancer Res **1996**;56:21-6
26. Belkina AC, Ciccolella CO, Anno R, Halpert R, Spidlen J, Snyder-Cappione JE. Automated optimized parameters for T-distributed stochastic neighbor embedding improve visualization and analysis of large datasets. Nature Communications **2019**;10:5415
27. Murphy JP, Kim Y, Clements DR, Konda P, Schuster H, Kowalewski DJ*, et al.* Therapy-Induced MHC I Ligands Shape Neo-Antitumor CD8 T Cell Responses during Oncolytic Virus-Based Cancer Immunotherapy. J Proteome Res **2019**;18:2666-75
28. Mijatovic-Rustempasic S, Tam KI, Kerin TK, Lewis JM, Gautam R, Quaye O*, et al.* Sensitive and specific quantitative detection of rotavirus A by one-step real-time reverse transcription-PCR assay without antecedent double-stranded-RNA denaturation. Journal of clinical microbiology **2013**;51:3047-54
29. Dupont WD, Plummer WD, Jr. Power and sample size calculations. A review and computer program. Controlled clinical trials **1990**;11:116-28
30. Groeneveldt C, Kinderman P, van Stigt Thans JJC, Labrie C, Griffioen L, Sluijter M*, et al.* Preinduced reovirus-specific T-cell immunity enhances the anticancer efficacy of reovirus therapy. Journal for ImmunoTherapy of Cancer **2022**;10:e004464
31. Loken SD, Norman K, Hirasawa K, Nodwell M, Lester WM, Demetrick DJ. Morbidity in immunosuppressed (SCID/NOD) mice treated with reovirus (Dearing 3) as an anti-cancer biotherapeutic. Cancer Biology & Therapy **2004**;3:734-8
32. Kim M, Garant KA, zur Nieden NI, Alain T, Loken SD, Urbanski SJ*, et al.* Attenuated reovirus displays oncolysis with reduced host toxicity. Br J Cancer **2011**;104:290-9
33. Dina Zita M, Phillips MB, Stuart JD, Kumarapeli AR, Snyder AJ, Paredes A*, et al.* The M2 Gene Is a Determinant of Reovirus-Induced Myocarditis. J Virol **2022**;96:e0187921
34. Samson A, Scott KJ, Taggart D, West EJ, Wilson E, Nuovo GJ*, et al.* Intravenous delivery of oncolytic reovirus to brain tumor patients immunologically primes for subsequent checkpoint blockade. Sci Transl Med **2018**;10:eaam7577
35. Collienne M, Loghmani H, Heineman TC, Arnold D. GOBLET: a phase I/II study of pelareorep and atezolizumab +/- chemo in advanced or metastatic gastrointestinal cancers. Future oncology (London, England) **2022**;18:2871-8

36. Sivanandam V, LaRocca CJ, Chen NG, Fong Y, Warner SG. Oncolytic Viruses and Immune Checkpoint Inhibition: The Best of Both Worlds. Molecular Therapy - Oncolytics **2019**;13:93-106
37. Kleinovink JW, Marijt KA, Schoonderwoerd MJA, van Hall T, Ossendorp F, Fransen MF. PD-L1 expression on malignant cells is no prerequisite for checkpoint therapy. Oncoimmunology **2017**;6:e1294299
38. Ricca JM, Oseledchyk A, Walther T, Liu C, Mangarin L, Merghoub T*, et al.* Pre-existing Immunity to Oncolytic Virus Potentiates Its Immunotherapeutic Efficacy. Molecular Therapy **2018**;26:1008-19
39. Tokunaga R, Zhang W, Naseem M, Puccini A, Berger MD, Soni S*, et al.* CXCL9, CXCL10, CXCL11/CXCR3 axis for immune activation - A target for novel cancer therapy. Cancer treatment reviews **2018**;63:40-7
40. Vitiello GAF, Ferreira WAS, Cordeiro de Lima VC, Medina TDS. Antiviral Responses in Cancer: Boosting Antitumor Immunity Through Activation of Interferon Pathway in the Tumor Microenvironment. Front Immunol **2021**;12:782852
41. Geoffroy K, Bourgeois-Daigneault M-C. The pros and cons of interferons for oncolytic virotherapy. Cytokine & Growth Factor Reviews **2020**;56:49-58
42. van Montfoort N, Mangsbo SM, Camps MGM, van Maren WWC, Verhaart IEC, Waisman A*, et al.* Circulating specific antibodies enhance systemic cross-priming by delivery of complexed antigen to dendritic cells in vivo. European Journal of Immunology **2012**;42:598-606
43. Ilett EJ, Bárcena M, Errington-Mais F, Griffin S, Harrington KJ, Pandha HS*, et al.* Internalization of Oncolytic Reovirus by Human Dendritic Cell Carriers Protects the Virus from Neutralization. Clinical Cancer Research **2011**;17:2767-76
44. Roulstone V, Khan K, Pandha HS, Rudman S, Coffey M, Gill GM*, et al.* Phase I trial of cyclophosphamide as an immune modulator for optimizing oncolytic reovirus delivery to solid tumors. Clin Cancer Res **2015**;21:1305-12
45. Ghiringhelli F, Menard C, Puig PE, Ladoire S, Roux S, Martin F*, et al.* Metronomic cyclophosphamide regimen selectively depletes CD4+CD25+ regulatory T cells and restores T and NK effector functions in end stage cancer patients. Cancer Immunol Immunother **2007**;56:641-8
46. Scurr M, Pembroke T, Bloom A, Roberts D, Thomson A, Smart K*, et al.* Low-Dose Cyclophosphamide Induces Antitumor T-Cell Responses, which Associate with Survival in Metastatic Colorectal Cancer. Clin Cancer Res **2017**;23:6771-80
47. Qiao J, Wang H, Kottke T, White C, Twigger K, Diaz RM*, et al.* Cyclophosphamide Facilitates Antitumor Efficacy against Subcutaneous Tumors following Intravenous Delivery of Reovirus. Clinical Cancer Research **2008**;14:259-69
48. Kottke T, Thompson J, Diaz RM, Pulido J, Willmon C, Coffey M*, et al.* Improved Systemic Delivery of Oncolytic Reovirus to Established Tumors Using Preconditioning with Cyclophosphamide-Mediated Treg Modulation and Interleukin-2. Clinical Cancer Research **2009**;15:561-9
49. Roulstone V, Mansfield D, Harris RJ, Twigger K, White C, de Bono J*, et al.* Antiviral antibody responses to systemic administration of an oncolytic RNA virus: the impact of standard concomitant anticancer chemotherapies. Journal for ImmunoTherapy of Cancer **2021**;9:e002673-e
50. Weinstein R. Basic principles of therapeutic plasma exchange. Transfusion and Apheresis Science **2023**;62:103675
51. Braun N, Bosch T. Immunoadsorption, current status and future developments. Expert opinion on investigational drugs **2000**;9:2017-38
52. Mostafa AA, Meyers DE, Thirukkumaran CM, Liu PJ, Gratton K, Spurrell J*, et al.* Oncolytic Reovirus and Immune Checkpoint Inhibition as a Novel Immunotherapeutic Strategy for Breast Cancer. Cancers **2018**;10

53. Augustine T, John P, Friedman T, Jiffry J, Guzik H, Mannan R*, et al.* Potentiating effect of reovirus on immune checkpoint inhibition in microsatellite stable colorectal cancer. Front Oncol **2022**;12
54. Evgin L, Kottke T, Tonne J, Thompson J, Huff AL, van Vloten J*, et al.* Oncolytic virus-mediated expansion of dual-specific CAR T cells improves efficacy against solid tumors in mice. Sci Transl Med **2022**;14:eabn2231

SUPPLEMENTARY FIGURES

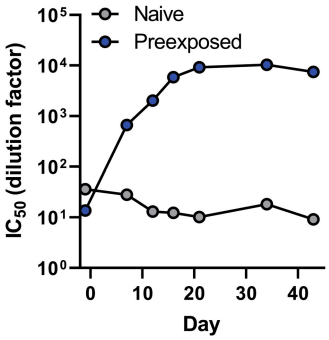


Figure S1. Kinetics of neutralizing antibodies after preexposure. Graph depicts IC_{50} values of pooled plasma (n=6 mice/group) of indicated groups that were harvested on indicated days and subjected to a Reo neutralization assay. IC_{50} values were calculated using non-linear regression analysis.

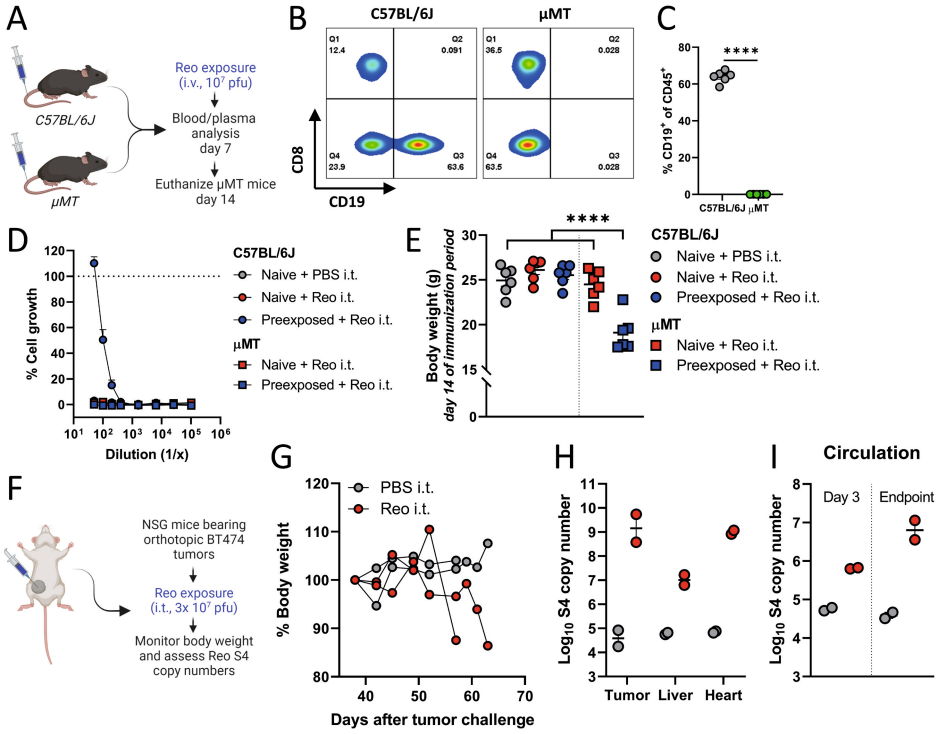


Figure S2. Neutralizing antibodies are required to prevent Reo-induced weight loss and viremia. (**A**) Overview of experiment described in (B-E). Male C57BL/6J or µMT mice (n=6/group) were exposed to Reo by intravenous (i.v.) injection (10^7 plaque-forming units (pfu)/injection) on day 0. (**B**) Representative flow cytometry plots of $CD19^+$ B cells in the circulation of C57BL/6J or µMT mice. (**C**) Quantification of $CD19^+$ B cells in the circulation. (**D**) Reo neutralization assay. Average dilution curves using plasma from indicated groups, harvested on day 7 after preexposure. (**E**) Body weight on day 14 after Reo exposure.

>>

>> (**F**) NSG mice (n=2/group) were inoculated orthotopically with BT474 tumor cells (5x10^6/mouse) in the mammary fat pad and received intratumoral Reo injections (10^7 plaque-forming units (pfu)/injection) on days 37-39. (**G**) Individual changes in body weight during the experiment from the moment of Reo administration. See next page for continuation of figure legend. (**H**) Presence of genomic copies of Reo S4 segment in the tumor, liver, and heart, as measured by quantitative reverse transcription PCR (RT-qPCR). (**I**) Presence of infectious Reo particles in the circulation, as measured by RT-qPCR. Plasma was obtained on day 3 and at the experimental endpoint, and 5 µL was transferred to a monolayer of KPC3 cells. Samples were harvested after 24 hours and subjected to RT-qPCR analysis. Difference between groups in (C) was determined using an unpaired t test, and an ordinary one-way analysis of variance (ANOVA) with Tukey's post hoc test was used to determine differences between groups in (E) Significance level: ****p<0.0001.

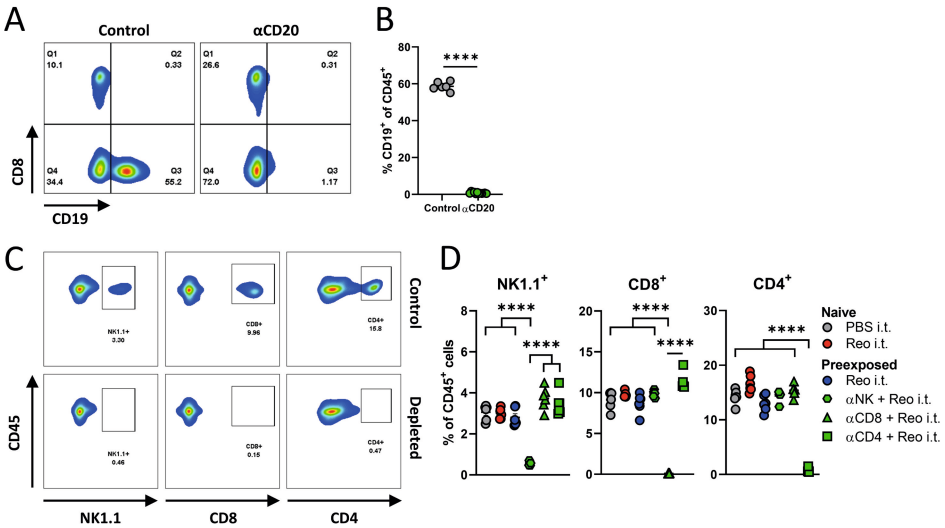


Figure S3. Depletion efficiency during preexposure. (**A**) Representative flow cytometry plots of CD19$^+$ B cells in the circulation after administration of αCD20. (**B**) Quantification of CD19$^+$ B cells in the circulation. (**C**) Representative flow cytometry plots of NK1.1$^+$, CD8$^+$, or CD4$^+$ cells in the circulation after administration of αNK, αCD8, or αCD4 antibodies. (**D**) Quantification of NK1.1$^+$, CD8$^+$, or CD4$^+$ cells in the circulation. Data represent mean±SEM. Differences between groups in (B) were determined using an unpaired t test, and an ordinary one-way analysis of variance (ANOVA) with Tukey's post hoc test was used to determine differences between groups in (D). Significance level: ****p<0.0001.

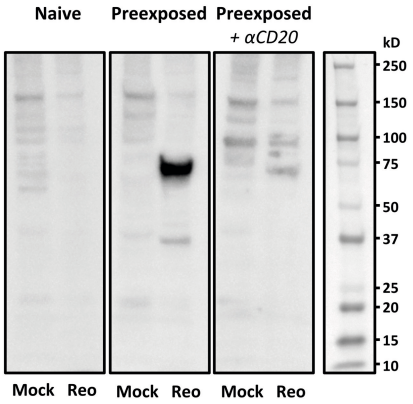


Figure S4. B-cell depletion during preexposure does not completely abrogate the presence of Reo-specific neutralizing antibodies. Western blot of Mock or Reo-infected lysates of HER911 cells using mouse plasma as primary antibody source.

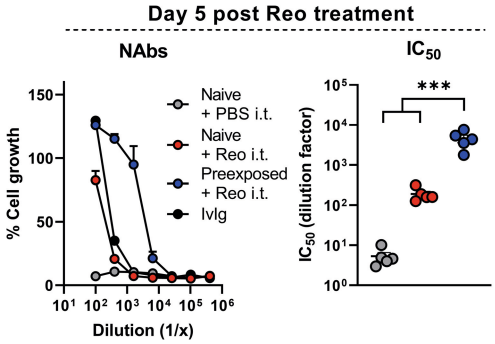


Figure S5. Reo-specific neutralizing antibodies are present 5 days after intratumoral Reo administration. Reo neutralization assay. Average dilution curves using plasma from naive or preexposed mice and individual IC_{50} values on day 5 post intratumoral Reo treatment. Data represent mean±SEM. IC_{50} values were calculated using non-linear regression analysis. Differences between groups were determined using an ordinary one-way analysis of variance (ANOVA) with Tukey's post hoc test. Significance level: ***p<0.001.

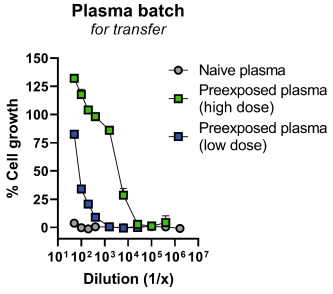


Figure S6. Neutralization capacity of plasma used for the transfer to NSG mice. Reo neutralization assay. Dilution curves were prepared using combined plasma from immunocompetent C57BL/6J naive mice (naive plasma) or C57BL/6J mice that were intravenously preexposed to Reo (preexposed plasma).

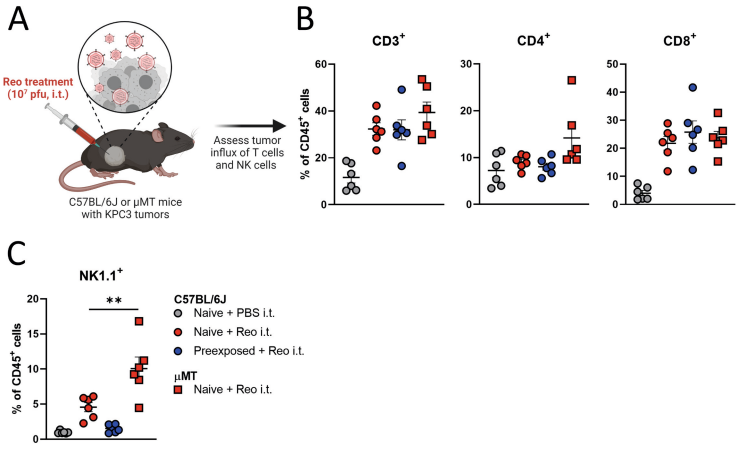


Figure S7. Intratumoral T-cell influx after Reo treatment in µMT or C57BL/6J mice. (**A**) Design of experiment described in (B, C). Male C57BL/6J or µMT mice (n=6/group) were subcutaneously inoculated with KPC3 cells (1x10^5/mouse) and received intratumoral (i.t.) Reo injections (10^7 pfu/injection) on days 13-15. Mice were sacrificed 7 days after Reo administration for ***ex vivo*** analysis. (**B**) Intratumoral frequency of CD3$^+$, CD4$^+$, and CD8$^+$ T cells within CD45$^+$ immune cells. (**C**) Intratumoral frequency of NK cells within CD45$^+$ immune cells. Data represent mean±SEM and differences between groups in (B) and (C) were determined using an ordinary one-way analysis of variance (ANOVA) with Tukey's post hoc test. Significance level: **p<0.01.

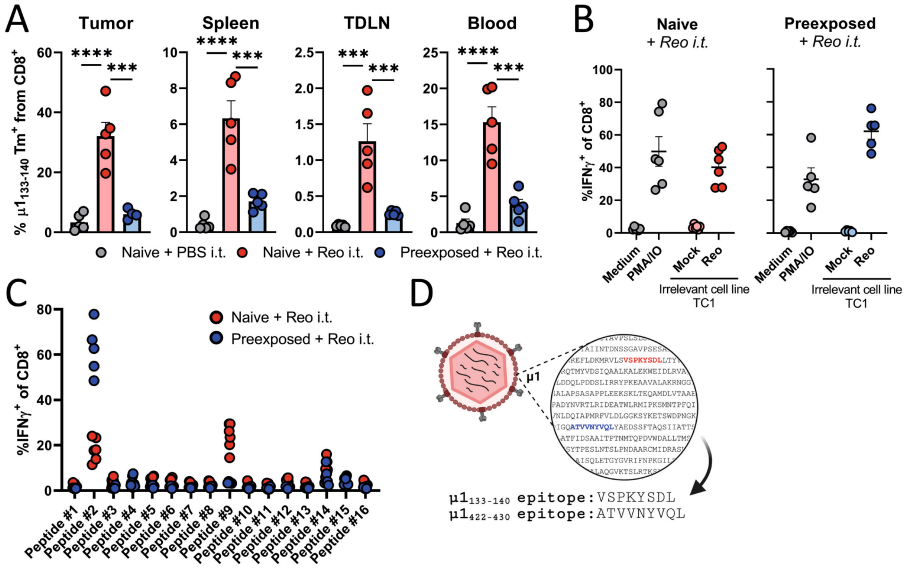


Figure S8. Preexposure affects the specificity of Reo-specific CD8$^+$ T cells. (**A**) Frequency of Reo-specific µ1$_{133-140}$ tetramer (Tm)$^+$ CD8$^+$ T cells in tumor, spleen, tumor-draining lymph node (TDLN), or blood. (**B**) Frequency of interferon gamma (IFNγ)$^+$ cells within the intratumoral CD8$^+$ T-cell population after coculture with indicated targets, as measured with intracellular cytokine staining. PMA/ionomycin (IO) was used as positive control. (**C**) Frequency of IFNγ$^+$ cells within the intratumoral CD8$^+$ T-cell population after coculture with indicated peptides. Each dot represents 1 tumor. (**D**) Schematic overview of sequence and location of both Reo-derived CD8$^+$ T-cell epitopes. Data represent mean±SEM. Differences between groups in (A) were determined using an ordinary one-way analysis of variance (ANOVA) with Tukey's post hoc test. Significance levels: ***p<0.001 and ****p<0.0001.

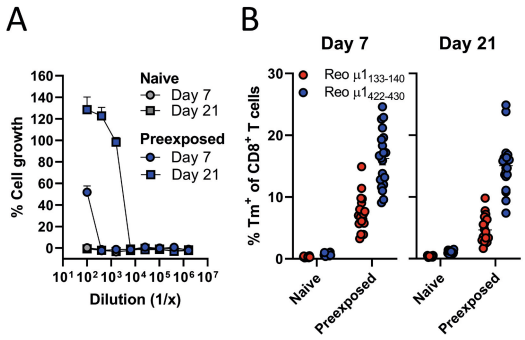


Figure S9. Reo preexposure induces Reo-specific NAbs and CD8⁺ T cells. (**A**) Reo neutralization assay. Average dilution curves using plasma harvested on indicated days. (**B**) Reo-specific $\mu1_{133\text{-}140}$ and $\mu1_{422\text{-}430}$ tetramer $(Tm)^+$ $CD8^+$ T cells in the circulation on indicated days. Data represent mean±SEM.

SUPPLEMENTARY TABLES

Table S1. List of antibodies used for flow cytometric analysis.

	Marker	*Clone*	*Fluorochrome*	*Supplier*
Lymphoid panel	CD45.2	104	FITC	eBioscience
	CD3	145-2C11	PE-CF594	BD Biosciences
	CD8α	53-6.7	Alexa Fluor 700	eBioscience
	Tetramer $\mu1_{133-140}$		APC	In-house
	Tetramer $\mu1_{422-430}$		PE	In-house
	CD4	RM4-5	APC	BioLegend
	NK1.1	Pk136	BV650	BD Biosciences
	CD44	IM-7	BV785	BioLegend
	CD62L	MEL-14	BV421	BioLegend
	CD69	H1.2F3	BV605	BioLegend
	KLRG-1	2F1	PE-Cy7	eBioscience
Intracellular cytokine staining panel	CD45.2	104	FITC	eBioscience
	CD3	145-2C11	PE-CF594	BD Biosciences
	CD8α	53-6.7	Alexa Fluor 700	eBioscience
	IFNγ	XMG1.2	APC	BioLegend

Table S2. Sequences of Reo-derived peptides tested using intracellular cytokine staining.

N	*Peptide*	*Allele*	*nM*	*Reo protein*
1	SSVTGIETI	H-2-Db	100.4	λ2
2	ATVVNYVQL	H-2-Db	56.5	μ1
3	HAITNFTKA	H-2-Db	50.1	μ1
4	SALEKTSQI	H-2-Db	1513.6	σ1
5	TGINNANEL	H-2-Db	84.0	λ1
6	HAITNFTKAEM	H-2-Db	46.2	μ1
7	LSTHNGVSL	H-2-Db	1207.8	μ-NS
8	KQLLNTETL	H-2-Db	11.1	λ1
9	VSPKYSDL	H-2-Kb	10.9	μ1
10	FSPGNDFTHM	H-2-Db	137.5	λ3
11	RMNINPTEI	H-2-Db	29.3	λ1
12	NMMVGFETI	H-2-Db	234.4	λ1
13	TRVVNLDQI	H-2-Db	1100.1	μ1
14	AAFLFKTV	H-2-Kb	25.8	σ2
15	INNAFEGRV	H-2-Kb	227.6	σ3
16	YSIMYPTRM	H-2-Kb	83.0	λ1

Table S3. List of primers used for RT-qPCR analysis.

Gene	*Forward*	*Reverse*
S4Q	5′-CGCTTTTGAAGGTCGTGTATCA-3′	5′-CTGGCTGTGCTGAGATTGTTTT-3′
β2M	5′-CTCGGTGACCCTGGTCTTT-3′	5′-CCGTTCTTCAGCATTTGGAT-3′
Bst2	5′-ACATGGCGCCCTCTTTCTATCACT-3′	5′-TGACGGCGAAGTAGATTGTCAGGA-3′
Cxcl9	5′-TGGAGTTCGAGGAACCCTAGT-3′	5′-AGGCAGGTTTGATCTCCGTT-3′
Cxcl10	5′-ACGAACTTAACCACCATCT-3′	5′-TAAACTTTAACTACCCATTGATACATA-3′
Cxcl11	5′-GTTCAAACAGGGGCGCTG-3′	5′-GCATTATGAGGCGAGCTTGC-3′
Ddx58	5′-AAGGCCACAGTTGATCCAAA-3′	5′-TTGGCCAGTTTTCCTTGTCG-3′
Ifit-1	5′-CTGGACAAGGTGGAGAAGGT-3′	5′-AGGGTTTTCTGGCTCCACTT-3′
Ifit-2	5′-TGCTCTTGACTGTGAGGAGG-3′	5′-ATCCAGACGGTAGTTCGCAA-3′
Ifit-3	5′-GTGCAACCAGGTCGAACATT-3′	5′- AGGTGACCAGTCGACGAATT-3′
Irf7	5′-GACCGTGTTTACGAGGAACC-3′	5′-GCTGTACAGGAACACGCATC-3′
Isg15	5′-GGAACGAAAGGGGCCACAGCA-3′	5′-CCTCCATGGGCCTTCCCTCGA-3′
Mx1	5′-GATGGTCCAAACTGCCTTCG-3′	5′-TTGTAAACCTGGTCCTGGCA-3′
Mzt2	5′-TCGGTGCCCATATCTCTGTC-3′	5′-CTGCTTCGGGAGTTGCTTTT-3′
Oas1b	5′-AGCATGAGAGACGTTGTGGA-3′	5′-GCGTAGAATTGTTGGTTAGGCT-3′
Ptp4a2	5′-AGCCCCTGTGGAGATCTCTT-3′	5′-AGCATCACAAACTCGAACCA-3′
Rsad2	5′-GGTGCCTGAATCTAACCAGAAG-3′	5′-CCACGCCAACATCCAGAATA-3′

ADDENDUM

$CD4^+$ T-cell depletion abrogates NAb production and improves the efficacy of reovirus monotherapy

BACKGROUND

Although NAbs hamper the efficacy of reovirus (Reo) when used as oncolytic agent, they are required to prevent Reo-induced weight loss and viremia. Indeed, B-cell deficient mice succumb around 2 weeks after reovirus therapy (**Chapter 5, Figure S2**) (1). We also demonstrated that complete abrogation of NAb production by $CD4^+$ T-cell depletion improved reovirus infection (**Chapter 5, Figure 3G**), but the lack of NAbs in these mice did not coincide with weight loss. Therefore, we explored the depletion of $CD4^+$ T cells as a strategy to study the effects of NAbs on the clinical efficacy of reovirus while separating unwanted Reo-induced viremia from the desired Reo-induced antitumor effects.

RESULTS & DISCUSSION

We preexposed immunocompetent C57BL/6J mice intravenously to Reo. $CD4^+$ T-cell depletion was initiated either before (B-exp) or after the first Reo preexposure (A-exp), or before the first intratumoral Reo injection and was continued for the duration of the experiment (**Figure 1A**). Depletion of $CD4^+$ T cells was efficient (**Figure 1B**) and subsequent absence of NAbs was sustained (**Figure 1C**), but only when $CD4^+$ depletion was initiated before the first Reo exposure (**Figure 1C**). The complete removal of NAbs, mediated by $CD4^+$ T-cell depletion during Reo preexposure or Reo administration, was not associated with changes in body weight (**Figure 1D**), but significantly delayed outgrowth of KPC3 tumors upon intratumoral Reo administration (**Figure 1E**), resulting in smaller tumors at later time points (**Figure 1F**). Combined, these results show that abrogation of Reo-specific NAb responses by $CD4^+$ T-cell depletion can improve the antitumor efficacy of Reo monotherapy, without the concomitant weight loss due to uncontrolled Reo replication that is normally observed when NAbs are absent.

$CD4^+$ T cells are essential for mounting effective B-cell responses. Especially the interactions between B cells and a specific type of $CD4^+$ T cell, named follicular helper $CD4^+$ T cell (Tfh), are important. Tfh cells release cytokines such as IL-2, IL-4, and IL-21 that contribute to the formation of germinal centers, where they promote the generation of antibody-producing plasma cells (2). Similar as what we observed for Reo, it is demonstrated that $CD4^+$ T cells are absolutely required for the generation of optimal antibody responses after infection with coronavirus (3), vaccinia virus (4), or vesicular stomatitis virus (5). It has also been observed earlier that $CD4^+$ T-cell depletion abrogates antibody responses, for instance after intramuscular immunization with an Adenovirus vector or a trimeric SIV Env gp140 protein (6). However, it is unclear why a complete lack of Reo-specific NAbs after $CD4^+$ T-cell depletion does not coincide with weight loss and viremia, which contrasts the observations in B-cell deficient μMT and NSG mice that succumb after Reo exposure.

The immune system can be considered a dynamic system where certain immune cells can 'take over' when other cells are absent or dysfunctional. In the absence of NAbs, it is possible that Reo-specific $CD8^+$ T cells might have provided protection from Reo-induced pathology. Indeed, depletion of $CD4^+$ T cells during Reo preexposure did not preclude the mounting of Reo-specific $CD8^+$ T-cell responses (**Figure 2A**). However, Reo-specific $CD8^+$ T cells could also be found in μMT mice (**Figure 2B**), but these mice still succumbed quickly after Reo exposure. This suggests that $CD8^+$ T cells might not be involved in the clearance of Reo-infected cells (and thus the clearance of Reo itself), or at least not in all settings. Thus, it would be very interesting to identify which other cell types or proteins might be able to provide protection against Reo-induced pathology in settings where NAbs are absent.

These observations provide exciting avenues for further research, especially in the context of preclinical research investigating the role of NAbs on OV therapy. Transient depletion of $CD4^+$ T cells during OV therapy is not applicable as a therapeutic strategy for cancer patients since this would increase the susceptibility to opportunistic pathogens and malignancies, but specific depletion or inhibition of follicular helper $CD4^+$ T cells (Tfh) cells (7), for example by inhibition of Tfh-specific transcription factor B-cell lymphoma 6 (Bcl-6) (8), might be a strategy to consider. It would also be interesting to investigate the specific depletion of regulatory $CD4^+$ T cells (Tregs), since it has been shown in the context of infection with influenza or respiratory syncytial virus that depletion of Tregs leads to reduced virus-specific B-cell responses (9,10). Furthermore, the depletion of Tregs might also result in stronger virus-specific $CD8^+$ T-cell responses that could contribute to protection against virus-induced pathology (11). However, as the effects of $CD4^+$ T-cell depletion on NAbs only work when applied before Reo exposure, this might only be of interest for the minority of patients that do not present with preexisting NAbs (**Chapter 5, Figure 1**). But, we also observed a small delay in tumor outgrowth in mice that received $CD4^+$ T-cell-depleting antibodies after Reo preexposure (A-exp group), even though these mice presented with similar NAb levels as preexposed mice that did not receive $CD4^+$ T-cell-depleting antibodies (**Figure 1C**). We cannot explain this observation, but it indicates that removal of $CD4^+$ T cells might also be employed to enhance the anticancer efficacy of Reo in preexposed individuals, in a NAb independent manner. Furthermore, it would also be interesting to investigate the effect of $CD4^+$ T-cell depletion on the efficacy of Reo&CD3-bsAb therapy, since this might result in increased viral persistence but simultaneously limit the number of T cells that can be employed by CD3-bsAbs and thereby impair, and not improve this combination therapy.

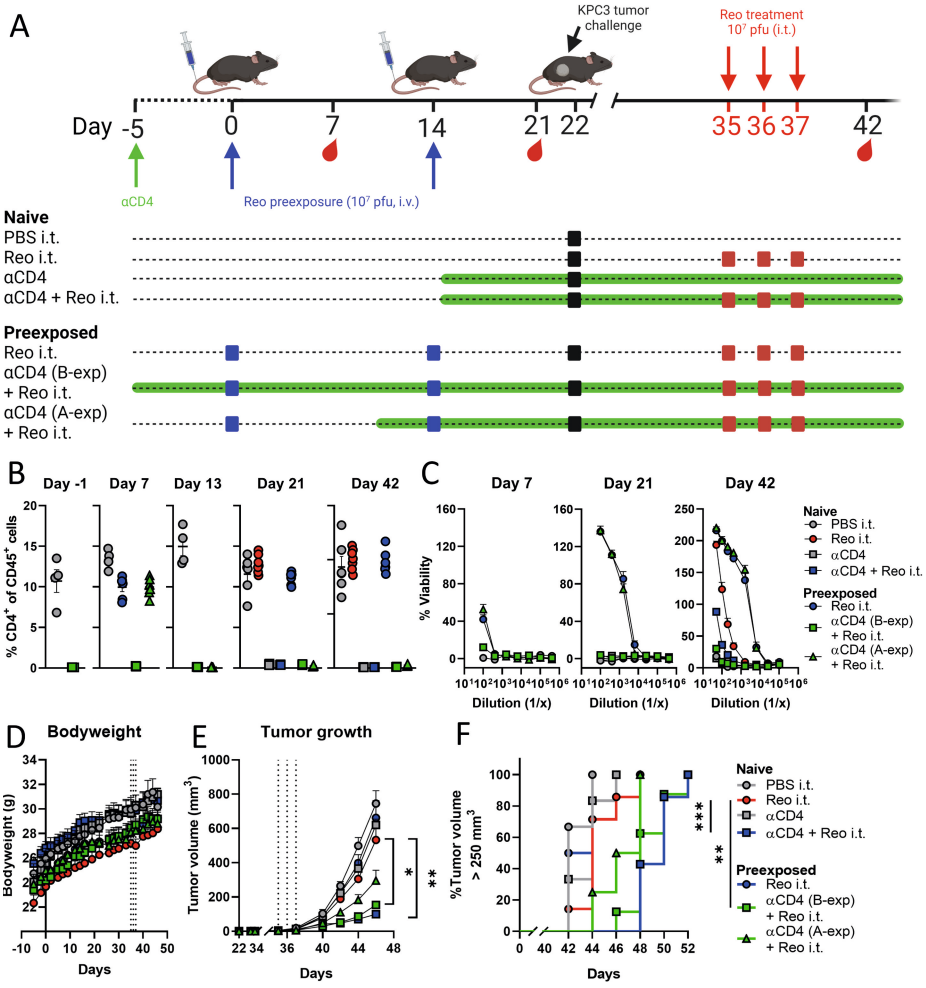


Figure 1. Abrogated production of Reo-specific neutralizing antibodies by CD4⁺ T-cell depletion improves Reo monotherapy efficacy without inducing weight loss. (**A**) Overview of experiment described in (B-F). Male C57BL/6J mice (n=6-8/group) were preexposed by intravenous injection of Reo (10^7 plaque-forming units (pfu)/injection) on days 0 and 14. Depletion of CD4⁺ T cells (αCD4, 100 µg/injection, intraperitoneally) was initiated either before preexposure 1 (B-exp), after preexposure 1 (A-exp), or before KPC3 tumor challenge, and was maintained by weekly injections of αCD4. Blood was drawn on indicated days for interim analysis. After preexposure, mice were inoculated with KPC3 cells ($1x10^5$/mouse) and received intratumoral Reo injections (10^7 pfu/injection) and tumor growth and body weight were monitored during the experiment. (**B**) Frequency of CD4⁺ T cells in the circulation. (**C**) Reo neutralization assay. Average dilution curves using plasma harvested on indicated days. (**D**) Average body weight curves. (**E**) Average tumor volume curves. (**F**) Kaplan-Meier graph showing accumulation of animals reaching tumor volume > 250 mm^3. Data represent mean±SEM. IC_{50} values were calculated using non-linear regression analysis. Differences between groups in (E) were determined using an ordinary two-way analysis of variance (ANOVA) with Tukey's post hoc test, and Mantel-Cox Log-rank tests were used to calculate significant differences between groups in (F). Significance levels: *p<0.05, **p<0.01, and ***p<0.001.

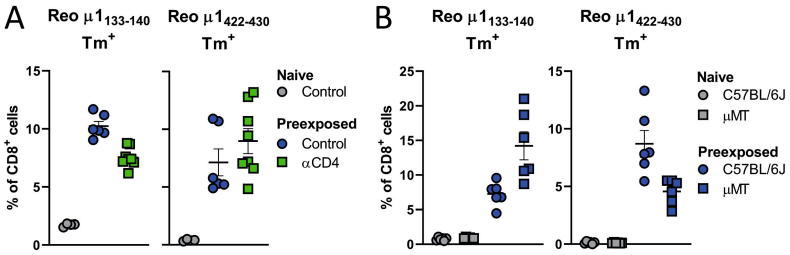


Figure 2. Reo-specific CD8⁺ T-cell responses are present after CD4⁺ T-cell depletion or in B-cell deficient μMT mice. (**A**) Frequency of Reo-specific CD8⁺ T cells in blood. Male immunocompetent C57BL/6J mice (n=6-8/group) were preexposed by intravenous (i.v.) injection of Reo (10^7 plaque-forming units (pfu)/injection) on day 0. Depletion of CD4⁺ T cells (αCD4, 100 μg/injection, intraperitoneally (i.p.)) was initiated before preexposure. Blood was harvested on day 7 for flow cytometry analysis. (**B**) Frequency of Reo-specific CD8⁺ T cells in blood. Male immunocompetent C57BL/6J mice or B-cell deficient μMT mice (n=6/group) were preexposed as described in (A) on day 0, and blood was harvested on day 7 for flow cytometry analysis. Data represent mean±SEM. Significance levels: ***p<0.001 and ****p<0.0001.

CONCLUSION

Combined with the data described in **Chapter 5**, these results show that Reo-specific NAb responses are required to prevent Reo-induced pathology, but they also directly hamper the antitumor efficacy of Reo monotherapy. Depletion of CD4⁺ T cells can abrogate NAb production and enhance the antitumor efficacy of Reo therapy, without concomitant Reo-induced viremia.

REFERENCES

1. Qiao J, Wang H, Kottke T, White C, Twigger K, Diaz RM*, et al.* Cyclophosphamide Facilitates Antitumor Efficacy against Subcutaneous Tumors following Intravenous Delivery of Reovirus. Clinical Cancer Research **2008**;14:259-69
2. Swain SL, McKinstry KK, Strutt TM. Expanding roles for CD4+ T cells in immunity to viruses. Nature Reviews Immunology **2012**;12:136-48
3. Chen J, Lau YF, Lamirande EW, Paddock CD, Bartlett JH, Zaki SR*, et al.* Cellular immune responses to severe acute respiratory syndrome coronavirus (SARS-CoV) infection in senescent BALB/c mice: CD4+ T cells are important in control of SARS-CoV infection. J Virol **2010**;84:1289-301
4. Sette A, Moutaftsi M, Moyron-Quiroz J, McCausland MM, Davies DH, Johnston RJ*, et al.* Selective CD4+ T cell help for antibody responses to a large viral pathogen: deterministic linkage of specificities. Immunity **2008**;28:847-58
5. Thomsen AR, Nansen A, Andersen C, Johansen J, Marker O, Christensen JP. Cooperation of B cells and T cells is required for survival of mice infected with vesicular stomatitis virus. International immunology **1997**;9:1757-66
6. Provine NM, Badamchi-Zadeh A, Bricault CA, Penaloza-MacMaster P, Larocca RA, Borducchi EN*, et al.* Transient CD4+ T Cell Depletion Results in Delayed Development of Functional Vaccine-Elicited Antibody Responses. J Virol **2016**;90:4278-88
7. Crotty S. T follicular helper cell differentiation, function, and roles in disease. Immunity **2014**;41:529-42
8. Pearce AC, Bamford MJ, Barber R, Bridges A, Convery MA, Demetriou C*, et al.* GSK137, a potent small-molecule BCL6 inhibitor with *in vivo* activity, suppresses antibody responses in mice. Journal of Biological Chemistry **2021**;297
9. León B, Bradley JE, Lund FE, Randall TD, Ballesteros-Tato A. FoxP3+ regulatory T cells promote influenza-specific Tfh responses by controlling IL-2 availability. Nat Commun **2014**;5:3495
10. Shao H-Y, Huang J-Y, Lin Y-W, Yu S-L, Chitra E, Chang C-K*, et al.* Depletion of regulatory T-cells leads to moderate B-cell antigenicity in respiratory syncytial virus infection. International Journal of Infectious Diseases **2015**;41:56-64
11. Dietze KK, Zelinskyy G, Gibbert K, Schimmer S, Francois S, Myers L*, et al.* Transient depletion of regulatory T cells in transgenic mice reactivates virus-specific CD8+ T cells and reduces hronic retroviral set points. Proc Natl Acad Sci U S A **2011**;108:2420-5



PART C

Blockade of TGF-β signaling to improve reovirus-based immuno-therapy



CHAPTER 6

Immunotherapeutic Potential of TGF-β Inhibition and Oncolytic Viruses

Christianne Groeneveldt[1], Thorbald van Hall[1], Sjoerd H. van der Burg[1], Peter ten Dijke[2] and Nadine van Montfoort[1#]

[1] Department of Medical Oncology, Oncode Institute, Leiden University Medical Center, 2333 ZA Leiden, The Netherlands

[2] Department of Cell and Chemical Biology, Oncode Institute, Leiden University Medical Center, 2300 RC Leiden, The Netherlands

[#] Corresponding author

Trends in Immunology 2020;41(5):406-420

ABSTRACT

In cancer immunotherapy, a patient's own immune system is harnessed against cancer. Immune checkpoint inhibitors release the brakes on tumor-reactive T cells and therefore are particularly effective in treating certain immune-infiltrated solid tumors. In contrast, solid tumors with immune-silent profiles show limited efficacy of checkpoint blockers due to several barriers. Recent discoveries highlight transforming growth factor-β (TGF-β)-induced immune exclusion and a lack of immunogenicity as examples of these barriers. In this review, we summarize preclinical and clinical evidence that illustrates how the inhibition of TGF-β signaling and the use of oncolytic viruses (OVs) can increase the efficacy of immunotherapy and discuss the promise and challenges of combining these approaches with immune checkpoint blockade.

HIGHLIGHTS

- Immune checkpoint blockade is not effective in immune-excluded and immune-desert tumors due to an immunosuppressive tumor microenvironment and the absence of activated T cells.
- TGF-β is a pleiotropic cytokine that contributes to immune exclusion and evasion in various cancer types.
- The therapeutic efficacy of oncolytic viruses is built on the recruitment of T cells and the induction of tumor-reactive immunity.
- Oncolytic virotherapy and inhibition of TGF-β signaling, either alone or in combination, are two emerging approaches to increase the susceptibility of immune-silent tumors to immune checkpoint therapy.

THE IMMUNE PROFILE OF SOLID TUMORS CAN DETERMINE THE EFFICACY OF IMMUNOTHERAPY

Our immune system is able to respond to invading pathogens and initiate a protective immune response. Although malignant cells are much more similar to the host than pathogens are, they still differ genetically, metabolically, and morphologically from normal cells and can therefore be recognized by the adaptive immune system, a trait called **immunogenicity** (see Glossary). In **Box 1** we provide more information about processes involved in antitumor immunity. **Immunotherapy** is being extensively studied as a new modality of cancer treatment for a wide variety of tumors. In contrast to conventional therapies that directly target the proliferation, survival, or metabolic activity of tumor cells, cancer immunotherapy is directed towards immune cells with the purpose of eliciting a durable and effective anticancer immune response.

Box 1: Priming of tumor-specific T cells

Recognition of tumors by T cells requires the expression of tumor antigens (TAs), aberrant proteins, or peptides beyond the normal repertoire that alert the adaptive immune system that the tumor cell is no longer healthy. Different classes of tumor antigens have been identified, of which **neoantigens** are the most tumor-specific. Neoantigens arise from genetic mutations in a tumor cell that give rise to a novel protein or peptide sequence. The number of mutations varies significantly per tumor type and it is believed that tumors with a high mutational burden are more immunogenic, display a higher immune infiltrate, and are more responsive to immune checkpoint inhibitors than tumors with a low mutational burden (1).

Whereas CTLs are believed to be the main T-cell subset responsible for eliminating cancer cells, $CD4^+$ T helper cells are of vital importance in shaping the tumor-specific T-cell response (2). Priming of naive $CD4^+$ and $CD8^+$ T cells towards effective tumor-specific $CD4^+$ helper and $CD8^+$ cytotoxic T cells, respectively, is a multifaceted process that requires uptake, processing, and presentation of TAs by dendritic cells (DCs) in the context of inflammation (3). The sensing of inflammatory signals, derived from **pathogen-associated molecular patterns** (PAMPs) or **damage-associated molecular patterns** (DAMPs) by a DC induces a differentiation process called maturation. DC maturation is characterized by upregulated amounts of costimulatory molecules, antigen processing, and presentation pathways, and the production of type 1 helper T cell (Th1) skewing cytokines.

The tumor microenvironment (TME) is usually not inflammatory in nature, and additionally, tumors use several strategies to actively suppress the immune system, leading to T-cell ignorance. Activating tumor-specific $CD4^+$ and $CD8^+$ T cells by applying TAs in the optimal context together with a DC maturing agent is in some cases achieved by cancer vaccine platforms, such as synthetic peptide-based vaccines or dendritic cell-based vaccines (4-6). However, tumors often have the ability to escape immune recognition and destruction, which highlights the need for effective immunotherapeutic strategies to overcome these barriers.

The tumor immune profile is an important determinant to guide immunotherapeutic strategies (7,8). Clinical responses to immune checkpoint inhibition mostly occur in patients with an **immune-infiltrated** tumor phenotype, which displays a pre-existing but often dysfunctional immune response (9). In contrast to immune-infiltrated tumors, **immune-excluded or immune-desert** (also described as immune-silent) tumors are less susceptible to checkpoint inhibition because **tumor-infiltrating T cells** (TILs) are absent (10). Strategies to convert immune-silent tumors into immune-active tumors are desperately needed to broaden the fraction of patients that might benefit from immune checkpoint therapy. In this review, we discuss two emerging approaches that

might be harnessed on their own or in combination to enhance the efficacy of immune checkpoint inhibition in immune-silent tumors (**Figure 1, Graphical Abstract**).

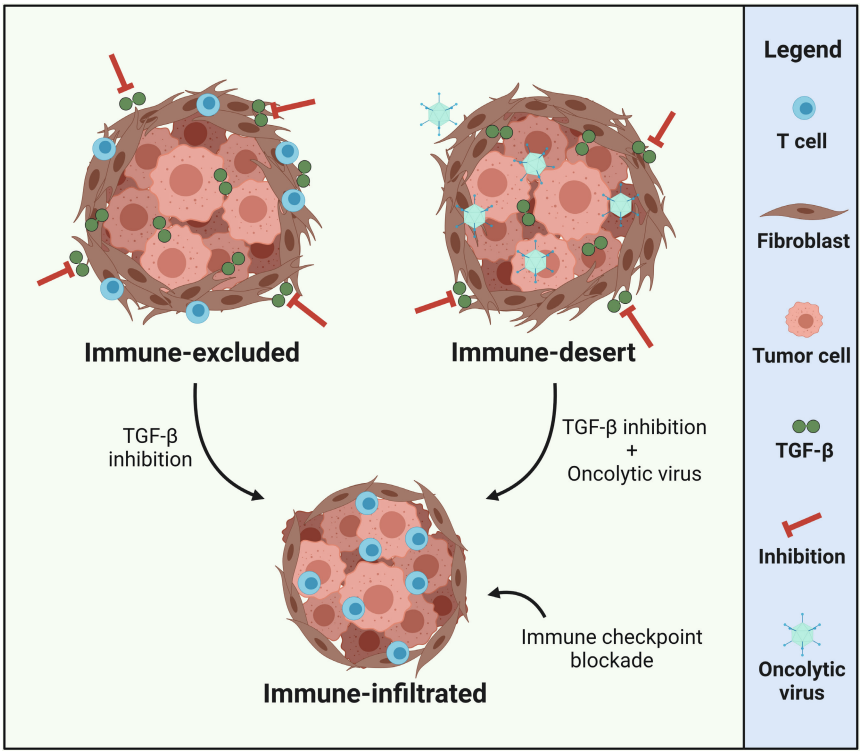


Figure 1, Graphical Abstract. Combining TGF-β inhibition with oncolytic viruses to increase efficacy of immune checkpoint blockade in solid tumors. Immune checkpoint blockade is mostly effective in immune-infiltrated tumors where T cells (blue) are present in the tumor nests (red) but may be dysfunctional. In immune excluded tumors, T cells are present but remain trapped in the stromal regions (brown) surrounding the tumor nests. TGF-β (dark green) inhibition is expected to change the phenotype of immune-excluded tumors towards an immune-infiltrated phenotype. In immune-desert tumors, a T cell response is absent. Combination strategies of oncolytic viruses with TGF-β-inhibition may also convert immune-desert tumors to immune-infiltrated tumors, facilitating effective immune checkpoint blockade for all immune phenotypes in solid tumors.

First, we discuss the inhibition of **transforming growth factor β** (**TGF-β**) signaling to enhance the efficacy of checkpoint blockade therapy given that recent evidence suggests that TGF-β may be a key factor in regulating immune exclusion and immunosuppression in solid tumors. Additionally, we highlight the potency of **oncolytic viruses** (**OVs**) to convert solid tumors from an immune-silent phenotype towards an immune-infiltrated phenotype. Lastly, we theorize how a combination of TGF-β inhibition, OVs and immune checkpoint blockade may be superior in efficacy compared to strategies that contain only two of these three aspects.

IMMUNE CHECKPOINT INHIBITION CAN REINVIGORATE DYSFUNCTIONAL ANTITUMOR RESPONSES IN IMMUNE-INFILTRATED TUMORS

The discovery of immune checkpoints boosted the development of immunotherapeutic strategies against certain cancers. **Programmed cell death protein 1** (PD-1) and **cytotoxic T lymphocyte-associated antigen 4** (CTLA-4) are well-recognized immune checkpoint receptors that can limit antitumor immunity using distinct mechanisms. CTLA-4 prevents T-cell activation by competing with the costimulatory molecule CD28 for binding to their common ligands CD80 and CD86 (11). In contrast, PD-1 induces **T-cell anergy** or **T-cell exhaustion** after binding to one of its ligands, PD-L1 or PD-L2, expressed on the surface of tumor cells and/or immune cells (10,12). The use of blocking antibodies specific for these immune checkpoint axes can prevent or overcome T lymphocyte dysfunction and reinvigorate potent $CD8^+$ T-cell-mediated antitumor immune responses, as has been demonstrated in clinical practice for hematological malignancies such as acute myeloid leukemia, as well as in solid tumors such as melanoma, lung, bladder and head and neck cancers (10,13). In addition to the CTLA4-CD80/86 and the PD-1-PD-L1/L2 axes, other coinhibitory receptor targets, such as lymphocyte activation gene 3 (LAG-3) (14), T-cell immunoglobulin and mucin-domain containing protein 3 (TIM-3) (15) and C-type lectin receptor NKG2A (16,17), are currently being investigated in either preclinical studies or clinical trials for a wide variety of both hematological and solid cancers. Although checkpoint inhibition is able to induce dramatic responses in some types of cancer, the response rate in general ranges from 10-40% and heavily depends on the cancer type and the development of resistance during disease progression (18). Factors associated with a beneficial response to checkpoint blockade therapies include a high total number of mutations in tumor cell DNA (1), the presence of an interferon gene signature, the expression of proinflammatory and T-cell-recruiting chemokines such as CXCL9 and CXCL10, the presence of $CD8^+$ T lymphocytes in close proximity to tumor cells, and high PD-L1 expression, in particular on infiltrating immune cells (10,19-22). An immune cell-infiltrated tumor without a clinical response may suggest a pre-existing but dysfunctional tumor-specific $CD8^+$ T-cell response (23).

One category of immune-silent tumors with relatively low susceptibility to checkpoint inhibition includes tumors with an immune-excluded phenotype, such as colorectal cancer, ovarian cancer, pancreatic ductal adenocarcinoma, and vulvar squamous cell carcinoma (24,25, reviewed in 26). Immune-excluded tumors are characterized by the presence of $CD8^+$ T cells in the tumor-surrounding tumor stromal regions, but these T cells fail to infiltrate into the tumor beds (**Figure 1**) (27). The presence of stroma including **cancer-associated fibroblasts** (**CAFs**), extracellular matrix components such as collagen, and cells of the myeloid lineage, such as the so-called **myeloid-derived suppressor cells** (**MDSCs**) (28) and **tumor-associated macrophages** (**TAMs**) (29), not only represents a physical barrier but also induces an

immunosuppressive **tumor microenvironment** (**TME**), which limits T-cell infiltration into tumor nests (26,30). Hence, it is necessary to overcome the physical barrier and modify the immunosuppressive TME in immune-excluded tumors to facilitate T-cell migration through the stromal region into the tumor cell nests, where these immune cells can fully exert their tumoricidal function. An additional type of immune-silent tumors that exhibits low susceptibility to checkpoint blockade is the immune-desert phenotype. Immune-desert tumors lack the presence of T cells completely and require preceding T-cell activation (31). Below, we discuss promising methods for achieving T-cell infiltration into immune-desert tumors.

OVERCOMING IMMUNOSUPPRESSION VIA TGF-β SIGNALING INHIBITION FOR IMMUNE-EXCLUDED TUMORS

TGF-β as a mediator of immunosuppression

The secreted cytokine TGF-β is one of the key factors believed to be responsible for immune exclusion and suppression in certain types of cancer, such as pancreatic cancer, non-small cell lung cancer, and colon cancer (32-34). In premalignant lesions, TGF-β signaling suppresses tumor growth by inducing apoptosis and inhibiting cell proliferation (35). However, during tumor progression, tumor cells become insensitive to TGF-β-induced cytostatic effects, and TGF-β functionally switches into acting as a tumor-promoting cytokine by promoting cancer cell migration and invasion, extracellular matrix (ECM) remodeling, **epithelial-to-mesenchymal transition** (**EMT**) and the formation of an immunosuppressive TME (36). TGF-β induces its prometastatic programs directly via cell surface TGF-β type I and type II serine/threonine kinase receptors (TGF-βRI and TGF-βRII) and intracellular SMAD-transcriptional effector proteins. Especially in human colon and pancreatic cancers, the TGF-β-induced cytostatic response is often inactivated by mutation of TGF-β receptors or SMADs (37). However, TGF-β is still produced in high amounts by cancer and stromal cells, which is associated with relapse and reduced survival (32,33,38). In **Box 2,** we provide further details regarding the TGF-β signaling pathway in cancer progression and metastasis, and how this pathway can be inhibited.

In addition to the regulation of tumor-promoting processes described above, TGF-β also inhibits the generation and function of $CD4^+$ and $CD8^+$ effector T cells and dendritic cells (DCs), while promoting the expansion of **regulatory T cells** (**Tregs**) and MDSCs (recently reviewed in 39). Early, pivotal studies showed that CD4-dnTGFβRII transgenic mice engineered to express a dominant-negative version of TGF-βRII in their $CD4^+$ and $CD8^+$ T cells rendered these mice resistant to tumor challenge with B16.F10 murine melanoma cells or EL-4 murine lymphoma cells (40). TGF-β inhibits the differentiation of $CD4^+$ T cells into effector cells by silencing the expression of master transcription factor T-bet (41), while stimulating the transition of naive $CD4^+$ cells into Tregs by inducing FoxP3 expression (42). In $CD8^+$ T cells, TGF-β represses eomesodermin (EOMES), an

important transcription factor that regulates the effector program of cytotoxic $CD8^+$ T cells (43). In a murine B16.F10 melanoma model, treatment with various small molecule kinase inhibitors specific for TGF-βRI not only directly inhibited phosphorylation of receptor-regulated SMAD proteins, but also induced ubiquitin-mediated degradation of SMAD4 mainly in $CD8^+$ **cytotoxic T lymphocytes** (**CTLs**), and thereby increased their effector function and suppressed tumor growth (43). The important role of TGF-β in T-cell suppression was further illustrated by the observation that TGF-β induced the surface expression of PD-1 on both activated human peripheral blood mononuclear cells (PBMCs) and murine B16.F10 tumor-infiltrating $CD8^+$ and $CD4^+$ T cells through SMAD3-dependent transcriptional activation, thereby reducing T-cell effector function and limiting the antitumor response (44). Additionally, T cells genetically modified to be resistant to TGF-β showed significantly enhanced tumor control in an adoptive T-cell transfer setting in a syngeneic murine B16.F10 melanoma model in comparison with T cells that could still respond to TGF-β (45).

Box 2: TGF-β signaling in cancer and metastasis

Transforming growth factor β (TGF-β) is a pleiotropic cytokine produced in a latent form by cancer cells, various immune cells, platelets, and stromal cells (39). The signaling pathways activated by TGF-β and its family members are highly conserved among species and are involved in development, homeostasis, and regeneration (46). Dysfunction of the TGF-β signaling pathway might lead to various pathologies such as fibrosis, congenital defects, dysfunction of the immune system, and cancer. In short, all three TGF-β isoforms, i.e. TGF-β1, -β2, and -β3 are cleaved into their active form by integrins or matrix metalloproteinases, resulting in a TGF-β dimer. Signaling takes place via TGF-β type I and II serine/threonine kinase receptors (TGF-βRI and TGF-βRII) that are expressed on the plasma membrane (**Figure I**). Upon TGF-β-induced heteromeric complex formation of TGF-βRI and TGF-βRII, TGF-βRII phosphorylates TGF-βRI, which subsequently leads to the phosphorylation of receptor-regulated SMADs (R-SMADs). R-SMADs form complexes with the common mediator SMAD4, which drives transcriptional regulation of various TGF-β target genes. Additionally, TGF-β family members can also signal in SMAD-independent manners by using non-canonical pathways such as the phosphatidylinositol-3 kinase (PI3K)-AKT and the p38 MAP kinase pathway (47).

TGF-β acts as a tumor suppressor in the early stages of tumor development, but this function is lost during the later phases of cancer progression. Instead, TGF-β signaling promotes epithelial-to-mesenchymal transition (EMT) by reducing the expression of epithelial markers, such as E-cadherin, while increasing the expression of mesenchymal markers, such as vimentin (48). The TGF-β-induced exploitation of EMT during cancer progression is assumed to contribute to the growth of the primary tumor as well as metastasis. Because of the various functions of TGF-β during tumor progression and metastasis, multiple strategies >>

>> have been developed to block TGF-β signaling (**Figure I**). Current TGF-β pathway inhibitors work on different levels by either (**A**) preventing TGF-β production or expression of its receptor by antisense oligonucleotides (synthetic nucleic acids with a complementary sequence that prevents mRNA translation), (**B**) preventing TGF-β activation via integrin-blocking antibodies (49), (**C**) inhibiting the interaction between TGF-β and its receptor with neutralizing antibodies to TGF-β, blocking antibodies to TGF-βRII or ligand traps (engineered soluble forms of the receptor that compete with the cell-bound receptor) or (**D**) preventing intracellular TGF-β receptor signal transduction via **small molecule kinase inhibitors** such as galunisertib (reviewed in 50).

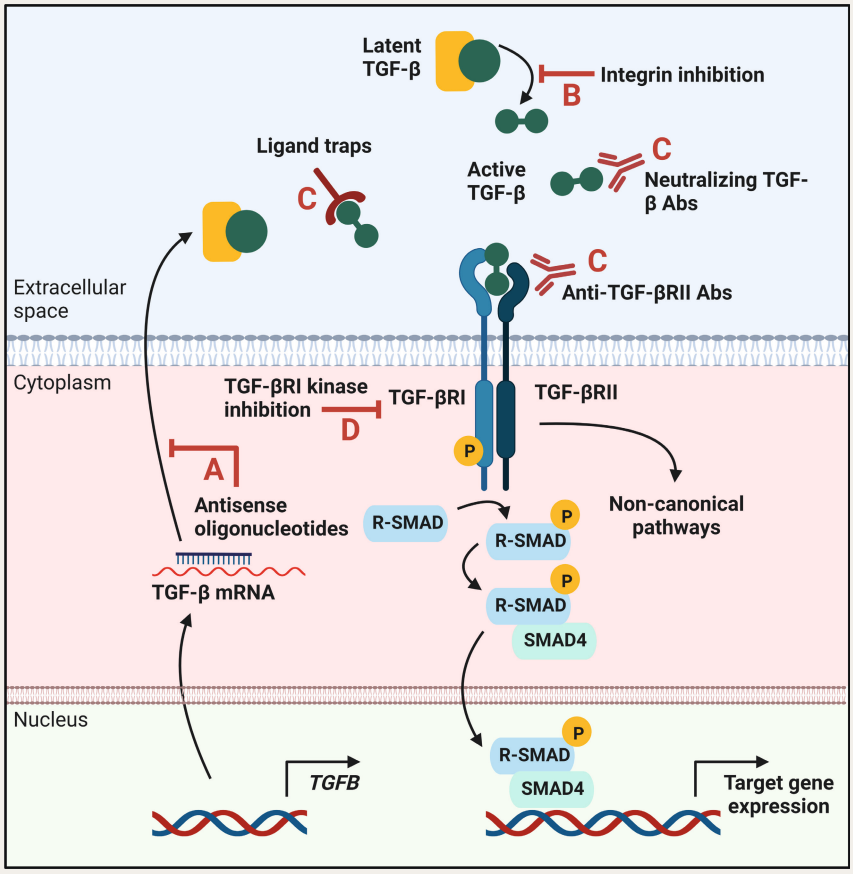


Figure I. Overview of TGF-β signaling across species. Arrows indicate processes. Latent TGF-β (dark green) is cleaved into its active form by integrins or matrix metalloproteinases, resulting in a TGF-β dimer. Active TGF-β induces heterodimerisation of TGF-βRI and TGF-βRII, ultimately leading to the phosphorylation of TGF-βRI. Subsequent phosphorylation of R-SMADs initiates the SMAD-mediated transcription of TGF-β target genes. TGF-β also signals via non-SMAD pathways, via the so-called non-canonical pathways. Interference in TGF-β signaling is possible using various strategies (indicated in dark red) by inhibiting **A:** TGF-β (receptor) production, **B:** TGF-β activation, **C:** ligand-receptor interaction or **D:** TGF-βRI receptor activation.

The results of these *in vivo* studies hint towards a potential beneficial effect of TGF-β inhibition on the induction of a potent antitumor response. Indeed, antibody-mediated inhibition of TGF-β was able to induce complete tumor regression when given as monotherapy in up to 20% of animals in the subcutaneous CCK168 model of chemically-induced cutaneous squamous cell carcinoma engrafted in FVB/NJ mice (51). Furthermore, rechallenge experiments suggested that TGF-β blockade induced immunological memory and long-term protection since both the parental cell line or similar chemically-induced cutaneous squamous cell carcinoma cell lines failed to grow in the animals that underwent complete regression (51). Similar effects were observed in a mouse model of murine 4T1-luciferase breast cancer, where complete regression was observed in 50% of animals after treatment with galunisertib (LY2157299 monohydrate), a small molecule that inhibits the kinase activity of TGF-βRI (52). Mice with durable regressions also rejected tumor rechallenge with both the 4T1-luciferase cell line and the parental, less immunogenic 4T1 cell line, thereby demonstrating established immunological memory (52). In addition, inhibition of TGF-β signaling using the same compound unleashed a potent and enduring CTL response in murine metastatic colorectal cancer models, reducing both primary tumor growth and blocking the appearance of liver metastases (53). Rechallenge experiments with the same tumor model demonstrated rejection of most tumors in the absence of any treatment, an effect that was mitigated upon antibody-mediated depletion of CTLs, again suggesting that TGF-β could limit adaptive immune responses by inhibiting CTL responses (53). Overall, TGF-β can heavily impair CTL responses and induce a generally immunosuppressed TME, thereby promoting tumor progression and metastasis.

TGF-β inhibition can increase the efficacy of immune checkpoint therapy

As described above, TGF-β inhibition induces regression of primary tumors, prevents metastasis formation, and induces protection against tumor rechallenge in various mouse tumor models when applied as a monotherapy. However, can TGF-β inhibition provide an added therapeutic effect to immune checkpoint therapy? A rationale for this strategy was demonstrated by a genomic and transcriptomic analysis that revealed enrichment in markers of EMT, cell adhesion, and ECM remodeling in PD-1 therapy-resistant melanoma patients in comparison to therapy-responding patients (54). All of these cellular processes are known to be regulated via TGF-β signaling (55). Moreover, transcriptomic analysis of human tumors from The Cancer Genome Atlas (TCGA) suggested that upregulation of ECM gene expression, such as genes encoding matrix metallopeptidases (MMPs) and collagen, was linked to the activation of TGF-β target genes in CAFs and that this pan-cancer signature predicted unresponsiveness to PD-1 blockade (56). Additionally, single-cell sequencing studies identified a population of TGF-β-driven CAFs that was associated with poor response to anti-PD-L1 therapy in human immune-excluded tumors, such as pancreatic cancer and bladder cancer (57). Finally, gene set enrichment analysis identified the genes *TGFB1* (encoding TGF-β1) and *TGFBR2* (encoding TGF-βRII) to be associated with nonresponse to anti-PD-L1 therapy and reduced overall survival in patients with urothelial cancer (58). Altogether, these

studies support the use of TGF-β signaling pathway inhibitors to sensitize immune-excluded tumors for immunotherapy. Indeed, combined treatment with anti-PD-L1 and anti-TGF-β antibodies in the immune-excluded EMT6 mouse mammary carcinoma model led to a significant decrease in the tumor burden, reprogramming of stromal fibroblasts and increased infiltration of $CD8^+$ T cells in comparison to either treatment alone (58). These effects were lost after antibody-mediated depletion of $CD8^+$ T cells, indicating that the effect of this combination therapy was based on a potent $CD8^+$ T-cell-driven antitumor immune response (58). In the 4T1 mouse model of metastatic breast cancer, TGF-β neutralization using the pan-isoform 1D11 monoclonal antibody during radiotherapy successfully decreased both primary tumor growth and the occurrence of metastasis and increased $CD4^+$ and $CD8^+$ T-cell infiltration (59). The addition of checkpoint blockade to this regimen led to complete tumor regression in 75% of mice, delayed tumor recurrence, and prolonged survival. Similar beneficial effects of combined checkpoint inhibition and TGF-β inhibition on tumor regression were observed in mouse models of 4T1 breast cancer (52), progressive metastatic liver disease (53), MC38 colorectal cancer (60), and on the metastatic spread to the lung of the colorectal tumor model CT26 (61). Additionally, *in vivo* treatment using the bifunctional fusion protein M7824, composed of an antibody targeting PD-L1 and a TGF-β ligand trap, has shown promising antitumor activity in a vast number of preclinical models, including **orthotopic** and subcutaneous mouse models of breast cancer, colon cancer, and renal adenocarcinoma, as well as in a xenograft model of human pharyngeal carcinoma (62). Last, a similar bifunctional fusion protein targeting CTLA-4 instead of PD-L1 was shown to inhibit tumor growth more efficiently than anti-CTLA-4 alone in human melanoma and triple-negative breast cancer models established in immunodeficient, humanized mice (63). Based on the promising effects observed in preclinical studies, various clinical trials are ongoing in which the combination of TGF-β inhibition and checkpoint blockade is investigated. For example, an ongoing Phase 1b/2 dose-escalation and cohort-expansion study with 75 participants (NCT02423343)[i] aims to evaluate the safety, tolerability, and efficacy of the combination of galunisertib and anti-PD-1 in advanced refractory solid tumors (Phase 1b) and in recurrent or refractory non-small cell lung cancer or hepatocellular carcinoma patients (Phase 2). This trial and others may provide more information about the ability of dual inhibition of immune checkpoint axes and the TGF-β pathway to establish tumor growth control and prevent metastasis.

RECRUITING TUMOR-SPECIFIC T CELLS IS THE FIRST PRIORITY IN IMMUNE-DESERT TUMORS

While immune-excluded tumors may benefit from combined checkpoint blockade and TGF-β inhibition, tumors with the immune-desert phenotype are less likely to benefit from this combination therapy (10,64). Immune-desert tumors are characterized by an absence of T lymphocytes in both the tumor and the surrounding stromal regions

(10). The absence of pre-existing antitumor immunity is the first barrier that needs to be overcome before checkpoint inhibitors and TGF-β blockade can be used.

Using oncolytic viruses to induce antitumor immunity

A promising immunotherapeutic strategy that may promote antitumor immunity is treatment with oncolytic viruses (OVs) (65). The use of OVs as anticancer agents is emerging and driven by the FDA approval of **talimogene laherparepvec** (**T-VEC**), a modified herpes simplex virus type 1 (HSV-1) that increased survival and demonstrated favorable tolerability in advanced-stage melanoma patients (66). OVs selectively replicate in transformed cells, either naturally or after genetic modification (**Figure 2A**). Accumulating evidence suggests that beyond their oncolytic activity, OVs have broad immunostimulatory properties. Mechanisms of action include the induction of local inflammation and priming and recruitment of tumor-reactive $CD4^+$ and $CD8^+$ T cells (**Figure 2B**) (67-70). In addition to their oncolytic and immunostimulatory properties, OVs can also be used as a delivery platform for tumor-specific expression of immunostimulatory transgenes such as cytokines, chemokines, costimulatory ligands, immune checkpoint inhibitors and TAs (**Figure 2C**) (71). More background on OVs is provided in **Box 3.**

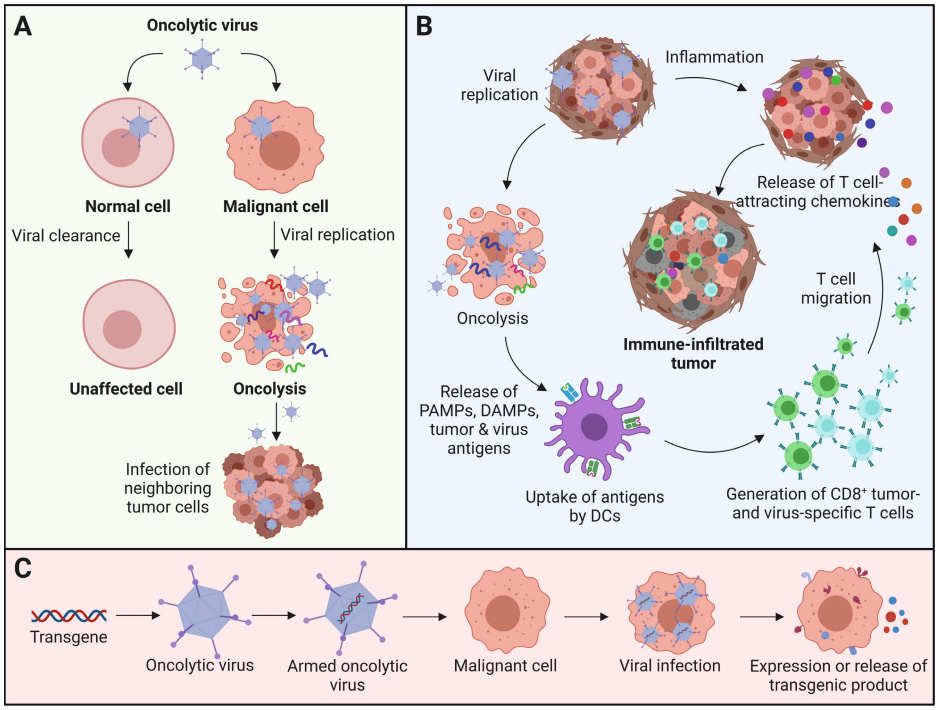


Figure 2. Properties of oncolytic viruses. (**A**) *Oncolytic properties.* Oncolytic viruses (OVs) selectively replicate in malignant cells, either naturally or after genetic modification. Normal cells remain unaffected due to viral clearance. Viral replication together with the induction of cell death pathways leads to lysis of tumor cells. Oncolysis causes the release of virus progeny, which infects new tumor cells.

>>

>> (**B**) *Immuno-stimulatory properties*. Virus replication causes oncolysis, which induces the release of tumor-specific and virus-specific antigens and **pathogen- and damage-associated molecular pattern molecules** (**PAMPs and DAMPs**, respectively). On the one hand, the subsequent uptake and presentation of antigens by dendritic cells leads to the induction of tumor- and virus-specific T cells. On the other hand, viral infection and replication induces an inflammatory response which causes the release of T cell-attracting chemokines. The tumor- and virus-specific T cells are attracted by these chemokines and migrate towards the tumor to exert their function. (**C**) *OVs as transgene delivery platform.* Some OVs (such as adenovirus and vaccinia virus) can be modified to encode transgenes (armed oncolytic viruses) such as cytokines or antibodies, ensuring specific delivery to the tumor microenvironment and further stimulation of an antitumor immune response.

Box 3: Oncolytic viruses as antitumor agents

Oncolytic viruses (OVs) are able to selectively infect, replicate in and lyse tumor cells that initially gained interest because of their tumor cell-lysing (oncolytic) capabilities. In contrast to normal cells, where virus infection initiates a type I interferon (IFN)-driven antiviral response program, deficiency of this pathway in many cancer cells favors cancer-specific OV replication (85,86). Tumor-specific driver mutations, such as an activated RAS pathway, and upregulation of cell-entry receptor expression can further promote selective replication in tumor cells (87,88). Furthermore, some OVs, including adenovirus and HSV, have been engineered to increase their tumor specificity (89,90), whereas a strain of oncolytic reovirus has been bioselected by growing on cells that lack expression of the entry receptor to broaden its tropism for different tumor cells (91).

Beyond their oncolytic activity, OVs are able to induce a tumor-reactive T-cell response by acting as ***in situ*** vaccines (70,79,92). The process of T-cell priming is particularly effective during virus infection because virus-derived nucleic acids optimally induce the maturation of dendritic cells (67,70). Simultaneously, dying tumor cells are a source of TAs, leading to the priming of tumor-reactive $CD4^+$ and $CD8^+$ T cells (93,94). This process is further enhanced by the OV-induced IFN response, which recruits immune cells to the tumor and promotes antigen presentation (78). Noteworthy, the OV-induced ***in situ*** vaccine strategy does not rely on prior identification of TAs or neoantigens for a given tumor or patient, which conceptually would provide a major advantage over other types of cancer vaccines (71).

OVs can also be used as platforms for the specific delivery of transgenes into the tumor bed (71). Cytokines and chemokines represent attractive transgenes because they have pleiotropic effects and are encoded by small genes (95). The cytokine granulocyte-macrophage colony-stimulating factor (GM-CSF), which promotes DC recruitment and maturation, has been the most widely studied transgene and has been encoded in many different OV platforms (96-98), including the leading clinically approved OV T-VEC (99). Other cargoes used to promote tumor-reactive

T-cell responses include ligands for costimulatory receptors such as CD40 ligand (100,101) or inducible co-stimulator (ICOS) ligand (102), checkpoint blockers such as anti-PD-1 antibodies (103), or **bispecific T-cell-engager**s (BiTEs) (104). Alternatively, OVs can also be armed with enzymes such as DNase or hyaluronidase to promote intratumoral penetration (105), or TAs such as MAGE-A3, which turn OVs into oncolytic vaccine vectors (106).

In addition to the direct elimination of primary treated tumors, OVs can induce long-term protection against secondary tumors (72-74). In an elegant rechallenge model, primary 4T1, EMT6, and E0771 murine breast cancer tumors were treated intratumorally with unarmed oncolytic Maraba virus MG1, after which the primary tumor was surgically resected (72). Thereafter, secondary tumors were implanted in the mammary fat pad and left untreated. Mice that were previously treated with Maraba virus showed significantly better tumor control of the untreated secondary tumor, and at least 20% of the animals showed complete tumor control. When T-cell deficient nude mice were used in a similar experiment, this effect was completely lost, suggesting that a functional adaptive immune system was necessary to induce T-cell memory and subsequent protection from secondary tumors. The capacity to confer immunological memory was similarly demonstrated for vesicular stomatitis virus (VSV), adenovirus, and HSV-1 in the 4T1 breast cancer model (73). Presurgical treatment with reovirus was only effective against the primary tumor in this study (73), but did induce protective memory in the EMT6 murine breast cancer model in another study (75). The OV-induced tumor-reactive immunity is believed to be not only a crucial aspect of the therapeutic efficacy of OVs (76,77) but may also be utilized to sensitize tumors for other types of immunotherapy by enhancing immunogenicity or by attracting activated $CD4^+$ and $CD8^+$ T cells to nonresponsive tumors (65,68).

Oncolytic virotherapy can synergize with immune checkpoint blockade

Several OV platforms have been demonstrated to increase the number of TILs and sensitize tumors for checkpoint therapy, both in preclinical studies and in clinical trials (68,72,75,78-81). For example, a randomized Phase 1b clinical trial (NCT02263508) [II] that investigated the combination of FDA-approved oncolytic HSV-1 T-VEC and pembrolizumab (anti-PD-1) in 21 patients with unresectable melanoma patients has shown promising results with a 61.9% objective response and a 33.3% complete response (82). Of note, responses have also occurred in patients whose tumors displayed a low $CD8^+$ T-cell density and no PD-L1 expression at baseline, which originally emerged as the first potential predictive biomarker for insensitivity to immune checkpoint blockade (83). This trial is currently continued as a Phase 3 trial to investigate the effect of combined treatment with T-VEC and pembrolizumab on progression-free survival and overall survival in comparison with pembrolizumab alone (NCT02263508)[II]. Furthermore, the combination of T-VEC and ipilimumab (anti-CTLA4 monoclonal antibody) has shown promising results in a randomized Phase 2 clinical

trial (NCT01740297)[111] with 198 patients with unresectable stage IIIB or IV melanoma that were randomly assigned half-half to combination therapy or ipilimumab alone (84). The combination therapy resulted in an objective response of 35.7% compared to 17.5% in the ipilimumab-only treated group (84). Driven by these encouraging initial studies and additional preclinical data, there are more than twenty ongoing clinical programs involving different OV platforms in combination with immune checkpoint inhibitors (65). Collectively, these studies not only highlight the potent role of OVs as anticancer agents but also illustrate their capacity to sensitize tumors for subsequent immunotherapy, although further robust testing is evidently warranted.

COMBINING OVS WITH TGF-β INHIBITION TO SENSITIZE SOLID TUMORS FOR IMMUNOTHERAPY

The lack of immunogenicity and the presence of stromal and immunosuppressive barriers are 2 major hurdles to effective immunotherapy for immune-desert tumors. Combined modulation of the stromal barrier by TGF-β inhibition and increasing immunogenicity using OVs might therefore be a potent strategy to sensitize immune-desert tumors for T-cell-based immunotherapy. Indeed, systemic treatment with a small molecule TGF-βRI inhibitor in combination with a single intratumoral injection of oncolytic HSV-1 variant MG18L resulted in complete tumor regression in 60% of treated subjects in an orthotopic model of patient-derived recurrent glioblastomas established in severe combined immunodeficient (SCID) mice lacking mature B and T cells (107). In a human MDA-MB-231 breast cancer xenograft model established in nude mice, 3 intratumoral injections of an oncolytic adenovirus armed with a soluble form of TGF-β receptor type II (sTGF-βRII) that functions as a ligand trap for TGF-β caused complete tumor regression in 7 out of 8 mice, which was better than the efficacy of the unarmed virus (3 out of 8 mice) and sTGF-βRII only (1 out of 8 mice) (108). Additionally, intravenous delivery of the same armed virus in this MDA-MB-231 breast cancer xenograft model significantly inhibited the progression of bone metastasis and prolonged survival when compared with the unarmed virus (109). A limitation of the studies performed in immunodeficient mice is that the role of T cells during the OV and TGF-β inhibition combination therapies remains underexplored. Combination treatment with intratumorally injected HSV1716, an attenuated unarmed oncolytic HSV-1, and a small molecule inhibitor of TGF-βRI was evaluated in immunocompetent models of murine rhabdomyosarcoma, resulting in tumor growth stabilization, significantly prolonged survival and even some complete responses compared to the single agents alone (89). In this study, the removal of T-cell responses via antibody-mediated depletion of $CD4^+$ and $CD8^+$ T cells or the use of athymic nude mice as recipients completely abolished the antitumor effect, indicating the importance of the T-cell response underlying efficacy of this combination treatment (89). Together, these preclinical studies suggest that the combination of TGFβ inhibition and OV therapy may be considered to putatively treat tumors with low immunogenicity and stromal or immunosuppressive barriers.

CONCLUDING REMARKS

In this review, we discussed two promising therapeutic strategies to overcome barriers to effective immunotherapy in relation to the tumor immune phenotype. For the classification of tumor immune profiles, we relied on the three main tumor immune phenotypes postulated by Chen and Mellman (9). We recognize that other classification strategies are possible, and more detailed profiles based on immunophenotyping of tumors are being investigated (26,110). Immune-infiltrated tumors have an ongoing T-cell response, but the dysfunctional state of these T cells needs to be overcome by immune checkpoint therapy. Clinical successes in various tumors with this immune phenotype have already been reported, and many efforts to identify novel targets, find biomarkers of efficacy, and understand secondary resistance mechanisms are ongoing, and more breakthroughs are anticipated. Tumors with an immune-excluded phenotype require modification of the immunosuppressive TME to allow T-cell infiltration into the tumor before checkpoint therapy can be applied. As discussed above, TGF-β inhibition has emerged as a multifunctional strategy to increase the efficacy of immunotherapy due to its capacity to modify the desmoplastic TME, increase the cytotoxic activity of $CD8^+$ (and possibly $CD4^+$) T cells, and reduce the frequency of Tregs. However, due to the pleiotropic effects on different cell types and the heterogenicity of the TGF-β superfamily, TGF-β is a challenging target in terms of pharmacology.

For immune-desert tumors, immunotherapy is a different, much harder, challenge. Treating these tumors with immune checkpoint blockade and TGF-β inhibition may be useful only when a prior treatment strategy has increased the immunogenicity of the tumor and induced tumor-reactive T-cell responses. OVs may represent potent tools to evoke potent $CD4^+$ and $CD8^+$ T-cell responses, as has been demonstrated by multiple preclinical studies mentioned above. The addition of TGF-β blockade may increase the efficacy of this combination therapy even further, but this remains to be vigorously investigated. TGF-β inhibition can not only lift the immunosuppressive and physical barriers to allow T-cell infiltration into the tumor bed, but also lift a physical barrier for penetration of OVs into tumors. Previous studies have shown that stromal components in the TME, such as TGF-β-producing CAFs and collagen, may impair viral spread in tumors, limiting the efficacy of OVs (111). Indeed, an oncolytic vaccinia virus armed with a **bispecific T-cell-engager** (**BiTE**) directed against fibroblast activation protein (FAP) and murine CD3 decreased the number of FAP-expressing CAFs, increased the viral titer and T-cell accumulation in the tumor and enhanced antitumor efficacy in comparison with the unarmed virus in the murine B16.F1 melanoma model (112). Furthermore, in a similar approach with oncolytic Adenovirus that secretes FAP-targeting BiTEs, T-cell accumulation and antitumor efficacy were enhanced in xenograft models of subcutaneous human lung carcinoma and pancreatic adenocarcinoma established in NSG mice supplemented with pre-stimulated human T cells (113). Nevertheless, a great deal of caution needs to be taken with these interpretations since TGF-β and CAFs can also promote the efficacy of OV replication. A study performed in xenografts

derived from patients with pancreatic cancer showed that tumor-derived TGF-β made the CAFs more sensitive to infection with various OVs, such as Vaccinia virus, VSV, and Maraba virus by downregulating their antiviral program (114). In turn, CAFs produced high amounts of fibroblast growth factor 2, which impeded the ability of the pancreatic cancer cells to detect and respond to virus infection.

Because of this complex interplay, the interference between TGF-β signaling and OV treatment needs to be investigated further in the context of checkpoint blockade therapy. In particular, the rational choice of targets and the timing of the combination strategy might be of key importance to effectively sensitize tumors for immunotherapy (see **Outstanding Questions**). For instance, in an inducible murine model of $BRAF^{V600E}PTEN^{-/-}$ melanoma with modest baseline responses to PD-1/PD-L1 blockade, TGF-β inhibition failed to augment the response to anti-PD-1 immunotherapy whereas anti-CTLA-4 immunotherapy did benefit from the combination, resulting in tumor growth control and increased survival (115). Mechanistic studies in mice with subcutaneously implanted $BRAF^{V600E}PTEN^{-/-}$ melanomas in C57BL/6 mice revealed that inhibition of TGF-β signaling promoted the proliferative expansion of stromal fibroblasts and increased the production of MMP9, which subsequently facilitated cleavage of PD-L1 on the surface of melanoma cells, ultimately leading to resistance to anti-PD-1 therapy (115). The authors also demonstrated that TGF-β inhibition following anti-PD-1 treatment had superior therapeutic efficacy compared to a continuous combination of TGF-β inhibition and PD-1 blockade (115).

Additionally, whether combinations of three separate strategies are achievable in terms of cost and the accumulating burden of adverse events in patients remains undetermined. Although side effects may be limited for all monotherapies (116-118), the question arises as to whether adding up these therapies still has manageable adverse effects. Encoding checkpoint blockers and TGF-β blocking agents in a single OV for intratumoral delivery may limit the therapeutic burden and systemic adverse effects (71), however, it remains to be assessed whether the antitumor efficacy of this strategy reaches its full potential when all agents are delivered to the tumor simultaneously. Additionally, not all OVs have sufficient space in their genome to allow the encoding of complicated and large molecules (119). Extensive preclinical studies need to be performed to elucidate the putative therapeutic effect of combined TGF-β inhibition and OV therapy to sensitize immune-desert tumors for immune checkpoint blockade or other immunotherapeutic strategies and to determine for which specific cancers these combinations can be helpful.

Although multiple challenges and questions remain to be addressed, combining immune checkpoint inhibition with strategies to overcome immune evasion and exclusion is expected to result in the induction of strong antitumor immune responses in a variety of cancers. It will be exciting to follow future progress in this area.

DECLARATIONS

Acknowledgments. We sincerely apologize to authors for not citing their excellent work due to space limitations. This work was financially supported by a PhD fellowship from Leiden University Medical Center (to CG), the Dutch Cancer Society Bas Mulder Award 11056 (to NvM), the Cancer Genomics Centre Netherlands (CGC.nl) and the Support Casper campaign by the Dutch foundation "Overleven met Alvleesklierkanker" (supportcasper.nl). All figures were created with BioRender software (BioRender.com).

Resources.

[I] This trial is listed in https://clinicaltrials.gov/ct2/show/NCT02423343
[II] This trial is listed in https://clinicaltrials.gov/ct2/show/NCT02263508
[III] This trial is listed in https://clinicaltrials.gov/ct2/show/NCT01740297

OUTSTANDING QUESTIONS

- Can we develop approaches to selectively inhibit TGF-β signaling in immune cells or in a specific CAF subset to restore immune surveillance and overcome immune evasion in solid tumors?
- Is replication of oncolytic virus required for its expected synergistic effect with TGF-β signaling inhibition and immune checkpoint therapy?
- Which biomarkers can predict susceptibility to the combination therapy of oncolytic viruses, TGF-β inhibition, and immune checkpoint inhibition?
- Which criteria should be used to select the appropriate oncolytic virus and immune checkpoint inhibitor for application in combination therapy? Does this differ between tumor types or even between patients?
- What would be the optimal timing for a combination approach of oncolytic virus therapy, TGF-β signaling inhibition, and checkpoint blockade?
- Would it be technically feasible and therapeutically effective to genetically engineer a single oncolytic virus expressing TGF-β signaling antagonists and immune checkpoint inhibitors to limit the therapy burden for patients?

GLOSSARY

Bispecific T-cell-engagers (**BiTEs**)**:** fusion proteins consisting of two different single-chain variable fragments of monoclonal antibodies for simultaneous tumor cell binding and T-cell activation.

Cancer-associated fibroblasts (**CAFs**)**:** cell type within the tumor stroma that can promote tumor progression by extracellular matrix remodeling and secretion of cytokines.

Cytotoxic T lymphocytes (**CTL**)**:** $CD8^+$ effector T cells, important for the elimination of intracellular pathogens and malignant cells.
Cytotoxic T lymphocyte-associated antigen-4 (**CTLA-4**)**:** immune checkpoint receptor that downregulates T-cell responses.
Damage-associated molecular patterns (**DAMPs**)**:** endogenous molecules that are released from damaged cells, initiating a noninfectious inflammatory response.
Dendritic cells (**DCs**)**:** antigen-presenting cells that are specialized in priming of naive T cells.
Epithelial-to-mesenchymal transition (**EMT**)**:** a process by which epithelial cells de-differentiate towards migratory and invasive mesenchymal stem cells.
Extracellular matrix (**ECM**): a network of extracellular macromolecules such as collagen.
Immune-desert: tumor phenotype without an evident immune response.
Immune-excluded: tumor phenotype where tumor-reactive T cells are unable to infiltrate into the tumor beds due to a physical or immunosuppressive barrier.
Immune-infiltrated: tumor phenotype where inflammation is present and T lymphocytes have infiltrated the tumor.
Immunogenicity: the ability to evoke an adaptive immune response.
Immunotherapy: treatment focused on mobilizing the host immune system to combat disease.
Myeloid-derived suppressor cells (**MDSCs**)**:** cells of the myeloid lineage with strong immunosuppressive properties that are associated with tumor progression.
Neoantigens: antigens that result from tumor-specific mutations and are absent from the normal genome.
Oncolytic viruses (**OVs**)**:** viruses that preferentially replicate in and kill cancer cells.
Orthotopic tumor model: an experimental model where a transplanted tumor is placed in the organ of the original tumor.
Pathogen-associated molecular patterns (**PAMPs**)**:** molecules derived from bacteria or viruses that evoke an inflammatory reaction.
Priming: process in which naive T cells encounter an antigen in the context of an activated dendritic cell and start clonal expansion.
Programmed cell death protein-1 (**PD-1**)**:** immune checkpoint receptor expressed on the cell surface of T cells, which negatively regulates T-cell responses.
Regulatory T cells: FoxP3-expressing $CD4^+$ T lymphocytes that functionally suppress effector T cells.
Small molecule kinase inhibitors: low molecular weight compounds that block the action of one or more enzymes called protein kinases.
Talimogene laherparepvec (**T-VEC**)**:** genetically modified oncolytic herpes simplex virus type 1, designed to produce GM-CSF. FDA-approved for the treatment of melanoma.
T-cell anergy: functionally inactivated state of T cells after antigen encounter.
T-cell exhaustion: progressive loss of effector function in T cells due to prolonged antigen stimulation

Transforming growth factor β: multifunctional secreted protein with three isoforms, involved in regulating and mediating many cellular processes.
Tumor antigens: proteins or substances produced in tumor cells that can be recognized by the adaptive immune system.
Tumor-associated macrophages (**TAMs**)**:** macrophages found in tumors that exhibit immunosuppressive properties.
Tumor-infiltrating lymphocytes (**TILs**)**:** white blood cells that have migrated into the tumor.
Tumor microenvironment (**TME**)**:** the molecules, cells, and vessels that surround and interact with the tumor cells.

REFERENCES

1. Goodman AM, Kato S, Bazhenova L, Patel SP, Frampton GM, Miller V*, et al.* Tumor Mutational Burden as an Independent Predictor of Response to Immunotherapy in Diverse Cancers. Mol Cancer Ther **2017**;16:2598-608
2. Ahrends T, Spanjaard A, Pilzecker B, Bąbała N, Bovens A, Xiao Y*, et al.* CD4+ T Cell Help Confers a Cytotoxic T Cell Effector Program Including Coinhibitory Receptor Downregulation and Increased Tissue Invasiveness. Immunity **2017**;47:848-61.e5
3. Prlic M, Williams MA, Bevan MJ. Requirements for CD8 T-cell priming, memory generation and maintenance. Current Opinion in Immunology **2007**;19:315-9
4. van der Burg SH, Arens R, Ossendorp F, van Hall T, Melief CJM. Vaccines for established cancer: overcoming the challenges posed by immune evasion. Nature Reviews Cancer **2016**;16:219
5. Kenter GG, Welters MJ, Valentijn AR, Lowik MJ, Berends-van der Meer DM, Vloon AP*, et al.* Vaccination against HPV-16 oncoproteins for vulvar intraepithelial neoplasia. N Engl J Med **2009**;361:1838-47
6. Aarntzen EHJG, De Vries IJM, Lesterhuis WJ, Schuurhuis D, Jacobs JFM, Bol K*, et al.* Targeting CD4+ T-Helper Cells Improves the Induction of Antitumor Responses in Dendritic Cell–Based Vaccination. Cancer Res **2013**;73:19-29
7. Ribas A, Tumeh PC. The Future of Cancer Therapy: Selecting Patients Likely to Respond to PD1/L1 Blockade. Clin Cancer Res **2014**;20:4982-4
8. Tumeh PC, Harview CL, Yearley JH, Shintaku IP, Taylor EJM, Robert L*, et al.* PD-1 blockade induces responses by inhibiting adaptive immune resistance. Nature **2014**;515:568-71
9. Chen DS, Mellman I. Elements of cancer immunity and the cancer-immune set point. Nature **2017**;541:321-30
10. Herbst RS, Soria J-C, Kowanetz M, Fine GD, Hamid O, Gordon MS*, et al.* Predictive correlates of response to the anti-PD-L1 antibody MPDL3280A in cancer patients. Nature **2014**;515:563-7
11. Leach DR, Krummel MF, Allison JP. Enhancement of antitumor immunity by CTLA-4 blockade. Science **1996**;271:1734-6
12. Gordon J. Freeman AJL, Yoshiko Iwai, Karen Bourque,Tatyana Chernova, Hiroyuki Nishimura, Lori J. Fitz, Nelly Malenkovich, Taku Okazaki, Michael C. Byrne, Heidi F. Horton, Lynette Fouser, Laura Carter, Vincent Ling, Michael R. Bowman,, Beatriz M. Carreno MC, Clive R. Wood, and Tasuku Honjo. Engagement of the PD-1 immunoinhibitory receptor by a novel B7 family member leads to negative regulation of lymphocyte activation. Journal of Experimental Medicine **2000**;192:1027-34
13. Topalian SL, Drake CG, Pardoll DM. Immune checkpoint blockade: a common denominator approach to cancer therapy. Cancer Cell **2015**;27:450-61
14. Maruhashi T, Okazaki I-m, Sugiura D, Takahashi S, Maeda TK, Shimizu K*, et al.* LAG-3 inhibits the activation of CD4+ T cells that recognize stable pMHCII through its conformation-dependent recognition of pMHCII. Nature Immunology **2018**;19:1415-26
15. Sakuishi K, Apetoh L, Sullivan JM, Blazar BR, Kuchroo VK, Anderson AC. Targeting Tim-3 and PD-1 pathways to reverse T cell exhaustion and restore anti-tumor immunity. J Exp Med **2010**;207:2187-94
16. van Montfoort N, Borst L, Korrer MJ, Sluijter M, Marijt KA, Santegoets SJ*, et al.* NKG2A Blockade Potentiates CD8 T Cell Immunity Induced by Cancer Vaccines. Cell **2018**;175:1744-55 e15
17. Andre P, Denis C, Soulas C, Bourbon-Caillet C, Lopez J, Arnoux T*, et al.* Anti-NKG2A mAb Is a Checkpoint Inhibitor that Promotes Anti-tumor Immunity by Unleashing Both T and NK Cells. Cell **2018**;175:1731-43 e13
18. Zou W, Wolchok JD, Chen L. PD-L1 (B7-H1) and PD-1 pathway blockade for cancer therapy: Mechanisms, response biomarkers, and combinations. Sci Transl Med **2016**;8:328rv4

19. Gajewski TF. The Next Hurdle in Cancer Immunotherapy: Overcoming the Non-T-Cell-Inflamed Tumor Microenvironment. Semin Oncol **2015**;42:663-71
20. Taube JM, Klein A, Brahmer JR, Xu H, Pan X, Kim JH*, et al.* Association of PD-1, PD-1 ligands, and other features of the tumor immune microenvironment with response to anti-PD-1 therapy. Clin Cancer Res **2014**;20:5064-74
21. Snyder A, Makarov V, Merghoub T, Yuan J, Zaretsky JM, Desrichard A*, et al.* Genetic basis for clinical response to CTLA-4 blockade in melanoma. N Engl J Med **2014**;371:2189-99
22. Van Allen EM, Miao D, Schilling B, Shukla SA, Blank C, Zimmer L*, et al.* Genomic correlates of response to CTLA-4 blockade in metastatic melanoma. Science **2015**;350:207-11
23. Miller BC, Sen DR, Al Abosy R, Bi K, Virkud YV, LaFleur MW*, et al.* Subsets of exhausted CD8(+) T cells differentially mediate tumor control and respond to checkpoint blockade. Nat Immunol **2019**;20:326-36
24. Galon J, Costes A, Sanchez-Cabo F, Kirilovsky A, Mlecnik B, Lagorce-Pagès C*, et al.* Type, Density, and Location of Immune Cells Within Human Colorectal Tumors Predict Clinical Outcome. Science **2006**;313:1960-4
25. Kortekaas KE, Santegoets SJ, Abdulrahman Z, van Ham VJ, van der Tol M, Ehsan I*, et al.* High numbers of activated helper T cells are associated with better clinical outcome in early stage vulvar cancer, irrespective of HPV or p53 status. Journal for ImmunoTherapy of Cancer **2019**;7:236
26. Galon J, Bruni D. Approaches to treat immune hot, altered and cold tumours with combination immunotherapies. Nature Reviews Drug Discovery **2019**;18:197-218
27. Salmon H, Franciszkiewicz K, Damotte D, Dieu-Nosjean MC, Validire P, Trautmann A*, et al.* Matrix architecture defines the preferential localization and migration of T cells into the stroma of human lung tumors. J Clin Invest **2012**;122:899-910
28. Lesokhin AM, Hohl TM, Kitano S, Cortez C, Hirschhorn-Cymerman D, Avogadri F*, et al.* Monocytic CCR2(+) myeloid-derived suppressor cells promote immune escape by limiting activated CD8 T-cell infiltration into the tumor microenvironment. Cancer research **2012**;72:876-86
29. Beatty GL, Winograd R, Evans RA, Long KB, Luque SL, Lee JW*, et al.* Exclusion of T Cells From Pancreatic Carcinomas in Mice Is Regulated by Ly6C(low) F4/80(+) Extratumoral Macrophages. Gastroenterology **2015**;149:201-10
30. Feig C, Jones JO, Kraman M, Wells RJB, Deonarine A, Chan DS*, et al.* Targeting CXCL12 from FAP-expressing carcinoma-associated fibroblasts synergizes with anti–PD-L1 immunotherapy in pancreatic cancer. Proc Natl Acad Sci U S A **2013**;110:20212-7
31. Kather JN, Suarez-Carmona M, Charoentong P, Weis C-A, Hirsch D, Bankhead P*, et al.* Topography of cancer-associated immune cells in human solid tumors. Elife **2018**;7:e36967
32. Shen W, Tao GQ, Zhang Y, Cai B, Sun J, Tian ZQ. TGF-beta in pancreatic cancer initiation and progression: two sides of the same coin. Cell & Bioscience **2017**;7:39
33. Calon A, Espinet E, Palomo-Ponce S, Tauriello DV, Iglesias M, Cespedes MV*, et al.* Dependency of colorectal cancer on a TGF-beta-driven program in stromal cells for metastasis initiation. Cancer Cell **2012**;22:571-84
34. Chae YK, Chang S, Ko T, Anker J, Agte S, Iams W*, et al.* Epithelial-mesenchymal transition (EMT) signature is inversely associated with T-cell infiltration in non-small cell lung cancer (NSCLC). Scientific reports **2018**;8:2918
35. David CJ, Massagué J. Contextual determinants of TGFβ action in development, immunity and cancer. Nature Reviews Molecular Cell Biology **2018**;19:419-35
36. Connolly EC, Freimuth J, Akhurst RJ. Complexities of TGF-beta targeted cancer therapy. Int J Biol Sci **2012**;8:964-78
37. Oyanagi H, Shimada Y, Nagahashi M, Ichikawa H, Tajima Y, Abe K*, et al.* SMAD4 alteration associates with invasive-front pathological markers and poor prognosis in colorectal cancer. Histopathology **2019**;74:873-82

38. Zhao J, Liang Y, Yin Q, Liu S, Wang Q, Tang Y, *et al.* Clinical and prognostic significance of serum transforming growth factor-beta1 levels in patients with pancreatic ductal adenocarcinoma. Braz J Med Biol Res **2016**;49:e5485
39. Batlle E, Massague J. Transforming Growth Factor-beta Signaling in Immunity and Cancer. Immunity **2019**;50:924-40
40. Gorelik L, Flavell RA. Immune-mediated eradication of tumors through the blockade of transforming growth factor-β signaling in T cells. Nat Med **2001**;7:1118-22
41. Gorelik L, Constant S, Flavell RA. Mechanism of transforming growth factor beta-induced inhibition of T helper type 1 differentiation. J Exp Med **2002**;195:1499-505
42. Chen W, Jin W, Hardegen N, Lei K-J, Li L, Marinos N, *et al.* Conversion of peripheral CD4+CD25- naive T cells to CD4+CD25+ regulatory T cells by TGF-beta induction of transcription factor Foxp3. J Exp Med **2003**;198:1875-86
43. Yoon J-H, Jung SM, Park SH, Kato M, Yamashita T, Lee I-K, *et al.* Activin receptor-like kinase5 inhibition suppresses mouse melanoma by ubiquitin degradation of Smad4, thereby derepressing eomesodermin in cytotoxic T lymphocytes. EMBO Mol Med **2013**;5:1720-39
44. Park BV, Freeman ZT, Ghasemzadeh A, Chattergoon MA, Rutebemberwa A, Steigner J, *et al.* TGFβ1-Mediated SMAD3 Enhances PD-1 Expression on Antigen-Specific T Cells in Cancer. Cancer discovery **2016**;6:1366-81
45. Zhang L, Yu Z, Muranski P, Palmer DC, Restifo NP, Rosenberg SA, *et al.* Inhibition of TGF-β signaling in genetically engineered tumor antigen-reactive T cells significantly enhances tumor treatment efficacy. Gene therapy **2013**;20:575-80
46. Zheng S, Long J, Liu Z, Tao W, Wang D. Identification and Evolution of TGF-β Signaling Pathway Members in Twenty-Four Animal Species and Expression in Tilapia. Int J Mol Sci **2018**;19:1154
47. Derynck R, Zhang YE. Smad-dependent and Smad-independent pathways in TGF-β family signalling. Nature **2003**;425:577-84
48. Xu J, Lamouille S, Derynck R. TGF-beta-induced epithelial to mesenchymal transition. Cell Res **2009**;19:156-72
49. Takasaka N, Seed RI, Cormier A, Bondesson AJ, Lou J, Elattma A, *et al.* Integrin αvβ8–expressing tumor cells evade host immunity by regulating TGF-β activation in immune cells. JCI Insight **2018**;3
50. Neuzillet C, Tijeras-Raballand A, Cohen R, Cros J, Faivre S, Raymond E, *et al.* Targeting the TGFbeta pathway for cancer therapy. Pharmacol Ther **2015**;147:22-31
51. Dodagatta-Marri E, Meyer DS, Reeves MQ, Paniagua R, To MD, Binnewies M, *et al.* α-PD-1 therapy elevates Treg/Th balance and increases tumor cell pSmad3 that are both targeted by α-TGFβ antibody to promote durable rejection and immunity in squamous cell carcinomas. Journal for immunotherapy of cancer **2019**;7:10.1186/s40425-018-0493-9
52. Holmgaard RB, Schaer DA, Li Y, Castaneda SP, Murphy MY, Xu X, *et al.* Targeting the TGFbeta pathway with galunisertib, a TGFbetaRI small molecule inhibitor, promotes anti-tumor immunity leading to durable, complete responses, as monotherapy and in combination with checkpoint blockade. J Immunother Cancer **2018**;6:47
53. Tauriello DVF, Palomo-Ponce S, Stork D, Berenguer-Llergo A, Badia-Ramentol J, Iglesias M, *et al.* TGFbeta drives immune evasion in genetically reconstituted colon cancer metastasis. Nature **2018**;554:538-43
54. Hugo W, Zaretsky JM, Sun L, Song C, Moreno BH, Hu-Lieskovan S, *et al.* Genomic and Transcriptomic Features of Response to Anti-PD-1 Therapy in Metastatic Melanoma. Cell **2016**;165:35-44
55. Akhurst RJ, Hata A. Targeting the TGFβ signalling pathway in disease. Nat Rev Drug Discov **2012**;11:790-811
56. Chakravarthy A, Khan L, Bensler NP, Bose P, De Carvalho DD. TGF-β-associated extracellular matrix genes link cancer-associated fibroblasts to immune evasion and immunotherapy failure. Nature Communications **2018**;9:4692

57. Dominguez CX, Muller S, Keerthivasan S, Koeppen H, Hung J, Gierke S, *et al.* Single-cell RNA sequencing reveals stromal evolution into LRRC15+ myofibroblasts as a determinant of patient response to cancer immunotherapy. Cancer Discov **2019**:CD-19-0644
58. Mariathasan S, Turley SJ, Nickles D, Castiglioni A, Yuen K, Wang Y, *et al.* TGFbeta attenuates tumour response to PD-L1 blockade by contributing to exclusion of T cells. Nature **2018**;554:544-8
59. Vanpouille-Box C, Diamond JM, Pilones KA, Zavadil J, Babb JS, Formenti SC, *et al.* TGFbeta Is a Master Regulator of Radiation Therapy-Induced Antitumor Immunity. Cancer Res **2015**;75:2232-42
60. Sow HS, Ren J, Camps M, Ossendorp F, ten Dijke P. Combined Inhibition of TGF-β Signaling and the PD-L1 Immune Checkpoint Is Differentially Effective in Tumor Models. Cells **2019**;8
61. Terabe M, Robertson FC, Clark K, De Ravin E, Bloom A, Venzon DJ, *et al.* Blockade of only TGF-beta 1 and 2 is sufficient to enhance the efficacy of vaccine and PD-1 checkpoint blockade immunotherapy. Oncoimmunology **2017**;6:e1308616
62. Lan Y, Zhang D, Xu C, Hance KW, Marelli B, Qi J, *et al.* Enhanced preclinical antitumor activity of M7824, a bifunctional fusion protein simultaneously targeting PD-L1 and TGF-beta. Sci Transl Med **2018**;10
63. Ravi R, Noonan KA, Pham V, Bedi R, Zhavoronkov A, Ozerov IV, *et al.* Bifunctional immune checkpoint-targeted antibody-ligand traps that simultaneously disable TGFbeta enhance the efficacy of cancer immunotherapy. Nat Commun **2018**;9:741
64. Duan J, Wang Y, Jiao S. Checkpoint blockade-based immunotherapy in the context of tumor microenvironment: Opportunities and challenges. Cancer Med **2018**;7:4517-29
65. Harrington K, Freeman DJ, Kelly B, Harper J, Soria J-C. Optimizing oncolytic virotherapy in cancer treatment. Nature Reviews Drug Discovery **2019**
66. Andtbacka RHI, Kaufman HL, Collichio F, Amatruda T, Senzer N, Chesney J, *et al.* Talimogene Laherparepvec Improves Durable Response Rate in Patients With Advanced Melanoma. J Clin Oncol **2015**;33:2780-8
67. Benencia F, Courrèges MC, Conejo-García JR, Mohamed-Hadley A, Zhang L, Buckanovich RJ, *et al.* HSV oncolytic therapy upregulates interferon-inducible chemokines and recruits immune effector cells in ovarian cancer. Molecular Therapy **2005**;12:789-802
68. Zamarin D, Holmgaard RB, Subudhi SK, Park JS, Mansour M, Palese P, *et al.* Localized Oncolytic Virotherapy Overcomes Systemic Tumor Resistance to Immune Checkpoint Blockade Immunotherapy. Sci Transl Med **2014**;6:226ra32-ra32
69. Atherton MJ, Stephenson KB, Tzelepis F, Bakhshinyan D, Nikota JK, Son HH, *et al.* Transforming the prostatic tumor microenvironment with oncolytic virotherapy. Oncoimmunology **2018**;7:e1445459-e
70. Brown MC, Holl EK, Boczkowski D, Dobrikova E, Mosaheb M, Chandramohan V, *et al.* Cancer immunotherapy with recombinant poliovirus induces IFN-dominant activation of dendritic cells and tumor antigen–specific CTLs. Sci Transl Med **2017**;9:eaan4220
71. Twumasi-Boateng K, Pettigrew JL, Kwok YYE, Bell JC, Nelson BH. Oncolytic viruses as engineering platforms for combination immunotherapy. Nature Reviews Cancer **2018**;18:419-32
72. Bourgeois-Daigneault M-C, Roy DG, Aitken AS, El Sayes N, Martin NT, Varette O, *et al.* Neoadjuvant oncolytic virotherapy before surgery sensitizes triple-negative breast cancer to immune checkpoint therapy. Sci Transl Med **2018**;10:eaao1641
73. Martin NT, Roy DG, Workenhe ST, van den Wollenberg DJM, Hoeben RC, Mossman KL, *et al.* Pre-surgical neoadjuvant oncolytic virotherapy confers protection against rechallenge in a murine model of breast cancer. Sci Rep **2019**;9:1865
74. Jiang H, Shin DH, Nguyen TT, Fueyo J, Fan X, Henry V, *et al.* Localized Treatment with Oncolytic Adenovirus Delta-24-RGDOX Induces Systemic Immunity against Disseminated Subcutaneous and Intracranial Melanomas. Clin Cancer Res **2019**;25:6801-14

75. Mostafa AA, Meyers DE, Thirukkumaran CM, Liu PJ, Gratton K, Spurrell J*, et al.* Oncolytic Reovirus and Immune Checkpoint Inhibition as a Novel Immunotherapeutic Strategy for Breast Cancer. Cancers (Basel) **2018**;10
76. Diaz RM, Galivo F, Kottke T, Wongthida P, Qiao J, Thompson J*, et al.* Oncolytic Immunovirotherapy for Melanoma Using Vesicular Stomatitis Virus. Cancer Res **2007**;67:2840-8
77. Moesta AK, Cooke K, Piasecki J, Mitchell P, Rottman JB, Fitzgerald K*, et al.* Local Delivery of OncoVEXmGM-CSF Generates Systemic Antitumor Immune Responses Enhanced by Cytotoxic T-Lymphocyte–Associated Protein Blockade. Clin Cancer Res **2017**;23:6190-202
78. Samson A, Scott KJ, Taggart D, West EJ, Wilson E, Nuovo GJ*, et al.* Intravenous delivery of oncolytic reovirus to brain tumor patients immunologically primes for subsequent checkpoint blockade. Sci Transl Med **2018**;10:eaam7577
79. Woller N, Gürlevik E, Fleischmann-Mundt B, Schumacher A, Knocke S, Kloos AM*, et al.* Viral Infection of Tumors Overcomes Resistance to PD-1-immunotherapy by Broadening Neoantigenome-directed T-cell Responses. Molecular therapy : the journal of the American Society of Gene Therapy **2015**;23:1630-40
80. Cervera-Carrascon V, Siurala M, Santos JM, Havunen R, Tahtinen S, Karell P*, et al.* TNFa and IL-2 armed adenoviruses enable complete responses by anti-PD-1 checkpoint blockade. Oncoimmunology **2018**;7:e1412902
81. Feola S, Capasso C, Fusciello M, Martins B, Tahtinen S, Medeot M*, et al.* Oncolytic vaccines increase the response to PD-L1 blockade in immunogenic and poorly immunogenic tumors. Oncoimmunology **2018**;7:e1457596
82. Ribas A, Dummer R, Puzanov I, VanderWalde A, Andtbacka RHI, Michielin O*, et al.* Oncolytic Virotherapy Promotes Intratumoral T Cell Infiltration and Improves Anti-PD-1 Immunotherapy. Cell **2017**;170:1109-19.e10
83. Davis AA, Patel VG. The role of PD-L1 expression as a predictive biomarker: an analysis of all US Food and Drug Administration (FDA) approvals of immune checkpoint inhibitors. Journal for ImmunoTherapy of Cancer **2019**;7:278
84. Chesney J, Puzanov I, Collichio F, Singh P, Milhem MM, Glaspy J*, et al.* Randomized, Open-Label Phase II Study Evaluating the Efficacy and Safety of Talimogene Laherparepvec in Combination With Ipilimumab Versus Ipilimumab Alone in Patients With Advanced, Unresectable Melanoma. Journal of clinical oncology : official journal of the American Society of Clinical Oncology **2018**;36:1658-67
85. Allagui F, Achard C, Panterne C, Combredet C, Labarriere N, Dreno B*, et al.* Modulation of the Type I Interferon Response Defines the Sensitivity of Human Melanoma Cells to Oncolytic Measles Virus. Curr Gene Ther **2017**;16:419-28
86. Kohlhapp FJ, Kaufman HL. Molecular Pathways: Mechanism of Action for Talimogene Laherparepvec, a New Oncolytic Virus Immunotherapy. Clin Cancer Res **2016**;22:1048-54
87. Shmulevitz M, Pan L-Z, Garant K, Pan D, Lee PWK. Oncogenic Ras Promotes Reovirus Spread by Suppressing IFN-β Production through Negative Regulation of RIG-I Signaling. Cancer Res **2010**;70:4912-21
88. Lin L-T, Richardson CD. The Host Cell Receptors for Measles Virus and Their Interaction with the Viral Hemagglutinin (H) Protein. Viruses **2016**;8:250
89. Hutzen B, Chen CY, Wang PY, Sprague L, Swain HM, Love J*, et al.* TGF-beta Inhibition Improves Oncolytic Herpes Viroimmunotherapy in Murine Models of Rhabdomyosarcoma. Mol Ther Oncolytics **2017**;7:17-26
90. Fueyo J, Gomez-Manzano C, Alemany R, Lee PSY, McDonnell TJ, Mitlianga P*, et al.* A mutant oncolytic adenovirus targeting the Rb pathway produces anti-glioma effect in vivo. Oncogene **2000**;19:2-12
91. van den Wollenberg DJ, Dautzenberg IJ, van den Hengel SK, Cramer SJ, de Groot RJ, Hoeben RC. Isolation of reovirus T3D mutants capable of infecting human tumor cells independent of junction adhesion molecule-A. PLoS One **2012**;7:e48064

92. Prestwich RJ, Ilett EJ, Errington F, Diaz RM, Steele LP, Kottke T, *et al.* Immune-mediated antitumor activity of reovirus is required for therapy and is independent of direct viral oncolysis and replication. Clin Cancer Res **2009**;15:4374-81
93. Gauvrit A, Brandler S, Sapede-Peroz C, Boisgerault N, Tangy F, Gregoire M. Measles virus induces oncolysis of mesothelioma cells and allows dendritic cells to cross-prime tumor-specific CD8 response. Cancer Res **2008**;68:4882-92
94. Delaunay T, Violland M, Boisgerault N, Dutoit S, Vignard V, Münz C, *et al.* Oncolytic viruses sensitize human tumor cells for NY-ESO-1 tumor antigen recognition by CD4+ effector T cells. Oncoimmunology **2017**;7:e1407897-e
95. de Graaf JF, de Vor L, Fouchier RAM, van den Hoogen BG. Armed oncolytic viruses: A kick-start for anti-tumor immunity. Cytokine & Growth Factor Reviews **2018**;41:28-39
96. Kemp V, van den Wollenberg DJM, Camps MGM, van Hall T, Kinderman P, Pronk-van Montfoort N, *et al.* Arming oncolytic reovirus with GM-CSF gene to enhance immunity. Cancer Gene Therapy **2018**
97. Cerullo V, Pesonen S, Diaconu I, Escutenaire S, Arstila PT, Ugolini M, *et al.* Oncolytic adenovirus coding for granulocyte macrophage colony-stimulating factor induces antitumoral immunity in cancer patients. Cancer Res **2010**;70:4297-309
98. Grossardt C, Engeland CE, Bossow S, Halama N, Zaoui K, Leber MF, *et al.* Granulocyte-macrophage colony-stimulating factor-armed oncolytic measles virus is an effective therapeutic cancer vaccine. Hum Gene Ther **2013**;24:644-54
99. Andtbacka RHI, Collichio F, Harrington KJ, Middleton MR, Downey G, Öhrling K, *et al.* Final analyses of OPTiM: a randomized phase III trial of talimogene laherparepvec versus granulocyte-macrophage colony-stimulating factor in unresectable stage III–IV melanoma. Journal for ImmunoTherapy of Cancer **2019**;7:145
100. Diaconu I, Cerullo V, Hirvinen ML, Escutenaire S, Ugolini M, Pesonen SK, *et al.* Immune response is an important aspect of the antitumor effect produced by a CD40L-encoding oncolytic adenovirus. Cancer Res **2012**;72:2327-38
101. Pesonen S, Diaconu I, Kangasniemi L, Ranki T, Kanerva A, Pesonen SK, *et al.* Oncolytic Immunotherapy of Advanced Solid Tumors with a CD40L-Expressing Replicating Adenovirus: Assessment of Safety and Immunologic Responses in Patients. Cancer Res **2012**;72:1621-31
102. Zamarin D, Holmgaard RB, Ricca J, Plitt T, Palese P, Sharma P, *et al.* Intratumoral modulation of the inducible co-stimulator ICOS by recombinant oncolytic virus promotes systemic anti-tumour immunity. Nature Communications **2017**;8:14340
103. Kleinpeter P, Fend L, Thioudellet C, Geist M, Sfrontato N, Koerper V, *et al.* Vectorization in an oncolytic vaccinia virus of an antibody, a Fab and a scFv against programmed cell death -1 (PD-1) allows their intratumoral delivery and an improved tumor-growth inhibition. Oncoimmunology **2016**;5:e1220467-e
104. Wing A, Fajardo CA, Posey AD, Shaw C, Da T, Young RM, *et al.* Improving CART-Cell Therapy of Solid Tumors with Oncolytic Virus–Driven Production of a Bispecific T-cell Engager. Cancer Immunol Res **2018**;6:605-16
105. Tedcastle A, Illingworth S, Brown A, Seymour LW, Fisher KD. Actin-resistant DNAse I Expression From Oncolytic Adenovirus Enadenotucirev Enhances Its Intratumoral Spread and Reduces Tumor Growth. Molecular therapy : the journal of the American Society of Gene Therapy **2016**;24:796-804
106. Pol JG, Acuna SA, Yadollahi B, Tang N, Stephenson KB, Atherton MJ, *et al.* Preclinical evaluation of a MAGE-A3 vaccination utilizing the oncolytic Maraba virus currently in first-in-human trials. Oncoimmunology **2018**;8:e1512329-e
107. Esaki S, Nigim F, Moon E, Luk S, Kiyokawa J, Curry W, Jr., *et al.* Blockade of transforming growth factor-beta signaling enhances oncolytic herpes simplex virus efficacy in patient-derived recurrent glioblastoma models. Int J Cancer **2017**;141:2348-58

108. Seth P, Wang ZG, Pister A, Zafar MB, Kim S, Guise T, *et al.* Development of oncolytic adenovirus armed with a fusion of soluble transforming growth factor-beta receptor II and human immunoglobulin Fc for breast cancer therapy. Hum Gene Ther **2006**;17:1152-60
109. Hu Z, Gerseny H, Zhang Z, Chen YJ, Berg A, Zhang Z, *et al.* Oncolytic adenovirus expressing soluble TGFbeta receptor II-Fc-mediated inhibition of established bone metastases: a safe and effective systemic therapeutic approach for breast cancer. Mol Ther **2011**;19:1609-18
110. Thommen DS, Schumacher TN. T Cell Dysfunction in Cancer. Cancer Cell **2018**;33:547-62
111. McKee TD, Grandi P, Mok W, Alexandrakis G, Insin N, Zimmer JP, *et al.* Degradation of fibrillar collagen in a human melanoma xenograft improves the efficacy of an oncolytic herpes simplex virus vector. Cancer Res **2006**;66:2509-13
112. Yu F, Hong B, Song X-T. A T-cell engager-armed oncolytic vaccinia virus to target the tumor stroma. Cancer Transl Med **2017**;3:122-32
113. de Sostoa J, Fajardo CA, Moreno R, Ramos MD, Farrera-Sal M, Alemany R. Targeting the tumor stroma with an oncolytic adenovirus secreting a fibroblast activation protein-targeted bispecific T-cell engager. Journal for immunotherapy of cancer **2019**;7:19-
114. Ilkow CS, Marguerie M, Batenchuk C, Mayer J, Ben Neriah D, Cousineau S, *et al.* Reciprocal cellular cross-talk within the tumor microenvironment promotes oncolytic virus activity. Nat Med **2015**;21:530-6
115. Zhao F, Evans K, Xiao C, DeVito N, Theivanthiran B, Holtzhausen A, *et al.* Stromal Fibroblasts Mediate Anti–PD-1 Resistance via MMP-9 and Dictate TGFβ Inhibitor Sequencing in Melanoma. Cancer Immunol Res **2018**;6:1459-71
116. Bajwa R, Cheema A, Khan T, Amirpour A, Paul A, Chaughtai S, *et al.* Adverse Effects of Immune Checkpoint Inhibitors (Programmed Death-1 Inhibitors and Cytotoxic T-Lymphocyte-Associated Protein-4 Inhibitors): Results of a Retrospective Study. J Clin Med Res **2019**;11:225-36
117. Kovacs RJ, Maldonado G, Azaro A, Fernández MS, Romero FL, Sepulveda-Sánchez JM, *et al.* Cardiac Safety of TGF-β Receptor I Kinase Inhibitor LY2157299 Monohydrate in Cancer Patients in a First-in-Human Dose Study. Cardiovasc Toxicol **2015**;15:309-23
118. Perez MC, Miura JT, Naqvi SMH, Kim Y, Holstein A, Lee D, *et al.* Talimogene Laherparepvec (TVEC) for the Treatment of Advanced Melanoma: A Single-Institution Experience. Ann Surg Oncol **2018**;25:3960-5
119. Bommareddy PK, Shettigar M, Kaufman HL. Integrating oncolytic viruses in combination cancer immunotherapy. Nature Reviews Immunology **2018**;18:498-513



CHAPTER 7

Intertumoral differences dictate the outcome of TGF-β blockade on the efficacy of viro-immunotherapy

Christianne Groeneveldt[1], Jurriaan Q. van Ginkel[1], Priscilla Kinderman[2], Marjolein Sluijter[1], Lisa Griffioen[1], Camilla Labrie[1], Diana J. M. van den Wollenberg[3], Rob C. Hoeben[3], Sjoerd H. van der Burg[1], Peter ten Dijke[4], Lukas J. A. C. Hawinkels[2], Thorbald van Hall[1], Nadine van Montfoort[2#]

[1] Department of Medical Oncology, Oncode Institute, Leiden University Medical Center, 2333 ZA, Leiden, The Netherlands

[2] Department of Gastroenterology and Hepatology, Leiden University Medical Center, 2333 ZA, Leiden, The Netherlands

[3] Department of Cell and Chemical Biology, Leiden University Medical Center, 2300 RC, Leiden, The Netherlands

[4] Department of Cell and Chemical Biology, Oncode Institute, Leiden University Medical Center, 2300 RC, Leiden, The Netherlands

[#] Corresponding author

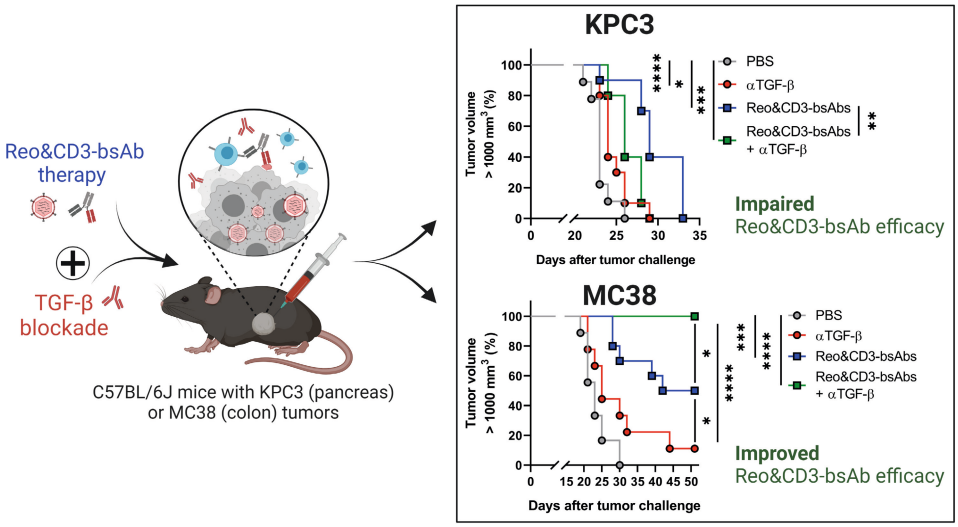
Cancer Research Communications 2023;3(2):325–337

ABSTRACT

The absence of T cells in the tumor microenvironment of solid tumors is a major barrier to cancer immunotherapy efficacy. Oncolytic viruses, including reovirus type 3 Dearing (Reo), can recruit $CD8^+$ T cells to the tumor and thereby enhance the efficacy of immunotherapeutic strategies that depend on high T-cell density, such as CD3-bispecific antibody (bsAb) therapy. Transforming growth factor-β (TGF-β) signaling might represent another barrier to effective Reo&CD3-bsAb therapy due to its immunoinhibitory characteristics. Here, we investigated the effect of TGF-β blockade on the antitumor efficacy of Reo&CD3-bsAb therapy in the preclinical pancreatic KPC3 and colon MC38 tumor models, where TGF-β signaling is active. TGF-β blockade impaired tumor growth in both KPC3 and MC38 tumors. Furthermore, TGF-β blockade did not affect reovirus replication in both models and significantly enhanced the Reo-induced T-cell influx in MC38 colon tumors. Reo administration decreased TGF-β signaling in MC38 tumors but instead increased TGF-β activity in KPC3 tumors, resulting in the accumulation of αSMA^+ fibroblasts. In KPC3 tumors, TGF-β blockade antagonized the antitumor effect of Reo&CD3-bsAb therapy, even though T-cell influx and activity were not impaired. Moreover, genetic loss of TGF-β signaling in $CD8^+$ T cells did not affect therapeutic responses. In contrast, TGF-β blockade significantly improved therapeutic efficacy of Reo&CD3-bsAb in mice bearing MC38 colon tumors, resulting in a 100% complete response. Further understanding of the factors that determine this inter-tumor dichotomy is required before TGF-β inhibition can be exploited as part of viro-immunotherapeutic combination strategies to improve their clinical benefit.

Significance: Blockade of the pleiotropic molecule TGF-β can both improve or impair the efficacy of viro-immunotherapy, depending on the tumor model. While TGF-β blockade antagonized Reo&CD3-bsAb combination therapy in the KPC3 model for pancreatic cancer, it resulted in 100% complete responses in the MC38 colon model. Understanding factors underlying this contrast is required to guide therapeutic application.

GRAPHICAL ABSTRACT



INTRODUCTION

Oncolytic viruses (OVs) are increasingly recognized as potent anticancer agents due to their preferential infection of cancerous cells and stimulation of host antitumor immunity (1). The mammalian reovirus type 3 Dearing strain (T3D) is one of the most prominent oncolytic viruses under clinical evaluation and displays an excellent safety record in clinical trials (2,3). Reoviruses show an inherent preference for replication in and lysis of transformed, but not healthy cells (4). Although reovirus has demonstrated moderate antitumor efficacy as monotherapy (5,6), studies have shown that its potential might be better utilized as a part of combinatorial approaches (7). For example, we recently demonstrated that sensitizing the tumor microenvironment (TME) of murine pancreatic KPC3 tumors with reovirus significantly enhanced the efficacy of otherwise non-effective CD3-bispecific antibodies (CD3-bsAbs). This enhanced efficacy could be attributed to the capability of reovirus to induce a fast interferon response which was followed by a potent influx of $CD8^+$ T cells (8). Others have shown that reovirus can sensitize the TME for immune checkpoint inhibition by enhancing the intratumoral density of tumor-specific $CD8^+$ T cells and upregulating immune checkpoint inhibitor Programmed Death-Ligand 1 (PD-L1) expression (9).

Although the use of OVs is very promising to attract T cells to solid tumors and improve the efficacy of immunotherapeutic strategies, these combination approaches rarely lead to complete cures. Various tumor types such as colorectal cancer, ovarian cancer, and pancreatic ductal adenocarcinoma (PDAC) (10-12) often present with high transforming growth factor-β (TGF-β) signaling, which might be another barrier to effective combinatorial immunotherapy (13-15). TGF-β acts as a tumor-promoting cytokine by stimulating cancer cell migration and invasion, extracellular matrix (ECM) remodeling, epithelial-to-mesenchymal transition (EMT), and the induction of an immunosuppressive TME (16). In particular, TGF-β acts as an immunosuppressive factor by inhibiting the generation and function of $CD4^+$ and $CD8^+$ effector T cells and dendritic cells (DCs), whilst promoting the expansion of regulatory T cells (Tregs) and myeloid-derived suppressor cells (17,18). Indeed, TGF-β blockade can promote the expansion of $CD8^+$ T cells, reduce the level of regulatory T cells (Tregs) and induce the polarization from pro-tumorigenic M2 macrophages to antitumor M1 macrophages (19,20).

Altogether, these observations hint towards a potential beneficial effect of TGF-β inhibition on the efficacy of immunotherapeutic strategies. For example, TGF-β inhibition has increased the efficacy of checkpoint blockade in mouse models for mammary carcinoma and metastatic breast cancer, and colorectal cancer (21-24). We hypothesized that the reovirus-induced increase in intratumoral T cells, combined with TGF-β inhibition to remove the immunosuppressive barrier in the TME, would also strongly enhance the efficacy of viro-immunotherapeutic strategies. In the present study, we investigated whether inhibition of TGF-β signaling further enhanced the

efficacy of reovirus and CD3-bispecific antibody therapy in preclinical tumor models with high TGF-β signaling.

MATERIAL & METHODS

Reovirus

The wild-type reovirus strain R124 (further referred to as Reo) was previously isolated from a heterogeneous reovirus Type 3 Dearing (T3D) stock (VR-824) obtained from the American Type Culture Collection (ATCC) by two rounds of plaque purification using HER911 cells (RRID:CVCL_1K15) (25). All experiments were performed using cesium chloride (CsCl)-purified stocks as described earlier (8). The total amount of particles was calculated based on OD_{260} values where 1 OD equals $2.10x10^{12}$ reovirus particles/mL, and the infectious titer was quantified by plaque assay on HER911 cells.

Cell lines and culture

The murine pancreatic cancer cell line KPC3 (RRID:CVCL_A9ZK) is a low-passage derivate of a primary KPC tumor with mutant *p53* and *K-ras* from a female C57BL/6 mouse (8,26). KPC3.TRP1 cells (RRID:CVCL_A9ZL) were generated as described (27) and selected for expression of tyrosine-related protein (TRP1) by cell sorting using an αTRP1 antibody (clone: TA99). The MC38 cell line (RRID: CVCL_B288) is a chemically-induced murine colon carcinoma. MC38.TRP1 cells were generated as described before for KPC3.TRP1 (27) by transfection of MC38 cells with a *TRP1/gp75*-coding plasmid using lipofectamine (Invitrogen) in a 1:3 ratio. Transfected cells were selected with 400 µg/mL geneticin (G418, ThermoFisher Scientific) and sorted twice for expression of TRP1 as described above. All cells were cultured at 37 °C in a humidified atmosphere containing 5% CO_2 in Iscove's Modified Dulbecco's Medium (IMDM; Invitrogen) supplemented with 8% fetal calf serum (FCS; Bodinco, Alkmaar, The Netherlands), 2 mM L-glutamine (Gibco), 100 µg/mL penicillin and 100 µg/mL streptomycin (Gibco). Cell lines were assured to be free of *Mycoplasma* by regular PCR analysis. Authentication of the cell lines was done by Short Tandem Repeat (STR) profiling (IDEXX BioAnalytics, Ludwigsburg, Germany) and cells of low passage number were used for all experiments.

Antibodies for in vivo administration

The CD3xTRP1 bispecific antibody (bsAb) used is a knob-into-hole bispecific based on murine IgG2a with an Fc Silent™ mutation, featuring one arm with an anti-mouse CD3e scFv based on the clone 145-2C11, and the other arm containing the TA99 clone directed against TRP1 (bAb0136; Absolute Antibody). Transforming growth factor-β (TGF-β) blockade was performed using the monoclonal TGF-β-blocking antibody (clone 1D11.16.8; InVivoMAb anti-mouse/human/rat/monkey/ hamster/canine/bovine TGF-β1, -2, -3; BioXCell).

Mouse experiments

Male C57BL/6J mice (RRID:IMSR_JAX:000664) (6-8 weeks old) were purchased from Charles River Laboratories (France). Male nonobese diabetic (NOD).Cg-Prkdc^{scid}Il2rg^{tm1Wjl}/SzJ (NSG) mice (RRID:IMSR_JAX:005557) (6-8 weeks old) were obtained from The Jackson Laboratory (Bar Harbor, Maine, USA). TGF-β receptor II (TβRII) knockout mice (TβRII$^{fl/fl}$) (28) were crossed with CD8a-driven Cre-knock-in mice (RRID:IMSR_JAX:008766) to generate CD8Cre$^{+/-}$TβRII$^{fl/fl}$ (CD8 TβRII KO) and CD8Cre$^{-/-}$TβRII$^{fl/fl}$ (TβRII WT) mice. Both male and female CD8 TβRII KO and TβRII WT mice (7-22 weeks old) were used in the experiment. Genomic PCR was conducted to analyze the genotypes of mice using ear DNA and gene-specific primers for the conditional TGF-βRII locus (28) and Cre construct (CRE transgene 5'-CAA TGG AAG GAA GTC GTG GT-3'; wt 5'-CAC ACA TGC AAG TCT AAA TCA GG-3'; CRE common 5'-TGG GAT TTA CAG GGC ATA CTG-3').

All mouse experiments were individually prepared, reviewed, ethically approved, and registered by the institutional Animal Welfare Body of Leiden University Medical Center and carried out under project license AVD1160020187004, issued by the competent authority on animal experiments in The Netherlands (named CCD: Centrale Commissie Dierproeven). Power calculation was performed to define optimal sample size. Experiments were performed following the Dutch Act on Animal Experimentation and EU Directive 2010/63/EU ("On the protection of animals used for scientific purposes") at the animal facility of the Leiden University Medical Center (LUMC), The Netherlands. Mice were housed in individually ventilated cages with no more than 5 mice/cage. After one week of acclimatization after transport, mice were inoculated in the right flank with subcutaneous KPC3(.TRP1) tumors (1x10^5 cells in 100 µL phosphate-buffered saline (PBS)/0.1% bovine serum albumin (BSA) or MC38(.TRP1) tumors (5x10^5 cells in 200 µL PBS/0.1% BSA). In the case of a rechallenge, mice that cleared the primary tumor were injected with the same number of cells in the alternate flank. Intratumoral reovirus administration was performed under isoflurane anesthesia by injection of 1x10^7 plaque-forming units (pfu) of reovirus or PBS as a control in a volume of 30 µL PBS. Intravenous administration of reovirus after tumor challenge was performed by injection of 1x10^8 pfu of reovirus in a total volume of 100 µL PBS in the tail vein. Treatment with CD3xTRP1 bsAbs consisted of 2-3 intraperitoneal (i.p.) injections of 12,5 µg antibody in 100 µL PBS, given every other day. αTGF-β was administered 2-3x/week by i.p. injections of 200 µg in 100 µL PBS.

Cages were randomly allocated to a certain treatment group by an independent researcher and treatments were given in a different order each time. During all experiments, tumors were measured 3-5 times a week in 3 dimensions using a caliper, in a blinded manner concerning the experimental group or genotype of the mice. For experiments where tumor growth was the experimental outcome, mice were sacrificed when the tumor volume exceeded 1000 mm^3. In the case where therapy response was determined: NR = no response; CR = complete response and PR = partial response (regression or constant tumor volumes for at least 7 days). For interim blood analysis,

blood was harvested by tail vein puncture. For intratumoral analysis experiments, mice were sacrificed at indicated days after treatment before tumors were collected. Tumors were divided into representative parts, which were either snap-frozen in liquid N2 and stored at -80 °C for further analysis or fixed in 4% formaldehyde (AddedPharma) for immunohistochemistry (see also **Supplementary Methods**). Alternatively, tumors were immediately processed to single cells suspensions for flow cytometry analysis.

Cell preparation and flow cytometry

Tumors were dissociated into a single-cell suspension as described before (8). Blood was incubated with red blood cell lysis buffer for 3 minutes at room temperature (RT) before use. Cells were incubated with Zombie AquaTM Fixable Viability Dye (BioLegend) in PBS at RT followed by incubation with 2.4G2 FcR blocking antibodies (clone 2.4G2; BD Biosciences) in FACS buffer (PBS, 0.5% BSA, and 0.2% NaN_3) for 20 minutes on ice. If applicable, cells were incubated with Reo $\mu1_{133\text{-}140}$ tetramer conjugated to APC or the Rpl18 tetramer conjugated to PE (both generated in-house) for 1 hour at RT in FACS buffer, after which surface markers (**Table S1**) were added directly to the tetramer mixture for 30 minutes of incubation at RT. For intracellular staining, cells were fixed and stained for transcription factors and nuclear proteins using the Foxp3 / Transcription Factor Staining Buffer Set (eBiosciences) according to the manufacturer's instructions. After completion of staining protocols, samples were fixed in 1% paraformaldehyde and acquired using a BD LSRFortessa™ X20 4L cell analyzer (BD Biosciences, San Jose, CA, USA) at the Flow cytometry Core Facility (FCF) of Leiden University Medical Center (LUMC) in Leiden, The Netherlands (https://www.lumc.nl/research/facilities/fcf). Data were analyzed using FlowJoTM Software Version 10 (Becton, Dickinson, and Company).

RNA isolation and RT-qPCR

A representative snap-frozen proportion (10-30 mg) of each tumor or organ was disrupted in lysis buffer (Promega) using a stainless bead and the TissueLyser LT (Qiagen). Total RNA of in vivo samples was using the ReliaPrep™ RNA Tissue Miniprep System (Promega) according to the manufacturer's protocol. Total RNA from in vitro samples was isolated from cell pellets using the NucleoSpin® RNA Kit (Macherey-Nagel™) according to the manufacturer's instructions. 500 ng of RNA was used to generate cDNA using the High-Capacity RNA-to-cDNATM Kit (ThermoFisher Scientific) according to the manufacturer's protocol. Reovirus genomic copies and expression levels of host genes (**Table S2**) in tumors were measured by RT-qPCR as previously described (8). Reovirus S4 copy numbers were determined based on a standard curve, generated with serial dilutions of plasmid pcDNA_S4. Log_{10} S4 copy numbers were calculated using a previously described formula (29). The expression of host genes was normalized to reference genes Mzt2 and Ptp4a2 using the Bio-Rad CFX Manager 3.1 Software (Bio-Rad).

Statistics

Sample size was calculated using the PS: Power and Sample Size Calculation program (Vanderbilt University, version 3.1.6) (30). For experiments where tumor growth was the experimental read-out, mice were excluded when tumor engraftment was not successful (1% of all tumor engraftments). For RT-qPCR analysis, samples were excluded when RNA concentration and/or sample purity were too low. For flow cytometry data, tumor samples were excluded when evidence for draining lymph node contamination was present. All graphs were prepared and statistical analyses were performed using the GraphPad Prism software (version 8.0.2) (RRID:SCR_002798). Statistical tests used for each figure are described in the figure legends. Significance levels are labeled with asterisks, with ns=non-significant, *p<0.05, **p<0.01, ***p<0.001, and ****p<0.0001.

RESULTS

Early blockade of TGF-β signaling delays tumor outgrowth of KPC3 and MC38 tumors

In our previous work, we demonstrated that preconditioning murine pancreatic KPC3 tumors with reovirus (Reo) potently sensitized these solid tumors for otherwise ineffective CD3-bispecific antibody (bsAb) therapy (abbreviated to Reo&CD3-bsAbs) (8). KPC3 tumors display many characteristics of human PDAC, including desmoplastic stroma containing α-smooth muscle actin ($\alpha SMA)^+$ fibroblasts and collagen, and the absence of $CD8^+$ T cells (**Figure 1A**). KPC3 tumors also display TGF-β signaling, as indicated by nuclear accumulation of epithelial and stromal phosphorylated Smad2, a signaling protein directly downstream of the TGF-β type I receptor. Similarly to the murine pancreatic KPC3 tumor model, murine colon MC38 tumors display phosphorylated Smad2, but they do not contain many αSMA^+ fibroblasts and collagen and show a basal presence of $CD8^+$ T cells (**Figure 1B**). Since TGF-β signaling is active in both KPC3 and MC38 tumor tumors (23) and TGF-β has many immunoinhibitory characteristics, we hypothesized that inhibition of TGF-β might enhance the efficacy of Reo&CD3-bsAb therapy in these models.

First, we assessed the effect of TGF-β blockade as a monotherapy. We employed the murine monoclonal antibody 1D11 (αTGF-β), which neutralizes all 3 isoforms of TGF-β (31). This antibody was effective in decreasing TGF-β signaling *in vitro*, as was determined using a transcriptional reporter assay (CAGA-Luciferase, **Figure S1A**) and phosphorylation of Smad2 (**Figure S1B**). We next assessed the effect of TGF-β inhibition *in vivo* by applying TGF-β blockade in immunocompetent mice bearing subcutaneous KPC3 or MC38 tumors. Interestingly, TGF-β blockade significantly delayed tumor outgrowth of both KPC3 and MC38 tumors, but only when TGF-β blockade was started early after tumor challenge (**Figure 1C, D**) and not when tumors were already established (**Figure S2A**). Especially in KPC3 tumors, this delay in tumor growth after early, but not late intervention with TGF-β blocking antibodies was accompanied by a decreased intratumoral collagen

deposition (**Figure 1E, F, Figure S2B**). The impaired outgrowth of KPC3 tumors after TGF-β blockade could not be attributed to a lower proliferation of tumor cells, since the frequency of Ki67^{+} cells was not affected (**Figure 1G**). Additionally, the same delay in KPC3 tumor growth after early TGF-β blockade could be observed in immunodeficient NSG mice that lack T, B, and NK cells, suggesting that this delay in tumor growth after TGF-β blockade is not immune-mediated (**Figure 1H**). Combined, these data demonstrate that early TGF-β blockade delays the outgrowth of both KPC3 and MC38 tumors, which could possibly lead to improved efficacy of Reo&CD3-bsAb therapy.

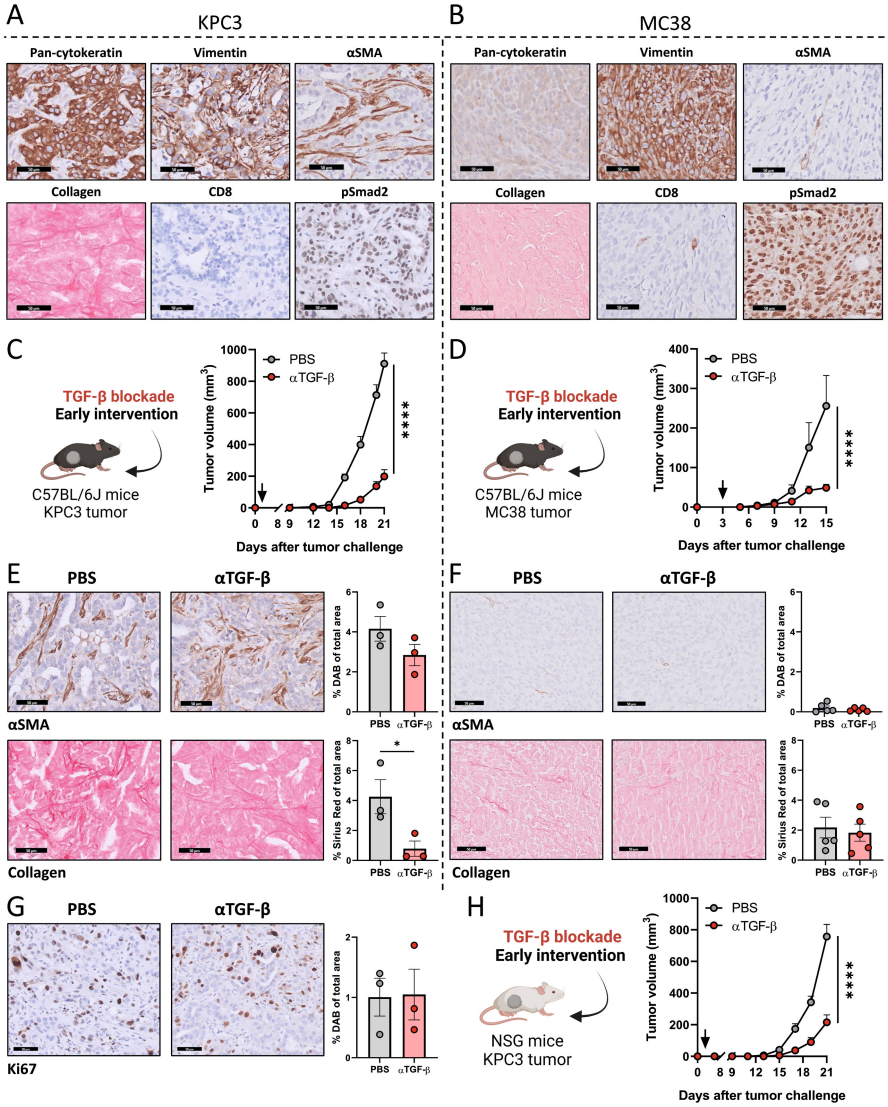


Figure 1. Early blockade of TGF-β signaling delays tumor outgrowth of KPC3 and MC38 tumors. (**A/B**) Representative images obtained from immunohistochemical (IHC) stainings of an untreated KPC3 (A) or MC38 (B) tumor for pan-cytokeratin, vimentin, smooth muscle actin-α (αSMA), collagen, CD8, and phosphorylated Smad2 (pSmad2). Scale bars equal 50 µm. >>

>> (**C/D**) Average tumor growth curves of immunocompetent KPC3 (C) or MC38 (D) tumor-bearing C57BL/6J mice (n=5/group) after TGF-β blockade. Mice were subcutaneously engrafted with KPC3 cells ($1x10^5$/mouse[5]) or MC38 cells ($5x10^5$/mouse) and received TGF-β-neutralizing antibodies (αTGF-β, 200 μg/injection every 3 days, starting from day 3 as indicated by the black arrow) as early intervention. (**E/F**) IHC stainings for αSMA and collagen in representative KPC3 (E) or MC38 (F) tumors after indicated treatments. Scale bars represent 50 μm and stainings were quantified using ImageJ. (**G**) IHC staining of Ki67 in KPC3 tumors treated with PBS or αTGF-β. Scale bars represent 50 μm and stainings were quantified using ImageJ. (**H**) Average tumor growth curves of immunodeficient KPC3-bearing NSG mice (n=8/group) after TGF-β blockade as early intervention, as described in (C). Data represent mean±SEM. Significance between PBS and αTGF-β in (E, F, G) was determined using unpaired t-tests. Significant differences in tumor growth between PBS and αTGF-β in (C, D, and H) were determined using an ordinary two-way analysis of variance (ANOVA) with Sidak's multiple comparisons test. Significance levels: *p<0.05 and ****p<0.0001.

TGF-β blockade does not impair Reo replication and the Reo-induced interferon response

Before investigating the effect of TGF-β blockade on the efficacy of Reo&CD3-bsAb therapy, we first analyzed whether TGF-β blockade would not affect the replication and immune-stimulatory properties of Reo in KPC3 and MC38 tumors. *In vitro,* Reo replication was not altered in KPC3 and MC38 cells after the addition of recombinant TGF-β or TGF-β inhibition (**Figure S3**). To confirm this *in vivo*, immunocompetent mice were treated with αTGF-β or left untreated and palpable tumors were injected with Reo. Reo replication and the Reo-induced expression of interferon-stimulated genes (ISGs) were compared between groups at the end of the experiment (**Figure 2A, B**). In both KPC3 and MC38 tumors, Reo replication (**Figure 2C, D**) and the Reo-induced expression of ISGs including T-cell-attracting chemokines *Cxcl9* and *Cxcl10* (**Figure 2E, F**) were not negatively affected after TGF-β blockade. Instead, the expression of various ISGs was higher in the groups that received Reo + αTGF-β compared to the group that received Reo only. Combined, these data indicate that TGF-β inhibition does not negatively influence the Reo-induced inflammatory response in the TME.

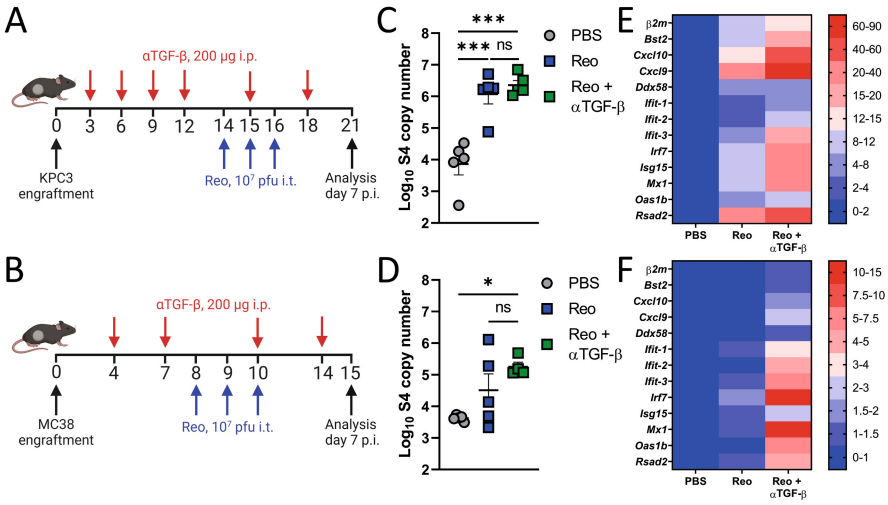


Figure 2. TGF-β blockade does not impair Reo replication and the Reo-induced interferon response in KPC3 and MC38 tumors. (**A**/**B**) Mice (n=4-5/group) were engrafted subcutaneously with KPC3 cells (1x10^5/mouse) (A) or MC38 cells (5x10^5/mouse) (B) and received TGF-β-neutralizing antibodies (αTGF-β, 200 μg/injection every 3 days) starting directly after tumor engraftment. Mice received Reo intratumorally on indicated days (10^7 plaque-forming units/injection)**.** Mice were sacrificed on day 21 (KPC3) or day 15 (MC38) for intratumoral analysis. (**C**/**D**) Reovirus genomic segment 4 (S4) copy number in KPC3 (C) or MC38 (D) tumor lysates, as determined by RT-qPCR. (**E**/**F**) Heatmap with relative expression of interferon response genes (ISGs) target genes in KPC3 (E) or MC38 (F) tumors after indicated treatments, as determined by RT-qPCR. Data represent mean±SEM. Significance between groups in (B) and (E) was determined using an ordinary two-way analysis of variance (ANOVA) with Tukey's post hoc test. Significance levels: ns=not significant, *p<0.05, ***p<0.001.

TGF-β blockade enhances the Reo-induced influx of T cells in MC38 tumors but not in KPC3 tumors

The efficacy of reovirus-based immunotherapy such as Reo&CD3-bsAb therapy relies on efficient Reo-induced intratumoral T-cell influx. Since TGF-β is known to promote an immunosuppressive and T-cell-excluding environment in the TME, we hypothesized that TGF-β blockade might further enhance the Reo-induced T-cell influx and function in these tumors. In KPC3 tumors, TGF-β blockade did not enhance the influx of total CD45$^+$ immune cells (**Figure 3A**) but significantly increased the frequency of NK cells after Reo administration (**Figure 3B**). Surprisingly, however, TGF-β blockade did not improve the Reo-induced influx of (reovirus-specific) CD8$^+$ T cells, nor their activation status (**Figure 3C-E**). TGF-β blockade also did not enhance total CD45$^+$ immune cell influx in MC38 tumors (**Figure 3F**), and again significantly improved the frequency of NK cells (**Figure 3G**).

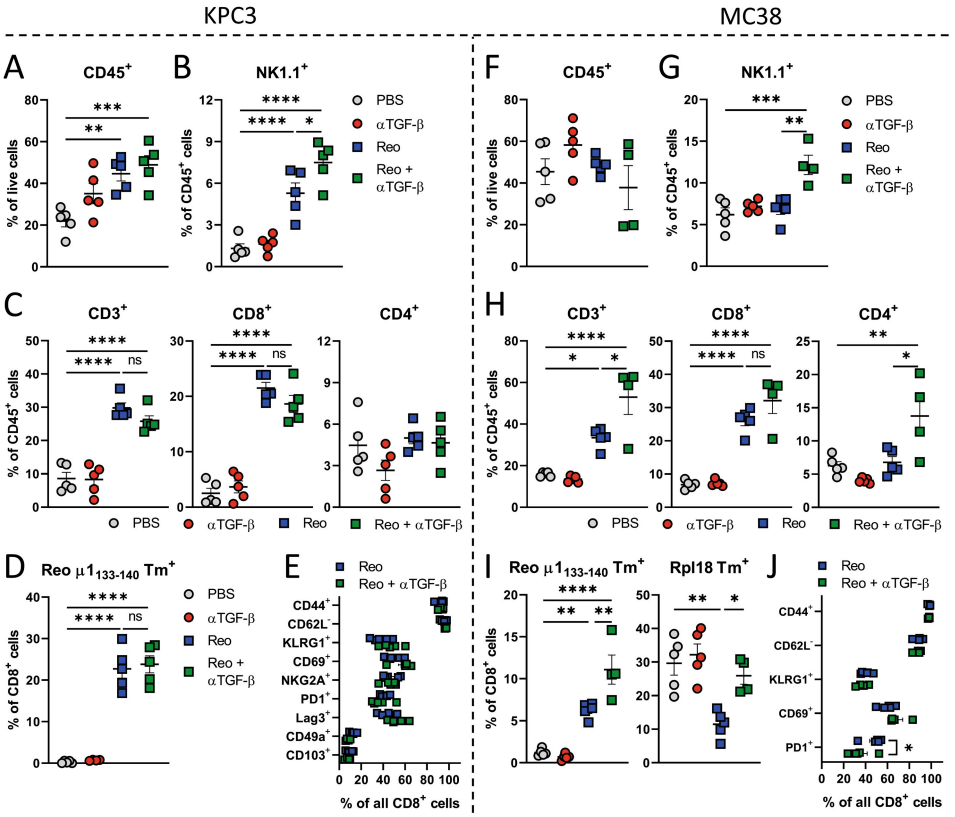


Figure 3. TGF-β blockade enhances the Reo-induced influx of T cells in MC38 tumors but not in KPC3 tumors. Experiments were performed according to the design described before in Figure 2A (KPC3) and Figure 2B (MC38). (**A**) Frequency of CD45$^+$ immune cells in KPC3 tumors after indicated treatments. (**B**) Frequency of NK cells within the CD45$^+$ immune cell population in KPC3 tumors. (**C**) Percentage of CD3$^+$, CD8$^+$, and CD4$^+$ T cells within CD45$^+$ immune cells in KPC3 tumors. (**D**) Frequency of reovirus-specific $\mu1_{133\text{-}140}$ T cells within the intratumoral CD8$^+$ T-cell population. (**E**) Expression of various markers on intratumoral CD8$^+$ T cells after receiving Reo only or Reo + αTGF-β. (**F**) Frequency of CD45$^+$ immune cells in MC38 tumors after indicated treatments. (**G**) Frequency of NK cells within the CD45$^+$ immune cell population in MC38 tumors. (**H**) Percentage of CD3$^+$, CD8$^+$, and CD4$^+$ T cells within CD45$^+$ immune cells in MC38 tumors. (**I**) Frequency of reovirus-specific $\mu1_{133\text{-}140}$ and tumor-specific Rpl18 T cells within the intratumoral CD8$^+$ T-cell population. (**J**) Expression of various markers on intratumoral CD8$^+$ T cells after receiving Reo only or Reo + αTGF-β. Data represent mean±SEM. Significance in (A-D) and (F-I) was determined using an ordinary one-way ANOVA with Tukey's multiple comparisons test. Significance between groups in (E) and (J) was determined using an ordinary two-way analysis of variance (ANOVA) with Tukey's post hoc test. Significance levels: ns=not significant, *p<0.05, **p<0.01, ***p<0.001 and ****p<0.0001.

Compared to KPC3 tumors, PBS-treated MC38 tumors already contained a higher basal frequency of $CD8^+$ T cells (6.808±0.57 vs 2.502±0.92) within the $CD45^+$ immune cell population. In contrast to KPC3 tumors, αTGF-β administration significantly increased the Reo-induced influx of total T cells in MC38 tumors (**Figure 3H**), as well as the frequency of reovirus-specific ($\mu1_{133\text{-}140}$ Tm^+) and tumor-specific (Rpl18 Tm^+) $CD8^+$ T cells compared to the group that received Reo only (**Figure 3I**). Expression of various activation markers on $CD8^+$ T cells was again comparable between both Reo-treated groups (**Figure 3J**). Combined, these data indicate that TGF-β blockade does not improve the Reo-induced T-cell influx and activation in KPC3 tumors. However, in MC38 tumors the frequency of T cells in the tumor, including reovirus- and tumor-specific T cells, is significantly enhanced when TGF-β signaling is inhibited.

Reovirus administration increases TGF-β signaling in KPC3, but not MC38 tumors

Next, we explored whether Reo administration affects TGF-β signaling in these tumors. Interestingly, when Reo was administered to mice bearing KPC3 tumors, a further increase in the presence of TGF-β1 levels in the tumor was observed (**Figure 4A**). Expression of various TGF-β target genes was also elevated within the tumor lysate (**Figure 4B**). Furthermore, Reo-treated tumors contained more αSMA-positive fibroblasts (**Figure 4C, D**), which are known to be induced by TGF-β (32). Together, these data suggest that TGF-β signaling is increased in KPC3 tumors after Reo administration, which provides an additional rationale to apply TGF-β blockade in combination with Reo-based viro-immunotherapy. In contrast, MC38 tumors displayed much lower total and active TGF-β1 levels in the tumor compared to KPC3 tumors, and the presence of active TGF-β was not increased upon Reo administration (**Figure 4E**). Additionally, expression of TGF-β target genes was decreased in Reo-treated MC38 tumors (**Figure 4F**) and the intratumoral presence of αSMA-positive fibroblasts was not increased (**Figure 4G, H**). We conclude that Reo differentially impacts TGF-β signaling in KPC3 and MC38 tumors, which might influence the added value of TGF-β blockade on the efficacy of Reo&CD3-bsAbs in these preclinical models.

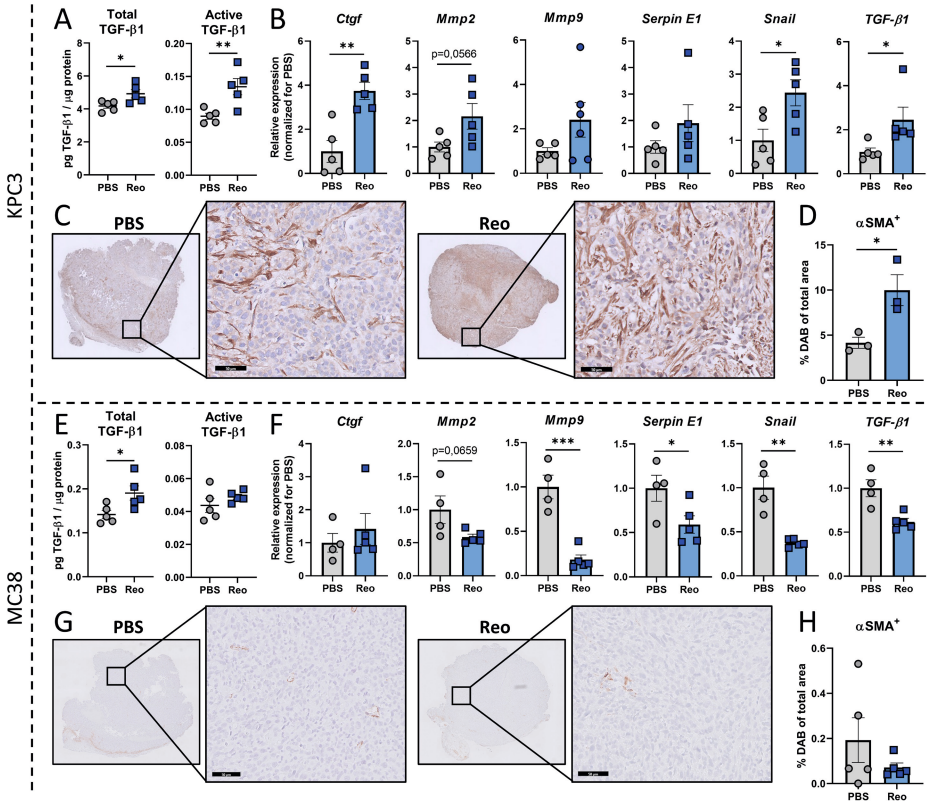


Figure 4. Reovirus administration increases TGF-β signaling in KPC3, but not MC38 tumors. (**A**) Levels of active and total TGF-β in tumor lysates of KPC3 tumors (n=4-5/group), treated intratumorally with PBS or Reo (3x 10^7 plaque-forming units) and harvested after 5 days. (**B**) Relative expression of TGF-β target genes in PBS- or Reo-treated KPC3 tumors (n=4-5/group), as determined by RT-qPCR. (**C**) Representative images obtained from immunohistochemical staining of PBS- or Reo-treated KPC3 tumors (n=3-5/group) for αSMA. Scale bars of magnification images equal 50 µm. (**D**) Quantification of positive DAB signal in sections stained for αSMA. (**E**) Levels of active and total TGF-β in tumor lysates of MC38 tumors (n=4-5/group), treated intratumorally with PBS or Reo (3x 10^7 plaque-forming units) and harvested after 5 days. (**F**) Relative expression of TGF-β target genes in PBS- or Reo-treated MC38 tumors (n=4-5/group), as determined by RT-qPCR. (**G**) Representative images obtained from immunohistochemical staining of PBS- or Reo-treated MC38 tumors (n=3-5/group) for αSMA. Scale bars of magnification images equal 50 µm. (**H**) Quantification of positive DAB signal in sections stained for αSMA. Data represent mean±SEM. Significance between PBS and Reo in (A, B), (D, E), and (H) was determined using unpaired t-tests. Significance levels: *p<0.05, **p<0.01 and ***p<0.001.

TGF-β blockade diminishes the efficacy of Reo&CD3-bsAb therapy in the pancreatic KPC3.TRP1 tumor model

We first employed the KPC3 tumor model to test our hypothesis that TGF-β blockade could improve the antitumor efficacy of Reo&CD3-bsAbs therapy. Immunocompetent mice were engrafted with a KPC3 tumor expressing tyrosine related protein 1 (TRP1) as a model antigen to be targeted by CD3-bsAbs (**Figure 5A**). As previously reported (8), Reo&CD3-bsAbs therapy induced steep regressions (**Figure 5B, C**), followed by tumor escape. Unexpectedly, however, TGF-β blockade did not improve Reo&CD3-bsAb therapy but abrogated its antitumor efficacy. Tumors of mice that received Reo&CD3-bsAbs as well as TGF-β blockade did not regress in size after receiving CD3-bsAbs but displayed similar tumor growth as observed in mice treated with TGF-β blockade alone (**Figure 5C, D**). Ultimately, Reo&CD3-bsAbs + αTGF-β treated mice did have significantly better survival compared to untreated mice, but their survival was significantly worse compared to mice that received Reo&CD3-bsAbs without TGF-β inhibition (**Figure 5E**).

The impaired efficacy of Reo&CD3-bsAbs, when combined with TGF-β blockade, could not be attributed to a lower presence of T cells, since tumors that received this triple combination therapy did not demonstrate lower intratumoral T-cell frequencies compared to the group that received Reo&CD3-bsAbs without αTGF-β (**Figure S4A**). Instead, there was a trend towards a higher T-cell presence in tumors after TGF-β blockade and Reo&CD3-bsAb therapy compared to the group that only received Reo&CD3-bsAb therapy, mimicking the increased T-cell influx after TGF-β blockade that was observed in MC38 tumors (**Figure 3H**). Expression levels of various T-cell activation markers were also similar between both groups (**Figure S4B**). Histological analysis confirmed that tumors of the Reo&CD3-bsAbs + αTGF-β group contained a high number of $CD3^+$ T cells that were spread throughout the whole tumor (**Figure S4C, D**). These data indicate that TGF-β inhibition did not impair the reovirus-induced quantity or location of effector T-cells in these end-stage KPC3.TRP1 tumors.

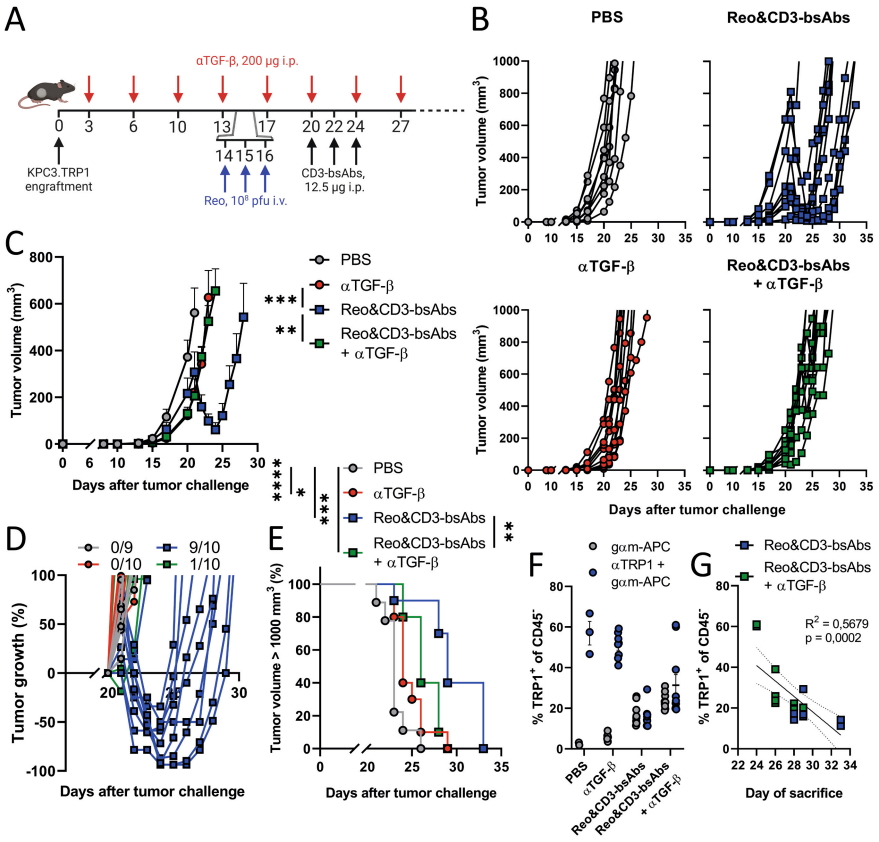


Figure 5. TGF-β blockade diminishes the efficacy of Reo&CD3-bsAb therapy in the KPC3.TRP1 tumor model. (**A**) Overview of the experiment described in (B-G). Mice (n=9-10/group) were subcutaneously engrafted with KPC3.TRP1 cells (1x10^5/mouse) and received TGF-β-neutralizing antibodies (αTGF-β, 200 µg/injection every 3 days) starting directly after tumor engraftment. Mice received Reo intravenously on days 14, 15, and 16 (10^8 plaque-forming units/injection) and received CD3-bsAbs intraperitoneally (12.5 µg/injection) on days 20, 22, and 24. Tumor growth was measured 3-5x/week. (**B**) Individual tumor growth curves of mice receiving indicated treatments. (**C**) Average tumor growth curves of mice receiving indicated treatments. One non-responding mouse in the Reo&CD3-bsAbs group is excluded for clarity (see also (B)). Significant differences in average tumor growth were calculated on day 23. (**D**) Relative changes in tumor volume of individual mice, calculated from the start of CD3-bsAb treatment. Indicated is the number of mice with tumor regressions in each group. (**E**) Kaplan-Meier survival graphs of mice after indicated treatments. (**F**) Quantification of TRP1 expression on CD45$^-$ cells within the end stage KPC3.TRP1 tumors after indicated therapies. Grey values indicate corresponding background staining of secondary goat-anti-mouse antibody only. (**G**) Correlation between TRP1 expression in tumors and the day of sacrifice. Data represent mean±SEM. Significance in (C) was determined using an ordinary one-way ANOVA with Tukey's multiple comparisons test. Log-rank tests were used to compare differences in survival in (E). Significance levels: *p<0.05, **p<0.01, ***p<0.001 and ****p<0.0001.

Since the impaired response to Reo&CD3-bsAb therapy after TGF-β blockade could not be attributed to a lower frequency of T cells, we next investigated whether an impaired quality of T cells might explain this effect. $CD8^+$ T cells are the main effector cells that infiltrate into the tumor after reovirus administration and are employed by CD3-bsAbs (27). *In vitro* experiments showed that the CD3-bsAb-induced cytotoxic efficacy of naive $CD8^+$ T cells was not impaired when TGF-β was added or neutralized (**Figure S5A**). Similarly, T cells of CD8 TβRII KO mice that selectively lacked TGF-β signaling in their $CD8^+$ T cells demonstrated similar cytotoxic capacity as TβRII wild-type (WT) T cells (**Figure S5B**). To confirm this *in vivo*, TβRII WT or CD8 TβRII KO mice were inoculated with KPC3.TRP1 tumor cells and received Reo&CD3-bsAb therapy as described earlier (**Figure S5C**). Interestingly, the efficacy of Reo&CD3-bsAb therapy was similar in TβRII WT and CD8 TβRII KO mice, while again Reo&CD3-bsAb + αTGF-β therapy demonstrated decreased antitumor effects and survival (**Figure S5D, E**).

Further flow cytometry analysis of end-stage tumors that received Reo&CD3-bsAbs as well as TGF-β blockade confirmed that TGF-β did not affect T-cell function. Tumors of mice that received Reo&CD3-bsAbs + αTGF-β demonstrated loss of TRP1 expression in the majority of $CD45^-$ cells, similar to tumors of mice treated with Reo&CD3-bsAb (**Figure 5F**), a phenomenon previously described in mice with successful tumor regressions upon Reo&CD3-bsAb treatment (8). Indeed, TRP1 expression in these groups negatively correlated with survival time until the experimental endpoint (**Figure 5G**), indicating that the best clinical response was correlated with the highest loss of TRP1 expression. Importantly, αTGF-β alone did not decrease the number of TRP1-expressing $CD45^-$ cells, indicating that the decreased frequency of TRP1-expressing cells after Reo&CD3-bsAb + αTGF-β was due to active attack and T-cell mediated killing of TRP1-expressing cells, and not because TGF-β blockade simply decreases TRP1 expression. Altogether, these data indicate TGF-β blockade impairs the efficacy of Reo&CD3-bsAb therapy in the KPC3 tumor model, even though the intratumoral T-cell frequency and their cytotoxic capacity were not negatively affected by TGF-β signaling inhibition.

TGF-β blockade significantly enhances the efficacy of Reo&CD3-bsAb therapy in the MC38.TRP1 model of colon cancer

We next investigated whether TGF-β blockade could improve the efficacy of Reo&CD3-bsAb therapy in the MC38 tumor model, which also displays high TGF-β signaling. Since MC38 tumor cells do not naturally express tumor antigen TRP1, we transfected MC38 cells with a plasmid encoding TRP1 and sorted $TRP1^+$ cells (**Figure S6A, B**), similar to what was previously done for KPC3. Hereafter, MC38.TRP1 cells were susceptible to T-cell mediated killing in the presence of CD3-bsAbs in an *in vitro* setting (**Figure S6C**), so we continued investigating whether TGF-β inhibition would improve the antitumor efficacy Reo&CD3-bsAb therapy in mice bearing MC38.TRP1 tumors (**Figure 6A**).

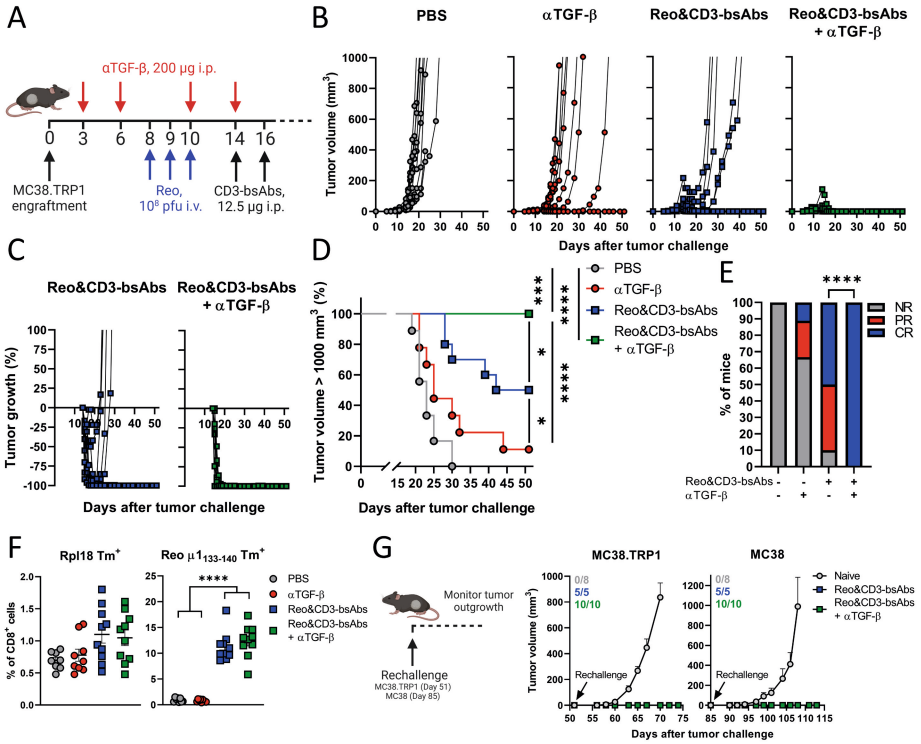


Figure 6. TGF-β blockade significantly enhances the efficacy of Reo&CD3-bsAb therapy in the MC38.TRP1 model of colon cancer. (**A**) Overview of the experiment described in (B-H). Mice (n=9-10/group) were subcutaneously engrafted with MC38.TRP1 cells (5x10^5/mouse) and received TGF-β-neutralizing antibodies (αTGF-β, 200 μg/injection every 3 days) starting directly after tumor engraftment. Mice received Reo (intravenously, 10^8 plaque-forming units/injection) and CD3-bsAbs (intraperitoneally, 200 μg/injection) on days 14 and 16. Tumor growth was measured 3x/week. (**B**) Individual tumor growth curves of mice receiving indicated treatments. (**C**) Relative changes in tumor volume of individual mice from the start of CD3-bsAb treatment. (**D**) Kaplan-Meier survival graphs of mice after indicated treatments. (**E**) Frequency of Non-Responders (NR), Partial Responders (PR; tumor regression/stagnation for more than 7 days), or Complete Responders (CR) within indicated treatment groups. (**F**) Frequency of Rpl18$^+$ and Reo μ1$_{133\text{-}140}$ CD8$^+$ T cells in the blood of mice after indicated treatments. (**G**) Rechallenge experiment. All CR mice from (D) were subcutaneously engrafted with MC38.(TRP1) tumor cells (5x10^5/mouse) in the alternate flank on day 51 (MC38.TRP1) or day 85 (MC38) and tumor outgrowth was measured 3x/week. Indicated is the number of mice within each group that rejected the rechallenge. Data represent mean±SEM. Log-rank tests were used to compare differences in survival in (D). A chi-square test was used to determine statistical differences in response in (E). Significance between groups in (F) was determined using an ordinary one-way ANOVA with Tukey's multiple comparisons test. Significance levels: *p<0.05, **p<0.01, ***p<0.001 and ****p<0.0001.

TGF-β blockade alone already delayed the outgrowth of MC38 tumors and induced complete tumor clearance in 1 out of 9 animals (=11.1%) (**Figure 6B**). In this model, Reo&CD3-bsAb therapy led to durable responses with complete tumor clearance in 50% of the animals (**Figure 6B**). Most interestingly, however, was the observation that here the efficacy of Reo&CD3-bsAb therapy was significantly improved by TGF-β inhibition. TGF-β inhibition combined with Reo&CD3-bsAb therapy led to very rapid tumor clearance in 100% of animals and significantly enhanced survival (**Figure 6C-E**). This increase in therapeutic efficacy could not be attributed to an increased presence of tumor-specific (Rpl18 Tm^+) or reovirus-specific ($\mu1_{133\text{-}140}$ Tm^+) $CD8^+$ T cells in the circulation, since their frequencies were similar between the group that received Reo&CD3-bsAb therapy and the group that received additional αTGF-β therapy (**Figure 6F**).

Since 50% of mice that received Reo&CD3-bsAb therapy and 100% of mice that received Reo&CD3-bsAb therapy in combination with αTGF-β completely cleared their tumor, we wondered whether tumor-specific immunologic memory was established. All mice that cleared the first tumor received a rechallenge at the alternate flank with MC38. TRP1 tumor cells, which was rejected (**Figure 6G**). Similarly, a third rechallenge with the parental MC38 cell line was also rejected, suggesting the establishment of an effective antitumor memory immune response. Combined, these data indicate that Reo&CD3-bsAb therapy alone is already effective in clearing MC38 tumors and establishing antitumor immunity, but the addition of αTGF-β significantly increases the primary antitumor response.

Altogether, we demonstrated that the addition of TGF-β blockade has the potential to improve the efficacy of Reo&CD3-bsAb therapy, but this benefit depends on the tumor model used. Although both KPC3 and MC38 tumors display active TGF-β signaling, the therapeutic efficacy of Reo&CD3-bsAbs was only drastically improved when TGF-β signaling was inhibited in MC38 tumors and not in KPC3 tumors. This differential effect of TGF-β blockade during Reo&CD3-bsAb combination therapy was associated with a different effect of Reo on TGF-β signaling in these tumors. Further understanding of inter-tumor differences that might contribute to this differential effect of TGF-β blockade is essential to improve, and not impair, the efficacy of viro-immunotherapeutic strategies.

DISCUSSION

In this study, we demonstrated that the combination therapy of reovirus and CD3-bispecific antibodies (Reo&CD3-bsAbs) can be significantly improved by additional neutralization of TGF-β. However, the added benefit of TGF-β blockade is model-dependent. Our data indicate that inhibition of TGF-β signaling might be a promising

strategy to enhance the efficacy of viro-immunotherapeutic strategies, but inter-tumor differences might also result in the diminishing of their efficacy after TGF-β blockade. TGF-β is mostly recognized as a tumor-promoting cytokine by inducing cancer cell migration and invasion (33,34) and as an immunosuppressive factor by inhibiting the generation and effector function of $CD4^+$ and $CD8^+$ effector T cells (17). The tumor-promoting and immunoinhibitory characteristics of TGF-β make it an attractive target for therapeutic intervention to enhance the efficacy of (viro-)immunotherapeutic strategies.

In preclinical research, 1D11 is a well-known antibody that prevents the binding of TGF-β isoforms to TGF-b receptors (31). TGF-β blockade using 1D11 only induced suppression of tumor growth when TGF-β blockade was initiated directly after tumor challenge (early intervention), and not when αTGF-β treatment was initiated when tumors were already established (late intervention). Similar observations were made in an MDA-MB-231 model of bone metastasis, where the reduced tumor burden in the bones after TGF-β inhibition was much more pronounced when TGF-β blockade was administered directly after tumor inoculation, compared to administration when metastases in the bones were already established (35). Additionally, treatment of established, orthotopic MDA-MB-231 tumors with 1D11 did not impact tumor growth, while stable overexpression of a soluble TGF-βRII (i.e. continued neutralization of TGF-β) almost completely blocked the growth of the same tumor (36). For KPC3 tumors, the impaired tumor growth suppression after early TGF-β blockade was not immune-mediated and could not be associated with impaired proliferation, but was associated with decreased intratumoral collagen disposition, as has also been observed in the murine mammary carcinoma 4T1 model and the human mammary carcinoma MDA-MB-231 model (36,37). These combined observations suggest that the TGF-β blockade-induced delay in tumor growth might be a result of microenvironmental changes, rather than a direct effect on tumor cells.

In our studies, we observed that TGF-β inhibition using 1D11 did not improve the efficacy of Reo&CD3-bsAb therapy in the murine pancreatic KPC3 model, but did significantly enhance the number of responders and overall survival in the murine colon MC38 model. A similar contrast was observed in a study where TGF-β inhibition enhanced the efficacy of checkpoint blockade in the MC38 tumor model but was unable to do so in a model for murine pancreatic cancer (23). The divergent effects of TGF-β blockade have also been observed in a panel of 12 models for metastatic breast cancer, where TGF-β using 1D11 suppressed the formation of lung metastasis in 42% of the models, did not induce a response in 33% of the models and induced an increase in lung metastasis in 25% of the models (38). An understanding of the factors underlying this dichotomy would be a first step towards predicting which individuals would most likely benefit from TGF-β neutralization in addition to viro-immunotherapy.

First, we took a closer look at the composition of the TME in both tumors. One big difference between the tumor models used is the immunogenicity and the related baseline frequency of tumor-infiltrated immune cells. The chemically-induced MC38 tumor model is more immunogenic compared to the genetically-induced KPC3 tumor model. Higher immunogenicity is associated with higher therapeutic efficacy of TGF-β inhibition, as was observed in a study where TGF-β inhibition using kinase inhibitor galunisertib resulted in stronger $CD8^+$ T-cell dependent control of tumor growth of immunogenic 4T1-Luciferase breast tumors, compared to poorly immunogenic 4T1 parental tumors (39). Similarly, TGF-β blockade in multiple squamous cell carcinoma (SCC) models using the pan-TGF-β neutralizing antibody was most effective in SCC tumors with the highest mutational loads (19). Immunogenic MC38 tumors already contain more T cells at baseline compared to poorly immunogenic KPC3 tumors, and TGF-β inhibition was able to further enhance the reovirus-induced influx of T cells in MC38 tumors. Interestingly, previous studies indicated that the main mechanism of action of TGF-β blockade to improve the efficacy of checkpoint blockade is by increasing T-cell infiltration into the tumor (21,40). Our data suggest that this might also be valid for other immunotherapeutic strategies, including Reo&CD3-bsAb therapy.

Another difference between the TME of both tumor models is the abundance of stroma in KPC3 tumors, which is absent in MC38 tumors. The tumor stroma consists, amongst other components, of fibroblasts, matrix proteins, and the vasculature (41). The importance of tumor stroma for the development, promotion, and invasion of cancer has become increasingly clear. In particular, cancer-associated fibroblasts can stimulate the growth, invasion, angiogenesis, and metastasis of tumors (42). As such, various stroma-related factors, such as an abundance of αSMA^+ fibroblasts and high expression of fibroblast activation protein (FAP), are associated with aggressive disease progression, recurrence, and therapy resistance in pancreatic and colorectal cancer (43-46). Matrix proteins such as type I collagens can promote the proliferation and invasiveness of tumor cells (47,48). High collagen content and cross-linking also contribute to tumor stiffness and drive metastatic growth (49). Interestingly, collagen can also decrease responses to immunotherapy by acting as a physical barrier to immune cell infiltration, as well as delivering inhibitory signals to immune cells such as T and NK cells by binding to the leukocyte-associated immunoglobulin-like receptor-1 (LAIR-1) (50). Although TGF-β inhibition was able to decrease αSMA^+ fibroblast and collagen content in KPC3 tumors, this decrease might not have been sufficient to enhance the efficacy of Reo&CD3-bsAb therapy similarly as was observed in MC38 tumors where the stromal compartment is mostly absent.

Additionally, besides the difference in T-cell infiltration or stromal composition, tumor-intrinsic differences might explain the differential effects of TGF-β inhibition on therapy outcome. Both KPC3 and MC38 tumor models used in this study display active signaling of TGF-β. Canonical TGF-β signaling involves the formation of a heterooligomer complex comprising Smad4 and other Smad proteins, that travels to the nucleus to induce

expression of TGF-β target genes (51). Alternatively, TGF-β signaling can also occur non-canonically, in a Smad4-independent manner. While canonical TGF-β signaling is involved in both tumor-promoting and tumor-suppressive pathways, non-canonical TGF-β signaling especially activates tumor-promoting pathways that facilitate EMT and cell migration, such as the RAS/RAF/MEK/ERK pathway. Interestingly, unlike KPC3, MC38 cells do not display Smad4-dependent signaling, even though Smad2 is phosphorylated (52). This lack of Smad4 expression results in enhanced tumorigenicity and metastatic potential, which could be reduced when Smad4 was introduced in these cells (52). Thus, Smad4 loss might result in the uncoupling of the TGF-β-mediated growth-suppressive function from its pro-oncogenic effects (53), which might explain why especially in the MC38 model TGF-β inhibition was very effective. Indeed, ablation of Smad4 expression in murine pancreatic 6694c2 tumors enhanced T-cell influx and improved the response to chemo-immunotherapy (54). Since both canonical and non-canonical TGF-β signaling pathways are intact in the KPC3 model, TGF-β inhibition might not only lead to the inhibition of its tumor-promoting pathways but also some of its tumor-suppressive aspects. This is eloquently demonstrated in the murine pancreatic BMFA3 tumor model, where treatment with an anti-TGFβR2 antibody significantly slowed the growth of *Tgfbr2*-mutant tumors but increased the growth of *Tgfbr*^{wt} tumors (55).

Another difference that we found between both models was the contrasting effect of Reo on TGF-β signaling. We observed that Reo administration leads to a further elevated presence of TGF-β in KPC3 tumors, which was accompanied by an increased expression of various TGF-β target genes and αSMA^{+} fibroblasts. An increase in TGF-β production after Reo administration has also been observed in other tumor models, as well as after other OV infections (56-59). In contrast, Reo administration led to decreased TGF-β signaling in MC38 tumors. This may imply that in KPC3 tumors blockade of TGF-β signaling is overruled by reovirus administration, while in MC38 tumors TGF-β blockade works synergistically with the Reo-induced decrease in TGF-β signaling and thereby results in significantly improved antitumor responses in these tumors. However, these opposite effects of Reo administration on TGF-β production and the expression of TGF-β target genes may not necessarily involve the canonical TGF-β signaling pathway, since MC38 tumor cells lack Smad4-mediated responses and the expression of many TGF-β target genes can also be induced or inhibited by other pathways.

In conclusion, we demonstrated that TGF-β blockade can differentially affect the efficacy of Reo&CD3-bsAb therapy in different preclinical tumor models, even if both models display active TGF-β signaling at baseline. These opposite effects might be attributed to the baseline T-cell density, immunogenicity, stromal composition, genetic factors including Smad4 deficiency, the effect of TGF-β blockade on the reovirus-induced T-cell influx into the tumor, or the effect of reovirus administration on TGF-β signaling. Further understanding of these inter-model differences that dictate whether TGF-β blockade promotes or impairs viro-immunotherapy is needed to guide further therapeutic developments. Since both oncolytic virus-based immunotherapeutic strategies (60),

as well as several therapeutic approaches to inhibit TGF-β signaling (51), are in clinical development, the implications of this research may be valuable for clinical practice.

DECLARATIONS

Acknowledgments. The authors are grateful to Prof. Stefan Karlsson (Lund University Hospital, Sweden) for the TβRII floxed mice. The authors appreciate the technical assistance from Stef G. T. Janson regarding the Western Blotting and Eveline S. M. de Jonge-Muller regarding the immunohistochemistry stainings, as well as Gaby Schaap and Jim Middelburg for their assistance with generating the MC38.TRP1 cell line. The authors gratefully acknowledge the operators of the Flow cytometry Core Facility (FCF) of the LUMC and the Animal Facility of the LUMC for their excellent support and care of the animals, respectively. All figures regarding experimental designs are created with BioRender.com.

Author contributions. Conceptualization, C.G., L.J.A.C.H., T.v.H., N.v.M.; Methodology, C.G., J.Q.v.G., P.K., M.S., L.G., C.L., D.v.d.W, R.H., L.J.A.C.H., T.v.H., N.v.M.; Formal analysis, C.G.; Investigation, C.G., J.Q.v.G., P.K.; Resources, D.v.d.W., R.H., M.S., L.J.A.C.H., P.t.D.; Writing – Original Draft, C.G., N.v.M.; Writing - Review & Editing, C.G., P.t.D., L.J.A.C.H., S.H.v.d.B., T.v.H, N.v.M.; Visualization, C.G.; Supervision, N.v.M.; Funding acquisition, S.H.v.d.B., T.v.H., N.v.M.. All authors approved the final version of the manuscript.

Funding. This work was financially supported by the Dutch Cancer Society Bas Mulder Award 11056 (to NvM), a PhD fellowship from Leiden University Medical Center (to CG), and the Support Casper campaign by the Dutch foundation 'Stichting Overleven met Alvleesklierkanker' (supportcasper.nl) project number SOAK 17.04 (to SHvdB, TvH, and NvM). RCH received funding for the work on oncolytic reoviruses from the Dutch Research Council (NWO)/STW Biotechnology and Safety program for the project 'Environmental safety evaluation of host range-modified oncolytic viruses' (project number 15414). PtD received funding from the Cancer Genomics Centre Netherlands (CGC.nl) through the NWO 'Zwaartekracht' program. Authors CG, JQvG, MS, LG, CL, SHvdB, PtD, and TvH are affiliated with Oncode Institute, an independent institute dedicated to understanding cancer and translating research into practice. Oncode Institute receives funding from the Dutch Cancer Society and ZonMw.

Conflicts of Interest. The authors declare no conflict of interest. The funders had no role in the design of the study; in the collection, analyses, or interpretation of data; in the writing of the manuscript, or in the decision to publish the results.

Data Availability. The data generated in this study are available upon reasonable request from the corresponding author.

REFERENCES

1. Groeneveldt C, van Hall T, van der Burg SH, Ten Dijke P, van Montfoort N. Immunotherapeutic Potential of TGF-β Inhibition and Oncolytic Viruses. Trends Immunol **2020**;41:406-20
2. Mahalingam D, Goel S, Aparo S, Patel Arora S, Noronha N, Tran H*, et al.* A Phase II Study of Pelareorep (REOLYSIN(®)) in Combination with Gemcitabine for Patients with Advanced Pancreatic Adenocarcinoma. Cancers (Basel) **2018**;10:160
3. Sborov DW, Nuovo GJ, Stiff A, Mace T, Lesinski GB, Benson DM*, et al.* A Phase I Trial of Single-Agent Reolysin in Patients with Relapsed Multiple Myeloma. Clinical Cancer Research **2014**;20:5946-55
4. Phillips MB, Stuart JD, Rodríguez Stewart RM, Berry JT, Mainou BA, Boehme KW. Current understanding of reovirus oncolysis mechanisms. Oncolytic Virother **2018**;7:53-63
5. Zhao X, Chester C, Rajasekaran N, He Z, Kohrt HE. Strategic Combinations: The Future of Oncolytic Virotherapy with Reovirus. Molecular cancer therapeutics **2016**;15:767-73
6. Kicielinski KP, Chiocca EA, Yu JS, Gill GM, Coffey M, Markert JM. Phase 1 clinical trial of intratumoral reovirus infusion for the treatment of recurrent malignant gliomas in adults. Mol Ther **2014**;22:1056-62
7. Müller L, Berkeley R, Barr T, Ilett E, Errington-Mais F. Past, Present and Future of Oncolytic Reovirus. Cancers **2020**;12:3219
8. Groeneveldt C, Kinderman P, van den Wollenberg DJM, van den Oever RL, Middelburg J, Mustafa DAM*, et al.* Preconditioning of the tumor microenvironment with oncolytic reovirus converts CD3-bispecific antibody treatment into effective immunotherapy. J Immunother Cancer **2020**;8:e001191
9. Samson A, Scott KJ, Taggart D, West EJ, Wilson E, Nuovo GJ*, et al.* Intravenous delivery of oncolytic reovirus to brain tumor patients immunologically primes for subsequent checkpoint blockade. Sci Transl Med **2018**;10:eaam7577
10. Kortekaas KE, Santegoets SJ, Abdulrahman Z, van Ham VJ, van der Tol M, Ehsan I*, et al.* High numbers of activated helper T cells are associated with better clinical outcome in early stage vulvar cancer, irrespective of HPV or p53 status. Journal for ImmunoTherapy of Cancer **2019**;7:236
11. Galon J, Bruni D. Approaches to treat immune hot, altered and cold tumours with combination immunotherapies. Nature Reviews Drug Discovery **2019**;18:197-218
12. Soleimani A, Pashirzad M, Avan A, Ferns GA, Khazaei M, Hassanian SM. Role of the transforming growth factor-β signaling pathway in the pathogenesis of colorectal cancer. Journal of Cellular Biochemistry **2019**;120:8899-907
13. Shen W, Tao GQ, Zhang Y, Cai B, Sun J, Tian ZQ. TGF-beta in pancreatic cancer initiation and progression: two sides of the same coin. Cell & Bioscience **2017**;7:39
14. Chae YK, Chang S, Ko T, Anker J, Agte S, Iams W*, et al.* Epithelial-mesenchymal transition (EMT) signature is inversely associated with T-cell infiltration in non-small cell lung cancer (NSCLC). Scientific reports **2018**;8:2918
15. Ganesh K, Massagué J. TGF-β Inhibition and Immunotherapy: Checkmate. Immunity **2018**;48:626-8
16. Angioni R, Sánchez-Rodríguez R, Viola A, Molon B. TGF-β in Cancer: Metabolic Driver of the Tolerogenic Crosstalk in the Tumor Microenvironment. Cancers (Basel) **2021**;13
17. Batlle E, Massague J. Transforming Growth Factor-beta Signaling in Immunity and Cancer. Immunity **2019**;50:924-40
18. Nixon BG, Gao S, Wang X, Li MO. TGFβ control of immune responses in cancer: a holistic immuno-oncology perspective. Nature Reviews Immunology **2022**;doi.org/10.1038/s41577-022-00796-z

19. Dodagatta-Marri E, Meyer DS, Reeves MQ, Paniagua R, To MD, Binnewies M*, et al.* α-PD-1 therapy elevates Treg/Th balance and increases tumor cell pSmad3 that are both targeted by α-TGFβ antibody to promote durable rejection and immunity in squamous cell carcinomas. Journal for immunotherapy of cancer **2019**;7:10.1186/s40425-018-0493-9
20. Jiao S, Subudhi SK, Aparicio A, Ge Z, Guan B, Miura Y*, et al.* Differences in Tumor Microenvironment Dictate T Helper Lineage Polarization and Response to Immune Checkpoint Therapy. Cell **2019**;179:1177-90.e13
21. Mariathasan S, Turley SJ, Nickles D, Castiglioni A, Yuen K, Wang Y*, et al.* TGFbeta attenuates tumour response to PD-L1 blockade by contributing to exclusion of T cells. Nature **2018**;554:544-8
22. Vanpouille-Box C, Diamond JM, Pilones KA, Zavadil J, Babb JS, Formenti SC*, et al.* TGFbeta Is a Master Regulator of Radiation Therapy-Induced Antitumor Immunity. Cancer Res **2015**;75:2232-42
23. Sow HS, Ren J, Camps M, Ossendorp F, ten Dijke P. Combined Inhibition of TGF-β Signaling and the PD-L1 Immune Checkpoint Is Differentially Effective in Tumor Models. Cells **2019**;8
24. Terabe M, Robertson FC, Clark K, De Ravin E, Bloom A, Venzon DJ*, et al.* Blockade of only TGF-beta 1 and 2 is sufficient to enhance the efficacy of vaccine and PD-1 checkpoint blockade immunotherapy. Oncoimmunology **2017**;6:e1308616
25. van den Wollenberg DJM, Dautzenberg IJC, van den Hengel SK, Cramer SJ, de Groot RJ, Hoeben RC. Isolation of reovirus T3D mutants capable of infecting human tumor cells independent of junction adhesion molecule-A. PLoS One **2012**;7:e48064-e
26. Hingorani SR, Wang L, Multani AS, Combs C, Deramaudt TB, Hruban RH*, et al.* Trp53R172H and KrasG12D cooperate to promote chromosomal instability and widely metastatic pancreatic ductal adenocarcinoma in mice. Cancer cell **2005**;7:469-83
27. Benonisson H, Altıntaş I, Sluijter M, Verploegen S, Labrijn AF, Schuurhuis DH*, et al.* CD3-Bispecific Antibody Therapy Turns Solid Tumors into Inflammatory Sites but Does Not Install Protective Memory. Molecular cancer therapeutics **2019**;18:312-22
28. Levéen P, Larsson J, Ehinger M, Cilio CM, Sundler M, Sjöstrand LJ*, et al.* Induced disruption of the transforming growth factor beta type II receptor gene in mice causes a lethal inflammatory disorder that is transplantable. Blood **2002**;100:560-8
29. Mijatovic-Rustempasic S, Tam KI, Kerin TK, Lewis JM, Gautam R, Quaye O*, et al.* Sensitive and specific quantitative detection of rotavirus A by one-step real-time reverse transcription-PCR assay without antecedent double-stranded-RNA denaturation. Journal of clinical microbiology **2013**;51:3047-54
30. Dupont WD, Plummer WD, Jr. Power and sample size calculations. A review and computer program. Controlled clinical trials **1990**;11:116-28
31. Bedinger D, Lao L, Khan S, Lee S, Takeuchi T, Mirza AM. Development and characterization of human monoclonal antibodies that neutralize multiple TGFβ isoforms. MAbs **2016**;8:389-404
32. Hata S, Okamura K, Hatta M, Ishikawa H, Yamazaki J. Proteolytic and Non-proteolytic Activation of Keratinocyte-Derived Latent TGF-β1 Induces Fibroblast Differentiation in a Wound-Healing Model Using Rat Skin. Journal of Pharmacological Sciences **2014**;124:230-43
33. Massague J. TGFbeta in Cancer. Cell **2008**;134:215-30
34. Connolly EC, Freimuth J, Akhurst RJ. Complexities of TGF-beta targeted cancer therapy. Int J Biol Sci **2012**;8:964-78
35. Biswas S, Nyman JS, Alvarez J, Chakrabarti A, Ayres A, Sterling J*, et al.* Anti-transforming growth factor ß antibody treatment rescues bone loss and prevents breast cancer metastasis to bone. PloS one **2011**;6:e27090-e
36. Liu J, Liao S, Diop-Frimpong B, Chen W, Goel S, Naxerova K*, et al.* TGF-β blockade improves the distribution and efficacy of therapeutics in breast carcinoma by normalizing the tumor stroma. Proc Natl Acad Sci U S A **2012**;109:16618-23

37. Grauel AL, Nguyen B, Ruddy D, Laszewski T, Schwartz S, Chang J, *et al.* TGFβ-blockade uncovers stromal plasticity in tumors by revealing the existence of a subset of interferon-licensed fibroblasts. Nature Communications **2020**;11:6315
38. Yang Y, Yang HH, Tang B, Wu AML, Flanders KC, Moshkovich N, *et al.* The Outcome of TGFβ Antagonism in Metastatic Breast Cancer Models In Vivo Reflects a Complex Balance between Tumor-Suppressive and Proprogression Activities of TGFβ. Clinical Cancer Research **2020**;26:643-56
39. Holmgaard RB, Schaer DA, Li Y, Castaneda SP, Murphy MY, Xu X, *et al.* Targeting the TGFbeta pathway with galunisertib, a TGFbetaRI small molecule inhibitor, promotes anti-tumor immunity leading to durable, complete responses, as monotherapy and in combination with checkpoint blockade. J Immunother Cancer **2018**;6:47
40. Tauriello DVF, Palomo-Ponce S, Stork D, Berenguer-Llergo A, Badia-Ramentol J, Iglesias M, *et al.* TGFbeta drives immune evasion in genetically reconstituted colon cancer metastasis. Nature **2018**;554:538-43
41. Bremnes RM, Dønnem T, Al-Saad S, Al-Shibli K, Andersen S, Sirera R, *et al.* The Role of Tumor Stroma in Cancer Progression and Prognosis: Emphasis on Carcinoma-Associated Fibroblasts and Non-small Cell Lung Cancer. Journal of Thoracic Oncology **2011**;6:209-17
42. Joshi RS, Kanugula SS, Sudhir S, Pereira MP, Jain S, Aghi MK. The Role of Cancer-Associated Fibroblasts in Tumor Progression. Cancers (Basel) **2021**;13
43. Sinn M, Denkert C, Striefler JK, Pelzer U, Stieler JM, Bahra M, *et al.* α-Smooth muscle actin expression and desmoplastic stromal reaction in pancreatic cancer: results from the CONKO-001 study. British Journal of Cancer **2014**;111:1917-23
44. Vathiotis IA, Moutafi MK, Divakar P, Aung TN, Qing T, Fernandez A, *et al.* Alpha-smooth Muscle Actin Expression in the Stroma Predicts Resistance to Trastuzumab in Patients with Early-stage HER2-positive Breast Cancer. Clin Cancer Res **2021**;27:6156-63
45. Kawase T, Yasui Y, Nishina S, Hara Y, Yanatori I, Tomiyama Y, *et al.* Fibroblast activation protein-α-expressing fibroblasts promote the progression of pancreatic ductal adenocarcinoma. BMC gastroenterology **2015**;15:109
46. Coto-Llerena M, Ercan C, Kancherla V, Taha-Mehlitz S, Eppenberger-Castori S, Soysal SD, *et al.* High Expression of FAP in Colorectal Cancer Is Associated With Angiogenesis and Immunoregulation Processes. Front Immunol **2020**;10
47. Nissen NI, Karsdal M, Willumsen N. Collagens and Cancer associated fibroblasts in the reactive stroma and its relation to Cancer biology. Journal of experimental & clinical cancer research : CR **2019**;38:115
48. Northcott JM, Dean IS, Mouw JK, Weaver VM. Feeling Stress: The Mechanics of Cancer Progression and Aggression. Frontiers in cell and developmental biology **2018**;6:17
49. Cox TR, Bird D, Baker AM, Barker HE, Ho MW, Lang G, *et al.* LOX-mediated collagen crosslinking is responsible for fibrosis-enhanced metastasis. Cancer Res **2013**;73:1721-32
50. Horn LA, Chariou PL, Gameiro SR, Qin H, Iida M, Fousek K, *et al.* Remodeling the tumor microenvironment via blockade of LAIR-1 and TGF-β signaling enables PD-L1–mediated tumor eradication. The Journal of Clinical Investigation **2022**;132
51. Principe DR, Timbers KE, Atia LG, Koch RM, Rana A. TGFβ Signaling in the Pancreatic Tumor Microenvironment. Cancers **2021**;13:5086
52. Zhang B, Halder SK, Kashikar ND, Cho YJ, Datta A, Gorden DL, *et al.* Antimetastatic role of Smad4 signaling in colorectal cancer. Gastroenterology **2010**;138:969-80.e1-3
53. Subramanian G, Schwarz RE, Higgins L, McEnroe G, Chakravarty S, Dugar S, *et al.* Targeting Endogenous Transforming Growth Factor β Receptor Signaling in SMAD4-Deficient Human Pancreatic Carcinoma Cells Inhibits Their Invasive Phenotype. Cancer Research **2004**;64:5200-11
54. Li J, Yuan S, Norgard RJ, Yan F, Sun YH, Kim I-K, *et al.* Epigenetic and Transcriptional Control of the Epidermal Growth Factor Receptor Regulates the Tumor Immune Microenvironment in Pancreatic Cancer. Cancer Discovery **2021**;11:736-53

55. Huang H, Zhang Y, Gallegos V, Sorrelle N, Zaid MM, Toombs J*, et al.* Targeting TGFβR2-mutant tumors exposes vulnerabilities to stromal TGFβ blockade in pancreatic cancer. EMBO Mol Med **2019**;11:e10515
56. Clements DR, Sterea AM, Kim Y, Helson E, Dean CA, Nunokawa A*, et al.* Newly Recruited CD11b+, GR-1+, Ly6Chigh Myeloid Cells Augment Tumor-Associated Immunosuppression Immediately following the Therapeutic Administration of Oncolytic Reovirus. J Immunol **2015**;194:4397-412
57. Beckham JD, Tuttle K, Tyler KL. Reovirus activates transforming growth factor beta and bone morphogenetic protein signaling pathways in the central nervous system that contribute to neuronal survival following infection. J Virol **2009**;83:5035-45
58. Stanifer ML, Rippert A, Kazakov A, Willemsen J, Bucher D, Bender S*, et al.* Reovirus intermediate subviral particles constitute a strategy to infect intestinal epithelial cells by exploiting TGF-β dependent pro-survival signaling. Cellular Microbiology **2016**;18:1831-45
59. Guo L, Smith JA, Abelson M, Vlasova-St Louis I, Schiff LA, Bohjanen PR. Reovirus infection induces stabilization and up-regulation of cellular transcripts that encode regulators of TGF-β signaling. PloS one **2018**;13:e0204622-e
60. Macedo N, Miller DM, Haq R, Kaufman HL. Clinical landscape of oncolytic virus research in 2020. Journal for ImmunoTherapy of Cancer **2020**;8:e001486
61. Schneider CA, Rasband WS, Eliceiri KW. NIH Image to ImageJ: 25 years of image analysis. Nature Methods **2012**;9:671-5
62. Hawinkels LJ, Paauwe M, Verspaget HW, Wiercinska E, van der Zon JM, van der Ploeg K*, et al.* Interaction with colon cancer cells hyperactivates TGF-β signaling in cancer-associated fibroblasts. Oncogene **2014**;33:97-107

SUPPLEMENTARY METHODS

Immunohistochemistry

Formalin-fixed tumor pieces were embedded in paraffin and then sectioned randomly at 4 µm and placed on Superfrost® Plus slides (VWR). Sections were dried overnight at 37 °C and stored at 4 °C until staining. Slides were deparaffinized and endogenous peroxidase was blocked with 0,3% hydrogen peroxidase (VWR) in methanol for 20 minutes. After rehydration, antigen retrieval was performed by boiling slides for 10 minutes in 0,01M sodium citrate (pH 6) (Merck). Non-specific binding was blocked using SuperBlock™ (ThermoFisher Scientific) before overnight incubation in PBS/1% BSA in a humified box at 4 °C or RT with rabbit anti-mouse CD3ε (clone D7A6E™, 1:200; Cell Signaling Technology), rat anti-mouse CD8a (clone 4SM15, 1:1600; eBioscience™), mouse anti-mouse α-smooth muscle actin (clone 1A4/ASM-1, 1:1600/1:3200; Progen), rabbit anti-mouse phosphorylated-Smad2 (clone 138D4, 1:50; Cell Signaling Technology), rabbit anti-mouse vimentin (clone D21H3, 1:400; Cell Signaling Technology), mouse anti-mouse pan-cytokeratin (clone PCK-26, 1:400; Sigma-Aldrich) or rabbit anti-mouse Ki67 (clone SP6, 1:300, Abcam). Hereafter, samples were incubated for 30 min at RT with biotinylated goat anti-rabbit, rabbit anti-rat, or goat anti-mouse secondary antibodies (1:200; Agilent), followed by incubation with avidin-biotin complex (VECTASTAIN® Elite® ABC HRP Kit; Vector Laboratories). Peroxidase activity was detected using the 2-component liquid DAB+ system (Agilent) according to the manufacturer's instructions for 5 min. Slides were counterstained in hematoxylin (Sigma Aldrich) for 15 seconds, dehydrated, and mounted using Entellan (Sigma Aldrich). Control sections were processed in parallel, but without incubation with the primary antibody. No labeling was observed in the control sections. Collagen was stained by incubating rehydrated slides in 0.1% Sirius Red (Direct Red 80; Sigma-Aldrich) in 1.3% picric acid (Sigma-Aldrich) for 90 minutes after which slides were washed, dehydrated, and mounted as described above. αSMA, CD3, collagen, and Ki67 immunohistochemistry stainings were quantified by measuring the positive DAB or Sirius Red signal using ImageJ, and researchers analyzing the tissues were blinded to treatment groups (61).

Western Blotting

Phosphorylation of the downstream TGF-β signaling molecule Smad2 (pSmad2) in KPC3 tumor cells was analyzed by western blot as described before (62). Briefly, KPC3 cells were lysed in radioimmunoprecipitation assay (RIPA) buffer containing protease and phosphatase inhibitors using a stainless bead and the TissueLyser LT (Qiagen). Proteins (30 µg) were separated on a 10% SDS–polyacrylamide gel under reducing conditions and then transferred to a 0.45 µM PVDF membrane (Merck). After blocking for 1h at RT with 5% milk powder (Campina) in Tris-HCl-buffered saline containing 0.05% Tween-20 (TBS-T; Merck, Darmstadt, Germany), the membrane was incubated overnight at 4°C with anti-pSmad2 (Ser465/467) (clone 138D4; Cell Signaling Technology, 1:1000) or anti-β-actin (clone C4; Santa Cruz, 1:5000), followed HRP-conjugated goat anti-rabbit or anti-mouse IgG (Agilent, 1:5000) at RT for 90 minutes. After washing, proteins were

detected on the Chemidoc imaging XRS+ system (Bio-Rad) using the Clarity Western ECL Substrate kit (Bio-Rad).

TGF-β1 ELISA

Snap-frozen KPC3 or MC38 tumor pieces were lysed in radioimmunoprecipitation assay (RIPA) buffer containing protease and phosphatase inhibitors using a stain-less bead and the TissueLyser LT (Qiagen). Homogenate was centrifuged at $13x10^3$ rpm for 15 minutes at 4 °C, after which supernatants were collected and stored at −80 °C until further analysis. Active and total mTGF-β1 levels were measured by using a Mouse TGF-β1 duoset ELISA kit according to the manufacturer's instructions (R&D Systems, Minneapolis, MN, USA). Absorbance was measured using the SpectraMax iD3 multi-mode plate reader (Molecular Devices). Final values were expressed per µg protein in the tumor lysate.

CAGA-Luciferase Reporter Assay

HepG2 (RRID:CVCL_0027) is a cell line derived from a human hepatoblastoma and was obtained from ATCC (HB-8065™). $1x10^6$ HepG2 cells per well were plated into a 6-wells plate. The next days, cells were transfected with 2 µg of TGF-β/Smad inducible $(CAGA)_{12}$ luciferase transcriptional reporter construct, which encodes 12 repeats of the AGCCAGACA sequence (identified as a SMAD3/SMAD4-binding element in the human *SERPIN 1* promoter [39]) using lipofectamine 2000 transfection reagent (1:5; ThermoFisher Scientific). After overnight incubation, cells were harvested and 20.000 cells/well were plated in a 96-wells plate. After attachment, HepG2 cells were serum-starved overnight. The next day, serum-free media were removed and replaced by medium containing TGF-β1 (0.001 - 5 ng/mL, Peprotech). In other wells, TGF-β1 was added in a concentration of 5 ng/mL in combination with increasing concentrations of the monoclonal TGFβ-blocking antibody (αTGF-β) 0.01 – 10 ng/mL, BioXCell). After overnight incubation, the luciferase signal was measured using the Luciferase Assay System (Promega) according to the manufacturer's instructions using the SpectraMax iD3 multi-mode plate reader (Molecular Devices).

Lactate dehydrogenase (LDH) assay

The ability of T cells to induce killing of tumor cells was evaluated using a colorimetric method for quantifying cellular cytotoxicity. In short, KPC3.TRP1, MC38 or MC38.TRP1 cells were irradiated at 8000 RAD and plated at a concentration of 30.000 cells/well. Splenocytes and lymph nodes were isolated from either treatment-naive C57BL/6J, CD8 TGF-βRII KO, or TGF-βRII WT mice and were enriched for CD8 T cells using the Mouse CD8 T Lymphocyte Enrichment Set – DM (BD Biosciences) or via nylon wool processing. Effector cells were added to tumor cells in an E/T ratio of 10:1 and CD3-bsAbs were added in a concentration of 1 µg/mL. In the experiment with naive splenocytes from C57BL/6J mice, αTGF-β (100 or 10 µg/mL) was added as well. After 48 hours of incubation, 20 µL of Triton-X100 was added to wells containing tumor cells alone for 30 minutes to serve as a positive control. Hereafter, 50 µL of supernatant was harvested

of all conditions and incubated for 30 minutes with 50 µL of lactate dehydrogenase reaction mix (Pierce LDH Cytotoxicity Assay Kit, ThermoFisher Scientific). Absorbance was measured at 490 using a SpectraMax iD3 multi-mode plate reader (Molecular Devices). The percentage of cytotoxicity was calculated using the positive control as 100 % cytotoxicity. All conditions were performed in triplicate.

SUPPLEMENTARY FIGURES

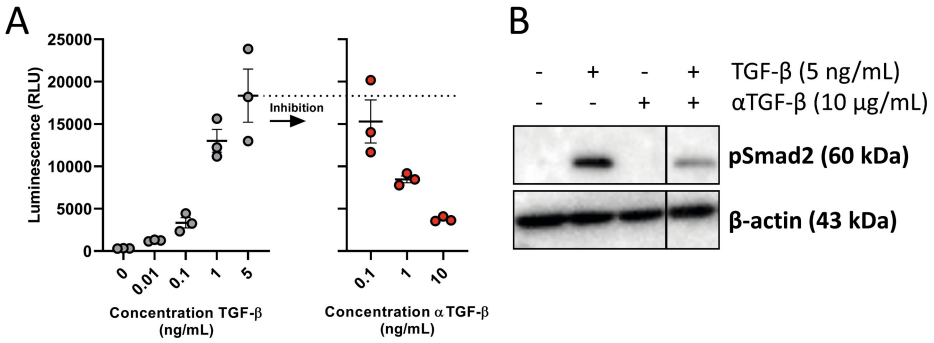


Figure S1. Inhibition of TGF-β signaling by the monoclonal antibody 1D11. (**A**) Induction of TGF-β signaling by TGF-β and subsequent inhibition of TGF-β signaling via TGF-β neutralizing antibodies (αTGF-β, 1D11), as measured by transcriptional CAGA-Luciferase reporter assay. Cells were incubated with TGF-β (0-5 ng/mL). In other wells with 5 ng/mL of TGF-β, αTGF-β was added (0.1-10 ng/mL). (**B**) Immunoblotting of phospho-Smad2 in KPC3 tumor cell line after TGF-β (5 ng/mL) and/or αTGF-β treatment (10 µg/mL). B-actin was measured as a loading control. Vertical black line indicates cutting of blot to eliminate irrelevant samples. Data represent mean±SEM.

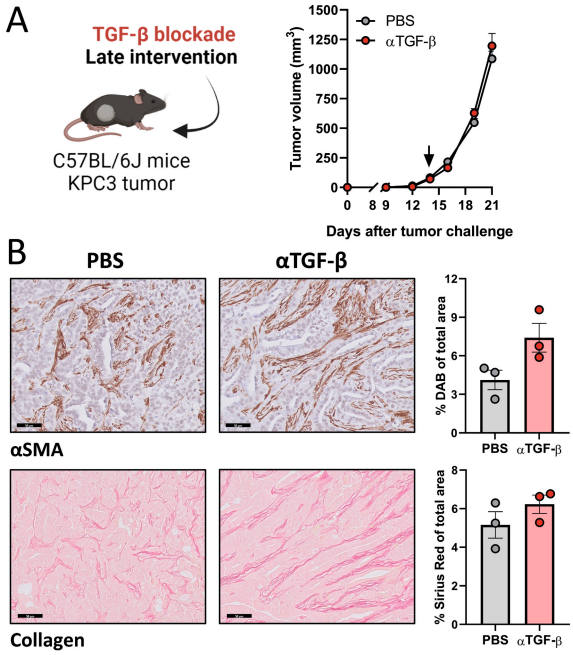


Figure S2. Late TGF-β blockade does not affect tumor outgrowth. (**A**) Average tumor growth curves of immunocompetent C57BL/6J mice (n=5/group) engrafted with KPC3 tumors (1x10^5 cells/mouse) and receiving αTGF-β (200 µg/injection every 3 days, starting on day 14, indicated by black arrow) as late intervention. (**B**) Immunohistochemistry stainings for αSMA and collagen in representative tumors after indicated treatments. Scale bars represent 50 µm and stainings were quantified using ImageJ. Data represent mean±SEM. Significance between PBS and αTGF-β was determined using unpaired t-tests.

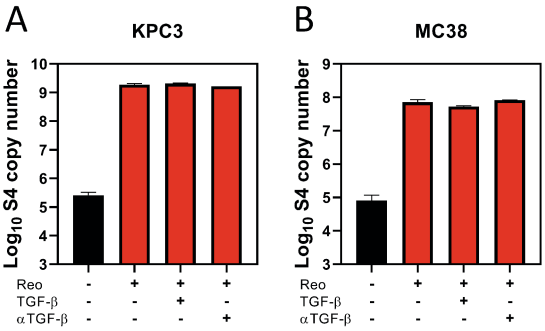


Figure S3. TGF-β addition or blockade does not affect reovirus replication in KPC3 and MC38 cells in vitro. Reovirus genomic segment 4 (S4) copy number in KPC3 (**A**) or MC38 (**B**) lysates, as determined by RT-qPCR. Cells were infected with reovirus for 24 hours (multiplicity of infection of 10) in the presence of TGF-β (5 ng/mL) or αTGF-β (10 µg/mL). Data represent mean±SEM.

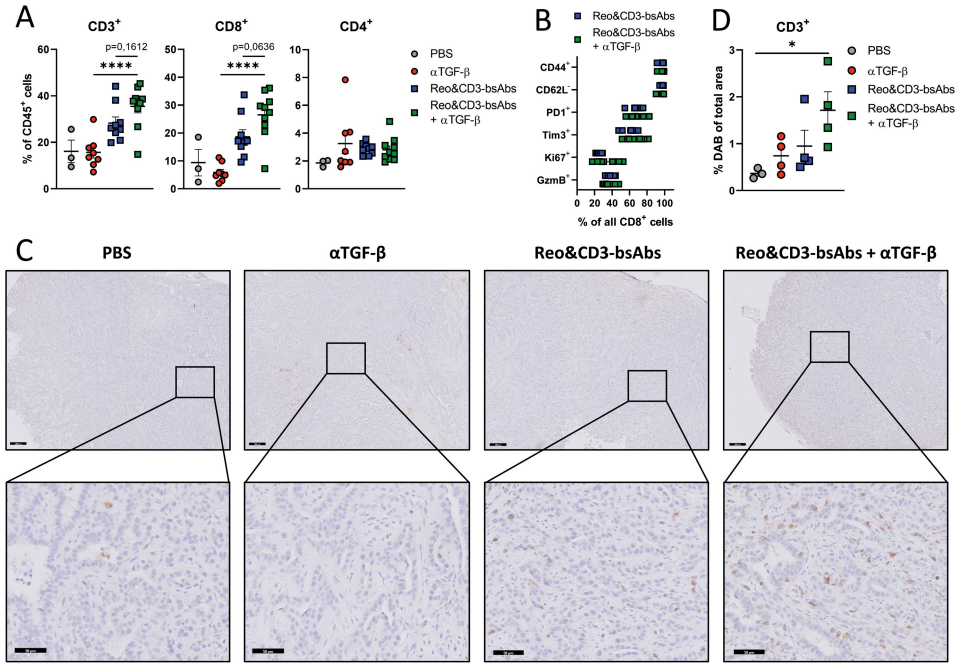


Figure S4. TGF-β blockade does not impair Reo&CD3-bsAb efficacy by decreasing T-cell influx or activation. (**A**) Frequency of $CD3^+$, $CD8^+$ and $CD4^+$ T cells within the total $CD45^+$ immune cell population in end-stage tumors after indicated treatments. (**B**) Expression of various markers on intratumoral CD8+ T cells after receiving Reo&CD3-bsAbs or Reo&CD3-bsAb + αTGF-β. (**C**) Immunohistochemistry staining for CD3 in representative tumors after indicated treatments. Scale bars represent 200 µm for overview and 50 µm for magnification, respectively. (**D**) Quantification of positive DAB signal in tumor coupes stained for CD3 after receiving indicated treatments. Data represent mean±SEM. Significance between groups in (A) and (D) was determined using an ordinary one-way ANOVA with Tukey's multiple comparisons test. Significance levels: ns=not significant, *p<0.05 and **p<0.01.

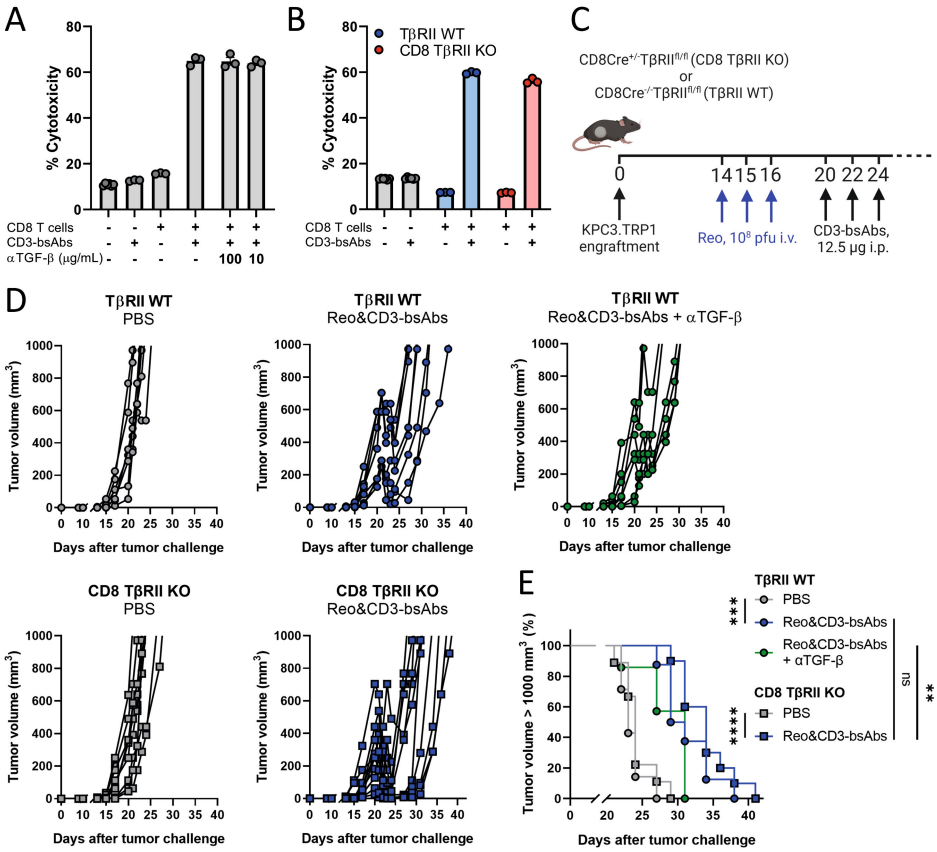


Figure S5. CD8-specific TGF-β blockade does not impair the efficacy of Reo&CD3-bsAb therapy. (**A**) Percentages of cytotoxicity of KPC3.TRP1 cells after in vitro co-culture with enriched $CD8^+$ T cells from naive mice and CD3-bsAbs, in combination with TGF-β neutralizing antibodies. (**B**) Percentage of cytotoxicity of KPC3.TRP1 cells after in vitro co-culture with enriched $CD8^+$ T cells from TβRII WT or CD8 TβRII KO mice and CD3-bsAbs. Data represents mean±SEM of triplicates. (**C**) Overview of the experiment described in (B-C). TβRII or CD8 TβRII KO mice (n=7-10/group) were subcutaneously engrafted with KPC3.TRP1 cells ($1x10^5$/mouse). Mice received Reo intravenously on days 14, 15, and 16 (10^8 plaque-forming units/injection) and received CD3-bsAbs intraperitoneally (12.5 μg/injection) on days 20, 22, and 24. Tumor growth was measured 3-5x/week. (**D**) Individual tumor growth curves of mice receiving indicated treatments. (**E**) Kaplan-Meier survival graphs of mice after indicated treatments. Log-rank tests were used to compare differences in survival in (E). Significance levels: ns= not significant, **p<0.01, ***p<0.001 and ****p<0.0001.

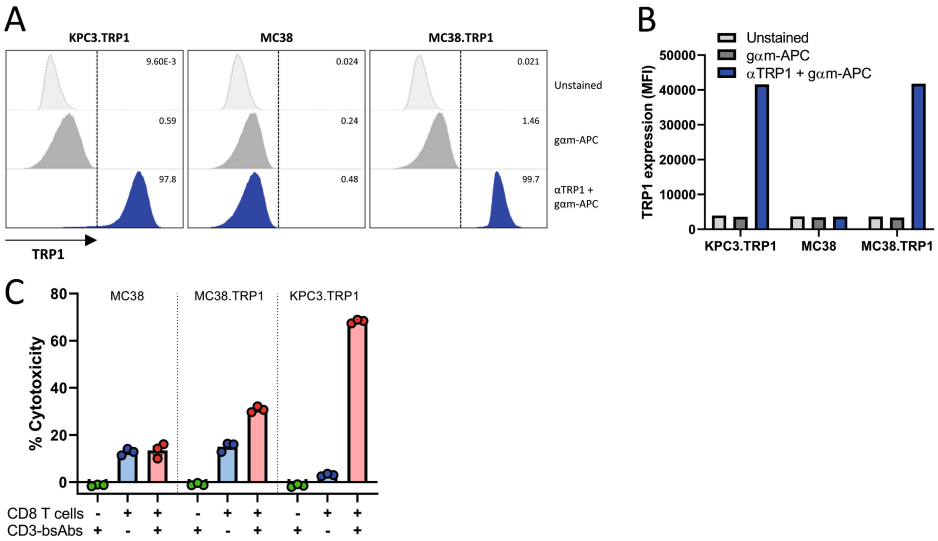


Figure S6. Introduction of TRP1 expression on MC38.TRP1 cells allows killing via CD3-bsAbs. (**A**) Percentage of TRP1 expression on MC38 cells after transfection and sorting, as measured by flow cytometry. Non-transfected MC38 cells are used as negative control and KPC3.TRP1 cells act as a positive control. (**B**) Comparison of mean fluorescence intensity (MFI) of TRP1 signal between KPC3.TRP1 and MC38.TRP1. (**C**) Percentages of cytotoxicity of KPC3.TRP1, MC38 and MC38.TRP1 cells after in vitro co-culture with nylon-wool enriched T cells from naive mice and CD3-bsAbs. Data represents mean±SEM of triplicates.

SUPPLEMENTARY TABLES

Table S1. List of antibodies used for flow cytometric analysis.

Marker	*Clone*	*Fluorochrome*	*Supplier*
CD45.2	104	FITC	eBioscience
CD3	145-2C11	PE-CF594	BD Biosciences
CD8α	53-6.7	Alexa Fluor 700	eBioscience
CD4	RM4-5	APC	BioLegend
Reo $\mu1_{133-140}$ Tetramer		APC	In-house
Rpl18 Tetramer		PE	In-house
CD44	IM-7	BV785	BioLegend
CD62L	MEL-14	BV421	BioLegend
PD-1	29F.1A12	APC-Cy7	BioLegend
Tim3	RMT3-23	PE	BioLegend
NKG2A	16A11	PE	eBioscience
KLRG-1	2F1	PE-Cy7	eBioscience
CD69	H1.2F3	BV605	BioLegend
Lag3	C9B7W	PE-Cy7	Invitrogen
CD49a	Ha31/8	BV786	BD Biosciences
CD103	2E7	BV711	BioLegend
Ki67	B56	BV711	BD Biosciences
GzmB	NGZB	PE-Cy7	BioLegend

Table S2. List of primers used for RT-qPCR analysis.

Gene	*Forward*	*Reverse*
S4Q	5′-CGCTTTTGAAGGTCGTGTATCA-3′	5′-CTGGCTGTGCTGAGATTGTTTT-3′
Ifit-1	5′-CTGGACAAGGTGGAGAAGGT-3′	5′-AGGGTTTTCTGGCTCCACTT-3′
Ifit-2	5′-TGCTCTTGACTGTGAGGAGG-3′	5′-ATCCAGACGGTAGTTCGCAA-3′
Ifit-3	5′-GTGCAACCAGGTCGAACATT-3′	5′- AGGTGACCAGTCGACGAATT-3′
Irf7	5′-GACCGTGTTTACGAGGAACC-3′	5′-GCTGTACAGGAACACGCATC-3′
Isg15	5′-GGAACGAAAGGGGCCACAGCA-3′	5′-CCTCCATGGGCCTTCCCTCGA-3′
Oas1b	5′-AGCATGAGAGACGTTGTGGA-3′	5′-GCGTAGAATTGTTGGTTAGGCT-3′
Ddx58	5′-AAGGCCACAGTTGATCCAAA-3′	5′-TTGGCCAGTTTTCCTTGTCG-3′
Cxcl9	5′-TGGAGTTCGAGGAACCCTAGT-3′	5′-AGGCAGGTTTGATCTCCGTT-3′
Cxcl10	5′-ACGAACTTAACCACCATCT-3′	5′-TAAACTTTAACTACCCATTGATACATA-3′
Mx1	5′-GATGGTCCAAACTGCCTTCG-3′	5′-TTGTAAACCTGGTCCTGGCA-3′
β2m	5′-CTCGGTGACCCTGGTCTTT-3′	5′-CCGTTCTTCAGCATTTGGAT-3′
Bst2	5′-ACATGGCGCCCTCTTTCTATCACT-3′	5′-TGACGGCGAAGTAGATTGTCAGGA-3′
Rsad2	5′-GGTGCCTGAATCTAACCAGAAG-3′	5′-CCACGCCAACATCCAGAATA-3′
Ctgf	5′-GGCCTCTTCTGCGATTTCG-3′	5′-CCATCTTTGGCAGTGCACACT-3′
Id-1	5′-ACCCTGAACGGCGAGATCA-3′	5′-TCGTCGGCTGGAACACAT-3′
Mmp2	5′-TTCTGTCCCGAGACCGCTAT-3′	5′-GTGTAGATCGGGGCCATCAG-3′

Table S2. Continued.

Gene	*Forward*	*Reverse*
Serpin E1	5′-GCCAACAAGAGCCAATCACA-3′	5′-AGGCAAGCAAGGGCTGAAG-3′
Snail	5′-AGCCCAACTATAGCGAGCTG-3′	5′-CCAGGAGAGAGTCCCAGATG-3′
TGF-β1	5′-CAACAATTCCTGGCGTTACC-3′	5′-TGCTGTCACAAGAGCAGTGA-3′
Mzt2	5′-TCGGTGCCCATATCTCTGTC-3′	5′-CTGCTTCGGGAGTTGCTTTT-3′
Ptp4a2	5′-AGCCCCTGTGGAGATCTCTT-3′	5′-AGCATCACAAACTCGAACCA-3′

ADDENDUM II

TGF-β blockade improves Reo&αPD-L1 therapy in the murine colon MC38 tumor model

BACKGROUND

In **Chapter 7**, we observed that TGF-β blockade differentially affects the efficacy of reovirus and CD3-bispecific antibody therapy (Reo&CD3-bsAbs). In the murine pancreatic KPC3 tumor model, the efficacy of Reo&CD3-bsAbs was impaired. Tumor regressions were prevented, and survival was shortened by TGF-β blockade. In contrast, in the murine MC38 colon carcinoma tumor model, TGF-β blockade significantly improved the efficacy of Reo&CD3-bsAb therapy, even leading to a 100% complete response rate. Since we also demonstrated that reovirus can enhance the efficacy of PD-L1 blockade in MC38 tumors in **Chapter 5**, we here investigated whether the efficacy of this combination therapy (Reo&αPD-L1) could also be improved by TGF-β blockade.

RESULTS & DISCUSSION

We engrafted immunocompetent C57BL/6J mice with subcutaneous MC38 tumors. Mice received TGF-β neutralizing antibodies (αTGF-β) starting a few days after tumor engraftment, and Reo&αPD-L1 therapy was administered on day 8, 11 and 14 (**Figure 1A**). Anti-TGF-β antibodies alone delayed tumor growth and induced complete tumor clearance in 10% of animals, and Reo&αPD-L1 therapy led to tumor clearance in 50% of animals (**Figure 1B-D**). However, the addition of αTGF-β to Reo&αPD-L1 therapy led to a total tumor clearance in 80% of animals and enhanced survival. Thus, the efficacy of Reo&αPD-L1 therapy can be improved by TGF-β blockade.

It is expected that PD-L1 blockade mediates its efficacy by reinvigorating dysfunctional tumor-specific T cells (1). However, the increased efficacy of Reo&αPD-L1 after αTGF-β could not be attributed to an increase in tumor-specific (Rpl18+) T cells, as similar frequencies were detected in the circulation of both groups receiving Reo&αPD-L1 therapy (**Figure 1E**). In **Chapter 7**, we also observed that Reo treatment does not improve the frequency of $Rpl18^+$ $CD8^+$ T cells, either in the circulation or in the tumor. Here, we confirmed that the frequency of $Rpl18^+$ $CD8^+$ T cells was not correlated with clinical outcome, since mice with a complete response (CR; in blue) did not always have the highest frequency of $Rpl18^+$ $CD8^+$ T cells (**Figure 1E**). Hence, we concluded that the triple combination of Reo, αPD-L1 and αTGF-β blockade demonstrates superior antitumor efficacy compared to all single arms or combinations of two arms, but that this improved efficacy was not associated with an increased frequency of tumor-specific $Rpl18^+$ $CD8^+$ T cells.

We next investigated whether antitumor immunologic memory was established by the different treatments. We therefore rechallenged the mice that completely cleared the primary tumor on the other flank and monitored tumor outgrowth (**Figure 1F**). Mice that cleared previous tumors had increased presence of Rpl18-specific T cells in the

circulation compared to naive mice, especially the group that received Reo&αPD-L1 therapy together with αTGF-β, suggesting that Rpl18-specific T-cell responses were boosted by the rechallenge with MC38 tumor cells (**Figure 1G**). While tumors grew out in 100% of naive mice, this was not the case in mice previously treated with Reo&αPD-L1 or Reo&αPD-L1+αTGF-β (**Figure 1H**).

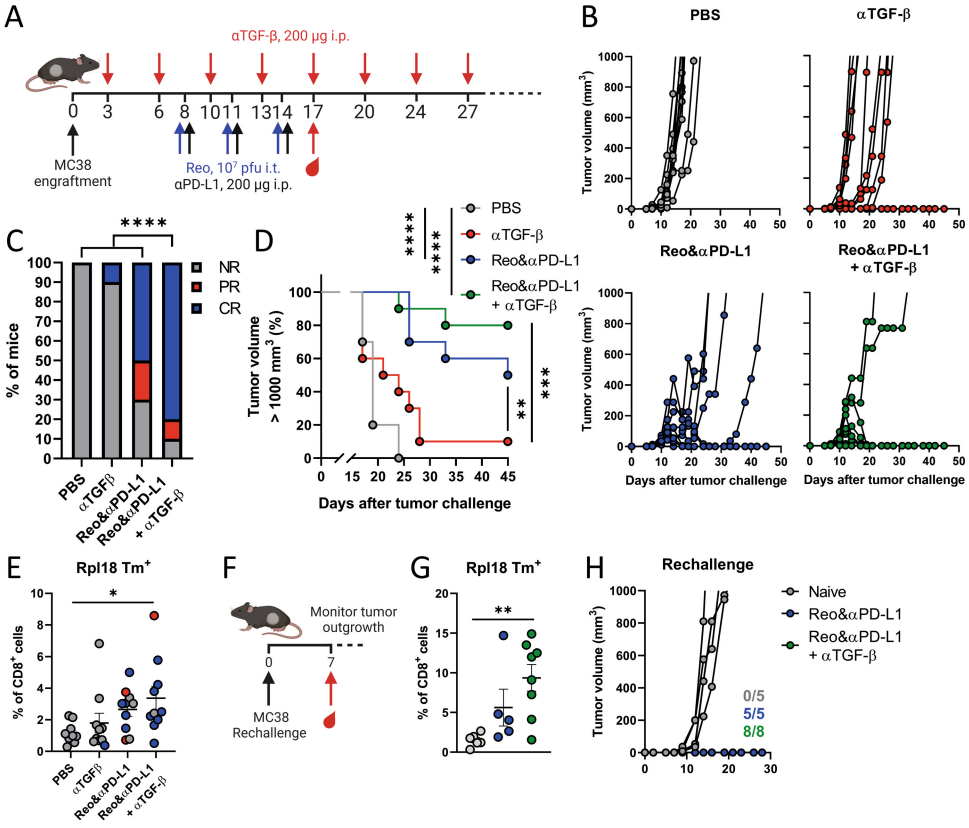


Figure 1. TGF-β blockade increases response rate after Reo&αPD-L1 in the MC38 model of colon cancer. (**A**) Overview of experiment described in (B-E). Immunocompetent C57BL/6J mice were subcutaneously engrafted with MC38 cells (5x10^5/mouse) and received TGF-β-neutralizing antibodies (αTGF-β, 200 µg/injection every 3 days) starting directly after tumor engraftment. Mice received Reo (intratumorally, 10^7 plaque-forming units/injection) and αPD-L1 (intraperitoneally, 200 µg/injection) on day 8, 11 and 14. Tumor growth was measured 3x/week. (**B**) Individual tumor growth curves of mice receiving indicated treatments. (**C**) Frequency of Non-Responders (NR), Partial Responders (PR) or Complete Responders (CR) within each treatment group. (**D**) Kaplan-Meier survival graphs of mice after indicated treatments. (**E**) Frequency of Rpl18$^+$ CD8$^+$ T cells in blood of mice after indicated treatments. (**F**) Design of rechallenge experiment. All CR mice from (D) were subcutaneously engrafted with MC38 tumor cells (5x10^5/mouse) in the alternate flank, and tumor outgrowth was measured 3x/week. (**G**) Frequency of Rpl18$^+$ CD8$^+$ T cells in blood of mice after rechallenge. (**H**) Individual tumor growth curves of mice that were rechallenged with MC38 tumor cells. Data represent mean±SEM. Significance between groups in (E) and (G) was determined using an ordinary one-way ANOVA with Tukey's multiple comparisons test. Chi-square test was used to determine statistical differences in response in (C). Log-rank tests were used to compare differences in survival in (D). Significance levels: *p<0.05, **p<0.01, ***p<0.001 and ****p<0.0001.

These data indicate that tumor-specific immune responses were established by our therapies, but that the efficacy of these therapies could not be explained by the increased frequency of tumor-specific Rpl18^{+} T cells. It would be interesting to investigate whether the improved protection was due to other MC38-specific T-cell responses, for instance those directed towards neo-epitope Adpgk (2). Alternatively, other cell types in the TME may be involved. For instance, tumor-associated M2 macrophages (TAMs) have been shown to hamper the efficacy of checkpoint blockade in the MC38 tumor model (3). Since anti-inflammatory M2 TAMs are induced by TGF-β (4,5), it is possible that neutralization of TGF-β hampered the function or reduced the level of these TAMs and thereby improved the efficacy of Reo&αPD-L1 therapy, without directly affecting the numbers of circulating tumor-specific T cells.

CONCLUSION

Combined, these data show that both Reo&CD3-bsAb and Reo&αPD-L1 therapy can be improved by TGF-β blockade in the MC38 tumor model. This further highlights the necessity to determine which factor(s), mechanism(s) or cell type(s) that are present in MC38 tumors permit or even contribute to this beneficial effect of TGF-β blockade, with the ultimate aim to employ this characteristic for effective viro-immunotherapy in other tumor models that are much harder to treat.

REFERENCES

1. Xu-Monette ZY, Zhang M, Li J, Young KH. PD-1/PD-L1 Blockade: Have We Found the Key to Unleash the Antitumor Immune Response? Front Immunol **2017**;8
2. Hos BJ, Camps MGM, van den Bulk J, Tondini E, van den Ende TC, Ruano D, *et al.* Identification of a neo-epitope dominating endogenous CD8 T cell responses to MC-38 colorectal cancer. Oncoimmunology **2019**;9:1673125
3. Arlauckas SP, Garris CS, Kohler RH, Kitaoka M, Cuccarese MF, Yang KS, *et al.* In vivo imaging reveals a tumor-associated macrophage-mediated resistance pathway in anti-PD-1 therapy. Sci Transl Med **2017**;9:eaal3604
4. Zhang F, Wang H, Wang X, Jiang G, Liu H, Zhang G, *et al.* TGF-β induces M2-like macrophage polarization via SNAIL-mediated suppression of a pro-inflammatory phenotype. Oncotarget **2016**;7:52294-306
5. Batlle E, Massague J. Transforming Growth Factor-beta Signaling in Immunity and Cancer. Immunity **2019**;50:924-40



CHAPTER 8

Summarizing Discussion and Future Perspectives

The exploitation of the immune system to battle tumors has revolutionized the field of anticancer therapy. However, improved clinical responses to immunotherapy occur in only a subgroup of patients with solid tumors. These tumors often present with an ongoing immune response, which includes the baseline presence of immune cells, particularly T cells. Tumors with this phenotype are known as immune-infiltrated tumors. Tumors with an immune-silent phenotype, for example a large proportion of pancreatic cancers, lack this basal influx of T cells and as such barely respond to T-cell-based immunotherapy. The central theme of this thesis was to investigate and exploit the immunostimulatory properties of oncolytic reovirus as a strategy to enhance the response of pancreatic cancers to T-cell-based immunotherapy.

The use of oncolytic viruses (OVs) as anticancer agents was kickstarted by occasional observations where tumor regressions coincided with natural virus infections (1). A very well-known example, already published in 1904, is that of a 42-year-old woman with leukemia that went into remission after an infection with influenza (2). In the years following the 1950s, many human pathogens were investigated for oncolytic activity, including measles, vaccinia, adenovirus, and reovirus. More recent investigations into the therapeutic benefit of OVs have led to several clinical candidates and one FDA/EMA-approved oncolytic virus. These investigations also resulted in the culmination of various topics of debate and outstanding questions concerning the optimal application of OVs in the clinic. Here, I have used these outstanding questions, accompanied by illustrative figures comprising published and unpublished data, to summarize and discuss how the accumulated data in this thesis provides new insights and may ultimately contribute to more effective viro-immunotherapy.

REOVIRUS: ONCOLYSIS OR IMMUNE STIMULATION?

OVs, including oncolytic reovirus, comprise an emerging and highly promising class of anticancer immunotherapeutics that exploit the natural ability of certain viruses to infect and preferentially lyse tumor cells while leaving healthy cells intact. However, newer studies demonstrated that OVs might also, or even better be utilized as agents that can induce local potent immune responses.

In our studies, we observed that intratumoral administration of 10^7 plaque-forming units (pfu) of oncolytic reovirus, a dose that is comparable to the amount of reovirus pfu/kg bodyweight used for patients in clinical trials, did not result in an increased presence of apoptosis marker cleaved caspase 3 in reovirus-treated, immune-silent murine pancreatic KPC3 tumors (**Chapter 5**). Although more recent insights demonstrated that reovirus can also cause necrosis (3), a caspase-independent pathway of cell death, we also did not observe a significant reovirus-induced inhibition on the outgrowth of murine pancreatic KPC3 tumors or other preclinical tumor models (**Figure 1**). These

observations suggest that in the models that we tested, the capacity of reovirus to act directly as an oncolytic agent is limited.

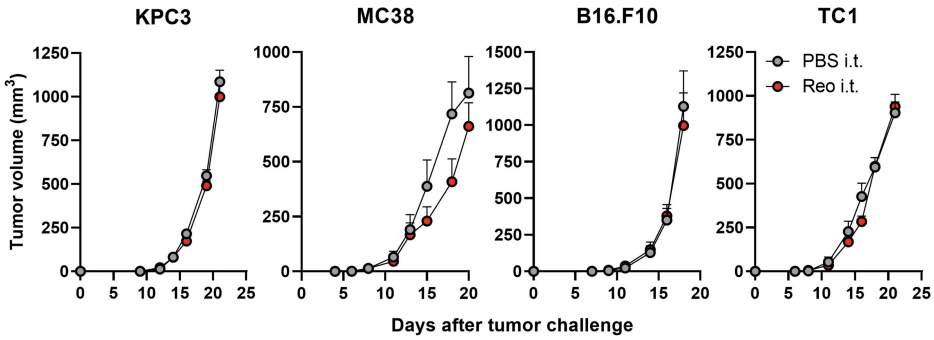


Figure 1. Reovirus administration does not affect tumor outgrowth in different preclinical tumor models. Average tumor growth curves of murine pancreatic KPC3, colon MC38, melanoma B16.F10, and lung TC1 tumors after intratumoral administration of reovirus (10^7 plaque-forming units). Data represent mean±SEM.

However, the administration of oncolytic reovirus did induce a fast interferon response (**Chapters 2, 3, 5, and 7**), including the expression of various T-cell-attracting chemokines and other interferon-stimulated genes (ISGs), which was followed by the influx of immune cells into these otherwise immune-silent tumors. Interestingly, the reovirus-induced influx of immune cells seems to be very specific for 'killer cells', since not $CD4^+$ T cells, but mostly $CD8^+$ T cells and to a lesser extent NK cells infiltrate into KPC3 tumors, as well as MC38, B16.F10, and TC1 tumors (**Figure 2**). The frequency of other immune cells, such as macrophages, dendritic cells, or neutrophils did not increase upon intratumoral reovirus administration. In contrast, whilst other OVs might also induce the influx of $CD8^+$ T cells or NK cells, often the influx of other immune cells is more prominent. For instance, after the injection of adenovirus Δ24-RGD in a syngeneic mouse model for glioblastoma (4), macrophages were the immune-cell population that was mostly enriched in the tumor. Alternatively, vesicular stomatitis virus (VSV) administration greatly enhanced the frequency of neutrophils in B16 murine melanoma tumors compared to other immune-cell populations (5). Although all these immune cells can be employed for anticancer therapy using various strategies, the observation that reovirus administration predominantly induces a potent influx of $CD8^+$ T cells in various preclinical tumor models makes reovirus especially attractive to combine with T-cell-based immunotherapy.

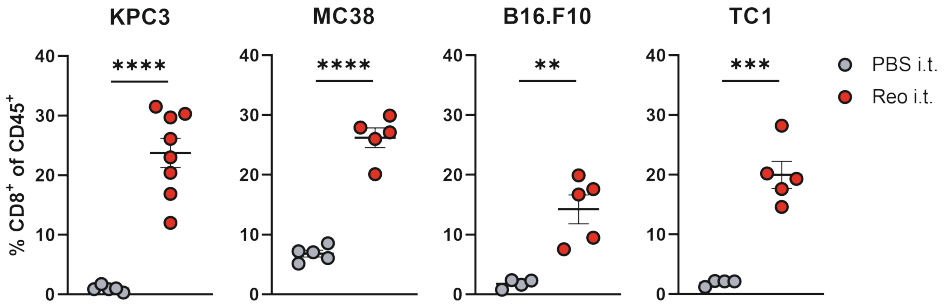


Figure 2. Reovirus administration induces an intratumoral influx of CD8⁺ T cells. Frequency of CD8⁺ T cells out of CD45⁺ immune cells in murine pancreatic KPC3, colon MC38, melanoma B16.F10, and lung TC1 tumors after intratumoral administration of reovirus (10^7 plaque-forming units). Data represent mean±SEM. Significance levels: **p<0.01, ***p<0.001, and ****p<0.0001.

Altogether, our observations demonstrate that in the case of oncolytic reovirus, the exploitation of its immunostimulatory potential should be prioritized over its use as an oncolytic agent. The oncolytic effect of reovirus might be improved by employing a much higher dosage or a modified virus that has more lytic potential, but it is unknown if this is possible without inducing adverse effects. Additionally, employing a higher dose or a more lytic virus might result in faster clearance of the virus by eliciting stronger antiviral immune responses. The fact that potent immunostimulatory effects can already be observed using a relatively low dose of reovirus further advocate that this characteristic of reovirus should be exploited for anticancer therapy.

REOVIRUS THERAPY: MONOTHERAPY OR COMBINATION THERAPY?

Applying OV therapy as monotherapy or in combination with other anticancer modalities is another important question that needs to be answered when considering clinical OV application. As was reviewed in 2020, a large proportion of clinical trials investigating the safety and efficacy of OVs were conducted with OV monotherapy (6).

However, in the case of reovirus, our data and studies by others demonstrated that the efficacy of reovirus as monotherapy is limited (7-9). As such, reovirus has often been used in combination with various other therapeutics to increase its anticancer efficacy (**Figure 3**). Given the immunostimulatory potential of reovirus (See section "Reovirus: oncolysis or immune stimulation"), especially the potential beneficial combination of reovirus with immunotherapeutic strategies warrants extensive investigation.

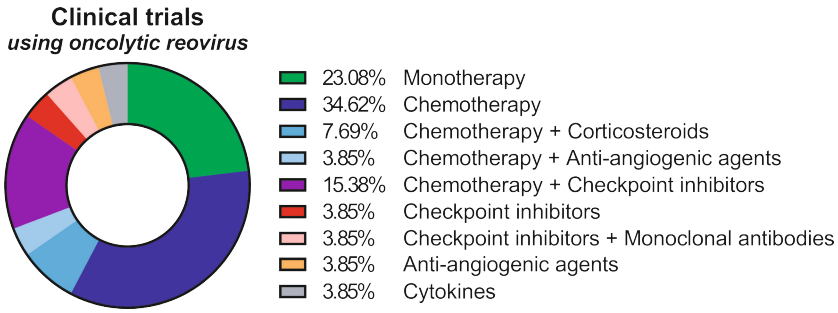


Figure 3. Combination agents used with oncolytic reovirus in clinical trials. A total of 26 clinical trials involving reovirus were assessed for their additional use of other therapeutics. Chemotherapy: reovirus with cyclophosphamide, carboplatin, paclitaxel, or gemcitabine. Chemotherapy + Corticosteroids: reovirus with bortezomib/carfilzomib and dexamethasone. Chemotherapy + Anti-angiogenic agents: reovirus with irinotecan/leucovorin/fluorouracil and bevacizumab (αVEGF). Chemotherapy + Checkpoint inhibitors: reovirus with gemcitabine/irinotecan/leucovorin/fluorouracil/bortezomib/carfilzomib/paclitaxel and pembrolizumab (αPD1)/avelumab (αPD-L1)/nivolumab (αPD-L1). Checkpoint inhibitors: reovirus with retifanlimab (αPD1). Checkpoint inhibitors + monoclonal antibodies: reovirus with atezolizumab (αPD-L1) and trastuzumab (αHER2). Anti-angiogenic agents: reovirus with lenalidomide/pomalidomide. Cytokines: reovirus with sagramostim (recombinant GM-CSF). Data was obtained from clinicaltrials.gov on 15-03-2023.

Reovirus and checkpoint blockade

When aiming to exploit the immunostimulatory properties of oncolytic reovirus, as was the goal of the research described in this thesis, reovirus is often combined with other immunotherapeutic agents. Within the group of immunotherapeutic agents, reovirus is most often combined with immune checkpoint inhibitors, especially those blocking the PD1-PD-L1 axis. Here, binding of PD-L1 (expressed on tumor cells or various immune cells) to PD1 (expressed on T cells) inhibits the effector function of T cells, including tumor-specific T cells. Blocking this pathway to enhance the efficacy of T cells that are primed after OV therapy is a logical choice, since OVs can stimulate the secretion of interferons that upregulate the expression of PD-L1 on tumor cells (10-14). Indeed, we also observed an increase in PD-L1 expression on both tumor cells ($CD45^-$) and immune cells ($CD45^+$) in KPC3 tumors after intratumoral reovirus administration (**Figure 4**).

Although reovirus administration attracts a wave of T cells to the tumor, the presence of these T cells does not affect tumor growth (**Figure 1**). This suggests that these incoming T cells are not tumor-specific. Thus, even though PD-L1 is expressed, the lack of tumor-specific T-cell responses limits the efficacy of checkpoint blockade in these KPC3 tumors (**Chapters 2 and 3**). In other, more immunogenic tumors, the combination of reovirus and checkpoint blockade can be very beneficial. This was also visible in our studies, where we observed that the combination of reovirus and αPD-L1 therapy was very effective in the immunogenic murine MC38 colon tumor model (**Chapter 5**). The efficacy of this combination therapy could even be further improved by TGF-β blockade (**Addendum II**). Other studies have also demonstrated a synergistic effect when reovirus is combined with checkpoint blockade. For instance, in the subcutaneous

B16 melanoma model, intratumoral reovirus administration combined with systemic αPD1 treatment led to a significantly increased survival of mice compared to both agents alone, which was attributed to increased antitumor T-cell responses and abrogation of T_{reg} activity (15). Similar observations were made in the syngeneic EMT6 breast cancer model, where the combination of reovirus and αPD1 increased survival and tumor-specific immune responses, even leading to protection against rechallenge (14). Lastly, in the orthotopic syngeneic GL261 brain tumor model, intravenous reovirus administration significantly enhanced the efficacy of αPD1 therapy (13).

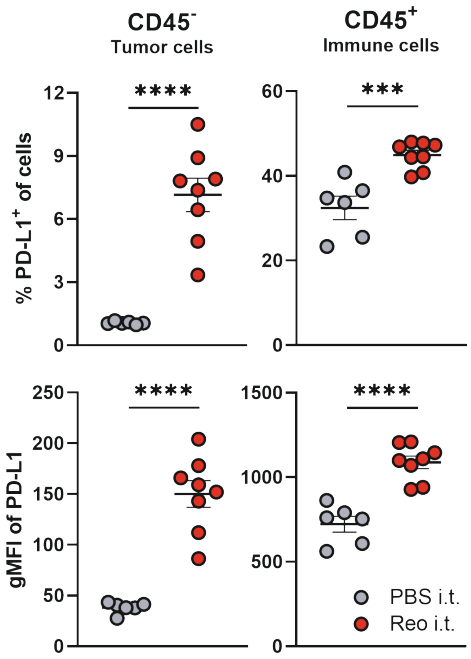


Figure 4. PD-L1 expression in KPC3 tumors after reovirus administration. Intratumoral reovirus administration increases the frequency of PD-L1⁺ cells, as well as the intensity (gMFI) of PD-L1 expression on both the tumor cell compartment (CD45⁻) and the immune cell compartment (CD45⁺) in KPC3 tumors. Significance levels: ***p<0.001 and ****p<0.0001.

Since the lack of tumor-specific T-cell responses, even after reovirus administration, prevents effective combination therapy in non-immunogenic tumors, it is necessary to employ other immunotherapeutic strategies to treat these tumors.

Reovirus and SLP vaccination

In our studies described in **Chapter 2 and 3**, we observed that a significant proportion of the CD8⁺ T cells that infiltrated into the tumor after reovirus administration was reovirus-specific, and not tumor-specific. Whereas a body of literature has shown that several OVs, including reovirus, can induce tumor-specific T-cell responses via antigenic spread, this seems to be restricted to immunogenic models with high mutational load or expression of tumor-associated or artificial antigens (16-20). Therefore, the exploitation

of virus-specific T cells may represent a solution for targeting low-immunogenic tumors to which tumor-specific responses are more difficult.

In **Chapter 3**, we exploited the ability of reovirus-specific T cells to recognize and kill virus-infected tumor cells. We demonstrated that a synthetic long peptide (SLP) vaccine-induced preinstalled pool of reovirus-specific $CD8^+$ T cells was recruited to the tumor upon intratumoral reovirus administration and effectively delayed tumor growth. Antiviral $CD8^+$ T cells were shown to reside in a range of both murine and human tumors, including melanomas, brain metastases, and endometrial, lung, and colorectal cancers (21-25). In contrast to most of the tumor-specific T cells present, the $CD8^+$ T cells specific for common viral pathogens, such as Cytomegalovirus (CMV), Eppstein-Barr virus (EBV), or Influenza virus exhibited phenotypes more in line with active effector cells, which could be activated upon stimulation with their cognate antigen (21,22). Furthermore, exploiting OV-specific T cells instead of other T cells specific for other viruses adds some sort of tumor-specificity to the system, due to the specific replication of the OV in malignant cells. In this way, only tumor cells are converted into target cells for the previously established OV-specific T cells.

Although this is a promising approach, a lot of steps are necessary before the combination of vaccination and OV therapy can be clinically applied. For instance, reovirus-epitopes for human HLA class I types need to be identified, to allow the specific priming of reovirus-specific T cells and not the induction of reovirus-specific NAb responses that would occur when for instance vaccines would be used that comprise complete reovirus proteins in their original conformation. Alternatively, it would be an option to provide overlapping sequences of reovirus proteins, which circumvents the need to identify reovirus-specific T-cell epitopes. Lastly, besides an SLP, other formats might be considered to deliver reovirus-specific T-cell epitopes, such as the mRNA-containing lipoplex nanoparticles that have recently been used to deliver neoantigens to prime tumor-specific T-cell responses in pancreatic cancer (26).

Reovirus and CD3-bsAbs

In addition to the exploitation of the specificity of reovirus-specific T cells, these T cells can also be employed to target cancer cells by bypassing their specificity. In **Chapter 2**, we made use of CD3-bispecific antibodies (bsAbs) to redirect the recruited reovirus-specific T cells to the tumor and induce tumor-specific killing. Since CD3-bsAbs activate T cells via binding to CD3, the interaction between MHC class I and the T-cell receptor is redundant and any T cell, including virus-specific T cells, can be employed to target tumor cells (27-29). Although T cells induced by vaccination or other strategies might also be employed by CD3-bsAbs (30), we were the first to demonstrate that the treatment of intratumoral reovirus injection followed by systemic CD3-bsAb administration (Reo&CD3-bsAbs) resulted in the fast regression of local and distant tumors. This effect was dependent on the expression of the targeted tumor antigen on tumor cells. Therefore, for the clinical application of reovirus and CD3-bsAbs, the

selection of the appropriate tumor antigen is of utmost importance. For effective bsAb therapy in humans, the ideal target antigen needs to be selectively and abundantly expressed on tumor cells but should also be essential for tumorigenesis, to avoid downregulation or immunologic selection for tumor cells without expression of the antigen. Although the ideal target for PDAC has not been identified, a plethora of tumor antigens is currently being evaluated (30). Additionally, various OV-CD3-bsAb platforms are extensively investigated in preclinical studies (31). Based on our data, we argue for a fast translation of this highly promising immunotherapeutic combination to the clinic.

In **Chapter 7**, we investigated whether the efficacy of Reo&CD3-bsAb therapy could be further improved by TGF-β blockade. As is reviewed in **Chapter 6**, TGF-β is one of the most potent and pleiotropic regulatory cytokines and is involved in almost all stages of tumor growth, including initiation, progression, and spread (32). TGF-β signaling influences virtually all innate and adaptive immune cells, which includes the stimulation of inhibitory regulatory T cells and the inhibition of cytotoxic $CD8^+$ T cells (33). Additionally, TGF-β plays a role in the exclusion of T cells from the tumor beds. Thus, in the context of cancer, these pleiotropic functions of TGF-β make it an interesting, but complex, target for therapy.

This complexity was also visible in our studies, since TGF-β blockade antagonized Reo&CD3-bsAb combination therapy in KPC3 tumors but enhanced the percentage of complete responses to this therapy from 50% to 100% in MC38 tumors. This demonstrates that intertumoral differences can determine whether TGF-β blockade improves or impairs the efficacy of (viro)-immunotherapeutic strategies, and an increased understanding of these intertumoral differences is required to predict which individuals would most likely benefit from TGF-β neutralization as an addition to Reo&CD3-bsAb therapy.

Reovirus and other forms of anticancer therapy

Besides the combination with immunotherapeutic strategies, reovirus is also often combined with chemotherapeutic agents (**Figure 3**), and synergistic effects were sometimes observed. This enhanced treatment efficacy might be mostly attributed to increased tumor cell death. For instance, the treatment of prostate cancer cell lines with reovirus combined with various chemotherapeutic agents led to increased cell death compared to both agents alone (34). Similarly, combined treatment of reovirus and docetaxel demonstrated superior antitumor efficacy in subcutaneous human prostate PC3 tumors engrafted in nude mice (34). Others have demonstrated the improved efficacy of reovirus therapy after combination with cisplatin, gemcitabine, vinblastine, and/or paclitaxel in the murine melanoma B16.F10 model (35), various non-small cell lung cancer cell lines (36) and the Cal27 tumor model for head and neck cancer (37). The combination of reovirus and chemotherapy was demonstrated to be safe in multiple clinical trials (38,39) and demonstrated antitumor responses in a Phase II study in patients with head and neck cancer (40). Combined, these data suggest that the

addition of chemotherapy might be mostly beneficial to enhance intratumoral cell death. However, since chemotherapeutic drugs have also demonstrated immunostimulatory potential (41,42), an interesting avenue for further research might be to investigate whether a combination of reovirus and chemotherapeutic drugs could not only lead to lead to enhanced oncolysis, but also to enhanced immune stimulation.

In conclusion, the research described in this thesis advocates for applying reovirus as part of a combinatorial approach, and not as monotherapy. However, exploitation of the immunostimulatory potential of reovirus requires careful evaluation of the immune phenotype of tumors to determine which immunotherapeutic strategy will induce optimal results when combined with reovirus. Although the field of cancer immunotherapy, including OV research, is predominantly focused on and might prefer the induction of potent endogenous tumor-specific T-cell responses, we demonstrated that virus-specific T cells can also be very useful to target tumor cells. Especially for low-immunogenic tumors where endogenous tumor-specific T cells are lacking, I propose that combining reovirus with CD3-bsAbs might lead to better anticancer efficacy compared to the commonly used checkpoint inhibitors. Alternatively, combining OVs with the adoptive transfer of *ex vivo* cultured tumor-specific T cells might be promising, where OV treatment can induce a local chemokine gradient to facilitate the recruitment and trafficking of these transferred T cells to the tumor and increase their antitumor efficacy (43-48). Lastly, further investigation into intertumoral differences is required to assess the factor, process, or cell type that determines whether TGF-β blockade will be beneficial for the efficacy of combined reovirus and T-cell-based immunotherapeutic strategies.

ROUTE OF ADMINISTRATION: LOCAL OR SYSTEMIC DELIVERY?

Another important outstanding question for OV therapy is the choice of administration route. Local delivery of OVs is clinical practice for the FDA/EMA-approved OV T-VEC (49,50) and is used in many preclinical studies, including the majority of studies described in this thesis, and ensures efficient delivery to the tumor site. However, in a large number of clinical studies, reovirus and other OVs are administered intravenously (6,51,52). A major and clinically-relevant advantage of intravenous delivery is that it does not rely on injectable tumor lesions, which are often lacking in the majority of cancer types. Additionally, multiple lesions can be targeted at once by systemic administration.

The effect of the administration route on OV delivery into tumors

Consideration of the route of OV administration is mostly focused on the efficient delivery of the OV itself to the tumor site (6,53). We observed that intravenous administration of reovirus resulted in very limited viral presence in tumors compared to intratumoral administration, even when a 10-fold higher dose of virus is used for

the infusion (**Chapters 2 and 3**). Similar observations were made in immunodeficient mice bearing human pancreatic BxPC3 tumors, where intratumoral administration of oncolytic Newcastle disease virus (NDV) led to the detection of viral RNA in 4 out of 6 tumors, while intravenous administration of NDV in the same dosage led to the detection of viral RNA in only 1 out of 6 tumors (54). This is most likely explained by the fact that systemic delivery results in the spread of the OV throughout the body, leaving fewer infectious particles available to infect tumor cells when compared to direct, intratumoral administration.

The low OV detection in tumors after intravenous administration is also observed in clinical studies. For instance, in a Phase I dose escalation study with an oncolytic vaccinia virus, evidence of viral infection in the tumor 8 days after intravenous administration could only be observed in 2 out of 8 tumor biopsies (55). Similarly, in a Phase I dose escalation study with an oncolytic adenovirus in patients with cutaneous and uveal melanoma, evidence of virus genomic particles in tumors could be detected in 4 out of 7 patients (56). Lastly, in a Phase I study with oncolytic reovirus in 9 patients with brain tumors, immunohistochemistry analysis revealed the presence of reovirus σ3 protein in 6 out of 9 patients, but in very low levels (13). Although these studies and others indicate that intravenous OV delivery is safe and well-tolerated, the detection of high titers at tumor sites is not yet demonstrated and might contribute to the moderate clinical responses observed after intravenous OV therapy. Future research should also reveal whether increased delivery of reovirus to tumors will result in increased antitumor responses and improved survival. These parameters might be correlated, since in a Phase II study investigating intravenous delivery of reovirus to 13 patients with metastatic melanoma, reovirus could be detected in tumor biopsies of only 2 patients, whom both displayed a longer progression-free survival (80 and 87 days) compared to the median survival of 45 days (57).

The effect of the administration route on the OV-induced immune response

Although efficient delivery of the OV itself is currently the main focus, the OV-induced immune response might be a more appropriate parameter to investigate, especially in the context of combining OV administration with T-cell-based immunotherapy (see also the section 'Reovirus therapy: monotherapy or combination therapy?'). In our studies, we observed that priming of reovirus-specific T cells does not depend on a specific route of administration (**Chapter 3**). In fact, reovirus infection of tumors was not even required to mount a potent systemic reovirus-specific T-cell response, suggesting that uptake of a virus particle by an antigen-presenting cell, without specific replication in tumors, is already sufficient for the priming of reovirus-specific $CD8^+$ T cells. But, although priming of reovirus-specific T cells was similar between injection methods, intratumoral administration induced more efficient trafficking of (reovirus-specific) $CD8^+$ T cells to the tumor, presumably due to increased expression of T-cell-attracting chemokines *Cxcl9* and *Cxcl10* and other ISGs (**Chapter 3**).

Although T-cell influx in tumors might be lower after intravenous OV administration compared to intratumoral administration, this may not necessarily result in lower efficacy of OV and T-cell-based immunotherapy. For example, we observed that intravenous reovirus administration followed by CD3-bsAbs was able to induce potent tumor regressions and significantly improve survival in both KPC3 (**Chapters 2, 5, and 7**) and MC38 (**Chapter 7**) tumor models. Direct comparisons between therapeutic outcomes of viro-immunotherapeutic strategies after intratumoral or intravenous OV administration are lacking, but effective antitumor responses have been observed after intravenous reovirus administration combined with αPD1 therapy in a murine brain tumor model (13), with an intravenously-administered vaccinia virus in combination with αPD1 therapy in murine pancreatic neuroendocrine tumors and metastases (58) and after intravenous administration of oncolytic alphavirus M1 in combination with αPD-L1 in murine melanoma B16.F10 and murine prostate RM-1 tumors (59). Thus, effective combination therapy is feasible when OVs are administered intravenously.

Combined, we demonstrated that the infection of tumors by reovirus is related to the route of administration, with intratumoral reovirus administration resulting in greater infection of tumors compared to intravenous administration. However, intratumoral administration is not required for effective combination therapy, since intravenously administered OVs are also capable to sensitize tumors for T-cell-based immunotherapy. Interestingly, reovirus infection is not restrained to the injected tumor site. This is evidenced in our studies where reovirus was administered to only one tumor in mice with bilateral tumors, we were also able to detect virus and T cells in the non-injected, distant tumor (**Chapter 2**). Similarly, the addition of CD3-bsAbs resulted also in potent antitumor responses in these tumors, even though they were not intratumorally injected with reovirus. Possibly, reovirus itself can migrate from one tumor to the next. However, since we also observed low levels of reovirus in the tumor-draining lymph node, it is also possible that reovirus migrated to the distant tumor by associating with immune cells, as has been observed before (60,61). These observations provide interesting avenues for further research. Altogether, our data suggest that combined reovirus and T-cell-based immunotherapy can result in effective antitumor responses after both intratumoral and intravenous reovirus administration, and even in the context of metastatic disease.

PREEXISTING IMMUNITY: BARRIER OR BRIDGE FOR EFFECTIVE THERAPY?

Another outstanding question that is closely related to determining the optimal route of OV administration, is whether preexisting immunity against an OV influences the efficacy of OV therapy. This is especially relevant in the context of systemic administration, where OVs might be more susceptible to clearance by preexisting neutralizing antibodies compared to local, intratumoral administration.

In **Chapter 4**, we summarized the current literature regarding the effect of preexisting immunity on both the OV infection and replication, as well as the OV-induced immune response. Preexisting immunity, especially in the form of neutralizing antibodies (NAbs), is prevalent against several viruses that besides their application as OVs, also circulate in the human population or are used as vectors for vaccination. These include Adenovirus serotype 5 (Ad5) (62,63), Herpes simplex virus type 1 (HSV-1) (64,65), Vaccinia virus (55,66,67), and reovirus (7,9,38,39,68-70). For Ad5 and HSV-1, their capacity to infect cells in order to replicate is impaired in preexposed animals (71,72). This illustrates the importance of investigating the possible effects of preexisting immunity on the efficacy of reovirus therapy.

The influence of (preexisting) NAbs on the efficacy of reovirus as an oncolytic agent

In **Chapter 5**, we confirmed that the majority of human cancer patients also present with circulating NAbs against reovirus. Therefore, we preexposed mice to reovirus to induce high levels of circulating NAbs, and observed that viral infection was significantly impaired in preexposed mice. NAbs also counteracted reovirus-mediated control of tumor growth, since the antitumor efficacy of reovirus was much improved in mice that could not produce NAbs, and again reduced in these mice upon the transfer of NAbs. Thus, NAbs hamper the effective use of reovirus as an oncolytic agent.

NAbs ensure fast removal of infectious reovirus particles and thus likely prevent a large proportion of reovirus particles to reach the tumor and exert their oncolytic effects. Since the majority of the human population has circulating reovirus-specific NAbs, this might explain why reovirus monotherapy has not yet reached optimal efficacy in prior clinical studies (7,73). Various strategies can be employed to enhance reovirus infection and the efficacy of reovirus therapy, for instance combining reovirus with chemotherapeutic agents that can ablate the production of NAbs upon reovirus exposure (74,75), or depletion of $CD4^+$ T cells (**Addendum I**). However, chemotherapy and $CD4^+$ T-cell depletion cannot eliminate preexisting Nabs, thus this may only be successfully employed in reovirus-naive individuals. Alternatively, an option might be to load reovirus on immune cells, such as T cells, dendritic cells, or monocytes before administration, to shield the virus and prevent NAb-mediated clearance (60,76,77).

The effect of (preexisting) NAbs on reovirus efficacy as a T-cell-attracting agent

Although the presence of preexisting NAbs hampers the use of reovirus as an oncolytic agent, the reovirus-induced influx of T cells was surprisingly not affected in preexposed mice (**Chapter 5**). A similar observation was made in a study where immunocompetent naive or NDV-exposed B16.F10-bearing C57BL/6J mice were intratumorally injected with NDV (78). While viral replication was decreased in preexposed mice, the intratumoral influx of $CD8^+$ T cells was comparable between naive and preexposed animals. These observations illustrate that the presence of reovirus in a tumor might not directly correlate with the presence of T cells.

It is commonly accepted that the reovirus-induced expression of ISGs is responsible for the attraction of T cells to the tumor. However, in the presence of NAbs, the reovirus-induced expression of ISGs was impaired, but a remaining moderate expression of some ISGs, including T-cell-attracting chemokine *Cxcl9*, was still observed. We hypothesize that this moderate expression might already have been sufficient to attract T cells to the tumor. Alternatively, it is possible that the administration of reovirus to preexposed mice did not completely preclude effective viral infection and ISG expression, but that this response was already quenched by NAbs at the moment of analysis. Additionally, the presence of the virus itself, the expression of ISGs, and the influx of T cells may differ kinetically in preexposed mice compared to naive mice.

Lastly, various studies comparing the proteome and the immunopeptidome note that there is a limited correlation between the presence of viral antigens and the presentation of epitopes (79,80). Thus, even though the presence of NAbs significantly decreases the number of genomic copies of reovirus, this might not preclude the presentation of reovirus-epitopes in MHC-I and the presence of reovirus-specific T cells in the tumor. Further studies to directly compare the kinetics of reovirus presence in the tumor, the expression of ISGs, as well as the intratumoral influx of T cells in naive versus reovirus-preexposed mice could hopefully answer these remaining questions.

Additionally, it would be interesting to investigate why the presence of NAbs shifts the specificity of reovirus-specific T cells from being specific for the $\mu1_{133\text{-}140}$ epitope to being specific for the $\mu1_{422\text{-}430}$ epitope. Since the reovirus-specific NAbs are also directed towards the reovirus μ1 protein, it is possible that reovirus particles bound to NAbs are processed differently, leading to the presentation of other epitopes on the surface of infected cells (81). Although we demonstrated in **Chapter 5** that these $\mu1_{422\text{-}430}$-specific T cells could still be employed by CD3-bsAbs, it would be interesting to investigate if inducing a preexisting pool of T cells with this specificity by SLP vaccination would also lead to impaired tumor growth upon intratumoral reovirus administration.

Do preexisting T cells influence the anticancer efficacy of reovirus therapy?

In parallel, the question was raised whether the presence of reovirus-specific T cells impairs the efficacy of reovirus therapy. Interestingly, the work presented in **Chapter 3** demonstrated that the preexisting presence of a large pool of reovirus-specific T cells enhanced the antitumor efficacy of reovirus monotherapy, without impairing reovirus infection in the tumor. Since we also demonstrated that depletion of $CD8^+$ T cells did not improve reovirus infection (**Chapter 5**), our data suggest that $CD8^+$ T cells are not involved in the clearance of reovirus.

Since mice were vaccinated with a reovirus-specific $CD8^+$ T-cell epitope-containing SLP before intratumoral reovirus administration, we did not induce preexisting reovirus-specific NAbs that could counteract viral infection and ISG expression upon subsequent therapy. Installing this pool of virus-specific T cells prior to intratumoral reovirus

administration resulted in a faster and bigger influx of T cells that were mostly reovirus-specific and caused a delay in tumor growth (**Chapter 3**). Thus, we demonstrated for the first time that the presence of preexisting reovirus-specific T cells does not impair, but instead improves the efficacy of reovirus monotherapy. For future experiments, it would be interesting to investigate whether having this preinduced pool of reovirus-specific T cells could also lead to enhanced efficacy of Reo&CD3-bsAb therapy.

Altogether, we concluded that the presence of NAbs prevents the use of reovirus as an oncolytic agent, but not its T-cell-attracting capacities. Therefore, reovirus can still be employed for effective combination therapy with T-cell-based immunotherapy. This is very promising for the clinical application of reovirus, where patients presenting with high levels of preexisting NAbs might not be eligible for effective reovirus as monotherapy but could still be susceptible to a combinatorial strategy comprising reovirus and T-cell-based immunotherapy. Additionally, we delivered conceptual evidence that taking advantage of a (preexisting) virus-specific immune cell population provides an exciting new approach in the cancer immunotherapy field.

CONCLUDING REMARKS

In this thesis, we unraveled the immunostimulatory potential of oncolytic reovirus and investigated how these immunostimulatory characteristics could be exploited for effective anticancer immunotherapy.

In summary (**Figure 5**), we demonstrated that administration of oncolytic reovirus does not lead to strong oncolytic effects in tumors (**1**), but instead unleashes a very potent immune response, including the priming of reovirus-specific $CD8^+$ T cells (**2**). For the first time, we showed that these reovirus-specific $CD8^+$ T cells can be employed for anticancer immunotherapy (**3**), by either bypassing their specificity (with CD3-bsAbs) or by exploiting their specificity (via installing a preinduced pool using SLP vaccination). Besides the induction of reovirus-specific $CD8^+$ T cells, reovirus administration also leads to very fast B-cell responses. We are the first to demonstrate that the presence of neutralizing antibodies (NAbs) restricts the use of reovirus as an oncolytic agent (**4**), but that the reovirus-induced influx of $CD8^+$ T cells is retained and the use of reovirus in combination with T-cell-based immunotherapy can still result in potent antitumor responses. Lastly, we showed that blockade of TGF-β does not impair reovirus infection and reovirus-induced expression ISG expression (**5**) or the reovirus-induced attraction and activation of T cells (**6**), but that intrinsic differences between preclinical tumor models can determine whether TGF-β blockade is a beneficial addition to combined reovirus and T-cell-based immunotherapy.

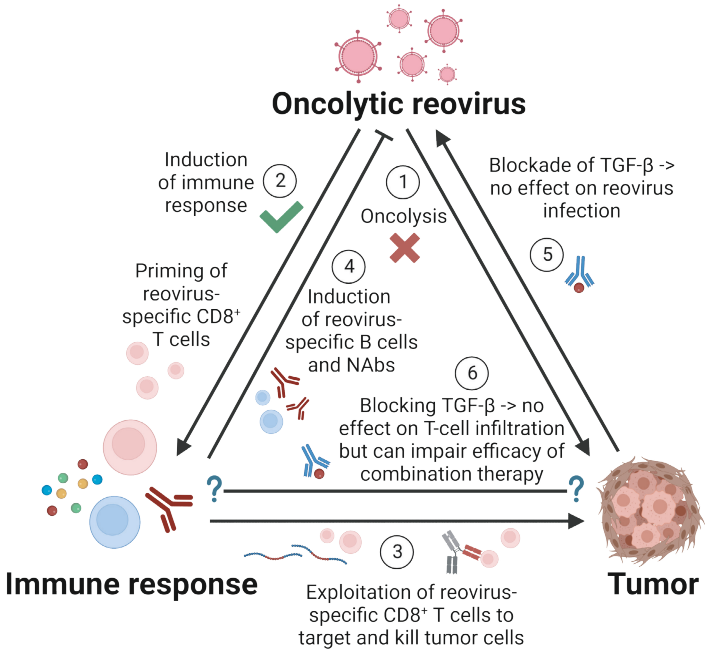


Figure 5. Harnessing the immunostimulatory potential of oncolytic reovirus for anticancer immunotherapy. Reovirus administration does not induce strong oncolysis (**1**) but unleashes a potent immune response (**2**). The reovirus-induced influx of T cells CD8$^+$ T cells can be exploited for anticancer immunotherapy, even if they are reovirus-specific (**3**). Reovirus-specific B-cell responses hamper the use of reovirus as an oncolytic agent, but not its T-cell-attracting ability (**4**). Blockade of TGF-β does not affect reovirus infection (**5**) or the reovirus-induced immune response (**6**), but intertumoral differences dictate whether TGF-β improves or impairs the efficacy of reovirus and T-cell-based immunotherapy.

Although we extensively investigated the use of oncolytic reovirus as an immunostimulatory agent to increase the efficacy of T-cell-based anticancer immunotherapy, there still are some fundamental questions that remained unanswered. For instance, we observed that CD4$^+$ T-cell depletion completely abrogates NAb production and improves the antitumor efficacy of reovirus. However, it is highly puzzling why these mice don't present with viremia and weight loss, in contrast to B-cell deficient mice that also don't have NAbs but do succumb to reovirus-induced pathology. Future studies should investigate the immunological processes underlying these observations. Additionally, we do not know why and how the presence of NAbs induces a shift in the specificity of reovirus-specific CD8$^+$ T cells that are present in the tumor, as well as the implications of this shift in specificity. We did observe that these T cells can still be employed by CD3-bsAbs, but it would be interesting to investigate whether preinstalling a pool of these 'other' T cells by SLP vaccination also leads to delayed tumor outgrowth upon intratumoral reovirus administration. Lastly, it is of utmost importance to identify the factor(s), mechanism(s), or cell type(s) that determine whether TGF-β blockade provides a benefit to the efficacy of reovirus and T-cell-based combination therapy.

Besides answering fundamental questions, a few topics need to be further investigated regarding the clinical translation of our observations. For example, to be able to exploit our novel concept of installing a preexisting T-cell pool that enhances reovirus efficacy in the clinic, prior identification of the human reovirus epitopes is needed. Subsequently, we need to determine which vaccination strategy would be most effective in inducing reovirus-specific $CD8^+$ T cells. Future research should also hunt for an appropriate tumor antigen that can be used for targeting by CD3-bsAbs. The question arises whether there is an appropriate tumor antigen that is expressed by multiple tumor types, or if tumor-specific (or even patient-specific) identification is necessary. Furthermore, it would be highly beneficial to identify or design a safe and non-invasive way to remove NAbs in seropositive patients and/or prevent NAb responses in seronegative patients, to further increase the efficacy of reovirus and T-cell-based combination therapy.

Altogether, the data accumulated in this thesis provides an increased understanding and new insights regarding the use of oncolytic reovirus for anticancer therapy. The collected data described here should prove instructive for future decisions regarding both fundamental investigations as well as the therapeutic application of oncolytic reovirus, and may ultimately contribute to more effective viro-immunotherapy for patients.

REFERENCES

1. Kelly E, Russell SJ. History of Oncolytic Viruses: Genesis to Genetic Engineering. Molecular Therapy **2007**;15:651-9
2. Dock G. The influence of complicating diseases upon leukaemia. The American Journal of the Medical Sciences **1904**;127:563
3. DeAntoneo C, Danthi P, Balachandran S. Reovirus Activated Cell Death Pathways. Cells **2022**;11:1757
4. Kleijn A, Kloezeman J, Treffers-Westerlaken E, Fulci G, Leenstra S, Dirven C, *et al.* The in vivo therapeutic efficacy of the oncolytic adenovirus Delta24-RGD is mediated by tumor-specific immunity. PLoS One **2014**;9:e97495
5. Leveille S, Goulet ML, Lichty BD, Hiscott J. Vesicular stomatitis virus oncolytic treatment interferes with tumor-associated dendritic cell functions and abrogates tumor antigen presentation. J Virol **2011**;85:12160-9
6. Macedo N, Miller DM, Haq R, Kaufman HL. Clinical landscape of oncolytic virus research in 2020. Journal for ImmunoTherapy of Cancer **2020**;8:e001486
7. Müller L, Berkeley R, Barr T, Ilett E, Errington-Mais F. Past, Present and Future of Oncolytic Reovirus. Cancers **2020**;12:3219
8. Forsyth P, Roldán G, George D, Wallace C, Palmer CA, Morris D, *et al.* A Phase I Trial of Intratumoral Administration of Reovirus in Patients With Histologically Confirmed Recurrent Malignant Gliomas. Molecular Therapy **2008**;16:627-32
9. Vidal L, Pandha HS, Yap TA, White CL, Twigger K, Vile RG, *et al.* A Phase I Study of Intravenous Oncolytic Reovirus Type 3 Dearing in Patients with Advanced Cancer. Clinical Cancer Research **2008**;14:7127-37
10. Benencia F, Courrèges MC, Conejo-García JR, Mohamed-Hadley A, Zhang L, Buckanovich RJ, *et al.* HSV oncolytic therapy upregulates interferon-inducible chemokines and recruits immune effector cells in ovarian cancer. Molecular Therapy **2005**;12:789-802
11. Steele L, Errington F, Prestwich R, Ilett E, Harrington K, Pandha H, *et al.* Pro-inflammatory cytokine/chemokine production by reovirus treated melanoma cells is PKR/NF-κB mediated and supports innate and adaptive anti-tumour immune priming. Mol Cancer **2011**;10:20
12. Kelly KR, Espitia CM, Zhao W, Wu K, Visconte V, Anwer F, *et al.* Oncolytic reovirus sensitizes multiple myeloma cells to anti-PD-L1 therapy. Leukemia **2018**;32:230-3
13. Samson A, Scott KJ, Taggart D, West EJ, Wilson E, Nuovo GJ, *et al.* Intravenous delivery of oncolytic reovirus to brain tumor patients immunologically primes for subsequent checkpoint blockade. Sci Transl Med **2018**;10:eaam7577
14. Mostafa AA, Meyers DE, Thirukkumaran CM, Liu PJ, Gratton K, Spurrell J, *et al.* Oncolytic Reovirus and Immune Checkpoint Inhibition as a Novel Immunotherapeutic Strategy for Breast Cancer. Cancers **2018**;10
15. Rajani K, Parrish C, Kottke T, Thompson J, Zaidi S, Ilett L, *et al.* Combination Therapy With Reovirus and Anti-PD-1 Blockade Controls Tumor Growth Through Innate and Adaptive Immune Responses. Mol Ther **2016**;24:166-74
16. Diaz RM, Galivo F, Kottke T, Wongthida P, Qiao J, Thompson J, *et al.* Oncolytic Immunovirotherapy for Melanoma Using Vesicular Stomatitis Virus. Cancer Res **2007**;67:2840-8
17. Wang G, Kang X, Chen KS, Jehng T, Jones L, Chen J, *et al.* An engineered oncolytic virus expressing PD-L1 inhibitors activates tumor neoantigen-specific T cell responses. Nature Communications **2020**;11:1395
18. Woller N, Gürlevik E, Fleischmann-Mundt B, Schumacher A, Knocke S, Kloos AM, *et al.* Viral Infection of Tumors Overcomes Resistance to PD-1-immunotherapy by Broadening Neoantigenome-directed T-cell Responses. Molecular therapy : the journal of the American Society of Gene Therapy **2015**;23:1630-40

19. Prestwich RJ, Ilett EJ, Errington F, Diaz RM, Steele LP, Kottke T*, et al.* Immune-mediated antitumor activity of reovirus is required for therapy and is independent of direct viral oncolysis and replication. Clin Cancer Res **2009**;15:4374-81
20. Brown MC, Holl EK, Boczkowski D, Dobrikova E, Mosaheb M, Chandramohan V*, et al.* Cancer immunotherapy with recombinant poliovirus induces IFN-dominant activation of dendritic cells and tumor antigen–specific CTLs. Sci Transl Med **2017**;9:eaan4220
21. Rosato PC, Wijeyesinghe S, Stolley JM, Nelson CE, Davis RL, Manlove LS*, et al.* Virus-specific memory T cells populate tumors and can be repurposed for tumor immunotherapy. Nature Communications **2019**;10:567
22. Simoni Y, Becht E, Fehlings M, Loh CY, Koo SL, Teng KWW*, et al.* Bystander $CD8^+$ T cells are abundant and phenotypically distinct in human tumour infiltrates. Nature **2018**;557:575-9
23. Erkes DA, Smith CJ, Wilski NA, Caldeira-Dantas S, Mohgbeli T, Snyder CM. Virus-Specific $CD8^+$ T Cells Infiltrate Melanoma Lesions and Retain Function Independently of PD-1 Expression. J Immunol **2017**;198:2979-88
24. Saini SK, Ørskov AD, Bjerregaard AM, Unnikrishnan A, Holmberg-Thydén S, Borch A*, et al.* Human endogenous retroviruses form a reservoir of T cell targets in hematological cancers. Nat Commun **2020**;11:5660
25. Bentzen AK, Marquard AM, Lyngaa R, Saini SK, Ramskov S, Donia M*, et al.* Large-scale detection of antigen-specific T cells using peptide-MHC-I multimers labeled with DNA barcodes. Nature Biotechnology **2016**;34:1037-45
26. Rojas LA, Sethna Z, Soares KC, Olcese C, Pang N, Patterson E*, et al.* Personalized RNA neoantigen vaccines stimulate T cells in pancreatic cancer. Nature **2023**
27. Mandikian D, Takahashi N, Lo AA, Li J, Eastham-Anderson J, Slaga D*, et al.* Relative Target Affinities of T-Cell–Dependent Bispecific Antibodies Determine Biodistribution in a Solid Tumor Mouse Model. Molecular cancer therapeutics **2018**;17:776-85
28. Offner S, Hofmeister R, Romaniuk A, Kufer P, Baeuerle PA. Induction of regular cytolytic T cell synapses by bispecific single-chain antibody constructs on MHC class I-negative tumor cells. Molecular Immunology **2006**;43:763-71
29. Mack M, Gruber R, Schmidt S, Riethmüller G, Kufer P. Biologic properties of a bispecific single-chain antibody directed against 17-1A (EpCAM) and CD3: tumor cell-dependent T cell stimulation and cytotoxic activity. J Immunol **1997**;158:3965-70
30. Middelburg J, Kemper K, Engelberts P, Labrijn AF, Schuurman J, van Hall T. Overcoming Challenges for CD3-Bispecific Antibody Therapy in Solid Tumors. Cancers **2021**;13:287
31. Heidbuechel JPW, Engeland CE. Oncolytic viruses encoding bispecific T cell engagers: a blueprint for emerging immunovirotherapies. Journal of Hematology & Oncology **2021**;14:63
32. Nixon BG, Gao S, Wang X, Li MO. TGFβ control of immune responses in cancer: a holistic immuno-oncology perspective. Nature Reviews Immunology **2022**;doi.org/10.1038/s41577-022-00796-z
33. Batlle E, Massague J. Transforming Growth Factor-beta Signaling in Immunity and Cancer. Immunity **2019**;50:924-40
34. Heinemann L, Simpson GR, Boxall A, Kottke T, Relph KL, Vile R*, et al.* Synergistic effects of oncolytic reovirus and docetaxel chemotherapy in prostate cancer. BMC Cancer **2011**;11:221
35. Pandha HS, Heinemann L, Simpson GR, Melcher A, Prestwich R, Errington F*, et al.* Synergistic effects of oncolytic reovirus and cisplatin chemotherapy in murine malignant melanoma. Clin Cancer Res **2009**;15:6158-66
36. Sei S, Mussio JK, Yang QE, Nagashima K, Parchment RE, Coffey MC*, et al.* Synergistic antitumor activity of oncolytic reovirus and chemotherapeutic agents in non-small cell lung cancer cells. Mol Cancer **2009**;8:47
37. Roulstone V, Twigger K, Zaidi S, Pencavel T, Kyula JN, White C*, et al.* Synergistic cytotoxicity of oncolytic reovirus in combination with cisplatin-paclitaxel doublet chemotherapy. Gene Ther **2013**;20:521-8

38. Comins C, Spicer J, Protheroe A, Roulstone V, Twigger K, White CM, *et al.* REO-10: A Phase I Study of Intravenous Reovirus and Docetaxel in Patients with Advanced Cancer. Clinical Cancer Research **2010**;16:5564-72
39. Lolkema MP, Arkenau H-T, Harrington K, Roxburgh P, Morrison R, Roulstone V, *et al.* A Phase I Study of the Combination of Intravenous Reovirus Type 3 Dearing and Gemcitabine in Patients with Advanced Cancer. Clinical Cancer Research **2011**;17:581-8
40. Karapanagiotou EM, Roulstone V, Twigger K, Ball M, Tanay M, Nutting C, *et al.* Phase I/II trial of carboplatin and paclitaxel chemotherapy in combination with intravenous oncolytic reovirus in patients with advanced malignancies. Clin Cancer Res **2012**;18:2080-9
41. Beyranvand Nejad E, van der Sluis TC, van Duikeren S, Yagita H, Janssen GM, van Veelen PA, *et al.* Tumor Eradication by Cisplatin Is Sustained by CD80/86-Mediated Costimulation of CD8+ T Cells. Cancer Res **2016**;76:6017-29
42. Galluzzi L, Humeau J, Buqué A, Zitvogel L, Kroemer G. Immunostimulation with chemotherapy in the era of immune checkpoint inhibitors. Nature Reviews Clinical Oncology **2020**;17:725-41
43. Rosewell Shaw A, Suzuki M. Oncolytic Viruses Partner With T-Cell Therapy for Solid Tumor Treatment. Front Immunol **2018**;9:2103
44. Krabbe T, Marek J, Groll T, Steiger K, Schmid RM, Krackhardt AM, *et al.* Adoptive T Cell Therapy Is Complemented by Oncolytic Virotherapy with Fusogenic VSV-NDV in Combination Treatment of Murine Melanoma. Cancers (Basel) **2021**;13
45. Rezaei R, Esmaeili Gouvarchin Ghaleh H, Farzanehpour M, Dorostkar R, Ranjbar R, Bolandian M, *et al.* Combination therapy with CAR T cells and oncolytic viruses: a new era in cancer immunotherapy. Cancer Gene Therapy **2022**;29:647-60
46. Feist M, Zhu Z, Dai E, Ma C, Liu Z, Giehl E, *et al.* Oncolytic virus promotes tumor-reactive infiltrating lymphocytes for adoptive cell therapy. Cancer Gene Therapy **2021**;28:98-111
47. Guedan S, Alemany R. CAR-T Cells and Oncolytic Viruses: Joining Forces to Overcome the Solid Tumor Challenge. Front Immunol **2018**;9
48. Ajina A, Maher J. Prospects for combined use of oncolytic viruses and CAR T-cells. J Immunother Cancer **2017**;5:90
49. Andtbacka RHI, Kaufman HL, Collichio F, Amatruda T, Senzer N, Chesney J, *et al.* Talimogene Laherparepvec Improves Durable Response Rate in Patients With Advanced Melanoma. Journal of Clinical Oncology **2015**;33:2780-8
50. Ribas A, Dummer R, Puzanov I, VanderWalde A, Andtbacka RHI, Michielin O, *et al.* Oncolytic Virotherapy Promotes Intratumoral T Cell Infiltration and Improves Anti-PD-1 Immunotherapy. Cell **2017**;170:1109-19 e10
51. Harrington KJ, Vile RG, Melcher A, Chester J, Pandha HS. Clinical trials with oncolytic reovirus: moving beyond phase I into combinations with standard therapeutics. Cytokine Growth Factor Rev **2010**;21:91-8
52. Samson A, Scott KJ, Taggart D, West EJ, Wilson E, Nuovo GJ, *et al.* Intravenous delivery of oncolytic reovirus to brain tumor patients immunologically primes for subsequent checkpoint blockade. Science translational medicine **2018**;10
53. Kaufman HL, Bommareddy PK. Two roads for oncolytic immunotherapy development. Journal for ImmunoTherapy of Cancer **2019**;7:26
54. de Graaf JF, Huberts M, Groeneveld D, van Nieuwkoop S, van Eijck CHJ, Fouchier RAM, *et al.* Comparison between intratumoral and intravenously administered oncolytic virus therapy with Newcastle disease virus in a xenograft murine model for pancreatic adenocarcinoma. Heliyon **2022**;8:e09915
55. Downs-Canner S, Guo ZS, Ravindranathan R, Breitbach CJ, O'Malley ME, Jones HL, *et al.* Phase 1 Study of Intravenous Oncolytic Poxvirus (vvDD) in Patients With Advanced Solid Cancers. Molecular Therapy **2016**;24:1492-501
56. García M, Moreno R, Gil-Martin M, Cascallò M, Ochoa de Olza M, Cuadra C, *et al.* A Phase 1 Trial of Oncolytic Adenovirus ICOVIR-5 Administered Intravenously to Cutaneous and Uveal Melanoma Patients. Hum Gene Ther **2019**;30:352-64

57. Galanis E, Markovic SN, Suman VJ, Nuovo GJ, Vile RG, Kottke TJ*, et al.* Phase II trial of intravenous administration of Reolysin(®) (Reovirus Serotype-3-dearing Strain) in patients with metastatic melanoma. Mol Ther **2012**;20:1998-2003
58. Inoue M, Kim M, Inoue T, Tait M, Byrne T, Nitschké M*, et al.* Oncolytic vaccinia virus injected intravenously sensitizes pancreatic neuroendocrine tumors and metastases to immune checkpoint blockade. Molecular Therapy - Oncolytics **2022**;24:299-318
59. Liu Y, Cai J, Liu W, Lin Y, Guo L, Liu X*, et al.* Intravenous injection of the oncolytic virus M1 awakens antitumor T cells and overcomes resistance to checkpoint blockade. Cell death & disease **2020**;11:1062
60. Berkeley RA, Steele LP, Mulder AA, van den Wollenberg DJM, Kottke TJ, Thompson J*, et al.* Antibody-Neutralized Reovirus Is Effective in Oncolytic Virotherapy. Cancer Imm Res **2018**;6:1161-73
61. Adair RA, Roulstone V, Scott KJ, Morgan R, Nuovo GJ, Fuller M*, et al.* Cell Carriage, Delivery, and Selective Replication of an Oncolytic Virus in Tumor in Patients. Science Translational Medicine **2012**;4
62. Nwanegbo E, Vardas E, Gao W, Whittle H, Sun H, Rowe D*, et al.* Prevalence of Neutralizing Antibodies to Adenoviral Serotypes 5 and 35 in the Adult Populations of The Gambia, South Africa, and the United States. Clinical and Vaccine Immunology **2004**;11:351-7
63. Hemminki O, Parviainen S, Juhila J, Turkki R, Linder N, Lundin J*, et al.* Immunological data from cancer patients treated with Ad5/3-E2F-Δ24-GMCSF suggests utility for tumor immunotherapy. Oncotarget **2015**;6:4467-81
64. Bradley H, Markowitz LE, Gibson T, McQuillan GM. Seroprevalence of Herpes Simplex Virus Types 1 and 2--United States, 1999-2010. Journal of Infectious Diseases **2014**;209:325-33
65. Puzanov I, Milhem MM, Minor D, Hamid O, Li A, Chen L*, et al.* Talimogene Laherparepvec in Combination With Ipilimumab in Previously Untreated, Unresectable Stage IIIB-IV Melanoma. Journal of Clinical Oncology **2016**;34:2619-26
66. Costantino V, Trent MJ, Sullivan JS, Kunasekaran MP, Gray R, MacIntyre R. Serological Immunity to Smallpox in New South Wales, Australia. Viruses **2020**;12:554-
67. Hwang T-H, Moon A, Burke J, Ribas A, Stephenson J, Breitbach CJ*, et al.* A Mechanistic Proof-of-concept Clinical Trial With JX-594, a Targeted Multi-mechanistic Oncolytic Poxvirus, in Patients With Metastatic Melanoma. Molecular Therapy **2011**;19:1913-22
68. Tai JH, Williams JV, Edwards KM, Wright PF, Crowe JJE, Dermody TS. Prevalence of Reovirus-Specific Antibodies in Young Children in Nashville, Tennessee. J Infect Disease **2005**;191:1221-4
69. White CL, Twigger KR, Vidal L, De Bono JS, Coffey M, Heinemann L*, et al.* Characterization of the adaptive and innate immune response to intravenous oncolytic reovirus (Dearing type 3) during a phase I clinical trial. Gene Therapy **2008**;15:911-20
70. Shmulevitz M, Pan L-Z, Garant K, Pan D, Lee PWK. Oncogenic Ras Promotes Reovirus Spread by Suppressing IFN-β Production through Negative Regulation of RIG-I Signaling. Cancer Res **2010**;70:4912-21
71. Dhar D, Spencer JF, Toth K, Wold WSM. Effect of Preexisting Immunity on Oncolytic Adenovirus Vector INGN 007 Antitumor Efficacy in Immunocompetent and Immunosuppressed Syrian Hamsters. J Virol **2009**;83:2130-9
72. Herrlinger U, Kramm CM, Aboody-Guterman KS, Silver JS, Ikeda K, Johnston KM*, et al.* Pre-existing herpes simplex virus 1 (HSV-1) immunity decreases, but does not abolish, gene transfer to experimental brain tumors by a HSV-1 vector. Gene Therapy **1998**;5:809-19
73. Galanis E, Hartmann LC, Cliby WA, Long HJ, Peethambaram PP, Barrette BA*, et al.* Phase I Trial of Intraperitoneal Administration of an Oncolytic Measles Virus Strain Engineered to Express Carcinoembryonic Antigen for Recurrent Ovarian Cancer. Cancer Research **2010**;70:875-82
74. Qiao J, Wang H, Kottke T, White C, Twigger K, Diaz RM*, et al.* Cyclophosphamide Facilitates Antitumor Efficacy against Subcutaneous Tumors following Intravenous Delivery of Reovirus. Clinical Cancer Research **2008**;14:259-69

75. Kottke T, Thompson J, Diaz RM, Pulido J, Willmon C, Coffey M*, et al.* Improved Systemic Delivery of Oncolytic Reovirus to Established Tumors Using Preconditioning with Cyclophosphamide-Mediated Treg Modulation and Interleukin-2. Clinical Cancer Research **2009**;15:561-9
76. Ilett EJ, Bárcena M, Errington-Mais F, Griffin S, Harrington KJ, Pandha HS*, et al.* Internalization of Oncolytic Reovirus by Human Dendritic Cell Carriers Protects the Virus from Neutralization. Clinical Cancer Research **2011**;17:2767-76
77. Ilett E, Kottke T, Donnelly O, Thompson J, Willmon C, Diaz R, *et al.* Cytokine Conditioning Enhances Systemic Delivery and Therapy of an Oncolytic Virus. Molecular Therapy **2014**;22:1851-63
78. Ricca JM, Oseledchyk A, Walther T, Liu C, Mangarin L, Merghoub T*, et al.* Pre-existing Immunity to Oncolytic Virus Potentiates Its Immunotherapeutic Efficacy. Molecular Therapy **2018**;26:1008-19
79. Croft NP, Smith SA, Wong YC, Tan CT, Dudek NL, Flesch IEA*, et al.* Kinetics of Antigen Expression and Epitope Presentation during Virus Infection. PLOS Pathogens **2013**;9:e1003129
80. Weinzierl AO, Lemmel C, Schoor O, Müller M, Krüger T, Wernet D*, et al.* Distorted Relation between mRNA Copy Number and Corresponding Major Histocompatibility Complex Ligand Density on the Cell Surface*S. Molecular & Cellular Proteomics **2007**;6:102-13
81. van Montfoort N, Mangsbo SM, Camps MGM, van Maren WWC, Verhaart IEC, Waisman A*, et al.* Circulating specific antibodies enhance systemic cross-priming by delivery of complexed antigen to dendritic cells in vivo. European Journal of Immunology **2012**;42:598-606



APPENDICES

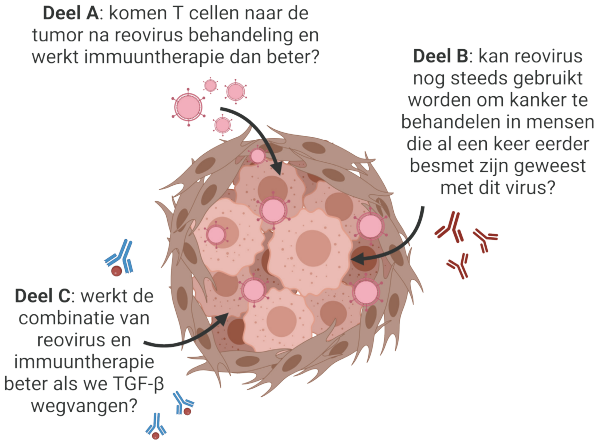
NEDERLANDSE SAMENVATTING VOOR NIET-INGEWIJDEN

Het immuunsysteem beschermt ons lichaam tegen indringers zoals virussen en bacteriën. Het bestaat uit veel verschillende soorten witte bloedcellen, die samenwerken om deze indringers te bestrijden en ons lichaam gezond te houden. Twee belangrijke spelers van het immuunsysteem zijn B cellen en T cellen. B cellen kunnen voorkomen dat een indringer een gezonde cel van het lichaam infecteert, door neutraliserende antilichamen te produceren die aan virussen of bacteriën kunnen binden en daarbij de indringer wegvangen. Mocht zo'n infectie toch plaatsgevonden hebben, dan komen de T cellen aan bod. Er bestaan verschillende soorten T cellen, maar met name de cytotoxische $CD8^+$ T cellen zijn erg goed in staat om een geïnfecteerde cel te herkennen en te doden. De $CD8^+$ T cellen kunnen dit doen doordat een geïnfecteerde cel kleine stukjes van het virus of de bacterie (ook wel antigenen genoemd) presenteert op de oppervlakte. Een T cel is speciaal opgeleid om deze stukjes te herkennen en elke cel die deze antigenen presenteert te doden. Elke T cel herkent maar één antigen, dit wordt T cel specificiteit genoemd. Nadat de geïnfecteerde cel door de T cel is opgeruimd blijven er altijd een aantal geheugen T cellen bestaan, die voor een snellere reactie kunnen zorgen als er op een later moment opnieuw een infectie plaatsvindt.

Naast virussen en bacteriën zijn tumorcellen ook (deels) lichaamsvreemd. Het idee om het immuunsysteem te gebruiken om kankercellen te doden, ook wel immuuntherapie genoemd, heeft geleid tot ongekende verbeteringen in de behandeling van verschillende soorten kanker. Er bestaan verschillende soorten immuuntherapieën, en veel daarvan zijn gericht op het activeren of toedienen van T cellen die stukjes eiwit herkennen die specifiek gepresenteerd worden op de oppervlakte van tumorcellen (tumor-specifieke antigenen). Deze T cellen worden tumor-specifieke T cellen genoemd. Maar, sommige soorten tumoren, zoals alvleesklierkanker, zijn nauwelijks gevoelig voor immuuntherapie. Dit komt onder andere doordat deze tumoren niet of nauwelijks tumor-specifieke antigenen presenteren op de oppervlakte. Het immuunsysteem herkent deze tumoren dus niet als lichaamsvreemd, en daardoor zijn er ook nauwelijks (tumor-specifieke) T cellen in deze tumoren te vinden. Omdat veel soorten immuuntherapie juist deze (tumor-specifieke) T cellen nodig hebben om hun werk te doen, werkt immuuntherapie niet goed in tumoren zoals alvleesklierkanker.

In dit proefschrift hebben we onderzocht of oncolytisch reovirus gebruikt kan worden om immuuntherapie beter te laten werken in deze tot op heden ongevoelige tumoren. Oncolytische virussen, zoals reovirus, zijn virussen die zich alleen in tumorcellen kunnen vermenigvuldigen en gezonde cellen met rust laten. Doordat deze virussen tumorcellen infecteren en zich daar vermenigvuldigen, kan dit uiteindelijk leiden tot de dood van de kankercel. Daarnaast, omdat deze virussen dus wel als lichaamsvreemd gezien worden door het immuunsysteem, kunnen deze virussen misschien ook wel gebruikt worden om T cellen naar de tumor toe te trekken en als zodanig de werking van immuuntherapie te verbeteren.

Dit proefschrift bestaat uit verschillende delen (**Figuur 1**). In **Deel A** hebben we eerst onderzocht of behandeling met oncolytisch reovirus er inderdaad voor zorgt dat er meer T cellen naar de tumor komen, en of we daarmee kunnen zorgen dat immuuntherapie beter werkt in tumoren die daar normaal niet op reageren. Aangezien oncolytisch reovirus een virus is waarmee veel mensen in hun kindertijd al een keer geïnfecteerd zijn, hebben veel mensen al geheugen opgebouwd tegen reovirus. Dit wordt ook wel 'reeds bestaande immuniteit' genoemd. In **Deel B** hebben we daarom onderzocht wat het effect van reeds bestaande immuniteit is op de werking van oncolytisch reovirus therapie is, zowel als het alleen wordt toegediend of als het gecombineerd wordt met immuuntherapie (zogenaamde viro-immuuntherapie). Als laatste hebben we in **Deel C** onderzocht wat er gebeurt met de werking van viro-immuuntherapie als we een molecuul genaamd transformerende groeifactor-β (TGF-β) wegvangen. TGF-β heeft heel veel verschillende functies, onder andere zorgt het ervoor dat T cellen minder goed de tumor kunnen binnenkomen en dat hun functie geremd wordt. We hebben bestudeerd of het wegvangen van TGF-β ervoor zorgt dat de T cellen beter de tumor konden inkomen en actiever zouden zijn, en of dit dan leidt tot een verbeterde werking van viro-immuuntherapie.



Figuur 1. Overzicht van de verschillende onderzoeksvragen die centraal staan in elk deel van deze thesis. In **Deel A** onderzoeken we of reovirus behandeling ervoor zorgt dat er meer T cellen de tumor binnenkomen, en of we daardoor deze tumoren effectiever kunnen behandelen met immuuntherapie. In **Deel B** kijken we of reovirus nog steeds gebruikt kan worden om kankerpatiënten te behandelen als zij al een keertje in hun leven besmet zijn geweest met reovirus en dus 'reeds bestaande immuniteit' hebben opgebouwd. Als laatste onderzoeken we in **Deel C** of we de effectiviteit van reovirus in combinatie met immuuntherapie kunnen verbeteren als we de cytokine transformerende groeifactor-β (TGF-β) wegvangen.

Deel A: het benutten van reovirus-specifieke t cellen voor de behandeling van kanker

In **Hoofstuk 2** zijn we begonnen met het bestuderen van de immuunreactie die plaatsvindt na toediening van reovirus. We gebruiken hiervoor muizen die een functioneel immuunsysteem hebben, en injecteren alvleesklier tumorcellen in de

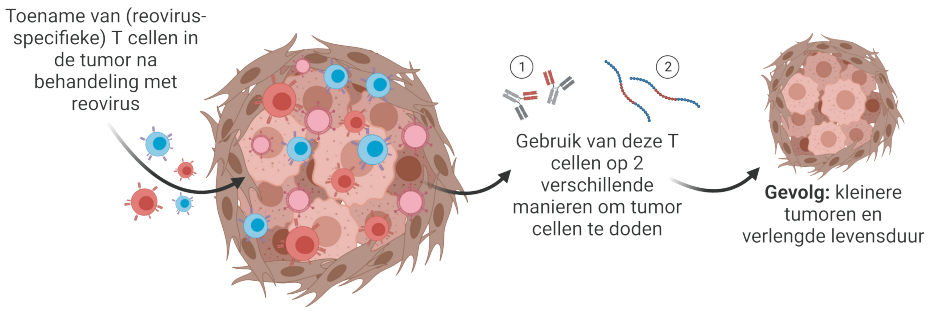
flank. In de flank groeit binnen 2 weken een tumor, waarin wij vervolgens reovirus intratumoraal (direct in de tumor) kunnen toedienen. We hebben gezien dat intratumorale toediening van reovirus leidt tot infectie van de tumorcellen en een snelle expressie van allerlei infectie-gerelateerde genen. De expressie van deze verschillende genen zorgt ervoor dat immuuncellen aangetrokken worden tot de tumor.

Deze toestroom van immuuncellen bestond met name uit $CD8^+$ cytotoxische (celdodende) T cellen, wat een goed teken is. We zagen echter ook dat een groot deel van deze $CD8^+$ T cellen niet tumor-specifiek was, maar reovirus-specifiek. Dit betekent dat ze alleen tumorcellen konden herkennen en doden die geïnfecteerd waren en daarom een stukje virus op hun oppervlakte presenteren, maar de rest van de tumorcellen die niet door het virus zijn geïnfecteerd worden niet herkend.

Om deze virus-specifieke $CD8^+$ T cellen aan te zetten om ook de niet geïnfecteerde kankercellen te doden, hebben we in **Hoofdstuk 2** gebruik gemaakt van CD3-bispecifieke antilichamen. CD3-bispecifieke antilichamen hebben 2 'armen', waarbij de ene 'arm' kan binden aan CD3 (een eiwit dat op de oppervlakte van alle T cellen aanwezig is) en de andere 'arm' kan binden aan een eiwit dat op de tumorcel tot expressie komt. Als beide 'armen' gebonden zijn, wordt de T cel geactiveerd en zal deze de tumorcel doden. Op deze manier kan iedere T cel, dus ook reovirus-specifieke T cellen, aangezet worden om tumorcellen te doden. We hebben inderdaad gezien dat de combinatie van reovirus behandeling (om T cellen naar de tumor te loodsen), gevolgd door CD3-bispecifieke antilichamen (om de T cellen aan te zetten tot het doden van tumorcellen), zeer effectief was en zorgde voor verkleinde tumoren en een langere levensduur van de muizen. We zagen zelfs dat deze combinatie effectief was als we reovirus intraveneus (dus via de bloedbaan) in plaats van direct in de tumor (intratumoraal) toedienden, en dat ook andere tumoren naast de behandelde tumor in de flank kleiner werden. Dus, het gebruik van reovirus in combinatie met CD3-bispecifieke antilichamen leidt tot een zeer effectieve therapie.

In **Hoofstuk 3** hebben we reovirus-specifieke $CD8^+$ T cellen op een andere manier benut. Hier hebben we eerst ontdekt welk kleine stukje van reovirus nu precies herkend wordt door de reovirus-specifieke T cellen. Toen we dit wisten, konden we heel gericht onderzoeken hoe snel reovirus-specifieke T cellen in de tumor komen, hoeveel er komen, en hoe actief ze zijn. We ontdekten dat de reovirus-specifieke $CD8^+$ T cellen in de tumor krachtige en actieve cellen zijn, en theoretisch gezien zouden ze dus tumorcellen die geïnfecteerd zijn met reovirus moeten herkennen en doden. We wilden daarom een manier vinden om zo veel mogelijk reovirus-specifieke T cellen in de tumor te krijgen, zodat er veel tumorcellen gedood zouden worden. We hebben dit gedaan door muizen te vaccineren met een synthetisch lang peptide (SLP) vaccin wat het kleine stukje van reovirus bevatte dat normaliter door reovirus-specifieke T cellen herkend wordt. Door deze vaccinatie strategie konden we ervoor zorgen dat deze muizen al heel veel circulerende reovirus-specifieke T cellen hadden, zonder dat ze ooit reovirus zelf

toegediend hadden gekregen. Op het moment dat de gevaccineerde muizen reovirus intratumoraal kregen toegediend, gingen de tumoren in muizen met veel circulerende reovirus-specifieke T cellen langzamer groeien. Wij denken dat dit komt doordat de T-cellen de reovirus-geïnfecteerde tumorcellen konden herkennen en aanvallen. Dus, het onderzoek beschreven in **Hoofdstukken 2 en 3** laat twee verschillende manieren zien waarop reovirus-specifieke T cellen kunnen worden benut voor effectieve anti-kankertherapie (**Figuur 2**).



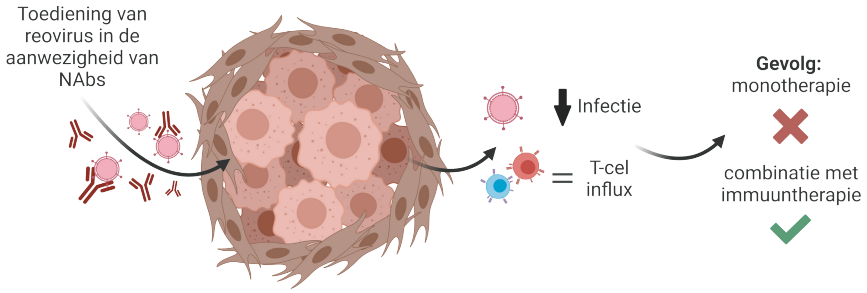
Figuur 2. Het benutten van reovirus-specifieke T cellen voor de behandeling van kanker. Het inspuiten van reovirus in de tumor zorgt voor een snelle toestroom van reovirus-specifieke T cellen. Deze reovirus-specifieke T cellen kunnen geactiveerd worden met CD3-bispecifieke antilichamen (1) en op die manier tumorcellen doden. Ook kan vaccinatie met een SLP (2) gebruikt worden om ervoor te zorgen dat er al heel veel reovirus-specifieke T cellen circuleren, die vervolgens allemaal naar de tumor migreren zodra reovirus daar geïnjecteerd wordt en daar geïnfecteerde tumorcellen kunnen doden. In beide gevallen leidt dit tot kleinere en/of langzamer groeiende tumoren, wat de levensduur verlengt.

Deel B: het effect van reeds bestaande immuniteit op reovirus therapie

Een groot deel van de menselijke bevolking is tijdens hun leven als eens met reovirus in aanraking gekomen. Hierdoor heeft het immuunsysteem van veel kankerpatiënten al geheugen tegen reovirus heeft opgebouwd, voordat de behandeling met reovirus plaatsgevonden heeft. We vroegen ons daarom af of deze reeds bestaande immuniteit gevolgen zou hebben voor de werkzaamheid van reovirus (combinatie)therapie.

Hoofdstuk 4 geeft een overzicht van de huidige literatuur over het effect van reeds bestaande immuniteit tegen verschillende oncolytische virussen, inclusief reovirus, op hun werkzaamheid bij gebruik als therapeutische middelen tegen kanker. In **Hoofdstuk 5** hebben we het gevolg van reeds bestaande immuniteit op de effectiviteit van reovirus therapie onderzocht. We hebben hier vooral gekeken naar het effect van reeds aanwezige neutraliserende antilichamen (NAbs), die door B cellen geproduceerd worden en reovirus snel kunnen wegvangen voordat het de tumorcel kan infecteren. We wilden weten of de aanwezigheid van deze NAbs verhindert dat het reovirus tumorcellen kan doden, maar ook of hierdoor de immuun-stimulerende werking van reovirus (dus het aantrekken van T cellen naar de tumor) beïnvloed wordt.

We hebben het bloed van 100 mensen onderzocht voor de aanwezigheid van NAbs, en konden in ruim 80% van de mensen deze NAbs terugvinden. Dit betekent dus dat een groot deel van de mensen al eens besmet is geweest met reovirus. Om te onderzoeken wat het effect van deze NAbs is, hebben we vervolgens een aantal muizen besmet met reovirus (zodat ze veel NAbs ontwikkelen), en een ander aantal controlemuizen onbesmet gelaten. Vervolgens hebben we bij alle muizen tumorcellen ingespoten in de flank, en toen de tumor gegroeid was hebben we reovirus intratumoraal geïnjecteerd. Eerst hebben we onderzocht of reovirus nog tumorcellen kan doden in de aanwezigheid van NAbs. Toen we de mate van reovirus infectie vergeleken tussen tumoren van muizen zonder NAbs en muizen met NAbs, zagen we dat reovirus infectie sterk verminderd is door de aanwezigheid van NAbs. Het tegenover gestelde zagen we in muizen die genetisch aangepast zijn zodat ze geen B cellen hebben, en daardoor dus ook geen NAbs kunnen produceren. In deze muizen zorgde reovirus behandeling ervoor dat tumoren langzamer groeien of zelfs kleiner worden. Dus, de aanwezigheid van NAbs zorgt ervoor dat reovirus niet goed in staat is om tumorcellen de doden en reovirus als monotherapie niet goed werkt (**Figuur 3**).



Figuur 3. Het effect van de reeds bestaande immuniteit op reovirus therapie. De aanwezigheid van neutraliserende antilichamen (NAbs) vermindert de infectie van reovirus in de tumor, en dit zorgt ervoor dat reovirus uiteindelijk minder tumorcellen kan doden. T cellen worden echter nog steeds wel aangetrokken richting de tumor, en deze T cellen kunnen nog steeds benut worden met immuuntherapie.

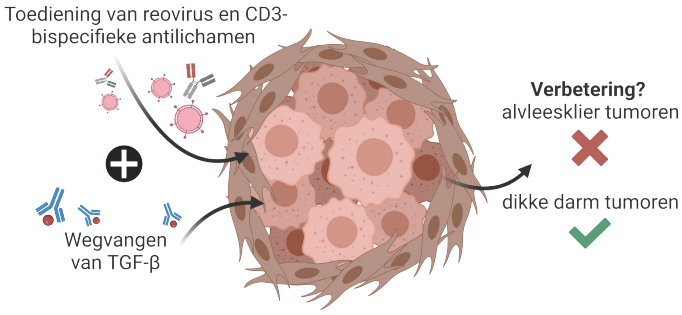
In **Hoofdstukken 2 en 3** hadden we ontdekt dat wanneer tumorcellen geïnfecteerd worden door reovirus, dit ervoor zorgt dat $CD8^+$ T cellen naar de tumor komen. Interessant genoeg was de hoeveelheid T cellen in de tumor niet aangetast door de aanwezigheid van NAbs, ondanks dat de infectie van tumorcellen sterk verminderd was. Omdat de hoeveelheid T cellen niet verminderd was in muizen die veel NAbs hadden, werkte immuuntherapie met behulp van CD3-bispecifieke antilichamen nog steeds. Dus, hoewel NAbs de werkzaamheid van reovirus als monotherapie belemmerden, was reovirus in combinatie met immunotherapeutische strategieën waarbij de T cellen benut worden nog steeds effectief (**Figuur 3**). In andere woorden, NAbs zorgen ervoor dat we reovirus niet goed op zichzelf kunnen gebruiken om tumorcellen te doden (oncolytische werking), maar het aantrekken van T cellen naar de tumor (immuunstimulerende werking) is nog steeds effectief. Deze resultaten betekenen dat we voor het behandelen van kankerpatiënten eigenlijk altijd reovirus moeten gebruiken in

combinatie met een andere soort immuuntherapie die op het gebruik van T cellen gebaseerd is, omdat we verwachten dat deze combinatie strategieën minder beïnvloed zullen zijn door de aanwezigheid van reeds bestaande NAbs in veel kankerpatiënten.

Deel C: het wegvangen van TGF-β om viro-immunotherapie te verbeteren

TGF-β is een molecuul wat heel veel verschillende functies heeft. Het speelt een rol bij het groeien en uitzaaien van tumoren, maar het beïnvloedt ook de functie van verschillende immuuncellen. In **Hoofdstuk 6** hebben we een groot aantal preklinische en klinische studies verzameld die gezamenlijk aangeven dat het wegvangen van TGF-β gecombineerd met het gebruik van oncolytische virussen mogelijk de werkzaamheid van immunotherapie zou kunnen vergroten.

Vervolgens hebben we dit in **Hoofdstuk 7** onderzocht. We hebben hier voor muizen gebruikt met alvleesklier tumoren of dikke darm tumoren, omdat in beide tumor soorten veel TGF-β aanwezig is. We ontdekten dat het wegvangen van TGF-β de werkzaamheid van reovirus en CD3-bispecifieke antilichamen sterk verbeterde in muizen met dikke darm tumoren, maar verrassend genoeg juist verslechterde in muizen met alvleesklier tumoren (**Figuur 4**). Een aantal aspecten verschillen erg tussen deze twee tumor types, zoals de hoeveelheid T cellen die voor behandeling al in de tumor aanwezig is. Een ander verschil tussen deze tumor types is de hoeveelheid stroma (bindweefselcellen en bloedvaten) in de tumor. Met name bindweefselcellen spelen ook een rol in de productie van TGF-β en kunnen de effectiviteit van immuuntherapie beïnvloeden. Helaas zijn we er niet achter gekomen welke factor kan verklaren waarom het wegvangen van TGF-β tot verschillende resultaten leidt. Deze data laten echter wel zien dat het heel belangrijk is om hier meer onderzoek naar te doen, aangezien we de combinatie van reovirus en CD3-bispecifieke antilichamen natuurlijk alleen willen verbeteren en juist niet verslechteren.



Figuur 4. Het wegvangen van TGF-β om viro-immunotherapie te verbeteren. Het wegvangen van transformerende groeifactor-β (TGF-β) zorgt ervoor dat de effectiviteit van reovirus en CD3-bispecifieke antilichamen (dit noemen we ook wel viro-immunotherapie) verslechterd wordt in een model voor alvleesklier kanker, maar juist verbeterd wordt in een model voor dikke darmkanker. Dit verschil kunnen we nog niet verklaren.

Conclusie

Gezamenlijk hebben de data die gepresenteerd worden in dit proefschrift laten zien dat het benutten van de immuun-stimulerende eigenschappen van oncolytisch reovirus een zeer doeltreffende manier is om de effectiviteit van immuuntherapie te vergroten. We hopen dat deze verzamelde inzichten gebruikt kunnen worden voor verder fundamenteel onderzoek, maar ook voor de therapeutische toepassing van oncolytisch reovirus, met het uiteindelijke doel om immuuntherapie beter te laten werken en dus kanker beter te kunnen behandelen.

LIST OF PUBLICATIONS

Publications included in this thesis

1. **Neutralizing antibodies impair the efficacy of reovirus as oncolytic agent but permit effective combination with T-cell-based immunotherapy.**
   Groeneveldt C, Kinderman P, Griffioen L, Rensing O, Labrie C, van den Wollenberg DJM, Hoeben RC, Coffey M, Loghmani H, Verdegaal EME, Welters MJP, van der Burg SH, van Hall T, van Montfoort N. *Manuscript submitted.*

2. **Preexisting immunity: Barrier or Bridge to Effective Oncolytic Virus Therapy?**
   Groeneveldt C*, van der Ende J*, van Montfoort N. *Cytokine Growth Factor Rev.* 2023 Jan 31:S1359-6101(23)00002-3. doi: 10.1016/j.cytogfr.2023.01.002.

3. **Intratumoral differences dictate the outcome of TGF-β blockade on the efficacy of viro-immunotherapy.**
   Groeneveldt C, van Ginkel JQ, Kinderman P, Sluijter M, Griffioen L, Labrie C, van den Wollenberg DJM, Hoeben RC, van der Burg SH, ten Dijke P, Hawinkels LJAC, van Hall T, van Montfoort N. *Cancer Res Comm.* 2023;3(2):325–337. doi:10.1158/2767-9764.CRC-23-0019.

4. **Preinduced reovirus-specific T-cell immunity enhances the anticancer efficacy of reovirus therapy.**
   Groeneveldt C, Kinderman P, van Stigt Thans JJC, Labrie C, Griffioen L, Sluijter M, van den Wollenberg DJM, Hoeben RC, den Haan JMM, van der Burg SH, van Hall T, van Montfoort N. *J Immunother Cancer.* 2022 Jul;10(7):e004464. doi: 10.1136/jitc-2021-004464.

5. **Preconditioning of the tumor microenvironment with oncolytic reovirus converts CD3-bispecific antibody treatment into effective immunotherapy.**
   Groeneveldt C, Kinderman P, van den Wollenberg DJM, van den Oever RL, Middelburg J, Mustafa DAM, Hoeben RC, van der Burg SH, van Hall T*, van Montfoort N*. *J Immunother Cancer.* 2020 Oct;8(2):e001191. doi: 10.1136/jitc-2020-001191.

6. **Immunotherapeutic Potential of TGF-β Inhibition and Oncolytic Viruses.**
   Groeneveldt C, van Hall T, van der Burg SH, Ten Dijke P, van Montfoort N. *Trends Immunol.* 2020 May;41(5):406-420. doi: 10.1016/j.it.2020.03.003.

Other Publications

7. **T-cell stimulating vaccines empower CD3 bispecific antibody therapy in solid tumors.**
   Middelburg J, Sluijter M, Schaap G, Göynük B, Lloyd K, Ovcinnikovs V, Zom GG, Marijnissen RJ, Groeneveldt C, Griffioen L, Sandker GGW, Heskamp S, van der

Burg SH, Arakelian T, Ossendorp F, Arens R, Schuurman J, Kemper K*, van Hall T*. *Manuscript submitted.*

8. **Preclinical Evaluation of the Gorilla-Derived Oncolytic Adenovirus AdV-lumc007 'GoraVir' for the Treatment of Pancreatic Ductal Adenocarcinoma.**
   Bots STF, Harryvan TJ, Groeneveldt C, Kinderman P, Kemp V, van Montfoort N, Hoeben, RC. *Manuscript accepted for publication in Mol Onc.*

9. **NKG2A is a late immune checkpoint on CD8 T cells and marks repeated stimulation and cell division.**
   Borst L, Sluijter M, Sturm G, Charoentong P, Santegoets SJ, van Gulijk M, van Elsas MJ, Groeneveldt C, van Montfoort N, Finotello F, Trajanoski Z, Kiełbasa SM, van der Burg SH, van Hall T. *Int J Cancer.* 2022 Feb 15;150(4):688-704. doi: 10.1002/ijc.33859.

10. **Dendritic cell vaccination and CD40-agonist combination therapy licenses T cell-dependent antitumor immunity in a pancreatic carcinoma murine model.**
    Lau SP, van Montfoort N, Kinderman P, Lukkes M, Klaase L, van Nimwegen M, van Gulijk M, Dumas J, Mustafa DAM, Lievense SLA, Groeneveldt C, Stadhouders R, Li Y, Stubbs A, Marijt KA, Vroman H, van der Burg SH, Aerts J, van Hall T, Dammeijer F, van Eijck CHJ. *J Immunother Cancer.* 2020 Jul;8(2):e000772. doi: 10.1136/jitc-2020-000772.

11. **Exploiting Preexisting Immunity to Enhance Oncolytic Cancer Immunotherapy.**
    Tähtinen S, Feola S, Capasso C, Laustio N, Groeneveldt C, Ylösmäki EO, Ylösmäki L, Martins B, Fusciello M, Medeot M, Tagliamonte M, Chiaro J, Hamdan F, Peltonen K, Ranki T, Buonaguro L, Cerullo V. *Cancer Res.* 2020 Jun 15;80(12):2575-2585. doi: 10.1158/0008-5472.CAN-19-2062.

12. **Biohybrid Vaccines for Improved Treatment of Aggressive Melanoma with Checkpoint Inhibitor.**
    Fontana F, Fusciello M, Groeneveldt C, Capasso C, Chiaro J, Feola S, Liu Z, Mäkilä EM, Salonen JJ, Hirvonen JT, Cerullo V, Santos HA. *ACS Nano.* 2019 Jun 25;13(6):6477-6490. doi: 10.1021/acsnano.8b09613.

13. **Disruption of a CD1d-mediated interaction between mast cells and NKT cells aggravates atherosclerosis.**
    Kritikou E, van Duijn J, Nahon JE, van der Heijden T, Bouwman M, Groeneveldt C, Schaftenaar FH, Kröner MJ, Kuiper J, van Puijvelde GHM, Bot I. *Atherosclerosis*. 2019 Jan;280:132-139. doi: 10.1016/j.atherosclerosis.2018.11.027.

14. **Inhibition of protein arginine methyltransferase 3 activity selectively impairs liver X receptor-driven transcription of hepatic lipogenic genes in vivo.**
Nahon JE*, Groeneveldt C*, Geerling JJ, van Eck M, Hoekstra M. *Br J Pharmacol*. 2018 Aug;175(15):3175-3183. doi: 10.1111/bph.14361.

* Shared authorship position

ABOUT THE AUTHOR

Christianne Groeneveldt was born on September 4, 1995 in Dordrecht. After completing her VWO degree in 2013 at the Wartburg College in Rotterdam, she started the bachelor Bio-Pharmaceutical Sciences at Leiden University. During her bachelor studies, she did an internship at the Division of BioTherapeutics of the Leiden Academic Centre for Drug Research, where she wrote a research proposal to investigate the effect of vascular adhesion molecule 1 (VCAM-1) on the progression of atherosclerosis under supervision of Dr. Janine Geerling. After obtaining her bachelor's degree, Christianne continued with the master Bio-Pharmaceutical Sciences at Leiden University in 2018. Here, she performed her first 9-month internship at the Division of BioTherapeutics of the LACDR, where she studied the role of protein arginine methyltransferase 3 (PRMT3) as a co-activator for liver x receptor α (LXRα)-mediated lipogenesis under the supervision of Dr. Joya Nahon and Dr. Menno Hoekstra in the group of Prof. Miranda van Eck. During her master's degree, Christianne worked as a teaching assistant for various (practical) courses. A second 6-month internship was performed at the Division of Pharmaceutical Biosciences at the University of Helsinki, Finland. Here, she investigated the effect of tumor membrane-based biohybrid vaccination and membrane-covered oncolytic adenovirus on the induction of antitumor responses against aggressive melanoma, under the supervision of Dr. Cristian Capasso in the group of Prof. Vincenzo Cerullo. She received the Koninklijke Nederlandse Maatschappij ter bevordering der Pharmacie (KNMP) Studentenprijs 2018 for this research. Directly after completing her master's degree (cum laude) in 2018, Christianne started her PhD project described in this thesis, which was performed at the Department of Medical Oncology of the Leiden University Medical Center under the supervision of co-promotor Dr. Nadine van Montfoort and promotores Prof. Thorbald van Hall and Prof. Sjoerd van der Burg. After completion of her PhD, Christianne is continuing her scientific career as a postdoc in the field of cancer immunotherapy in the group of Prof. Joachim Aerts at the Department of Pulmonary Medicine of the Erasmus Medical Center in Rotterdam.

ABOUT THE COVER

Imagine a tumor as a castle that is slowly being built in a dark forest of a certain land, without the landowner knowing about it. When this castle is finally discovered, it is already completed and contains strong walls and many varieties of defense mechanisms. Of course, the landowner wants to send knights with the order to attack and destroy the castle. But, since this castle is built in a dark forest and thus surrounded by trees, it is invisible to the knights. Similarly, tumors are often not visible to our immune system, and immune cells therefore cannot enter and destroy the tumor. Because these tumors are not infiltrated and attacked by immune cells, immunotherapy (which often aims to enhance the function of these immune cells) is not effective. Oncolytic reovirus can be employed to overcome this problem. Reovirus can be imagined as a fire. Igniting a fire in the castle can already do some damage, but more importantly, also makes the castle more visible to the knights that were sent by the landowner. Because the fire 'lights up' the castle, these knights can more easily find it, enter it and destroy it. Thus, by administering oncolytic reovirus (the fire), the tumor (the castle) is more visible to immune cells (the knights), which ultimately enhances the efficacy of anticancer immunotherapy.

DANKWOORD

De afgelopen jaren zijn voorbijgevlogen, en ik wil hier graag een aantal mensen bedanken die een bijdrage geleverd hebben aan deze leerzame, uitdagende, maar zeker ook zeer leuke tijd.

Sjoerd, bedankt voor je nuchtere en directe kijk op experimenten en resultaten en het regelmatig opwerpen van de vraag 'wat kunnen we ermee?'. Dank ook voor je altijd razendsnelle en nuttige feedback, ik waardeer het enorm.

Thorbald, jij vroeg tijdens besprekingen minder vaak 'wat kunnen we ermee?' maar meer 'hoe werkt dat nou precies?'. Ik heb veel geleerd van onze discussies over de lay-out van figuren, de volgorde van alinea's en het feit dat meer data niet altijd resulteert in een duidelijker verhaal.

Nadine, wat ben ik blij dat je me 5 jaar geleden de kans gaf dit mooie promotie-avontuur aan te gaan. Ik heb enorm veel van je geleerd en waardeerde het altijd als jij weer eens een positieve draai wist te geven aan iets wat ik alleen maar als negatief kon zien.

Priscilla, erg fijn dat ik in het begin van mijn PhD alle fijne kneepjes van het vak van jou kon leren. Bedankt voor je hulp bij sacrifices in de vroege ochtenden of in het weekend, dit heeft geleid tot waardevolle resultaten en mooie publicaties.

Jim, wat was het fijn dat we bijna tegelijkertijd als buren met onze promotie begonnen en dus vaak konden brainstormen over onze projecten. Heel veel succes met de laatste loodjes, en dankjewel dat je mijn paranimf wilt zijn!

Marit, bedankt voor alle momenten dat ik even lekker frustraties kon uiten in ons kantoor op D1. Na bijna 10 jaar samen studeren en promoveren scheiden hier onze wegen, erg leuk dat we dit kunnen afsluiten door elkaars paranimf te zijn.

Lisa, ik vond het enorm fijn dat ik altijd bij jou terecht kon voor het bespreken van doem-denk scenario's en morele vraagstukken. Bedankt ook voor het opsporen van de kleinste foutjes of scheve lijntjes in mijn papers en presentaties, dit was confronterend maar erg nuttig!

Camilla, als koningin van het i.v. injecteren en het snijden van coupes heb jij me regelmatig uit de brand geholpen, ik waardeer het enorm! Bedankt ook voor al je liefdevolle (maar toch harde) schouderklapjes, ik zal ze missen.

Gaby, eindelijk kwam daar iemand die wel weet wat 'Trekkertrek' is en wat 'barre gaanders' zijn. Volgens mij was het 'meant-to-be' dat je bij de ONCO terecht bent gekomen! Bedankt voor je kritische blik, mijn figuren en presentaties zijn hierdoor zeker verbeterd.

Marjolein, als ik hulp nodig had in de vroege uurtjes was jij altijd beschikbaar, ontzettend dank daarvoor! Bedankt ook voor je berichtjes in de ochtend over zaken in D5-48, ze zorgden er altijd voor dat ik gelijk klaarwakker was.

Lien, dankzij jouw organisatorische talenten verloopt alles op het lab als een geoliede machine. Veel van jouw werk heeft achter de schermen plaatsgevonden, maar ik waardeer het enorm!

Ook de collega's van de 'humane kant' wil ik graag bedanken: Anouk, Anneloes, Els, Linda, Marij, Monique, Nikki, Sanne, Saskia en Vera. Dank voor jullie hulp en de gezelligheid bij congressen en/of gezamenlijke theetjes! Thanks also to 'new' colleagues Hester, Paula, Pieter and Tsolere for suggestions, help or 'gezelligheid'.

Peter en Luuk, bedankt voor de fijne samenwerking op het gebied van TGF-β. Rob en Diana, bedankt voor de vele epjes met reovirus en jullie kritische blik op mijn manuscripten. Ook de andere leden van de OVIT-LUMC groep bedankt voor de gezellige meetings, interessante discussies en nuttige feedback.

Mijn studenten Jordi, Jurriaan en Jasper (in mijn hoofd de 3Js), met jullie enthousiasme en inzet hebben jullie een waardevolle bijdrage geleverd aan 1 van de hoofdstukken van dit proefschrift, hartelijk dank daarvoor!

Aan aantal mensen wil ik bedanken voor het bijdragen aan gezellige momenten en het zorgen voor afleiding van het promoveren in de afgelopen jaren. Kim en Louise (en Marit), het is altijd gezellig om samen met jullie herinneringen op te halen aan onze studententijd en soms toch even de naam van onze appgroep eer aan te doen. Emma, na de middelbare school hebben we menig stedentripje en roadtrip gemaakt. Fijn dat ik nu ook voor een rustgevende boswandeling bij jou terecht kan! Pinar, sinds het begin van onze studie hebben we lief en leed(!) met elkaar gedeeld. Ik heb genoten van onze regelmatige uitstapjes naar een museum/restaurant/koffietentje/boekwinkel/tuincentrum!

Als laatste wil ik mijn familie enorm bedanken. Marnick & Marije, wat is het leuk om jullie gezin te zien groeien met de komst van Noortje en Jurre. Bedankt voor de momenten dat ik even kon langskomen om te 'Zwitsal snuiven', dit werkte altijd erg ontspannend in drukke tijden. Madelon en Rosalien, jullie gekke acties en domme woordgrappen bezorgen mij altijd hoofdpijn van het lachen. Ik hoop op nog veel meer zussenuitstapjes in de toekomst! Walther, wat is het leuk om nog een 'klein' broertje te hebben die wel mee wil naar musea en ook kan genieten van een goed geschiedenisverhaal. Ik heb genoten van de momenten dat je gezellig kwam logeren in Oegstgeest! Lieve pap & mam, bedankt voor jullie onvoorwaardelijke steun, niet alleen de afgelopen jaren maar ook alle tijd daarvoor. Jullie nuchtere houding en 'niet lullen maar poetsen' mentaliteit dient voor mij als voorbeeld en probeer ik graag toe te passen op mijn eigen leven. Fijn dat ik af en toe lekker kan komen uitwaaien in de polder en dat er voor mij altijd een plekje vrij is voor de houtkachel!